Corcoran, WM. H & others

Momentum transfer in fluids 1956

MOMENTUM TRANSFER IN FLUIDS

MOMENTUM TRANSFER IN FLUIDS

By

WM. H. CORCORAN, J. B. OPFELL

and

B. H. SAGE

Chemical Engineering Laboratory
California Institute of Technology
Pasadena, California

1956

ACADEMIC PRESS INC • PUBLISHERS • NEW YORK

LIBRARY OF CONGRESS CATALOG CARD NUMBER:

56-6612

PRINTED IN THE UNITED STATES OF AMERICA

PREFACE

The movement of fluids is important to all branches of engineering and science. Fluid mechanics is one of the areas of mutual interest to scientist and engineer. It is the purpose of this book to present a small portion of this field which we believe to be of special interest to chemical engineers.

In spite of the large number of excellent texts and treatises in the field, none seemed to be available which had the desired combination of details relating to laminar and turbulent shear-flow, boundary-layer analysis, and a statistical treatment of turbulence. It is hoped that the present short discussion provides a sufficient background in these subjects to give the reader a reasonable understanding of the nature of local fluid motions which are of primary importance in thermal and material transport. The described conditions of flow are limited to those frequently encountered in industrial practice. Consideration is given to situations where variations in the molecular properties of the fluid with position are encountered.

Each year sees the accumulation of additional experimental facts and ingenious methods of analysis. The studies have been summarized and placed in consistent form by many authors. The efforts of Lamb, Goldstein, and Howarth are particularly noteworthy although many excellent textbooks by other authors have been written. The field is growing rapidly, however, and the annual increase in experimental information concerning the mechanics of fluid flow, particularly in the field of turbulence, is sufficiently great as to necessitate the frequent preparation of textbooks and review volumes.

The behavior of laminar boundary layers and the transition from these boundary flows to the main body of a turbulently flowing stream have been stressed to a much greater extent than is usual in an elementary textbook in fluid mechanics. Schlichting's approach to laminar boundary flow has been used, and laminar and turbulent boundary flow for a compressible fluid has been given a short treatment. The material has been presented on the assumption that the reader is familiar with the calculus and the elementary principles of differential equations. Tensor and vector notations have not been used in the main body of the text. Their elimination, however, has prevented the clarity of analysis and precision of description that these rather elegant mathematical tools permit. For this reason a brief description of tensors has been included in one appendix along with

the corresponding derivation of the basic relationships of flow in three dimensions.

One chapter in the early part of the text has been devoted to the basic equations of the motion of fluids. This discussion need not be mastered before the later discussions of turbulence and boundary layer are considered. The basic equations of motion involving the Navier-Stokes equations in rectangular Cartesian, cylindrical, and spherical coordinate systems are useful in predicting the velocity distribution in many situations encountered in chemical engineering practice. For this reason the equations have been presented in sufficient detail to permit their significance and interpretation to be understood without an extensive mathematical background.

The statistical theories of turbulence have been described in some detail following the basic ideas of Howarth and Kármán. The recently available data on the statistical nature of turbulent shear-flow have been included together with some discussion of eddy viscosity. The concepts have been presented in an early part of the text because of their historical interest and their widespread acceptance by the engineering profession.

In spite of the widespread interest in supersonic flow and shock phenomena, these matters have not been included since they have been so ably treated by Howarth, Shapiro, Courant, and others. An effort has been made, however, to establish a background that will permit the solution of problems in which the molecular properties of the fluid undergo change with respect to the spatial coordinates of the system.

A number of examples have been presented. These examples have not been chosen for their simplicity but rather as illustrations of the extent to which the differential equations may be applied to physical situations. For convenience in solving problems, tabulations of conversion factors and fluid properties have been given.

Many persons have contributed to this volume. The first four chapters were prepared in somewhat different form just after World War II, and a number of the authors' students contributed to the assembly of these parts of the book. The material was rewritten in the summer of 1954 and the chapters on turbulence and boundary layer were added. Appreciation is expressed to Professor S. Corrsin, Dr. Donald Coles, and Professor R. P. Dilworth for their reviews and suggestions concerning the chapters on turbulence and boundary layer and Appendix II, respectively. Professor W. N. Lacey made a marked contribution by his review of the manuscript, and his suggestions materially improved the clarity of presentation. Olga S. Opfell helped to put the manuscript into a form suitable for publication; Virginia Berry and June Gray prepared the illustrations; Elizabeth

McLaughlin assisted the authors in the preparation of the original copy, and Evelyn Anderson and Patricia Moen with the final typing. B. Lawson Miller aided in the review of proof material.

Throughout the text an effort has been made to acknowledge properly all sources of specific information. Special appreciation is due the following copyright owners, who have made available large numbers of figures and tables: G. Braun, Karlsruhe, Germany; Chemical Engineering Progress; The Clarendon Press, Oxford, England; Deutscher-Ingenieur-Verlag, Düsseldorf; Her Majesty's Stationery Office, London; Industrial and Engineering Chemistry; Transactions of the American Society of Mechanical Engineers; and United Engineering Trustees, Inc.

Professor Hunter Rouse of the Iowa Institute of Hydraulic Research at the State University of Iowa furnished the authors with a photograph relating to the Reynolds classic experiment. Much information presented by Professor Sidney Goldstein of the Hebrew Institute of Technology, Haifa, Israel, was utilized in the chapter on turbulence. L. G. Dunn while at the Jet Propulsion Laboratory of the California Institute of Technology and G. B. Schubauer of the National Bureau of Standards made available experimental records of turbulence. The conversion factors prepared by F. D. Rossini for the National Bureau of Standards are fully quoted. D. D. Wagman of the same bureau prepared a table of constants and conversion factors involving units of energy which has been incorporated. The National Advisory Committee for Aeronautics kindly permitted wide use of its many publications as the basis for figures and discussions in the text.

To all of these and the many workers in the field of fluid mechanics who have made available such a wealth of data the authors wish to express their thanks.

In closing, the authors wish to express their admiration of W. N. Lacey and their appreciation of the opportunity of having been among his students. To have worked with him is a privilege each of us values. His friendly cooperation and meticulous consideration have contributed much to this volume.

PASADENA, JUNE 1956

WM. H. CORCORAN
J. B. OPFELL
B. H. SAGE

CONTENTS

CHAPTER I

INTRODUCTION TO MOMENTUM TRANSFER

The motion of any body of fluid involves momentum. The science of fluid mechanics is frequently concerned with the transfer of momentum from one part of the flowing system to another and to the surroundings. An understanding of the physical nature of momentum and the application of this concept to systems of variable weight are useful in the prediction of the physical behavior of fluids in motion.

Throughout this discussion primary emphasis will be placed upon a consideration of the conservation of momentum rather than upon a balance of forces. The advantages of this approach become clear in the application of fluid mechanics to the evaluation of material and energy transfers.

In describing the flow of fluids it is desirable to adopt certain conventions and symbols in order to simplify the application of Newtonian mechanics to such processes. In the present chapter an effort is made to familiarize the reader with these conventions and symbols. The general nature of flow processes and some of the simpler relationships also are described. Primary emphasis is given to a description of the general characteristics of isothermal fluid flow and to a presentation of the groundwork upon which a quantitative treatment may be based. It is assumed that the reader has some familiarity with mechanics and an understanding of the elements of thermodynamics. It is particularly necessary that the concept of dynamic physical equilibrium be developed along with an understanding of the physical nature of flow processes and the concepts of steady state. Throughout this treatment it will be assumed that local microscopic[1] equilibrium (*1*) obtains. This assumption does not imply in any way that the conditions at a point are invariant in respect to time but only that the properties of the fluid may be described in terms of the thermodynamic state of the system at any given time.

---

[1] The term microscopic will be used to refer to conditions or behavior at a point in a fluid, in contradistinction to the term macroscopic which applies to bulk or aggregate conditions or behavior.

I-1. Fundamental Variables

In the discussion of flow problems the undefined quantities (*2*) or concepts in terms of which all other physical variables will be expressed are force, length, time, and temperature. These quantities cannot themselves be expressed in terms of a smaller number of physical variables although other independent quantities may be substituted for some or all of them. In physics it is usual to take mass, length, time, and temperature as undefined. However, the widespread acceptance of force in engineering discussions makes its use more desirable.

In discussing undefined concepts, the reservation should be made that, from the principles of mechanics (*3*), a variable can be constructed involving only mass, length, and time which can be successfully identified with the temperature of a thermodynamic system (*4*).

I-2. Frames of Reference

It may be desirable to view a flowing system from a position at rest with respect to part or all of the boundary surfaces or at rest with respect to a part of the flow. In certain instances a frame of reference or a coordinate system which moves in some other prescribed manner is useful. In a centrifugal pump it may be desirable to view the flow from a position fixed in the casing so that both the rotor and the flow are in motion relative to the coordinate system, or it may be desirable to associate the frame of reference with the rotor or possibly with an element in the fluid. Often such shifts of reference introduce marked simplifications into the treatment of specific problems.

I-3. Definition of Element of Volume

Fluids will be considered to be continuous unless otherwise specified. It will be assumed that the properties of the smallest portions into which matter may be physically divided are the same as those of the substance in bulk except for effects introduced by gradients (*5*) in associated fields, such as gravity. In the first part of this treatment no regard is taken of the statistical behavior of the molecules making up a small volume of matter. An infinitesimal portion of a flowing system may be bounded at a given instant by imaginary surfaces in such a manner that the values of all the physical properties, such as specific weight, composition, and viscosity of the fluid within the surfaces, vary by only infinitesimal amounts from an

average value. Such a portion of the system will be identified as an element of volume. From this definition it follows that the dimensions of an element of volume may vary widely, depending on the conditions of the problem.

I-4. Conservation of Momentum

The momentum per unit volume of fluid is given by the following defining expression:

$$M_{x,v} = \frac{\sigma u_x}{g} = \rho u_x. \tag{I.01}$$

Equation (I.01) is limited to movement in the x-direction. Momentum is a vector quantity and must be evaluated in both magnitude and direction. Throughout the following discussion all flows will be limited to the x-direction and the subscripts indicating this fact will be omitted.

In dealing with a system of variable weight which is fixed in space, it is convenient to consider the momentum flux to or from the element of volume. The momentum flux at a section per unit area may be expressed as

$$\dot{M} = \frac{\dot{m} u}{g} = \frac{\sigma u^2}{g} \tag{I.02}$$

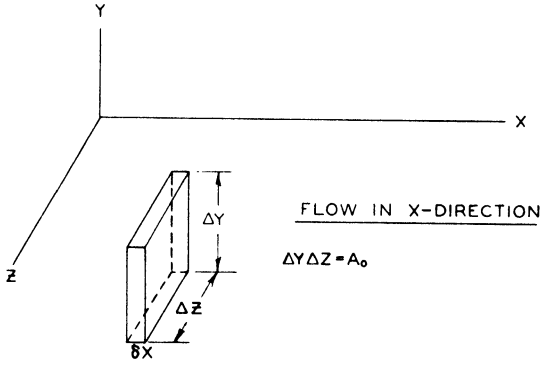

FIG. I-1. Element of volume in a flowing stream.

The weight of the system of fixed total volume may vary with time as a result of change in specific weight of the fluid. Equation (I.02) serves as the defining relationship for the rate of transfer of momentum across a section per unit area. A cross section of area A_0 constitutes one side of an element of volume with length δx shown in Fig. I-1. The momentum of the fluid in the element of volume shown in this figure may be indicated in the following way where the velocity and specific weight are functions of position in the yz-plane:

$$\delta M = \left[\oint_0^{A_0} \frac{\sigma u}{g} dA_0 \right] \delta x. \tag{I.03}$$

In the case for which the velocity and specific weight do not vary from one part to another of this section of area A_0, Eq. (I.03) simplifies to

$$\delta M = A_0 \frac{\sigma u}{g} \delta x. \tag{I.04}$$

Newton postulated that the time rate of change of momentum of a system is equal to the forces acting on it. This fact may be expressed for a system of volume $A_0\,\delta x$ in the following way:

$$\delta F = A_0 \left(\frac{\partial \dot{M}}{\partial x}\right)_\theta \delta x + \left(\frac{\partial \left[\oint_0^{A_0} \frac{\sigma u}{g} dA_0\right]}{\partial \theta}\right)_x \delta x. \tag{I.05}$$

Equation (I.05) applies to the volume element of area A_0 and length δx shown in Fig. I-1. If Eq. (I.05) is applied at a point and the defining relationship for the momentum flux given by Eq. (I.02) is combined with Eq. (I.05), there is obtained

$$\delta F = \frac{1}{g}\left(\frac{\partial \sigma u^2}{\partial x}\right)_\theta \delta x + \frac{1}{g}\left(\frac{\partial \sigma u}{\partial \theta}\right)_x \delta x. \tag{I.06}$$

Equation (I.06) represents the conservation of momentum by equating the force to the differences in the flux at the up- and downstream boundaries of the element and the change in momentum of the system per unit of time. It should be noted that in the interests of generality the virtual changes in force and direction have been employed, along with the partial derivatives to describe this situation.

Equation (I.06) may be rewritten as

$$\delta F = \frac{\sigma u}{g}\left(\frac{\partial u}{\partial x}\right)_\theta \delta x + \frac{u}{g}\left(\frac{\partial \sigma u}{\partial x}\right)_\theta \delta x + \frac{1}{g}\left(\frac{\partial \sigma u}{\partial \theta}\right)_x \delta x. \tag{I.07}$$

The equation of continuity for the type of flow presently considered may be written as

$$\left(\frac{\partial \sigma}{\partial \theta}\right)_x = -\left(\frac{\partial \sigma u}{\partial x}\right)_\theta \tag{I.08}$$

which is only an expression of the fact that the sum of the material entering and leaving the element of volume shown in Fig. I-1 is equal to the change

in weight of the material present in the volume element. A combination of Eqs. (I.07) and (I.08) yields

$$\delta F = \frac{\sigma u}{g}\left(\frac{\partial u}{\partial x}\right)_\theta \delta x + \frac{1}{g}\left(\frac{\partial \sigma u}{\partial \theta}\right)_x \delta x - \frac{u}{g}\left(\frac{\partial \sigma}{\partial \theta}\right)_x \delta x \tag{I.09}$$

which is an expression of the conservation of momentum and the equation of continuity. Under conditions of steady flow, where there is no change with time, Eq. (I.09) assumes the following simple form:

$$\delta F = \frac{\sigma u}{g}\frac{du}{dx}\delta x. \tag{I.10}$$

I-5. Pressure Gradient

The foregoing discussion of the conservation of momentum yields an expression for the total change in force per unit area. If it is desired to relate this to the pressure gradient, still neglecting all external fields including gravity, then, for incompressible uniform flow the result is

$$\delta F = \left[\frac{1}{A_0}\int_0^L \tau_{yx}\, dL\right]\delta x - \frac{dP}{dx}\delta x \tag{I.11}$$

$$= -\left\{\tau_{yx} - \left(\tau_{yx} + \left(\frac{\partial \tau_{yx}}{\partial y_d}\right)_x \Delta y_d\right)\right\}\frac{\delta x}{\Delta y_d} + \left\{P - \left(P + \left(\frac{\partial P}{\partial x}\right)_y \delta x\right)\right\}$$

where A_0 is the peripheral surface area of the volume element and L is the peripheral distance around the volume element. Equation (I.11) is thus a general expression for the force balance.

Where flow between parallel plates is being considered, Eq. (I.11) becomes

$$\delta F = \left(\frac{\partial \tau_{yx}}{\partial y_d}\right)_x \delta x - \left(\frac{\partial P}{\partial x}\right)_y \delta x \tag{I.12}$$

which may be rewritten in terms of a gradient in the following way:

$$\frac{\delta F}{\delta x} = \left(\frac{\partial \tau_{yx}}{\partial y_d}\right)_x - \left(\frac{\partial P}{\partial x}\right)_y. \tag{I.13}$$

In the case of flow in a circular conduit, Eq. (I.11) assumes the form

$$\frac{\delta F}{\delta x} = \frac{1}{r}\left(\frac{\partial r\, \tau_{rx}}{\partial r}\right)_x + \left(\frac{\partial P}{\partial x}\right)_r. \tag{I.14}$$

A combination of Eqs. (I.07) and (I.13), limited to incompressible, uniform flow for a Newtonian fluid, results in

$$\left(\frac{\partial \tau_{yx}}{\partial y_d}\right)_x - \left(\frac{\partial P}{\partial x}\right)_y = \frac{1}{g}\left(\frac{\partial \sigma u}{\partial \theta}\right)_x \tag{I.15}$$

which may be re-expressed for the additional condition of steady flow:

$$\left(\frac{\partial P}{\partial x}\right)_y = \left(\frac{\partial \tau_{yx}}{\partial y_d}\right)_x . \tag{I.16}$$

Under conditions of steady flow Eq. (I.16) may be integrated to give

$$\tau_{yx} = \left(\frac{\partial P}{\partial x}\right)_y y_d + C = \left(\frac{\partial P}{\partial x}\right)_x y_d + (\tau_{yx})_0. \tag{I.17}$$

The second equality was obtained by setting $y = 0$ and evaluating the constant. In the case of flow in a circular conduit, the analogous expression may be written as

$$\tau_{rx} = -\left(\frac{\partial P}{\partial x}\right)_r \frac{r}{2} + \frac{C}{r} = -\left(\frac{\partial P}{\partial x}\right)_r \frac{r}{2} \tag{I.18}$$

where τ_{rx} is zero at $r = 0$. It should be emphasized that the expressions as written apply only to an element of flow symmetrical with respect to the axis of the stream. It is apparent from Eqs. (I.16) and (I.17) that, for this case of steady, uniform flow of an incompressible fluid, they may be extended to represent a force balance between the shear at the walls and the pressure gradient. This elementary treatment of the conservation of momentum does not take into account the effect of flow normal to the axis of principal motion nor does it consider any type of fluctuating velocity. The expressions, except for the limitations stated, are general.

I-6. Thermodynamics of Flowing Systems

The systems usually considered by Gibbs (*6*) in thermodynamical treatments were those at equilibrium or those whose properties differed from the equilibrium values only by infinitesimal amounts. Thus the only states of a system[1] considered (*7*) were those in which conditions within the system were constant with respect to time. Where necessary, due allowance was made for the modifying effect of gravitational, centrifugal, electrical, and magnetic fields on the properties of the system. Thus, under isothermal

[1] The state of a system may be described as its condition at a particular instant.

conditions, a mixture of gases in a thin, flat cell, rotating at constant angular velocity about an axis parallel to one of the long dimensions, as shown in Fig. I-2, would come to thermodynamic equilibrium if the effect of electric, magnetic, and gravitational fields could be neglected, even though to an observer stationary with respect to the cell there would be measurable pressure changes in going from the axis toward the outer ends because of the centrifugal field.

The concepts of thermodynamics can often be extended, however, to cover the case of flowing systems by extending the concept of the "state of a system" to that of the "state of a volume element;" that is, by describing the conditions and assuming local microscopic equilibrium (*1*) of the matter in a volume element at a particular instant. By summing over all the volume elements in a given region, measures of extensive thermodynamic properties as well as averages of intensive properties can be obtained.

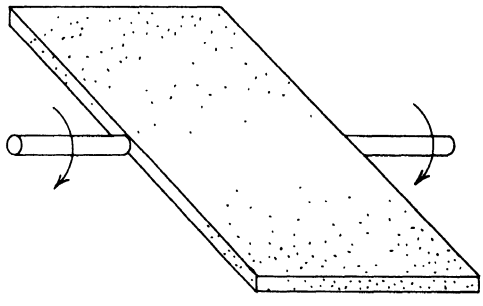

FIG. I-2. Rotating flat cell.

Some care is required in order to determine the thermodynamic state in the volume element. The independent variables must be measured from a reference frame which moves with the volume element, or the variables measured in other ways must be corrected in order to give the properties in the proper frame of reference. The pressure measured when the instrument moves with the flow is often quite different from the apparent pressure measured by a stationary instrument. Likewise, the measured temperature depends on whether the instrument moves with the flow or remains fixed relative to the walls. In the latter case the impact of the flow on the instrument will give a higher measured temperature. The terms "pressure" and "temperature" will be used only in the thermodynamic sense and will relate directly to the state of the fluid in the volume element as measured in a reference frame moving with the element. Classical thermodynamics alone can give no information as to the rate at which processes occur in any system. It is extremely useful, however, in predicting the nature of a specified local flow process as long as local microscopic equilibrium is assumed.

I-7. Stress and Deformation

Materials are distorted or deformed to a greater or lesser extent by forces acting on them. In general, the limiting value of the ratio of the force acting at a real or imaginary surface to the area of the surfaces as the latter is diminished without limit is called the stress.

With some materials, known as elastic solids, the deformation is, at least approximately, proportional to the stress over a considerable range whether the forces are acting in compression or shear. Usually, the proportionality constants also are essentially the same whether the stress is being increased or decreased, except for inertia effects. Thus, if τ_{yx} is the shearing stress or force per unit area being exerted tangentially on the volume element by neighboring elements, as shown in Fig. I-3, and dx/dy is the tangent of the angular deformation from the original position, then

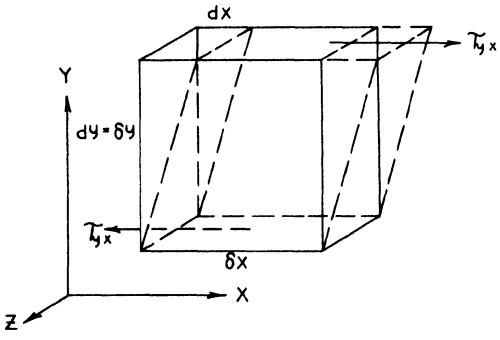

FIG. I-3. Shear stress on a volume element.

$$\tau_{yx} = k\frac{dx}{dy} \tag{I.19}$$

where k is the constant of proportionality known as the shear modulus. The study of the deformation of elastic solids is called "elasticity." Gibbs (*6*) and Goranson (*4*) discuss the thermodynamic relations of strained elastic solids.

With other materials, known as Newtonian fluids or more simply as fluids, the shear is proportional to the relative rate of deformation so that, if the illustrated deformation is produced by the shear in the time interval $d\theta$,

$$\tau_{yx} = \eta\frac{d}{dy_d}\left(\frac{dx}{d\theta}\right) = \eta\frac{du}{dy_d} \tag{I.20}$$

where η is the constant of proportionality known as the absolute viscosity, which is independent of the stress-time relation. It can be seen that a fluid will not support a shearing stress at equilibrium. Gases and simple liquids have been found experimentally to be Newtonian fluids to a close approximation.

The actual behavior of gases and liquids may often be satisfactorily approximated by that of perfect gases and incompressible liquids, respectively. For a perfect gas the relative deformation under pressure is

$$\frac{1}{V}\left(\frac{\partial V}{\partial P}\right)_T = -\frac{1}{P} \tag{I.21}$$

whereas for an incompressible liquid,

$$\frac{1}{V}\left(\frac{\partial V}{\partial P}\right)_T = 0. \tag{I.22}$$

Equations (I.21) and (I.22), for example, may be considered to give the fractional change in volume per unit change in pressure.

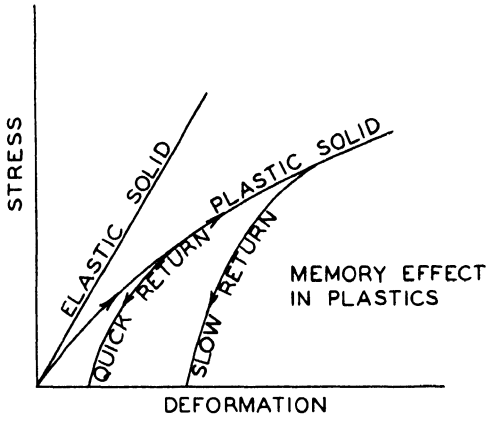

FIG. I-4. Stress-strain curves for elastic and plastic solids.

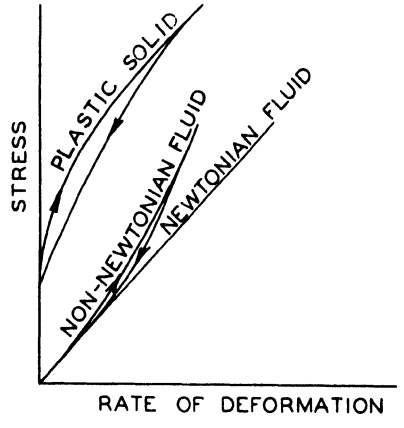

FIG. I-5. Stress *versus* rate of strain for various substances.

The non-Newtonian fluids, which are exemplified by colloidal solutions, such as gels, have apparent viscosities which vary with the magnitude of shear stress and depend also on whether the stress is increasing or decreasing, even after inertia effects are discounted. Plastic solids, which deform like elastic solids under small stresses and flow like fluids under larger stresses which have exceeded a minimum value, are in the same category. The apparent elastic constant and apparent viscosity, however, depend on the magnitude of the stress whether it increases or decreases with time. Plastics, resins, pitches, clays, etc., are broadly classed as plastic solids.

There are no sharp demarcations between these various groups of materials, which differ in degree and not in kind in their behavior. Performance of various materials under shear is shown qualitatively in Figs. I-4 and I-5. A much more complete classification and terminology of such materials is available (*8*).

I-8. Types of Fluid Flow

Two broad types of fluid flow are steady and unsteady. In the latter case, the macroscopic conditions at a given point in the flow change with time, whereas, in the former, the over-all or macroscopic conditions have achieved constant values with respect to time at each point, although conditions may change with respect to down-stream position. Under such circumstances the flow is called nonuniform. If the conditions of flow at a given point in the cross-section of the stream do not change with down-stream position, the flow is considered uniform. Normally, for incompressible fluids the changes in pressure are neglected in considering uniform flow. Strictly speaking, it is not possible to obtain uniform flow for a compressible fluid and it is only encountered in the frictionless flow of an incompressible fluid if the variation in pressure is considered a pertinent parameter.

Each of these types of fluid flow may be further subdivided into laminar and turbulent flow. In the former, elements of volume of the fluid which are often treated as thin sheets or lamina slip past one another without mixing so that each fluid element, although deformed, never loses its identity. In the case of turbulent flow there are many secondary motions, in addition to the broad motion of the fluid, which can be considered random in nature and which effect the mixing of adjacent portions of the fluid.

In unsteady flow starting from rest, the motion is laminar, but, as the velocity of flow increases to a sufficient extent, a transition to turbulent flow will occur. This transition will also occur as a result of many other influences, some of which are associated with steady flow systems.

I-9. Time Averages

The properties of a flowing system will vary from point to point in steady, laminar flow and change microscopically with time at a given point in steady, turbulent flow. Variations of stream conditions with respect to time and position are encountered in all types of unsteady motion. Often the variations in the local value of a property are small compared with the gross changes encountered. It is useful to consider the instantaneous conditions as made up of a steady average value and a fluctuating component. In unsteady, turbulent motion, the macroscopic conditions will be changing, but the concept of an average value will be useful if its time rate of change is small compared to the rate of change of the fluctuating quantity. Under such circumstances the average condition may be treated as independent of the local fluctuations at a given time.

If G_i is the instantaneous value of an intensive property at a given point in a flowing system, it follows from the foregoing discussion that:

$$G_i = \overline{G} + G_f. \tag{I.23}$$

Here $\overline{G}$ is the time average of the property and G_f is the fluctuation value at time θ_0. Then

$$\overline{G} = \frac{1}{\theta} \int_{\theta_0 - \theta/2}^{\theta_0 + \theta/2} G_i \, d\theta. \tag{I.24}$$

The time interval θ over which the averaging is done is long enough so that $\overline{G}(\theta) \approx \overline{G}(\theta')$ for any value of θ' for which $\theta' > \theta$. Stated in another way, the time must be long enough so that the average value does not change significantly as a result of variation in the length of interval chosen. It follows similarly that:

$$\overline{G}_f = \frac{1}{\theta} \int_{\theta_0 - \theta/2}^{\theta_0 + \theta/2} G_f \, d\theta = \frac{1}{\theta} \int_0^{\theta} G_f \, d\theta = 0. \tag{I.25}$$

For simplicity, when the averaging process is not emphasized, the bar over the symbol for the value of the property will be omitted, so that

$$G = \overline{G} \tag{I.26}$$

and the word "average" will be used to designate "time average."

I-10. Flow Equation for an Important Special Case

Before considering the more general application of the conservation of momentum and energy to the mechanics of fluids, it is desirable to develop the flow characteristics in a number of special situations.

The analysis of steady, isothermal flow of an incompressible, homogeneous, Newtonian fluid in a straight, horizontal, smooth conduit of uniform cross section is a problem of practical interest. The intensive properties of the fluid will be considered to be independent of state. If flow in such a conduit is considered at a distance from the ends of the conduit which is large compared to the hydraulic radius,[1] the flow characteristics will depend

[1] The hydraulic radius is the ratio of the transverse cross-sectional area to the transverse wetted perimeter.

only on conditions within the conduit and will not be influenced by the end conditions. Such a flow process is idealized in many aspects and will be identified as a form of idealized viscous flow. Under these circumstances there will be no net flow normal to the axis of the main stream and no average accelerations normal to the axis of flow. For this reason there will be no pressure change along any path perpendicular to the axis flow other than that associated with external fields, such as gravity. In many instances this latter effect will be neglected but in special situations it may be of controlling importance. Since the fluid is homogeneous and incompressible and the process is isothermal, all the intensive properties of the fluid will be invariant. If the flow is steady and the fluid incompressible, there can be no acceleration in the direction of motion since the conduit has a uniform cross section.

I-11. Flow in a Circular Pipe

As shown in Fig. I-6, a straight circular conduit of radius r_0 with fluid flowing under the restrictions set forth in the preceding paragraph will be considered. The average change in pressure with distance along the conduit,

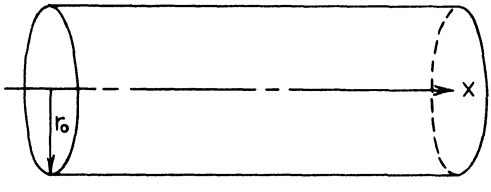

FIG. I-6. Flow in straight circular conduit.

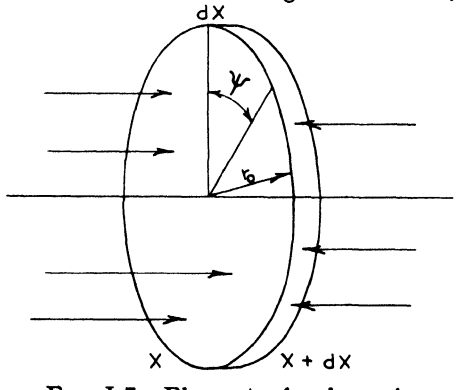

FIG. I-7. Element of volume in straight circular conduit.

dP/dx, is considered to be the pressure gradient. It represents the change in pressure between the points x and $x + dx$ in the stream. The difference in the total force per unit length exerted upon a disk of fluid with radius r, as shown in Fig. I-7, may be given by

$$-\pi r^2 \frac{dP}{dx}. \tag{I.27}$$

In steady, uniform flow this difference in force per unit length produces no axial acceleration of the volume element of fluid and is balanced by

shearing forces acting at the periphery of the element. If τ_{yx} is the average shearing stress at the periphery, it follows that:

$$2\pi r \tau_{rx} dx = -\left(\frac{dP}{dx}\right)\pi r^2 dx. \tag{I.28}$$

For symmetric flow, τ_{rx} must be constant at a given value of r and independent of the polar angle ψ. It follows from Eq. (I.28) that:

$$\tau_{rx} = -\left(\frac{dP}{dx}\right)\frac{r}{2}. \tag{I.29}$$

If Eq. (I.29) is applied at a radius equal to that of the conduit, it follows that:

$$(\tau_{rx})_0 = -\left(\frac{dP}{dx}\right)\frac{r_0}{2}. \tag{I.30}$$

A combination of Eqs. (I.29) and (I.30) yields

$$\frac{\tau_{rx}}{(\tau_{rx})_0} = \frac{r}{r_0}. \tag{I.31}$$

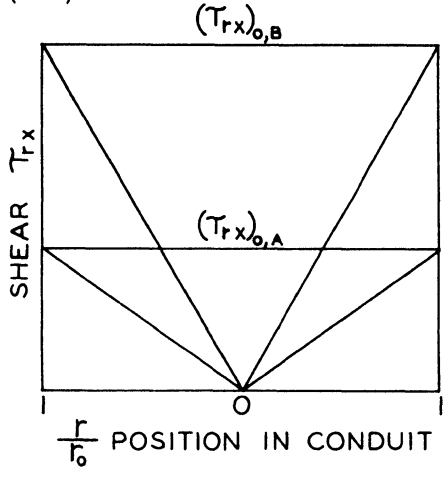

FIG. I-8. Shear *versus* radius for two symmetrical flow patterns.

The shearing stress thus varies linearly from zero at the center of the conduit to a maximum at the wall. Equation (I.31) is one of the more general relationships in fluid mechanics and is the starting point of many useful relations for describing the characteristics of a steady, uniform stream. For two different symmetric conditions the variation in shear with radius is shown in Fig. I-8.

The volumetric rate at which fluid crosses the face of the disk at x in Fig. I-7, for any case in which characteristics of the flow are independent of the polar angle, may be evaluated from

$$\dot{V} = \int_0^r 2\pi r u_x dr = \pi r^2 U_x. \tag{I.32}$$

In this expression, $\dot{V}$ is the average volumetric rate of flow through the section, u_x is the average velocity in the x or axial direction at radius r, and U_x is the average bulk velocity through the disk. The total volumetric rate of flow through the cross section of pipe in Fig. I-6 is given by

$$\dot{V}_0 = \int_0^{r_0} 2\pi r u_x \, dr = \pi r_0^2 U_{x,0} = A_0 U_{x,0} \tag{I.33}$$

where $\dot{V}_0$ is the average volumetric rate of flow through the cross section of the conduit, $U_{x,0}$ is the average bulk velocity, and A_0 is the total cross sectional area of the conduit.

The rate of energy exchange as friction[1] per unit length of flow may be established from the following expression for a volume element of radius r:

$$\frac{j}{dx} = -\frac{dP}{dx}\dot{V}. \tag{I.34}$$

In the case of the conduit as a whole, Eq. (I.34) reduces to

$$\frac{j_0}{dx} = -\frac{dP}{dx}\dot{V}_0. \tag{I.35}$$

Hence from Eqs. (I.34) and (I.35) it follows that:

$$\frac{1}{\dot{V}_0}\frac{j_0}{dx} = -\frac{dP}{dx}. \tag{I.36}$$

It is often implicitly assumed that the fluid under consideration possesses an equation of state such that the following thermodynamic expression applies:

$$\left(\frac{\partial E}{\partial P}\right)_T = 0. \tag{I.37}$$

For many liquids this condition is nearly satisfied. The average rate of energy exchange as friction per unit volume per unit length of flow is then constant, irrespective of the type of flow, as long as the pressure gradient is uniform over a cross section. Since the specific volume is constant, this fact follows directly from Eq. (I.36) and the thermodynamic relationship for the isothermal change in internal energy with pressure. Such a result may be expressed in another way. From Eqs. (I.29), (I.32), and (I.34),

$$\frac{j}{dx} = 2\pi r \tau_{yx} U_x \tag{I.38}$$

and similarly for the entire conduit,

$$\frac{j_0}{dx} = 2\pi r_0 (\tau_{yx})_0 U_{x,0}. \tag{I.39}$$

[1] For a discussion of the concept of friction see ref. 6, Chapters II and VI.

Example 1

Friction in Incompressible Flow.

It is desired to evaluate the friction associated with the flow of 1 lb. of an incompressible liquid in a uniform, circular conduit which is 1000 ft. in length. Experiment indicated that the difference in pressure at the two ends of this horizontal conduit was 127 lb./in.^{2} when the gross flow rate was 5.7 cu. ft./sec. For the purposes of these calculations the fluid may be considered to have a specific weight of 64 lb./cu. ft. The friction per unit length is given by Eq. (I.35),

$$\frac{\dot{J}_0}{dx} = -\frac{dP}{dx}\dot{V}_0 \tag{1 E}$$

It should be realized that this is the friction per unit time per unit length and is not the friction per unit weight associated with the travel through the conduit. Integration of Eq. (1 E) results in

$$\dot{J}_0 = -\dot{V}_0 \int_{P_1}^{P_2} dP = \dot{V}(P_1 - P_2). \tag{2 E}$$

Substituting the appropriate numerical value results in

$$\dot{J}_0 = 5.7 \times 127 \times 144 = 1.04 \times 10^5 \text{ ft.lb./sec.} \tag{3 E}$$

The value of $\dot{J}_0$ represents the friction per second in the entire conduit since the fluid is incompressible and the conduit is uniform and horizontal. If these conditions did not apply, Eq. (1 E) would be somewhat more complicated. The friction per pound of fluid passing through the conduit is simply obtained from

$$J = \frac{\dot{J}_0}{\dot{V}_0 \sigma} = \frac{1}{\sigma}\int_{P_1}^{P_2} dP = \frac{127 \times 144}{64} = 286 \frac{\text{ft. lb.}}{\text{lb}} \tag{4 E}$$

Equation (4 E) yields the degradation associated with the shearing force resulting from the viscosity of the fluid, which in the end accounts for the degradation of the kinetic energy in either turbulent or viscous flow. In this instance no regard need be taken of the velocity distribution as long as the flow is uniform. Changes in velocity distribution in the direction of flow will introduce uncertainties in this simple evaluation of friction.

I-12. The Bernoulli Equation

Much has been written about an expression proposed by Bernoulli which is based primarily upon the conservation of momentum. The momentum flux across a section of unit area is given by

$$\dot{M} = \frac{\dot{m}\,u}{g}. \tag{I.40}$$

For steady flow, Eq. (I.40) gives the change in momentum flux as

$$d\dot{M} = \frac{\dot{m}}{g}\,du. \tag{I.41}$$

From the superposition concept, the change in pressure may be divided into that associated with an applied external field and that associated with the dynamic characteristics of the system, as indicated,

$$dP = dP_s + dP_d. \tag{I.42}$$

In the presence of a gravitational field, the change in pressure under static conditions may be established from

$$dP_s = -\sigma\,dh. \tag{I.43}$$

The conservation of momentum for steady, uniform flow may be written as

$$dP_d = -\frac{\dot{m}}{g}\,du - J_v\,dx. \tag{I.44}$$

The quantity J_v represents the loss in momentum associated with dissipative processes in the flowing system and is directly related to the shear at the wall. A combination of Eqs. (I.42), (I.43), and (I.44) results in

$$dP = -\frac{\dot{m}}{g}\,du - J_v\,dx - \sigma\,dh. \tag{I.45}$$

In many thermodynamic treatments, (7) it is convenient to consider the dissipative processes associated with a unit weight of material. A simple relationship exists between the sum of the dissipative processes in a unit volume and those in a unit weight. Likewise, the friction associated with a unit weight of material while traveling a distance dx may be considered as infinitesimal and has been identified in the following equation as j:

$$J_v\,dx = \sigma J\,dx = \sigma j. \tag{I.46}$$

Combining Eqs. (I.45) and (I.46) and substituting σu for the weight rate of flow per unit of cross sectional area, there is obtained

$$dP = -\frac{\sigma u}{g} du - \sigma j - \sigma dh \tag{I.47}$$

which may be rewritten as

$$V dP = -\frac{u}{g} du - j - dh. \tag{I.48}$$

This may be integrated between states A and B to give

$$\int_A^B V dP = \frac{u_A^2 - u_B^2}{2g} - J + h_A - h_B. \tag{I.49}$$

If it is desired to express Eq. (I.48) in somewhat different form, the first term may be written as

$$V dP = d PV - P dV. \tag{I.50}$$

A combination of Eqs. (I.48) and (I.50) results in

$$d PV = -\frac{u}{g} du - j - d h + P dV. \tag{I.51}$$

The integration of Eq. (I.51) between states A and B yields

$$P_A V_A + \frac{u_A^2}{2g} + h_A = P_B V_B + \frac{u_B^2}{2g} + h_B - \int_A^B P dV + J. \tag{I.52}$$

Equation (I.52) does not include situations where energy is mechanically added to the flowing system between the sections A and B. An example of the simplification that results if Eq. (I.51) is applied to a process at constant elevation with an incompressible fluid and with no dissipative processes is obtained

$$2g V(P_A - P_B) = u_B^2 - u_A^2. \tag{I.53}$$

It is emphasized that strictly this simple derivation of Bernoulli's equation should be applied to a single stream filament since no regard has been taken of the changes in velocity across the section. For many situations it is possible to substitute the gross velocity for the point velocity. However,

this substitution may introduce significant uncertainties, particularly in laminar flow with a parabolic velocity distribution. To take such velocity distribution into account, Eq. (I.47) may be rewritten as

$$dP = -\left(\frac{1}{A_0 g}\int_0^{A_0} \sigma u\, dA_0\right) du - \frac{1}{A_0}\int_0^{A_0} \sigma j\, dA_0 - d\left(\frac{1}{A_0}\int_0^{A_0} \sigma h\, dA_0\right). \quad \text{(I.54)}$$

This equation takes into account the variation in velocity over the cross sectional area as well as the variation in specific weight and the change in the center of gravity of the flowing stream at each location. The derivation of Bernoulli's equation as set forth in the foregoing section leaves much to be desired in the way of precise analysis and of extension to types of flow other than the one-dimensional steady process considered here. A derivation taking most of these factors into account is presented in Appendix I.

I-13. Flow Between Parallel Flat Plates

Many practical situations are approximated by considering the flow of fluids between parallel plates. These plates are considered to be of large extent relative to their separation. A schematic view of two parallel plates is shown in Fig. I-9. The conventions adopted for the Cartesian coordinates are indicated in this figure. For most applications the flow is treated as two dimensional and all the characteristics

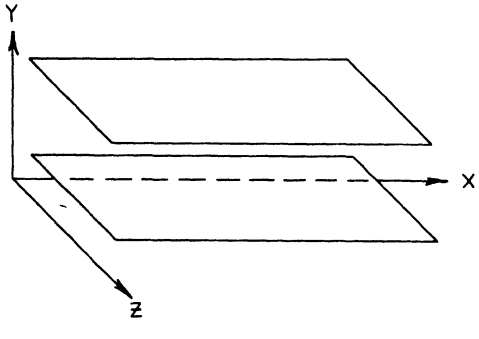

FIG. I-9. Flow between parallel plates.

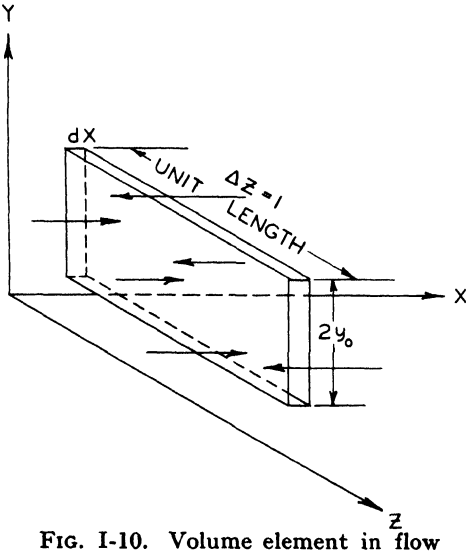

FIG. I-10. Volume element in flow between two parallel plates.

are only functions of the position between plates and the downstream distance. In the case of uniform flow, the characteristics are independent of the down-stream distance and the flow may be considered one dimensional.

This assumption follows the convention established earlier of neglecting the changes in pressure as a measure of uniformity.

The balance of the forces upon a rectangular parallelepiped, which is considered the volume element, results in a series of expressions similar to those found for the flow in circular conduits. In this instance the volume element is of unit width, corresponding to the dimension in the z-direction, and of thickness dx with depth $2\ y_0$, as shown in Fig. I-10. The shear at any point in the flow between parallel plates may be established from

$$\tau_{yx} = -\ y \frac{dP}{dx} \tag{I.55}$$

where y is the distance from the center plane between the plates. When Eq. (I.55) is applied to the wall, it assumes the form

$$(\tau_{yx})_0 = -\ y_0 \frac{dP}{dx}. \tag{I.56}$$

A combination of Eqs. (I.55) and (I.56) results in

$$\frac{\tau_{yx}}{(\tau_{yx})_0} = \frac{y}{y_0}. \tag{I.57}$$

For flow between parallel plates it may be shown that

$$\dot{V} = 2 \int_0^y u_x\, dy = 2\, y\, U_x. \tag{I.58}$$

In Eq. (I.58), $\dot{V}$ is the average volumetric rate of flow per unit width through the element of depth $2\ y$. If this equation is applied to the entire channel, the result is

$$\dot{V}_0 = 2 \int_0^{y_0} u_x\, dy = 2\, y_0\, U_{x,0}. \tag{I.59}$$

In this instance, $\dot{V}$ is the average total volumetric flow rate per unit width of plate.

Equations (I.34) and (I.35) are also applicable to flow between parallel plates:

$$\frac{j}{dx} = -\frac{dP}{dx} \dot{V}. \tag{I.60}$$

Hence for the entire stream, there is obtained

$$\frac{\dot{j}_0}{dx} = -\frac{dP}{dx}\dot{V}_0 \tag{I.61}$$

which is the same as the expression (I.35) for flow in circular conduits. A combination of Eqs. (I.60) and (I.61) yields an expression analogous to Eq. (I.36) for the flow in a circular conduit:

$$\frac{1}{\dot{V}_0}\frac{\dot{j}_0}{dx} = -\frac{dP}{dx}. \tag{I.62}$$

From Eqs. (I.55), (I.58), and (I.60), there is obtained

$$\frac{\dot{j}}{dx} = 2\tau_{yx}U_x. \tag{I.63}$$

When Eq. (I.63) is applied to the entire stream, it assumes the form

$$\frac{\dot{j}_0}{dx} = 2(\tau_{yx})_0 U_{x,0}. \tag{I.64}$$

These equations give average rates at which the fluid motion, under the shear stresses imposed, is transferring mechanical energy into internal energy as friction in the volume element under consideration.

I-14. Laminar Flow in a Cylindrical Pipe

From Eq. (I.20) converted to a cylindrical pipe and from Eq. (I.31), the shear stress on the periphery of an annular element of volume, having radii r and $r + dr$ and a length dx, is given by

$$\tau_{rx} = \frac{(\tau_{rx})_0}{r_0}r = -\eta\frac{du_x}{dr}. \tag{I.65}$$

The volume element is shown in Fig. I-11. It is known from experiment that the net flow is only in the axial direction and that the flow processes consist in the orderly movement of annular filaments of a molecular scale past one another. The integration of Eq. (I.65) yields

$$u_x = C - \frac{(\tau_{rx})_0}{2\eta r_0}r^2. \tag{I.66}$$

In the foregoing equation, C is the constant of integration. At the center of the conduit, where $r = 0$,

$$u_x = u_{x,m}. \tag{I.67}$$

Thus

$$C = u_{x,m}. \tag{I.68}$$

A combination of Eqs. (I.66) and (I.68) yields an expression for the velocity as a function of radius,

$$u_x = u_{x,m} - \frac{(\tau_{rx})_0}{2\eta r_0} r^2. \tag{I.69}$$

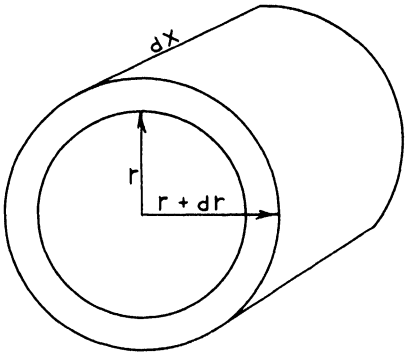

FIG. I-11. Annular volume element in a cylindrical pipe.

It is known experimentally that, except for gases at low pressures, the velocity of the fluid in contact with a solid wall is zero. Under these circumstances, when $r = r_0$

$$u_x = 0. \tag{I.70}$$

From the preceding expressions, including Eq. (I.29), it follows that:

$$u_{x,m} = \frac{(\tau_{rx})_0 r_0}{2\eta} = -\frac{r_0^2}{4\eta}\frac{dP}{dx}. \tag{I.71}$$

From Eqs. (I.69) and (I.71), there results

$$u_x = u_{x,m}\left(1 - \frac{r^2}{r_0^2}\right). \tag{I.72}$$

Since the velocity distribution is parabolic, the volumetric flow rate may be established from

$$\dot{V}_0 = \pi r_0^2 U_x = \int_0^{r_0} 2\pi r u_x \, dr = 2\pi u_{x,m} \int_0^{r_0} r\left(1 - \frac{r^2}{r_0^2}\right) dr = \frac{\pi r_0^2 u_{x,m}}{2}. \tag{I.73}$$

Under these circumstances the gross velocity may be related to the maximum velocity by

$$U_x = \tfrac{1}{2} u_{x,m}. \tag{I.74}$$

A combination of Eqs. (I.71) and (I.73) results in the following useful expression:

$$-\frac{dP}{dx} = \frac{8\eta \dot{V}_0}{\pi r_0^4} = \frac{8\eta U_x}{r_0^2}. \tag{I.75}$$

I-15. Steady, Uniform, Laminar Flow Between Parallel Plates

From Eqs. (I.20) and (I.57) it follows, when y is the distance from the centerline of the channel, that

$$\tau_{yx} = (\tau_{yx})_0 \frac{y}{y_0} = -\eta \frac{du_x}{dy}. \tag{I.76}$$

Integration of Eq. (I.76) yields

$$u_x = C - \frac{(\tau_{yx})_0 y^2}{2\eta y_0}. \tag{I.77}$$

In the case of symmetric flow when

$$u_x = u_{x,m} \tag{I.78}$$

a combination of Eqs. (I.77) and (I.78) results in

$$u_x = u_{x,m} - \frac{(\tau_{yx})_0 y^2}{2\eta y_0}. \tag{I.79}$$

At the wall when

$$y = y_0 \tag{I.80}$$

the following boundary condition obtains:

$$u_x = 0. \tag{I.81}$$

From Eqs. (I.55), (I.79), and (I.81) there is obtained

$$u_{x,m} = \frac{(\tau_{yx})_0 y_0}{2\eta} = -\frac{y_0^2}{2\eta}\frac{dP}{dx}. \tag{I.82}$$

Under these circumstances the velocity distribution is given by

$$u_x = u_{x,m}\left(1 - \frac{y^2}{y_0^2}\right). \tag{I.83}$$

and it is seen that the velocity distribution is parabolic. Equation (I.83) indicates that the velocity distribution for the steady, uniform, laminar flow of a fluid of constant viscosity between parallel plates is parabolic. The volumetric rate of flow per unit width is given by

$$\dot{V}_0 = 2\,y_0\,U_x = 2\int_0^{y_0} u_x\,dy = 2\,u_{x,m}\int_0^{y_0}\left(1 - \frac{y^2}{{y_0}^2}\right)dy = \frac{4}{3}\,y_0\,u_{x,m}. \quad \text{(I.84)}$$

From this it follows that the gross velocity is related to the maximum velocity by

$$U_x = \frac{2}{3}\,u_{x,m} = -\frac{{y_0}^2}{3\,\eta}\frac{dP}{dx} \quad \text{(I.85)}$$

which may be written as

$$-\frac{dP}{dx} = \frac{3\,\eta\,\dot{V}_0}{2\,{y_0}^3} = \frac{3\,\eta\,U_x}{{y_0}^2}. \quad \text{(I.86)}$$

For flow between parallel plates the algebraic relationships among the gross velocity, pressure gradient, and maximum velocity are different from those for flow in a circular conduit.

I-16. Dimensionless Parameters

The use of dimensionless parameters affords a simple approach to the problem of fluid motion. The correct relations can be obtained by simple reasoning which, however, is lacking in rigor. In a more complete treatment of the attack, a more fundamental approach is necessary.

Consider in the simple approach the same steady, uniform flow as was described in Section (I-10). This fluid motion can be described in part by the bulk velocity U, a length L perpendicular to the flow, the viscosity η, the density ρ, and the pressure difference ΔP between two cross sections along the conduit. The force from the inertia of the flowing fluid is the product of the fluid mass and the acceleration and will be dimensionally equivalent to the product of volume, density, and velocity divided by time. This statement may be written as

$$V\frac{\sigma U}{g\,\theta} = L^3\rho\frac{U}{L/U} = L^2\rho\,U^2. \quad \text{(I.87)}$$

The viscous force is dimensionally equivalent to the product of shearing stress and length squared which may be stated as

$$\tau_{yx} L^2 = \eta \frac{U}{L} L^2 = \eta U L. \tag{I.88}$$

The forces causing dissipation of kinetic energy as friction are equal to the product of the pressure difference and an area:

$$F_D = L^2 \Delta P. \tag{I.89}$$

For the case under consideration these quantities may determine the flow characteristics, and on this basis any two of the three ratios formed from them may be used to define the flow. It is convenient to employ the ratio of the inertia forces to the viscous forces and the ratio of the friction forces to the inertia forces for such purposes.

If these ratios describe the flow, there must be an analytical relation connecting them which describes completely the fluid motion. This relation is necessary since it is known experimentally that either the velocity, pressure difference, or characteristic length is established if the other variables are fixed. Such a relationship may be indicated by

$$\phi\left(\frac{\text{inertia forces}}{\text{viscous forces}}, \quad \frac{\text{friction forces}}{\text{inertia forces}}\right) = 0 \tag{I.90}$$

which may be rewritten as

$$\phi\left(\frac{L U \rho}{\eta}, \quad \frac{g \Delta P}{\sigma U^2}\right) = \phi\,(\mathrm{Re}, \mathrm{Eu}) = 0. \tag{I.91}$$

The quantity $L U \rho/\eta$ is identified as the Reynolds number, and the quantity $g \Delta P/\sigma U^2$ is known as the Euler number. If desired, Eq. (I.90) may be rewritten

$$\frac{g \Delta P}{\sigma U^2} = \phi_1\,(\mathrm{Re}). \tag{I.92}$$

The Euler number is often expressed in terms of the pressure gradient dP/dx. Under such circumstances the Euler number is defined as

$$\mathrm{Eu} = -\frac{g L}{\sigma U^2} \frac{dP}{dx}. \tag{I.93}$$

A large body of facts has confirmed that there is a single function ϕ_1 which presents, to a remarkably high degree of accuracy, the behavior of fluids for widely varying conditions of flow (*9*).

Example 2

Distribution of Oil and Water Flowing Between Horizontal Parallel Plates. It is desired to predict the flow characteristics of a binary flowing stream made up of an oil phase and a water phase moving in laminar motion between parallel plates. The plates are spaced 2 in. apart and the oil and water are each introduced at a rate of 0.1 cu. ft./sec./ft. of width of the plate. The arrangement is shown in Fig. I-12.

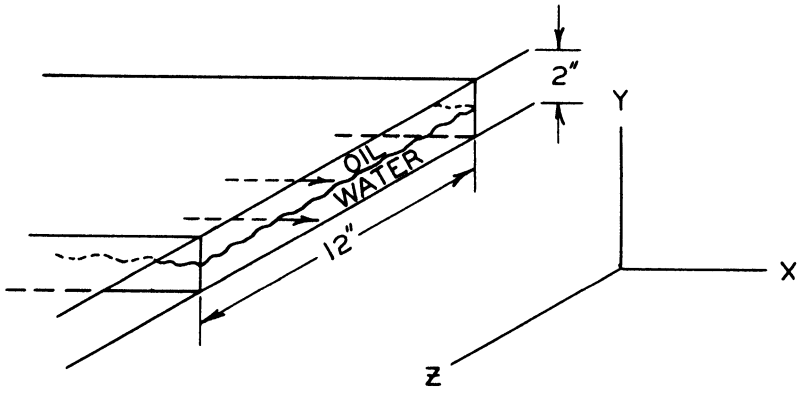

FIG. I-12. Flow of oil and water between parallel plates.

It is desired to determine the elevation of the oil-water interface, the velocity distribution, and the pressure gradient. At the state of the flowing system, the absolute viscosities of the oil and water are 100 and 0.897 centipoises, respectively.

The shear at an elevation y_d per unit width is given by

$$\delta F_{r,1} = \tau_{yx}\,\delta x. \tag{1 E}$$

At a second plane that is at a distance dy_d above the first, the shearing force is

$$\delta F_{\tau,2} = \left(\tau_{yx} + \frac{d\tau_{yx}}{dy_d}\,dy_d\right)\delta x. \tag{2 E}$$

The net shearing force on the volume element is, then,

$$\delta F_{\tau,2} - \delta F_{\tau,1} = \frac{d\tau_{yx}}{dy_d}\,dy_d\,\delta x. \tag{3 E}$$

The force at the upstream side of the volume element is given by

$$\delta F_{P,3} = P\,\delta y_d. \tag{4 E}$$

At the downstream face,

$$\delta F_{P,4} = \left(P + \frac{dP}{dx}\,dx\right)\delta y_d. \tag{5 E}$$

For steady, uniform flow, where the momentum in the volume element is independent of time, it follows from the conservation of momentum that:

$$\delta F_{\tau,2} - \delta F_{\tau,1} = \delta F_{P,4} - \delta F_{P,3}. \tag{6 E}$$

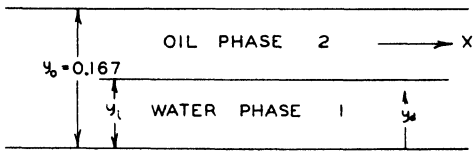

FIG. I-13. Spacing of interface in two-dimensional flow of oil and water.

A combination of Eqs. (1 E) through (5 E) then gives

$$\frac{d\tau_{yx}}{dy_d}\,\delta x\,dy_d = \frac{dP}{dx}\,dx\,\delta y_d \tag{7 E}$$

or

$$\frac{d\tau_{yx}}{dy_d} = \frac{dP}{dx}. \tag{8 E}$$

Equation (8 E) is the same as was derived earlier in Eq. (I.16). For each phase,

$$\tau_{yx,1} = \eta_1 \frac{du_{x,1}}{dy_d}. \tag{9 E}$$

Since the flow is two dimensional, it may be described simply as in Fig. I-13. Assuming isothermal conditions and neglecting any dispersion or solubility of one phase in the other, Eq. (8 E) may be integrated to give

$$\tau_{yx} = \frac{dP}{dx}\,y_d + C_1 \tag{10 E}$$

The applicable boundary conditions are:

$$\begin{aligned} y_d &= y_i, \\ \tau_{yx} &= \tau_{yx,i}, \\ u_{i,1} &= u_{i,2}. \end{aligned} \tag{11 E}$$

Substituting the boundary conditions in Eq. (8 E) and integrating, there is obtained

$$\tau_{yx} = (\tau_{yx})_i + \frac{dP}{dx}(y_d - y_i) = \eta \frac{du_x}{dy_d}. \tag{12 E}$$

Integrating again, with dP/dx independent of y,

$$y_d(\tau_{yx})_i + \frac{dP}{dx}\left(\frac{y_d^2}{2} - y_i\, y_d\right) = \eta\, u_x + C_2. \tag{13 E}$$

Considering the aqueous phase, it is observed that for

$$\begin{aligned} y_d &= 0, \\ u_x &= 0. \end{aligned} \tag{14 E}$$

From Eq. (13 E) it follows that:

$$C_2 = 0. \tag{15 E}$$

Then Eq. (13 E) may be written in the following way for the aqueous phase:

$$y_d(\tau_{yx})_i + \frac{dP}{dx}\left(\frac{y_d^2}{2} - y_d\, y_i\right) = \eta_1\, u_x. \tag{16 E}$$

When the equation of continuity is combined with Eq. (16 E) for the aqueous phase, the result is

$$\eta_1 \dot{V}_1 = \eta_1 \int_0^{y_i} u_x\, dy_d = \frac{(\tau_{yx})_i\, y_i^2}{2} - \frac{dP}{dx}\frac{y_i^3}{3} \tag{17 E}$$

in the oil phase, when

$$\begin{aligned} y_d &= y_0, \\ u_x &= 0. \end{aligned} \tag{18 E}$$

Using the appropriate boundary condition and rewriting Eq. (13 E) for the oil phase,

$$(\tau_{yx})_i\,(y_d - y_0) + \frac{dP}{dx}\left(\frac{y_d^2}{2} - y_d\, y_i + y_i\, y_0 - \frac{y_0^2}{2}\right) = \eta_2\, u_x. \tag{19 E}$$

Likewise,

$$\eta_2 \dot{V}_2 = \eta_2 \int_{y_i}^{y_0} u_x\, dy_d = (\tau_{yx})_i \frac{(y_i - y_0)^2}{2} - \frac{dP}{dx}\frac{(y_0 - y_1)^3}{3}. \tag{20 E}$$

Remembering that

$$u_{i,1} = u_{i,2}. \tag{21 E}$$

Eqs. (16 E) and (19 E) may be combined to give

$$u_{x,i} = \frac{(\tau_{yx})_i\, y_i}{\eta_1} - \frac{y_i^2}{2\eta_1}\frac{dP}{dx} = (\tau_{yx})_i \frac{(y_i - y_0)}{\eta_2} - \frac{1}{2\eta_2}\frac{dP}{dx}(y_i - y_0)^2. \quad (22\text{ E})$$

Rearranging,

$$\frac{\eta_2}{\eta_1}\left[(\tau_{yx})_i\, y_i - \frac{y_i^2}{2}\frac{dP}{dx}\right] = (\tau_{yx})_i\,(y_i - y_0) - \frac{dP}{dx}\frac{(y_i - y_0)^2}{2}. \quad (23\text{ E})$$

Solving Eqs. (17 E), (20 E), and (23 E) simultaneously for y_i, dP/dx, and $(\tau_{yx})_i$, there is obtained

$$\begin{aligned} y_i &= 0.0404 \text{ ft.} \\ (\tau_{yx})_i &= -0.00460 \text{ lb./ft.}^2 \\ \frac{dP}{dx} &= -0.256 \text{ lb./ft.}^3 \end{aligned} \quad (24\text{ E})$$

Iterative methods are a convenient approach to the solution of these three equations.

From Eqs. (16 E) and (19 E) it is possible to evaluate the velocity distribution in each of the phases:

$$u_{x,1} = 307\, y_d - 6.840\, y_d^2; \qquad 0 \leqslant y_d \leqslant 0.0404 \text{ ft.}, \quad (25\text{ E})$$

$$u_{x,2} = 1.24 + 2.74\, y_d - 61.2\, y_d^2; \qquad 0.0404 \leqslant y_d \leqslant 0.1667 \text{ ft.} \quad (26\text{ E})$$

The methods of solution employed may be extended readily to other conditions. As a matter of interest it is possible to substitute the expressions for velocity in Eqs. (16 E) and (19 E) and check the pressure gradient and gross rate of flow.

Example 3

Laminar Flow in an Annulus.

In many industrial applications fluid is permitted to flow in an annular space between concentric cylinders. For this reason it is of interest to investigate in some detail the behavior of a viscous fluid in isothermal laminar flow through a concentric annulus, as is shown in Fig. I-14. The flow takes place between the inner cylinder A and the outer cylinder B. The concentric circular cylinders then afford a uniform annular channel for the flow. It is obvious that, as the ratio of the difference in radii to

the outer radius becomes smaller, the flow pattern approaches that found between parallel plates. In many practical situations, however, such an approximation is not satisfactory, and a more detailed analysis is required.

Figure I-15 shows an element of volume in cylindrical coordinates which will form the basis of the analysis. For present purposes it is convenient to consider a force balance for steady flow. This may be written in expanded form as

$$2\pi r\,dr\left(\frac{dP}{dx}\right)dx + 2\pi(r+dr)\left(\tau_{rx} + \frac{d\tau_{rx}}{dr}dr\right)dx - 2\pi r\,\tau_{rx}\,dx = 0. \quad (1\text{ E})$$

Combining terms yields

$$r\left(\frac{dP}{dx}\right)dr + r\,d\tau_{rx} + \tau_{rx}\,dr = \left(\frac{dP}{dx}\right)r\,dr + d(r\,\tau_{rx}) = 0. \quad (2\text{ E})$$

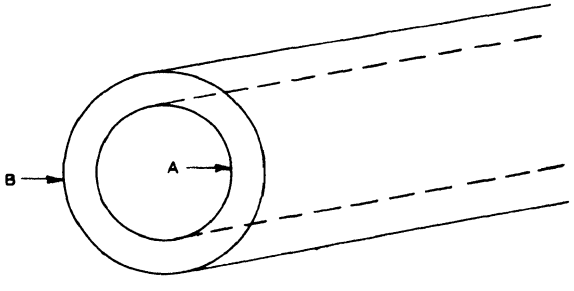

FIG. I-14. Concentric annulus.

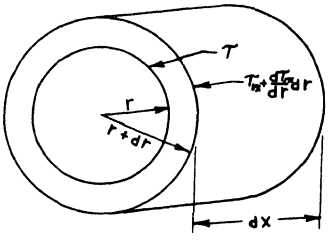

FIG. I-15. Element of volume in cylindrical coordinates.

Equation (2 E) may be integrated from the inner radius r_i to some arbitrary radius r. The appropriate integration may be shown as

$$\frac{dP}{dx}\int_{r_i}^{r} r\,dr + \int_{r_i(\tau_{rx})_i}^{r\tau_{rx}} d(r\,\tau_{rx}) = 0 \quad (3\text{ E})$$

which may be integrated to yield

$$-\frac{dP}{dx}\left(\frac{r^2 - r_i^2}{2}\right) = r\,\tau_{rx} - r_i(\tau_{rx})_i. \quad (4\text{ E})$$

Since the flow is laminar, it follows that:

$$\tau_{rx} = -\eta\frac{du_x}{dr}. \quad (5\text{ E})$$

In Eq. (5 E) since isothermal conditions have been assumed, the viscosity η is assumed to be independent of the spatial coordinate. A combination of Eqs. (4 E) and (5 E) results in

$$-\frac{dP}{dx}\left(\frac{r^2-r_i^2}{2}\right)=-\eta r\frac{du_x}{dr}-r_i(\tau_{rx})_i \tag{6 E}$$

which may be expressed in the following integral form:

$$-\frac{dP}{dx}\int_{r_i}^{r,r_0}\frac{r^2-r_i^2}{2r}dr=-\eta\int_0^{u,0}du-r_i(\tau_{rx})_i\int_{r_i}^{r,r_0}\frac{dr}{r}. \tag{7 E}$$

The limits of the integration in Eq. (7 E) are obvious from the boundary conditions of the problem. The two sets of limits have been included in order to obtain two simultaneous equations which must be applicable, one applying over the entire annulus from the inner radius r_i to the outer radius r_0 and the other, from the inner radius to some arbitrarily chosen radius r:

$$-\frac{dP}{dx}\left(\frac{r_0^2-r_i^2}{4}\right)+\frac{r_i^2}{2}\frac{dP}{dx}\ln\frac{r_0}{r_i}+r_i(\tau_{rx})_i\ln\frac{r_0}{r_i}=0, \tag{8 E}$$

$$-\frac{dP}{dx}\left(\frac{r^2-r_i^2}{4}\right)+\frac{r_i^2}{2}\frac{dP}{dx}\ln\frac{r}{r_i}+r_i(\tau_{rx})_i\ln\frac{r}{r_i}=-\eta u. \tag{9 E}$$

Equation (8 E) may be solved directly for the product $r_i(\tau_{yx})_i$. The resulting expression assumes the form

$$r_i(\tau_{rx})_i=\frac{dP}{dx}\left\{\frac{r_0^2-r_i^2}{4\ln(r_0/r_i)}-\frac{r_i^2}{2}\right\}. \tag{10 E}$$

If Eq. (10 E) is substituted in Eq. (9 E), there is obtained

$$\frac{dP}{dx}\left(\frac{r^2-r_i^2}{4}\right)-\frac{dP}{dx}\frac{r_i^2}{2}\ln\frac{r}{r_i}+\frac{1}{2}\frac{dP}{dx}\left\{r_i^2-\frac{r_0^2-r_i^2}{\ln(r_0/r_i)^2}\right\}\ln\frac{r}{r_i}=\eta u. \tag{11 E}$$

If Eq. (11 E) is solved for the point velocity, it is found that

$$u=\frac{1}{\eta}\frac{dP}{dx}\left\{\frac{r^2-r_i^2}{4}-\frac{r_0^2-r_i^2}{4\ln r_0/r_i}\ln\frac{r}{r_i}\right\}. \tag{12 E}$$

Equation (12 E) describes the velocity in terms of the pressure gradient and the viscosity together with a series of nonlinear terms involving the radius. It permits the velocity to be calculated as a function of the radius for any specified annulus.

It is now desired to determine the point at which the velocity gradient is zero. This may be determined by differentiating Eq. (12 E) with respect to the radius. The result is

$$\frac{du_x}{dr} = \frac{1}{\eta}\frac{dP}{dx}\left\{\frac{r}{2} - \frac{r_0^2 - r_i^2}{4 \ln (r_0/r_i)}\frac{1}{r}\right\}. \tag{13 E}$$

If Eq. (13 E) is set equal to zero corresponding to the point of maximum velocity, it is found that the radius at which the velocity is a maximum is given by

$$r_{u\,max} = \sqrt{\frac{r_0^2 - r_i^2}{\ln r_0^2/r_i^2}}. \tag{14 E}$$

In many situations it is desired to determine the behavior of annular flow in terms of the bulk transport of material through the space between the two circular cylinders. From the definition of bulk flow it follows that:

$$U = \frac{\dot{V}}{A_0} = \frac{\int_{r_i}^{r_0} 2\pi r u_x dr}{\pi(r_0^2 - r_i^2)} \tag{15 E}$$

If Eq. (15 E) is combined with Eq. (12 E), the result is

$$U = \frac{1}{2\eta(r_0^2 - r_i^2)}\frac{dP}{dx}\int_{r_i}^{r_0}\left(r^3 - r r_i^2 - \frac{r_0^2 - r_i^2}{\ln r_0/r_i} r \ln \frac{r}{r_0}\right) dr. \tag{16 E}$$

After appropriate simplification, Eq. (16 E) assumes the form

$$U = \frac{\dot{V}}{A_0} = \frac{1}{4\eta}\frac{dP}{dx}\left\{\frac{r_0^2 - r_i^2}{\ln r_0^2/r_i^2} - \frac{r_0^2 + r_i^2}{2}\right\} \tag{17 E}$$

In obtaining Eq. (17 E) it is not necessary to make any approximation, and therefore the relatively simple expression is an exact description of the gross volumetric velocity for the flow between concentric cylinders. Equation (17 E) reduces to an expression for the gross velocity between parallel plates when the radii of the inner and outer cylinder approach one another.

In order to illustrate the application of the foregoing analysis, it is assumed that it is desired to determine the character of the flow in the annulus between 1-in. and 2-in. admiralty condenser tubing of 18-gage metal. Under these circumstances the inner and outer radii are found to be

$$r_i = 0.0416 \text{ ft.} \tag{18 E}$$

$$r_0 = 0.0792 \text{ ft.} \tag{19 E}$$

If water is flowing at a bulk velocity of 0.1 ft./sec. and has an absolute viscosity of 0.897 centipoise, a kinematic viscosity of 10^{-5} ft.^{2}/sec. is found. Under these circumstances a Reynolds number of 750 is obtained, thus indicating that the flow is laminar and that the foregoing analysis is applicable. For convenience, Eq. (17 E) may be rewritten as

$$-\frac{dP}{dx} = 4\eta U \Big/ \left(\frac{r_0^2 + r_i^2}{2} - \frac{r_0^2 - r_i^2}{\ln r_0^2/r_i^2}\right). \tag{20 E}$$

When the numerical values of the foregoing paragraph are substituted in Eq. (20 E), the result is

$$-\frac{dP}{dx} = \frac{4\,(0.897)\,(0.0000209)\,(0.1)}{\left(\dfrac{0.0416^2 + 0.0792^2}{2} - \dfrac{0.0792^2 - 0.0416^2}{2 \ln\,(0.0792/0.0416)}\right)} \tag{21 E}$$

The conversion of centipoises to the dimensions of absolute viscosity in pounds seconds per square foot must not be overlooked. The reader is referred to Appendix III for a set of conversion units for viscosity.

Solving Eq. (21 E) for the pressure gradient results in

$$-\frac{dP}{dx} = 1.565 \times 10^{-2} \text{ lb./ft.}^2\text{/ft.} \tag{22 E}$$

If the annulus had been 100 ft. in length, the total pressure drop would be given by

$$\Delta P = 0.01087 \text{ lb./in.}^2 \tag{23 E}$$

The small pressure drop of 0.01087 lb./in.^{2} is an indication of the extremely small pressure drops associated with slow viscous flow of liquid of low viscosity. For example, if it is desired to determine the equivalent change in pressure for crude oil flowing at a bulk velocity of 1 ft./sec., somewhat different results are obtained. If it is assumed that the crude oil has a viscosity of 400 centipoises, the pressure gradient from Eq. (17 E) is given by

$$-\frac{dP}{dx} = 69.9 \text{ lb./ft.}^2\text{/ft.} \tag{24 E}$$

The corresponding difference in pressure then becomes

$$\Delta P = 48.5 \text{ lb./in.}^2 \tag{25 E}$$

In this instance the flow at somewhat higher velocity and with a much higher viscosity yields a much larger pressure gradient. This is to be expected since the pressure gradient varies directly with the viscosity and the gross velocity for a given configuration.

If attention is again returned to the flow of water through the same annulus, it is possible to establish a number of additional characteristics of the flow. For example, the distribution of shear may be simply established. Equation (6 E) may be rewritten as

$$r_i(\tau_{rx})_i = \frac{dP}{dx}\left[\frac{r_0^2 - r_i^2}{4 \ln (r_0/r_i)} - \frac{r_i^2}{2}\right] \tag{26 E}$$

All of the quantities in Eq. (26 E) have been established for the flow of water in the annulus at a gross velocity of 0.1 ft./sec. Substitution of these values yields

$$\begin{aligned} r_i(\tau_{rx})_i &= -1.565 \times 10^{-2}\left[\frac{0.0792^2 - 0.0416^2}{4 \ln (0.0792/0.0416)} - \frac{0.0416^2}{2}\right] \\ &= -1.400 \times 10^{-5} \text{ lb./ft.} \end{aligned} \tag{27 E}$$

Likewise Eq. (4 E) may be rewritten as

$$\tau_{rx} = -\frac{1}{r}\left[\frac{dP}{dx}\left(\frac{r^2 - r_i^2}{2} - r_i(\tau_{rx})_i\right]\right. . \tag{28 E}$$

The substitution of the appropriate values for each of the quantities in Eq. (28 E) results in

$$\tau_{rx} = -\frac{1}{r}\left[-1.565 \times 10^{-2}\left(\frac{r^2}{2} - 8.65 \times 10^{-4}\right) + 1.400 \times 10^{-5}\right], \tag{29a E}$$

$$\tau_{rx} = -\frac{1}{r}\left[2.752 \times 10^{-5} - 0.782 \times 10^{-2} r^2\right], \tag{29b E}$$

$$\tau_{rx} = 0.782 \times 10^{-2} r - \frac{2.752 \times 10^{-5}}{r} \tag{29c E}$$

The shear is shown in the accompanying Table I-1 as a function of radius. Figure I-16 shows the variation graphically. In this instance the shear passes through zero at the point corresponding to maximum velocity which was found in Eq. (14 E) to occur at a radius of 0.0595 ft. The shear has not been indicated as changing sign in the figure although this convention has

been carried over in the table. It is of interest to note that the shear at the smaller radius is larger than that at the outer radius, and the locus of points of zero shear does not occur at the center of the annular space.

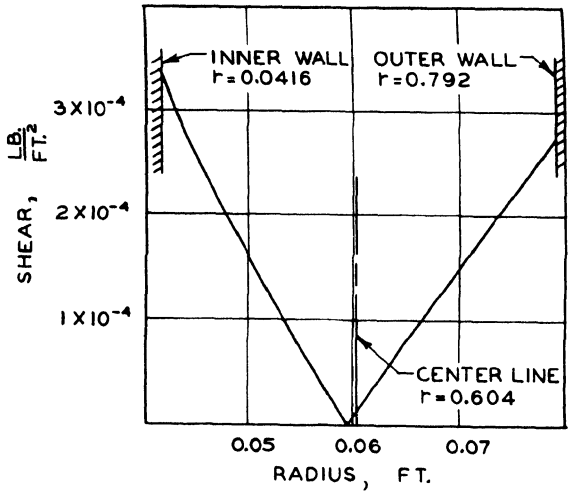

FIG. I-16. Variation in shear with radius.

The velocity in the annular space may be determined directly from Eq. (11 E). Substitution of the appropriate values for the flow of water at a gross velocity of 0.1 ft./sec. yields the following numerical expression for the point velocity in the annulus:

$$u = -0.834 \times 10^3 \left[-4.32 \times 10^{-4} + \frac{r^2}{4} - 17.68 \times 10^{-4} \ln \frac{r}{r_i} \right]. \quad (30\,E)$$

The corresponding values of the velocity are tabulated in Table (I E) and are shown in Fig. I-17. Again it is noted that the velocity distribution is not symmetrical with respect to the walls of the annulus. It is apparent that the maximum velocity is approximately 1½ times the gross velocity. If the flow were not considered to be isothermal, as might well be the case where thermal exchange was involved, the foregoing analysis would not suffice. If the viscosity is a function of the radius, as would be the case in nonisothermal flow, it would require the solution of a nonlinear differential equation and could most easily be solved by numerical methods. Furthermore, if the flow were not steady, the simplifications made in the analysis of the force balance could not be made, and again the problem would probably require a numerical solution.

TABLE I-1. Velocity and Shear Distribution in an Annulus[1]

Radius ft.	Position		Shear lb./ft.	Velocity ft./sec.
	r/r_i	$\ln r/r_i$		
0.0416	1.000	0*	-3.36×10^{-4}	0
0.0450	1.080	0.077	-2.58×10^{-4}	0.0525
0.0500	1.202	0.184	-1.59×10^{-4}	0.110
0.0550	1.322	0.279	-0.70×10^{-4}	0.143
0.0595	1.430	0.358	0.00×10^{-4}	0.151
0.0650	1.562	0.446	0.86×10^{-4}	0.138
0.0700	1.682	0.520	1.54×10^{-4}	0.104
0.0750	1.803	0.589	2.19×10^{-4}	0.0559
0.0792	1.905	0.645	2.73×10^{-4}	0

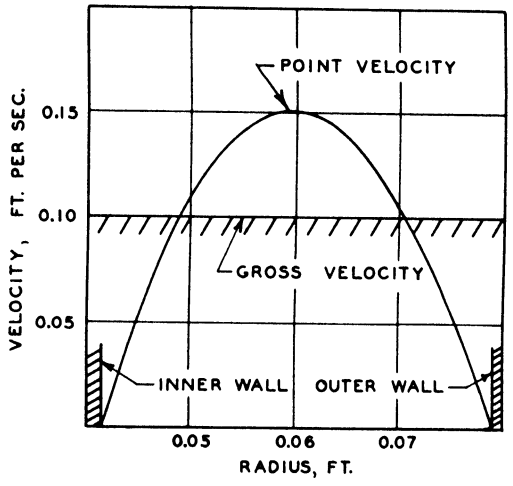

FIG. I-17. Variation in velocity with radius.

I-17. Transition from Laminar to Turbulent Flow

It is found experimentally that the value of the Reynolds number determines in a large measure whether the flow is laminar or turbulent. In circular pipes the flow usually is laminar for $\mathrm{Re} < 2000$ and turbulent for $\mathrm{Re} > 3000$. For parallel plates the transition occurs at somewhat higher values (*10*) of the Reynolds number. Between the limits indicated, there is a transition region, and the path followed depends on other factors than those described above. In the transition region the functional relationship ϕ_1

[1] Radius of inner wall, 0.0416 ft.; radius of outer wall, 0.0792 ft.

of Eq. (I.92) will not be single valued for a particular Reynolds number but will depend on the history of the flow. By exercising special care, laminar flow in pipes may be extended well beyond the normal limit to Reynolds numbers as high as 97,000 (*11*). Any disturbance introduced into the flow causes transition to turbulent motion which will spread throughout the stream.

The study of the mechanism of the transition from laminar to turbulent flow has been described only recently with even a reasonable degree of approximation (*12, 13*). Near the boundary of the stream the transitions between laminar and turbulent flow are even less well understood. At present, these transitions are often empirically established. There appears to be some hysteresis in transitions between laminar and turbulent flow.

I-18. Friction Coefficients

In engineering practice, the Euler number is identified with several factors describing the loss of momentum in the stream. Confusion exists as to the use of these factors, and care is necessary in order to ascertain just which factor is used in a particular application. The Fanning friction factor or coefficient f is defined as

$$f = \tfrac{1}{2}\phi_1(\mathrm{Re}) = \frac{\Delta P}{2\rho U^2}. \tag{I.94}$$

Another common coefficient, which is often designated as λ, is defined as

$$\lambda = 2\phi_1(\mathrm{Re}) \tag{I.95}$$

so that

$$4f = \lambda. \tag{I.96}$$

One approach utilizes a friction factor as a coefficient to the Euler number ratio and defines the Fanning friction factor by [cf. Eq. (I.20)]

$$(\tau_{yx})_0 = f\frac{\rho U^2}{2}. \tag{I.97}$$

A combination with Eq. (I.30) for flow in a circular pipe results in

$$-\frac{dP}{dx} = 2\frac{(\tau_{rx})_0}{r_0} = 4\frac{(\tau_{rx})_0}{D_0} = \frac{4f\rho U^2}{2D_0} = \frac{\lambda\rho U^2}{2D_0}. \tag{I.98}$$

When applying Eq. (I.98), it is convenient to define the Reynolds number as

$$\mathrm{Re} = D_0 \frac{U\rho}{\eta}. \tag{I.99}$$

For parallel plates, it follows from Eq. (I.56) that:

$$-\frac{dP}{dx} = \frac{(\tau_{yx})_0}{y_0} = \frac{2f\rho U^2}{2 \cdot 2 y_0} = \frac{1}{2}\frac{\lambda \rho U^2}{4 y_0}. \tag{I.100}$$

Under these circumstances the Reynolds number is defined as

$$\mathrm{Re} = 2 y_0 \frac{U\rho}{\eta} = \frac{L U \rho}{\eta}. \tag{I.101}$$

It can be seen that the descriptions of the pressure gradients vary with the cross section. In order that a single variable can be used to describe the shape of conduit, a ratio called the hydraulic radius r_h has been widely employed in fluid mechanics. This parameter is defined here as the ratio of the cross sectional area of the stream to the transverse wetted perimeter. For a circular conduit

$$r_h = \frac{\frac{1}{4}\pi D_0^2}{\pi D_0} = \frac{D_0}{4} \tag{I.102}$$

so that the Reynolds number may be described in terms of the diameter or in terms of the hydraulic radius Re_h. It is defined as

$$\mathrm{Re}_h = 4 r_h \frac{U\rho}{\eta} = D_0 \frac{U\rho}{\eta}. \tag{I.103}$$

For pipes, Eq. (I.98) becomes

$$-\frac{dP}{dx} = \frac{(\tau_{rx})_0}{r_h} = \frac{f_h \rho U^2}{2 r_h} = \frac{1}{4}\frac{\lambda_h}{r_h}\frac{\rho U^2}{2}. \tag{I.104}$$

For parallel plates of infinite extent,

$$r_h = \frac{1 \cdot 2 y_0}{2 \cdot 1} = y_0 \tag{I.105}$$

and Eq. (I.100) becomes

$$-\frac{dP}{dx} = \frac{(\tau_{yx})_0}{r_h} = \frac{f_h}{r_h}\frac{\rho U^2}{2} = \frac{1}{4}\frac{\lambda_h}{r_h}\frac{\rho U^2}{2}. \tag{I.106}$$

Equation (I.106) is identical with Eq. (I.104), but the Reynolds number for the flow between parallel plates is twice the value based on the characteristic plate separation, as is indicated by

$$\mathrm{Re}_h = 2\,\mathrm{Re}. \tag{I.107}$$

Another useful relation is obtained from Eqs. (I.100) or (I.106) by considering the second and fourth members and solving for the gross velocity:

$$U = \sqrt{\frac{8}{\lambda_h}}\sqrt{\frac{(\tau_{yx})_0}{\rho}}. \tag{I.108}$$

In the case of laminar flow these relations must agree with the analytic solutions already obtained. For circular conduits, Eq. (I.75) may be rewritten as

$$-\frac{dP}{dx} = \frac{32\eta U}{D_0^2} = \frac{32\eta}{D_0 U\rho}\frac{\rho U^2}{D_0} = \frac{32}{D_0}\frac{\rho U^2}{\mathrm{Re}}. \tag{I.109}$$

However, from Eq. (I.98),

$$-\frac{dP}{dx} = 2f\frac{\rho U^2}{D_0} = \frac{\lambda}{2}\frac{\rho U^2}{D_0}. \tag{I.110}$$

From the preceding expressions, it follows that:

$$\lambda = \frac{64}{\mathrm{Re}}; \qquad f = \frac{16}{\mathrm{Re}}. \tag{I.111}$$

For parallel plates, it follows from Eq. (I.86) that:

$$-\frac{dP}{dx} = \frac{3\eta U}{y_0^2} = \frac{12\eta}{2y_0 U\rho}\frac{\rho U^2}{2y_0} = \frac{12}{2y_0}\frac{\rho U^2}{\mathrm{Re}}. \tag{I.112}$$

Combination with Eq. (I.100) results in

$$\lambda = \frac{48}{\mathrm{Re}}; \qquad f = \frac{12}{\mathrm{Re}}. \tag{I.113}$$

Equation (I.113) may be rewritten in terms of the Reynolds number based upon the hydraulic radius:

$$\lambda_h = \frac{96}{\mathrm{Re}_h}; \qquad f_h = \frac{24}{\mathrm{Re}_h}. \tag{I.114}$$

It is seen that neither Eq. (I.113) nor Eq. (I.114) is identical with Eq. (I.111) which applied to flow in a circular conduit.

Gross parameters designed to account for variation in the shape of the conduit usually do not accomplish the resolution in detail although their use may markedly reduce the differences between the predicted and actual flow in conduits of different shapes. An empirical approach would relate the numerical constants of Eqs. (I.111) and (I.114) to chosen shape parameters. The Reynolds number Re_h is sometimes used in the application of experimental information about turbulent flow in circular conduits to situations involving flow between parallel plates.

I-19. Smooth and Rough Circular Pipes

From a compilation of existing experimental data, the relationship expressed by Eq. (I.95) for turbulent flow in circular conduits was found by Blasius (*14*) to be well represented by the empirical equation,

$$\lambda = 4f = \frac{0.316}{(\mathrm{Re})^{1/4}}. \tag{I.115}$$

An improved relation for the same conditions, advanced by Nikuradse (*15*) on the basis of more extensive and carefully made measurements, was

$$\lambda = 0.0032 + \frac{0.221}{\mathrm{Re}^{0.237}}. \tag{I.116}$$

For turbulent flow in smooth circular conduits, experimental velocity traverses show that the velocity distribution is more nearly constant in the center of the channel than predicted by the parabolic laminar distribution of Eqs. (I.72) and (I.83). Thus in turbulent flow there are smaller velocity gradients near the center of the conduit, and the greater part of the gradients are localized in the vicinity of the walls.

The interior surfaces of actual conduits are never perfectly smooth. As a beginning to a rational analysis, the random irregularities of real walls may be replaced by idealized rough surfaces involving repetition of a unit protuberance in a uniform frequency. If desired, a spectrum of irregularities of continuously varying intensity may be substituted for the uniform synthetic roughness described. Rough surfaces that are geometrically similar possess equal ratios of spacing of the roughness element to height and geometrically similar shapes of protuberances. Much experimental work has been done with artificially roughened surfaces. Nikuradse made measure-

ments with circular conduits coated with sand grains of uniform size in order to secure constant surface conditions. He obtained data yielding the friction

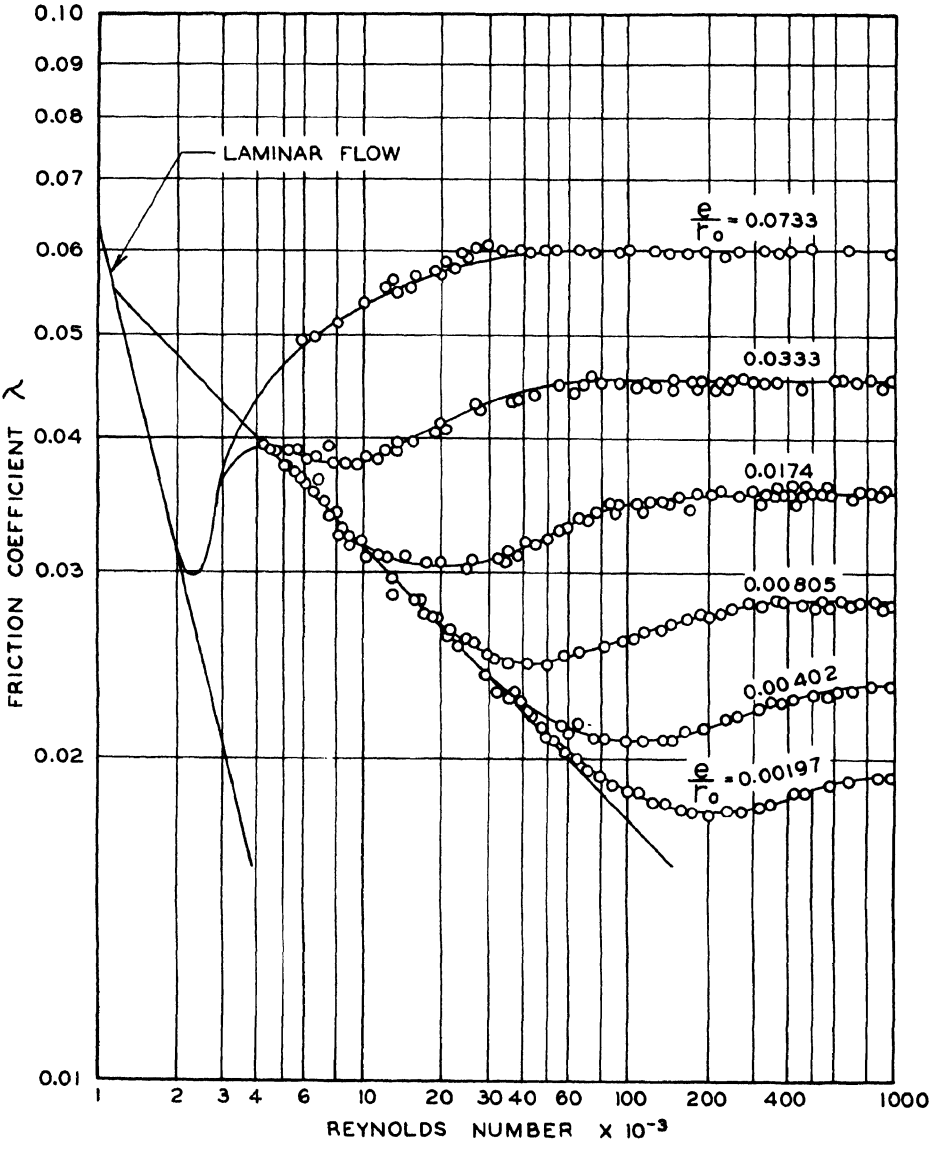

FIG. I-18 A. Friction coefficient λ *versus* the Reynolds number for artificially roughened conduits (*14*).

coefficient λ as a function of the Reynolds number for various relative roughnesses e/r_0 where e is the height of a particle. These data are shown in Fig. I-18 A. The same curves are shown in Fig. I-18 B without experimental

points in order to permit quantitative information to be obtained from the figure.

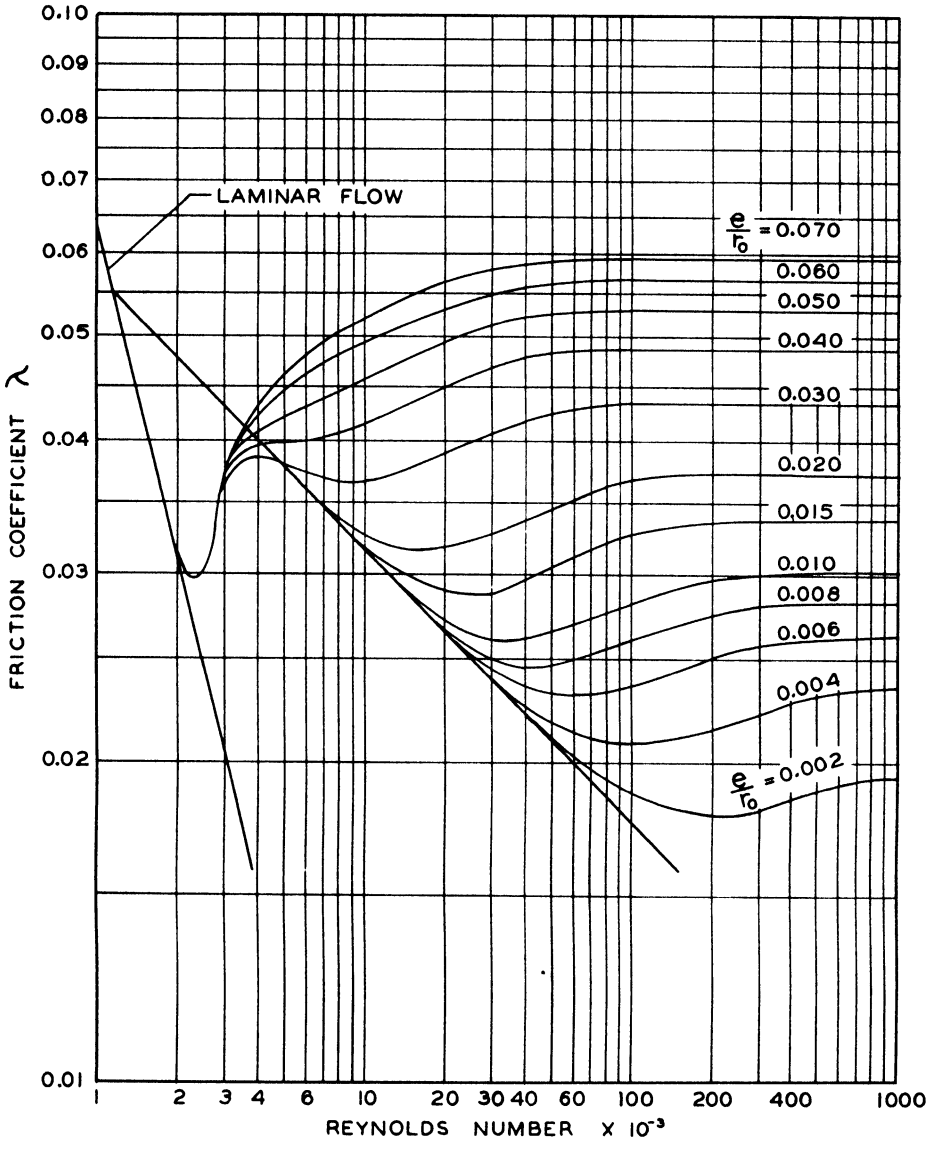

FIG. I-18 B. Friction coefficient λ *versus* the Reynolds number for artificially roughened conduits (*14*).

The influence of such surface roughness can be explained on the basis of the flow pattern. There is a single-valued relationship between λ and the Reynolds number for smooth pipes which indicates that the extent of the

turbulent motion does not depend on the nature of the smooth walls of the conduit. As the relative smoothness is decreased, the protuberances enter the laminar boundary layer flowing next to the wall and, at a sufficiently high Reynolds number, will project into the turbulent region. Under such circumstances the main body of the flow is not influenced greatly by the viscous shearing stresses on the tops of the protuberances. The distortion of the flow pattern introduces resistances overshadowing those resulting from local changes in the velocity distribution in the laminar layer. The viscosity and the related Reynolds number do not influence the flow characteristics appreciably for a sufficiently high degree of roughness. The friction coefficient λ is, therefore, independent of the Reynolds number. With increasing roughness, the velocity or the Reynolds number at which the laminar layer will no longer cover the protuberances will decrease. For this reason the transition from the relationship describing the behavior with a smooth wall to that associated with a rough wall will occur at a lower Reynolds number.

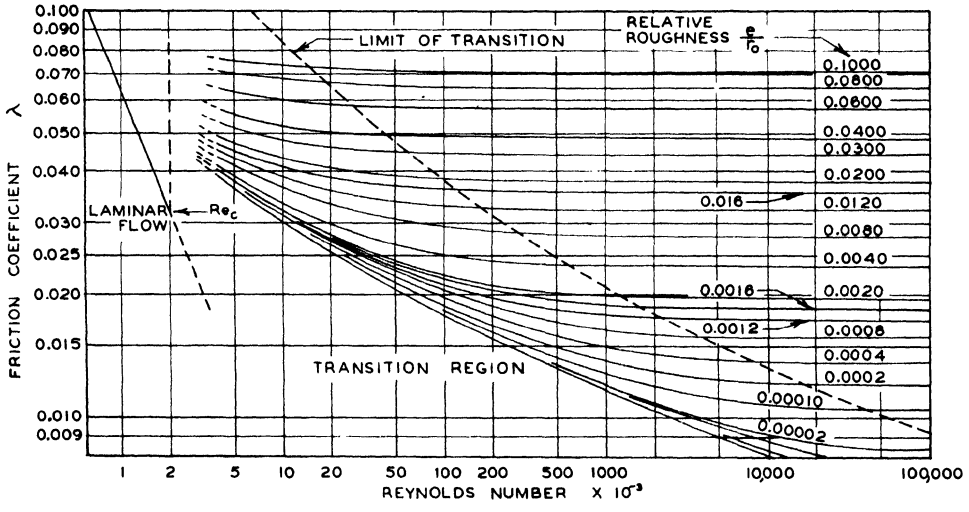

FIG. I-19. Friction coefficient λ *versus* the Reynolds number for clean, commercial pipe (*16*).

Moody (*16*) compiled available experimental data on friction factors for clean, commercial pipes and established the friction factor as a function of the Reynolds number for various values of the relative roughness e/r_0. This empirical information covers a wide range of commercial pipe sizes and types as is shown in Figs. I-19 and I-20.[1] Figure I-19 shows the effect of the

[1] These figures are based upon Ref. 16 and are presented by permission of the copyright owner.

Reynolds number upon the friction coefficient. There is a broad transition region without the complicated instability shown for artificially roughened conduits of Figs. I-18. Figure I-20 shows Moody's appraisal of the relative roughness of a number of commercial pipes. The absolute average roughness is taken as a constant for each material of construction and methods of fabrication. The relative roughness decreases directly with an increase in pipe diameter. These two charts permit a reasonable evaluation of friction

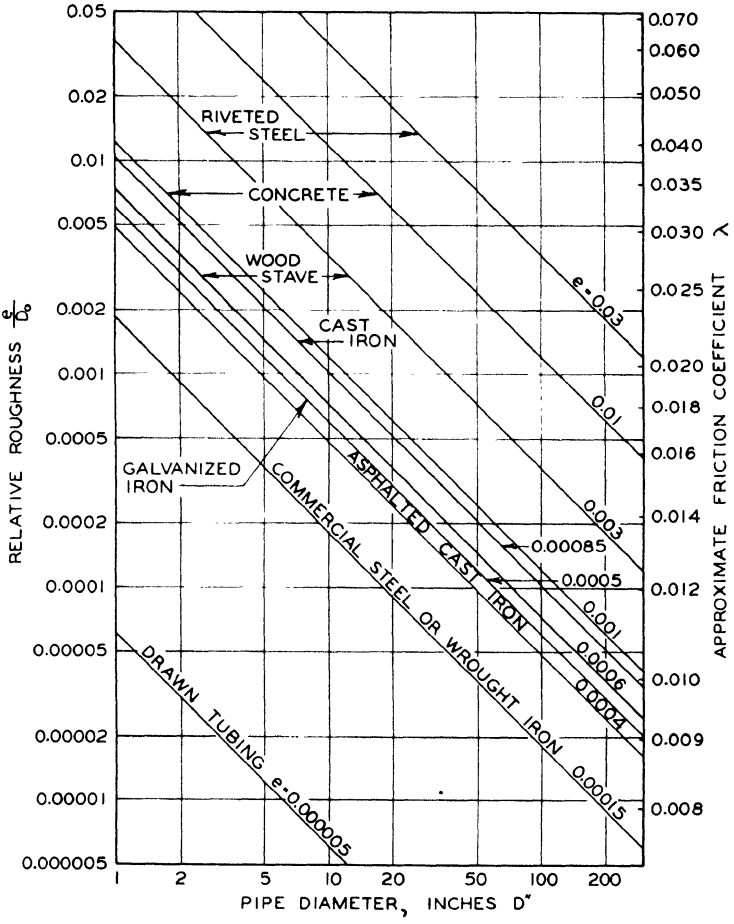

FIG. I-20. Relative roughness *versus* pipe diameter for clean, commercial pipe (*16*).

coefficients for clean, commercial pipes. The relationship of the friction factor to the Reynolds number does not resemble Nikuradse's data in detail. A possible explanation of the failure of commercial pipe data to follow those for smooth conduits, as is the case with sand coated surfaces, can be found in the size distribution of the protuberances in commercial pipes. The sand

coated pipe contains roughness elements of a uniform size which penetrate the laminar boundary region at about the same Reynolds number. The larger roughness elements of commercial pipes penetrate the boundary layer at a sequence of values above the transition Reynolds number. For commercial pipes there is no turbulent flow in which the laminar boundary layer masks all the protuberances. The smaller roughness elements are gradually uncovered at the increasing Reynolds number so that the transition to the characteristic flow for rough conduits is more continuous for commercial pipes than for smooth conduits.

Nomenclature

A_0 Cross sectional area, ft.^{2}
C Constant of integration
D_0 Outside diameter, ft.
d Differential operator
E Specific internal energy, internal energy of a unit weight system, B. t. u./lb.
e Height of roughness element, ft.
Eu Euler number
F Force per unit area, lb./ft.^{2}
$\boldsymbol{F}$ Force, lb.
F_D Dissipative force, lb.
f Fanning friction factor, dimensionless
f_h Fanning friction factor calculated by using mean hydraulic radius
G Pure or derived intensive property
$\overline{G}$ Average value, often time average
$\boldsymbol{G}$ Extensive property
G_f Fluctuating value of intensive property
$\overline{G_f}$ Average fluctuating value of intensive property
G_i Instantaneous value of intensive property
g Acceleration due to gravity, ft./sec.^{2}
h Elevation above datum plane, ft.
J Friction per unit weight associated with flow through a specified conduit, ft.lb./lb.
$\dot{\boldsymbol{J}}$ Friction associated with flow through a specified conduit, ft. lb.
$\dot{J}_0$ Total friction associated with flow through a specified conduit, ft. lb.
J_v Time rate of change of momentum per unit volume, lb./ft.^{3}
j Friction, infinitesimal, ft. lb./lb.
$\dot{j}$ Friction per unit time per unit cross sectional area, ft.lb./sec.ft.^{2}
$\dot{\boldsymbol{j}}$ Friction per unit time in specified length of conduit, ft.lb./sec.
$\dot{j}_0$ Friction per unit time in differential length of total conduit, ft.lb./sec.
k Constant of proportionality
L Length, ft.
l Distance from plane of symmetry, ft.
l_0 Distance from plane of symmetry to the wall, ft.
ln Natural logarithm
$\boldsymbol{M}$ Total momentum for system of variable weight, lb./sec.
$\dot{M}$ Momentum flux per unit area, lb./ft.^{2}
$M_{x,v}$ Momentum in the x-direction per unit volume of flow, lb.sec./ft.^{3}
$\dot{m}$ Weight rate of flow per unit area, lb./sec.ft.^{2}
P Pressure, lb./in.^{2} or lb./ft.^{2}
P_d Pressure associated with dissipative effects, lb./ft.^{2}
P_s Pressure arising from the effect of gravity, lb./ft.^{2}
r Polar radius in cylindrical and spherical coordinates, ft.

r_h Hydraulic radius, ft.
r_i Radius at interface, ft.
r_0 Radius of conduit, ft.
Re The Reynolds number
Re_h The Reynolds number with hydraulic radius as characteristic length
T Absolute temperature, °R.
U Average velocity over an area, or gross velocity, ft./sec.
U_x Average velocity over an area in the x-direction, ft./sec.
$U_{x,0}$ Average velocity in the x-direction over entire channel, ft./sec.
u Point velocity or time average point velocity, ft./sec.
u_i Velocity at interface, ft./sec.
u_x Point velocity in the x-direction, ft./sec.
$u_{x,m}$ Maximum time average velocity, ft./sec.
V Specific volume, ft.^{3}/lb.
$\dot{V}$ Total volumetric rate of flow through a section, ft.^{3}/sec.
$\dot{V}_0$ Volumetric rate of flow for the conduit as a whole, ft.^{3}/sec.
x Distance measured parallel to primary axis of flow, ft.
y Distance from axis of flow, ft.
y_d Distance deficiency, distance from wall, ft.
y_i Position of interface, ft.
$2y_0$, y_0 Transverse distance between channel walls, ft.
z One of the Cartesian coordinates, ft.
Δ Difference in
δ Infinitesimal increment
η Absolute viscosity, lb.sec./ft.^{2}
θ, θ', θ_0 Time, sec.
λ Friction coefficient
λ_h Friction coefficient calculated by using mean hydraulic radius
ρ Density, σ/g, lb.sec.^{2}/ft.^{4}
σ Specific weight, lb./ft.^{3}
τ_{rx} Shear in the x-direction in plane perpendicular to the r-axis, lb./ft.^{2}
τ_{yx} Shear in the x-direction in plane perpendicular to the y-axis, lb./ft.^{2}
τ_{rx}, τ_{yx} Shear, lb./ft.^{2}
$(\tau_{rx})_0$, $(\tau_{yx})_0$ Shear at wall, lb./ft.^{2}
$(\tau_{yx})_i$ Shear at interface, lb./ft.^{2}
ϕ, ϕ_1 Function of
ψ Polar angle

SUBSCRIPTS

A, B Refers to states A, B, etc.
P Refers to pressure
r In the r-direction
X Held constant
x In the x-direction
y In the y-direction
θ Held constant
τ Refers to shear
1, 2 Refers to states 1, 2, etc.

References

1. Kirkwood, J. G., and Crawford, B., Jr., *J. Phys. Chem.* **56**, 1048 (1952).
2. Bridgman, P. W., "The Logic of Modern Physics." Macmillan, New York, 1938.
3. Tolman, R. C., "The Principles of Statistical Mechanics." Oxford U. P., New York, 1938.
4. Goranson, R. W., "Thermodynamic Relations in Multi-Component Systems," Chapters V—IX. Carnegie Institution of Washington, Washington, D. C., 1930.
5. Lamb, H., "Hydrodynamics." Dover, New York, 1945.
6. Gibbs, J. W., "Collected Works," Vol. 1. Longmans, Green, New York, 1931.

7. Lacey, W. N., and Sage, B. H., "Thermodynamics of One-Component Systems." California Institute of Technology, Pasadena, 1940, 1947.
8. Classification of rheological properties, *Nature* **149**, 702 (1942).
9. Walker, W. H., Lewis, W. K., McAdams, W. H., and Gilliland, L. R., "The Principles of Chemical Engineering," p. 78. McGraw-Hill, New York, 1937.
10. Goldstein, S., "Modern Developments in Fluid Dynamics," Vol. 1, p. 319. Oxford U. P., New York, 1938.
11. Gibson, A. H., *Proc. Roy. Soc.* **A 88**, 376 (1910).
12. Lin, C. C., *Quart. Appl. Math.* **3**, 117 (1945).
13. Reissner, E., Mindlin, R. D., and Tranter, C. J., *Quart. Appl. Math.* **4**, 277 (1946).
14. von Blasius, H., *Mitt. Forschungsarb. Ver. deut. Ing.* **131**, 22 (1913).
15. Nikuradse, J., *Forsch.-Gebiete Ingenieurw.* **3**, *Forschungsheft* **356** (1932).
16. Moody, D. F., *Trans. Am. Soc. Mech. Engrs.* **66**, 671 (1944).

CHAPTER II

SOME SIMPLE PROPERTIES OF TURBULENT FLOW

Many situations in which turbulent flow prevails are encountered in nature. For this reason the greater part of the present discussion is directed toward an understanding of the macroscopic aspects of turbulence. The Reynolds experiment, shown in Fig. II-1, in which a filament of dyed fluid is introduced into a flowing fluid is an excellent example of the transition from laminar to turbulent flow. The filament of dyed fluid remains continuous and possesses sharp boundaries until the velocity in the channel has been increased to a critical value. At this point the filament is broken up by the random motion of small elements of the flowing stream. The magnitude of these elements and their velocities vary markedly with time at a given point. Under most conditions a decrease in the flow rate will yield a somewhat lower velocity at which the dyed filament again becomes continuous than was obtained for the onset of turbulent flow upon an increase in velocity. The magnitude of this hysteresis depends upon the particular geometry of the flow channel and on the nature of the fluid involved.

The energy required for the maintenance of turbulence comes from the primary flow. It is probable that these transfers of kinetic energy from the primary flow involve large scale, irregular, periodic motion which degenerates into random motions of decreasing magnitude. In a turbulently flowing stream the proportion of the friction that results from turbulent dissipation increases with the Reynolds number. Since kinetic energy is required for the maintenance of turbulence as well as for the accomplishment of the fluid transport, it is to be expected that the total energy transfer necessary for the maintenance of the turbulent flow of a fluid is greater than that required for the similar flow of a fluid in laminar motion. From such reasoning it may be deduced that the shear at the wall of a stream for a given gross velocity will be greater for turbulent flow than for streamline flow. Since the viscosity of the fluid is not changed[1] by the transition from

---

[1] This statement neglects the effects of shear upon viscosity. Such effects are probably not large except at extremely high shears. The effect of temperature gradients and shear on viscosity can be evaluated from the Onsager reciprocity (*1*) relationships, which have been well described by Denbigh (*2*) and de Groot (*3*).

one type of flow to another, the velocity gradient at the boundary of the stream must be greater in turbulent than in streamline flow. It has been shown by Millikan (*4*) and Corrsin (*5*) that for both laminar and turbulent flow under steady, uniform conditions the velocity distribution will be so

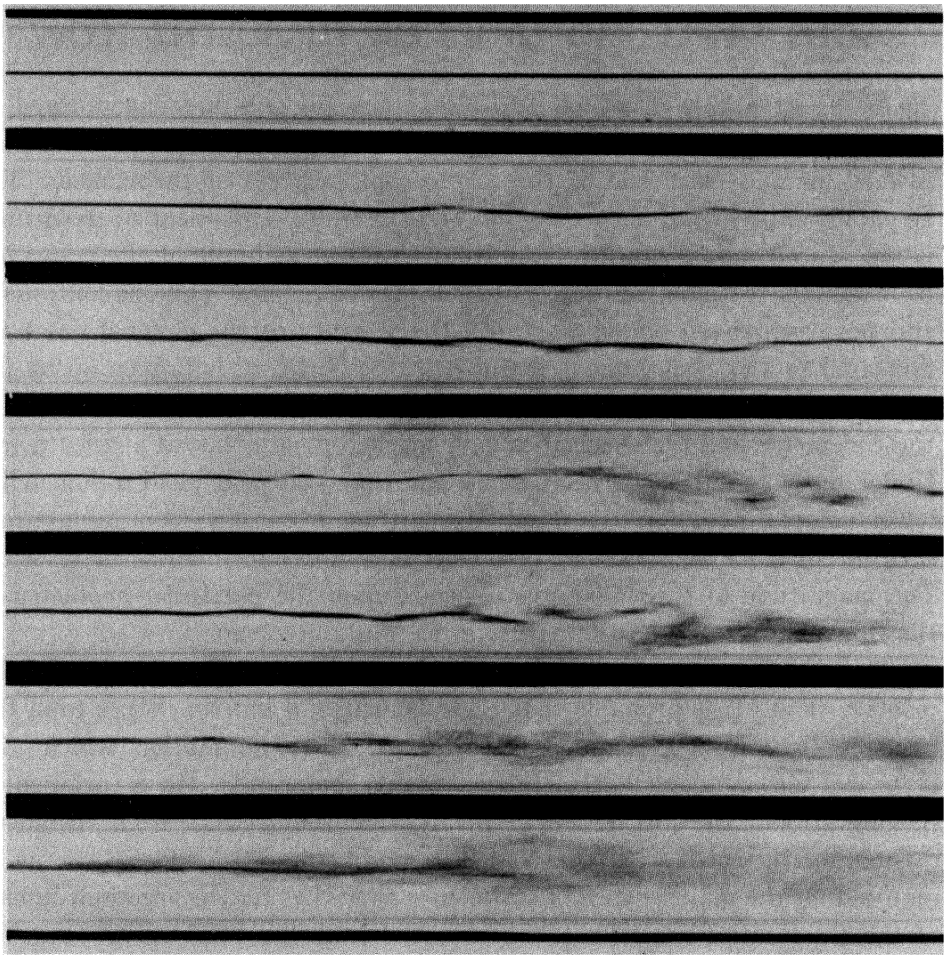

FIG. II-1. Reynolds' apparatus showing instability of flow through a tube. (From the frontispiece of H. Rouse, "Fluid Mechanics for Hydraulic Engineers," McGraw-Hill, New York, 1938. Presented here by permission of the copyright owner, United Engineering Trustees, Inc., New York.)

adjusted as to yield the minimum total dissipation of kinetic energy during a specified flow process. The variational methods (*6*) used by them do not appear to be as widely applied in fluid mechanics as the theorems of steady state thermodynamics (*2*) would permit.

II-1. Concepts of Flow

If an observer who is stationary with respect to the solid boundary of the steady, turbulent flow of a viscous fluid were able to measure the instantaneous velocity at a fixed point, it would be possible to resolve this vectorial quantity u_i into three mutually perpendicular components: $u_{x,i}$, $u_{y,i}$, and $u_{z,i}$. In steady flow the time average of any component can be made to differ by an arbitrarily small amount from a chosen fixed value, by averaging over a long enough time interval. For the x-component, the mathematical expression becomes

$$\frac{1}{\theta}\int_{\theta_0-\theta/2}^{\theta_0+\theta/2} u_{x,i}\,d\theta = \overline{u}_x + \delta_x. \tag{II.01}$$

In Eq. (II.01), $\overline{u}_x$ is a constant and δ_x can be made smaller than any preassigned quantity by taking the time θ sufficiently large, as was just discussed. Similar equations may be written for the y- and z-components of the velocity.

Any component of the instantaneous velocity such as $u_{x,i}$ can be expressed as the sum of the average value $\overline{u}_x$ and of a superimposed fluctuation component $u_{x,f}$ which has a time average equal to δ_x:[1]

$$u_{x,i} = \overline{u}_x + u_{x,f}. \tag{II.02}$$

It is possible to characterize turbulent flow for nonsteady conditions in the above manner if the rate of change in the average value of each component with respect to time is small compared to the corresponding rate of change in the associated local fluctuating velocity.

The average values of velocity should be taken with respect to both space and time. In the case of homogeneous, turbulent flow the average is independent of the volume of the field considered since such turbulence is independent of the position in the field (*7*). It remains for ergodic (*8*) theory to show that a description of a sufficiently large volume of homogeneous turbulence at one instant in time is equivalent to the description of the behavior at one point in space taken over a sufficiently long time. Some limitations exist (*1*) in this generalization, but they are not of direct concern to the physical situation as long as the variations in velocity are continuous with respect to space and time.

---

[1] The fact that the time average of $\overline{u}_{x,f}$ is δ_x can be seen by substitution of Eq. (II.02) into Eq. (II.01).

Much of the statistical description of turbulence which is not considered in this chapter is concerned with the velocity fluctuations at a particular time. This is in contradistinction to the functioning of most instruments used in this field which evaluate the variations in velocity with time at a point in space.

II-2. Temperature Fluctuations

In Fig. II-2 is shown a variation in temperature with time in a jet of air controlled at a nominal temperature of 100.00° F. and an average velocity of 6 ft./sec. By means of conventional statistical analysis, it was found that over a period of 9 sec. the least squares deviation was from a base temperature of 100.006° F. and the corresponding arithmetical average was 100.006° F.

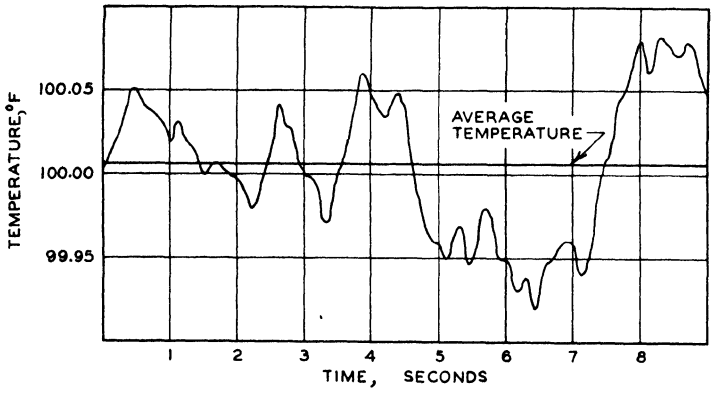

FIG. II-2. Deviation of temperature with time at a point in an air jet.

The standard deviation from the former temperature was 0.042° F. The period of 9 sec. corresponded to a segment of the gas stream 54 ft. in length. If the data shown in Fig. II-2 were averaged over 0.5 sec., an average temperature from 99.935° F. to 100.065° F. would have been obtained.

The root-mean-square deviation from a number of base temperatures is shown in Fig. II-3. A minimum deviation of the square root of the sum of the squares was found for a temperature of 100.006° F. Under these circumstances it must be realized that the standard deviation will in some measure depend on the size of the sample of the flow from which it was established. The data of Fig. II-2 were obtained with a 0.0005 in. platinum resistance thermometer and do not include any of the high-frequency fluctuations that exist in turbulent flow. However, the data do indicate the physical nature of fluctuating scalar quantities in the flow of fluids.

II-3. Transfer of Momentum as a Result of Turbulence

Consider two different layers of fluid, A and B, of different thicknesses shown in Fig. II-4. Each layer is bounded by a pair of mutually parallel planes which may be considered to extend indefinitely. Consider the two layers to be moving, each as a solid body, with instantaneous velocities always parallel to the planes. Without loss of generality, except as stated

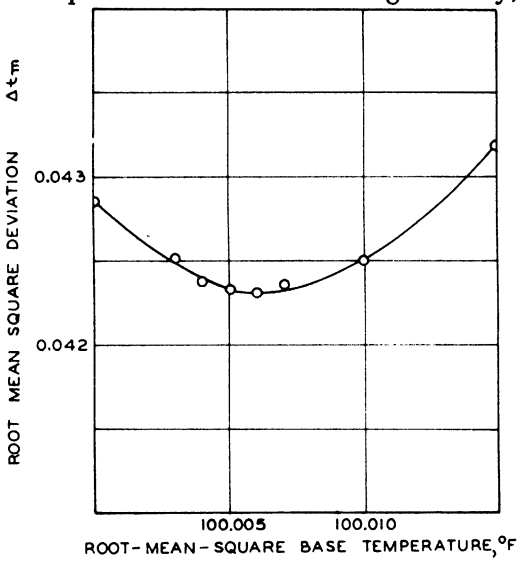

FIG. II-3. Root-mean-square deviation from base temperature in an air jet.

in the preceding sentence, the coordinates may be taken as fixed on the layer A with the xz-plane parallel to the bounding planes and the x-axis parallel to the relative instantaneous velocity of B with respect to layer A. At a given instant, in addition to the above-described motion, a quantity of fluid is transferred parallel to the y-axis uniformly from each surface element of layer A to layer B with a velocity $u_{y,i}$. The mass transfer per unit area per unit time is $u_{y,i}\,\sigma/g$,[1] and the time rate of exchange of momentum per unit area is $u_{x,i}\,u_{y,i}\,\sigma/g$. From the general statement of the conservation of momentum, the time average of the rate of exchange of momentum per unit area may be set equal to a component of the average[2]

[1] In this treatment the density of the fluid ρ is equal to the specific weight σ divided by the acceleration due to gravity g.

[2] Unless otherwise stated, the "average" value of a quantity at a point will represent a time average. In a more general way the average value of $u(x, y, z, \theta)$ may be considered as

$$\bar{u} = \frac{\int\int\int\int u(x, y, z, \theta)\, dx\, dy\, dz\, d\theta}{\int\int\int\int dx\, dy\, dz\, d\theta}.$$

shearing stress $\overline{\tau_{yx}}$. The stress $\overline{\tau_{yx}}$ acts on a plane perpendicular to the y-axis and in a direction parallel to the x-axis. It acts to reduce the velocity of layer B relative to that of layer A. In this simplified application of the conservation of momentum no regard is taken of the molecular viscous forces associated with a velocity gradient.

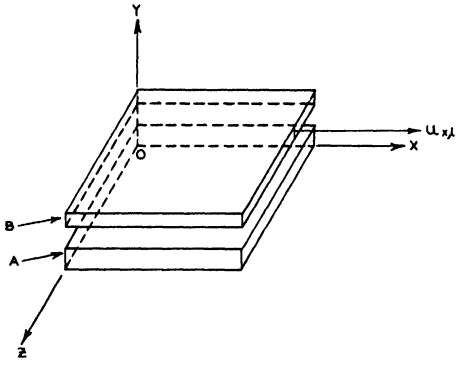

FIG. II-4. Volume elements moving parallel in a fluid stream.

From the foregoing discussion the time average of the turbulent shearing stress may be written in the following way:

$$\overline{\tau_{yx_e}} = -\overline{u_{x,i}\, u_{y,i}\, \sigma/g}. \tag{II.03}$$

If each instantaneous value of velocity is expressed in terms of the sum of an average and a fluctuating component, as in Eq. (II.02), it follows from Eq. (II.03) that when the effect of fluctuations of density on the shear is not considered:

$$\overline{\tau_{yx_e}} = -\frac{\overline{\sigma}}{g}\overline{[\overline{u}_y + u_{y,f}]\,[u_x + u_{x,f}]}. \tag{II.04}$$

If macroscopic steady state flow is assumed, the average values of $u_{x,i}$ and $u_{y,i}$ may be considered as constants and the variation in the specific weight averaged independently from the velocity:

$$\overline{\tau_{yx_e}} = -\frac{\overline{\sigma}}{g}[\overline{u_y}\,\overline{u_x} + \overline{u_y}\,\overline{u_{x,f}} + \overline{u_x}\,\overline{u_{y,f}} + \overline{u_{y,f}\,u_{x,f}}]. \tag{II.05}$$

Since the average values of the fluctuating components can be made arbitrarily small, as may be seen from Eq. (II.01), it follows that:

$$\overline{\tau_{yx_e}} = -\frac{\overline{\sigma}}{g}[\overline{u_y}\,\overline{u_x} + \overline{u_{y,f}\,u_{x,f}}]. \tag{II.06}$$

Since it was assumed that the segments of fluid in Fig. II-4 were moving parallel to one another, the y-component of velocity is zero. Therefore, Eq. (II.06) may be written as

$$\overline{\tau_{yx_e}} = -\frac{\overline{\sigma}}{g}\overline{u_{y,f}\,u_{x,f}}. \tag{II.07}$$

Only the turbulent component of the shear has been included in these expressions. The combined effect of turbulence and molecular viscous forces will be discussed later.

II-4. Measurement of Velocity

For a detailed knowledge of the characteristics of a flow of a fluid, it is necessary to make measurements of velocity as a function of time at various points in the flowing fluid. Pitot tubes are ordinarily used to obtain average values of velocity. A description and bibliography pertaining to this instrument are available (*9*, *10*).

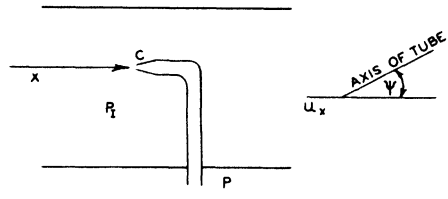

FIG. II-5. Measurement of stream velocity with Pitot tube.

The general application of the Pitot tube is restricted to average velocities in steady flow. In transient macroscopic flow, the inertia of the fluid in the pressure measuring system is often sufficient to introduce errors in the measurement of velocity. As a first approximation, the velocity relative to the axis of the tube inlet shown in Fig. II-5 may be evaluated from

$$u_x = \beta(c)\sqrt{2gh} = \beta(c, \psi)\sqrt{\frac{2g}{\sigma}(P_I - P)}. \qquad \text{(II.08)}$$

This equation can be derived from the Bernoulli equation. If the effect of the change in pressure upon the specific weight is neglected, the coefficient β is close to unity for a wide variety of shapes at the tip C of the tube as long as the principal axis of the tube inlet is parallel to that of the main stream. Marked deviations may be experienced if the axis of the tube is not parallel to the main stream. Such measurements are sometimes attempted in order to obtain components of velocity and in this instance the coefficient β is roughly approximated by $\cos\psi$. The details of such Pitot tubes are described in the literature.

Information may be obtained concerning the mechanics of turbulent flow by measuring instantaneous values of velocity in steadily flowing fluid streams. By means of special instruments, it is possible to measure approximately the instantaneous values of velocity in different parts of turbulently flowing fluids. Thus, the way is open for the determination of turbulent shear stresses as well as for the establishment of correlations between simultaneous events at different points in the system.

Hot-wire anemometers, which in their simple application consist of small, heated wires placed with axes transverse to the direction of the stream, are

sometimes employed for recording the average value of the longitudinal velocity (*11*) as well as the variations resulting from turbulence (*12, 13*).

In general, these instruments have been most useful in measurements involving average velocities of less than 100 ft./sec., the sensitivity decreasing at higher average velocities. The usual technique employed in the operation of hot-wire anemometers for the determination of average speeds consists of ascertaining the current necessary to maintain a constant average temperature and, hence, of electrical resistance of the wire at the average speed. The wire may be connected in one arm of a Wheatstone bridge circuit, and the current supplied to the bridge may be adjusted so that the bridge is balanced. After calibration, the measurement of the current supplied to maintain a chosen temperature of the wire affords a measure of the average speed in the vicinity of the wire.

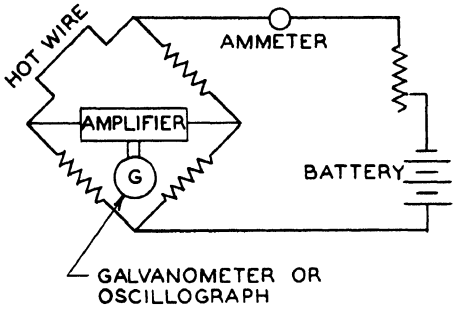

FIG. II-6. Circuit for hot-wire anemometer.

It is possible to measure the turbulent fluctuations in velocity with a hot-wire anemometer if the wire is sufficiently small and if the electrical equipment is adapted to transient conditions. This measurement is usually carried out by adding a vacuum tube amplifier to the detecting circuit of the Wheatstone bridge just described (*12, 14, 15*) and by describing the diameter of the hot wire. The heating current is adjusted in the usual manner until the bridge is balanced, and the small fluctuations in potential across the detecting circuit are amplified and observed on a cathode ray oscillograph or averaged in a statistical manner by means of a suitable type of integrating circuit. Such a circuit is indicated schematically in Fig. II-6. Even with rather small wires from 0.0001 to 0.0005 in. in diameter, there is a lag in the resistance temperature from the equilibrium value as a result of the heat capacity of the small hot wire. The amplifier shown in Fig. II-6 is provided with a compensation circuit which takes such effects into account for a first degree of approximation. In addition, it is desirable to consider the end effects which may be of secondary importance if the wire is long. The reader is referred to the work of King (*16*) and Dryden (*12, 13*) for details. It may be noted that

$$\frac{i^2 \overline{R}}{R - R_a} = a + b\sqrt{\overline{u}} \tag{II.09}$$

for time average conditions. The time constant (*17*), which describes the lag of the resistance of the wire in following the velocity of gas, may be expressed as

$$M' = \frac{k\,C_w}{a\,R_0}\frac{\overline{R} - R_a}{i^2\,R_a} = K_1\left(\frac{\overline{R} - R_a}{i^2\,R_a}\right). \tag{II.10}$$

Likewise, the ratio of average fluctuation to the average velocity may be obtained from

$$\frac{\sqrt{\overline{u_f^2}}}{U} = \frac{\sqrt{\overline{e^2}}}{R_a\phi(\overline{R}/R_a\,i)}. \tag{II.11}$$

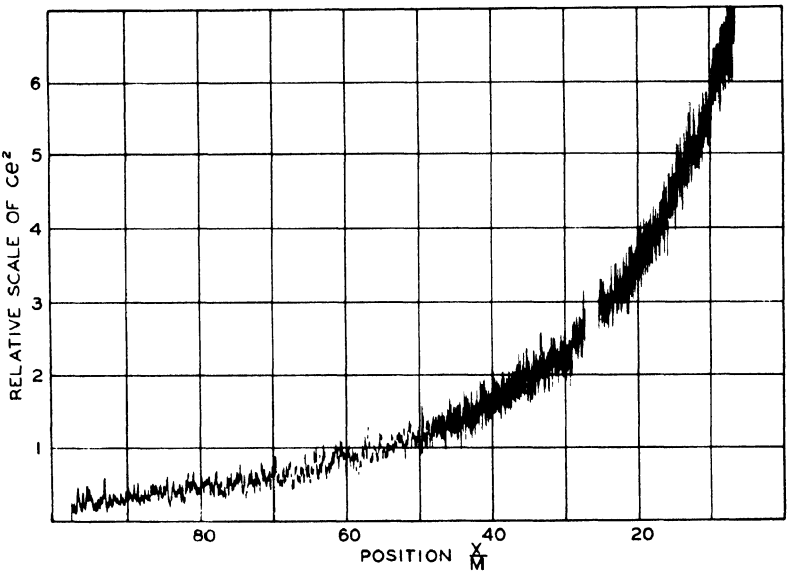

FIG. II-7 A. The quantity $\overline{u_f^2}$, expressed as $\overline{c\,e^2}$, as a function of downstream position behind a grid for the Reynolds number of 20,000. Grid constructed of 0.375-in. rods on 2.25-in. spacing (*17*).

It is often a simple matter to establish the electronic compensation for the hot wire directly by use of a square-wave, electromotive-force generator (*17*) and a sine-wave generator. The magnitude of $\overline{e^2}$ may be determined from a vacuum thermocouple by suitable calibration (*17*) with a square-wave generator. A typical record of a quantity proportional to $\overline{e^2}$ as a function of downstream position behind a grid in a wind tunnel is shown in Fig. II-7 A. The grid had a square opening 2.25 in. on each side and a wire diameter of 0.375 in. The data of Fig. II-7 A indicate an increase in the magnitude of the fluctuations as their frequency per unit arc length of the

mean curve is decreased near the grids. It should be realized that the frequency response of the pen of the recorder is not more than 1 or 2 per second. Thus the change in fluctuations shown is extremely slow as compared with the main body of the turbulent fluctuations. The corresponding value of $\sqrt{\overline{u_{x,f}^2}}/U$ or fraction turbulence is shown in Fig. II-7 B. If it is desired to study the variation of the kinetic energy of the spectrum of turbulence as a function of frequency, a more complicated approach must be employed (*17*). The frequency may be advantageously compared with the output of a random noise generator of known spectral characteristics. It is beyond the scope of this section to consider such measurements in detail.

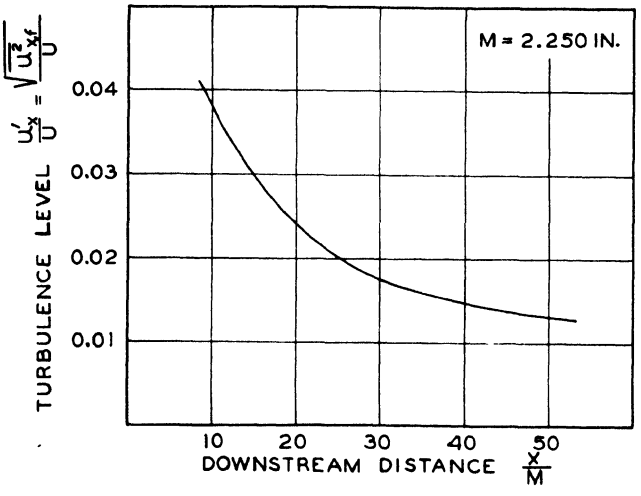

FIG. II-7 B. Fraction turbulence as a function of position downstream from a grid for the Reynolds number of 20,000. Same grid as Fig. 7 A.

It is possible to define a coefficient R_y which is a direct measure of the correlation in time of the turbulent fluctuations of the velocity in a flowing fluid at two points in the flow which may be located in any position relative to each other. Thus, if $u_{x,f,A}$ and $u_{x,f,B}$ represent the fluctuating velocities at points A and B, respectively, which lie on a line parallel to the y-axis, the x-axis being taken parallel to the mean flow, the correlation coefficient R_y between these quantities is defined as[1]

[1] It is shown in a number of books on statistics (*18*, *19*) that, if the simultaneous fluctuations $u_{x,f,A}$ and $u_{x,f,B}$, for example, are plotted on rectangular graph paper, the straight line which best fits the points in the sense that the sum of the squares of the distances from the points to the line is a minimum is

$$u_{x,f,A} = \frac{\sqrt{\overline{u_{x,f,A}^2}}}{\sqrt{\overline{u_{x,f,B}^2}}} R_y u_{x,f,B}.$$

$$R_y = \frac{\overline{u_{x,t,A}\, u_{x,t,B}}}{\sqrt{\overline{u^2_{x,t,A}}}\sqrt{\overline{u^2_{x,t,B}}}}. \qquad \text{(II.12)}$$

The behavior shown in Fig. II-8 corresponds to the lateral velocity correlation R_y as used by Batchelor (*7*). The corresponding longitudinal correlation $(R_y)_l$ would be defined as

$$(R_y)_l = \frac{\overline{u_{y,t,A}\, u_{y,t,B}}}{\sqrt{\overline{u^2_{y,t,A}}}\sqrt{\overline{u^2_{y,t,B}}}} \qquad \text{(II.13)}$$

It can be seen from Eq. (II.12) that $R_y = 1$ when A and B are coincident, since $u_{x,t,A}$ and $u_{x,t,B}$ are at all times equal. It has been established experimentally that, as $A \to B$, $R_y \to 1$. When points A and B are taken farther and farther apart, the time average of the product of the turbulent fluctuations of the velocity approaches zero; i.e., there is no correlation between the components. Hence when B recedes from A, $R_y \to 0$. The general variation of R_y with the distance apart y of A and B is indicated in Fig. II-8. It can be shown that

$$\frac{\partial R_y}{\partial y} \to 0 \qquad \text{as} \qquad y \to 0. \qquad \text{(II.14)}$$

Also in viscous fluid with turbulent energy dissipation,

$$\frac{\partial^2 R_y}{\partial y^2} \neq 0 \qquad \text{as} \qquad y \to 0. \qquad \text{(II.15)}$$

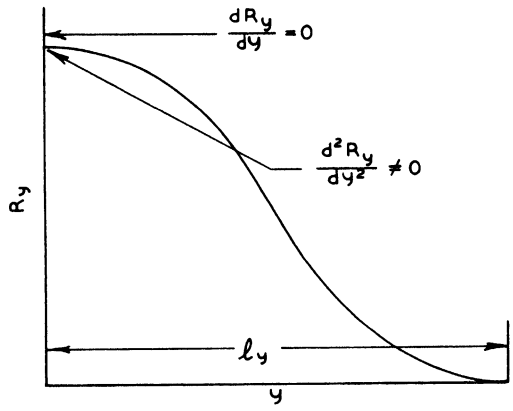

FIG. II-8. Lateral velocity correlation R_y as a function of distance separating correlated points (*17*).

It should be emphasized that the behavior shown in Fig. II-8 is only qualitative. In isotropic turbulence, the correlation R_y is in reality a function of only a single scalar quantity, although this is not true for nonisotropic or nonhomogeneous turbulence.

Several electrical methods have been developed for the measurement of correlation coefficients. Prandtl and Reichardt (*20*), for example, have applied the two amplified potential fluctuations obtained from separate bridge circuits connected to two hot wires to the vertical and horizontal

plates of a cathode ray oscilloscope. Pictures having a long exposure time were obtained and analyzed for the degree of correlation between the fluctuation of the two velocities measured by the hot wires. A method described by Goldstein (*21*) involves the separate application of the two amplified potentials to the two coils of an alternating-current galvanometer.

II-5. Characteristic Length

A characteristic quantity useful in the analysis of the correlation of turbulence and having the dimensions of length may be defined from the correlation coefficient as follows:

$$l_y = \int_0^\infty R_y \, dy. \tag{II.16}$$

It is found experimentally that the value of R_y is zero for all values of y above a certain value (*22*), which is designated by y_1, so that the value of l_y becomes constant for all values of y greater than y_1.

II-6. Mixing Length

It has been shown earlier that the fluctuating components of flow in two adjacent layers parallel to the xz-plane and moving in the x-direction give rise to a shear. The magnitude of the average value may be established from

$$\overline{\tau_{yx_t}} = -\frac{\overline{\sigma}}{g} \overline{u_{x,f} \, u_{y,f}}. \tag{II.17}$$

For purposes of practical application it would be advantageous if the quantity $\overline{u_{x,f} \, u_{y,f}}$ were expressed in terms which are more easily measurable than the fluctuating velocities. With this objective in mind, Prandtl postulated

$$\overline{u_{x,f} \, u_{y,f}} = -l^2 \left(\frac{du_x}{dy}\right)^2 \tag{II.18}$$

where l is a quantity having the dimension of length and is characteristic of the turbulence existing at the point in question. The primary justification

for the postulate arises from the utility of the expressions obtained by its use. If Eq. (II.18) is assumed, it is possible to calculate the Prandtl mixing length l from quantities which are easily measured.

The substitution of Eq. (II.18) in Eq. (II.17)[1] results in

$$\tau_{yx_e} = \frac{\sigma}{g} l^2 \left(\frac{du_x}{dy}\right)^2 \tag{II.19}$$

Equation (I.57) for the idealized flow[2] between parallel plane plates separated by a distance $2\,y_0$ yields

$$(\tau_{yx})_0 \frac{y}{y_0} = \frac{\sigma}{g} l^2 \left(\frac{du_x}{dy}\right)^2 - \tau_{yx_v}. \tag{II.20}$$

The molecular contribution to the shear τ_{yx_v} may be neglected in the central portions of the flow channel. Equations (II.19) and (II.20) may be solved for l as follows:

$$l = \sqrt{\frac{(\tau_{yx})_0 g}{\sigma}} \sqrt{\frac{y}{y_0}} \frac{dy}{du_x}. \tag{II.21}$$

The corresponding expression for idealized flow in a circular cylindrical conduit follows from Eq. (I.31):

$$l = \sqrt{\frac{(\tau_{rx})_0 g}{\sigma}} \sqrt{\frac{r}{r_0}} \frac{dr}{du_x}. \tag{II.22}$$

It is to be emphasized that Eqs. (II.21) and (II.22) apply only to idealized flow since Eqs. (I.57) and (I.31) are so limited.

II-7. Eddy Viscosity[3]

Equation (II.19) may be written as

$$\frac{\tau_{yx_e}}{\rho} = \left(l^2 \frac{du_x}{dy}\right) \frac{du_x}{dy} \tag{II.23}$$

or

$$\frac{\tau_{yx_e}}{\rho} = \varepsilon_m \frac{du_x}{dy}. \tag{II.24}$$

---

[1] Henceforth, except in special cases in which it is desired to emphasize the contrast between average and instantaneous values of shear stress, etc. the bar will be omitted.

[2] Idealized flow is defined here as the steady, isothermal movement in a straight, horizontal, smooth conduit of an incompressible, homogeneous, Newtonian fluid.

[3] A more extended discussion of eddy viscosity is given in Chapter VI.

The quantity ε_m, usually called the eddy viscosity,[1] is the turbulent analog of the molecular kinematic viscosity ν. Hereafter the term "kinematic viscosity" will refer to the molecular kinematic viscosity. The eddy viscosity can be thought of as the ratio of a quantity which is a measure of the turbulent shearing stress between two layers of fluid moving parallel to each other and the product of the density and velocity gradient. The shearing stress results from the exchange of momentum between the layers because of transverse turbulent fluctuations in velocity. The kinematic viscosity ν can be thought of as the ratio of the stress that results from the exchange of momentum associated with molecular motion and the product of the density and velocity gradient.

II-8. Dimensionless Relations

It is of value to obtain expressions which are independent of the absolute values of the physical quantities, which may change from one application to another. Inspection of Eq. (II.22) shows that it may be written in the following dimensionless form:

$$\frac{l\,du_x/dr}{\sqrt{\dfrac{(\tau_{rx})_0\,g}{\sigma}}} = \sqrt{\frac{r}{r_0}}. \tag{II.25}$$

The quantity $\sqrt{(\tau_{rx})_0\,g/\sigma}$ has the dimensions of velocity and may be designated as a characteristic velocity associated with the shearing stress at the wall and the density of the fluid:

$$u_* = \sqrt{\frac{(\tau_{rx})_0}{\rho}} = \sqrt{\frac{(\tau_{rx})_0\,g}{\sigma}}. \tag{II.26}$$

The quantity u_* is usually called the "friction velocity" and when it is substituted in Eq. (II.25), then

$$\frac{l\,du_x/dr}{u_*} = \sqrt{\frac{r}{r_0}}. \tag{II.27}$$

A similar expression may be written for flow between parallel plates:

$$\frac{l\,du_x/dy}{u_*} = \sqrt{\frac{y}{y_0}} \tag{II.28}$$

---

[1] The definition of eddy viscosity used in this work follows the practice of Kármán (*23*) and differs from that used by Bakhmeteff (*24*) in that the latter defines the eddy viscosity as $\rho\,l^2\,du_x/dy$.

where the friction velocity assumes the form

$$u_* = \sqrt{\frac{(\tau_{yx})_0}{\rho}} = \sqrt{\frac{(\tau_{yx})_0 g}{\sigma}}. \tag{II.29}$$

Some authors prefer to employ the distance from the wall instead of from the axis to express position. The subscript d is used to describe this deficiency distance. For circular conduits the deficiency radius is defined as

$$r_d = r_0 - r. \tag{II.30}$$

In two-dimensional conduits the corresponding deficiency distance may be established from

$$y_d = y_0 - y. \tag{II.31}$$

Equations (II.27) and (II.28) may be written in somewhat different form using Eqs. (II.30) and (II.31), respectively, so that

$$\frac{l\, du_x/dr}{u_*} = \sqrt{1 - \frac{r_d}{r_0}}, \tag{II.32}$$

$$\frac{l\, du_x/dy}{u_*} = \sqrt{1 - \frac{y_d}{y_0}}. \tag{II.33}$$

Two dimensionless parameters which will be found useful in the analysis of turbulent flow are defined by the following equations:

$$r_d{}^+ = \frac{u_* r_d}{\nu} = \frac{r_d}{\nu}\sqrt{\frac{(\tau_{rx})_0 g}{\sigma}}, \tag{II.34}$$

$$u_x{}^+ = \frac{u_x}{u_*} = \frac{u_x}{\sqrt{\frac{(\tau_{rx})_0 g}{\sigma}}}. \tag{II.35}$$

It can be seen that both $r_d{}^+$ and $u_x{}^+$ are dimensionless since the right side of Eq. (II.34) is dimensionless.

The equations corresponding to (II.34) and (II.35) for two-dimensional flow are, respectively,

$$y_d{}^+ = \frac{u_* y_d}{\nu} = \frac{y_d}{\nu}\sqrt{\frac{(\tau_{yx})_0 g}{\sigma}}, \tag{II.36}$$

$$u_x{}^+ = \frac{u_x}{u_*} = \frac{u_x}{\sqrt{\frac{(\tau_{yx})_0 g}{\sigma}}} \tag{II.37}$$

II-9. Flow Near Boundary

If turbulent flow in a conduit with solid walls is considered, it is evident that the fluctuation components of the velocity normal to the solid wall can be made arbitrarily as small as desired by choosing a point sufficiently close to the boundary of the stream. This concept indicates that the longitudinal shearing stress as the result of turbulence can be made smaller than any preassigned quantity by considering a region sufficiently close to the wall. The quantitative implications of this behavior are apparent in Eq. (II.17).

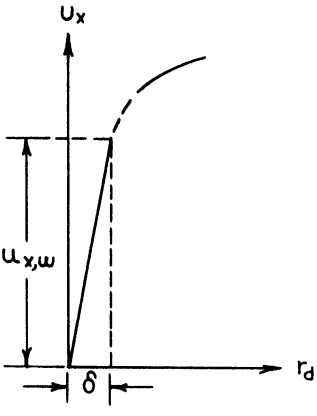

FIG. II-9. Velocity distribution near wall for a turbulently flowing fluid.

From Eq. (I.31), it follows that

$$\tau_{rx} = (\tau_{rx})_0 \frac{r}{r_0} \tag{II.38}$$

for idealized flow. The shear stress near the wall in any turbulent stream must be transmitted through the fluid near the wall by molecular transfer of momentum. In order that the high shear stresses encountered in turbulently flowing fluids can be transmitted by molecular transfer of momentum, high velocity gradients are to be expected in the fluid near the wall. This fact can be seen from Eq. (I.65). The average longitudinal velocity in a conduit containing turbulently flowing fluid would be zero at the wall, rising to a high value a short distance out from the wall, and then increasing more gradually as the axis of the stream is approached. A graphical representation of such a velocity distribution is given in Fig. II-9. The thickness of the laminar boundary layer is represented by δ. The average velocity gradient across the boundary layer is $u_{x,w}/\delta$. Application of Eq. (I.65) yields

$$\frac{(\tau_{rx})_0}{\eta} = \frac{u_{x,w}}{\delta}. \tag{II.39}$$

From Eq. (II.26) and the definition of kinematic viscosity,

$$\frac{u_{x,w}}{\delta} = \frac{u_*^2}{\nu}. \tag{II.40}$$

Rewriting Eq. (II.40), there is obtained

$$\delta = \frac{\nu}{u_*} \frac{u_{x,w}}{u_*}. \tag{II.41}$$

Equation (II.40) may be written in another way if the velocity gradient in the boundary layer is taken as u_x/r_d, where $u_x \leqslant u_{x,w}$ and $r_d < \delta$:

$$\frac{u_x}{r_d} = \frac{u_*^2}{\nu}, \tag{II.42}$$

or

$$\frac{u_x}{u_*} = \frac{u_* r_d}{\nu}. \tag{II.43}$$

From Eqs. (II.34) and (II.35) it follows that Eq. (II.43) may be rewritten as:

$$u_x^+ = r_d^+. \tag{II.44}$$

It must be remembered that the relation in Eq. (II.42) applies only in the laminar boundary layer for isothermal flow.

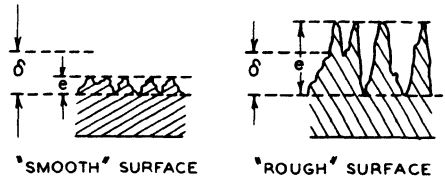

FIG. II-10. Height of roughness based on laminar boundary layer.

The expression for uniform flow between parallel plates which corresponds to Eq. (II.44) may be written as

$$u_x^+ = y_d^+. \tag{II.45}$$

It is convenient to define the condition of the surface of the inside of a conduit for a given flow as "rough" in case the maximum height of the protuberances e in a statistical sense is greater than the thickness of the laminar boundary layer δ and as "smooth" in case the maximum height is less than that thickness. This semiquantitative idea is portrayed in Fig. II-10.

NOMENCLATURE

a, b	Constants in King equation for hot-wire anemometer
C_w	Heat capacity of hot wire
c	Refers to geometry of tip of Pitot tube
d	Differential operator
e	Height of roughness element, ft.
$\overline{e^2}$	Mean-square voltage fluctuation
g	Acceleration due to gravity, ft./sec.
h	Fluid head
i	Hot-wire current
K_1	Constant in lag time equation for hot wire
k	Constant in equation for lag time of hot wire
l	Prandtl mixing length, ft.
l_y	Characteristic length, ft.
M	Mesh opening in grid (see Fig. II-7b)
M'	Lag time constant of hot wire
P	Pressure, lb./in.^{2} or lb./ft.^{2}

P_I Inlet pressure, lb./in.^{2} or lb./ft.^{2}

$\overline{R}$ Time average resistance hot wire at a fixed temperature

R_a Resistance of hot wire at a fixed ambient temperature

R_0 Resistance of hot wire at 32° F.

R_y Lateral velocity correlation coefficient

$(R_y)_l$ Longitudinal velocity correlation coefficient

r Polar radius in cylindrical and spherical coordinates, ft.

r_d Radial deficiency distance parameter, ft.

r_d^+ Radial friction distance for circular conduit, dimensionless

r_0 Radius of conduit, ft.

t_m Root-mean-square temperature

U Average velocity over an area or gross velocity, ft./sec.

u Point velocity or time average point velocity, ft./sec.

u_* Friction velocity, ft./sec.

$u(x, y, z, \theta)$ Velocity at a point at a given time, ft./sec.

$\overline{u}$ Average velocity with respect to time and space, ft./sec.

u' Root-mean-square value of velocity fluctuation, ft./sec.

$\overline{u_f}^2$ Mean square value of fluctuating component of velocity, ft.^{2}/sec.^{2}

u_x Point velocity in the x-direction, ft./sec.

$\overline{u}_x$ Time average velocity at a point, ft./sec.

u_x^+ Velocity to friction velocity ratio for the x-direction, dimensionless

$u_{x,f}$ Fluctuating velocity component in the x-direction, ft./sec.

$\overline{u_{x,f}\, u_{y,f}}$ Time average of the products of the fluctuating velocities in the x- and y-directions

$u_{x,f,A}$ Fluctuating velocity component in the x-direction at point A, ft./sec.

$u_{x,f,B}$ Fluctuating velocity component in the x-direction at point B, ft./sec.

$u_{x,i}$ Instantaneous velocity in the x-direction, ft./sec.

$u_{x,w}$ Velocity in the x-direction in laminar boundary layer, ft./sec.

$\overline{u}_y$ Time average velocity in the y-direction, ft./sec.

$u_{y,f}$ Instantaneous velocity fluctuation in the y-direction, ft./sec.

$u_{y,f,A}$ Instantaneous velocity fluctuation in the y-direction at point A, ft./sec.

$\overline{u_{y,f,A}}$ Average instantaneous velocity fluctuation in the y-direction at point A, ft./sec.

$u_{y,f,B}$ Instantaneous velocity fluctuation in the y-direction at point B, ft./sec.

$\overline{u_{y,f\,B}}$ Average instantaneous velocity fluctuation in the y-direction at point B, ft./sec.

$u_{y,i}$ Instantaneous velocity in the y-direction, ft./sec.

$u_{z,i}$ Instantaneous velocity in the z-direction, ft./sec.

x Position downstream from grid, ft.

y Distance from axis of flow, ft.

y_d Distance deficiency, distance from wall, ft.

y_d^+ Friction distance parameter for two-dimensional conduit, dimensionless

y_0 Half the distance between parallel plates, ft.

z Distance perpendicular to the y- and z-directions, ft.

α Temperature resistivity coefficient of hot wire

$\beta_{(c)}$ Dimensionless function of shape of Pitot tube

$\beta_{(c,\psi)}$ Dimensionless function of shape and angle of attack of Pitot tube

δ Thickness of laminar boundary layer, ft.

δ_x Difference between the time average velocity at a point averaged over an infinitely long period and the average value computed over a finite period, ft./sec.

ε_m Eddy viscosity, ft.^{2}/sec.

η Absolute viscosity, lb.sec./ft.^{2}

θ Time, sec.
ν Kinematic viscosity, ft.^{2}/sec.
ρ Density, σ/g, lb.sec.^{2}/ft.^{4}
σ Specific weight, lb./ft.^{3}
$\overline{\sigma}$ Time average specific weight. lb./ft.^{3}
$(\tau_{rx})_0$ Shear at wall, lb./ft.^{2}
τ_{yx} Shearing stress in the x-direction lying in a plane perpendicular to the y-direction, lb./ft.^{2}
$\overline{\tau_{yx}}$ Average shearing stress in the x-direction lying in a plane perpendicular to the y-direction, lb./ft.^{2}
$(\tau_{yx})_0$ Shearing stress at wall, lb./ft.^{2}
ψ Aspect angle of Pitot tube
$-$ Time average value, used over a symbol

SUBSCRIPTS

v Molecular viscous component
ε Turbulent component

References

1. Onsager, L., *Phys. Rev.* **37**, 405 (1951).
2. Denbigh, K. G., "Thermodynamics of the Steady State." Methuen, London, 1951.
3. DeGroot, S. R., "Thermodynamics of Irreversible Processes." North Holland, Amsterdam, 1952.
4. Millikan, C. B., *Phil. Mag.* **7**, Ser. 7, No. 44, 641 (1929).
5. Corrsin, S., *J. Aeronaut. Sci.* **20**, 357 (1953).

5 *a*. Rouse H., "Fluid Mechanics for Hydraulic Engineers," McGraw-Hill, New York, 1938.

6. Margenau, H., and Murphy, G. M., "The Mathematics of Physics and Chemistry." Van Nostrand, New York, 1943.
7. Batchelor, G. K., "The Theory of Homogeneous Turbulence." Cambridge U. P., New York, 1953.
8. Khintchine, A. *Mathematische Annalen* **109**, 604 (1934).
9. "Fluid Meters, Their Theory and Application," A.S.M.E., New York, 1937.
10. Goldstein, S., "Modern Developments in Fluid Dynamics," Vol. 1. Oxford U. P., New York, 1938.
11. King, R. O., *Engineering* **117**, 136, 259 (1924).
12. Dryden, H. E., and Kuethe, A. N., *Natl. Advisory Comm. Aeronaut. Tech. Rept.* **320** (1929).
13. Mock, W. C., Jr., and Dryden, H. L., *Natl. Advisory Comm. Aeronaut. Tech. Rept.* **448** (1932).
14. Mock, W. C., Jr., *Natl. Advisory Comm. Aeronaut. Tech. Rept.* **598** (1937).
15. Ziegler, M., *Koninkl. Ned. Akad. Wetenschap. Proc.* **34**, No. 5, 663 (1931).
16. King, L., *Phil. Trans. Roy. Soc.* **A 214**, 372 (1914).
17. Davis, L., Jet Propulsion Lab. Progr. Rept. 3-22, Pasadena, California, June, 1952.
18. Kenney, J. F., "Mathematics of Statistics." Van Nostrand, New York, 1939.
19. Rietz, H. L., "Mathematical Statistics." Open Court, New York, 1927.
20. Prandtl, L., and Reichardt, H., *Deutsche Forschung Heft* **21**, 110 (1934).
21. Goldstein, S., *op. cit.* (ref. **10**), p. 270.
22. Taylor, G. I., *Proc. Roy. Soc.* **A 151**, 421 (1935).
23. von Kármán, T., *Trans. Am. Soc. Mech. Engrs.* **61**, 705 (1939).
24. Bakhmeteff, B., "The Mechanics of Turbulent Flow." Princeton Univ. Press, Princeton, 1941.

CHAPTER III

SOME MACROSCOPIC CHARACTERISTICS OF TURBULENT FLOW

From the more general considerations of the preceding chapters, a number of relationships may be derived which are applicable to certain types of turbulent flow. From these expressions it is possible to predict the velocity distribution to a reasonable approximation in terms of a limited number of parameters. These relationships are based for the most part upon Kármán's similarity theory, the Prandtl mixing length, and the Taylor vorticity-transport hypothesis. It is not possible from these relatively simple theories and hypotheses to derive relationships which apply with accuracy to the behavior of the fluid throughout the flow channel. Certain of the macroscopic theories of turbulence yield predictions that apply with fair accuracy to the flow conditions near the axis of symmetry whereas others are descriptive of the situation in the vicinity of the wall. Even with these limitations the generalized relationships that may be derived are sufficiently descriptive of actuality to make them of engineering utility.

The present chapter deals with the derivation of such generalized relationships and presents a limited comparison with available experimental data. The significance and utility of mixing length and other macroscopic turbulence parameters are considered. The greater part of the material presented here is based upon the compilation prepared by Goldstein (*1*).

III-1. The Similarity Hypothesis

The similarity hypothesis proposed by Kármán (*2*) can be completely expressed only in mathematical terms. Goldstein (*1*) presents a somewhat simplified version of the hypothesis and summarizes the results of interest. For the case of idealized turbulent flow between parallel flat plates, the following expressions describe the more important results of this approach:

$$l = -k \frac{\left(\frac{du}{dy_d}\right)}{\left(\frac{d^2u}{dy_d^2}\right)}, \tag{III.01}[1]$$

$$\tau_{yx} = \rho l^2 \left(\frac{du}{dy_d}\right)^2, \tag{III.02}[2]$$

$$\frac{-1}{\rho}\frac{dP}{dx} = l^2 \left(\frac{du}{dy_d}\right)\left(\frac{d^2u}{dy_d^2}\right). \tag{III.03}$$

In the above expressions y_d is the normal distance from the nearest wall, x is the distance in the direction of flow, and u is the time-average point velocity in the x-direction. The results obtained from using any two of the three equations may lead to slightly different interpretations of the flow. For idealized turbulent flow in circular conduits, the corresponding equations may be expressed as

$$l = \frac{k\left(\frac{du}{dr}\right)}{\left(\frac{d^2u}{dr^2} - \frac{1}{r}\frac{du}{dr}\right)}, \tag{III.04}$$

$$\tau_{rx} = \rho l^2 \left(\frac{du}{dr}\right)^2, \tag{III.05}$$

$$\frac{1}{r}\frac{dr\,\tau_{rx}}{dr} = \rho l^2 \left(\frac{du}{dr}\right)\left(\frac{d^2u}{dr^2} - \frac{1}{r}\frac{du}{dr}\right) \tag{III.06}$$

when r is the distance from the center of the conduit and u is the average point velocity in the x-direction.

Equation (III.01) can be deduced from dimensional arguments without recourse to the full mathematical background if it is assumed that

(1) the value of l, the Kármán mixing length, at any point in the turbulent stream depends only upon the velocity distribution in the vicinity of the point, and

(2) the derivatives of order higher than the second of velocity with respect to position in the stream may be neglected in their effect upon the mixing length.

---

[1] The subscript x for the x-component of velocity is omitted in most equations in Chapters III and IV inasmuch as only the x-component of velocity is discussed.

[2] The shear τ_{yx} in this chapter is exerted by the fluid nearest the axis of symmetry upon that nearer the wall and is positive in the direction of flow.

A frame of reference moving with the average velocity of the point under consideration may be employed, and the mixing length will not directly involve the average point velocity u. Utilizing the pi theorem (*3*), Eq. (III.01) may be rewritten as

$$\phi\left(l, \frac{du}{dy_d}, \frac{d^2u}{dy_d^2}\right) = 0 \tag{III.07}$$

from which is obtained the dimensionless group,

$$l\frac{\left(\frac{d^2u}{dy_d^2}\right)}{\left(\frac{du}{dy_d}\right)} = k \tag{III.08}$$

$$l = -k\frac{\left(\frac{du}{dy_d}\right)}{\left(\frac{d^2u}{dy_d^2}\right)} \tag{III.09}$$[1]

Elaboration of the simple approach (*4*) given above shows that in addition the mixing length l may depend upon the following ratios of higher derivatives of the velocity:

$$\frac{\left(\frac{d^2u}{dy_d^2}\right)}{\left(\frac{d^3u}{dy_d^3}\right)}; \quad \frac{\left(\frac{d^3u}{dy_d^3}\right)}{\left(\frac{d^4u}{dy_d^4}\right)}.$$

The simpler result of Eq. (III.09) is valid only if all the quotients of the higher derivatives are proportional to each other, a circumstance which may be shown (*4*) to occur only for flow in the absence of a pressure gradient.

It should be noted that Eq. (III.09) does not yield determinate values when either du/dy_d or d^2u/dy_d^2 is equal to zero, and is intractable for the center of the channel unless L'Hospital's rule can be employed to advantage.

---

[1] This equation is the same as Eq. (III.01).

III-2. Idealized Turbulent Flow Between Parallel Plates Based on Similarity Hypothesis

Equation (I.57) can be rewritten for two-dimensional flow between parallel flat plates as

$$\tau_{yx} = (\tau_{yx})_0 \left(1 - \frac{y_d}{y_0}\right). \tag{III.10}$$

Upon combining Eqs. (III.01), (III.02), (II.26), and (III.10) the following expression results:

$$\frac{\left(\frac{d^2u}{dy_d^2}\right)}{\left(\frac{du}{dy_d}\right)^2} = -\frac{k_1}{u_* \sqrt{1 - \frac{y_d}{y_0}}} \tag{III.11}$$

where the friction velocity u_* is defined by Eq. (II.26). Equation (III.11) may be integrated directly to yield

$$\frac{1}{\left(\frac{du}{dy_d}\right)} = -2k_1 \frac{y_0}{u_*} \sqrt{1 - \frac{y_d}{y_0}} + C_1. \tag{III.12}$$

In order to evaluate the constant of integration, it was assumed that at the high Reynolds numbers the laminar boundary layer is thin and therefore du/dy_d is large near the wall. The exact value of du/dy_d will depend upon the thickness of the boundary layer, but as a first approximation, it was taken as infinite. Utilizing the boundary condition

$$\frac{du}{dy_d} = \infty \tag{III.13}$$

at

$$y_d = 0 \tag{III.14}$$

the constant of integration of Eq. (III.12) was found to be

$$C_1 = 2k_1 \frac{y_0}{u_*}. \tag{III.15}$$

When the quantity is incorporated in Eq. (III.12) and the equation rearranged, the following expression results:

$$\frac{du}{dy_d} = \frac{u_*}{2k_1 y_0} \frac{1}{1 - \sqrt{1 - \frac{y_d}{y_0}}} \tag{III.16}$$

in which y_0 is the half-width of the channel. Using the substitution

$$w^2 = 1 - \frac{y_d}{y_0} \tag{III.17}$$

the equation becomes

$$u = -\frac{u_*}{k_1}\int \frac{w\,dw}{1-w} + C_2. \tag{III.18}$$

By performing the indicated integration and substituting the original variable in the integrand, there is obtained

$$u = \frac{1}{k_1}\left[\sqrt{1-\frac{y_d}{y_0}} + \ln\left(1-\sqrt{1-\frac{y_d}{y_0}}\right)\right] + C_2. \tag{III.19}$$

Noting that

(III.20)

when

$$_{,d} = y_0 \tag{III.21}$$

it is apparent that

$$C_2 = u_m \tag{III.22}$$

or

$$\frac{u_m - u}{u_*} = -\frac{1}{k_1}\left[\sqrt{1-\frac{y_d}{y_0}} + \ln\left(1-\sqrt{1-\frac{y_d}{y_0}}\right)\right]. \tag{III.23}$$

This is a dimensionless expression for the velocity deficiency as a function of position in the channel and may be used to check in part the validity of the similarity hypothesis by comparison with experimental data. Figure III-1 presents such a comparison based upon the data of Dönch (*5*), Nikuradse (*6*), and Page (*7*). In conformity with the procedures adopted by Goldstein (*8*), a small additive constant has been incorporated in Eq. (III.23) which results in the following final form:

$$\frac{u_m - u}{u_*} = -\frac{1}{k_1}\left[\sqrt{1-\frac{y_d}{y_0}} + \ln\left(1-\sqrt{1-\frac{y_d}{y_0}}\right)\right] + b_1. \tag{III.24}$$

This additional constant permits an improvement in the agreement between the predicted and experimental data at values between 0.3 and 0.7 of the

quantity $1 - y_d/y_0$. For optimum agreement the constants in Eq. (III.24) result in the following numerical values:

$$k_1 = 0.295 \tag{III.25}$$

and

$$b_1 = -0.172. \tag{III.26}$$

Reference to Fig. III-1 indicates that b_1 is small in comparison to the scale of the figure. The addition of this second constant produces only a small vertical displacement of the predicted curve from that given in Eq. (III.23).

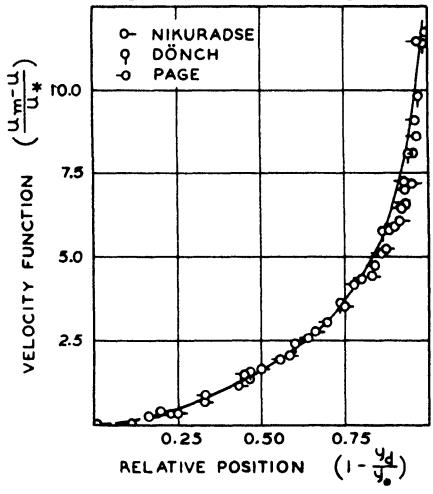

FIG. III-1. Velocity distribution between parallel plates predicted by similarity hypothesis using Eq. (III.24) (*1*).

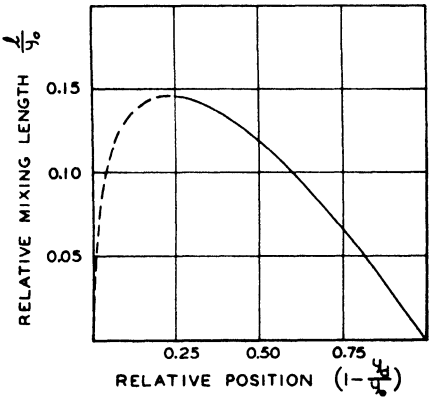

FIG. III-2. Kármán mixing length between parallel plates predicted by similarity hypothesis using Eq. (III.27) (*1*).

The variation of the Kármán mixing length (*9*), discussed earlier, with position in the channel is presented in Fig. III-2 in terms of the dimensionless ratio l/y_0. This curve is based upon the following expression using a numerical value of the constant k_1 of 0.295 (*10*):

$$\frac{l}{y_0} = 2k_1\left(1 - \sqrt{1 - \frac{y_d}{y_0}}\right)\sqrt{1 - \frac{y_d}{y_0}}. \tag{III.27}$$

This expression was obtained either by differentiating Eq. (III.23) twice and combining with Eq. (III.01) or by combining Eqs. (III.11), (III.16), and (III.01). The Kármán mixing length is zero when

$$y_d = 0 \tag{III.28}$$

and

$$y_d = y_0. \tag{III.29}$$

This last condition is a limitation to the application of these hypotheses at the center of a flowing stream. Such behavior indicates that the eddy viscosity is also zero at the axis of symmetry which is not substantiated by experimental measurements.

A second dimensionless expression for velocity deficiency as a function of position in the channel may be obtained from Eqs. (III.01) and (III.03). Equating the forces acting on an element of volume between parallel plates, as was done in deriving Eq. (I.56), there is obtained

$$-\frac{dP}{dx} = \frac{(\tau_{yx})_0}{y_0}, \tag{III.30}$$

or, dividing by the density,

$$-\frac{1}{\rho}\frac{dP}{dx} = -\frac{g_c}{\sigma}\frac{dP}{dx} = \frac{1}{y_0}\frac{g_c}{\sigma}(\tau_{yx})_0 = \frac{1}{y_0}u_*^2. \tag{III.31}$$

The last equality follows since

$$u_* = \sqrt{\frac{g_c}{\sigma}(\tau_{yx})_0} \tag{III.32}$$

by definition. Combining Eq. (III.31) with Eq. (III.03) results in

$$\frac{u_*^2}{y_0} = l^2\left(\frac{du}{dy_d}\right)\left(\frac{d^2u}{dy_d^2}\right). \tag{III.33}$$

Combining Eqs. (III.33) and (III.01), the following expression is obtained:

$$\frac{\left(\frac{d^2u}{dy_d^2}\right)}{\left(\frac{du}{dy_d}\right)^3} = -\frac{y_0}{u_*^2}k_2. \tag{III.34}$$[1]

[1] The subscript is applied to the constant k of Eq. (III.34) to distinguish it from the constant used in the equations derived by combination of Eqs. (III.01) and (III.02). Although both constants originate in the k of Eq. (III.01), it has been found that somewhat different numerical values are required in order to fit the experimental data.

The minus sign in the above expression arises from the fact that du/dy_d is positive and d^2u/dy_d^2 is negative over the range of conditions of interest. Equation (III.34) may be integrated directly to give

$$\frac{1}{\left(\frac{du}{dy_d}\right)^2} = 2\frac{y_0}{u_*^2} y_d k_2 + C_3. \tag{III.35}$$

At the wall of the channel, where

$$y_d = 0, \tag{III.36}$$

$$\frac{1}{\left(\frac{du}{dy_d}\right)^2} = C_3. \tag{III.37}$$

Under these circumstances it follows that the constant C_3 must be zero inasmuch as the velocity gradient becomes very large at the wall. By rearranging Eq. (III.35) after taking the square root of both sides, there results

$$\frac{du}{dy_d} = \frac{u_*}{k_2\sqrt{2\,y_0}} \frac{1}{\sqrt{y_d}}. \tag{III.38}$$

This expression may also be integrated directly to yield the following equation with a second constant C_4:

$$u = \frac{u_*}{k_2}\sqrt{\frac{2}{y_0}}\sqrt{y_d} + C_4. \tag{III.39}$$

The quantity C_4 may be evaluated by noting that, when

$$y_d = y_0 \tag{III.40}$$

then

$$u = u_m. \tag{III.41}$$

Substitution of the last two equations in (III.39) gives

$$C_4 = u_m - u_*\frac{\sqrt{2}}{k_2}. \tag{III.42}$$

A combination of Eqs. (III.39) and (III.42) results in

$$\frac{u_m - u}{u_*} = \frac{\sqrt{2}}{k_2}\left(1 - \sqrt{\frac{y_d}{y_0}}\right). \tag{III.43}$$

The predictions of Eq. (III.43) are compared in Fig. III-3 with the experimental data of Dönch (*5*), Nikuradse (*6*), and Page (*7*). An additive constant was incorporated in Eq. (III.43) in order to permit better agreement with experiment at values of $1 - y_d/y_0$ between 0.3 and 0.7. The values of the constants required for satisfactory agreement with experiment are

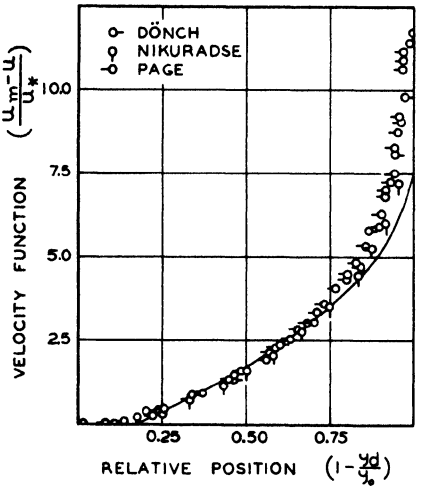

FIG. III-3. Velocity distribution between parallel plates predicted by similarity hypothesis using Eq. (III.46) (*1*).

$$k_2 = 0.165 \qquad \text{(III.44)}$$

and

$$b_2 = -0.736. \qquad \text{(III.45)}$$

Then

$$\frac{u_m - u}{u_*} = -0.736 + \frac{\sqrt{2}}{0.165}\left(1 - \sqrt{\frac{y_d}{y_0}}\right). \qquad \text{(III.46)}$$

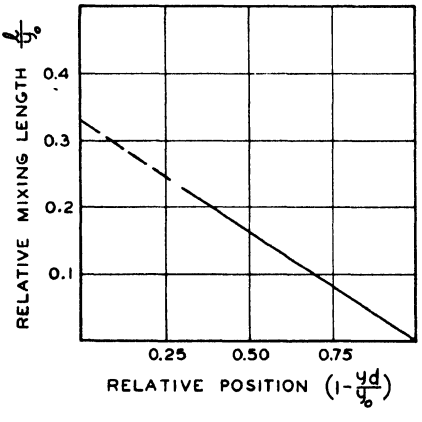

FIG. III-4. Kármán mixing length between parallel plates predicted by similarity hypothesis and linear approximation of Eq. (III.47) (*1*).

Figure III-3 indicates that even with this relatively large value of b_2 the agreement is not satisfactory for the region near the wall. Equation (III.46) may be used in combination with Eq. (III.01) to give

$$\frac{l}{y_0} = 2 k_2 \frac{y_d}{y_0}. \qquad \text{(III.47)}$$

Values of l/y_0 are shown in Fig. III-4. Upon the basis of Eq. (III.47), the mixing length is zero at the wall and increases to a maximum value $2 k_2 y_0$ at the center of the channel.

It is of interest that Eq. (III.43) predicts a finite value of u at the wall whereas Eq. (III.23) gives an infinite negative value at the boundary. Thus both of these expressions are useful only near the center of the stream.

III-3. Idealized Turbulent Flow in a Circular Channel — Similarity Hypothesis

Equations for flow in smooth circular conduits corresponding to Eqs. (III.23) and (III.43) may be developed by utilizing Eqs. (III.04), (III.05), and (III.06). By combining Eqs. (III.04) and (III.05) there is obtained

$$\tau_{rx} = \frac{\rho k_3^2 \left(\frac{du}{dr}\right)^4}{\left(\frac{d^2u}{dr^2} - \frac{1}{r}\frac{du}{dr}\right)^2} \tag{III.48}$$

which can be rearranged, using the definition of u_*, to yield

$$\frac{\left(r\frac{d^2u}{dr^2} - \frac{du}{dr}\right)}{\left(\frac{du}{dr}\right)^2} = \frac{k_3}{u_*}\sqrt{r_0}\sqrt{r}. \tag{III.49}$$

Equation (III.49) may be integrated directly into the following form:

$$-\frac{r}{\left(\frac{du}{dr}\right)} = \frac{2}{3}\frac{k_3}{u_*}\sqrt{r_0}\,r^{3/2} + C_5. \tag{III.50}$$

From the boundary condition

$$\frac{du}{dr} \cong \infty \tag{III.51}$$

when

$$r = r_0 \tag{III.52}$$

the constant C_5 is evaluated as

$$C_5 = -\frac{2}{3}\frac{k_3 r_0^2}{u_*}. \tag{III.53}$$

By combining Eq. (III.53) with Eq. (III.50) and rearranging, there results

$$-\frac{1}{r\left(\frac{du}{dr}\right)}\frac{r}{r_0} = \frac{2}{3}\frac{k_3}{u_*}\left[\left(\frac{r}{r_0}\right)^{3/2} - 1\right]. \tag{III.54}$$

By introducing the variable

$$\frac{r}{r_0} = V \tag{III.55}$$

the equation may be simplified somewhat and written in the following integral form:

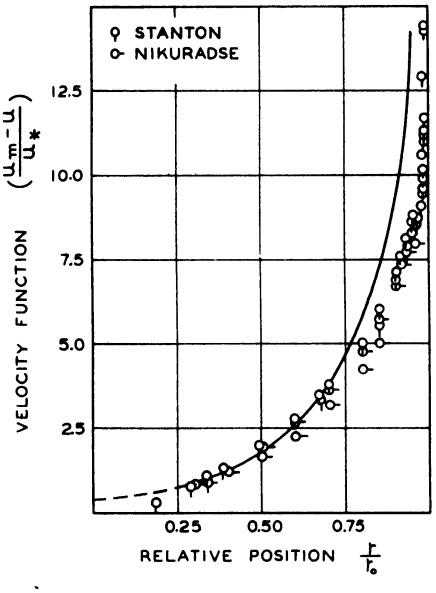

FIG. III-5. Velocity distribution in a pipe predicted by similarity hypothesis using Eq. (III.56).

$$\frac{u_m - u}{u_*} = \frac{3}{2\,k_3}\int_0^{r/r_0} \frac{V\,dV}{V^{3/2} - 1} + b_3. \tag{III.56}$$

The integral was evaluated by Goldstein (*12*). Figure III-5 compares the results from Eq. (III.56) with the experimental data of Stanton (*13*) and Nikuradse (*14*). An additive constant b_3 has been included to permit a better fit between theory and experiment at r/r_0 equal to 0.3 and 0.7. The constants required for the best fit are

$$k_3 = 0.171 \tag{III.57}$$

and

$$b_3 = 0.420. \tag{III.58}$$

It is to be noted that the agreement is poor near the wall. It should also be noted that Eq. (III.56) predicts a value of negative infinity for the velocity at the wall.

Figure III-6 presents the Kármán mixing length in terms of the dimensionless ratio l/r_0 based upon the following equation:

$$\frac{l}{r_0} = \frac{2}{3}\,k_3\left(\sqrt{\frac{r_0}{r}} - \frac{r}{r_0}\right) \tag{III.59}$$

which was obtained from a combination of Eqs. (III.49), (III.54), and (III.04). It should be observed from Eq. (III.59) that l is zero at the wall and infinite at the center of the conduit.

A second relationship may be obtained for the velocity deficiency in circular conduits by combining Eqs. (III.04) and (III.06):

$$\frac{1}{r}\frac{dr\,\tau_{rx}}{dr} = \frac{2\,(\tau_{rx})_0}{r_0} = \frac{\rho\, k_4^2 \left(\frac{du}{dr}\right)^3}{\left(\frac{d^2u}{dr^2} - \frac{1}{r}\frac{du}{dr}\right)^2}. \tag{III.60}$$

This equation may be rearranged in the following form:

$$\frac{\left(\frac{d^2u}{dr^2} - \frac{1}{r}\frac{du}{dr}\right)^2}{\left(\frac{du}{dr}\right)^3} = \frac{k_4^2}{2}\frac{r_0}{u_*^2}. \tag{III.61}$$

Inspection reveals that this equation has r^2 as an integrating factor which permits the following result to be obtained:

$$\frac{r^2}{\left(\frac{du}{dr}\right)^2} = -\frac{k_4^2}{3}\frac{r_0}{u_*^2}r^3 + C_6. \tag{III.62}$$

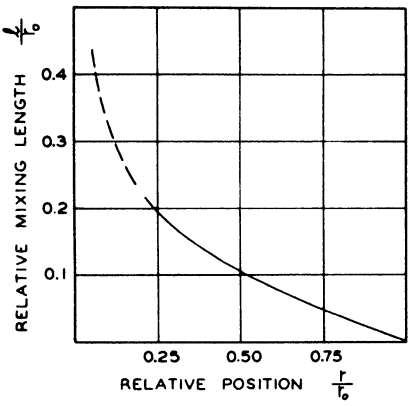

FIG. III-6. Kármán mixing length in a pipe predicted by similarity hypothesis using Eq. (III.59) (*1*)

Utilizing the boundary condition

$$\frac{du}{dr} \cong \infty \tag{III.63}$$

when

$$r = r_0 \tag{III.64}$$

the constant C_6 may be evaluated as

$$C_6 = \frac{k_4^2}{3}\frac{r_0^4}{u_*^2}. \tag{III.65}$$

The combination of Eqs. (III.62) and (III.65) results in

$$\frac{r^2}{\left(\frac{du}{dr}\right)^2} = \frac{k_4^2}{3}\frac{r_0}{u_*^2}(r_0^3 - r^3). \tag{III.66}$$

By rearrangement of Eq. (III.66), there is obtained

$$\frac{1}{r_0^2\left(\frac{du}{dr}\right)^2}\left(\frac{r}{r_0}\right)^2 = \frac{3u_*^2}{k_4^2}\left[1-\left(\frac{r}{r_0}\right)^3\right]. \tag{III.67}$$

After introduction of the auxiliary variable

$$\frac{r}{r_0} = V. \tag{III.68}$$

Eq. (III.67) may be rewritten as

$$\frac{z^2}{\left(\frac{du}{dz}\right)^2} = \frac{k_4^2}{3u_*^2}(1-V^3) \tag{III.69}$$

which may be integrated to yield

$$\frac{u_m-u}{u_*} = \frac{\sqrt{3}}{k_4}\int_0^{r/r_0}\frac{V\,dV}{\sqrt{1-V^3}} + b_4 \tag{III.70}$$

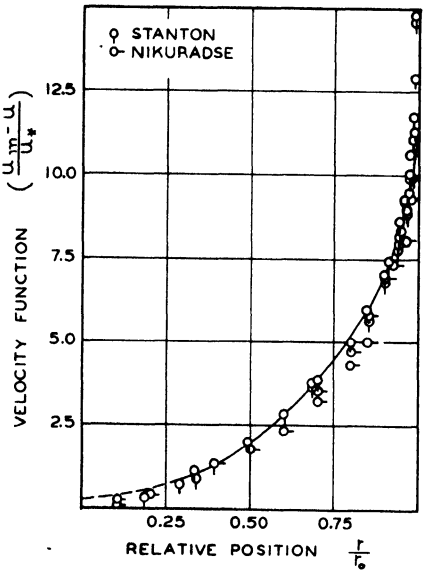

FIG. III-7. Velocity distribution in a pipe predicted by similarity hypothesis using Eq. (III.70) (*1*).

where b_4 is a corrective constant to improve the agreement between analysis and experiment for values of r/r_0 between 0.3 and 0.7. The integration in Eq. (III.70) has been evaluated by Goldstein (*15*). Figure III-7 compares the results of Eq. (III.70) with experimental data of Stanton and Nikuradse. The values of the constants for optimum agreement are

$$k_4 = 0.128 \tag{III.71}$$

and

$$b_4 = 0.251. \tag{III.72}$$

The agreement between the experimental data and the predictions is satisfactory. The velocity is, however, greater than zero at the wall, a fact which is contrary to the physical situation.

The Kármán mixing length is presented in Fig. III-8 as a function of the ratio l/r_0. In this instance the curve is based upon the function

$$\frac{l}{r_0} = \frac{2}{3} k_4 \left(\frac{r_0^2}{r^2} - \frac{r}{r_0} \right) \quad \text{(III.73)}$$

which was obtained from a combination of Eqs. (III.61), (III.66), and (III.04). It indicates that the mixing length l is zero at the wall and infinity at the center of the conduit.

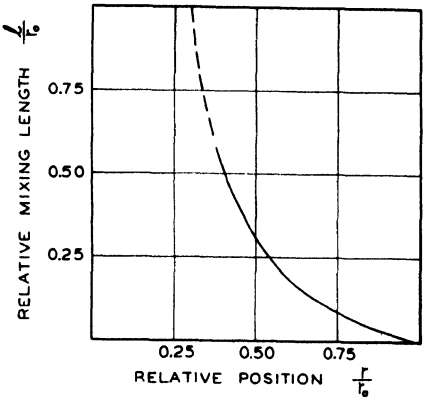

FIG. III-8. Kármán mixing length in a pipe predicted by similarity hypothesis using Eq. (III.73) (*1*).

The similarity hypothesis is the only one so far proposed which yields an expression for the mixing length l, which may be used to advantage in estimating the velocity distribution in uniform, steady flow. Other mixing length hypotheses require further assumptions regarding the variation of l with position. The assumptions of the similarity hypothesis are largely untested and, moreover, even in the relatively simple cases to which the approach has been applied, there are regions of flow where the assumptions break down. Goldstein (*16*) cites the following ways in which these failures are known to occur:

1. The restriction of the consideration of the turbulent mechanism at any point to the immediate neighborhood of the point requires that l should be small compared with any characteristic linear dimension of the flowing system, and this situation does not always exist.

2. The assumption of similarity implies constant values of the ratios

$$\overline{u_{x,f}^2} : \overline{u_{y,f}^2} : \overline{u_{z,f}^2} : \overline{u_{x,f}\, u_{y,f}} : \overline{u_{y,f}\, u_{z,f}} : \overline{u_{z,f}\, u_{x,f}}$$

where $u_{x,f}$, $u_{y,f}$, and $u_{z,f}$ are the turbulent fluctuation velocity components in the x-, y-, and z-directions, respectively. Experimental investigations (*17*) show that constant ratios are not obtained when comparing the center of the channel where little correlation exists between the instantaneous velocity components with the region of the wall where the viscous effects become of controlling importance.

III-4. The Momentum Transfer Hypothesis

It was shown in Chapter II that the Reynolds stress may be expressed as

$$\overline{\tau_{yx_s}} = -\rho \overline{u_{x,f} u_{y,f}}. \tag{III.74}$$[1]

In order to utilize this expression in predicting the distribution of average velocity, it is necessary to determine how the quantity depends upon both the average point velocity u and the boundary conditions. For this dependence, Prandtl proposed the following relationship:[2]

$$\overline{u_{x,f} u_{y,f}} = l_P^2 \frac{du}{dy} \left| \frac{du}{dy} \right|. \tag{III.75}$$

With this relationship Eq. (III.74) for the Reynolds stress assumes the following form when applied to idealized turbulent flow between flat, parallel plates:

$$\overline{\tau_{yx_s}} = -\rho l_P^2 \frac{du}{dy} \left| \frac{du}{dy} \right|. \tag{III.76}$$

In the case of flow in uniform, circular conduits it assumes the form

$$\overline{\tau_{rx_s}} = -\rho l_P^2 \frac{du}{dr} \left| \frac{du}{dr} \right|. \tag{III.77}$$

Before Eqs. (III.76) and (III.77) may be applied to the solution of particular flow problems, it is necessary that an assumption be made regarding the variation of l_P with position in the channel. The experimental data of Nikuradse which were utilized in the preparation of Figs. III-1 to III-8 may also be used to compute values for the Kármán mixing length as a function of position in the channel. Figure III-6 presents the results of such computation. It will be observed that in the region near the wall the mixing length is approximately a linear function of the distance from the wall. Therefore, as a first approximation, it may be assumed that

$$l_P = k_5 y_d. \tag{III.78}$$

Justification for extension of such a linear variation to the entire channel rests upon the accuracy of the predicted velocity distributions which are obtained.

---

[1] Equation (III.74) is the same as Eq. (II.07).

[2] For a discussion of the justification of such a hypothesis and the reason for the absolute value notation see ref. *18*.

III-5. Idealized Turbulent Flow Between Parallel Plates — Momentum Transfer Hypothesis

The momentum transfer hypothesis may be used to establish the velocity distribution in steady, uniform flow. Equation (III.76) may be combined with Eq. (III.78) to eliminate the mixing length l_P:

$$\overline{\tau_{yx_\varepsilon}} = \rho k_5^2 y_d^2 \frac{du}{dy_d}\left|\frac{du}{dy_d}\right|. \tag{III.79}$$

Likewise, Eq. (III.79) when combined with Eq. (III.10) gives for the central portion of the stream

$$(\tau_{yx})_0\left(1 - \frac{y_d}{y_0}\right) = \rho k_5^2 y_d^2 \frac{du}{dy_d}\left|\frac{du}{dy_d}\right| \tag{III.80}$$

which may be rewritten as

$$(\tau_{yx})_0 y = \rho k_5^2 y_0^3 \left(1 - \frac{y}{y_0}\right)^2 \left(\frac{du}{dy}\right)^2. \tag{III.81}$$

This equation may be combined with the friction velocity which is defined as

$$u_* = \sqrt{\frac{(\tau_{yx})_0}{\rho}} \tag{III.82}$$

and rearranged to give

$$\frac{du}{d(y/y_0)} = \frac{u_*}{k_5} \frac{\sqrt{y/y_0}}{\left(1 - \frac{y}{y_0}\right)}. \tag{III.83}$$

Equation (III.83) may be integrated with the following results:

$$u = -\frac{u_*}{k_5}\left\{\ln\left(\frac{1 + \sqrt{y/y_0}}{1 - \sqrt{y/y_0}}\right) - 2\sqrt{y/y_0}\right\} + C_7. \tag{III.84}$$

The constant of integration of Eq. (III.84) may be evaluated by setting

$$u = u_m \tag{III.85}$$

at

$$y = 0 \tag{III.86}$$

so that

$$C_7 = u_m. \tag{III.87}$$[1]

If the value of the constant C_7 in Eq. (III.87) is incorporated in Eq. (III.84) and the resulting expression rearranged, an equation for the dimensionless velocity deficiency is obtained:

$$\frac{u_m - u}{u_*} = \frac{1}{k_5}\left\{\ln\left(\frac{1+\sqrt{y/y_0}}{1-\sqrt{y/y_0}}\right) - 2\sqrt{y/y_0}\right\}. \tag{III.88}$$

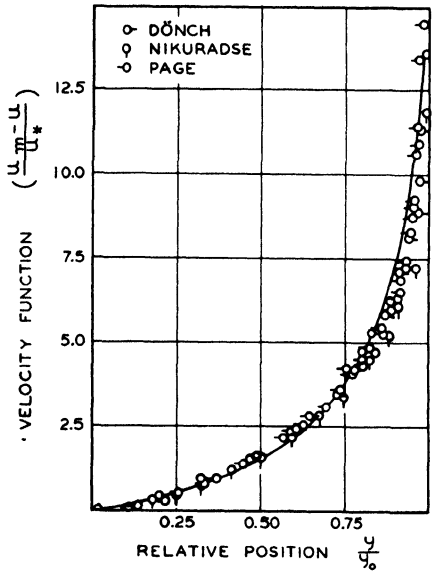

FIG. III-9. Velocity distribution between parallel plates predicted by momentum transfer hypothesis (*1*).

This equation shows the conditions

$$\frac{du}{dy} = 0 \tag{III.89}$$

at the center of the conduit and

$$\frac{du}{dy} = -\infty \tag{III.90}$$

at the wall. The velocity at the wall is predicted as negative infinity, which is far from the physical situation. A comparison of this equation with the experimental measurements of Dönch (*5*), Nikuradse (*6*), and Page (*7*) is shown in Fig. III-9. A value of

$$k_5 = 0.23 \tag{III.91}$$

was chosen to produce good agreement between the theory and experiment at

$$\frac{y}{y_0} = 0.7. \tag{III.92}$$

The agreement between the predicted and experimental measurements is satisfactory except near the wall.

---

[1] It is emphasized that in this chapter y is taken as the distance normal to the direction of flow measured from the axis of the stream.

A similar derivation may be carried out for flow through circular conduits. The equations in this instance correspond directly to those for two-dimensional flow with

$$y_d = r_d \tag{III.93}$$

and

$$y = r. \tag{III.94}$$

The dimensionless velocity-deficiency equation is then

$$\frac{u_m - u}{u_*} = \frac{1}{k_6}\left\{\ln\left(\frac{1 + \sqrt{r/r_0}}{1 - \sqrt{r/r_0}}\right) - 2\sqrt{r/r_0}\right\}. \tag{III.95}$$

This equation is compared with the experimental results of Stanton and Nikuradse in Fig. III-10. A value of k_6 of 0.20 was chosen to yield the best fit of the predicted and experimental data at a value of

$$\frac{r}{r_0} = 0.7. \tag{III.96}$$

The agreement is less satisfactory than in the case of the analysis for parallel plates, the theoretical curve diverging markedly from the experimental data near the wall.

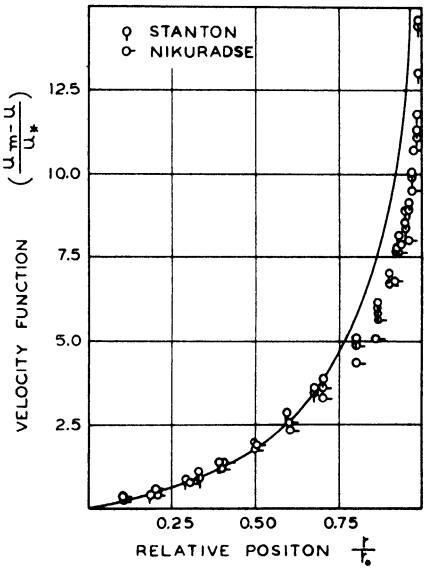

FIG. III-10. Velocity distribution in a circular conduit predicted by momentum transfer hypothesis (*1*).

It is interesting to note that Eqs. (III.88) and (III.95) may be applied to flow between both rough and smooth parallel walls and in rough or smooth circular conduits. Such applications are limited to conditions in which the surface irregularities are at least a magnitude smaller than the wall separation or pipe diameter (*19*). The experimental data presented in Fig. III-10 were taken from experimental work with smooth conduits. If the comparison had been made with Nikuradse's data for artificially roughened pipes (*20*), a similar degree of agreement would have been realized with a value of

$$k_6 = 0.24. \tag{III.97}$$

III-6. Transport Characteristics

The transport of momentum as a result of turbulence necessitates fluctuation of the velocity in a direction normal to that of the primary motion. For most conditions of momentum transfer, pressure fluctuation in the turbulent flow does not contribute to the phenomenon (*21*). An example of momentum transfer with steady, uniform, one-dimensional flow is found when momentum in the x-direction is transferred in the plane by turbulent motion. The streamlines initially parallel to the x-axis remain parallel to this axis throughout the motion. If the turbulent motion is two dimensional in the yz-plane, it may be shown (*21*) that vorticity[1] is a transport property. The latter fact may be used to develop expressions for velocity deficiency in two-dimensional flow.

III-7. The Vorticity Transport Hypothesis

The vorticity transport hypothesis initially proposed by G. I. Taylor is a result of his theoretical investigations of fluid flow. The mathematical statement of the generalized concept is involved and will not be reproduced here. However, for the case when the average velocity is only in the x-direction and is a function of y only, the full equation of motion, neglecting viscosity, may be written as

$$-\frac{\partial}{\partial x}\left(\frac{P}{\rho}+\tfrac{1}{2}(u+u_{x,t})^2+\tfrac{1}{2}u_{y,t}^2\right)=\frac{\partial}{\partial\theta}(u+u_{x,t})-u_{y,t}\left(\zeta-\frac{du}{dy}\right) \qquad \text{(III.98)}$$

[1] Vorticity is a vector quantity which is directly related to the angular velocity of a fluid element. It may be defined most precisely in mathematical terms (*22, 23*). Its general meaning, however, may be explained (*24*) by imagining an infinitesimally small sphere at any point of a fluid in motion to be suddenly solidified. If the resultant solid is found to have rotation, then the fluid possesses vorticity. Mathematically, the components of the vorticity in the x-, y-, and z-directions are expressed as

$$\omega_x=\frac{1}{2}\left(\frac{\partial u_z}{\partial y}-\frac{\partial u_y}{\partial z}\right)$$

$$\omega_y=\frac{1}{2}\left(\frac{\partial u_x}{\partial z}-\frac{\partial u_z}{\partial x}\right)$$

$$\omega_z=\frac{1}{2}\left(\frac{\partial u_y}{\partial x}-\frac{\partial u_x}{\partial y}\right)$$

If each component of the vorticity is zero, the fluid motion is termed irrotational. Other authors define the vorticity as twice this value (see Chapter V).

where ζ is the turbulent vorticity. Considering average quantities in this expression for steady flow, a marked simplification results, since the average of $u_{x,t}^2$ and $u_{y,t}^2$ will not vary with x,

$$\frac{1}{\rho}\frac{dP}{dx} = \overline{u_{x,t}\zeta}. \tag{III.99}$$

From expressions similar to Eq. (III.99), Taylor postulated that the effect of turbulence is to communicate momentum at a rate of $\rho\,\overline{u_{y,t}\zeta}$ to a unit volume per unit time. Utilizing a modification of the Prandtl hypothesis as given in Eq. (III.75), Taylor set

$$\overline{u_{y,t}\zeta} = l_T^2 \frac{d^2u}{dy^2}\left|\frac{du}{dy}\right| \tag{III.100}$$

from which there is obtained

$$\frac{1}{\rho}\frac{dP}{dx} = l_T^2 \frac{d^2u}{dy^2}\left|\frac{du}{dy}\right|. \tag{III.101}$$

This expression is identical with Eq. (III.03) obtained by Kármán (*2*) on the basis of the similarity hypothesis.

Utilizing Eqs. (III.30), (III.78), and (III.101) and the definition

$$u_* = \sqrt{\frac{(\tau_{yx})_0}{\rho}} \tag{III.102}$$

it is possible to write

$$\left|\frac{du}{dy}\right|\frac{d^2u}{dy^2} = \frac{-u_*^2}{k_7^2\, y_d^2\, y_0} \tag{III.103}$$

which may be rewritten as

$$\left|\frac{du}{dy}\right|\frac{d^2u}{dy^2} = \frac{-u_*^2}{k_7^2\left(1-\frac{y}{y_0}\right)^2 y_0^3}. \tag{III.104}$$

Equation (III.104) may be integrated in the following form:

$$\left(\frac{du}{dy}\right)^2 = \frac{2}{k_7^2}\frac{u_*^2}{y_0^2}\frac{1}{\left(1-\frac{y}{y_0}\right)} + C_8. \tag{III.105}$$

The constant may be evaluated by setting

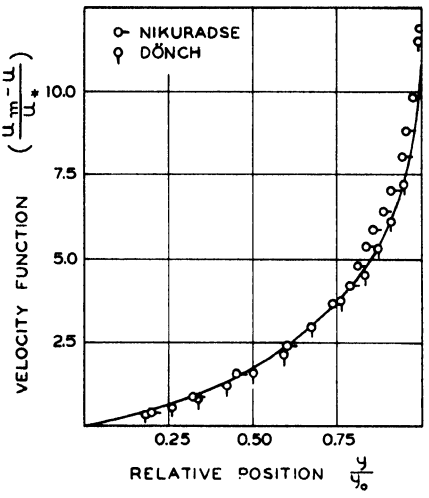

FIG. III-11. Velocity distribution between parallel plates predicted by vorticity transfer theory (*1*).

$$\frac{du}{dy} = 0 \tag{III.106}$$

at

$$y = 0. \tag{III.107}$$

By combining the results, there is obtained

$$\left(\frac{du}{dy}\right)^2 = \frac{2}{k_7^2}\frac{u_*^2}{y_0^2}\frac{(y/y_0)}{\left(1 - \frac{y}{y_0}\right)} \tag{III.108}$$

which may be integrated to give

$$u = -\frac{\sqrt{2}}{k_7}u_*\left\{\sin^{-1}\sqrt{y/y_0} - \right.$$
$$\left. - \sqrt{y/y_0}\sqrt{1 - \frac{y}{y_0}}\right\} + C_9 \tag{III.109}$$

The constant may be calculated by setting

$$u = u_m \tag{III.110}$$

at

$$y = 0 \tag{III.111}$$

which results upon rearrangement in the dimensionless, velocity deficiency equation

$$\frac{u_m - u}{u_*} = \frac{\sqrt{2}}{k_7}\left\{\sin^{-1}\sqrt{y/y_0} - \sqrt{y/y_0}\sqrt{1 - \frac{y}{y_0}}\right\}. \tag{III.112}$$

This expression is compared with the experimental data of Dönch (*5*) and Nikuradse (*6*) in Fig. III-11. The constant k_7 was given a value of 0.23 in order to obtain satisfactory agreement between theory and experiment at y/y_0 of 0.7. This equation satisfies the conditions

$$\frac{du}{dy} = 0 \tag{III.113}$$

at

$$y = 0 \tag{III.114}$$

and

$$\frac{du}{dy} = -\infty \tag{III.115}$$

at

$$y = y_0. \tag{III.116}$$

However, the predicted value of u is finite at the wall. The agreement is good in the center of the channel but poor near the boundary of the stream.

For flow in circular conduits, it is necessary to utilize the vorticity-transfer hypothesis (*25*) written for cylindrical coordinates:

$$\frac{1}{\rho}\frac{dP}{dx} = l_T^2\left(\frac{d^2u}{dr^2} + \frac{1}{r}\frac{du}{dr}\right)\left|\frac{du}{dr}\right|. \tag{III.117}$$

Equation (III.117) may be combined with Eqs. (III.30) and (III.78), and the definition of u_* to obtain

$$2\frac{u_*^2}{r_0} = k_8^2\,(r_0 - r)^2\left(\frac{d^2u}{dr^2} + \frac{1}{r}\frac{du}{dr}\right)\left|\frac{du}{dr}\right|. \tag{III.118}$$

This equation in turn may be rearranged with the following result:

$$\frac{2\,u_*^2}{k_8^2\left(1 - \dfrac{r}{r_0}\right)^2} = \left|\frac{du}{d(r/r_0)}\right|\left(\frac{d^2u}{d(r/r_0)^2} + \frac{1}{(r/r_0)}\frac{du}{d(r/r_0)}\right). \tag{III.119}$$

The foregoing expression may be converted to an integrable form by multiplying both sides by $2(r/r_0)^2$:

$$\frac{4\,u_*^2(r/r_0)^2}{k_8^2\left(1 - \dfrac{r}{r_0}\right)^2} = \frac{d}{d(r/r_0)}\left(\frac{r}{r_0}\frac{du}{d(r/r_0)}\right)^2 \tag{III.120}$$

Performing the integration, there is obtained

$$-\frac{4\,u_*^2}{k_8^2}\left[1 - \frac{r}{r_0} - 2\ln\left(1 - \frac{r}{r_0}\right) - \frac{1}{\left(1 - \dfrac{r}{r_0}\right)}\right] = \left(\frac{r}{r_0}\frac{du}{d(r/r_0)}\right)^2 + C_{10}. \tag{III.121}$$

The constant C_{10} may be evaluated by noting that

$$\frac{du}{dr} = 0 \tag{III.122}$$

at

$$r = 0. \tag{III.123}$$

Taking the square root of both sides results in

$$\frac{du}{d(r/r_0)} = -2\frac{u_*}{k_8}\left(\frac{r_0}{r}\right)\left[\frac{r}{r_0} - 1 + 2\ln\left(1 - \frac{r}{r_0}\right) + \frac{1}{\left(1 - \dfrac{r}{r_0}\right)}\right]^{1/2}. \tag{III.124}$$

Equation (III.124) may be integrated, and the value of u is then

$$u = -2\frac{u_*}{k_8}\int\left(\frac{r_0}{r}\right)\left[\frac{r}{r_0} - 1 + 2\ln\left(1-\frac{r}{r_0}\right) + \frac{1}{\left(1-\frac{r}{r_0}\right)}\right]^{1/2} d\left(\frac{r}{r_0}\right) + C_{11}. \tag{III.125}$$

The value of the constant C_{11} may be obtained by setting

$$u = u_m \tag{III.126}$$

at

$$r = 0. \tag{III.127}$$

After evaluating C_{11} and rearranging Eq. (III.125), the velocity-deficiency equation becomes

$$\frac{u_m - u}{u_*} = \frac{2}{k_8}\int_0^{r/r_0}\left(\frac{r_0}{r}\right)\left[\frac{r}{r_0} - 1 + 2\ln\left(1-\frac{r}{r_0}\right) + \frac{1}{\left(1-\frac{r}{r_0}\right)}\right]^{1/2} d\left(\frac{r}{r_0}\right). \tag{III.128}$$

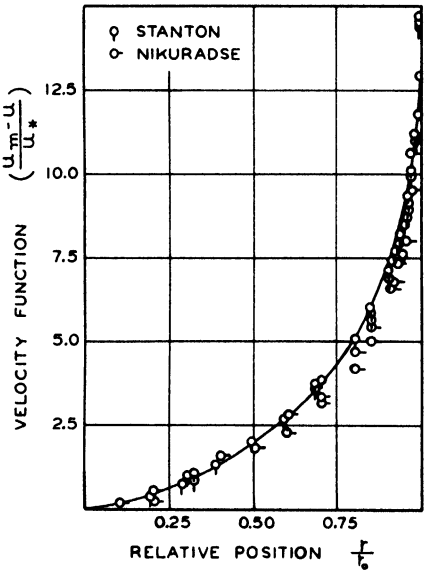

FIG. III-12. Velocity distribution in a pipe predicted by vorticity transfer theory (*1*).

This equation satisfies the conditions that

$$u = 0 \tag{III.129}$$

at

$$r = 0 \tag{III.130}$$

and

$$\frac{du}{dr} = \infty \tag{III.131}$$

at

$$r = r_0. \tag{III.132}$$

The velocity at the wall is finite despite the infinite value of the derivative. The integral was evaluated by Taylor (*26*) and is plotted in Fig. III-12. In this figure k_8 was taken to be 0.19. Comparison with the experimental data of Stanton and Nikuradse shows good agreement, even in the vicinity of the wall. However, the infinite value of the derivative du/dr is a limitation in this analysis.

III-8. Simplified Velocity Deficiency Relations

Somewhat simpler expressions may be obtained for the velocity deficiency by considering a region near the wall in which the shear may be assumed to be constant with respect to radius. In this region of boundary flow it follows that

$$\tau_{yx} = (\tau_{yx})_0. \tag{III.133}$$

If this assumption is applied to the Kármán similarity hypothesis for two-dimensional flow, Eq. (III.11) may be written as

$$\frac{\left(\frac{d^2u}{dy_d^2}\right)}{\left(\frac{du}{dy_d}\right)^2} = \frac{k_9}{u_*} \tag{III.134}$$

which may be integrated to obtain

$$\frac{1}{\left(\frac{du}{dy_d}\right)} = \frac{k_9}{u_*} y_d + C_{12}. \tag{III.135}$$

From this it follows that the constant of integration C_{12} in 0 since at the wall

$$\frac{du}{dy_d} \cong \infty \tag{III.136}$$

and

$$y_d = 0. \tag{III.137}$$

From the foregoing it follows that Eq. (III.135) assumes the form

$$\frac{du}{dy_d} = \frac{u_*}{k_9} \frac{1}{y_d}. \tag{III.138}$$

Equation (III.138) may also be obtained from the Prandtl momentum-transfer hypothesis by combining Eqs. (III.76) and (III.78) and from the assumption that the shear is constant in the region of boundary flow as indicated by Eq. (III.133). Equation (III.138) may be integrated to give

$$u = \frac{u_*}{k_9} \ln y_d + C_{13}. \tag{III.139}$$

Subject to experimental investigation, Prandtl assumed that Eq. (III.139) might apply to the entire channel as well as to the region near the wall.

Such an assumption permitted him to evaluate the constant of integration. Under these circumstances it follows that, when

$$y_d = y_0 \tag{III.140}$$

then

$$u = u_m. \tag{III.141}$$

Substitution of these boundary conditions in Eq. (III.139) results in

$$\frac{u_m - u}{u_*} = \frac{1}{k_9} \ln \left(\frac{y_0}{y_d} \right). \tag{III.142}$$

For flow in circular conduits, there is obtained the following analogous expression, since the Prandtl hypothesis applies to both two-dimensional flow between flat parallel plates and flow in circular conduits:

$$\frac{u_m - u}{u_*} = \frac{1}{k_{10}} \ln \left(\frac{r_0}{r_d} \right). \tag{III.143}$$

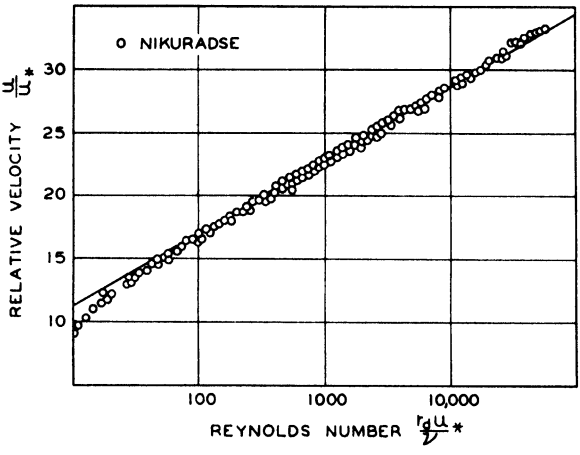

FIG. III-13. Experimental velocity distribution in circular conduits (*1*).

Comparison of equations of the form of Eqs. (III.142) and (III.143) with experimental velocity-deficiency data indicates good agreement. Figure III-13 is based upon Nikuradse's measurements which were also used in the preparation of Figs. III-5, III-7, III-10, and III-12. Figure III-13 presents u/u_* as a function of $u_* r_d/\nu$. Since ν is presumed to be constant, this figure is equivalent to Eq. (III.143). Similar agreement should be obtained for Eq. (III.142). In both cases it is found that a value of the constant approximately equal to 0.4 is required for best agreement with the experimental

data. When this value for k_9 and k_{10} is substituted in Eqs. (III.142) and (III.143), there are obtained the following forms of a velocity-deficiency equation:

$$\frac{u_m - u}{u_*} = 2.5 \ln \left(\frac{y_0}{y_d}\right) \tag{III.144}$$

or

$$\frac{u_m - u}{u_*} = 5.75 \log \left(\frac{y_0}{y_d}\right) \tag{III.145}$$

and the analogous expressions for flow in a circular conduit:

$$\frac{u_m - u}{u_*} = 2.5 \ln \left(\frac{r_0}{r_d}\right) \tag{III.146}$$

or

$$\frac{u_m - u}{u_*} = 5.75 \log \left(\frac{r_0}{r_d}\right). \tag{III.147}$$

It should be pointed out that Eq. (III.138), in common with the Kármán equations (III.16) and (III.54), gives a finite value for the velocity gradient in the center of the channel. This is in marked variance with experimental observation.

The Prandtl mixing length l_P may be calculated on the basis of the velocity gradient in Eq. (III.138) and the following defining relation:

$$l_P = \frac{u_* \sqrt{1 - \frac{y}{y_0}}}{\left(\frac{du}{dy_d}\right)}. \tag{III.148}$$

This equation, which defined the Prandtl mixing length, was derived from Eqs. (III.76) and (III.10) together with the definition of u_*. By substitution of Eq. (III.138) in Eq. (III.148), the results

$$l_P = k_9 y_d \sqrt{1 - \frac{y_d}{y_0}}. \tag{III.149}$$

The mixing length from Eq. (III.149) is zero at the wall and the center of the channel and passes through a maximum at

$$y_d = \frac{2}{3} y_0. \tag{III.150}$$

This fact is shown in Fig. III-14. Similar predictions of this mixing length are obtained for flow in circular conduits. The information of Fig. III-14 may be compared with the variation of l computed on the basis of the Kármán similarity hypothesis in Figs. III-2, III-4, III-6, and III-8. Indirect experimental evidence (*27*) indicates that the zero value of the mixing length at the center of the conduit is improbable.

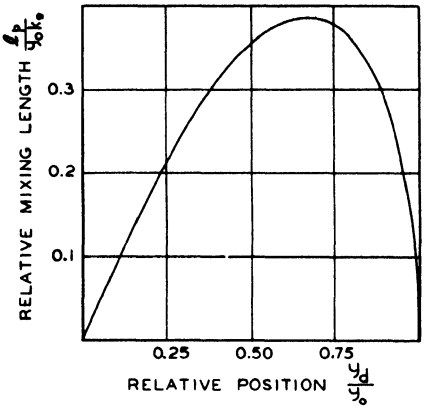

FIG. III-14. Prandtl mixing length for flow between parallel plates using Eq. (III.149).

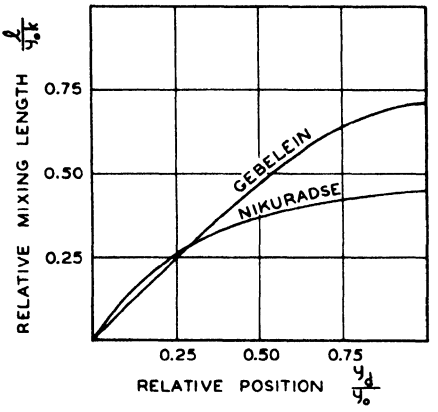

FIG. III-15. Gebelein's prediction of mixing length between parallel plates (*6*, *28*).

It is of interest to note that several investigators, notably Gebelein (*28*), have utilized the principles of statistical mechanics to investigate the problems of fluid flow. The Prandtl mixing length eliminates some of the inconsistencies noted in the preceding paragraphs. Although no attempt will be made to present an analysis, the theoretical mixing lengths obtained by Gebelein are depicted in Fig. III-15 along with a curve based upon the values calculated from Nikuradse's data of Fig. III-1. The agreement is better in certain respects than that for the three hypotheses discussed in this chapter. The absence of a zero value of the mixing length at the center of the channel is a notable improvement in prediction obtained from this approach.

Nomenclature

$b_1, \ldots, b_4$ Adjusting constant, dimensionless
$C_1, \ldots, C_{13}$ Integration constant
g_c Acceleration due to gravity, ft./sec.^{2}
k Proportionality constant
$k_1, \ldots, k_{10}$ Empirical constant, dimensionless
l Kármán mixing length, ft.
l_P Prandtl mixing length, ft.
l_T Taylor mixing length, ft.

P Thermodynamic pressure, lb./ft.^{2}
r Radial distance, ft.
r_0 Radius of circular conduit, ft.
u Velocity in the x-direction, ft./sec.
u_m Maximum velocity, ft./sec.
$u_{x,f}$ Fluctuating velocity in the x-direction, ft./sec.
$u_{y,f}$ Fluctuating velocity in the y-direction, ft./sec.
$u_{z,f}$ Fluctuating velocity in the z-direction, ft./sec.
u_* Friction velocity, ft./sec.
v Parameter, dimensionless
w Parameter, dimensionless
x Distance in the direction of flow, ft.
y Distance from plane of symmetry, ft.
y_d Perpendicular distance from the wall, ft.
$2\,y_0$ Separation distance between parallel plates, ft.
z Distance in the z-direction, ft.
ζ Turbulent vorticity, reciprocal seconds
θ Time, sec.
ν Kinematic viscosity, ft.^{2}/sec.
ρ Density, lb.sec.^{2}/ft.^{4}
σ Specific weight, lb./ft.^{3}
τ_{rx} Shear stress in the x-direction acting on a surface perpendicular to the r-direction, lb./ft.^{2}
τ_{yx} Shear stress in the x-direction acting a surface parallel to the wall, lb./ft.^{2}
$(\tau_{yx})_0$ Shear stress exerted by the fluid on the wall, lb./ft.^{2}
τ_{yx_e} The Reynolds stress in parallel plates conduit, lb./ft.^{2}
τ_{rx_e} The Reynolds stress in a circular conduit, lb./ft.^{2}
$\phi(\,)$ An unspecified function; different functional relationships among the variables are implied from time to time
ω_x Component of vorticity in the x-direction, reciprocal seconds
ω_y Component of vorticity in the y-direction, reciprocal seconds
ω_z Component of vorticity in the z-direction, reciprocal seconds
$-$ Time average, used over a symbol

References

1. Goldstein, S., "Modern Developments in Fluid Dynamics," Vols. 1 and 2; Vol. 2, pp. 347-352. Oxford U. P., New York, 1938.
2. von Kármán, T., *Nachr. Ges. Wiss. Göttingen* (1930); *Proc. 3rd Intern. Congr. Appl. Mech., Stockholm*, pp. 35-93 (1930).
3. Buckingham, E., *Trans. Am. Soc. Mech. Engrs.* **37**, 263 (1915).
4. Goldstein, S., *op. cit.* (reference *1*), Vol. 2, p. 351.
5. Dönch, F., *Forschungsarb. Ver. deut. Ing.* No. **282** (1926).
6. Nikuradse, J., *Forschungsarb. Ver. deut. Ing.* No. **289** (1929).
7. Page, F., Jr., Schlinger, W. G., Breaux, D. K., and Sage, B. H., *Am. Doc.*, Inst. Washington, D. C., No. **3294** (1951).
8. Goldstein, S., *op. cit.* (reference *1*), Vol. 2, p. 352.
9. von Kármán, T., *J. Aeronaut. Sci.* **1**, 1 (1934).
10. Deissler, R. G., *Natl. Advisory Comm. Aeronaut., Tech. Note* **2138** (1950).
11. Page, F., Jr., Schlinger, W. G., Breaux, D. K., and Sage, B. H., *Ind. Eng. Chem.* **44**, 424 (1952).
12. Goldstein, S., *op. cit.* (reference *1*), Vol. 2, p. 354.
13. Stanton, T. E., *Proc. Roy. Soc.* **A 85**, 366 (1911).
14. Nikuradse, J., *Forsch. Gebiete Ingenieurw. Forschungsheft* **No. 356** (1932).
15. Goldstein, S., *op. cit.* (reference *1*), Vol. 2, p. 355.

16. Goldstein, S., *op. cit.* (reference *1*), Vol. 2, p. 350.
17. Goldstein, S., *op. cit.* (reference *1*), Vol. 1, p. 194.
18. Goldstein, S., *op. cit.* (reference *1*), Vol. 1, pp. 206-8.
19. Goldstein, S., *op. cit.* (reference *1*), Vol. 2, p. 344.
20. Nikuradse, J., *Forsch. Gebiete Ingenieurw., Forschungsheft* **No. 361** (1933).
21. Goldstein, S., *op. cit.* (reference *1*), Vol. 1, p. 209.
22. Page, L., "Introduction to Theoretical Physics." Van Nostrand, New York, 1935.
23. Weatherburn, C. E., "Advanced Vector Analysis." Bell, London, 1924.
24. Stokes, G. G., *Trans. Cambridge Phil. Soc.* **8**, 309 (1845).
25. Goldstein, S., *op. cit.* (reference *1*), Vol. 1, pp. 213-4.
26. Taylor, G. J., *Proc. Roy. Soc.* **A 159**, 496 (1937).
27. Schlinger, W. G., and Sage, B. H., *Ind. Eng. Chem.* **45**, 2636 (1953).
28. Gebelein, H., "Turbulenz." Springer, Berlin, 1935.

CHAPTER IV

VELOCITY DISTRIBUTION AND FRICTION FACTORS FOR TURBULENT FLOW

The present chapter deals with the application of generalized relationships for turbulent flow, which were derived in the preceding chapters, to the prediction of velocity profiles and their comparison with experimental measurements. The influence of the roughness of the conduit upon the velocity distribution is considered. Emphasis is placed upon the prediction of the local velocity and friction in terms of quantities that are usually known for a particular flow. A comparison is given of the results obtained from the semimicroscopic approach of the preceding chapters with the more macroscopic consideration of the flow process as exemplified by the Fanning friction factor. Some generalizations of the characteristics of the flow, based in part upon theory modified to improve the agreement with experiment, are presented. The presentation is based on that previously made by Bakhmeteff (*1*).

IV-1. Velocity Distribution at Boundary in Circular Conduits

It is desirable to present the velocity distribution in a generalized form so that it will be used for a wide variety of conditions. The proof of the theoretical predictions rests upon detailed comparisons of the generalized results with existing experimental data.

The equations developed in Chapter III are primarily applicable to the central portion of the uniformly flowing stream and do not yield satisfactory results near the wall of the conduit. Prandtl (*2*) suggested that the following equation (see Eq. III.143) might be applied to the central position of the conduit:

$$u = \frac{u_*}{k} \ln (r_d) + C_1. \qquad \text{(IV.01)}$$

This equation was developed from the momentum transfer theory (*3*) (see Chapter III) for flow near the walls of circular conduits. The application of Prandtl's suggestion to uniform flow in the center of the conduit was made using Eq. (IV.01) in the form

$$\frac{u}{u_*} = A_1 + \frac{2.303}{k} \log\left(-\frac{r_d u_*}{\nu}\right). \tag{IV.02}$$

In this equation, A_1 is a constant. Using 0.40 as the value of k (*2*) and 5.5 for the constant A_1, Eq. (IV.02) becomes

$$\frac{u}{u^*} = 5.5 + 5.75 \log\left(\frac{r_d u_*}{\nu}\right) \tag{IV.03}$$

which is in good agreement with Nikuradse's data (*4*) obtained for turbulent flow in smooth circular conduits. It gives a generalized velocity distribution in fair agreement with experiment from the edge of the boundary flow to the center of the conduit.

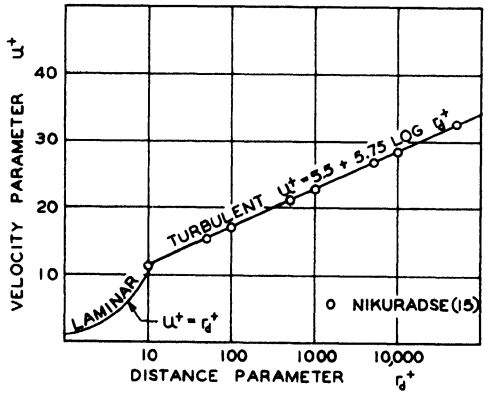

FIG. IV-1. Generalized velocity distribution near boundary of turbulent stream (*4*).

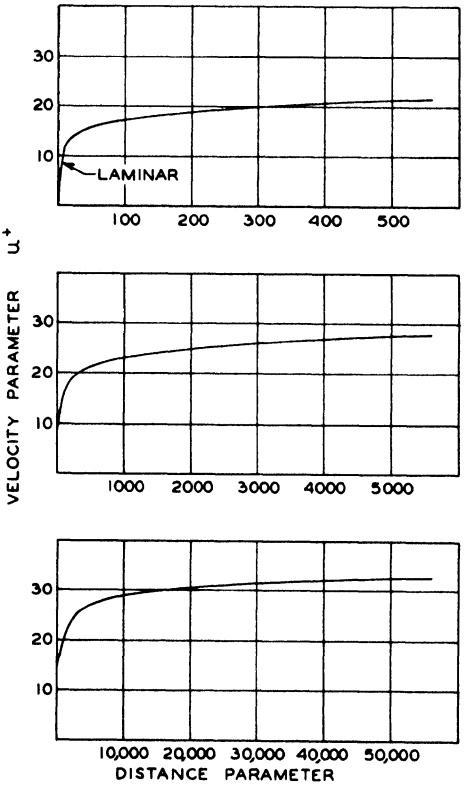

FIG. IV-2. Generalized velocity distribution in linear coordinates (*4*).

To complete the analysis of the generalized velocity distribution, it is necessary to provide an equation describing the velocity distribution from

the wall to the edge of the laminar boundary flow.[1] Such a relation[2] may be expressed as

$$u^+ = r_d^+. \tag{IV.04}$$

Figure IV-1 shows the result of combining Eqs. (IV.03) and (IV.04) to provide a simple generalized velocity distribution for turbulent flow in smooth circular conduits. Figure IV-2 is a series of plots of u^+ *versus* r_d^+ in Cartesian coordinates with different scales for the distance parameters, showing that Eqs. (IV.03) and (IV.04) yield curves similar in form to the actual velocity distribution.

Figure IV-1 indicates that the experimental data in the region of r_d^+ between 8 and 30 are not well described by Eqs. (IV.03) and (IV.04). This region in the outer part of the boundary flow, which has been called the "buffer layer," as noted earlier, was not considered in the original analysis. It is of value to consider the treatment of this transition region as well as other details of the generalized velocity distribution.

The generalized equations just described for the velocity distribution in turbulent flow also yield a discontinuity in the first derivative of the velocity with respect to the distance from the wall at the center of the channel. The discontinuity in this first derivative has its origin in the fact that the expressions were derived upon the basis that the mixing length l is zero at the axis of symmetry. It has been suggested (see Fig. III-15) that the mixing length may be a maximum at this point.

IV-2. Transition Region

Deissler (*5*) developed a number of expressions describing the variations in the velocity parameter with the distance parameter for both compressible and incompressible flow in circular conduits. In the case of an incompressible fluid where the variation in shear near the wall was neglected, the following expression was reported (*5*):

$$y_d^+ = \frac{1}{n} \frac{\dfrac{1}{\sqrt{2\pi}} \displaystyle\int_0^{nu^+} \exp\left\{-\frac{(n u^+)^2}{2}\right\} d(n u^+)}{\dfrac{1}{\sqrt{2\pi}} \exp\left\{-\frac{(n u^+)^2}{2}\right\}} \tag{IV.05}$$

[1] Here, as in the remainder of the discussion, the laminar layer is taken as that region bounded by the channel wall and the envelope defined by the intersections of the extrapolated velocity position relations in the turbulent and laminar sublayer regions.

[2] Equation (IV.04) is the same as Eq. (II.44).

which reduces to the following equality at small values of y_d^+:

$$u^+ = y_d^+. \tag{IV.06}$$

Equation (IV.05) employs (*5*) the probability integral to describe the relationship in the laminar and transition regions. The constant of proportionality η must be established for the particular conditions of flow.

Dunn (*6*) reported a suggestion by Rannie for a somewhat simpler relationship between u^+ and y_d^+ for the laminar and transition regions of uniform boundary flow:

$$u^+ = \frac{1}{\sqrt{K_1}} \tanh (y_d^+ \sqrt{K_1}) = \frac{1}{0.0695} \tanh (0.0695\, y_d^+). \tag{IV.07}$$

By proper choice of the square root of K_1 in Eq. (IV.07), it is possible to obtain a continuous first derivative of the velocity with respect to position between the transition region and the main turbulent flow. However, it is not possible for the second derivative of the velocity with respect to position to be continuous at the edge of the boundary flow. The value of the square root of K_1 shown in the second part of Eq. (IV.07) appears to describe the behavior for uniform flow in the transition region with fair accuracy.

In the turbulent core, Deissler (*5*) proposed the following expression which describes the velocity distribution and which is analogous to Eq. (IV.02):

$$u^+ = 3.8 + \frac{1}{0.36} \ln (y_d^+). \tag{IV.08}$$

If it is desired to take into account the variation in shear with position in the turbulent core, the following somewhat more complicated expression is suggested (*5*):

$$u^+ = 3.8 + \frac{1}{0.36}\left[\sqrt{1 - \frac{y_d^+}{y_0^+}} + \ln\left(1 - \sqrt{1 - \frac{y_d^+}{y_0^+}}\right)\right]. \tag{IV.09}$$

In the case of a circular conduit y_0^+ can be replaced by r_0^+. Throughout this portion of the discussion the quantity y_d^+ has been used as the distance parameter for flow either in a circular conduit or between parallel plates. This is equivalent to neglecting the effect of curvature of the wall upon the boundary flow. It is to be expected that such simplifications would not be admissible when the radius of curvature is of the same order as the thickness of the boundary flow.

IV-3. Flow Between Parallel Plates

The velocity distribution between parallel plates has been studied in some detail. Figure IV-3 presents the results of different investigators for flow between parallel plates and in circular conduits. In preparing the figure u^+ was assumed to be the same function of r_d^+ and y_d^+. The distance and velocity parameters used in correlating the flow between parallel plates are

$$y_d^+ = \frac{y_d}{\nu}\sqrt{\frac{g_c}{\sigma}(\tau_{yx})_0}\,; \qquad u^+ = \frac{u}{u_*} = \frac{u}{\sqrt{\frac{g_c}{\sigma}(\tau_{yx})_0}}. \tag{IV.10}$$

The measurements of Laufer (*7*) and Skinner (*8*) and Deissler (*5*) are shown. The agreement is not particularly satisfactory and shows that, insofar as these measurements are concerned, there exists a significant variation in the relationship between u^+ and y_d^+ as determined by different investigators.

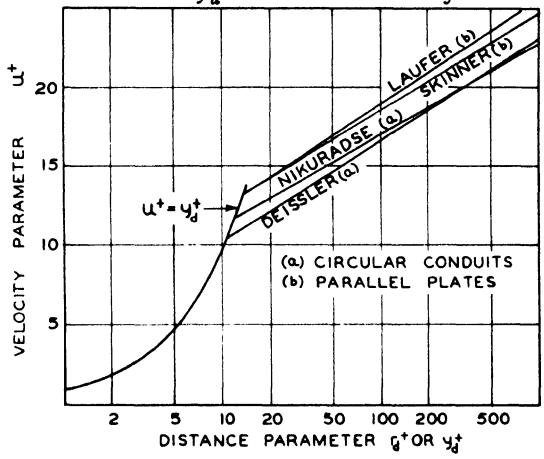

FIG. IV-3. Comparison of velocity distribution from several investigators (*10*).

The velocity distribution between parallel plates was more recently measured for the purposes of thermal transfer investigations (*9*). These measurements were made at the relatively low Reynolds numbers, varying between 7000 and 50,000. The data showed (*10*) a systematic variation in the relationship of u^+ to y_d^+ with the increasing Reynolds number. The experimental results are shown in Fig. IV-4, which includes the behavior corresponding to laminar flow with varying shear at a Reynolds number of 2000 and the upper limiting behavior corresponding to constant shear with u^+ equal to y_d^+. These results indicate a systematic variation in the velocity distribution for the Reynolds numbers below 20,000. Values of the velocity parameter are recorded in Table (IV-I) as a function of the distance

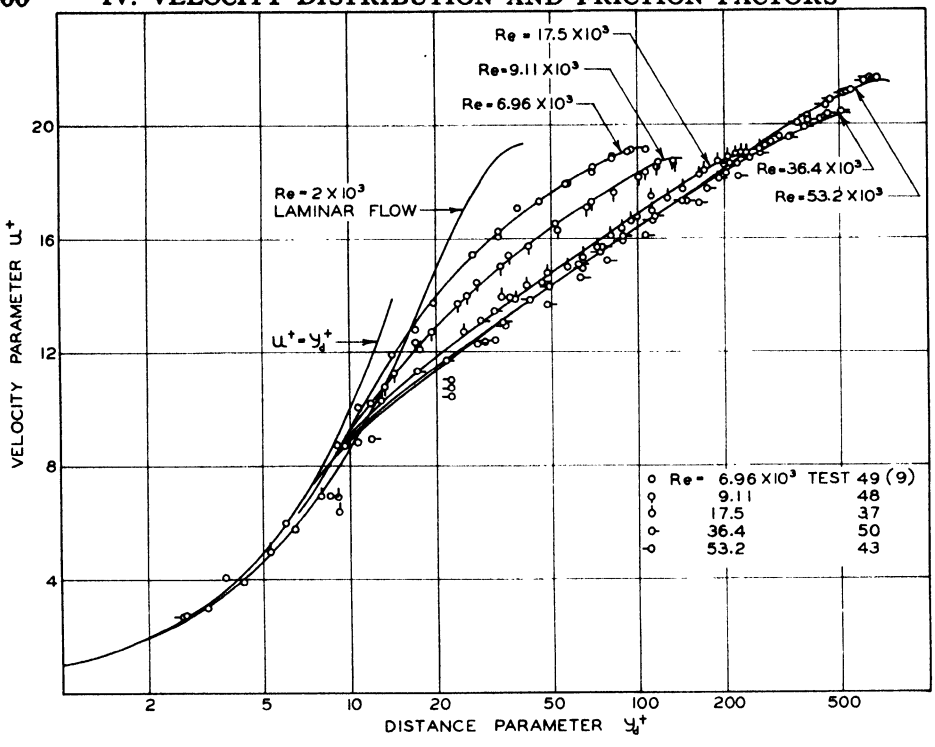

FIG. IV-4. Experimental velocity distribution for flow of air between parallel plates (*10*).

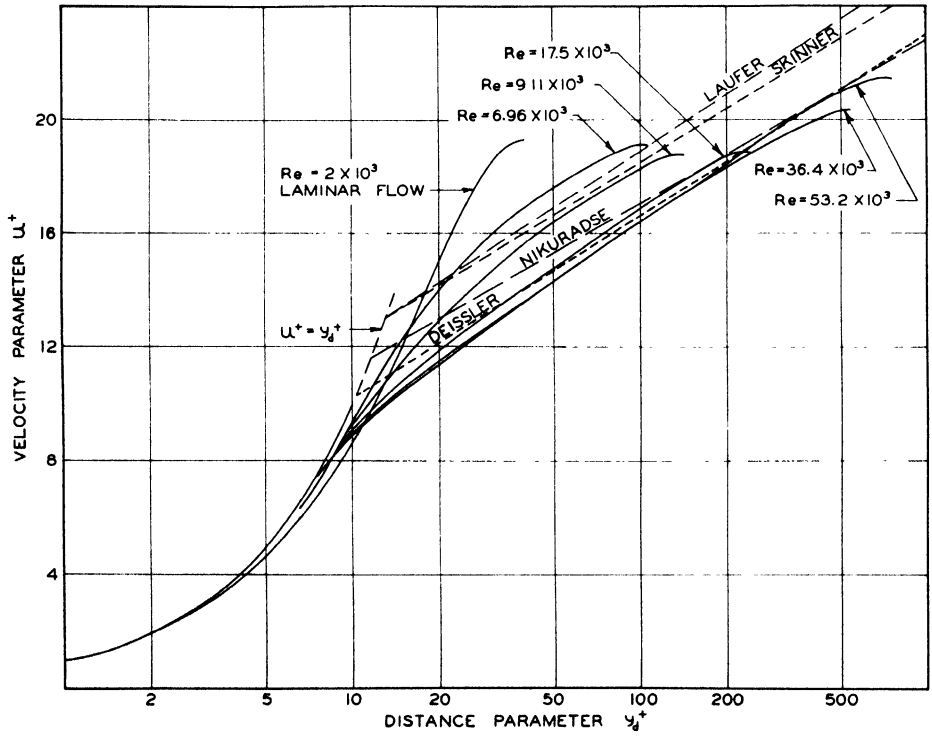

FIG. IV-5. Velocity distribution in turbulent flow (*10*).

parameter. The data for values of the distance parameter below 27 may be used for flow in circular conduits as well as for the flow between parallel plates.

It is of interest to compare on one plot the several types of velocity distribution which have been found by experiment. In Fig. IV-5 is shown a comparison of the recent experimental data (*10*) with the earlier measurements of Laufer (*7*), Skinner (*8*), Nikuradse (*4*), and Deissler (*5*). It is believed that the measurements of Deissler most properly represent the behavior near the center of the channel for flow between parallel plates. The data of Schlinger (*10*) for the transition Reynolds number range are in good agreement with the data of Deissler for the Reynolds numbers above 20,000.

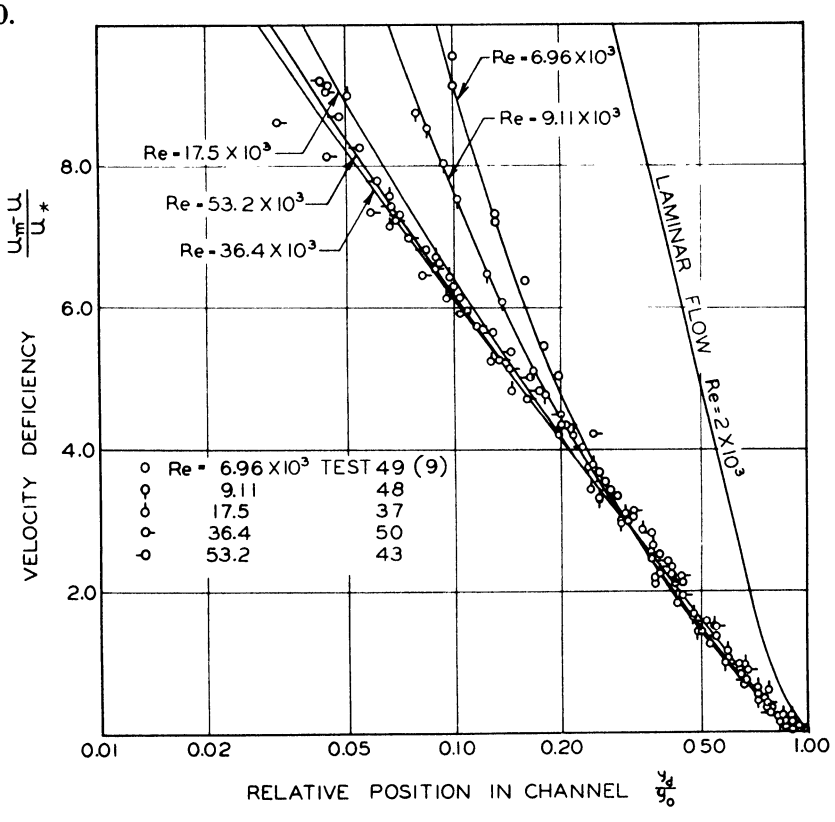

FIG. IV-6. Experimental values of velocity deficiency (*10*).

IV-4. Behavior Near Center of Channel

It is convenient to consider the velocity distribution near the center of the channel on the basis of the velocity deficiency, which is defined by the following expression:

$$u_d = \frac{u_m - u}{u_*} = \frac{u_m - u}{\sqrt{\frac{g_c}{\sigma}(\tau_{yx})_0}}. \qquad \text{(IV.11)}$$

Experimental measurements (*9*, *10*) of the velocity deficiency for the Reynolds numbers between 7000 and 53,000 are shown in Fig. IV-6. It is apparent that for the Reynolds numbers above 20,000 the velocity deficiency is a single-valued function of the position in the channel. For the lower Reynolds numbers, however, the velocity deficiency from the wall to about one-fifth the distance to the center is influenced by the Reynolds number. In laminar flow the velocity deficiency over the width of the channel is a function of the Reynolds number. The velocity deficiency as a function of even values

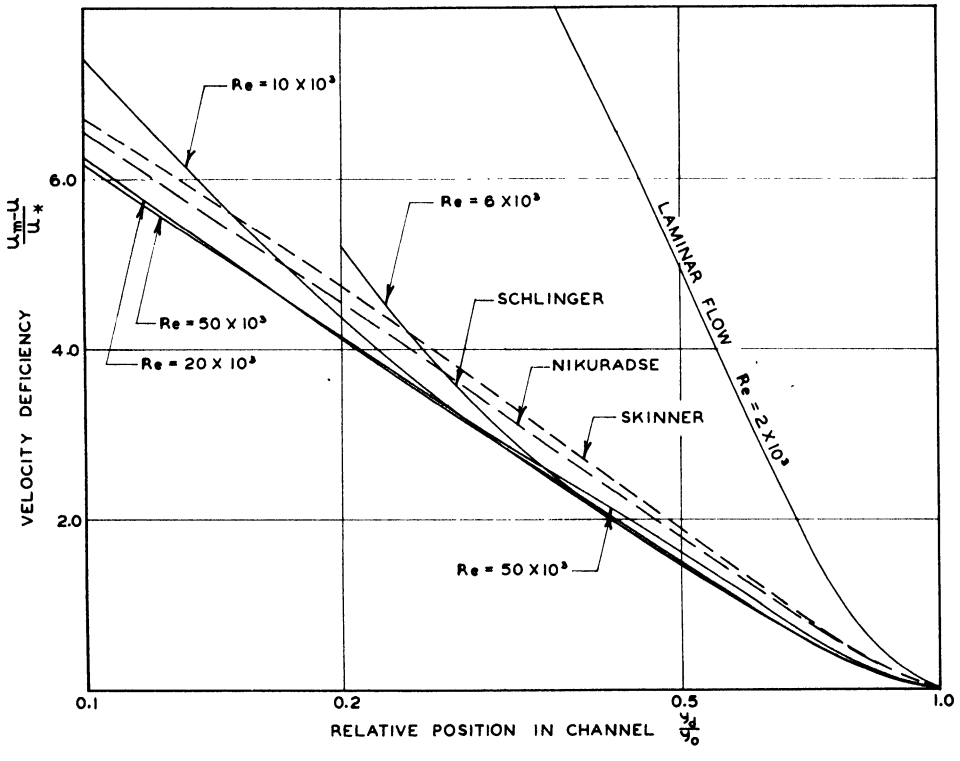

FIG. IV-7. Velocity deficiencies from different investigators (*10*).

of the Reynolds numbers is included in Fig. IV-7. It appears that the measurements of Nikuradse (*4*) for circular conduits and of Skinner (*8*) for flow between parallel plates are in fair agreement with Schlinger's measurements (*10*).

IV-5. Bulk Velocities

If it is desired, the velocity distribution for turbulent flow in smooth circular conduits may be applied to the specific problem of evaluating the average bulk velocity U. It has been shown (*1*) that

$$\frac{U}{u_*} = \frac{u_m}{u_*} - D. \tag{IV.12}$$

From experiment, D has been found to assume the following value:

$$D = \frac{3}{2k}. \tag{IV.13}$$

Taking k as 0.4, then D becomes 3.75. From Eq. (IV.03) it follows that:

$$\frac{u_m}{u_*} = 5.5 + 5.75 \log \left(\frac{r_0 u_*}{\nu}\right). \tag{IV.14}$$

From a combination of Eqs. (IV.13) and (IV.14), it is apparent that

$$\frac{U}{u_*} = 5.5 - 3.75 + 5.75 \log \left(\frac{r_0 u_*}{\nu}\right) \tag{IV.15}$$

or

$$\frac{U}{u_*} = 1.75 + 5.75 \log \left(\frac{r_0 u_*}{\nu}\right). \tag{IV.16}$$

Equations (IV.01) through (IV.04) and (IV.12) through (IV.14) apply specifically to flow in smooth circular conduits. An equation of the form of Eq. (IV.02) is also applicable to flow between infinite parallel planes with smooth surfaces, with r_d being replaced by the distance from the wall y_d.

IV-6. Resistance to Flow

In many industrial operations it is desirable to estimate the resistance to flow of a turbulent stream. It is the purpose of the following discussion to evaluate the shear at the wall in terms of the general conditions of flow. In steady, uniform flow it is a relatively simple matter to relate the shear at the wall to the pressure gradient. The following section will deal with the prediction of resistance coefficients or factors that have been found useful in evaluating the pressure gradient in circular conduits for uniform flow.

IV-7. Resistance Factor λ

The resistance factor λ for flow in smooth circular conduits may be obtained by considering Eqs. (IV.15) and (IV.16).

$$\frac{U}{u_*} = A_2 + B_1 \log\left(\frac{r_0 u_*}{\nu}\right). \tag{IV.17}$$

It has been shown in Chapter I from Eqs. (I.96) and (I.97) that

$$\frac{(\tau_{rx})_0}{\rho} = \frac{f}{2} U^2 = \frac{\lambda}{8} U^2 = u_*^2. \tag{IV.18}$$

In circular conduits the Reynolds number is defined by

$$\mathrm{Re} = \frac{2 r_0 U}{\nu}. \tag{IV.19}$$

Equation (IV.17) may be written in the following form:

$$\frac{1}{\sqrt{\lambda}} = C_2 + B_2 \log (\mathrm{Re} \sqrt{\lambda}). \tag{IV.20}$$

Equation (IV.20) only applies to the Reynolds numbers which are sufficiently large so that a region of uniform, stable turbulence exists in the center of the conduit, as shown in Fig. IV-1.

Data from Nikuradse yield the following values of the constants (*11*) for a form of Eq. (IV.20):

$$\frac{1}{\sqrt{\lambda}} = -0.8 + 2 \log (\mathrm{Re} \sqrt{\lambda}). \tag{IV.21}$$

If, in Eq. (IV.17), the quantity r_0 were to be replaced by y_0, half the distance between two infinite parallel plates, an equation of the same type as Eq. (IV.20) would be obtained. The constants should be evaluated from experimental data for two-dimensional flow between smooth parallel plates (*9*, *12*).

IV-8. Laminar Film Thickness

At the transition from the laminar to the turbulent region, the friction distance parameter has been observed to have a constant value, analogous to the value of 2000 for the Reynolds number often used as the transition

point from streamline to stable, uniform, steady, turbulent flow. The thickness of a uniform, laminar, boundary flow may be approximated by

$$y_\delta{}^+ = \frac{u_* \delta}{\nu} = N = \text{constant} \tag{IV.22}$$

or

$$\delta = \frac{\nu N}{u_*}. \tag{IV.23}$$

Since Eq. (IV.18) gives a relation between U and u_*, the following expression is obtained by combination of Eqs. (IV.18) and (IV.23):

$$\delta = \frac{\nu N}{U}\sqrt{\frac{8}{\lambda}}. \tag{IV.24}$$

From rewriting the definition of the Reynolds number given by equation (IV.19) to yield

$$\mathrm{Re} = \frac{D_0 U}{\nu} \tag{IV.25}$$

the following result is obtained from Eq. (IV.24):

$$\frac{\delta}{D_0} = \frac{\nu N}{D_0 U}\sqrt{\frac{8}{\lambda}} = \frac{N}{\mathrm{Re}}\sqrt{\frac{8}{\lambda}} \tag{IV.26}$$

where λ may be written as a function of the Reynolds number as in Eq. (IV.20). When the conduit diameter is replaced by the distance between the parallel boundaries of a stream, Eq. (IV.26) is valid for such two-dimensional flow.

IV-9. Velocity Distribution in Rough Conduits

In smooth conduits the Reynolds number may be used to characterize the flow. With flow in rough conduits a second parameter, identified as the wall roughness, is needed to describe the conditions of the flow. Before proceeding with such an analysis, it is desirable to clarify the designation of surface roughness. If only artificially roughened[1] surfaces are involved (*13, 14*), it is possible to describe the surface by establishing the

[1] Nikuradse in his experimental work (*4, 14*) used conduits artificially roughened with different size sand grains and thus controlled values of r_0/e.

depth of the roughness e,[1] measured normal to the surface. The walls of circular conduits may be classified by comparison of the ratio r_0/e. Similarly, the roughness of the surfaces of parallel plates bounding a flow may be compared by using the relative values of y_0/e.

Of particular interest in the present discussion is the region of the relatively high Reynolds numbers in which the laminar boundary flows are relatively thin and the resistance factor λ is independent of the Reynolds number. In this region the friction is proportional to the square of the average velocity and wholly "rough" flow exists. The velocity distribution equations and the expressions relating λ to r_0/e (or y_0/e) apply only to fully developed "rough" flow. Nikuradse (*14*) showed that when

$$\frac{e\,u_*}{\nu} \geqslant 100 \tag{IV.27}$$

a hydraulically rough surface is obtained. When

$$\frac{e\,u_*}{\nu} \leqslant 4 \tag{IV.28}$$

a hydraulically smooth surface is realized. The region between 4 and 100 is the transition between a smooth and rough surface. The following equation describes the velocity distribution in a rough-walled conduit:

$$u = \frac{u_*}{k} \ln (r_d) + C_1. \tag{IV.29}$$[2]

The form of the above relationship was suggested by Prandtl (*15*). It may be rewritten in terms of the maximum velocity encountered at the center of the channel, and the velocity u_w at the inner edge of the laminar boundary flow. With these changes there is obtained

$$\frac{u_w}{u_*} = \frac{u_m}{u_*} - 5.75 \log \left(\frac{r_0}{r_{d,w}} \right). \tag{IV.30}$$

In the above expression, a value of $k = 0.4$ as suggested by Prandtl (*15*) was introduced. Different wall conditions exist as a result of the variation

---

[1] The smooth or moderately rough walled conduits are identified as those where the statistical effective height e of the surface protuberances is less than the thickness of the laminar boundary flow. Rough walls are those where e is greater than the boundary thickness.

[2] This equation is the same as Eq. (IV.01).

in the roughness of the surface. For this reason u_w/u_* is not a constant as it was in smooth-walled conduits. Also the quantity $r_{d,w}$ may be expected to depend on the roughness e in the following manner:

$$r_{d,w} = m\,e. \tag{IV.31}$$

In Eq. (IV.31), m is a function of the shape and size of the wall protuberances.

Equation (IV.30) for the general case is

$$\frac{u_m - u}{u_*} = 5.75 \log\left(\frac{r_0}{r_d}\right). \tag{IV.32}$$

By combining Eq. (IV.31) with Eq. (IV.32) and a similar expression written for the edge of the boundary layer, the result is

$$\frac{u}{u_*} = \left(\frac{u_w}{u_*} - 5.75 \log (m)\right) + 5.75 \log\left(\frac{r_d}{e}\right). \tag{IV.33}$$

By substituting the variable A_r for the parenthetical expression in Eq. (IV.33), a simpler appearing equation is obtained:

$$\frac{u}{u_*} = A_r + 5.75 \log\left(\frac{r_d}{e}\right) \tag{IV.34}$$

which is more tractable for the analysis of experimental data than Eq. (IV.33). Equation (IV.34) is of the same form as was found for smooth conduits except that the first term of the right-hand side A_r is no longer constant but is a function of the surface conditions. Replacing r_d by y_d in Eq. (IV.34) yields an expression suitable for analysing two-dimensional flow between parallel plates.

IV-10. Friction Factor

The maximum velocity of flow in a straight circular conduit may be obtained from Eq. (IV.34):

$$\frac{u_m}{u_*} = A_r + 5.75 \log\left(\frac{r_0}{e}\right). \tag{IV.35}$$

The following expression has been found to be a good approximation for both smooth and rough conduits with D taken as a constant:

$$\frac{u_m - U}{u_*} = D. \tag{IV.36}$$

A combination of Eqs. (IV.35) and (IV.36) results in

$$\frac{U}{u_*} = A_r - D + 5.75 \log\left(\frac{r_0}{e}\right). \tag{IV.37}$$

The resistance factor λ is related to the velocity terms by

$$\frac{U}{u_*} = \sqrt{\frac{8}{\lambda}}. \tag{IV.38}$$

Substitution of Eq. (IV.38) in Eq. (IV.37) results in

$$\frac{1}{\sqrt{\lambda}} = \frac{A_r - D}{\sqrt{8}} + \frac{5.75}{\sqrt{8}} \log\left(\frac{r_0}{e}\right). \tag{IV.39}$$

For flow between parallel plates r_0 is replaced by y_0 in Eq. (IV.39).

IV-11. Experimental Results for Flow in Circular Conduits

Nikuradse (*14*) provided experimental data for comparison with the foregoing predictions. Values of A_r were computed from Eq. (IV.39) using experimental resistance data and a value of D of 4.07. The results of Nikuradse's calculations are plotted in Fig. IV-8 as a function of the

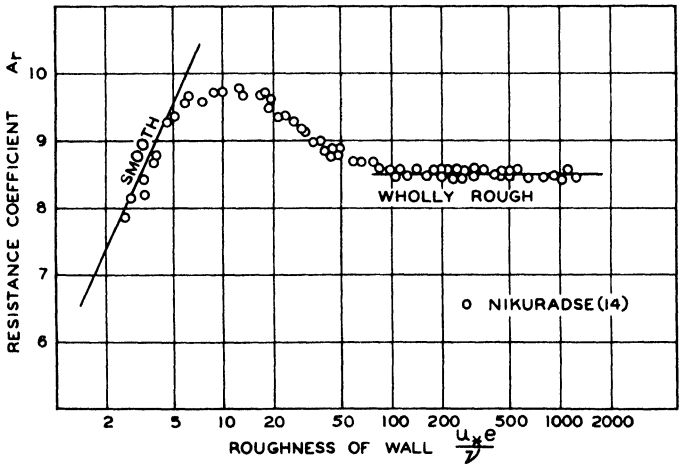

FIG. IV-8. Effect of roughness of wall on resistance coefficient (*14*).

logarithm of the dimensionless parameter $(u_* e/\nu)$ which is not directly dependent upon the Reynolds number. The value of A_r was found to increase to a maximum and then decrease slightly to a nearly constant value. The

variation in the quantity A_r occurs outside the region of fully developed "rough" flow in which the resistance factor is independent of the Reynolds

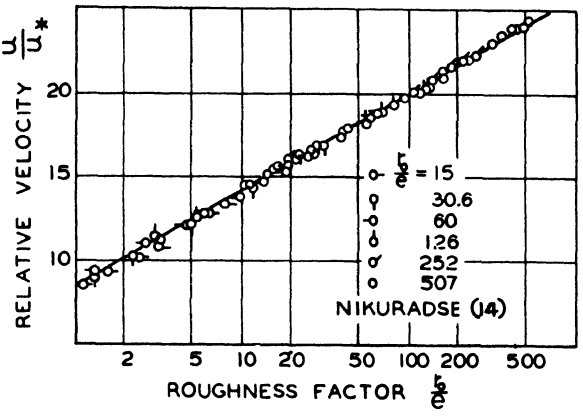

FIG. IV-9. Velocity distribution as function of roughness of wall for fully developed rough flow (*14*).

number. The value of A_r for rough flow was taken as 8.48. Substituting A_r and D in Eqs. (IV.34) and (IV.39) gives

$$\frac{u}{u_*} = 8.48 + 5.75 \log \left(\frac{r_d}{e}\right). \tag{IV.40}$$

and

$$\frac{1}{\sqrt{\lambda}} = 1.56 + 2.03 \log \left(\frac{r_0}{e}\right). \tag{IV.41}$$

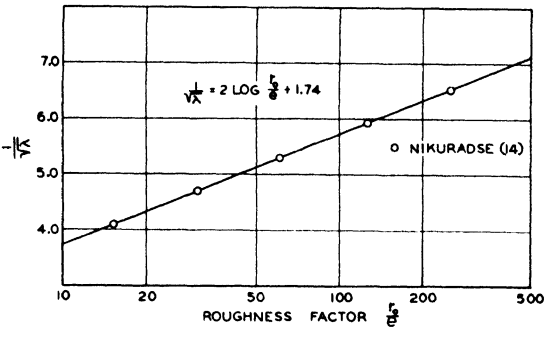

FIG. IV-10. Influence of roughness of wall on resistance factor for rough flow (*14*).

Nikuradse (*14*) presented Eq. (IV.41) in the following form:

$$\frac{1}{\sqrt{\lambda}} = 1.74 + 2 \log \left(\frac{r_0}{e}\right). \tag{IV.42}$$

The straight line in Fig. IV-9 shows the velocity distribution in flow through a rough-walled conduit as described by Eq. (IV.40). Similarly the line in Fig. IV-10 depicts Eq. (IV.42).

The first term of the right-hand side of Eq. (IV.39) is shown in Fig. IV-11 as a horizontal straight line. Nikuradse's data were included for comparison. Figures IV-8 and IV-11 show that for geometrically similar roughnesses similar flow conditions are obtained over a wide range of relative roughness.

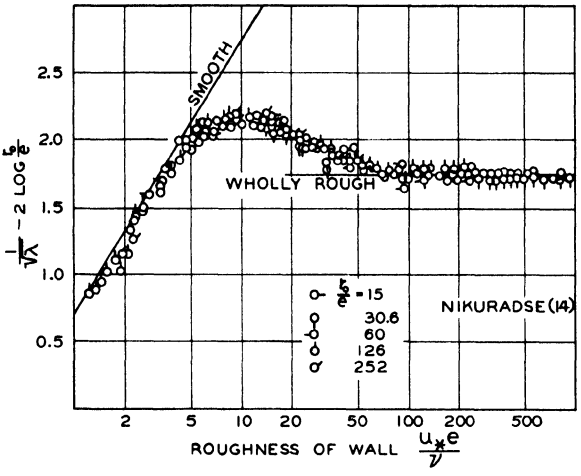

FIG. IV-11. Effect of velocity and roughness of wall on resistance (*14*).

In Figs. IV-8 and IV-11 straight lines are presented to show the relationships of the pertinent parameters for flow in "smooth" conduits. The lines have been established by transforming the equations for flow in "smooth" conduits. The transform for Fig. IV-8 is obtained from

$$\frac{u}{u_*} = 5.5 + 5.75 \log \left(\frac{r_d u_*}{\nu} \right). \qquad \text{(IV.43)}^1$$

In this instance the following substitution is made in Eq. (IV.43):

$$\log \left(\frac{r_d u_*}{\nu} \right) = \log \left(\frac{r_d}{e} \frac{e u_*}{\nu} \right) = \log \left(\frac{r_d}{e} \right) + \log \left(\frac{e u_*}{\nu} \right) \qquad \text{(IV.44)}$$

to give

$$A_r = \frac{u}{u_*} - 5.75 \log \left(\frac{r_d}{e} \right) = 5.5 + 5.75 \log \left(\frac{e u_*}{\nu} \right) \qquad \text{(IV.45)}$$

which describes the straight line for a smooth conduit shown in Fig. IV-8.

---

[1] This equation is the same as Eq. (IV.03).

The resistance equation for flow in a "smooth" conduit was established by Bakhmeteff (*1*) in the following form:

$$\frac{1}{\sqrt{\lambda}} = 0.5 + 2 \log \left(\frac{r_0 u_*}{\nu} \right). \tag{IV.46}$$

By making the same rearrangements as in obtaining Eq. (IV.44), it is possible to rewrite Eq. (IV.46) as

$$\frac{1}{\sqrt{\lambda}} - 2 \log \left(\frac{r_0}{e} \right) = 2 \log \left(\frac{e u_*}{\nu} \right) + 0.5 \tag{IV.47}$$

which describes the straight line for smooth conduits shown in Fig. IV-11.

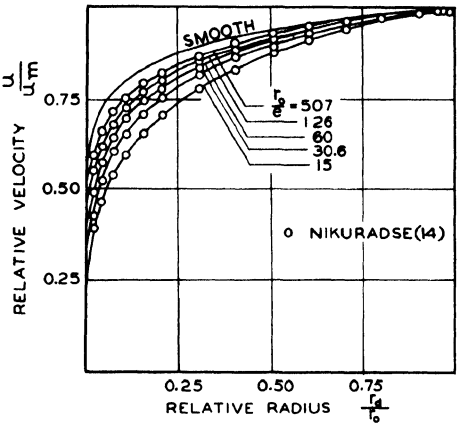

FIG. IV-12. Velocity distributions for several degrees of roughness of wall (*14*).

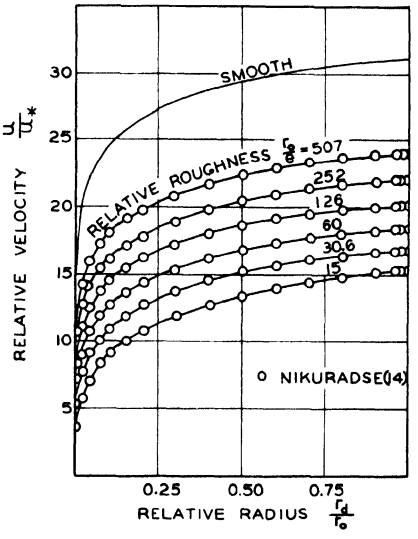

FIG. IV-13. Effect of roughness of wall on velocity distribution (*14*).

Experimental velocity distributions are shown in Fig. IV-12 for different relative roughnesses in the interior of the conduit. The data for flow in smooth conduits are included as a limiting case. In Fig. IV-13 the experimental data are depicted with u/u_* as the dependent variable in place of u/u_m used in Fig. IV-12.

The empirical coefficients which were obtained from Nikuradse's experimental work with artificially roughened conduits are limited in application to flows where the roughness is geometrically similar to that used by Nikuradse. It is possible that other types of surface roughness will yield different sets of coefficients, but the general form of the expressions should be the same.

TABLE IV-1. Generalized Velocity Distribution for Flow of Air Between Parallel Plates.[1]

(Values are velocity parameter u^+)

Reynolds number $\times 10^{-3}$

$y_d{}^{+2}$	2	4	6	8	10	15	20	30	40	50
2	1.95	1.96	1.96	1.96	1.98	2.00	2.00	2.00	2.00	2.00
4	3.79	3.85	3.88	3.88	3.88	3.88	3.92	3.92	3.92	3.92
6	5.54	5.68	5.76	5.78	5.80	5.80	5.84	5.85	5.86	5.87
8	7.17	7.43	7.56	7.62	7.66	7.68	7.68	7.70	7.72	7.74
10	8.71	9.20	9.30	9.25	9.18	9.08	9.04	9.03	9.00	9.00
15	12.10	12.52	12.45	11.85	11.28	10.76	10.72	10.68	10.64	10.60
20	14.84	14.88	14.39	13.33	12.54	11.88	11.72	11.52	11.48	11.48
25	16.93	16.80	15.78	14.46	13.66	12.82	12.48	12.24	12.24	12.24
30	18.38	17.82	16.64	15.16	14.25	13.36	13.05	12.73	12.73	12.73
35	19.19	18.45	17.20	15.73	14.88	13.84	13.44	13.24	13.24	13.24
40	19.34	18.61	17.48	16.13	15.33	14.28	13.84	13.60	13.60	13.60
45	...	...	...	16.56	15.72	14.65	14.21	14.00	14.00	14.00
50	...	...	...	16.91	16.04	14.98	14.55	14.36	14.36	14.36
60	...	...	...	17.40	16.57	15.52	15.12	14.95	14.95	14.95
70	...	...	...	17.86	17.06	15.95	15.52	15.40	15.40	15.40
80	...	...	...	18.20	17.39	16.32	15.90	15.80	15.80	15.80
90	...	...	...	18.49	17.68	16.67	16.28	16.12	16.12	16.12
100	...	...	...	18.74	17.98	17.01	16.60	16.40	16.40	16.40

[1] See ref. 10. [2] Parameter defined by Eq. (IV.10).

Nomenclature

A_1 Constant
A_2 Constant
A_r A function of the roughness of the walls of the conduit
B_1 Constant
C_1 Constant
C_2 Constant
D Constant
D_0 Diameter of circular conduit, ft.
e Depth of roughness, ft.
f Fanning friction factor, dimensionless
g_c Acceleration due to gravity, ft./sec.^{2}
K_1 Constant
k Proportionality constant, dimensionless
l Mixing length, ft.
m Proportionality constant
N Constant
n Empirical constant
r_d Radius deficiency, ft.
$r_d{}^+$ Dimensionless radial position parameter
$r_{d,w}$ Value of r_d at inner edge of laminar boundary flow, ft.

Re	Reynolds number, dimensionless
r_0	Radius of circular conduit, ft.
r_0^+	Value of r_d^+ at $r_d = r_0$
U	Gross velocity, ft./sec.
u	Component of velocity in the x-direction, ft./sec.
u_d	Velocity deficiency, ft./sec.
u_m	Maximum velocity, ft./sec.
u_w	Velocity at inner edge of laminar boundary flow, ft./sec.
u^+	Dimensionless velocity parameter
u_*	Friction velocity $\sqrt{\frac{(\tau_{yx})_0}{\rho}}$ or $\sqrt{\frac{(\tau_{rx})_0}{\rho}}$ ft./sec.
y_d^+	Dimensionless position parameter
$2\,y_0$	Separation of parallel plates, ft.
y_0^+	Value of y_d^+ at $y_d = y_0$
y_δ^+	Value of y_d^+ at $y_d = \delta$
δ	Laminar flow thickness
λ	Resistance factor, dimensionless
ν	Kinematic viscosity, ft.^{2}/sec.
ρ	Density, lb.sec.^{2}/ft.^{4}
σ	Specific weight, lb./ft.^{3}
$(\tau_{yx})_0$	Shear at wall, lb./ft.^{2}

References

1. Bakhmeteff, B. A., "The Mechanics of Turbulent Flow," p. 70. Princeton Univ. Press, Princeton, 1941.
2. Prandtl, L., Div. G in "Aerodynamic Theory" (W. F. Durand, ed.), Vol. 3. p. 84 Springer, Berlin, 1943.
3. Goldstein, S., "Modern Developments in Fluid Dynamics," Vol. 2, pp. 331-336. Oxford U. P., New York, 1938.
4. Nikuradse, J., *Forsch. Gebiete Ingenieurw. Forschungsheft* **No. 356** (1932).
5. Deissler, R. G., *Natl. Advisory Comm. Aeronaut. Tech. Note* **2138** (1950).
6. Dunn, L. G., Powell, W. B., and Seifert, H. S., Heat transfer studies relating to power plant development, *Roy. Aeronaut. Soc.* Brighton, England, *3rd Anglo-American Aeronaut. Conf.* (1951).
7. Laufer, J., *Natl. Advisory Comm. Aeronaut. Tech. Note* **2123** (1953).
8. Skinner, G. T., thesis, California Institute of Technology, Pasadena, 1950.
9. Page, F., Jr., Schlinger, W. G., Breaux, D. K., and Sage, B. H., *Ind. Eng. Chem.* **44**, 424 (1952).
10. Schlinger, W. G., and Sage, B. H., *Ind. Eng. Chem.* **45**, 2636 (1953).
11. Goldstein, S., *op. cit.* (reference *3*), p. 338.
12. Page, F., Jr., Corcoran, W. H., Schlinger, W. G., and Sage, B. H., *Ind. Eng. Chem.* **44**, 419 (1952).
13. Goldstein, S., *op. cit.* (reference *3*), p. 376, Section 167.
14. Nikuradse, J., *Forsch. Gebiete Ingenieurw. Forschungsheft* **No. 361** (1931).

CHAPTER V

GENERAL EQUATIONS OF FLUID MOTION

The foregoing chapters have been directed almost entirely to the prediction of the velocity and friction as functions of position in the flowing stream. The treatment has been only semimicroscopic in character and limited to consideration of quantities that are susceptible to direct measurements. If it is desired to investigate in greater detail the mechanics of the flow of the fluid, a much more detailed approach must be utilized. Such mathematical analyses rapidly become sufficiently complex so that their utility in the solution of engineering problems is limited. The point of view and general method of approach, however, are of definite interest as an indication of the methods which will ultimately permit the prediction of the detailed behavior of a flowing fluid. Furthermore, these relationships have a number of direct applications and in such cases the accuracy of the prediction is surprisingly good. The present chapter will treat the derivation of the general equations of fluid motion.[1] For the most part these derivations will be based upon the conservation of material and the conservation of momentum. The first relationship is well known as "the equation of continuity." The latter principle yields three similar equations applicable one to each of the three coordinates. These relationships are known as the "Navier-Stokes equation."

The first relationship to be established in this chapter is that expressing the conservation of matter.

V-1. Equation of Continuity

Because of the law of the conservation of matter, the time rate of change of mass within an element of volume of a homogeneous[2] flowing fluid is

[1] In this chapter the previous convention that an unmodified symbol indicates the average value of that quantity will be altered to the convention indicated in the nomenclature that an unmodified symbol will signify the instantaneous value of the quantity in question. The time-average values of quantities will be designated by a bar over the appropriate symbol.

[2] The restriction homogeneous is used so that the equations to be developed are mathematically correct inasmuch as the analyses will be confined to regions where all functions of interest are continuous and differentiable. If the region of study were heterogeneous in nature then such functions would not exist.

directly related to the rate at which mass flows into the volume element across the bounding surfaces of the element.

Consider a volume element, as shown in Fig. V-1, with edges parallel to the $x-y-z$ Cartesian coordinate axes, of lengths dx, dy, dz, and with center at (x, y, z). The Cartesian axes will be considered as fixed relative to the observer as will the volume element itself. If the components of the velocity of the fluid at (x, y, z) are u_x, u_y, u_z in the x-, y-, z-directions, respectively, then the mass of the fluid flowing out through the right $dx\,dz$-face in unit time is

$$\left\{\rho u_y + \left(\frac{\partial \rho u_y}{\partial y}\right)_{x,z,\theta} \frac{dy}{2}\right\} dx\,dz$$

and that flowing in through the left $dx\,dz$-face in unit time is

$$\left\{\rho u_y - \left(\frac{\partial \rho u_y}{\partial y}\right)_{x,z,\theta} \frac{dy}{2}\right\} dx\,dz.$$

The net gain of mass by flow through these two faces per unit time is, therefore,

$$-\left(\frac{\partial \rho u_y}{\partial y}\right)_{x,z,\theta} dx\,dy\,dz.$$

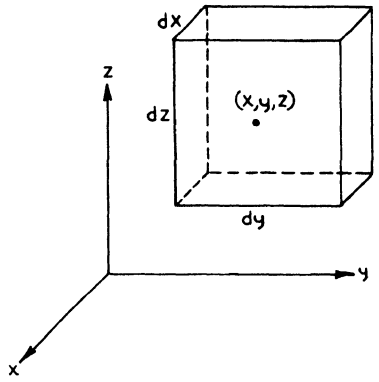

FIG. V-1. Element of volume.

Similarly, the net gain in the x-direction is

$$-\left(\frac{\partial \rho u_x}{\partial x}\right)_{y,z,\theta} dx\,dy\,dz$$

and in the z-direction,

$$-\left(\frac{\partial \rho u_z}{\partial z}\right)_{x,y,\theta} dx\,dy\,dz.$$

This rate of gain of mass by flow through the bounding surfaces of the volume element must equal the rate of increase of mass within the volume element, by the law of the conservation of matter, provided that no nuclear reactions or relativistic processes are occurring (*1*). The latter gain, however, is

$$\left(\frac{\partial \rho}{\partial \theta}\right)_{x,y,z} dx\,dy\,dz.$$

Hence

$$\left(\frac{\partial \rho}{\partial \theta}\right)_{x,y,z} + \left(\frac{\partial \rho u_x}{\partial x}\right)_{y,z,\theta} + \left(\frac{\partial \rho u_y}{\partial y}\right)_{x,z,\theta} + \left(\frac{\partial \rho u_z}{\partial z}\right)_{x,y,\theta} = 0. \qquad \text{(V.01)}$$

Equation (V.01) is the equation of continuity or of conservation of matter and is not restricted to systems of constant composition if the total mass and not the mass of a component is considered. Supplementary relations are necessary in case diffusion processes are occurring in order to describe the behavior of each component of the fluid. Chemical reactions introduce an additional complication and are not considered in this discussion (*2*).

In theoretical treatments of fluid motion it is sometimes convenient to introduce the concept of a pipe of infinitesimal cross section which has one end within a fluid element of volume. If the pipe adds material to the element, it is known as a source; if it removes material, a sink; and at the point where the pipe ends there is an infinite discontinuity in the density if the material is added or withdrawn at a finite rate. In such a case Eq. (V.01) must be modified by the addition to the right side of a term expressing the instantaneous rate of addition of material at the point (x, y, z).

Equation (V.01) may be written in another useful form by expanding the partial derivatives of the products of the density and the velocity components:

$$\left(\frac{\partial \rho}{\partial \theta}\right)_{x,y,z} + u_x\left(\frac{\partial \rho}{\partial x}\right)_{y,z,\theta} + u_y\left(\frac{\partial \rho}{\partial y}\right)_{x,z,\theta} + u_z\left(\frac{\partial \rho}{\partial z}\right)_{x,y,\theta} + \rho\left\{\left(\frac{\partial u_x}{\partial x}\right)_{y,z,\theta} + \left(\frac{\partial u_y}{\partial y}\right)_{x,z,\theta} + \left(\frac{\partial u_z}{\partial z}\right)_{x,y,\theta}\right\} = 0 \tag{V.02}$$

or

$$\frac{d\rho}{d\theta} = -\rho\left\{\left(\frac{\partial u_x}{\partial x}\right)_{y,z,\theta} + \left(\frac{\partial u_y}{\partial y}\right)_{x,z,\theta} + \left(\frac{\partial u_z}{\partial z}\right)_{x,y,\theta}\right\} \tag{V.03}$$

as by the ordinary rule for the expansion of a total derivative in terms of its independent variables when the density is considered to be a function of time and position only.

$$\begin{aligned}\frac{d\rho}{d\theta} &= \left(\frac{\partial \rho}{\partial \theta}\right)_{x,y,z} + \left(\frac{\partial \rho}{\partial x}\right)_{y,z,\theta}\frac{dx}{d\theta} + \left(\frac{\partial \rho}{\partial y}\right)_{x,z,\theta}\frac{dy}{d\theta} + \left(\frac{\partial \rho}{\partial z}\right)_{x,y,\theta}\frac{dz}{d\theta} \\ &= \left(\frac{\partial \rho}{\partial \theta}\right)_{x,y,z} + u_x\left(\frac{\partial \rho}{\partial x}\right)_{y,z,\theta} + u_y\left(\frac{\partial \rho}{\partial y}\right)_{x,z,\theta} + u_z\left(\frac{\partial \rho}{\partial z}\right)_{x,y,\theta}.\end{aligned} \tag{V.04}$$

Many authors in the field of fluid mechanics use the symbol $D/D\theta$ for $d/d\theta$ in Eqs. (V.03) and (V.04) because they desire to emphasize that the derivatives $dx/d\theta$, $dy/d\theta$, and $dz/d\theta$ have been assumed to be the components of the hydrodynamic velocity. In this connection another interpretation may be placed on Eq. (V.04). If the center of an element of volume of a fluid

moves from (x, y, z) to $(x + dx, y + dy, z + dz)$ in the time $d\theta$, Eq. (V.04) expresses the rate of change of density with time as the fluid flows along.

The equation of continuity, as shown in Eqs. (V.01) or (V.03), may also be derived by considering the distortion of a fluid element of volume which moves with the flow (*3*). Further, it may be derived without using approximations and without requiring any special orientation and shape for the fluid element of volume. This latter derivation requires the use of an important theorem of calculus known variously as Gauss' or Green's theorem. In this discussion it will be called Green's theorem in order to avoid confusion. Since later this theorem will be needed frequently, it will be given here and illustrated by the derivation.

The theorem states that if ξ_x, ξ_y, and ξ_z are the components of a quantity in the x-, y-, and z-directions, respectively, and that if ξ_x, ξ_y, and ξ_z are finite and continuous functions of x, y, and z throughout some region of space R as are their first derivatives with respect to x, y, and z, respectively, then

$$\int\int_R\int \left(\frac{\partial \xi_x}{\partial x} + \frac{\partial \xi_y}{\partial y} + \frac{\partial \xi_z}{\partial z}\right) dx\,dy\,dz = \int\int_\Sigma (\xi_x\,dy\,dz + \xi_y\,dx\,dz + \xi_z\,dx\,dy) \tag{V.05}$$

where the triple integral is taken throughout the region R, and the double integral is taken over the entire surface of the region R. The former integral is known as a volume integral and the latter, a surface integral. The theorem is proved in most advanced calculus texts (*4*, *5*).

There are several conventions which must be observed in connection with the double or surface integral. First, $dx\,dy$, $dy\,dz$, and $dx\,dz$ are the projections of the element of area dA of the surface of the region R on the xy-, yz-, and xz-planes, respectively, as shown in Fig. V-2. The element of area dA is considered to have a positive and a negative direction associated with it; the positive direction is taken as that direction perpendicular to the element of surface dA of the region R and going away from it, i.e., is the outward normal to the element of surface dA. The projected elements of area $dx\,dy$, $dy\,dz$, and $dx\,dz$ also have positive directions which are

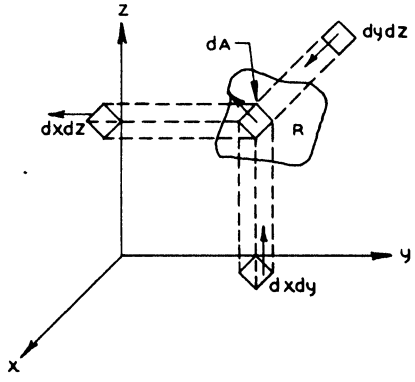

FIG. V-2. Projection of area in Cartesian coordinates.

the same as those of the outward normal projected in the z-, x-, and y-directions, respectively. Thus in Fig. V-2 the positive direction of $dy\,dz$ is the $+x$-direction; of $dx\,dy$, the $+z$; and of $dx\,dz$, the $-y$-direction. If the direction in which ξ_x is assumed positive is the same as the positive direction of $dy\,dz$, then $\xi_x\,dy\,dz$ is taken as positive in Eq. (V.05), otherwise negative, and similarly for the other components and projected surface elements.

To derive the equation of continuity, let ξ_x be the mass rate of flow per unit area in the x-direction, i.e., $\xi_x = \rho\,u_x$, and similarly $\xi_y = \rho\,u_y$, and $\xi_z = \rho\,u_z$. Then from Green's theorem, Eq. (V.05) becomes

$$\iint_R \iint \left[\left(\frac{\partial \rho\,u_x}{\partial x}\right)_{y,z,\theta} + \left(\frac{\partial \rho\,u_y}{\partial y}\right)_{x,z,\theta} + \left(\frac{\partial \rho\,u_z}{\partial z}\right)_{x,y,\theta}\right] dx\,dy\,dz$$

$$= \iint_\Sigma [\rho\,u_x\,dy\,dz + \rho\,u_y\,dx\,dz + \rho u_z\,dx\,dy]. \qquad \text{(V.06)}$$

Now the surface or double integral gives the rate at which mass flows out through the surface of the region R in the flowing fluid which is equal to the rate of decrease of mass within the surface. Hence

$$\iint_\Sigma [\rho\,u_x dy\,dz + \rho\,u_y\,dx\,dz + \rho_z u_z\,dx\,dy] = -\iint_R \int \left(\frac{\partial \rho}{\partial \theta}\right)_{x,y,z} dx\,dy\,dz. \qquad \text{(V.07)}$$

Or, combining Eqs. (V.06) and (V.07),

$$\iint_R \iint \left[\left(\frac{\partial \rho}{\partial \theta}\right)_{x,y,z} + \left(\frac{\partial \rho\,u_x}{\partial x}\right)_{y,z,\theta} + \left(\frac{\partial \rho\,u_y}{\partial y}\right)_{x,z,\theta} + \left(\frac{\partial \rho\,u_z}{\partial z}\right)_{x,y,\theta}\right] dx\,dy\,dz = 0. \qquad \text{(V.08)}$$

Equation (V.08) is restricted to a homogeneous system which is equivalent to the requirement that ξ_x and $\partial \xi_x/\partial x$, etc., are finite and continuous.

Since the size and shape of the region R can be varied arbitrarily, the integrand must vanish for each point in the flow in order to satisfy Eq. (V.08). Hence Eq. (V.01) is obtained.

In a volume element of a homogeneous fluid, the pressure and temperature have been assumed to be definable (see Section I-3) and continuous, i.e., they may be expressed as functions of the linear dimensions of the volume element. Thus for the fluid there will be, in general, an equation of state of the form

$$\rho = \rho(P, T). \qquad \text{(V.09)}$$

Here the possibility of diffusion and variation of composition is excluded. Equation (V.03) may then be written

$$\left(\frac{\partial \rho}{\partial T}\right)_P \frac{dT}{d\theta} + \left(\frac{\partial \rho}{\partial P}\right)_T \frac{dP}{d\theta} + \rho \left\{ \left(\frac{\partial u_x}{\partial x}\right)_{y,z,\theta} + \left(\frac{\partial u_y}{\partial y}\right)_{x,z,\theta} + \left(\frac{\partial u_z}{\partial z}\right)_{x,y,\theta} \right\} = 0 \tag{V.10}$$

to emphasize that ρ can be considered a thermodynamic function of P and T alone. The operator $d/d\theta$ has the same significance as in Eq. (V.03).

For a liquid which is both incompressible and thermally inexpansible, i.e., for which

$$\left(\frac{\partial \rho}{\partial P}\right)_T = \left(\frac{\partial \rho}{\partial T}\right)_P = 0 \qquad \text{or} \qquad \rho = \rho_0 \tag{V.11}$$

there is obtained from Eq. (V.03) or (V.10)

$$\left(\frac{\partial u_x}{\partial x}\right)_{y,z,\theta} + \left(\frac{\partial u_y}{\partial y}\right)_{x,z,\theta} + \left(\frac{\partial u_z}{\partial z}\right)_{x,y,\theta} = 0. \tag{V.12}$$

The left-hand side of Eq. (V.12) is known mathematically as the divergence of the velocity so that Eq. (V.03) is sometimes written in vector shorthand as

$$\frac{d\rho}{d\theta} + \rho \operatorname{div} \boldsymbol{u} = 0 \tag{V.13}$$

and Eq. (V.12) becomes

$$\operatorname{div} \boldsymbol{u} = 0. \tag{V.14}$$

Considering a volume element of constant mass, it can be seen from Eq. (V.13) by dividing by ρ and substituting m_0/v for ρ that div $\boldsymbol{u}$ represents the relative rate of expansion of the fluid.

The equation of continuity has been derived in the Cartesian coordinate system. This system is useful when any or all of the surfaces bounding the flow are planes; however, cylindrical, spherical, and other coordinate systems can be more useful depending upon the bounding surfaces. The equation of continuity may be rederived for each coordinate system by transposing from Cartesian coordinates or by using a general equation such as Eq. (V.13) (*6*) and tabulating the special results for each coordinate system. The techniques for obtaining each particular result are explained in most texts on vector analysis (*7*, *8*) and in Appendix II. Extensive tabulations of the results are given in Margenau and Murphy (*9*) and in Adams (*10*).

The results will be given here for the important cases of cylindrical and spherical coordinates. Cylindrical coordinates are shown in Fig. V-3. The equation of continuity in cylindrical coordinates becomes

$$\left(\frac{\partial \rho}{\partial \theta}\right)_{r,\psi,x} + \frac{1}{r}\left\{\left(\frac{\partial r\rho u_r}{\partial r}\right)_{\psi,x,\theta} + \left(\frac{\partial \rho u_\psi}{\partial \psi}\right)_{r,x,\theta} + \left(\frac{\partial r\rho u_x}{\partial x}\right)_{r,\psi,\theta}\right\} = 0 \qquad \text{(V.15)}$$

where r is the radial direction, ψ the azimuth, and x the axial direction.[1] The designations u_r, u_ψ, and u_x denote the components of the velocity in the radial, azimuthal, and axial directions, respectively. This form of Eq. (V.01) is especially useful in the consideration of flow in cylinders (e.g. pipes); i.e., where one of the flow boundaries can be taken as

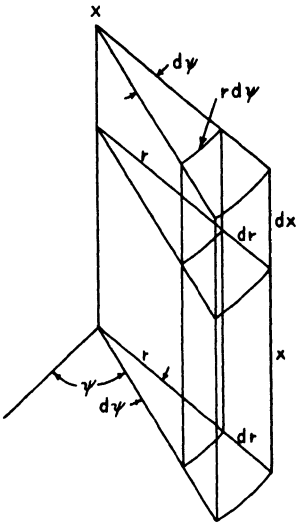

ELEMENT OF VOLUME = $r\,d\psi\,dr\,dx$

FIG. V-3. Volume element in cylindrical coordinates.

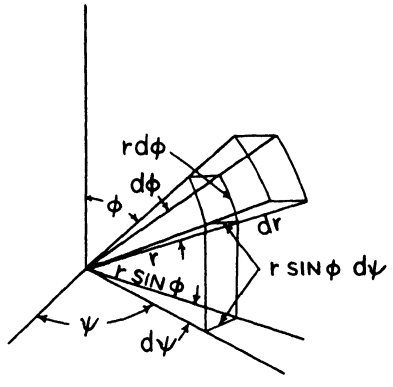

ELEMENT OF VOLUME = $r^2 \sin\phi\, dr\, d\psi\, d\phi$

FIG. V-4. Volume element in spherical coordinates.

$$r = r_0, \qquad \text{a constant.} \qquad \text{(V.16)}$$

Figure V-4 shows the spherical coordinates. The equation of continuity in spherical coordinates is

$$\left(\frac{\partial \rho}{\partial \theta}\right)_{r,\phi,\psi} + \frac{1}{r^2 \sin\phi}\left\{\left(\frac{\partial \rho\, r^2 u_r \sin\phi}{\partial r}\right)_{\phi,\psi,\theta} + \left(\frac{\partial \rho\, r\, u_\phi \sin\phi}{\partial \phi}\right)_{r,\psi,\theta} + \left(\frac{\partial \rho r u_\psi}{\partial \psi}\right)_{r,\phi,\theta}\right\} = 0 \qquad \text{(V.17)}$$

[1] In many books on mathematical physics z is taken as the axial direction and ϕ, as the azimuthal.

where r is the radial direction, ψ the azimuth, and ϕ the colatitude; and u_r, u_ψ, and u_ϕ are the components of the velocity in the radial, azimuthal, and colatitude directions. This form of Eq. (V.01) is most useful when one of the surfaces bounding the flow is a sphere or a portion of one, i.e., for which

$$r = r_0, \qquad \text{a constant.} \tag{V.18}$$

V-2. Boundary Conditions for the Equation of Continuity

The only boundaries to a homogeneous flowing fluid which will be considered here are solid walls or imaginary surfaces in the fluid itself. The imaginary surfaces may have any properties desired to ascribe to them, but the situation at a solid-fluid interface may be more complicated than it is possible to consider in this discussion. Therefore, it is assumed that there are no solution or crystallization processes occurring at the interface between the solid walls and the fluid and that the walls are continuous, smooth, and nonporous. Thus it may be assumed further that the interfacial energy is negligible compared to the internal energy of the fluid.

As mentioned in Chapter I, the relative velocity between a real fluid and a solid wall is generally negligible. Consequently, if u' is the velocity of a point on the surface of a solid wall and u, the velocity of the fluid in contact with that point,

$$u' - u = 0 \tag{V.19}$$

and if

$$u' = 0 \tag{V.20}$$

then u must be 0.

An important branch of theoretical fluid dynamics considers the behavior of a "perfect" fluid, i.e., a fluid which has no viscosity. In place of Eq. (V.19), equations may be derived expressing the fact that the relative velocity of the fluid normal to the wall is zero (*3*, *6*), but in general for this hypothetical case the relative tangential velocity need not be.

The equation of continuity is not of much value by itself since, even for a system of constant composition, it introduces five unknown quantities such as P, T, u_x, u_y, and u_z which are, for example, functions of the four independent variables x, y, z, and θ. Consequently, the discussion of methods of solution of partial differential equations, such as Eq. (V.01), together with their boundary conditions, such as Eq. (V.19), will be deferred until more relations among the unknown variables have been derived.

Three more equations relating these variables can be found by the law of the conservation of momentum, or equivalently by a force balance which

can be calculated by adding all the forces acting on a region or volume element of a fluid. Because of the complexity of the situation, it is desirable to discuss separately each type of force which acts on the fluid. In general the acceleration of the fluid is produced by external forces, such as gravitational and electric fields, and by forces exerted by adjacent portions of the fluid on one another.

V-3. Acceleration of the Flowing Fluid

The acceleration of a flowing fluid at any particular point in the flow as, for example, at the center of an element of volume is given by the rate of change of the velocity at that point. Thus

$$a_x = \frac{du_x}{d\theta} = \left(\frac{\partial u_x}{\partial \theta}\right)_{x,y,z} + \left(\frac{\partial u_x}{\partial x}\right)_{y,z,\theta}\frac{dx}{d\theta} + \left(\frac{\partial u_x}{\partial y}\right)_{x,z,\theta}\frac{dy}{d\theta} + \left(\frac{\partial u_x}{\partial z}\right)_{x,y,\theta}\frac{dz}{d\theta} \tag{V.21}$$

or

$$a_x = \frac{du_x}{d\theta} = \left(\frac{\partial u_x}{\partial \theta}\right)_{x,y,z} + u_x\left(\frac{\partial u_x}{\partial x}\right)_{y,z,\theta} + u_y\left(\frac{\partial u_x}{\partial y}\right)_{x,z,\theta} + u_z\left(\frac{\partial u_x}{\partial z}\right)_{x,y,\theta}. \tag{V.22}$$

Similarly, for the components of the acceleration of the fluid in the other coordinate directions,

$$a_y = \frac{du_y}{d\theta} = \left(\frac{\partial u_y}{\partial \theta}\right)_{x,y,z} + u_x\left(\frac{\partial u_y}{\partial x}\right)_{y,z,\theta} + u_y\left(\frac{\partial u_y}{\partial y}\right)_{x,z,\theta} + u_z\left(\frac{\partial u_y}{\partial z}\right)_{x,y,\theta} \tag{V.23}$$

and

$$a_z = \frac{du_z}{d\theta} = \left(\frac{\partial u_z}{\partial \theta}\right)_{x,y,z} + u_x\left(\frac{\partial u_z}{\partial x}\right)_{y,z,\theta} + u_y\left(\frac{\partial u_z}{\partial y}\right)_{x,z,\theta} + u_z\left(\frac{\partial u_z}{\partial z}\right)_{x,y,\theta}. \tag{V.24}$$

These equations may be written in several other forms, some of which will be given later (Cf. Appendix II), which are more convenient for particular problems.

V-4. External Forces Acting on a Flowing Fluid

Because of the possible influence of magnetic and electrical fields and the usual influence of gravitational fields on the matter of a flowing fluid, there may be external forces acting on an element of volume of the fluid, such as that shown in Fig. V-1. If the mass of the element is constant, the forces are

$$\rho\Phi_x\,dx\,dy\,dz, \qquad \rho\Phi_y\,dx\,dy\,dz, \qquad \text{and} \qquad \rho\Phi_z\,dx\,dy\,dz$$

in the x-, y-, and z-direction, respectively. Thus Φ_x is the acceleration in the x-direction produced by the external fields, etc.

If the fields are conservative, i.e., broadly speaking, there are no losses due to friction, the forces are derivable from a potential, (*11*) which means that there exists a potential function Ω such that

$$\Phi_x = -\left(\frac{\partial \Omega}{\partial x}\right)_{y,z,\theta}, \tag{V.25}$$

$$\Phi_y = -\left(\frac{\partial \Omega}{\partial y}\right)_{x,z,\theta}, \tag{V.26}$$

$$\Phi_z = -\left(\frac{\partial \Omega}{\partial z}\right)_{x,y,\theta} \tag{V.27}$$

The minus sign is a convention adopted from the study of electricity.

In pure gravitational fields the potential is

$$\Omega = g_c h \tag{V.28}$$

where h is the vertical distance above a reference plane, and g_c is the acceleration due to gravity. Equations (V.25), (V.26), and (V.27) then become

$$\Phi_x = -g_c\left(\frac{\partial h}{\partial x}\right)_{y,z,\theta}, \tag{V.29}$$

$$\Phi_y = -g_c\left(\frac{\partial h}{\partial y}\right)_{x,z,\theta}, \tag{V.30}$$

$$\Phi_z = -g_c\left(\frac{\partial h}{\partial z}\right)_{x,y,\theta}. \tag{V.31}$$

Electric and magnetic fields (*11*) are rarely of technical importance in the case of one-component systems, though the behavior of a jet of molten metal or fused salt under the influence of either or both types of external field would be a possible example. Chemical reactions usually accompany the electrolysis of multicomponent systems, therefore that case falls outside the scope of this discussion, and magnetic fields are rarely of technical importance even for multicomponent systems. Hence, unless stated to the contrary, external fields will always be taken to be pure gravitational fields.

V-5. Forces Acting on the Surface of a Portion of a Flowing Fluid

The element of volume of the flowing fluid shown in Fig. V-5 has its center at (x, y, z) at time θ and its edges of length dx, dy, and dz parallel to the respective coordinate axes. The surface stresses acting on three of the six faces are shown; the other three are similar, except that the direction

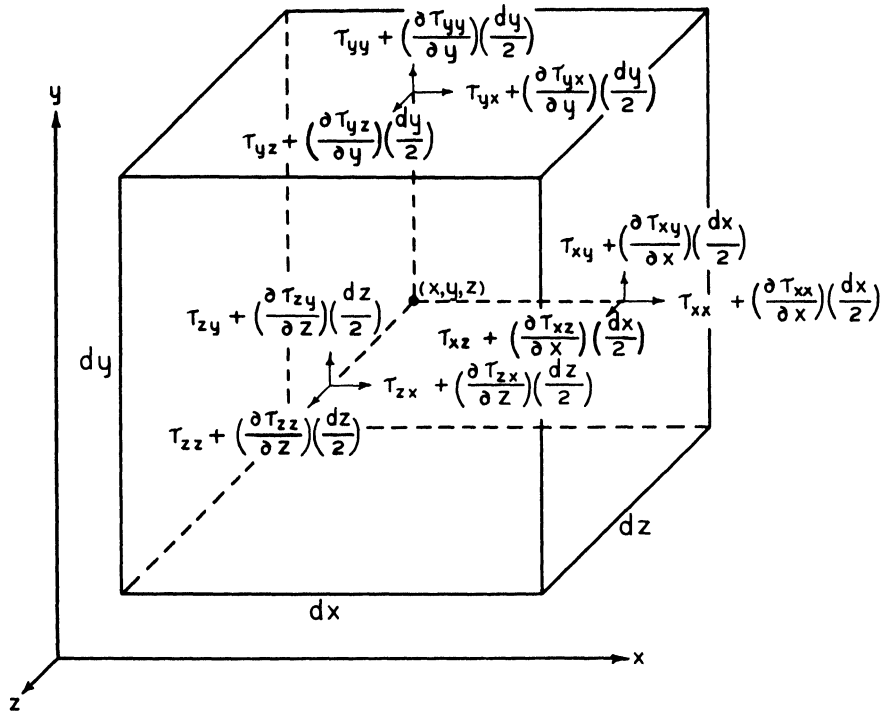

FIG. V-5. Surface stresses on element of volume.

of the stresses and the signs of their gradients are reversed. Here τ_{xx} represents the stress[1] at the point (x, y, z) which acts on an element of surface passing through (x, y, z) perpendicular to the x-axis, and acts in the x-direction; τ_{xy}, the stress on an element of surface passing through (x, y, z) perpendicular to the x-axis, and acting in the y-direction; etc. It should be noted that τ is being used to represent a stress in general terms even though it is more often specifically used as a shear stress.

---

[1] In this chapter contravariant and covariant tensors are not distinguished since only Cartesian coordinates are used where the distinction would be of importance (Cf. Appendix II).

The net force acting in the x-direction on the element of volume shown in Fig. V-6 is:

$$\left[\tau_{xx}+\left(\frac{\partial\tau_{xx}}{\partial x}\right)_{y,z,\theta}\frac{dx}{2}\right]dy\,dz+\left[-\tau_{xx}-\left(\frac{\partial(-\tau_{xx})}{\partial x}\right)_{y,z,\theta}\frac{dx}{2}\right]dy\,dz$$
$$+\left[\tau_{zx}+\left(\frac{\partial\tau_{zx}}{\partial z}\right)_{x,y,\theta}\frac{dz}{2}\right]dx\,dy+\left[-\tau_{zx}-\left(\frac{\partial(-\tau_{zx})}{\partial z}\right)_{x,y,\theta}\frac{dz}{2}\right]dx\,dy \tag{V.32}$$
$$+\left[\tau_{yx}+\left(\frac{\partial\tau_{yx}}{\partial y}\right)_{x,z,\theta}\frac{dy}{2}\right]dx\,dz+\left[-\tau_{yx}-\left(\frac{\partial(-\tau_{yx})}{\partial y}\right)_{x,z,\theta}\frac{dy}{2}\right]dx\,dz$$
$$=\left[\left(\frac{\partial\tau_{xx}}{\partial x}\right)_{y,z,\theta}+\left(\frac{\partial\tau_{yx}}{\partial y}\right)_{x,z,\theta}+\left(\frac{\partial\tau_{zx}}{\partial z}\right)_{x,y,\theta}\right]dx\,dy\,dz.$$

Similarly, the net force in the y-direction is

$$\left[\left(\frac{\partial\tau_{xy}}{\partial x}\right)_{y,z,\theta}+\left(\frac{\partial\tau_{yy}}{\partial y}\right)_{x,z,\theta}+\left(\frac{\partial\tau_{zy}}{\partial z}\right)_{x,y,\theta}\right]dx\,dy\,dz$$

and in the z-direction,

$$\left[\left(\frac{\partial\tau_{xz}}{\partial x}\right)_{y,z,\theta}+\left(\frac{\partial\tau_{yz}}{\partial y}\right)_{x,z,\theta}+\left(\frac{\partial\tau_{zz}}{\partial z}\right)_{x,y,\theta}\right]dx\,dy\,dz.$$

V-6. Momentum Equations for a Flowing Fluid

By Newton's second law of motion,[1] the time rate of change of momentum equals the net force acting on the element of volume of the flowing fluid. Since the element may be chosen so that its mass is constant, the product of the acceleration in the x-direction and the mass can be equated to the surface and external forces acting in the x-direction to give

$$\rho\frac{du_x}{d\theta}dx\,dy\,dz=\rho\Phi_x\,dx\,dy\,dz+\left[\left(\frac{\partial\tau_{xx}}{\partial x}\right)_{y,z,\theta}+\left(\frac{\partial\tau_{yx}}{\partial y}\right)_{x,z,\theta}+\left(\frac{\partial\tau_{zx}}{\partial z}\right)_{x,y,\theta}\right]dx\,dy\,dz. \tag{V.33}$$

---

[1] For the sake of completeness it should be mentioned that again relativistic effects radiation pressure, nuclear reactions, etc. are neglected. See Ref. 1.

Similar expressions may be obtained for the y- and z-directions so, upon dividing through by $\rho\, dx\, dy\, dz$, the result is

$$\frac{du_x}{d\theta} = \Phi_x + \frac{1}{\rho}\left[\left(\frac{\partial \tau_{xx}}{\partial x}\right)_{y,z,\theta} + \left(\frac{\partial \tau_{yx}}{\partial y}\right)_{x,z,\theta} + \left(\frac{\partial \tau_{zx}}{\partial z}\right)_{x,y,\theta}\right], \tag{V.34}$$

$$\frac{du_y}{d\theta} = \Phi_y + \frac{1}{\rho}\left[\left(\frac{\partial \tau_{xy}}{\partial x}\right)_{y,z,\theta} + \left(\frac{\partial \tau_{yy}}{\partial y}\right)_{x,z,\theta} + \left(\frac{\partial \tau_{zy}}{\partial z}\right)_{x,y,\theta}\right], \tag{V.35}$$

$$\frac{du_z}{d\theta} = \Phi_z + \frac{1}{\rho}\left[\left(\frac{\partial \tau_{xz}}{\partial x}\right)_{y,z,\theta} + \left(\frac{\partial \tau_{yz}}{\partial y}\right)_{x,z,\theta} + \left(\frac{\partial \tau_{zz}}{\partial z}\right)_{x,y,\theta}\right]. \tag{V.36}$$

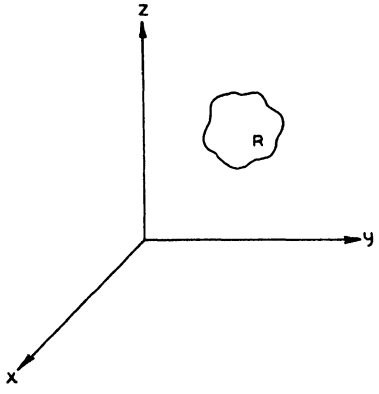

FIG. V-6. Arbitrary region of flowing fluid.

These fundamental relations which are known as the momentum equations may also be derived for an arbitrary region of the flowing fluid by means of Green's theorem. In the application of the theorem take an arbitrary region of the flowing fluid, as in Fig. V-6, and apply Newton's second law of motion to it. Where the volume integrals are extended over the entire region R and the surface integral over the entire surface of R, the result for the x-direction is

$$\frac{d}{d\theta}\iiint_R \rho\, u_x\, dx\, dy\, dz = \iiint_R \rho\, \Phi_x\, dx\, dy\, dz + \iint_\Sigma [\tau_{xx}\, dy\, dz + \tau_{yx}\, dx\, dz + \tau_{zx}\, dx\, dy]. \tag{V.37}$$

Here $\rho\, u_x\, dx\, dy\, dz$ is the momentum in the x-direction of an element of volume of the region R; $\rho\, \Phi_x\, dx\, dy\, dz$ is the external force acting in the x-direction on an element of volume; and $\tau_{xx}\, dy\, dz + \tau_{yx}\, dy\, dx + \tau_{zx}\, dy\, dx$ is the surface force acting in the x-direction on an element of surface of the region R.

In order to evaluate the left-hand integral in Eq. (V.37), it is best to evaluate first the integral

$$\frac{d}{d\theta}\iiint_R \xi\, dx\, dy\, dz$$

where ξ is any continuous and finite function of x, y, z, and θ with continuous and finite first derivatives and where the symbol R is written below the integral signs to emphasize that the integration is taken throughout the volume of the region R. By the definition of a total derivative,

$$\frac{d}{d\theta}\int\int\int_R \xi\, dx\, dy\, dz \tag{V.38}$$
$$= \lim_{\Delta\theta\to 0} \frac{1}{\Delta\theta}\left\{\int\int\int_{R(\theta+\Delta\theta)} \xi(\theta+\Delta\theta)\, dx\, dy\, dz - \int\int\int_{R(\theta)} \xi(\theta)\, dx\, dy\, dz\right\}$$

since the volume of the region R as well as the value of ξ may vary with time. Add and subtract

$$\frac{1}{\Delta\theta}\int\int\int_{R(\theta)} \xi(\theta+\Delta\theta)\, dx\, dy\, dz$$

to the right-hand side of Eq. (V.38) inside the braces. Then

$$\frac{d}{d\theta}\int\int\int_R \xi\, dx\, dy\, dz = \lim_{\Delta\theta\to 0}\frac{1}{\Delta\theta}\int\int\int_{R(\theta)} [\xi(\theta+\Delta\theta)-\xi(\theta)]\, dx\, dy\, dz \tag{V.39}$$
$$+ \lim_{\Delta\theta\to 0}\frac{1}{\Delta\theta}\int\int\int_{\Delta R(\theta)} \xi(\theta+\Delta\theta)\, dx\, dy\, dz$$

where

$$\Delta R(\theta) = R(\theta+\Delta\theta) - R(\theta) \tag{V.40}$$

the expansion of the region R in the time $\Delta\theta$. Since the integrating and limiting operations may be interchanged in the first term on the right side, it may be written as

$$\int\int\int_R \left\{\lim_{\Delta\theta\to 0}\frac{\xi(\theta+\Delta\theta)-\xi(\theta)}{\Delta\theta}\right\} dx\, dy\, dz$$

and then from the definition of a partial derivative the term becomes

$$\int\int\int_R \left(\frac{\partial\xi}{\partial\theta}\right)_{x,y,z} dx\, dy\, dz.$$

The second term on the right in Eq. (V.39) in the limit is given by $\xi\, dR/d\theta$ which is ξ times the rate of change of the volume of the region R. This term

may, however, be rewritten (*12*) in terms of the rate of expansion of the surface of the region R to give

$$\frac{\xi\, dR}{d\theta} = \int_{\Sigma}\int \xi\,[u_x\, dy\, dz + u_y\, dx\, dz + u_z\, dx\, dy] \tag{V.41}$$

since $u_x\, dy\, dz$ gives the volume swept out by the x-component of the velocity and the element of area perpendicular to it in unit time, etc. The symbol Σ indicates that the integration is taken over the entire surface of the region R. Thus Eq. (V.38) becomes

$$\begin{aligned}\frac{d}{d\theta}\int_{R}\int\int \xi\, dx\, dy\, dz &= \int_{R}\int\int \left(\frac{\partial \xi}{\partial \theta}\right)_{x,y,z} dx\, dy\, dz \\ &+ \int_{\Sigma}\int \xi(u_x\, dy\, dz + u_y\, dx\, dz + u_z\, dx\, dy).\end{aligned} \tag{V.42}$$

The second term on the right-hand side of Eq. (V.42) may be transformed by means of Green's theorem, Eq. (V.05), so that the equation becomes

$$\begin{aligned}&\frac{d}{d\theta}\int_{R}\int\int \xi\, dx\, dy\, dz \\ &= \int_{R}\int\int \left[\left(\frac{\partial \xi}{\partial \theta}\right)_{x,y,z} + \left(\frac{\partial \xi\, u_x}{\partial x}\right)_{y,z,\theta} + \left(\frac{\partial \xi\, u_y}{\partial y}\right)_{x,z,\theta} + \left(\frac{\partial \xi\, u_z}{\partial z}\right)_{x,y,\theta}\right] dx\, dy\, dz\end{aligned} \tag{V.43}$$

or, expanding the derivatives of the ξ-velocity products and remembering the expansion of a total derivative with respect to θ in x, y, z, and θ [Eq. (V.04)],

$$\begin{aligned}&\frac{d}{d\theta}\int_{R}\int\int \xi\, dx\, dy\, dz \\ &= \int_{R}\int\int \left[\frac{d\xi}{d\theta} + \xi\left\{\left(\frac{\partial u_x}{\partial x}\right)_{y,z,\theta} + \left(\frac{\partial u_y}{\partial y}\right)_{x,z,\theta} + \left(\frac{\partial u_z}{\partial z}\right)_{x,y,\theta}\right\}\right] dx\, dy\, dz.\end{aligned} \tag{V.44}$$

This result is that mentioned in the first paragraph after Eq. (V.37). Therefore, returning to the evaluation of the left-hand integral in Eq. (V.37), substitute

$$\rho\, u_x = \xi \tag{V.45}$$

in Eq. (V.44), and expand the derivative of the product, giving

$$\frac{d}{d\theta}\iiint_R \rho\, u_x\, dx\, dy\, dz$$

$$= \iiint_R \left[u_x\left\{\frac{d\rho}{d\theta} + \rho\left\{\left(\frac{\partial u_x}{\partial x}\right)_{y,z,\theta} + \left(\frac{\partial u_y}{\partial y}\right)_{x,z,\theta} + \left(\frac{\partial u_z}{\partial z}\right)_{x,y,\theta}\right\}\right\} + \rho\,\frac{du_x}{d\theta}\right] dx\, dy\, dz. \tag{V.46}$$

The portion of the integrand between brackets, $\{\}$, is zero since it is equivalent to Eq. (V.03), the equation of continuity. Therefore

$$\frac{d}{d\theta}\iiint_R \rho\, u_x\, dx\, dy\, dz = \iiint_R \rho\,\frac{du_x}{d\theta}\, dx\, dy\, dz. \tag{V.47}$$

Note that this result would also have been obtained for any continuous variable other than u_x. Thus, if ξ is any function of x, y, z, and θ which satisfies the same conditions as ξ above,

$$\frac{d}{d\theta}\iiint_R \rho\,\xi\, dx\, dy\, dz = \iiint_R \rho\,\frac{d\xi}{d\theta}\, dx\, dy\, dz. \tag{V.48}$$

Returning to Eq. (V.37), substitute in it the result obtained in Eq. (V.47) and transform the surface integral by Green's theorem, Eq. (V.05), giving

$$0 = \iiint_R \left[\rho\,\frac{du_x}{d\theta} - \rho\,\Phi_x - \left(\frac{\partial \tau_{xx}}{\partial x}\right)_{y,z,\theta} - \left(\frac{\partial \tau_{yx}}{\partial y}\right)_{x,z,\theta} - \left(\frac{\partial \tau_{zx}}{\partial z}\right)_{x,y,\theta}\right] dx\, dy\, dz. \tag{V.49}$$

Since the region R throughout which the integration is taken is arbitrary, the integrand must be identically zero, giving Eq. (V.34). Equations (V.35) and (V.36) are obtained in the same way.

However, not all of the surface stresses given in Eqs. (V.34), (V.35), and (V.36) and shown in Fig. V-5 are independent. To find their interrelations, consider the moments of all the forces acting on the volume element of Fig. V-5 about axes through the geometrical center of the element and parallel to each of the coordinate axes. Since the fluid properties and, in particular, the density are assumed to be continuous functions, they may be expressed as functions of the linear dimensions of the volume element. Therefore, the center of gravity and the center of rotation differ from the geometrical center at most by distances of the order of magnitude of the square of the dimensions of the volume element, i.e., by negligible amounts compared to the dimensions of the element.

The normal stresses τ_{xx}, τ_{yy}, and τ_{zz} act along lines passing through the geometrical center of the element, and the resultants of the external forces act along lines passing through the center of gravity. Therefore, these forces exert moments which are of a higher order of smallness compared to those exerted by the surface shear stresses τ_{xy}, etc., and hence they can be neglected in comparison.

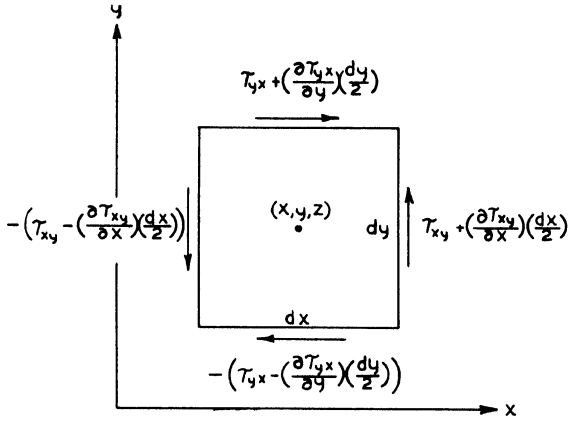

FIG. V-7. Moments exerted by surface stresses.

In Fig. V-7 is shown a section of the volume element of Fig. V-5 through the point (x, y, z) and perpendicular to the z-axis. The moment exerted by the shear stresses which are shown must equal the product of the moment of inertia of the element about the axis through the point (x, y, z) and parallel to the z-axis by its angular acceleration about the same point, since the moments of the other forces acting in this plane are of a higher order of smallness and may be neglected.

Therefore,

$$\left[\tau_{xy}+\left(\frac{\partial\tau_{xy}}{\partial x}\right)_{y,z,\theta}\frac{dx}{2}\right]dy\,dz\,\frac{dx}{2}+\left[\tau_{xy}-\left(\frac{\partial\tau_{xy}}{\partial x}\right)_{y,z,\theta}\frac{dx}{2}\right]dy\,dz\,\frac{dx}{2}$$
$$-\left[\tau_{yx}+\left(\frac{\partial\tau_{yx}}{\partial y}\right)_{x,z,\theta}\frac{dy}{2}\right]dx\,dz\,\frac{dy}{2}-\left[\tau_{yx}-\left(\frac{\partial\tau_{yx}}{\partial y}\right)_{x,z,\theta}\frac{dy}{2}\right]dx\,dz\,\frac{dy}{2}$$
$$\cong\rho\,dx\,dy\,dz\left(\frac{(dx)^2+(dy)^2}{12}\right)\alpha \tag{V.50}$$

where α is the angular acceleration (*13*). Simplifying

$$\tau_{xy}-\tau_{yx}\cong\rho\left(\frac{(dx)^2+(dy)^2}{12}\right)\alpha. \tag{V.51}$$

Since the dimensions of the volume element may be made as small as desired, in the limit, at the point (x, y, z),

$$\tau_{xy} = \tau_{yx} \tag{V.52}$$

and similarly

$$\tau_{xz} = \tau_{zx}, \tag{V.53}$$

$$\tau_{yz} = \tau_{zy}. \tag{V.54}$$

V-7. Acceleration of the Flowing Fluid (Continued)

In order to utilize the momentum equations, (V.34), (V.35), and (V.36), it is necessary to evaluate the surface stresses in terms of known or calculable quantities. To achieve this purpose, it is necessary to examine the motion of an element of volume of the flowing fluid more closely.

It has been proved (*6*, *11*) that the motion of an element of volume of a flowing fluid may be analyzed into three independent motions: a pure translation of the element as a whole, a pure rotation of the element as a whole about an instantaneous center, and a pure distortion or strain of the element.

Assuming the result, it is possible to determine the magnitude of each of these types of motion by considering the behavior of an element of volume of the fluid, as shown in Fig. V-8, which has edges of length dx, dy, and dz parallel to the respective coordinate axes at time θ. If the components of the fluid velocity at the corner point (x, y, z) nearest the origin are u_x, u_y, and u_z, the components of the velocity in the x-, y-, and z-direction at every other corner point will differ from these by amounts depending on the lengths of the edges and the gradients of the velocity in the relevant directions.

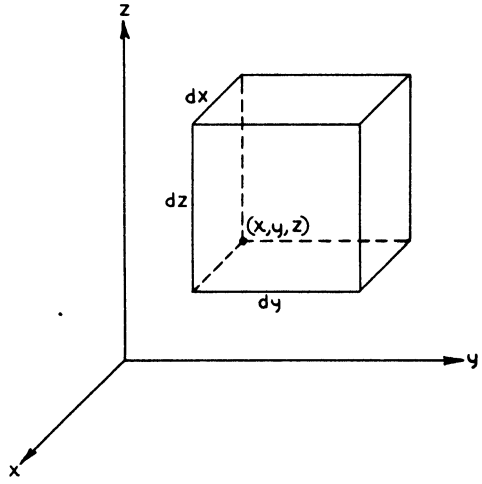

FIG. V-8. Element of volume.

In order to avoid possible confusion, only the motion of one face of the volume element will be considered, the results being easily extensible to

the motions of the other faces and, therefore, to the motion of the element itself. Take, for example, the face nearest the xy-plane shown in Fig. V-9.

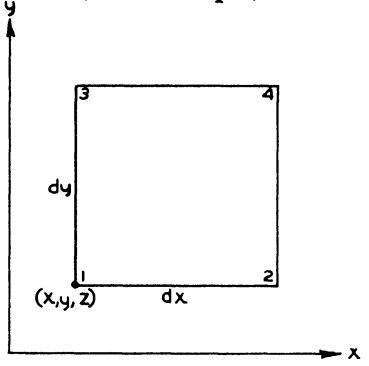

FIG. V-9. Volume face nearest plane.

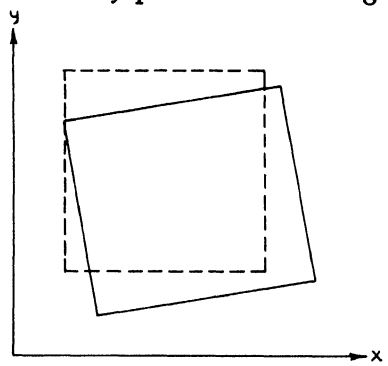

FIG. V-10. Distortion of face of volume element.

The velocity components in the x- and y-directions at the various corners at time θ will be, therefore:

Corner Point	Direction x	Direction y
1	u_x	u_y
2	$u_x + \left(\frac{\partial u_x}{\partial x}\right)_{y,z,\theta} dx$	$u_y + \left(\frac{\partial u_y}{\partial x}\right)_{y,z,\theta} dx$
3	$u_x + \left(\frac{\partial u_x}{\partial y}\right)_{x,z,\theta} dy$	$u_y + \left(\frac{\partial u_y}{\partial y}\right)_{x,z,\theta} dy$
4	$u_x + \left(\frac{\partial u_x}{\partial y}\right)_{x,z,\theta} dy + \left(\frac{\partial u_x}{\partial x}\right)_{y,z,\theta} dx$	$u_y + \left(\frac{\partial u_y}{\partial x}\right)_{y,z,\theta} dx + \left(\frac{\partial u_y}{\partial y}\right)_{x,z,\theta} dy$

At time $\theta + d\theta$, the face may have moved to the position shown in Fig. V-10. For pictorial purposes the distortion has been drawn as finite, so that the motion of the face cannot be *exactly* analyzed into a motion of pure translation, of pure rotation, and of pure distortion.

Approximately, however, a finite motion may be analyzed in the following manner into the separate types described. In the time increment $d\theta$, the magnitude of the translation of the face of the element in the x-direction is

$u_x\,d\theta$, the rate of translation in the x-direction shown in Fig. V-11 is u_x, and the acceleration of the linear translation in the x-direction is $(\partial u_x/\partial\theta)_{x,y,z}$. Similar results hold for the y-direction and for the z-direction in other faces.

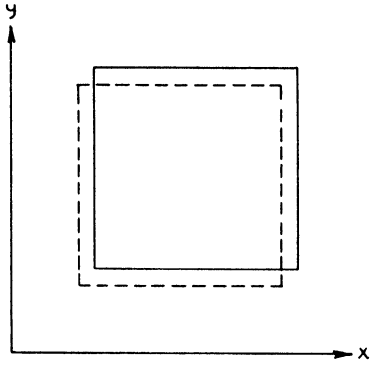

FIG. V-11. Translation of face of volume element.

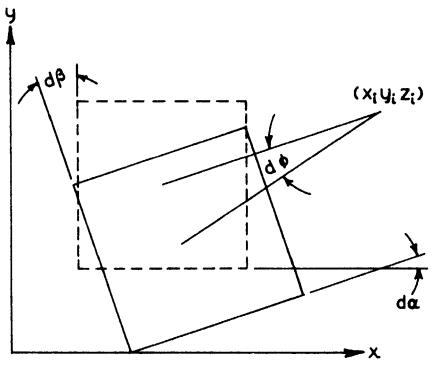

FIG. V-12. Rotation of face of volume element.

As shown in Fig. V-12, the motion of pure rotation is about an axis parallel to the z-axis and passing through the instantaneous center (x_i, y_i, z_i). It can be measured by the angle $d\phi$ through which the line connecting the axis and the center of the element rotate in the time $d\theta$. It may also be measured by the angle through which the edges of this face rotate in the same time interval; however, the latter are rotating at different rates so that the average of the angles through which two adjacent edges rotate is a better measure of $d\phi$. Taking the edges nearest the coordinate axes (the others differ in velocity from these only by infinitesimals) and remembering that, for infinitesimal angles, the angle and its tangent are equal,

$$d\alpha = \frac{\left(\dfrac{\partial u_y}{\partial x}\right)_{y,z,\theta} dx\,d\theta}{dx} \qquad \text{and} \qquad d\beta = \frac{-\left(\dfrac{\partial u_x}{\partial y}\right)_{x,z,\theta} dy\,d\theta}{dy} \tag{V.55}$$

where the gradients are those corresponding to Fig. V-9 and the table on page 132. If $d\phi$ is then taken as the average of the angles $d\alpha$ and $d\beta$, the following result is obtained:

$$d\phi = \frac{1}{2}\left[\left(\frac{\partial u_y}{\partial x}\right)_{y,z,\theta} - \left(\frac{\partial u_x}{\partial y}\right)_{x,z,\theta}\right] d\theta. \tag{V.56}$$

Therefore the rate of rotation or angular velocity about (x_i, y_i, z_i) is

$$\omega_z = \frac{1}{2}\left[\left(\frac{\partial u_y}{\partial x}\right)_{y,z,\theta} - \left(\frac{\partial u_x}{\partial y}\right)_{x,z,\theta}\right] \tag{V.57}$$

where ω_z is the z-component of the angular velocity because the rotation is about an axis parallel to the z-axis. The signs of the terms in Eq. (V.57) may be shown to be correct for rotation about any other instantaneous center if it is remembered that counterclockwise rotation is defined as positive.

From a similar analysis of the motion of the other faces of the element of Fig. V-8, the other components of the angular velocity are found to be

$$\omega_y = \frac{1}{2}\left[\left(\frac{\partial u_x}{\partial z}\right)_{x,y,\theta} - \left(\frac{\partial u_z}{\partial x}\right)_{y,z,\theta}\right], \tag{V.58}$$

$$\omega_x = \frac{1}{2}\left[\left(\frac{\partial u_z}{\partial y}\right)_{x,z,\theta} - \left(\frac{\partial u_y}{\partial z}\right)_{x,y,\theta}\right]. \tag{V.59}$$

The motion of pure distortion may be further analyzed into a motion of pure linear distortion or extension, and a motion of pure angular distortion. Take the second of these so that the deformation appears as shown in Fig. V-13.

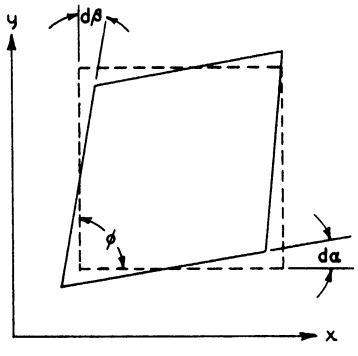

FIG. V-13. Pure angular distortion of face of volume element.

The pure angular deformation of the face of the element may be measured by the changes in the corner angles in the time $d\theta$. Since the lengths of the edges are unchanged, the changes in all the angles are the same except for signs. Since the angular deformation is the difference between the angles through which the adjacent sides have rotated in the time $d\theta$, the change in the angle ϕ at the corner nearest the origin (the conditions at the other corners differ only by infinitesimals) is

$$\begin{aligned} -d\phi &= d\alpha - (-d\beta) \\ &= \frac{\left(\frac{\partial u_y}{\partial x}\right)_{y,z,\theta} dx\, d\theta}{dx} - \frac{\left(\frac{\partial u_x}{\partial y}\right)_{x,z,\theta} dy\, d\theta}{dy} \\ &= \left[\left(\frac{\partial u_y}{\partial x}\right)_{y,z,\theta} + \left(\frac{\partial u_x}{\partial y}\right)_{x,z,\theta}\right] d\theta \end{aligned} \tag{V.60}$$

again remembering that counterclockwise rotation is taken as positive and that the angle and its tangent are equal for infinitesimal angles. Thus the rate of angular deformation is

$$2\zeta_z = \left[\left(\frac{\partial u_y}{\partial x}\right)_{y,z,\theta} + \left(\frac{\partial u_x}{\partial y}\right)_{x,z,\theta}\right] \tag{V.61}$$

and it is defined as $2\zeta_z$ because the distortion is for the face normal to the z-axis, and because the symmetry of an equation soon to be derived is improved by introducing the arbitrary factor 2. The rates of angular distortion for the faces normal to the y- and x-axis are, respectively, by a similar analysis:

$$2\zeta_y = \left[\left(\frac{\partial u_x}{\partial z}\right)_{x,y,\theta} + \left(\frac{\partial u_z}{\partial x}\right)_{y,z,\theta}\right], \tag{V.62}$$

$$2\zeta_x = \left[\left(\frac{\partial u_z}{\partial y}\right)_{x,z,\theta} + \left(\frac{\partial u_y}{\partial z}\right)_{x,y,\theta}\right]. \tag{V.63}$$

The pure linear distortion of the face of the element, as shown in Fig. V-14, may be analyzed most profitably by further decomposing it into a pure linear distortion without change of volume and a pure linear distortion in which the lengths of the edges are altered proportionally, i.e., a pure ex-

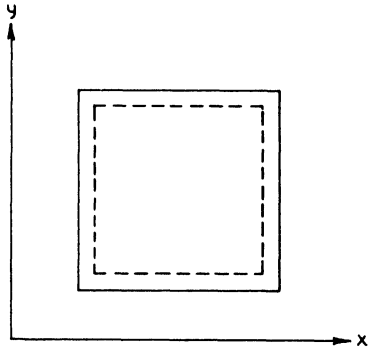

FIG. V-14. Pure linear distortion of face of volume element.

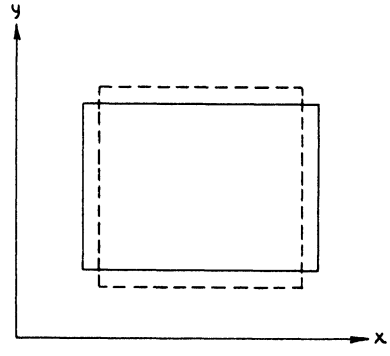

FIG. V-15. Pure linear distortion without change of volume.

pansion or compression. The linear distortion of the first sort, as shown in Fig. V-15, may be measured by the relative displacement of opposite edges during the time interval $d\theta$. Where u_x' is the velocity of the edge nearest the y-axis and parallel to it after the velocity due to the second type of distortion has been allowed for, the linear distortion for the x-direction is

$$\left\{\left[u_x' + \left(\frac{\partial u_x'}{\partial x}\right)_{y,z,\theta} dx\right] - u_x'\right\} d\theta = \left(\frac{\partial u_x'}{\partial x}\right)_{y,z,\theta} dx\, d\theta. \tag{V.64}$$

The rate of linear deformation is then $(\partial u_x'/\partial x)_{y,z,\theta}\, dx$, and the acceleration in the x-direction is $u_x(\partial u_x'/\partial x)_{y,z,\theta}$.

By drawing segments connecting consecutive bisectors of the edges of the face of the element, as shown in Fig. V-16, it may be seen that this type of pure linear distortion contains elements of pure angular distortion within it. A similar construction in Fig. V-13 shows that pure angular distortion also contains elements of pure linear distortion of this type, both of which interrelations may be emphasized by a rotation of the coordinate axes through 45°.

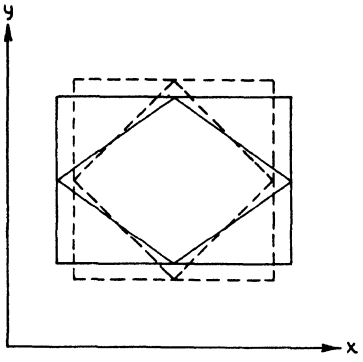

FIG. V-16. Analysis of pure linear distortion without change of volume.

The second type of pure linear distortion is closely related to the divergence of the velocity since, as was shown in Section V-1, this quantity gives the relative volume rate of expansion of the fluid. Since the increases in the lengths of the edges were assumed proportional to those lengths, the change in the volume of the fluid element is proportional to the cube of any edge, e.g. Δx, so that the relative rate of expansion of the edge Δx, $\left(\frac{1}{\Delta x}\frac{d}{d\theta}\Delta x\right)_{y,z,\theta}$, is equal to one-third the divergence of the velocity for this type of distortion as may be seen by substituting $(\Delta x)^3$ for V. [The total relative rate of expansion of the edge Δx is $(\partial u_x/\partial x)_{y,z,\theta}$.] The rate of expansion is thus given by $(\Delta x/3)\,(\partial u_x/\partial x)_{y,z,\theta}$, and the acceleration for this type of distortion in the x-direction by $u_x\,(\partial u_x/\partial x)_{y,z,\theta}$.

If no such decomposition of the pure linear distortion of the face of the element is made (see Fig. V-14), a measure of this distortion in the x-direction is given by

$$\left[u_x + \left(\frac{\partial u_x}{\partial x}\right)_{y,z,\theta} dx\right] d\theta - u_x\, d\theta = \left(\frac{\partial u_x}{\partial x}\right)_{y,z,\theta} dx\, d\theta \qquad \text{(V.65)}$$

of the rate by $(\partial u_x/\partial x)_{y,z,\theta}\,dx$, and of the acceleration in the x-direction by $u_x\,(\partial u_x/\partial x)_{y,z,\theta}$.

The various relations which have been developed to express the motion of an element of volume of a flowing fluid may be related to the expressions which were derived to express the acceleration of a fluid [Eqs. (V.22), (V.23), and (V.24)]. If $\frac{1}{2}u_y\,(\partial u_y/\partial x)_{y,z,\theta} + \frac{1}{2}u_z\,(\partial u_z/\partial x)_{y,z,\theta}$ be added and subtracted from Eq. (V.22), the result may be rearranged to give

$$a_x = \left(\frac{\partial u_x}{\partial \theta}\right)_{x,y,z} + u_x\left(\frac{\partial u_x}{\partial x}\right)_{y,z,\theta} + \frac{1}{2}u_y\left[\left(\frac{\partial u_y}{\partial x}\right)_{y,z,\theta} + \left(\frac{\partial u_x}{\partial y}\right)_{x,z,\theta}\right]$$
$$+ \frac{1}{2}u_y\left[\left(\frac{\partial u_x}{\partial y}\right)_{x,z,\theta} - \left(\frac{\partial u_y}{\partial x}\right)_{y,z,\theta}\right] + \frac{1}{2}u_z\left[\left(\frac{\partial u_x}{\partial z}\right)_{x,y,\theta} + \left(\frac{\partial u_z}{\partial x}\right)_{y,z,\theta}\right]$$
$$+ \frac{1}{2}u_z\left[\left(\frac{\partial u_x}{\partial z}\right)_{x,y,\theta} - \left(\frac{\partial u_z}{\partial x}\right)_{y,z,\theta}\right]. \qquad \text{(V.66)}$$

On substituting Eqs. (V.61), (V.62), (V.57), and (V.58) in Eq. (V.66) the acceleration in the x-direction is given as

$$a_x = \left(\frac{\partial u_x}{\partial \theta}\right)_{x,y,z} + u_x\left(\frac{\partial u_x}{\partial x}\right)_{y,z,\theta} + u_y\zeta_z + u_z\zeta_y - u_y\omega_z + u_z\omega_y \qquad \text{(V.67)}$$

and by a similar procedure Eqs. (V.23) and (V.24) become

$$a_y = \left(\frac{\partial u_y}{\partial \theta}\right)_{x,y,z} + u_y\left(\frac{\partial u_y}{\partial y}\right)_{x,z,\theta} + u_z\zeta_x + u_x\zeta_z - u_z\omega_x + u_x\omega_z, \qquad \text{(V.68)}$$

$$a_z = \left(\frac{\partial u_z}{\partial \theta}\right)_{x,y,z} + u_z\left(\frac{\partial u_z}{\partial z}\right)_{x,y,\theta} + u_x\zeta_y + u_y\zeta_x - u_x\omega_y + u_y\omega_x. \qquad \text{(V.69)}$$

The symmetrical form of these equations is the justification for the arbitrary factor 2 in Eqs. (V.61), (V.62), and (V.63).

V-8. Evaluation of the Surface Stresses in a Flowing Fluid

The equations which have been derived thus far are quite general, and they may be applied to both Newtonian and non-Newtonian fluids as well as to elastic and plastic solids.[1] This discussion is limited to the case of Newtonian fluids, but the analysis has been extended to the more general cases (*14—16*) which are of great technical importance.

The analysis of the motion of a fluid element of volume given in the last section shows that this motion may be separated into a translation of the element as a whole, a rotation of the element as a whole, and a distortion of the element. The definition of a Newtonian fluid given in Chapter I, Section I-7 and Eq. (I.20) indicates that any motion of the fluid element as a whole, i.e. as a rigid body, would not produce any viscous stresses, and that the deformation of the element would be the only source of such stresses.

---

[1] See Chapter I, Section I-7 for the definitions of these types of materials.

In order to evaluate, in terms of known or calculable quantities, the surface stresses used in the momentum Eqs. (V.34), (V.35), and (V.36), it is necessary to construct a generalization of Eq. (I.20) which retains the basic assumption for Newtonian fluids that the surface shear stresses are linear functions of the rates of strain and which also satisfies the relations which have been derived. This is the point where the analysis of the motion of an elastic solid, a plastic solid, a non-Newtonian fluid, and a Newtonian fluid diverge. In the first case the stresses are determined by the strains; in the second by both the strains and the rates of strain; and in the third the stresses are a more general function of the rates of strain than a simple linear combination. A rigorous derivation of the generalization is rather difficult, and it can best be given only by use of the tensor calculus (*3, 6, 11, 17, 18*).

The generalization, however, can be made plausible with the help of a few of the results of the more rigorous analysis. Thus a comparison of Fig. V-8, which shows the surface shear stresses acting on the faces of the element of volume parallel to the z-axis, with Fig. V-13, which shows the pure angular distortion of the face normal to the z-axis, makes it plausible that there is a cause and effect relation between them, i.e.,

$$\tau_{xy} = \tau_{yx} = \eta\left[\left(\frac{\partial u_y}{\partial x}\right)_{y,z,\theta} + \left(\frac{\partial u_x}{\partial y}\right)_{x,z,\theta}\right] \tag{V.70}$$

and similarly for the other coordinate directions,

$$\tau_{xz} = \tau_{zx} = \eta\left[\left(\frac{\partial u_x}{\partial z}\right)_{x,y,\theta} + \left(\frac{\partial u_z}{\partial x}\right)_{y,z,\theta}\right], \tag{V.71}$$

$$\tau_{yz} = \tau_{zy} = \eta\left[\left(\frac{\partial u_y}{\partial z}\right)_{x,y,\theta} + \left(\frac{\partial u_z}{\partial y}\right)_{x,z,\theta}\right] \tag{V.72}$$

where η is the absolute viscosity. The direction of positive τ used in Chapters I and II presumed the direction of positive y to be away from the wall [Cf. Eq. (I.20)].

The evaluation of the normal stresses τ_{xx}, τ_{yy}, and τ_{zz} is more difficult. It has been shown (*3, 6, 11, 17, 18*) that whatever orientation of the coordinate axes is taken, the sum of the three normal stresses is constant, i.e. an invariant. Thus, if τ_{ave} is taken as the average normal stress,

$$\tau_{ave} = \frac{1}{3}(\tau_{xx} + \tau_{yy} + \tau_{zz}). \tag{V.73}$$

It is not hard to show (*19*) that for an inviscid fluid (i.e., a fluid without viscosity),

$$\tau_{ave} = \tau_{xx} = \tau_{yy} = \tau_{zz} = -P \tag{V.74}$$

where P is the thermodynamic pressure (see Chapter I, Section I-6). The minus sign occurs because, in order to make the momentum equations more symmetrical, the normal stresses were taken as tensions, whereas P is a pressure. [See Fig. V-5.)

It is plausible, therefore, to identify τ_{ave} with the normal surface stresses which produce pure expansion or compression of the fluid, i.e. pure linear distortion of the second type, and to assume that the residual normal stresses $\tau_{xx} - \tau_{ave}$, $\tau_{yy} - \tau_{ave}$, and $\tau_{zz} - \tau_{ave}$ are the result of the pure linear distortion of the first type which involves deformation of the element of volume of the fluid without change of volume and which is similar to pure angular deformation.

Just as a rotation of the coordinate axes through 45° reveals interrelations between angular deformation and pure linear deformation of the first type, the same rotation partially interconverts shear and normal stresses (see Fig. V-5). Therefore the explicit expression for the residual normal stresses must contain a term similar to those for the shear stresses as in Eqs. (V.70), (V.71), and (V.72). The exact analysis indicates that these stresses should also be a general linear function of the relative rates of expansion of the edges of the element of volume, or, for example,

$$\tau_{xx} = \tau_{ave} + \eta\left[\left(\frac{\partial u_x}{\partial x}\right)_{y,z,\theta} + \left(\frac{\partial u_x}{\partial x}\right)_{y,z,\theta}\right] + \lambda_1\left(\frac{\partial u_x}{\partial x}\right)_{y,z,\theta} + \lambda_2\left(\frac{\partial u_y}{\partial y}\right)_{x,z,\theta} + \lambda_3\left(\frac{\partial u_z}{\partial z}\right)_{x,y,\theta} \tag{V.75}$$

where λ_1, λ_2, and λ_3 are constants (or more precisely, functions of state).

It has been implicitly assumed that the fluid is isotropic, i.e., it has the same properties in all directions. Since the fluid is isotropic, symmetry gives

$$\lambda_1 = \lambda_2 = \lambda_3 = \lambda. \tag{V.76}$$

Nonisotropic or anisotropic fluids are relatively rare, being confined to the class of liquids known as liquid crystals. Many colloidal solutions, however, are anisotropic. Therefore, the explicit expressions for the normal surface stresses are

$$\tau_{xx} = \tau_{\text{ave.}} + 2\eta\left(\frac{\partial u_x}{\partial x}\right)_{y,z,\theta} + \lambda\left[\left(\frac{\partial u_x}{\partial x}\right)_{y,z,\theta} + \left(\frac{\partial u_y}{\partial y}\right)_{x,z,\theta} + \left(\frac{\partial u_z}{\partial z}\right)_{x,y,\theta}\right], \quad \text{(V.77)}$$

$$\tau_{yy} = \tau_{\text{ave.}} + 2\eta\left(\frac{\partial u_y}{\partial y}\right)_{x,z,\theta} + \lambda\left[\left(\frac{\partial u_x}{\partial x}\right)_{y,z,\theta} + \left(\frac{\partial u_y}{\partial y}\right)_{x,z,\theta} + \left(\frac{\partial u_z}{\partial z}\right)_{x,y,\theta}\right], \quad \text{(V.78)}$$

$$\tau_{zz} = \tau_{\text{ave.}} + 2\eta\left(\frac{\partial u_z}{\partial z}\right)_{x,y,\theta} + \lambda\left[\left(\frac{\partial u_x}{\partial x}\right)_{y,z,\theta} + \left(\frac{\partial u_y}{\partial y}\right)_{x,z,\theta} + \left(\frac{\partial u_z}{\partial z}\right)_{x,y,\theta}\right]. \quad \text{(V.79)}$$

Adding these equations,

$$\tau_{xx} + \tau_{yy} + \tau_{zz} = 3\,\tau_{\text{ave.}} + (2\eta + 3\lambda)\left[\left(\frac{\partial u_x}{\partial x}\right)_{y,z,\theta} + \left(\frac{\partial u_y}{\partial y}\right)_{x,z,\theta} + \left(\frac{\partial u_z}{\partial z}\right)_{x,y,\theta}\right], \quad \text{(V.80)}$$

Therefore, in general, from Eq. (V.73)

$$\lambda = -\frac{2}{3}\eta \quad \text{(V.81)}$$

and λ can be eliminated from Eqs. (V.77), (V.78), and (V.79).

Equations (V.70), (V.71), (V.72), (V.77), (V.78), (V.79), and (V.80) are the desired generalization of Eq. (I.20) for the general case of the flow of a Newtonian fluid with the exception that the average normal stress $\tau_{\text{ave.}}$ has not been evaluated.

It has been shown by Chapman and Cowling (*20*) from the kinetic theory of gases alone that

$$P = -\tau_{\text{ave.}} \quad \text{(V.82)}$$

which is identical with Eq. (V.74). For a perfect gas composed of rigid, smooth spheres the surface stresses to a very good approximation are given by the above-mentioned equations. An even better approximation, however, was obtained by the same authors for this case which gave Eq. (V.82) again but more complicated expressions for the surface stresses involving terms which are usually very small, depending on temperature and pressure gradients as well as velocity gradients.

For real gases, however, especially near the critical state, it is very likely that the average normal stress τ_{ave} depends on the rate of expansion of the gas, since the intermolecular forces exert attractions among the molecules of the gas which would delay their free expansion and hence diminish the normal stress which they collectively could exert. As an approximation to the behavior of highly compressed gases (*21*), Eq. (V.82) may be modified by the inclusion of a term on the right-hand side of the

form η' div u, where η' is a second coefficient of viscosity, since div u represents the rate of expansion of the gas. Under these conditions, however, the applicability of the concept of thermodynamic pressure is beginning to be questionable so that even this assumption may be incorrect in some situations.

For a liquid, since the rate of expansion can only be very small as large pressure or temperature variations produce but small density changes [see Eq. (V.10)], it seems reasonable to assume that Eq. (V.82) applies. The lack of a satisfactory molecular theory of the liquid state prevents any more accurate approximations.

It may also be necessary to modify the equations for the surface stresses to include terms similar to those obtained by Chapman and Cowling to allow for the effects of pressure and especially temperature variations.

The above critical comments must not be taken to mean that the equations under discussion are only very crude approximations; on the contrary, they have been shown experimentally to be very excellent approximations (i.e., within the experimental error) of the actual behavior of real gases and liquids.

V-9. Navier-Stokes Equations

Thus the general equations expressing the conservation of momentum for a Newtonian fluid which result from combining from Eqs. (V.34), (V.35), (V.36), (V.70), (V.71), (V.72), (V.77), (V.78), (V.79), (V.81), and (V.82), are

$$\rho a_x = \rho \Phi_x - \frac{\partial P}{\partial x} + \frac{1}{3}\frac{\partial}{\partial x}\left\{\eta\left(\frac{\partial u_x}{\partial x} + \frac{\partial u_y}{\partial y} + \frac{\partial u_z}{\partial z}\right)\right\} + \frac{\partial}{\partial x}\left(\eta\frac{\partial u_x}{\partial x}\right) + \frac{\partial}{\partial y}\left(\eta\frac{\partial u_x}{\partial y}\right) + \frac{\partial}{\partial z}\left(\eta\frac{\partial u_x}{\partial z}\right), \tag{V.83}$$

$$\rho a_y = \rho \Phi_y - \frac{\partial P}{\partial y} + \frac{1}{3}\frac{\partial}{\partial y}\left\{\eta\left(\frac{\partial u_x}{\partial x} + \frac{\partial u_y}{\partial y} + \frac{\partial u_z}{\partial z}\right)\right\} + \frac{\partial}{\partial x}\left(\eta\frac{\partial u_y}{\partial x}\right) + \frac{\partial}{\partial y}\left(\eta\frac{\partial u_y}{\partial y}\right) + \frac{\partial}{\partial z}\left(\eta\frac{\partial u_y}{\partial z}\right), \tag{V.84}$$

$$\rho a_z = \rho \Phi_z - \frac{\partial P}{\partial z} + \frac{1}{3}\frac{\partial}{\partial z}\left\{\eta\left(\frac{\partial u_x}{\partial x} + \frac{\partial u_y}{\partial y} + \frac{\partial u_z}{\partial z}\right)\right\} + \frac{\partial}{\partial x}\left(\eta\frac{\partial u_z}{\partial x}\right) + \frac{\partial}{\partial y}\left(\eta\frac{\partial u_z}{\partial y}\right) + \frac{\partial}{\partial z}\left(\eta\frac{\partial u_z}{\partial z}\right). \tag{V.85}$$

These equations are known as the Navier-Stokes equations[1] in honor of some of the men who first derived them. For simplicity, the subscripts on the partial derivatives have been omitted on these final equations and on most of the subsequent equations, but they must always be understood as applying.

In the usual case where gravity is the only important external force and the fluid is incompressible, the first two terms on the right side of Eqs. (V.83), (V.84), and (V.85) may be combined to give $-(\partial/\partial x)(P+\sigma h)$, $-(\partial/\partial y)(P+\sigma h)$, and $-(\partial/\partial z)(P+\sigma h)$, respectively, where

$$\sigma = g_c \rho. \tag{V.86}$$

Since the fluid is incompressible, the third term on the right side disappears [see Eq. (V.03)] so that for a perfect liquid, the Navier-Stokes equations become

$$\rho a_x = -\frac{\partial}{\partial x}(P+\sigma h) + \frac{\partial}{\partial x}\left(\eta \frac{\partial u_x}{\partial x}\right) + \frac{\partial}{\partial y}\left(\eta \frac{\partial u_x}{\partial y}\right) + \frac{\partial}{\partial z}\left(\eta \frac{\partial u_x}{\partial z}\right), \tag{V.87}$$

$$\rho a_y = -\frac{\partial}{\partial y}(P+\sigma h) + \frac{\partial}{\partial x}\left(\eta \frac{\partial u_y}{\partial x}\right) + \frac{\partial}{\partial y}\left(\eta \frac{\partial u_y}{\partial y}\right) + \frac{\partial}{\partial z}\left(\eta \frac{\partial u_y}{\partial z}\right), \tag{V.88}$$

$$\rho a_z = -\frac{\partial}{\partial z}(P+\sigma h) + \frac{\partial}{\partial x}\left(\eta \frac{\partial u_z}{\partial x}\right) + \frac{\partial}{\partial y}\left(\eta \frac{\partial u_z}{\partial y}\right) + \frac{\partial}{\partial z}\left(\eta \frac{\partial u_z}{\partial z}\right). \tag{V.89}$$

For the case of objects moving through a large volume of fluid, the results obtained by assuming that the viscosity is zero in the Navier-Stokes equations [when the last four terms on the right sides of Eqs. (V.83), (V.84), and (V.85) disappear] are remarkably accurate for all portions of the flow, except in the immediate vicinity of the obstacle, provided that no velocities comparable to that of sound are involved. Many solutions of the equations under this restriction are discussed in texts on hydrodynamics (*3*, *6*) and aerodynamics. Such problems are, however, usually of little importance in chemical engineering.

V-10. Navier-Stokes Equations in Cylindrical Coordinates

In distinction to the situation which exists for ordinary differential equations, the task of bringing the solution of a partial differential equation into agreement with the boundary conditions is usually of the same order of

---

[1] See Appendix II for vector form of Navier-Stokes equations and generalized coordinate transformations.

difficulty as that of solving the equation originally. Consequently any simplification in the boundary conditions is of great convenience.

For example, in case the boundary to the flow is a cylinder, cylindrical instead of Cartesian coordinates can be used, and the boundary conditions are satisfied at

$$r = r_0 \tag{V.90}$$

instead of at

$$\sqrt{x^2 + y^2} = r_0 \tag{V.91}$$

where r_0 is the radius of the cylinder. This apparently slight simplification is often of great practical importance; and so the Navier-Stokes equations together with the accelerations and the angular velocities will be given in cylindrical coordinates:

$$\begin{aligned}\rho \frac{du_r}{d\theta} = \rho \Phi_r - \frac{\partial P}{\partial r} + \frac{1}{3}\frac{\partial}{\partial r}\left[\frac{\eta}{r}\left(\frac{\partial r\, u_r}{\partial r} + \frac{\partial u_\psi}{\partial \psi} + \frac{\partial r\, u_x}{\partial x}\right)\right] \\ + \frac{1}{r}\left[\frac{\partial}{\partial r}\left(\eta r \frac{\partial u_r}{\partial r}\right) + \frac{1}{r}\frac{\partial}{\partial \psi}\left(\eta \frac{\partial u_r}{\partial \psi}\right) + r\frac{\partial}{\partial x}\left(\eta \frac{\partial u_r}{\partial x}\right)\right] \\ - \frac{1}{r^2}\left[\eta u_r + 2\eta \frac{\partial u_\psi}{\partial \psi}\right],\end{aligned} \tag{V.92}$$

$$\begin{aligned}\rho \frac{du_\psi}{d\theta} = \rho \Phi_\psi - \frac{1}{r}\frac{\partial P}{\partial \psi} + \frac{1}{3r}\frac{\partial}{\partial \psi}\left[\frac{\eta}{r}\left(\frac{\partial r\, u_r}{\partial r} + \frac{\partial u_\psi}{\partial \psi} + \frac{\partial r\, u_x}{\partial x}\right)\right] \\ + \frac{1}{r}\left[\frac{\partial}{\partial r}\left(\eta r \frac{\partial u_\psi}{\partial r}\right) + \frac{1}{r}\frac{\partial}{\partial \psi}\left(\eta \frac{\partial u_\psi}{\partial \psi}\right) + r\frac{\partial}{\partial x}\left(\eta \frac{\partial u_x}{\partial x}\right)\right] \\ - \frac{1}{r^2}\left[\eta u_\psi - 2\eta \frac{\partial u_r}{\partial \psi}\right]\end{aligned} \tag{V.93}$$

$$\begin{aligned}\rho \frac{du_x}{d\theta} = \rho \Phi_x - \frac{\partial P}{\partial x} + \frac{1}{3}\frac{\partial}{\partial x}\left[\frac{\eta}{r}\left(\frac{\partial r\, u_r}{\partial r} + \frac{\partial u_\psi}{\partial \psi} + \frac{\partial r\, u_x}{\partial x}\right)\right] \\ + \frac{1}{r}\left[\frac{\partial}{\partial r}\left(\eta r \frac{\partial u_x}{\partial r}\right) + \frac{1}{r}\frac{\partial}{\partial \psi}\left(\eta \frac{\partial u_x}{\partial \psi}\right) + r\frac{\partial}{\partial x}\left(\eta \frac{\partial u_x}{\partial x}\right)\right]\end{aligned} \tag{V.94}$$

where

$$\frac{du_r}{d\theta} = \frac{\partial u_r}{\partial \theta} + u_r \frac{\partial u_r}{\partial r} + \frac{u_\psi}{r}\frac{\partial u_r}{\partial \psi} + u_x \frac{\partial u_r}{\partial x} - \frac{u_\psi^2}{r}, \tag{V.95}$$

$$\frac{du_\psi}{d\theta} = \frac{\partial u_\psi}{\partial \theta} + u_r \frac{\partial u_\psi}{\partial r} + \frac{u_\psi}{r}\frac{\partial u_\psi}{\partial \psi} + u_x \frac{\partial u_\psi}{\partial x} + \frac{u_r u_\psi}{r}, \tag{V.96}$$

$$\frac{du_x}{d\theta} = \frac{\partial u_x}{\partial \theta} + u_r \frac{\partial u_x}{\partial r} + \frac{u_\psi}{r}\frac{\partial u_x}{\partial \psi} + u_x \frac{\partial u_x}{\partial x} \tag{V.97}$$

and

$$\omega_r = \frac{1}{2}\left(\frac{1}{r}\frac{\partial u_x}{\partial \psi} - \frac{\partial u_\psi}{\partial x}\right), \tag{V.98}$$

$$\omega_\psi = \frac{1}{2}\left(\frac{\partial u_r}{\partial x} - \frac{\partial u_x}{\partial r}\right), \tag{V.99}$$

$$\omega_x = \frac{1}{2}\frac{1}{r}\left(\frac{\partial r\, u_\psi}{\partial r} - \frac{\partial u_r}{\partial \psi}\right). \tag{V.100}$$

V-11. Navier-Stokes Equations for Spherical Coordinates

In case the boundary to the flow is a sphere, equal simplification of the solution is usually obtained by solving in terms of spherical coordinates. The corresponding forms of the Navier-Stokes equations in spherical coordinates are:

$$\begin{aligned}\rho\frac{du_r}{d\theta} = \rho\Phi_r &- \frac{\partial P}{\partial r} + \frac{1}{3}\frac{\partial}{\partial r}\left[\frac{\eta}{r^2\sin\phi}\left(\frac{\partial r^2 u_r \sin\phi}{\partial r} + \frac{\partial r\, u_\phi \sin\phi}{\partial \phi} + \frac{\partial r\, u_\psi}{\partial \psi}\right)\right] \\ &+ \frac{1}{r^2\sin\phi}\left[\frac{\partial}{\partial r}\left(\eta r^2 \sin\phi \frac{\partial u_r}{\partial r}\right) + \frac{\partial}{\partial \phi}\left(\eta \sin\phi \frac{\partial u_r}{\partial \phi}\right) + \frac{1}{\sin\phi}\frac{\partial}{\partial \psi}\left(\eta \frac{\partial u_r}{\partial \psi}\right)\right] \\ &- \frac{2\eta}{r^2}\left[u_r + u_\phi \cot\phi + \frac{\partial u_\phi}{\partial \phi} + \frac{1}{\sin\phi}\frac{\partial u_\psi}{\partial \psi}\right],\end{aligned} \tag{V.101}$$

$$\begin{aligned}\rho\frac{du_\phi}{d\theta} = \rho\Phi_\phi &- \frac{1}{r}\frac{\partial P}{\partial \phi} + \frac{1}{3r}\frac{\partial}{\partial \phi}\left[\frac{\eta}{r^2\sin\phi}\left(\frac{\partial r^2 u_r \sin\phi}{\partial r} + \frac{\partial r\, u_\phi \sin\phi}{\partial \phi} + \frac{\partial r\, u_\psi}{\partial \psi}\right)\right] \\ &+ \frac{1}{r^2\sin\phi}\left[\frac{\partial}{\partial r}\left(\eta r^2 \sin\phi \frac{\partial u_\phi}{\partial r}\right) + \frac{\partial}{\partial \phi}\left(\eta \sin\phi \frac{\partial u_\phi}{\partial \phi}\right) + \frac{1}{\sin\phi}\frac{\partial}{\partial \psi}\left(\eta \frac{\partial u_\phi}{\partial \psi}\right)\right] \\ &- \frac{2\eta}{r^2}\left[\frac{\cot\phi}{\sin\phi}\frac{\partial u_\psi}{\partial \psi} - \frac{\partial u_r}{\partial \phi} + \frac{u_\phi}{2\sin^2\phi}\right],\end{aligned} \tag{V.102}$$

$$\begin{aligned}\rho\frac{du_\psi}{d\theta} = \rho\Phi_\psi &- \frac{1}{r\sin\phi}\frac{\partial P}{\partial \psi} \\ &+ \frac{1}{3r\sin\phi}\frac{\partial}{\partial \psi}\left[\frac{\eta}{r^2\sin\phi}\left(\frac{\partial r^2 u_r \sin\phi}{\partial r} + \frac{\partial r\, u_\phi \sin\phi}{\partial \phi} + \frac{\partial r\, u_\psi}{\partial \psi}\right)\right] \\ &+ \frac{1}{r^2\sin\phi}\left[\frac{\partial}{\partial r}\left(\eta r^2 \sin\phi \frac{\partial u_\psi}{\partial r}\right) + \frac{\partial}{\partial \phi}\left(\eta \sin\phi \frac{\partial u_\psi}{\partial \phi}\right) + \frac{1}{\sin\phi}\frac{\partial}{\partial \psi}\left(\eta \frac{\partial u_\psi}{\partial \psi}\right)\right] \\ &- \frac{\eta}{r^2\sin^2\phi}\left[u_\psi - 2\sin\phi\frac{\partial u_r}{\partial \psi} - 2\cos\phi\frac{\partial u_\phi}{\partial \psi}\right]\end{aligned} \tag{V.103}$$

where

$$\frac{du_r}{d\theta} = \frac{\partial u_r}{\partial \theta} + u_r \frac{\partial u_r}{\partial r} + \frac{u_\phi}{r}\frac{\partial u_r}{\partial \phi} + \frac{u_\psi}{r \sin\phi}\frac{\partial u_r}{\partial \psi} - \frac{u_\phi^2 + u_\psi^2}{r}, \tag{V.104}$$

$$\frac{du_\phi}{d\theta} = \frac{\partial u_\phi}{\partial \theta} + u_r \frac{\partial u_\phi}{\partial r} + \frac{u_\phi}{r}\frac{\partial u_\phi}{\partial \phi} + \frac{u_\psi}{r \sin\phi}\frac{\partial u_\phi}{\partial \psi} + \frac{u_r u_\phi}{r} - \frac{u_\psi^2 \cot\phi}{r} \tag{V.105}$$

and

$$\frac{du_\psi}{d\theta} = \frac{\partial u_\psi}{\partial \theta} + u_r \frac{\partial u_\psi}{\partial r} + \frac{u_\phi}{r}\frac{\partial u_\psi}{\partial \phi} + \frac{u_\psi}{r \sin\phi}\frac{\partial u_\psi}{\partial \psi} + \frac{u_r u_\psi}{r} + \frac{u_\psi u_\phi \cot\phi}{r} \tag{V.106}$$

also

$$\omega_r = \frac{1}{2r \sin\phi}\left[\frac{\partial}{\partial \phi}(u_\psi \sin\phi) - \frac{\partial u_\phi}{\partial \psi}\right], \tag{V.107}$$

$$\omega_\phi = \frac{1}{2r \sin\phi}\left[\frac{\partial u_r}{\partial \psi} - \frac{\partial r\, u_\psi \sin\phi}{\partial r}\right] \tag{V.108}$$

$$\omega_\psi = \frac{1}{2r}\left[\frac{\partial r\, u_\phi}{\partial r} - \frac{\partial u_r}{\partial \phi}\right]. \tag{V.109}$$

V-12. Dimensionless Form of the Equations of Motion

For any particular flow situation, the Navier-Stokes equations and the equation of continuity [Eqs. (V.83), (V.84), (V.85), and (V.03), respectively] may be reduced to a dimensionless form by substitution of "reduced" variables. The results which are obtained are important in two respects. First, they emphasize the importance of dimensional analysis; and, secondly, the reduced equations are in a very convenient form for numerical calculation since all the variables are reduced to a comparable basis.

It is usually possible to determine, at least approximately, the complete behavior of a particular flow situation by the specification of a few characteristic parameters of the flow. Thus, if values of the pressure gradient $(\partial P/\partial x)_0$, density ρ_0, a characteristic length L_0, velocity U_0, and viscosity η_0, which are in some fashion representative of the flow as a whole, are known, "reduced" dimensionless variables may be defined in the following way:

$$
\begin{aligned}
x' &= x L_0^{-1} & a_x' &= a_x L_0 U_0^{-2} & \theta' &= \theta U_0 L_0^{-1} \\
y' &= y L_0^{-1} & a_y' &= a_y L_0 U_0^{-2} & \Omega' &= \Omega U_0^{-2} = g_c h' L_0 U_0^{-2} \\
z' &= z L_0^{-1} & a_z' &= a L_0 U_0^{-2} & & \\
u_x' &= u_x U_0^{-1} & h' &= h L_0^{-1} & \left(\frac{\partial P}{\partial x}\right)^1 &= \left(\frac{\partial P}{\partial x}\right)\left(\frac{\partial P}{\partial x}\right)_0^{-1}. \\
u_y' &= u_y U_0^{-1} & \rho' &= \rho \rho_0^{-1} & & \\
u_z' &= u_z U_0^{-1} & \eta' &= \eta \eta_0^{-1} & &
\end{aligned}
\tag{V.110}
$$

If the proper substitutions are made from Eq. (V.110) in the equation of continuity, the simplified result is

$$
\frac{\partial \rho'}{\partial \theta'} + \frac{\partial \rho' u_x'}{\partial x} + \frac{\partial \rho' u_y'}{\partial y} + \frac{\partial \rho' u_z'}{\partial z} = 0. \tag{V.111}
$$

The x-component of the Navier-Stokes equation as given in Eq. (V.83) becomes

$$
\begin{aligned}
\rho_0 \rho' U_0^2 L_0^{-1} a_x' = &- \rho_0 \rho' g_c \frac{\partial h'}{\partial x'} - \left(\frac{\partial P}{\partial x}\right)_0 \left(\frac{\partial P}{\partial x}\right)' \\
&+ \frac{\eta_0 U_0}{3 L_0^2} \frac{\partial}{\partial x'}\left[\eta'\left(\frac{\partial u_x'}{\partial x'} + \frac{\partial u_y'}{\partial y'} + \frac{\partial u_z'}{\partial z'}\right)\right] \\
&+ \frac{\eta_0 U_0}{L_0^2}\left[\frac{\partial}{\partial x'}\left(\eta' \frac{\partial u_x'}{\partial x'}\right) + \frac{\partial}{\partial y'}\left(\eta' \frac{\partial u_x'}{\partial y'}\right) + \frac{\partial}{\partial z'}\left(\eta' \frac{\partial u_x'}{\partial z'}\right)\right].
\end{aligned}
\tag{V.112}
$$

The y- and z-members of the Navier-Stokes equation may be similarly treated. In turn Eq. (V.112) may be rearranged to give

$$
\begin{aligned}
\rho' a_x' = &- \rho' g_c L_0 U_0^{-2} \frac{\partial h'}{\partial x'} - L_0 \rho_0^{-1} U_0^{-2} \left(\frac{\partial P}{\partial x}\right)_0 \left(\frac{\partial P}{\partial x}\right)' \\
&+ \frac{1}{3} \eta_0 L_0^{-1} U_0^{-1} \rho_0^{-1} \frac{\partial}{\partial x'}\left[\eta'\left(\frac{\partial u_x'}{\partial x'} + \frac{\partial u_y'}{\partial y'} + \frac{\partial u_z'}{\partial z'}\right)\right] \\
&+ \eta_0 L_0^{-1} U_0^{-1} \rho_0^{-1}\left[\frac{\partial}{\partial x'}\left(\eta' \frac{\partial u_x'}{\partial x'}\right) + \frac{\partial}{\partial y'}\left(\eta' \frac{\partial u_x'}{\partial y'}\right) + \frac{\partial}{\partial z'}\left(\eta' \frac{\partial u_x'}{\partial z'}\right)\right]
\end{aligned}
\tag{V.113}
$$

and similarly for the other equations.

The use of the dimensionless form of the Navier-Stokes equation appears more rational when certain of the groupings of terms are recognized as commonly used dimensionless parameters. The ones that appear are the Froude number,

$$\mathrm{Fr} = \sqrt{\frac{U_0^2}{g_c L_0}} \tag{V.114}$$[1]

the Euler number,

$$\mathrm{Eu} = \frac{L_0}{\rho_0 U_0^2}\left(\frac{\partial P}{\partial x}\right)_0 \tag{V.115}$$

and the Reynolds number,

$$\mathrm{Re} = \frac{L_0 U_0 \rho_0}{\eta_0}. \tag{V.116}$$

By introducing the dimensionless numbers, Eq. (V.113) may be written as

$$\rho' a_x' = -\rho' \mathrm{Fr}^{-2}\frac{\partial h'}{\partial x'} - \mathrm{Eu}\left(\frac{\partial P}{\partial x}\right)' + \frac{1}{3\,\mathrm{Re}}\frac{\partial}{\partial x'}\left[\eta'\left(\frac{\partial u_x'}{\partial x'} + \frac{\partial u_y'}{\partial y'} + \frac{\partial u_z'}{\partial z'}\right)\right]$$
$$+ \frac{1}{\mathrm{Re}}\left[\frac{\partial}{\partial x'}\left(\eta'\frac{\partial u_x'}{\partial x'}\right) + \frac{\partial}{\partial y'}\left(\eta'\frac{\partial u_x'}{\partial y'}\right) + \frac{\partial}{\partial z'}\left(\eta'\frac{\partial u_x'}{\partial z'}\right)\right] \tag{V.117}$$

and similarly for the other equations.

For isothermal flow where the fluid is incompressible and its viscosity is independent of any pressure changes, Eq. (V.117) becomes

$$a_x' = -\mathrm{Fr}^{-2}\frac{\partial h'}{\partial x'} - \frac{\mathrm{Eu}}{\rho'}\left(\frac{\partial P}{\partial x}\right)' + \frac{\nu'}{\mathrm{Re}}\left[\frac{\partial^2 u_x'}{\partial (x')^2} + \frac{\partial^2 u_y'}{\partial (y')^2} + \frac{\partial^2 u_z'}{\partial (z')^2}\right] \tag{V.118}$$

and similarly for the other equations. Equation (V.111) becomes

$$\frac{\partial u_x'}{\partial x'} + \frac{\partial u_y'}{\partial y'} + \frac{\partial u_z'}{\partial z'} = 0. \tag{V.119}$$

Equation (V.117) and the other two equations which are similar to it for the y- and z-components together with Eq. (V.111) can be solved if sufficient restrictions are placed upon the flow situation so that one of the five unknown quantities (such as those mentioned on page 121) is eliminated as a variable. For example, the equations are solvable if the temperature is assumed to be constant. A complete solution would give the values of all flow variables throughout the flow so that the characteristic parameter could be determined. The various dimensionless coefficients or ratios could then be calculated and their interrelations determined throughout the flow from the equations.

---

[1] The Froude number is sometimes defined as $U_0^2/g_c L_0$ and as $g_c L_0/U_0^2$.

The preceding analysis is more basic than that of dimensional analysis since, except for the case summarized in Eqs. (V.118) and (V.119), the state of the fluid determines functions such as η and ρ. These functions vary in different manners for different fluids where there are equivalent changes in the state conditions. Thus no universal relation true for all fluids can be determined among the dimensionless ratios Re, Fr, and Eu.

Example 1

Exact Solutions of the Equations of Motion for Idealized Laminar Flow.[1]

Since only four of the five independent equations relating the five unknown quantities mentioned on page 121 have been derived, it is necessary, as noted above, to impose sufficient restrictions on the flow to eliminate one of the unknowns as a variable in order to be able to give a complete solution. As an illustration of the application of the equations of motion derived thus far, the two cases of idealized laminar flow treated in Chapter I, Sections I-14 and I-15 will be reanalyzed.

In idealized laminar flow, as defined here for the circular pipe shown in Fig. V-17, the temperature is constant; only velocities in the x-direction are not zero; the viscosity and density are functions of temperature only; the potential Ω is zero; and the flow is in steady state. Also the pressure drop per unit length of conduit is taken to be a constant.

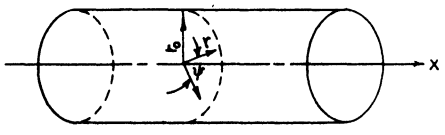

FIG. V-17. Coordinate system for flow in circular pipe.

Equation (V.15) may be expanded to give the basic equation used as a starting point in the study of idealized flow. The result is

$$\frac{\partial \rho}{\partial \theta} + u_r \frac{\partial \rho}{\partial r} + \frac{u_\psi}{r} \frac{\partial \rho}{\partial \psi} + u_x \frac{\partial \rho}{\partial x} + \frac{\rho}{r}\left[\frac{\partial r\, u_r}{\partial r} + \frac{\partial u_\psi}{\partial \psi} + \frac{\partial r\, u_x}{\partial x}\right] = 0. \qquad (1\,E)$$

Since ρ is a constant,

$$\frac{\partial r\, u_r}{\partial r} + \frac{\partial u_\psi}{\partial \psi} + \frac{\partial r\, u_x}{\partial x} = 0. \qquad (2\,E)$$

---

[1] See Chapter I, Section I-10 for the definition of idealized flow.

There are no radial or azimuthal components of velocity. Therefore

$$\frac{\partial u_x}{\partial x} = 0. \tag{3 E}$$

Further, since Ω is zero, Eq. (V.92) becomes

$$\frac{\partial P}{\partial r} = 0 \tag{4 E}$$

when Eqs. (2 E) and (3 E) are used along with the fact that

$$u_r = 0. \tag{5 E}$$

Similarly Eq. (V.93) becomes

$$\frac{\partial P}{\partial \psi} = 0 \tag{6 E}$$

since

$$u_\psi = 0. \tag{7 E}$$

Since steady-state conditions are assumed, Eqs. (V.94) and (V.97) give

$$-\frac{\partial P}{\partial x} + \frac{1}{r}\frac{\partial}{\partial r}\left(\eta r \frac{\partial u_x}{\partial r}\right) = 0 \tag{8 E}$$

because u_r and u_ψ are zero and the symmetry of the flow conditions gives

$$\frac{\partial u_x}{\partial \psi} = 0. \tag{9 E}$$

Thus for idealized laminar flow in a pipe the pressure gradient may be expressed in terms of the viscous forces in the following manner:

$$\frac{dP}{dx} = \frac{1}{r}\frac{\partial}{\partial r}\left(\eta r \frac{\partial u_x}{\partial r}\right). \tag{10 E}$$

Equation (10 E) may be solved for the idealized flow by integrating once with respect to r so that

$$\frac{r^2}{2}\frac{dP}{dx} = \eta r \frac{\partial u_x}{\partial r} + A(x) \tag{11 E}$$

where $A(x)$ is an arbitrary function of x and corresponds to a constant of integration in ordinary integration. Since the flow is symmetrical about the axis,

$$\frac{\partial u_x}{\partial r} = 0 \tag{12 E}$$

at

$$r = 0 \tag{13 E}$$

so that

$$A(x) = 0. \tag{14 E}$$

In the idealized flow T has been taken as constant and

$$\left(\frac{\partial \eta}{\partial P}\right)_T = 0 \tag{15 E}$$[1]

and then η is also a constant. Therefore a second radial integration may be made to give

$$\frac{r^2}{4}\frac{dP}{dx} = \eta u_x + B(x). \tag{16 E}$$

The velocity u_x is 0 when

$$r = r_0 \tag{17 E}$$

and so

$$B(x) = \frac{r_0^2}{4}\frac{dP}{dx} \tag{18 E}$$

Thus, finally,

$$u_x = \frac{dP}{dx}\frac{(r^2 - r_0^2)}{4\eta}. \tag{19 E}$$

Comparison of Eq. (19 E) with Eqs. (I.71) and (I.72) shows that the same results have been obtained.

---

[1] In case it is desired to make the restrictions as weak as possible, it is not necessary to assume $(\partial\eta/\partial P)_T = 0$, because $(\partial P/\partial r) = 0$ and a radial integration would not be disturbed by a functional dependence of η on P. Equation (11 E) would then, however, involve a quantity η which was a function of total pressure and hence of the axial distance x.

In case the isothermal restriction is removed and the other restrictions of idealized laminar flow are retained, the results are identical through Eq. (11 E). In case the viscosity is independent of temperature, which is a very artificial restriction, the above analysis is unmodified. In the more general case when η is a function of T, Eq. (14 E) is still valid and Eq. (11 E) becomes

$$\frac{\partial u_x}{\partial r} = \frac{r}{2\eta}\frac{dP}{dx} \qquad (20\,E)$$

which together with the equation giving the energy balance (*22*) may be solved numerically.

Figure V-18 shows the orientation of parallel plates through which idealized laminar flow occurs. Here the same idealized conditions are used as for the circular pipe.

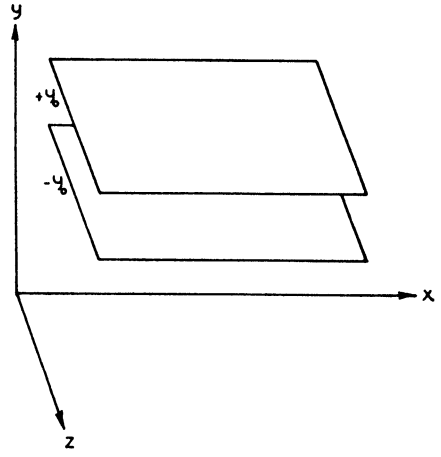

FIG. V-18. Schematic diagram for idealized laminar flow between parallel plates.

From Eq. (V.03)

$$\frac{d\rho}{d\theta} = -\rho\left[\frac{\partial u_x}{\partial x} + \frac{\partial u_y}{\partial y} + \frac{\partial u_z}{\partial z}\right]. \qquad (21\,E)$$

Since ρ is a constant for the idealized flow,

$$\frac{\partial u_x}{\partial x} + \frac{\partial u_y}{\partial y} + \frac{\partial u_z}{\partial z} = 0. \qquad (22\,E)$$

For laminar flow under these conditions,

$$u_y = u_z = 0 \qquad (23\,E)$$

since the motion is wholly in the x-direction. Equation (22 E) then becomes

$$\frac{\partial u_x}{\partial x} = 0. \qquad (24\,E)$$

Further, since Ω is zero for the idealized flow Eq. (V.84) becomes

$$\frac{\partial P}{\partial y} = 0 \qquad (25\,E)$$

and Eq. (V.85),

$$\frac{\partial P}{\partial z} = 0. \tag{26 E}$$

Since steady state prevails, Eqs. (V.83) and (V.22) give

$$\rho\, u_x \frac{\partial u_x}{\partial x} = -\frac{\partial P}{\partial x} + \frac{\partial}{\partial x}\left(\eta \frac{\partial u_x}{\partial x}\right) + \frac{\partial}{\partial y}\left(\eta \frac{\partial u_x}{\partial y}\right) \tag{27 E}$$

because by symmetry

$$\frac{\partial u_x}{\partial z} = 0. \tag{28 E}$$

Substitution of Eq. (24 E) into Eq. (27 E) and noting Eqs. (25 E) and (26 E) allows Eq. (27 E) to be written as

$$\frac{dP}{dx} = \frac{\partial}{\partial y}\left(\eta \frac{\partial u_x}{\partial y}\right). \tag{29 E}$$

Integrating once with respect to y results in the expression

$$y \frac{dP}{dx} = \eta \frac{\partial u_x}{\partial y} + A(x). \tag{30 E}$$

From symmetry of flow,

$$\frac{\partial u_x}{\partial y} = 0 \tag{31 E}$$

when

$$y = 0 \tag{32 E}$$

so that

$$A(x) = 0. \tag{33 E}$$

Since T is a constant and

$$\left(\frac{\partial \eta}{\partial P}\right)_T = 0 \tag{34 E}$$

in the idealized flow, η is a constant,[1] and a second integration with respect to y gives

$$\frac{y^2}{2} \frac{dP}{dx} = \eta\, u_x + B(x). \tag{35 E}$$

---

[1] See parallel footnote for circular pipe used in connection with Eq. (15 E), page 150.

In evaluating $B(x)$ it may be noted that the velocity is zero at the walls

$$u_x = 0 \tag{36 E}$$

when

$$y = \pm y_0. \tag{37 E}$$

Combining Eqs. (36 E) and (37 E) with Eq. (35 E) gives

$$B(x) = \frac{y_0^2}{2}\frac{dP}{dx} \tag{38 E}$$

so that finally

$$u_x = \frac{dP}{dx}\frac{y^2 - y_0^2}{2\eta}. \tag{39 E}$$

Comparison of Eq. (39 E) with Eqs. (I.82) and (I.83) shows that the same results have been obtained.

As in the case of the idealized laminar flow in the cylindrical pipe, the removal of the isothermal restriction requires that Eq. (30 E) be integrated numerically along with the energy equation.

Example 2

Idealized Laminar Velocity Distribution Between Journal and Bearing.

The Navier-Stokes equations can be solved easily for the distribution of velocity in idealized flow in an unloaded, weightless, bearing as shown in Fig. V-19. By symmetry the velocity of the fluid does not have components in the r- or x-directions and is a function of the distance from the shaft center r only.

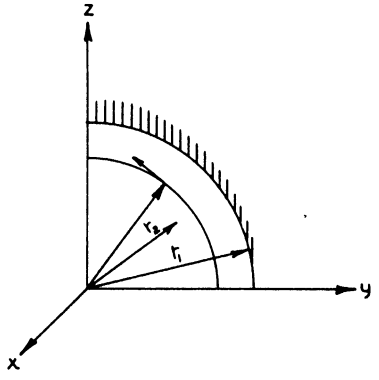

FIG. V-19. Schematic arrangement of concentric bearing.

The solution will be made employing the Navier-Stokes equations in Cartesian coordinates (V.83), (V.84), and (V.85) in order to illustrate change of variables. The student may find a solution more easily by use of the Navier-Stokes equations in cylindrical coordinates (V.92), (V.93), and (V.94).

Some terms present in the solution from the equations in cylindrical coordinates are not fully explained in this text. These terms are derived in the following solution.

The y- and z-components of velocity may be written in terms of the constant velocity u of the fluid passing a fixed point as follows:

$$u_y = -u \sin \psi = -\frac{z\,u}{r} = -z\,\omega, \tag{1 E}$$

$$u_z = u \cos \psi = \frac{y\,u}{r} = y\,\omega \tag{2 E}$$

where

$$\omega = \frac{u}{r} = f(r). \tag{3 E}$$

The velocity-coordinate derivatives may be evaluated as follows:

$$\frac{\partial u_y}{\partial y} = -\frac{z\,y}{r}\frac{d\omega}{dr}, \tag{4 E}$$

$$\frac{\partial u_z}{\partial y} = \omega + \frac{y^2}{r}\frac{d\omega}{dr}, \tag{5 E}$$

$$\frac{\partial u_y}{\partial z} = -\omega - \frac{z^2}{r}\frac{d\omega}{dr}, \tag{6 E}$$

$$\frac{\partial u_z}{\partial z} = \frac{y\,z}{r}\frac{d\omega}{dr} \tag{7 E}$$

Here $\partial\omega/\partial r$ is properly $d\omega/dr$, and $\partial^2\omega/\partial r^2$ is $d^2\omega/dr^2$.

The second velocity-coordinate derivatives needed may be evaluated next.

$$\frac{\partial^2 u_y}{\partial y^2} = -\frac{z}{r}\frac{d\omega}{dr} + \frac{z\,y^2}{r^3}\frac{d\omega}{dr} - \frac{y^2}{r^2}\frac{z}{r}\frac{d^2\omega}{dr^2}, \tag{8 E}$$

$$\frac{\partial^2 u_y}{\partial z^2} = -\frac{3\,z}{r}\frac{d\omega}{dr} + \frac{z^3}{r^3}\frac{d\omega}{dr} - \frac{z^3}{r^2}\frac{d^2\omega}{dr^2}, \tag{9 E}$$

$$\frac{\partial^2 u_z}{\partial y^2} = \frac{3\,y}{r}\frac{d\omega}{dr} - \frac{y^3}{r^3}\frac{d\omega}{dr} + \frac{y^3}{r^2}\frac{d^2\omega}{dr^2}, \tag{10 E}$$

$$\frac{\partial^2 u_z}{\partial z^2} = \frac{y}{r}\frac{d\omega}{dr} - \frac{y\,z^2}{r^3}\frac{d\omega}{dr} + \frac{y\,z^2}{r^2}\frac{d^2\omega}{dr^2}. \tag{11 E}$$

By making use of the preceding equations and the fact that

$$r^2 = y^2 + z^2 \tag{12 E}$$

the following results can be obtained for use in the Navier-Stokes equations:

$$u_y \frac{\partial u_y}{\partial y} + u_z \frac{\partial u_y}{\partial z} = - y \omega^2, \tag{13 E}$$

$$u_y \frac{\partial u_z}{\partial y} + u_z \frac{\partial u_z}{\partial z} = - z \omega^2, \tag{14 E}$$

$$\frac{\partial^2 u_y}{\partial y^2} + \frac{\partial^2 u_y}{\partial z^2} = - z \frac{d^2\omega}{dr^2} - \frac{3 z}{r} \frac{d\omega}{dr}, \tag{15 E}$$

$$\frac{\partial^2 u_z}{\partial y^2} + \frac{\partial^2 u_z}{\partial z^2} = y \frac{d^2\omega}{dr^2} + \frac{3 y}{r} \frac{d\omega}{dr}. \tag{16 E}$$

Since the flow is idealized,

$$\frac{\partial u_x}{\partial x} + \frac{\partial u_y}{\partial y} + \frac{\partial u_z}{\partial z} = 0 \tag{17 E}$$

from Eq. (V.01), the equation of continuity. Also, since Ω is zero, Eqs. (V.84) and (V.85) when combined with Eqs. (V.23), (V.24), and (13 E) through (16 E) become, respectively,

$$- \omega^2 y + \nu z \left(\frac{d^2\omega}{dr^2} + \frac{3}{r} \frac{d\omega}{dr} \right) = - \frac{1}{\rho} \frac{y}{r} \frac{dP}{dr}, \tag{18 E}$$

$$- \omega^2 z - \nu y \left(\frac{d^2\omega}{dr^2} + \frac{3}{r} \frac{d\omega}{dr} \right) = - \frac{1}{\rho} \frac{z}{r} \frac{dP}{dr} \tag{19 E}$$

where the kinematic viscosity ν replaces η/ρ and the pressure P is a function of r only. If Eq. (18 E) is multiplied by z and Eq. (19 E) by y, the result, when the two equations are subtracted, is

$$\frac{d^2\omega}{dr^2} + \frac{3}{r} \frac{d\omega}{dr} = 0. \tag{20 E}$$

The solution to Eq. (20 E) may be obtained by two simple quadratures and is

$$\omega = \frac{C}{r^2} + D. \tag{21 E}$$

If ω is taken as zero for

$$r = r_1 \tag{22 E}$$

and as ω_0 for

$$r = r_2 \tag{23 E}$$

then C and D may be evaluated. The resulting expression for ω is

$$\omega = \omega_0 \left(\frac{\frac{1}{r^2} - \frac{1}{r_1^2}}{\frac{1}{r_2^2} - \frac{1}{r_1^2}} \right). \tag{24 E}$$

The tangential stress is

$$\tau_{r\phi} = \eta r \frac{d\omega}{dr} = - \frac{2\eta\omega_0}{r^2 \left(\frac{1}{r_2^2} - \frac{1}{r_1^2} \right)}. \tag{25 E}$$

The torque per unit length of x is

$$\{(2\pi r)\tau_{r\phi} r\} = - \frac{4\pi\eta\omega_0}{\frac{1}{r_2^2} - \frac{1}{r_1^2}}. \tag{26 E}$$

The dependence of pressure on the r-coordinate may be obtained from (18 E) multiplied by y added to (19 E) multiplied by z to give

$$\frac{dP}{dr} = \rho\omega^2 r. \tag{27 E}$$

This equation is also integrable by simple quadrature.

Equation (26 E) is employed in the use of rotating-cylinder viscometers. Corrections for torque on the ends of the rotating cylinder and for bearing friction must be made.

V-13. Initial and Boundary Conditions for the Equations of Motion

In the general case of the motion of a fluid, sufficient mathematical conditions must be given in order to obtain a definite solution to the equations of motion. Just what constitutes sufficient conditions is difficult to state from a purely mathematical standpoint, and they vary from situation to situation. Yet it generally is possible to ascertain the conditions from

physical reasoning. Thus, in the last section, the physical situation at the boundaries to the flow gave the mathematical condition that the relative velocity at the wall was zero. In the general case, the physical situation at the boundaries to the flow is generally known and may be made to yield the mathematical "boundary" conditions, and the physical situation throughout the flow is generally known at some instant, usually

$$\theta = 0 \tag{V.120}$$

giving the mathematical "initial" conditions. (The latter conditions did not appear in the analysis of the last section because the motion was steady.) If the physical analysis is adequate, these physical conditions will determine the complete behavior of the fluid, and hence furnish sufficient mathematical conditions for the equations of motion to yield a definite solution. For illustrations of the determination and use of boundary and initial conditions, see Lamb (*3*), Boelter (*23*), and Goldstein (*24*).

V-14. Comments on the Solution of the Equations of Motion

Very few exact solutions of the equations of motion have been derived (*3*, *24*), although a number of approximate solutions have been obtained by neglecting various terms in the equations. The chief mathematical difficulty which has prevented the obtaining of an exact solution in the general case lies in the fact that, in the equation of continuity (V.03) and the Navier-Stokes equations (V.22), (V.23), (V.24), (V.83), (V.84), and (V.85), terms appear involving the product of two unknown quantities, $u_x\,(\partial u_x/\partial x)$, for example. In mathematical terms, the equations are nonlinear, the term linear equation being restricted to those in which every term contains at most one unknown quantity to the first power only. The nonlinearity prevents the use of the method of separation of variables (*25*) or the method of the Laplace transform (*26*, *27*) in the exact or analytical solution of the equations. Many of the approximate solutions which have been obtained were secured by neglecting all the nonlinear terms in the equation of motion and any others that would interfere with the mathematical techniques. Since it occasionally occurs that the equations of motion may be legitimately simplified to permit the use of these techniques, the range of applicability of the mathematics will be outlined so that the texts given in the footnotes may be consulted for details.

The method of separation of variables may be applied to homogeneous, linear, partial differential equations. A homogeneous linear equation is one

that contains no terms *not* involving an unknown quantity to the first power only. In the use of this method, the solution of the equation must be expressible as products of factors each of which is a function of only one independent variable. As for the method of the Laplace transform, it may be applied to linear, partial differential equations with only rather weak restrictions on the parameters.

There are many special methods for solving particular partial differential equations, and many partial differential equations may be greatly simplified by suitable transformations or mathematical tricks. Excellent discussions of methods of attack on partial differential equations are given in Frank and von Mises (*12*), Bateman (*28*), and Courant and Hilbert (*29*).

In general, the exact or analytic solutions to linear partial differential equations give either infinite series or complicated integrals, both involving coefficients which are often extremely difficult to evaluate numerically. Consequently, as a rule, only approximate numerical answers can be obtained. Further, the partial differential equations to be solved must often be unjustifiably simplified to yield linear equations with constant coefficients or coefficients which are artificially prescribed. Finally, if any boundary surfaces other than plane, circular, cylindrical, spherical, or a few others are introduced, the exact solution becomes much more difficult if not impossible.

On the other hand, there is an approximate numerical method of solving partial differential equations which is being rapidly developed at present (*30, 31*). This method makes no restriction on the form of the partial differential equation to be solved; can allow for any necessary variation in the parameters such as η with T, for example; and can yield answers of any desired degree of accuracy depending on the time expended on the solution. In common with all numerical methods of solution, however, only a single physical problem may be solved at a time, and general trends, optimum conditions, etc. can be obtained only by solving many separate problems individually. This method consists essentially in replacing the given partial differential equation with a partial finite difference equation (*32*). If an approximate analytic solution to the problem can be obtained without too much difficulty, it is often more efficient to consider that the "exact" solution is the sum of the analytic approximation and a further approximation obtained by numerical means as suggested above, i.e., that the numerical process be applied to "residual" quantities only.

The Navier-Stokes equations are most readily solved for laminar flow. In the case of the turbulent flow they are almost impossible to solve exactly. The difficulty arises from the fact that turbulent flow continuously generates

eddies which are gradually dissipated as they move through the fluid. An exact solution for the case of turbulent flow at constant rate, for example, would require the calculation of the history of all the eddies formed from an initial disturbance including that disturbance causing transition from laminar to turbulent flow, as well as the history of all the eddies formed by the eddies, etc.

For sufficiently viscous fluids, narrow conduits, and low velocities, i.e. for the small enough Reynolds numbers, laminar flow is usually stable, so that many practical problems do arise in chemical engineering technology which involve laminar flow.

V-15. General Discussion of Turbulent Flow

There are two broad types of attack on the problem of turbulence being advanced today. The first, the statistical approach, is the more difficult and less developed of the two though ultimately it promises to yield an accurate solution to the problem. It ignores the detailed history of the individual eddy motions in turbulent flow which, as previously discussed, is hopelessly complex. Instead, the statistical approach assumes that turbulent flow may be described by distributions of velocities, temperatures, and pressures at any point in the flow at any instant. By a distribution of velocities, for example, is meant a functional relationship between a velocity and the probability of its occurrence where the probability depends on position, and, in the case of unsteady flow, on time as well. In general the distributions will vary from point to point and instant to instant. From the probabilities, the average conditions can be calculated. For any given probability the velocities, pressures, and temperatures given by the distributions must satisfy the equations of motion, and the distributions themselves must satisfy the laws of probability.

The second approach to the problem of turbulent flow consists in making some assumptions as to the mechanism of turbulence. The Prandtl mixing length hypothesis, for example, assumes that turbulence consists essentially in the sudden motion of masses of fluid from one layer in the fluid to another. Here the masses of fluid suffer no changes in transit and upon striking the second layer give up their properties that they had in the first layer and assume the properties of the second layer. (See Chapter III and Goldstein (*24*) for further discussion.)

V-16. Reynolds (*33*) Transformation of the Equations of Motion

Reynolds introduced a transformation of the equations of motion which is of great importance in turbulence theories because it separates the effects caused by average conditions from those produced by fluctuations. This transformation utilizes the concepts of average and fluctuation quantities introduced in Chapter I which are redefined here for the average, instantaneous, and fluctuation values of a variable G:

$$G = \overline{G} + G_f, \tag{V.121}$$

$$\overline{G} = \frac{1}{\theta} \int_{\theta_0 - \frac{1}{2}\theta}^{\theta_0 + \frac{1}{2}\theta} G \, d\theta \tag{V.122}$$

where G is the instantaneous value of the variable at a given point at time θ_0, $\overline{G}$ is the time average value, and G_f is the fluctuation value. The period of the integration θ is taken long enough so that $\overline{G}$ is not sensibly changed by taking a longer time. In steady flow, θ may be taken as long as desired, but as discussed in Chapter I the concept of a fluctuation value can be applied to unsteady flow only if the general conditions are changing very slowly compared to the fluctuations.

Before performing the Reynolds transformation it is necessary to obtain some useful relations concerning average quantities. From Eqs. (V.121) and (V.122), it follows that the average of a fluctuation value is zero:

$$\overline{G_f} = 0 \tag{V.123}$$

and the double average is the average,

$$\overline{\overline{G}} = \overline{G} \tag{V.124}$$

where G is any variable. If I is any variable, including possibly G, there is obtained from Eq. (V.123)

$$\overline{\overline{G}\, I_f} = 0 \tag{V.125}$$

since $\overline{G}$ is constant. Hence

$$\overline{G\, I} = \overline{(\overline{G} + G_f)(\overline{I} + I_f)} = \overline{G}\,\overline{I} + \overline{G_f I_f}. \tag{V.126}$$

It is possible to invert the order of a partial differentiation with respect to one variable and a partial integration with respect to another under broad continuity conditions (*4*, *34*). Consequently

$$\overline{\frac{\partial G}{\partial L}} = \frac{1}{\theta}\int_{\theta_0-\frac{1}{2}\theta}^{\theta_0+\frac{1}{2}\theta}\frac{\partial G}{\partial L}\,d\theta = \frac{\partial}{\partial L}\left\{\frac{1}{\theta}\int_{\theta_0-\frac{1}{2}\theta}^{\theta_0+\frac{1}{2}\theta} G\,d\theta\right\} = \frac{\partial \overline{G}}{\partial L} \tag{V.127}$$

or the average of the partial of G with respect to a distance is the partial of the average of G with respect to the distance.

If the partial derivative is taken with respect to time, the same result is obtained for slightly different reasons. Thus

$$\overline{\frac{\partial G}{\partial \theta}} = \frac{1}{\theta_1}\int_{\theta_0-\frac{1}{2}\theta_1}^{\theta_0+\frac{1}{2}\theta_1}\frac{\partial G}{\partial \theta}\,d\theta = \frac{1}{\theta_1}\frac{\partial}{\partial \theta}\int_{\theta_0-\frac{1}{2}\theta_1}^{\theta_0+\frac{1}{2}\theta_1} G\,d\theta = \frac{\partial}{\partial \theta}\left\{\frac{1}{\theta_1}\int_{\theta_0-\frac{1}{2}\theta_1}^{\theta_0+\frac{1}{2}\theta_1} G\,d\theta\right\} \tag{V.128}$$

because the third member is obtained from the second by the theorem for differentiating integrals (*34*, *35*), and $1/\theta_1$ and $\partial/\partial\theta$ may be interchanged in the fourth member since $1/\theta_1$ is a constant as far as this differentiation is concerned.

The Reynolds transformation consists in substituting the sum of the average and fluctuation values of all dependent variables for the instantaneous values in the equations of motion and then taking the time average of the equations, term by term, by application of Eq. (V.122). This procedure yields the type of information generally desired about turbulent flow since only the average conditions are usually of interest, and the transformation permits the detailed flow processes to be ignored provided certain fluctuation quantities can be calculated.

Thus, if the average and fluctuation values of the density and the velocity components of the fluid are substituted for the instantaneous values in the equation of continuity, Eq. (V.03), and in Eq. (V.04), i.e., if

$$\begin{aligned} \rho &= \overline{\rho} + \rho_f, \\ u_x &= \overline{u_x} + u_{xf}, \\ u_y &= \overline{u_y} + u_{yf}, \\ u_z &= \overline{u_z} + u_{zf} \end{aligned} \tag{V.129}$$

are substituted in Eq. (V.03), the result is

$$\frac{d(\overline{\rho} + \rho_f)}{d\theta} = -(\overline{\rho} + \rho_f)\left[\frac{\partial \overline{u_x}}{\partial x} + \frac{\partial \overline{u_y}}{\partial y} + \frac{\partial \overline{u_z}}{\partial z} + \frac{\partial u_{xf}}{\partial x} + \frac{\partial u_{yf}}{\partial y} + \frac{\partial u_{zf}}{\partial z}\right]. \tag{V.130}$$

The average of Eq. (V.130), on applying Eq. (V.122) term by term and simplifying with Eqs. (V.128), (V.127), (V.126), (V.125), (V.124), and (V.123), is

$$\overline{\frac{d(\bar{\rho}+\rho_f)}{d\theta}} = -\bar{\rho}\left[\frac{\partial \overline{u_x}}{\partial x}+\frac{\partial \overline{u_y}}{\partial y}+\frac{\partial \overline{u_z}}{\partial z}\right]-\overline{\rho_f\left[\frac{\partial u_{xf}}{\partial x}+\frac{\partial u_{yf}}{\partial y}+\frac{\partial u_{zf}}{\partial z}\right]}. \quad \text{(V.131)}$$

It should be noted that

$$\overline{\frac{dG}{d\theta}} \neq \frac{d\bar{G}}{d\theta} \quad \text{(V.132)}$$

where

$$G = \bar{\rho} + \rho_f. \quad \text{(V.133)}$$

When the fluid is incompressible,

$$\frac{d\rho}{d\theta} = 0 \qquad \text{and} \qquad \rho_f = 0 \quad \text{(V.134)}$$

so that Eq. (V.131) reduces to

$$\frac{\partial \overline{u_x}}{\partial x}+\frac{\partial \overline{u_y}}{\partial y}+\frac{\partial \overline{u_z}}{\partial z} = 0 \quad \text{(V.135)}$$

which is the average of the equation of continuity for an incompressible fluid.

Before performing the Reynolds transformation on the Navier-Stokes equations, it is desirable to transform them first by means of a relation, which will now be derived, in order to obtain quantities useful in mixing-length turbulence theories.

If ξ is any arbitrary, finite, continuous function of x, y, z, and θ with finite and continuous derivatives, then the general theorem for partial differentiation gives

$$\frac{d\rho\,\xi}{d\theta} = \frac{\partial \rho\,\xi}{\partial \theta}+u_x\frac{\partial \rho\,\xi}{\partial x}+u_y\frac{\partial \rho\,\xi}{\partial y}+u_z\frac{\partial \rho\,\xi}{\partial z} = \rho\frac{d\xi}{d\theta}+\xi\frac{d\rho}{d\theta}. \quad \text{(V.136)}$$

From Eq. (V.03), the equation of continuity, Eq. (V.136) may be transformed into

$$\frac{\rho\,d\xi}{d\theta} = \rho\,\xi\left[\frac{\partial u_x}{\partial x}+\frac{\partial u_y}{\partial y}+\frac{\partial u_z}{\partial z}\right]+\frac{\partial \rho\,\xi}{\partial \theta}+u_x\frac{\partial \rho\,\xi}{\partial x}+u_y\frac{\partial \rho\,\xi}{\partial y}+u_z\frac{\partial \rho\,\xi}{\partial z} \quad \text{(V.137)}$$

or noting the rule for differentiation of a product,

$$\rho \frac{d\xi}{d\theta} = \frac{\partial \rho\, \xi}{\partial \theta} + \frac{\partial \rho\, \xi\, u_x}{\partial x} + \frac{\partial \rho\, \xi\, u_y}{\partial y} + \frac{\partial \rho\, \xi\, u_z}{\partial z}. \tag{V.138}$$

If ξ is taken as u_x, u_y, and u_z in turn and the result substituted in Eqs. (V.34), (V.35), and (V.36), respectively, the momentum equations, the result is

$$\frac{\partial \rho\, u_x}{\partial \theta} = \rho \Phi_x + \frac{\partial}{\partial x}(\tau_{xx} - \rho\, u_x u_x) + \frac{\partial}{\partial y}(\tau_{yx} - \rho\, u_y u_x) + \frac{\partial}{\partial z}(\tau_{zx} - \rho\, u_z u_x), \tag{V.139}$$

$$\frac{\partial \rho\, u_y}{\partial \theta} = \rho \Phi_y + \frac{\partial}{\partial x}(\tau_{xy} - \rho\, u_x u_y) + \frac{\partial}{\partial y}(\tau_{yy} - \rho\, u_y u_y) + \frac{\partial}{\partial z}(\tau_{zy} - \rho\, u_z u_y), \tag{V.140}$$

$$\frac{\partial \rho\, u_z}{\partial \theta} = \rho \Phi_z + \frac{\partial}{\partial x}(\tau_{xz} - \rho\, u_x u_z) + \frac{\partial}{\partial y}(\tau_{yz} - \rho\, u_y u_z) + \frac{\partial}{\partial z}(\tau_{zz} - \rho\, u_z u_z). \tag{V.141}$$

On substituting the sum of the average and fluctuation values of the density, components of the velocity and surface stresses, into Eqs. (V.139), (V.140), and (V.141) and taking the average of the equations term by term according to Eq. (V.122), the Reynolds transformation is effected. The averages of these equations are complicated, even after simplification with Eqs. (V.123) through (V.128), because of the appearance of triple product sums of the form $\overline{\rho}\,\overline{u_x}\,\overline{u_y} + \overline{\rho}\,\overline{u_{xf}\,u_{yf}} + \overline{\rho_f\,u_{yf}}\,\overline{u_{xf}} + \overline{\rho_f\,u_{xf}\,u_{yf}} + \ldots$ which arise, for example, from the term $\rho\, u_x\, u_y$. If the fluid is incompressible, the sum just mentioned simplifies greatly since only the first two terms remain. If the fluid is compressible, it may still be true that only the first two terms are important since the turbulent eddies may be so small and transient that they do not produce important fluctuations in pressure or temperature and hence in density. In order to secure the latter simplification, the treatment of turbulent flow is restricted to the range of well-developed turbulence since near the transition from turbulent to laminar flow the eddies are large and are dissipated only relatively slowly. Thus larger fluctuations in pressure and temperature may be expected than in the region of fully developed turbulence.

For an incompressible fluid or a fluid which is incompressible as far as the turbulent fluctuations are concerned, the momentum equations become

$$\frac{\partial \overline{\rho}\,\overline{u_x}}{\partial \theta} = \overline{\rho}\,\Phi_x + \frac{\partial}{\partial x}\left(\overline{\tau_{xx}} - \overline{\rho}\,\overline{u_x}\,\overline{u_x} - \overline{\rho}\,\overline{u_{xf}\,u_{xf}}\right) + \frac{\partial}{\partial y}\left(\overline{\tau_{yx}} - \overline{\rho}\,\overline{u_y}\,\overline{u_x} - \overline{\rho}\,\overline{u_{yf}\,u_{xf}}\right) + \frac{\partial}{\partial z}\left(\overline{\tau_{zx}} - \overline{\rho}\,\overline{u_z}\,\overline{u_x} - \overline{\rho}\,\overline{u_{zf}\,u_{xf}}\right) \tag{V.142}$$

$$\frac{\partial \overline{\rho}\,\overline{u_y}}{\partial \theta} = \overline{\rho}\,\Phi_y + \frac{\partial}{\partial x}\left(\overline{\tau_{xy}} - \overline{\rho}\,\overline{u_x}\,\overline{u_y} - \overline{\rho}\,\overline{u_{xf}\,u_{yf}}\right) + \frac{\partial}{\partial y}\left(\overline{\tau_{yy}} - \overline{\rho}\,\overline{u_y}\,\overline{u_y} - \overline{\rho}\,\overline{u_{yf}\,u_{yf}}\right) + \frac{\partial}{\partial z}\left(\overline{\tau_{zy}} - \overline{\rho}\,\overline{u_z}\,\overline{u_y} - \overline{\rho}\,\overline{u_{zf}\,u_{yf}}\right) \tag{V.143}$$

$$\frac{\partial \overline{\rho}\,\overline{u_z}}{\partial \theta} = \overline{\rho}\,\Phi_z + \frac{\partial}{\partial x}\left(\overline{\tau_{xz}} - \overline{\rho}\,\overline{u_x}\,\overline{u_z} - \overline{\rho}\,\overline{u_{xf}\,u_{zf}}\right) + \frac{\partial}{\partial y}\left(\overline{\tau_{yz}} - \overline{\rho}\,\overline{u_y}\,\overline{u_z} - \overline{\rho}\,\overline{u_{yf}\,u_{zf}}\right) + \frac{\partial}{\partial z}\left(\overline{\tau_{zz}} - \overline{\rho}\,\overline{u_z}\,\overline{u_z} - \overline{\rho}\,\overline{u_{zf}\,u_{zf}}\right). \tag{V.144}$$

In the development of the last three equations Φ has been assumed to be constant with respect to time for each coordinate direction. Where the fluids are incompressible, the bars may be omitted from the densities.

For a fluid which is essentially incompressible as far as turbulent fluctuations are concerned, the equation of continuity becomes

$$-\overline{\rho}\left[\frac{\partial \overline{u}_x}{\partial x} + \frac{\partial \overline{u}_y}{\partial y} + \frac{\partial \overline{u}_z}{\partial z}\right] = \frac{\partial \overline{\rho}}{\partial \theta} + \overline{u}_x\frac{\partial \overline{\rho}}{\partial x} + \overline{u}_y\frac{\partial \overline{\rho}}{\partial y} + \overline{u}_z\frac{\partial \overline{\rho}}{\partial z}. \tag{V.145}$$

Equations (V.142), (V.143), and (V.144) have the same form as the instantaneous momentum equations (V.139), (V.140), and (V.141) if the instantaneous values of the variables are replaced by average values and the viscous stresses τ_{ij} are changed to $\overline{\tau_{ij}} - \overline{\rho}\,\overline{u_{if}\,u_{jf}}$. The latter term of this stress is known as the Reynolds stress and arises from the transport of momentum by the velocity fluctuations just as τ_{ij} arises from the transport of momentum by molecular agitation (*36*).

Cylindrical Coordinates

The Reynolds transformation of the equations of motion in cylindrical coordinates yields for the equation of continuity of an incompressible fluid

$$\frac{\partial r\overline{u}_r}{\partial r} + \frac{\partial \overline{u}_\psi}{\partial \psi} + \frac{\partial r\overline{u}_x}{\partial x} = 0. \tag{V.146}$$

For a fluid which is only incompressible as far as the turbulent fluctuations are concerned, the equation of continuity becomes

$$\frac{\partial \overline{\rho}}{\partial \theta} + \frac{1}{r}\left[\frac{\partial r\,\overline{\rho}\,\overline{u}_r}{\partial r} + \frac{\partial \overline{\rho}\,\overline{u}_\psi}{\partial \psi} + \frac{\partial r\,\overline{\rho}\,\overline{u}_x}{\partial x}\right] = 0. \tag{V.147}$$

The momentum equations in cylindrical coordinates take the forms:

$$\rho a_r = \rho \Phi_r + \frac{1}{r}\left[\frac{\partial r\,\tau_{rr}}{\partial r} + \frac{\partial \tau_{\psi r}}{\partial \psi} + \frac{\partial r\,\tau_{xr}}{\partial x}\right] - \frac{\tau_{\psi\psi}}{r}, \tag{V.148}$$

$$\rho a_\psi = \rho \Phi_\psi + \frac{1}{r}\left[\frac{\partial r\,\tau_{r\psi}}{\partial r} + \frac{\partial \tau_{\psi\psi}}{\partial \psi} + \frac{\partial r\,\tau_{x\psi}}{\partial x}\right] + \frac{\tau_{r\psi}}{r}, \tag{V.149}$$

and

$$\rho a_x = \rho \Phi_x + \frac{1}{r}\left[\frac{\partial r\,\tau_{rx}}{\partial r} + \frac{\partial \tau_{\psi x}}{\partial \psi} + \frac{\partial r\,\tau_{xx}}{\partial x}\right]. \tag{V.150}$$

The cylindrical analog of Eq. (V.138) for the r-component of ξ is

$$\rho \frac{\delta \xi_r}{\delta \theta} = \frac{\partial \rho\,\xi_r}{\partial \theta} + \frac{1}{r}\left[\frac{\partial r\,\rho\,\xi_r\,u_r}{\partial r} + \frac{\partial \rho\,\xi_r\,u_\psi}{\partial \psi} + \frac{\partial r\,\rho\,\xi_r\,u_x}{\partial x}\right] - \frac{\rho\,\xi_\psi\,u_\psi}{r}. \tag{V.151}$$

The form of the last term changes with the component of ξ.

Taking ξ_i as u_r, u_ψ, and u_x in turn and substituting the results in Eqs. (V.148), (V.149), and (V.150), respectively, the result is

$$\frac{\partial \rho\,u_r}{\partial \theta} = \rho \Phi_r + \frac{1}{r}\left[\frac{\partial}{\partial r}(r\,\tau_{rr} - \rho\,r\,u_r\,u_r) + \frac{\partial}{\partial \psi}(\tau_{\psi r} - \rho\,u_\psi\,u_r) + \frac{\partial}{\partial x}(r\,\tau_{xr} - \rho\,r\,u_x\,u_r)\right] - \frac{1}{r}[\tau_{\psi\psi} - \rho\,u_\psi\,u_\psi], \tag{V.152}$$

$$\frac{\partial \rho\,u_\psi}{\partial \theta} = \rho \Phi_\psi + \frac{1}{r}\left[\frac{\partial}{\partial r}(r\,\tau_{r\psi} - \rho\,r\,u_r\,u_\psi) + \frac{\partial}{\partial \psi}(\tau_{\psi\psi} - \rho\,u_\psi\,u_\psi) + \frac{\partial}{\partial x}(r\,\tau_{x\psi} - \rho\,r\,u_x\,u_\psi)\right] + \frac{1}{r}[\tau_{r\psi} - \rho\,u_r\,u_\psi], \tag{V.153}$$

$$\frac{\partial \rho u_x}{\partial \theta} = \rho \Phi_x + \frac{1}{r}\left[\frac{\partial}{\partial r}(r\tau_{rx} - \rho r u_r u_x) + \frac{\partial}{\partial \psi}(\tau_{\psi x} - \rho u_\psi u_x) + \frac{\partial}{\partial x}(r\tau_{xx} - \rho r u_x u_x)\right]. \tag{V.154}$$

If the Reynolds transformation is performed on these momentum equations, the result for a fluid which is incompressible as far as turbulent fluctuations are concerned becomes

$$\frac{\partial \overline{\rho}\,\overline{u_r}}{\partial \theta} = \overline{\rho}\Phi_r + \frac{1}{r}\left[\frac{\partial}{\partial r}(r\overline{\tau_{rr}} - \overline{\rho} r \overline{u_r}\,\overline{u_r} - \overline{\rho} r \overline{u_{rf} u_{rf}}) + \frac{\partial}{\partial \psi}(\overline{\tau_{\psi r}} - \overline{\rho}\,\overline{u_\psi}\,\overline{u_r} - \overline{\rho}\,\overline{u_{\psi f} u_{rf}}) + \frac{\partial}{\partial x}(r\overline{\tau_{xr}} - \overline{\rho} r \overline{u_x}\,\overline{u_r} - \overline{\rho} r \overline{u_{xf} u_{rf}})\right] + \frac{1}{r}[\overline{\tau_{\psi\psi}} - \overline{\rho}\,\overline{u_\psi}\,\overline{u_\psi} - \overline{\rho}\,\overline{u_{\psi f} u_{\psi f}}], \tag{V.155}$$

$$\frac{\partial \overline{\rho}\,\overline{u_\psi}}{\partial \theta} = \overline{\rho}\Phi_\psi + \frac{1}{r}\left[\frac{\partial}{\partial r}(r\overline{\tau_{r\psi}} - \overline{\rho} r \overline{u_r}\,\overline{u_\psi} - \overline{\rho} r \overline{u_{\psi f} u_{rf}}) + \frac{\partial}{\partial \psi}(\overline{\tau_{\psi\psi}} - \overline{\rho}\,\overline{u_\psi}\,\overline{u_\psi} - \overline{\rho}\,\overline{u_{\psi f} u_{\psi f}}) + \frac{\partial}{\partial x}(r\overline{\tau_{x\psi}} - \overline{\rho} r \overline{u_x}\,\overline{u_\psi} - \overline{\rho} r \overline{u_{xf} u_{\psi f}})\right] + \frac{1}{r}[\overline{\tau_{r\psi}} - \overline{\rho}\,\overline{u_r}\,\overline{u_\psi} - \overline{\rho}\,\overline{u_{rf} u_{\psi f}}], \tag{V.156}$$

$$\frac{\partial \overline{\rho}\,\overline{u_x}}{\partial \theta} = \overline{\rho}\Phi_x + \frac{1}{r}\left[\frac{\partial}{\partial r}(r\overline{\tau_{rx}} - \overline{\rho} r \overline{u_r}\,\overline{u_x} - \overline{\rho} r \overline{u_{xf} u_{rf}}) + \frac{\partial}{\partial \psi}(\overline{\tau_{\psi x}} - \overline{\rho}\,\overline{u_\psi}\,\overline{u_x} - \overline{\rho}\,\overline{u_{\psi f} u_{xf}}) + \frac{\partial}{\partial x}(r\overline{\tau_{xx}} - \overline{\rho} r \overline{u_x}\,\overline{u_x} - \overline{\rho} r \overline{u_{xf} u_{xf}})\right]. \tag{V.157}$$

In the equations just developed, the external field was assumed to be constant with respect to time. For an incompressible fluid, the density is constant and the bar may be removed.

Example 3

Application of the Reynolds Transformation of the Equations of Motion to the Case of Idealized Flow between Parallel Plates — Expression of the Reynolds Shearing Stress.

For idealized turbulent flow between parallel plates spaced $2\,y_0$ apart as shown in Fig. V-20, the average velocities in the y- and z-directions are zero since the axes are oriented so that the mean motion is in the x-direction, i.e.,

$$\overline{u_y} = \overline{u_z} = 0. \tag{1 E}$$

Since the flow is steady and the fluid incompressible,

$$\frac{\partial \rho\,\overline{u_x}}{\partial \theta} = \frac{\partial \rho\,\overline{u_y}}{\partial \theta} = \frac{\partial \rho\,\overline{u_z}}{\partial \theta} = 0. \tag{2 E}$$

Since the external fields are neglected,

$$\Phi_x = \Phi_y = \Phi_z = 0. \tag{3 E}$$

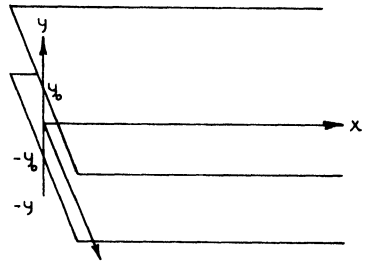

FIG. V-20. Schematic diagram for idealized turbulent flow between parallel plates.

Except for pressure, the average conditions in the flow are presumably independent of x and z so that

$$\frac{\partial \rho\,\overline{u_x}\,\overline{u_x}}{\partial x} = \frac{\partial \rho\,\overline{u_{xf}\,u_{xf}}}{\partial x} = \frac{\partial \rho\,\overline{u_{zf}\,u_{xf}}}{\partial z} = \frac{\partial \rho\,\overline{u_{xf}\,u_{yf}}}{\partial x}$$

$$= \frac{\partial \rho\,\overline{u_{zf}\,u_{yf}}}{\partial z} = \frac{\partial \rho\,\overline{u_{xf}\,u_{zf}}}{\partial x} = \frac{\partial \rho\,\overline{u_{zf}\,u_{zf}}}{\partial z} = 0. \tag{4 E}$$

Even if the independence of the average conditions from x and z is not employed, the third, fifth, and sixth members are zero since

$$\overline{u_{zf}\,u_{xf}} = \overline{u_{zf}\,u_{yf}} = \overline{u_{xf}\,u_{zf}} = 0 \tag{5 E}$$

and because the z fluctuations in velocity are independent of the x and y fluctuations, i.e., for a given x or y fluctuation, the probability of a given positive or negative z fluctuation is the same so that the average of each of the products is zero.

From Eqs. (V.70), (V.71), and (V.72), the Reynolds transformation yields

$$\overline{\tau_{zx}} = \overline{\tau_{xz}} = 0, \tag{6 E}$$

$$\overline{\tau_{zy}} = \overline{\tau_{yz}} = 0, \tag{7 E}$$

$$\overline{\tau_{xy}} = \overline{\tau_{yx}} = \overline{\eta}\,\frac{\partial \overline{u_x}}{\partial y} \tag{8 E}$$

provided the pressure and especially the temperature fluctuations are not severe enough to cause appreciable changes in the viscosity.

Therefore Eq. (V.142) becomes

$$\frac{\partial \overline{\tau_{xx}}}{\partial x} + \frac{\partial \overline{\tau_{yx}}}{\partial y} + \frac{\partial}{\partial y}(-\rho \overline{u_{yf} u_{xf}}) = 0. \tag{9 E}$$

Equation (V.143) becomes

$$\frac{\partial}{\partial y}(\overline{\tau_{yy}} - \rho \overline{u_{yf} u_{yf}}) = 0 \tag{10 E}$$

since

$$\frac{\partial \overline{\tau_{xy}}}{\partial x} = 0 \tag{11 E}$$

because of the independence of average conditions from x. Similarly, Eq. (V.144) becomes

$$\frac{\partial \overline{\tau_{zz}}}{\partial z} = 0. \tag{12 E}$$

From Eqs. (V.77), (V.78), (V.79), and (V.82) since the fluid is incompressible

$$\overline{\tau_{xx}} = -\overline{P} + 2\overline{\eta}\frac{\partial \overline{u_x}}{\partial x}, \tag{13 E}$$

$$\overline{\tau_{yy}} = -\overline{P}, \tag{14 E}$$

$$\overline{\tau_{zz}} = -\overline{P}. \tag{15 E}$$

Either from the independence of conditions from x or the equation of continuity, Eq. (V.135), there results

$$\frac{\partial \overline{u_x}}{\partial x} = 0. \tag{16 E}$$

Consequently

$$\overline{\tau_{xx}} = \overline{\tau_{yy}} = \overline{\tau_{zz}} = -P. \tag{17 E}$$

Combining Eq. (10 E) with (17 E) gives

$$\frac{\partial \overline{P}}{\partial y} + \frac{\partial \rho \overline{u_{yf} u_{yf}}}{\partial y} = 0 \tag{18 E}$$

or, as may be noted here, the average pressure in the y-direction is a function of the change in turbulence in the y-direction as obtained in the second term where the potential field is neglected. Upon differentiating Eq. (18 E) with respect to x and reversing the order of differentiation, there is obtained

$$\frac{\partial}{\partial y}\left(\frac{\partial \overline{P}}{\partial x}\right) + \frac{\partial}{\partial y}\left(\frac{\partial \rho\, \overline{u_{yf}\, u_{yf}}}{\partial x}\right) = 0. \tag{19 E}$$

However, from the independence condition,

$$\frac{\partial \rho\, \overline{u_{yf}\, u_{yf}}}{\partial x} = 0. \tag{20 E}$$

Therefore

$$\frac{\partial}{\partial y}\left(\frac{\partial \overline{P}}{\partial x}\right) = 0. \tag{21 E}$$

Upon differentiating Eq. (12 E) with respect to x, reversing the order of differentiation and substituting Eq. (17 E), the result is

$$\frac{\partial}{\partial z}\left(\frac{\partial \overline{P}}{\partial x}\right) = 0 \tag{22 E}$$

so that $\partial \overline{P}/\partial x$ is a function only of x, if that. Also

$$\frac{\partial \overline{P}}{\partial z} = 0. \tag{23 E}$$

Equation (9 E) becomes, on substituting Eqs. (17 E) and (8 E),

$$-\frac{\partial \overline{P}}{\partial x} + \frac{\partial}{\partial y}\left(\overline{\eta}\,\frac{\partial \overline{u_x}}{\partial y}\right) - \frac{\partial}{\partial y}\left(\rho\, \overline{u_{yf}\, u_{xf}}\right) = 0 \tag{24 E}$$

which, upon differentiation with respect to x, shows that $\partial^2 \overline{P}/\partial x^2$ is zero and thus $\partial \overline{P}/\partial x$ is a constant. Integrating Eq. (24 E) with respect to y, since $\partial \overline{P}/\partial x$ is not a function of y,

$$\rho\, \overline{u_{yf}\, u_{xf}} = -y\,\frac{\partial \overline{P}}{\partial x} + \overline{\eta}\,\frac{\partial \overline{u_x}}{\partial y} + A(x) \tag{25 E}$$

where $A(x)$ is an arbitrary function of x. When

$$y = 0 \tag{26 E}$$

for a given fluctuation in u_x, there is an equal probability of a positive or negative fluctuation in u_y because of the symmetry of the flow, so that the average of $u_{yf}\,u_{xf}$ is zero. Therefore, since by symmetry

$$\frac{\partial \overline{u}_x}{\partial y} = 0 \qquad \text{at} \qquad y = 0, \tag{27 E}$$

$$A(x) = 0. \tag{28 E}$$

Then, finally, the Reynolds stress may be expressed

$$-\rho\,\overline{u_{yf}u_{xf}} = y\frac{d\overline{P}}{dx} - \overline{\eta}\frac{\partial \overline{u}_x}{\partial y}. \tag{29 E}$$

Nomenclature

$A(x)$	An arbitrary function of x
a_r	Acceleration in the r-direction, ft./sec.^{2}
a_x	Acceleration in the x-direction, ft./sec.^{2}
a_y	Acceleration in the y-direction, ft./sec.^{2}
a_z	Acceleration in the z-direction, ft./sec.^{2}
a_ϕ	Acceleration in the ϕ-direction, ft./sec.^{2}
a_ψ	Acceleration in the ψ-direction, ft./sec.^{2}
$B(x)$	An arbitrary function of x
C	An arbitrary constant
D	An arbitrary constant
Eu	Euler number, dimensionless
Fr	Froude number, dimensionless
$f(r)$	A function of r alone
G	A general property of the fluid
g_c	Acceleration due to gravity, ft./sec.^{2}
h	Vertical distance above a reference plane, ft.
I	A generalized property of the fluid
L	A general length variable, ft.
m_0	Constant mass of fluid in the element of volume, lb.sec.^{2}/ft.
P	Thermodynamic pressure, lb./ft.^{2}
$R(\theta)$	The volume of the region R at the time θ
r	Radius, ft.
Re	The Reynolds number, dimensionless
T	Thermodynamic temperature, °R.
U_0	Gross velocity, ft./sec.
u	Point vector velocity, ft./sec.
u_r	Velocity in the r-direction, ft./sec.
u_x	Component of velocity in the x-direction, ft./sec.
u_y	Component of velocity in the y-direction, ft./sec.
u_z	Component of velocity in the z-direction, ft./sec.
u_ϕ	Velocity in the ϕ-direction, ft./sec.
u_ψ	Velocity in the ψ-direction, ft./sec.
V	Total volume, ft.^{3}
x	Rectangular Cartesian coordinate, ft. Altitude in polar cylindrical coordinates, ft.
y	Rectangular Cartesian coordinate, ft.
z	Rectangular Cartesian coordinate, ft.
α	Angular acceleration, sec.$^{-2}$ An angle, radians
β	An angle, radians
ζ_x	Component of rate of angular deformation in the x-direction, sec.$^{-1}$
ζ_y	Component of rate of angular deformation in the y-direction, sec.$^{-1}$
ζ_z	Component of rate of angular deformation in the z-direction, sec.$^{-1}$
η	Absolute viscosity, lb.sec./ft.^{2}

θ Time, sec.
λ A viscosity coefficient, lb.sec./ft.^{2}
ν Kinematic viscosity, ft.^{2}/sec.
ξ_i ith component of an arbitrary vector field
ρ Density, lb.sec.^{2}/ft.^{4}
Σ Surface of the region R
σ Specific weight, lb./ft.^{3}
τ_{ij} ijth component of stress, lb./ft.^{2}
Φ_r Component of acceleration due to conservative external field of force in the r-direction, ft./sec.^{2}
Φ_x Component of acceleration due to conservative external field of force in the x-direction, ft./sec.^{2}
Φ_y Component of acceleration due to conservative external field of force in the y-direction, ft./sec.^{2}
Φ_z Component of acceleration due to conservative external field of force in the z-direction, ft./sec.^{2}
Φ_ϕ Component of acceleration due to conservative external field of force in the ϕ-direction, ft./sec.^{2}
Φ_ψ Component of acceleration due to conservative external field of force in the ψ-direction, ft./sec.^{2}
ϕ Colatitude, radians
ψ Azimuth, radians
Ω Potential of conservative external field of force, ft.^{2}/sec.^{2}
ω_r Component of angular velocity in the r-direction, sec.$^{-1}$
ω_x Component of angular velocity in the x-direction, sec.$^{-1}$
ω_y Component of angular velocity in the y-direction, sec.$^{-1}$
ω_z Component of angular velocity in the z-direction, sec.$^{-1}$
ω_ϕ Component of angular velocity in the ϕ-direction, sec.$^{-1}$
ω_ψ Component of angular velocity in the ψ-direction, sec.$^{-1}$
d Operator for total derivative
$D/D\theta$ Operator for substantial differentiation
$d/d\theta$ Operator for total differentiation with respect to time. Also operator for substantial differentiation when dx/d, dy/d, dz/d are identified with components of hydrodynamic velocity
$\delta/\delta\theta$ Operator for intrinsic differentiation with respect to time
$\iint_\Sigma$ Integral over the entire surface of the boundary of the region R
$\iiint_R$ Integral over the entire space occupied by the region R
$-$ Time-average value, used over a symbol

SUBSCRIPTS AND SUPERSCRIPTS

Distinguishes the values of a variable at two different points
Indicates the dimensionless form of a variable
ave An arithmetical average as distinct from a time average
f Indicates a fluctuation value
i Instantaneous
o Indicates a constant or a characteristic value of a variable usually taken at the boundary of the stream
P Differentiation at constant P
r Differentiation at constant r
r-component
T Differentiation at constant T
x Differentiation at constant x
x-component
y Differentiation at constant y
y-component
z Differentiation at constant z
z-component
θ Differentiation at constant θ
ϕ Differentiation at constant ϕ
ϕ-component
ψ Differentiation at constant ψ
ψ-component
1 Indicates a boundary condition
2 Indicates a boundary condition

References

1. Eckart, C., *Phys. Rev.* **58**, 919 (1940).
2. Eckart, C., *Phys. Rev.* **58**, 269 (1940).
3. Lamb, H., "Hydrodynamics," p. 4. Dover, New York, 1945.
4. Wilson, E. B., "Advanced Calculus," p. 341. Ginn, New York, 1912.
5. Burington, R. S., and Torrance, C. C., "Higher Mathematics," p. 264. McGraw-Hill, New York, 1939.
6. Milne-Thomson, L. M., "Theoretical Hydrodynamics," p. 64. Macmillan, New York, 1938.
7. Phillips, H. B., "Vector Analysis." Wiley, New York, 1933.
8. Gibbs, J. W., and Wilson, E. B., "Vector Analysis." Yale U. P., New Haven, 1925.
9. Margenau, H., and Murphy, G. M., "The Mathematics of Physics and Chemistry," Chapter 5. Van Nostrand, New York, 1943.
10. "Smithsonian Mathematical Formulae" (E. P. Adams, ed.). Smithsonian Institute, Washington, D. C., 1922.
11. Page, L., "Introduction to Theoretical Physics." Van Nostrand, New York, 1935.
12. Frank, P., and von Mises, R., "Die Differential- und Integralgleichungen der Mechanik und Physik," p. 374. Vieweg, Braunschweig, 1925.
13. Timoshenko, S., and Young, D. H., "Engineering Mechanics." McGraw-Hill, New York, 1937.
14. Prager, W., "Theory of Plasticity." Brown Univ., Providence, Rhode Island, 1941.
15. Burk, R. E. (ed.), "The Chemistry of Large Molecules." Interscience, New York, 1943.
16. Love, A. E. H., "A Treatise on the Mathematical Theory of Elasticity." Cambridge U. P., New York, 1934.
17. McConnell, A. J., "Applications of the Absolute Differential Calculus." Blackie, London, 1931.
18. Lass, H., "Vector and Tensor Analysis." McGraw-Hill, New York, 1950.
19. Lamb, H., *op. cit.* (reference *3*), p. 1.
20. Chapman, S., and Cowling, T. G., "The Mathematical Theory of Nonuniform Gases." Cambridge U. P., New York, 1953.
21. Lamb, H., *op. cit.* (reference *3*), p. 645.
22. Kirkwood, J. G., and Crawford, B., Jr., *J. Phys. Chem.* **56**, 1048 (1952).
23. Boelter, L. M. K., Cherry, V. H., and Johnson, H. A., "Heat Transfer, University of California Syllabus Series." Univ. of California Press, Berkeley, 1936.
24. Goldstein, S., "Modern Developments in Fluid Dynamics," Vol. 1. Oxford U. P., New York, 1938.
25. Churchill, R. V., "Fourier Series and Boundary Value Problems." McGraw-Hill, New York, 1941.
26. Churchill, R. V., "Modern Operational Mathematics in Engineering." McGraw-Hill, New York, 1944.
27. Carslaw, H. S., and Jaeger, J. C., "Operational Methods in Applied Mathematics." Oxford U. P., New York, 1947.
28. Bateman, H., "Partial Differential Equations of Mathematical Physics." Dover, New York, 1944.
29. Courant, R., and Hilbert, D., "Methods of Mathematical Physics." Interscience, New York, 1953.
30. Hartree, D. R., "Numerical Analysis." Oxford U. P., New York, 1952.

31. Milne, W. E., "Numerical Solutions of Differential Equations." Wiley, New York, 1953.
32. Jordán, K., "Calculus of Finite Differences." Chelsea, New York, 1947.
33. Reynolds, O., *Phil. Trans. Roy. Soc.* **A 186, 123** (1894).
34. Burington, R. S., and Torrance, C. C., *op. cit.* (reference *5*), p. 298.
35. Wilson, E. B., *op. cit.* (reference *4*), p. 27.
36. Millikan, R. A., Roller, D., and Watson, E. C., "Mechanics, Molecular Physics, Heat and Sound." Ginn, New York, 1937.

CHAPTER VI

SOME PROPERTIES OF TURBULENCE

Much has been written about the phenomenon of turbulent flow. Some of the outstanding scientific and engineering personnel of this country and Europe devoted the greater part of their professional career to developing an understanding of the physical nature of turbulence and to describing its characteristics in mathematical terms. Boussinesq (*1*) first suggested a qualitative analog to molecular motion and presented the idea of a turbulent viscosity. Reynolds (*2*) added to the knowledge of the physical characteristics of turbulent flow. Prandtl contributed much to the knowledge of turbulence, and Kármán (*3*) and Taylor (*4*) made some of the first attempts to apply statistics to this random type of phenomenon. Taylor added much to what is known concerning the influence of vorticity upon momentum transport in turbulent flow. The monograph by Batchelor (*5*) outlines the recent progress that has been made in the theory of turbulence.

The review by Liepmann (*6*) points the way to new approaches to this difficult field of science. Kármán indicated (*7*) that a true mathematical description of turbulence may well await the development of a new branch of mathematics directed to a description of this complicated physical process. No attempt will be made here to consider the recent application of stochastic analysis to turbulence. Wiener (*8*) and Rice (*9*) described the application of random-walk concepts to situations other than turbulence. Liepmann (*6*) summarized the application and limitation of such methods to non-Gaussian processes such as turbulence. It is the purpose of the present discussion to present some of the physical manifestations of turbulence and to describe in an analytical fashion a limited number of the quantitative characteristics. Some quantitative description of the statistical characteristics of turbulence will be included. It is hoped that the discussion of the physical manifestations of turbulence may prove useful to those workers in the field of material and thermal transport who are not familiar with the nature of this phenomenon.

VI-1. Measurement of the Physical Nature of Turbulence

It is an empirical fact that all fluid shear-flow is turbulent at a sufficiently high Reynolds number. It is characterized (*6*) by essentially nonlinear terms in the equations of motion which are associated with the accelerations of transport in Eulerian[1] coordinates. In addition, the viscous terms in the equations of motion are of an order higher than the nonlinear acceleration terms, and, as indicated by Liepmann, the motion is invariably in three dimensions. The variations in the velocity in a fluid stream can best be described by equations of the following form:

$$u_i = \overline{u} + u_f, \tag{VI.01}$$

$$u_{x,i} = \overline{u_x} + u_{x,f}. \tag{VI.02}$$

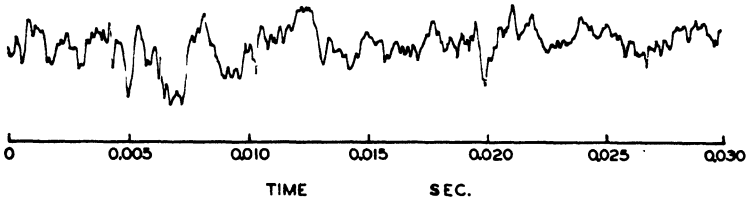

Isotropic turbulence: oscillogram of u-fluctuations 50 inches downstream from a 1.0 inch grid. root-mean-square value = 1.3 percent of mean speed. Mean speed = 50 feet per second.

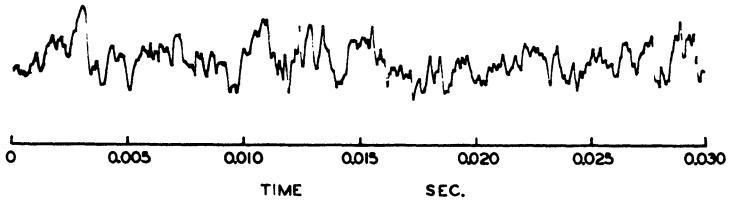

Boundary layer turbulence: oscillogram of u-fluctuations at 0.09 inch from wall in turbulent boundary layer 3 inches thick. root-mean-square value = 8.2 percent of free stream speed. Free stream speed = 50 feet per second.

FIG. VI-1. Sample of Variations in Point Velocity with Time

Equation (VI.01) applies in the direction of flow and subscript x refers to the x-component of the fluid velocity. The description of local turbulence is primarily concerned with the fluctuating velocity u_f.

Figure VI-1 shows an oscillogram of the randomly varying velocities which may be encountered in turbulent flow. Such measurements are

[1] In Euler's coordinates the control surface remains stationary and the system is open in the thermodynamic sense (*10*). The need for care in the application of the conservation of momentum, material, and energy in such systems was indicated by Corrsin (*11*).

obtained by optical methods (*12*) and conventional anemometric techniques (*13—16*).

If it is desired to consider the characteristics of turbulent transport, it is sometimes desirable to treat the time-average value of some scalar quantity such as temperature. Figures VI-2 and VI-3 show, respectively, the temperature distributions around a small heated wire in a turbulently flowing stream confined between parallel plates[1] and in a jet where the flow is nearly potential (*17*). Following the concept of Schubauer (*18*),

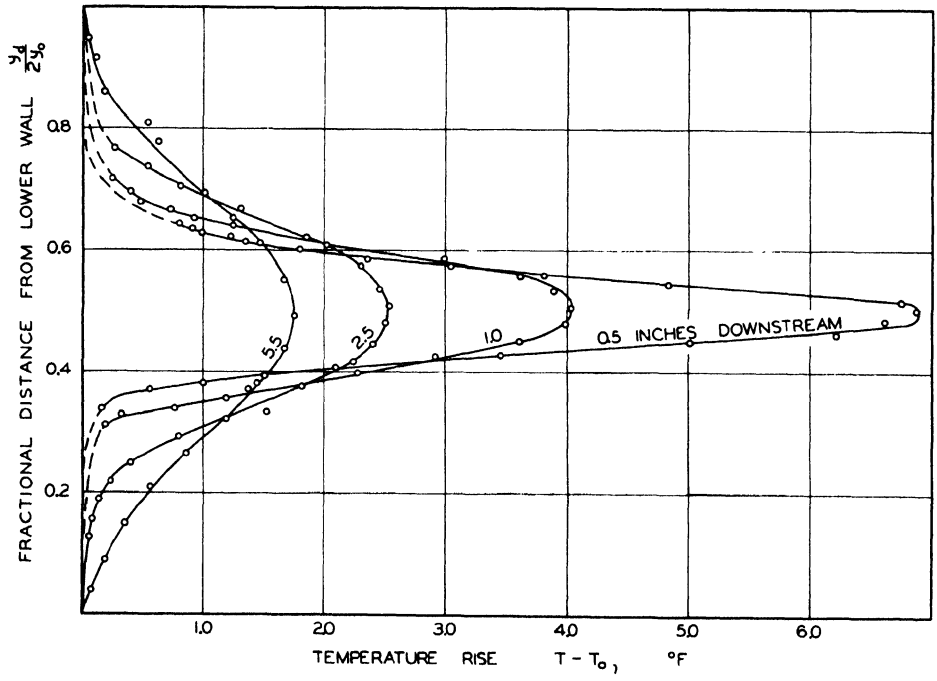

FIG. VI-2. Temperature profile in wake of heated cylinder in turbulent air stream (*17*).

a characteristic width Y_c of each of the profiles may be defined as the width measured perpendicular to the axis of the stream throughout which the temperature rise above that of the stream at a distance from the cylinder is greater than half the maximum value:

$$Y_c = 2\, y_{\Delta t_m/2}. \tag{VI.03}$$

From this definition it follows that one measure of the characteristics of a turbulent stream is established from the angle generated by the characteristic widths of the temperature wake of the wire as is indicated qualitatively

[1] In this instance the cylinder was 0.0318 in. in diameter and was placed in a duct 11 in. wide and 0.70 in. high. It was located 70 in. downstream from the entrance to the duct. The local velocity in the vicinity of the wire was approximately 35 ft./sec. and the bulk air temperature was 100° F.

in Fig. VI-4. It is apparent that the more turbulent the stream the wider the angle formed by the characteristic widths of the stream in the downstream position. It may be shown (*17*) that the characteristic width

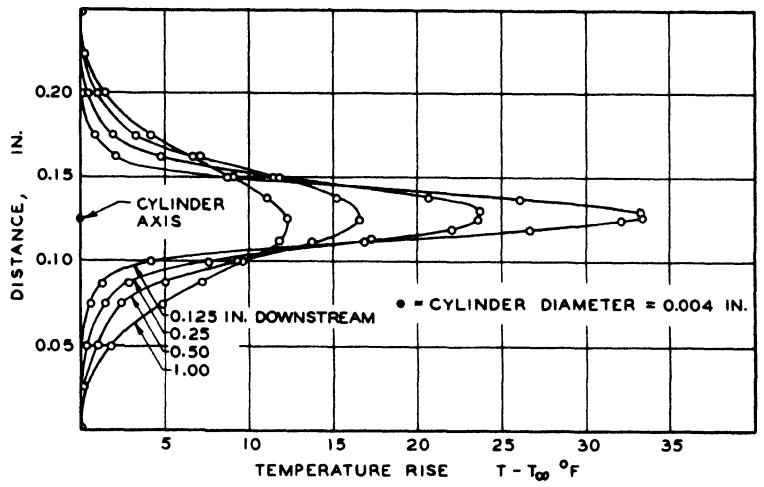

FIG. VI-3. Temperature profile in wake of heated cylinder in jet of air.

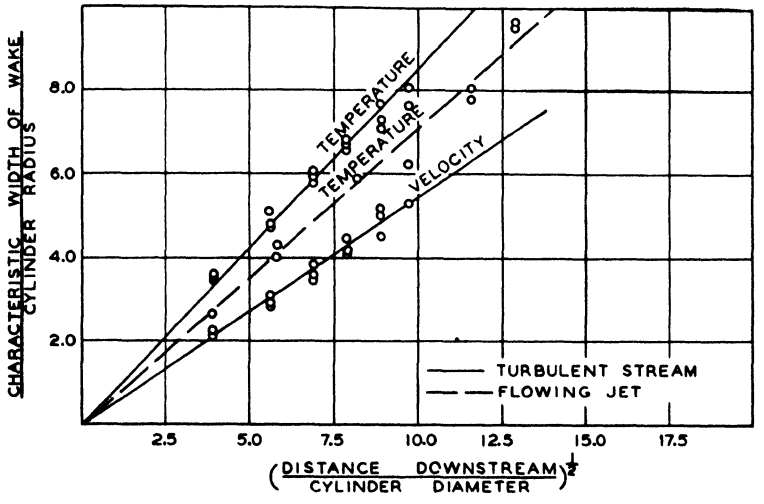

FIG. VI-4. Characteristic width of temperature and velocity profiles.

normalized in terms of the diameter of the cylinder should increase linearly with the square root of the normalized downstream distance. Schubauer (*18*) offered a correlation, shown in Fig. VI-5, between the angular width due to turbulence alone and the intensity of the turbulence measured as ζ, the

ratio of the root-mean-square of the fluctuating velocity and the average point velocity in the direction of flow:

$$\zeta = \frac{\sqrt{\overline{u_{x,f}^2}}}{\overline{u_x}}. \tag{VI.04}$$

Drew (*19*) proposed an analytical expression for the temperature distribution in laminar flow behind a line source in the following form which serves as a useful approximation for the temperature distribution in the wake of a small cylinder:

$$T - T_\infty = \frac{\dot{Q}_L}{2\pi\sigma C_p \kappa} K_0\left\{\frac{U}{2\kappa}\sqrt{x_a^2 + y_a^2}\right\} \exp\left\{\frac{x_a U}{2\kappa}\right\}. \tag{VI.05}$$

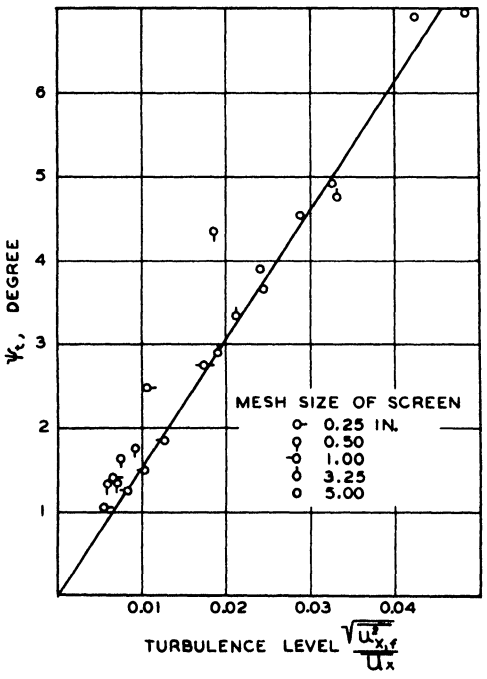

FIG. VI-5. Relation of turbulent angle of divergence to level of turbulence (*18*).

For large values of x_a, this may be simplified to (*17*, *18*)

$$T - T_\infty = \Delta t_m \exp\left\{-\frac{y_a^2 U}{\Delta \kappa x_a}\right\}. \tag{VI.06}$$

This expression assumes a line source and constant velocity, conductivity, and specific heat. It may be written for turbulent flow as

$$T - T_\infty = \Delta t_m \exp\left\{-\frac{y_a^2 U}{4(\kappa + \varepsilon_c) x_a}\right\}. \tag{VI.07}$$

After substituting $x_a \psi_m/(2 \cdot 57.3)$ for the values of y_a at which the temperature rise is equal to half the maximum value and solving for the angle ψ_m, there is obtained

$$\psi_m = 190.8\sqrt{\frac{\kappa}{x_a U}} = 57.3\,\frac{Y_c}{x_a} \tag{VI.08}$$

and the corresponding expression may be written for the eddy transport

$$\psi = 190.8\sqrt{\frac{\kappa + \varepsilon_c}{x_a U}}. \tag{VI.09}$$

Equations (VI.08) and (VI.09) may then be solved for the angle contributed by the turbulence

$$\psi_t = \sqrt{\psi^2 - \psi_m^2}. \tag{VI.10}$$

Figure VI-5 shows Schubauer's results (*18*) for the relation of the level of turbulence to the divergent angle resulting from turbulence defined by Eq. (VI.10). Over a broad range of conditions of turbulence, the data of Fig. VI-5 may be approximated by

$$\zeta = 0.066\,\psi_t = 12.59\sqrt{\frac{\varepsilon_c}{x_a U}}. \tag{VI.11}$$

Townsend (*20, 21*) showed that Schubauer's neglect of turbulent distortion of the diffusing hot spots or sheets can lead to inaccuracies.

VI-2. Correlations

Since turbulence is random in nature, a more detailed discussion of the correlation concept applied to this phenomenon than was given earlier in this volume is worth while. The correlation in the field of isotropic homogeneous turbulence may best be described for present purposes by two-point-correlation tensors which were introduced by Kármán and Howarth (*3, 22*) and discussed by Michal (*23*) and others. An abbreviated discussion of tensors and their application to these and other problems of fluid mechanics and the mathematical development of the concept of correlation are presented in Appendix II. Following the notation of Kármán and Howarth, the pressure correlation for the general turbulent case is $\overline{P(x_1, x_2, x_3)\, P'(x_1 + \xi_1, x_2 + \xi_2, x_3 + \xi_3)}$ and the double and triple velocity correlations are, respectively,

$$\overline{u_f^2}\, R_{ij} = \overline{u_{i,f}(x_1, x_2, x_3)\, u'_{j,f}(x_1 + \xi_1, x_2 + \xi_2, x_3 + \xi_3)}, \tag{VI.12}$$

$$\{\overline{u_f^2}\}^{3/2}\, T_{ijk} = \overline{u_{i,f}(x_1, x_2, x_3)\, u_{j,f}(x_1, x_2, x_3)\, u'_{k,f}(x_1 + \xi_1, x_2 + \xi_2, x_3 + \xi_3)}. \tag{VI.13}$$

The above equations are written for two points $B(x_1, x_2, x_3)$ and $B'(x_1 + \xi_1, x_2 + \xi_2, x_3 + \xi_3)$ and are discussed in Appendix II.

In the case of incompressible flow, Kármán and Howarth (*22*) have shown that

$$\overline{P(x_1, x_2, x_3)\, u'_{j,f}(x_1 + \xi_1, x_2 + \xi_2, x_3 + \xi_3)} = 0, \tag{VI.14}$$

$$\sum_{j=1}^{j=3} \frac{\partial R_{ij}}{\partial \xi_j} = 0, \tag{VI.15}$$

$$\sum_{k=1}^{k=3} \frac{\partial T_{ijk}}{\partial \xi_k} = 0. \tag{VI.16}$$

Thus it may be shown (*14*, *22*, *24—26*) that the dissipative function may be written as

$$\dot{e}_v = \sum_{i=1}^{i=3} \sum_{j=1}^{j=3} \tau_{ij} \frac{\partial u_{i,f}}{\partial x_j} = -15\eta \overline{u_f^2} f''(0) \tag{VI.17}$$

where $f''(0)$ is the second derivative of the longitudinal correlation parameter evaluated at $r = 0$ (see Appendix II).

It is perhaps of interest to note that the same type of correlation functions are found for the temperature. The correlation function for temperature may be expressed as

$$\overline{t_f(x_1, x_2, x_3)\, t_f'(x_1 + \xi_1, x_2 + \xi_2, x_3 + \xi_3)}.$$

This expression is of the same form as that noted for the pressure correlation. The entire problem of correlations is complicated, and, when correlations involving more than two quantities or points are considered, their interpretation becomes difficult. Uberoi (*27*) reviewed the accepted theory of correlations as applied to isotropic turbulence, extended his discussion to the more general field of homogeneous turbulence, and found that the quadruple and double velocity correlations are related in the same way as though the four velocities involved were jointly Gaussian. The results were used in incompressible and homogeneous turbulence to correlate fluctuating static pressures wherein such a pressure correlated with two velocity components at a point (*28*, *29*).

Utilizing the experimental work of Dryden (*30*) and Corrsin (*31*), Kovasznay (*32*) obtained for the case of locally isotropic turbulence reasonable agreement between the calculated and measured second-order correlation as shown in Fig. VI-6. The agreement between theory and experiment appears rather satisfactory in this case which involves only measurements downstream from a grid in a steady air stream. At large distances downstream from the grid marked divergences from Kovasznay's predictions were realized.

Batchelor and Townsend (*33*, *34*) considered correlation during the early and latter stages of the decay of turbulence behind grids and found the same general form of relationship that was recorded by Dryden (*30*) and Corrsin (*31*).

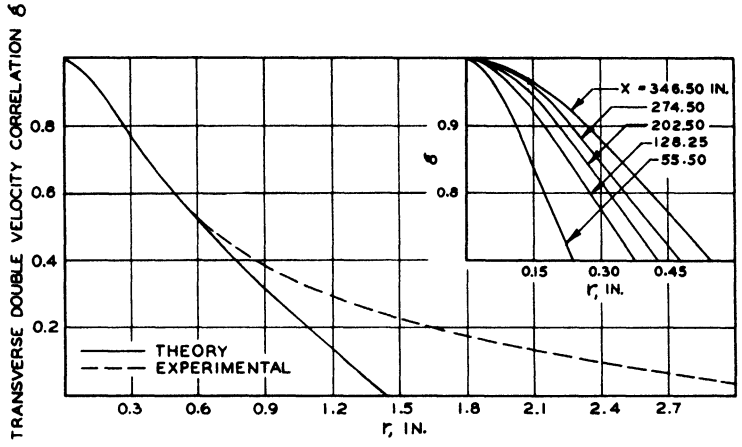

FIG. VI-6. Comparison of experimental and predicted transverse double velocity correlation (*32*).

Isotropic Turbulence

The concept of isotropic turbulence as applied to a turbulent stream with fixed boundaries is not particularly descriptive of the flow conditions encountered. If attention is focused, however, upon a local region the concept of isotropy becomes of general utility. Following the mathematical formulation of quantum mechanics, the Fourier transforms of the correlation functions are usually discussed. In this case the independent variable of position is replaced by one denoting wave number. Kolmogoroff (*35—37*) introduced three hypotheses, the first of which is perhaps one of the most general ideas concerning turbulence that has gained wide acceptance.

Kolmogoroff considered that for large enough Reynolds numbers the small-scale fluctuating motion is always statistically isotropic, irrespective of the nature of the flow. His hypothesis affords an effective description of the transition between the more discrete and nonisotropic turbulence associated with low wave numbers and the motion of the molecules associated with the internal energy of the system in a thermodynamic sense. Kolmogoroff (*35*) also suggested that the energy spectrum of the small-scale turbulence discussed above will not depend upon the details of the flow process but will be dependent upon the magnitude of the dissipation function per unit volume and thus will be associated with the entropy sources of irreversible thermodynamics (*38—40*).

VI-3. Characteristic Properties

The concept of local isotropic turbulence based upon the first similarity hypothesis (*6*) of Kolmogoroff (*35*) was considered in some detail by Kovasznay (*32*), who discussed the mechanism of energy transport between wave numbers under the assumptions that the mechanism is not affected by viscosity and that the energy flux depends only upon the wave number and the spectrum. If the local turbulent velocity components are identified by $u_{x,f}$, $u_{y,f}$, and $u_{z,f}$, it follows from the definition of isotropy that

$$\overline{u_f^2} = \overline{u_{x,f}^2} = \overline{u_{y,f}^2} = \overline{u_{z,f}^2}. \tag{VI.18}$$

A characteristic length of a locally isotropic turbulence is given from dimensional reasoning by Kolmogoroff as

$$l_c = \nu^{3/4}\, \dot{e}_\nu^{1/4}\, \rho^{1/4}. \tag{VI.19}$$

In a similar fashion a characteristic velocity is

$$u_c = \nu^{1/4}\, \dot{e}_\nu^{1/4}\, \rho^{-1/4}. \tag{VI.20}$$

On the basis of Eqs. (VI.19) and (VI.20), the characteristic Reynolds number of the fluctuation, following Kolmogoroff, is unity:

$$\mathrm{Re}_c = \frac{l_c\, u_c}{\nu} = 1 \tag{VI.21}$$

showing that, for motion in which l_c and u_c are representative of the velocity and length, the inertia and viscous forces are of comparable magnitude.

VI-4. Kinetic Energy

The turbulent kinetic energy per unit volume of the isotropic system is defined by

$$\mathcal{E}_\nu = \frac{\sigma}{2\, g_c} (\overline{u_{x,f}^2} + \overline{u_{y,f}^2} + \overline{u_{z,f}^2}) \frac{3\sigma}{2\, g_c} \overline{u_f^2}. \tag{VI.22}$$

In turn, the one-dimensional kinetic-energy spectrum may be defined by the following integral equation in which k is the wave number argument of the Fourier transform $\mathfrak{F}(k)$ of the velocity correlation (*5*):

$$u_f^2 = \int_0^\infty \mathfrak{F}(k)\, dk. \tag{VI.23}$$

The turbulent kinetic energy per unit volume is then given by

$$\mathcal{E}_\nu = \frac{3\sigma}{2g_c}\overline{u_f^2} = \frac{3\sigma}{2g_c}\int_0^\infty \mathcal{F}(k)\,dk. \tag{VI.24}$$

Following dimensional arguments, Liepmann (*6*) indicated that the kinetic-energy spectrum can be expressed in terms of the characteristic length l_c and the phase velocity u_c of Eqs. (VI.19) and (VI.20) for a viscous fluid. Under these circumstances the energy spectrum may be re-expressed as

$$\mathcal{F}(k) = \nu^{5/4}\,\dot{e}_\nu^{1/4}\,\Phi(k\,\nu^{3/4}\,\dot{e}_\nu^{-1/4}). \tag{VI.25}$$

The form of $\phi(k\,\nu^{3/4}\,\dot{e}_\nu^{-1/4})$ is still uncertain. Batchelor (*5*) discusses these matters in greater detail and points out some of the limitations. Independently of Kolmogoroff, Onsager (*39*) proposed that the effect of kinematic viscosity upon the kinetic-energy spectrum must vanish in the spectral region where there is a steady flow rate out of the spectral axes, i.e. steady with respect to k as well as θ. Under these circumstances Heisenberg (*41*) and others (*35—37, 39, 42*) showed that the turbulent spectrum of kinetic-energy may be described as

$$\mathcal{F}(k) = C\,\dot{e}_\nu^{2/3}\,k^{-5/3}. \tag{VI.26}$$

Corresponding relationships may be derived for the correlation but such matters appear beyond the scope of this discussion (*32*).

A description of local isotropic turbulence contributes only indirectly to the basic understanding of momentum transport. As indicated in Eq. (VI.26), the kinetic energy per unit volume of wave-number space associated with the large wave numbers is small. An understanding of the kinetic-energy distribution at large wave numbers, however, is of importance in relating the energy content per unit volume set forth in Eqs. (VI.24) and (VI.26) and the internal energy of the system in a thermodynamic sense. The specific internal energy of a one-component system may be expressed as solely a function of pressure and temperature (*10*).

$$E = \Phi_E(P, T). \tag{VI.27}$$

From the extensive properties of internal energy,

$$E_\nu = \sigma E. \tag{VI.28}$$

The kinetic energy considered in Eqs. (VI.22) and (VI.23) is that associated with turbulence, whereas the dissipation is concerned with that portion of

the turbulent spectrum which contributes directly to the internal energy. In considering the conservation of energy in a system involving decay of turbulence, it is necessary to differentiate clearly between the turbulent energy and the internal energy of the system. The energy balance for turbulent, one-dimensional, gross flow of an incompressible fluid may be written for a unit weight (*43*) as

$$\frac{2}{3}\frac{g_c}{\sigma}\frac{\partial \mathcal{E}_v}{\partial \theta} = \sum_{k=1}^{k=3} \frac{\partial \overline{u^2_{k,f}}}{\partial \theta} = -\sum_{j=1}^{j=3}\sum_{k=1}^{k=3}\left\{\frac{1}{2}\overline{u_j}\frac{\partial \overline{u_{k,f}{}^2}}{\partial x_j} + \overline{u_k\, u_{j,f}}\frac{\partial \overline{u_{k,f}}}{\partial x_j}\right.$$

$$\left. + \frac{1}{2}\frac{\partial}{\partial x_j}\{\overline{u^2_f}\,\overline{u_{j,f}}\} - \overline{u_{k,f}\, u_{j,f}}\frac{\partial \overline{u_k}}{\partial x_j}\right\} \qquad \text{(VI.29)}$$

$$-\sum_{k=1}^{k=3}\left\{\overline{u_{k,f}\frac{\partial P}{\partial x_k}} - \nu\,\overline{u_{k,f}\,\nabla^2 u_{k,f}}\right\}.$$

In Eq. (VI.29) the first term on the right-hand side is the gain in kinetic energy per unit weight as a result of turbulent motion. The second is the increase of turbulent kinetic energy as a result of the slowing down of the stream, whereas the third term represents the net gain in energy as the result of turbulent transport. The next to last term is the work in a thermodynamic sense associated with the fluctuating pressure that is transformed to turbulent energy, whereas the last is the net gain in turbulent energy resulting from viscous forces (*43*).

VI-5. Spectrum of Turbulence

The recent interest in the statistical aspects of turbulence has resulted in the application of spectral concepts to the quantitative evaluation of the fluctuation in velocity. In order to consider the spectrum of turbulence from either a theoretical or experimental point of view, the fluctuations are considered to be made up of a set of components subject to analysis in much the same way as noise (*8*, *9*). It is convenient to consider the wave number k as a function of the gross average velocity and the radial frequency (*8*):

$$k = \frac{2\pi n}{\overline{u}_x}. \qquad \text{(VI.30)}$$

This equation defines in a sense a three-dimensional wave number. In the case of most experimental work it is more convenient to consider only one-

dimensional spectra. The one-dimensional analog of Eq. (VI.30) may be written as

$$k_1 = \frac{2\pi n_1}{\overline{u}_x}. \tag{VI.31}$$

It is also convenient to consider the kinetic-energy spectrum in one dimension on an absolute basis to be defined by the following equation:

$$\mathfrak{F}_1(k_1) = \frac{2}{\pi} \int_0^\infty \overline{u^2}_f R_{11} \exp\{-i k_1 \xi_1\} \, d\xi_1. \tag{VI.32}$$

The three-dimensional kinetic-energy spectrum is related (*5*) to the measurable one-dimensional spectral function as follows:

$$\mathfrak{F}(k) = \frac{k^3}{3} \frac{d}{dk} \left(\frac{1}{k} \frac{d\mathfrak{F}_1(k_1)}{dk} \right). \tag{VI.33}$$

From the basic Fourier transformation of the double correlation tensor

$$\mathfrak{F}_1(k_1) = \frac{2}{\pi} \int_0^\infty \overline{u_f{}^2} f(r) \cos(k_1 r) \, dr, \tag{VI.34}$$

since R_{11} is an even function. In the limit when the wave number approaches zero it is possible to define the longitudinal scale of the fluctuating velocity by

$$L_x = \frac{\pi}{2} \frac{\mathfrak{F}_1(0)}{\overline{u_f{}^2}} = \int_0^\infty f(r) \, dr. \tag{VI.35}$$

If the spectrum is assumed to be independent of the kinematic viscosity, then Kolmogoroff's hypotheses indicate that over a restricted range of k the one-dimensional spectrum is proportional to $k^{-5/3}$ (*6*, *35—37*, *39*). The more recent theory of Kovasznay (*32*) indicates that for a less restricted range of k the kinetic-energy spectrum as a function of wave number may be given by the following somewhat more complicated expression:

$$\mathfrak{F}_1(k_1) = \mathfrak{F}_0 \left(\frac{k_1}{k_0} \right)^{-5/3} \left[1 - \left(\frac{k_1}{k_0} \right)^{4/3} \right]^2 \tag{VI.36}$$

which may be written as

$$\sqrt{\frac{\mathfrak{F}_1(k_1)}{k_1}} = \sqrt{\mathfrak{F}_0 k_0{}^{5/3}} \, k_1{}^{-4/3} - \sqrt{\mathfrak{F}_0 k_0{}^{-1}}. \tag{VI.37}$$

The expression indicates that the parameters $\mathfrak{F}_0$ and k_0 can be obtained from the slope and intercept of $\sqrt{\mathfrak{F}_1(k_1)/k_0}$ as a function of $k_1^{-4/3}$. The relationship between the longitudinal spectrum and the wave number is given in Fig. VI-7. The measurements of Davis (*44*) and Simmons (*46*) were included

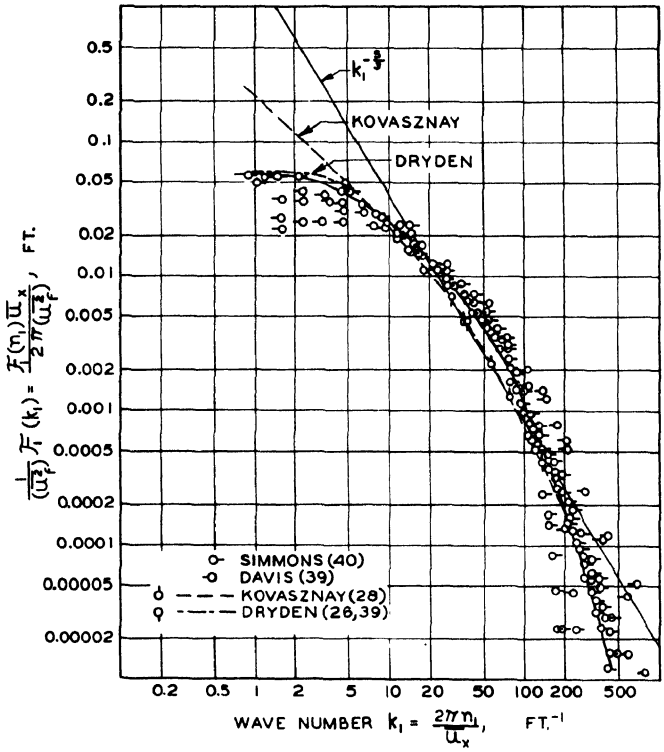

FIG. VI-7. Comparison of experimental and predicted kinetic-energy spectrum of velocity fluctuations (*32, 44, 46*).

for comparison with the theoretical equations of Kolmogoroff, Kovasznay, and Dryden which have been given, respectively, as Eqs. (VI.27), (VI.36), and the following expression:

$$\mathfrak{F}_1(k_1) = \frac{\mathfrak{F}_1(0)}{1 + \dfrac{\pi^2 k_1^2}{4\,\overline{(u_f^2)}}\,[\mathfrak{F}_1(0)]^2}. \tag{VI.38}$$

The approximation of Dryden fits the range of low wave numbers whereas that of Kovasznay describes the spectrum well only at high wave numbers. The values of the empirical parameters of Eq. (VI.36) were determined from the measurements of Simmons (*46*). The solid curve in Fig. VI-7 represents the apparent trend of Simmons' data.

As a matter of interest the spectrum of turbulent kinetic energy is presented in Fig. VI-8 from the measurements of Davis (*44*) for the behavior in the wake of a series of grids. A comparison of the longitudinal and transverse spectrum of the turbulence behind a grid is presented in Fig. VI-9. In this instance it is seen that the transverse kinetic-energy spectrum appears to increase slightly with an increase in wave number before decreasing in the normal manner. The contrast between the longitudinal and the transverse spectrum is a direct mathematical consequence of isotropy and was first noted by Heisenberg (*41*). From the theory of Batchelor (*5*) such behavior does not appear to be unexpected. It is interesting that the work of Davis (*44*) and Townsend and Stewart (*45*) indicates very little effect of grid configuration upon the spectrum of turbulence and the work of Simmons (*46*) appears to confirm that the spectrum of kinetic energy is nearly independent of the gross Reynolds number of the primary flow except at the end of the spectrum having high wave numbers.

Corrsin (*47*) studied the kinetic-energy spectrum of turbulence in jets. The spectrum of an unheated jet one inch in diameter is shown in

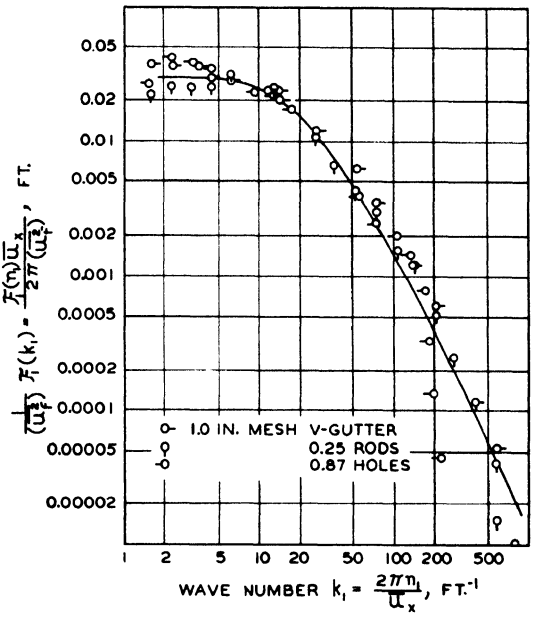

FIG. VI-8. Longitudinal spectrum of kinetic energy in wake of grids for gross velocity of 40 ft./sec. (*44*).

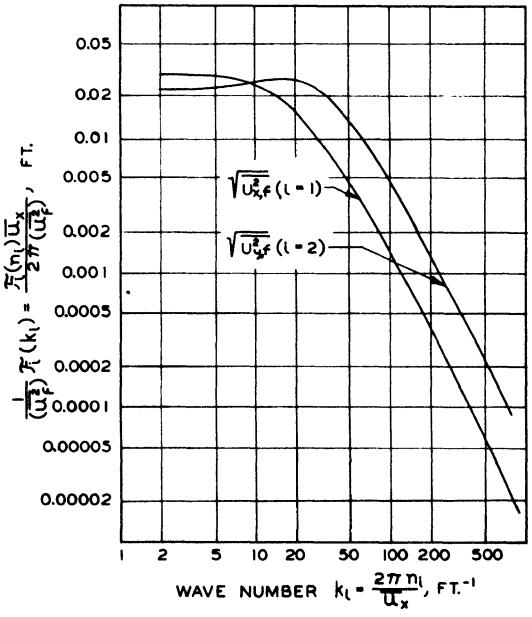

FIG. VI-9. Comparison of longitudinal and transverse kinetic-energy spectrum of turbulence downstream from grid (*44*).

Fig. VI-10. The measurements were made at a distance 20 inches downstream from the beginning of the free jet. There was no significant effect of radial position upon the spectrum since data obtained on the axis of the jet ($r = 0.0$ ft.) and in the region of maximum shear around the periphery ($r = 0.13$ ft.) were nearly identical. For the case of an unheated jet the correlation for the axial-velocity components at points located symmetrically with respect to the axis of flow as a function of radius is shown in Fig. VI-11. Corrsin found a negative correlation over regions remote from the axis of the jet. Such behavior is similar to that found for transverse correlation in isotropic turbulence. A characteristic length L_y of 0.4 in. was found for the transverse velocity correlations in this jet. This quantity represents the area under the curve in Fig. VI-11. The corresponding characteristic scale L_x, which is $\pi/2$ times the value of the one-dimensional spectrum at a wave number of zero, was 1.3 in.

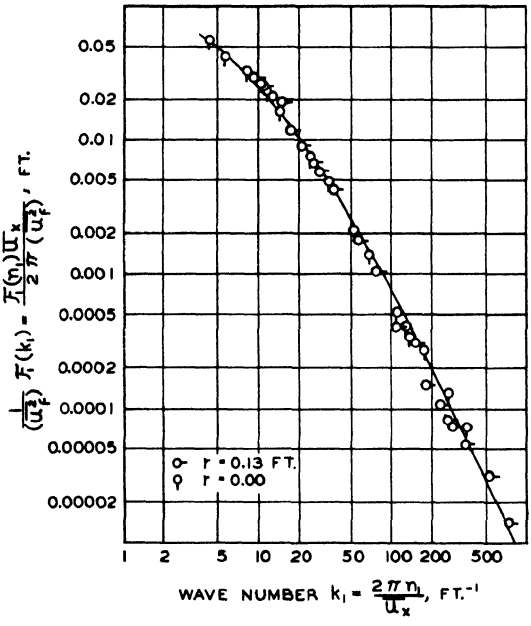

FIG. VI-10. One-dimensional spectrum of kinetic energy of velocity fluctuations in an isothermal jet, 1 in. in diameter (*47*).

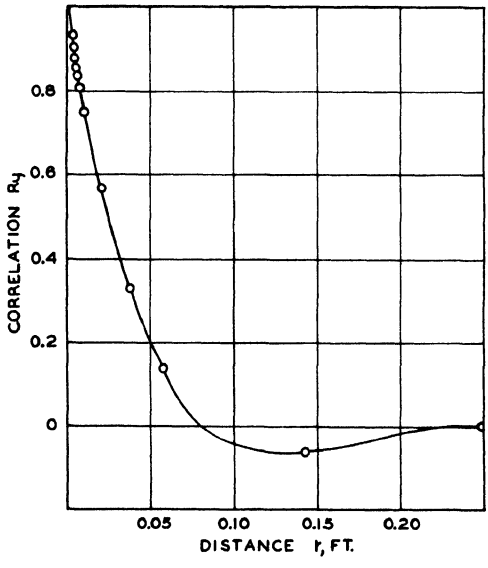

FIG. VI-11. Correlation of symmetric axial velocities measured from axis of isothermal jet (*47*).

Ribner and Tucker (*48*) considered from a theoretical standpoint the effect of contraction in the stream section upon the spectrum of turbulence in an incompressible fluid. They made a Fourier synthesis of Taylor's theory (*49*) which involved assumptions allowing linearization of the problem. Uberoi (*50*) noted that the procedure gave a mod-

erately good prediction of the shift in relative turbulence levels, $u_{x,f}/u_{y,f}$, through moderate contraction ratios. Figure VI-12 shows the estimated differences in the one-dimensional kinetic-energy spectrum taking into account the change in area between the upstream, A, and downstream, B, section. In this instance the spectrum is shown as a function of a dimensionless wave number in which γ_1 is a reducing parameter which should

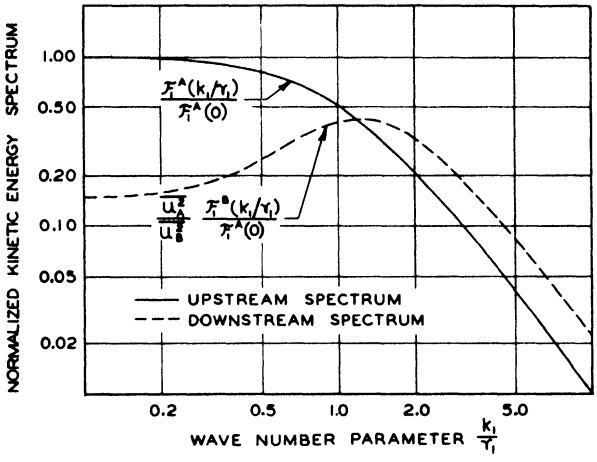

FIG. VI-12. One-dimensional longitudinal kinetic-energy spectrum upstream and downstream of contraction (*48*).

equalize the areas under the two curves if they were replotted on linear scales. The normalized kinetic-energy spectrum at the upstream point is established by the following relationship which is similar to Eq. (VI.38):

$$\frac{\mathcal{F}_1^A\left(\frac{k_1}{\gamma_1}\right)}{\mathcal{F}_1^A(0)} = \frac{1}{1+\left(\frac{k_1}{\gamma_1}\right)^2}. \tag{VI.39}$$

In Fig. VI.12, the ratio of downstream to upstream velocity was 29.8. With the method of correlation proposed in Eq. (VI.39), which was followed by Tucker (*48*), there is a marked difference at the small wave numbers between the upstream and downstream distribution of kinetic energy in the longitudinal spectrum. Such behavior is not surprising since it is improbable that the kinetic energy of the large wave-number components would be influenced by change in section in the same way as the small wave-number components. The predictions of Tucker indicate a substantial shift in the spectrum to the higher wave numbers. In the case of the one-dimensional transverse

spectrum, there was little change as a result of the contraction in section. If the theory proposed by Tucker is correct, these effects should be readily susceptible to experimental measurement.

VI-6. Decay of Turbulence

Turbulence in shear flow statistically reaches a relatively steady state which varies across the section of flow as has been described. If the shear gradients are reduced, however, by decreasing the velocity or by some other means, the magnitude of the turbulence will decrease. Most of the measurements of the decay of turbulence have been based on studies of the behavior downstream from grids inserted in a steady, uniform stream. The grid

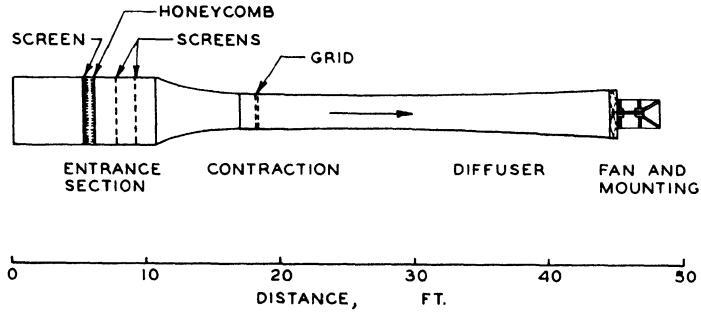

FIG. VI-13. Schematic view of 24 × 24-in. wind tunnel with grids in place (*44*).

introduces a large number of small jets which rapidly blend into a relatively uniform stream of higher intensity of turbulence than is found upstream of the grid, such as that indicated in Fig. VI-13. The variation in velocity with position across the channel is shown in Fig. VI-14 at downstream distances of 3, 5, and 7 in. In this instance the grid was a punched-plate grid with circular openings of 0.875 in. diameter and center spacings of 1 in. (1-in. mesh). It is apparent from Fig. VI-14 that, at a distance of approximately seven times the grid mesh, most of the point-to-point fluctuations in average velocity have been eliminated from the flow.

Davis (*44*, *51*) found from anemometric measurements that turbulence decays gradually and reaches a level of less than 2 per cent at a distance of 50 times the center spacing for the flow conditions shown in Fig. VI-13. There appears to be little difference as to the rate of decay as a result of change in grid form or scale relative to the wind tunnel. Figure VI-15 shows the decay of turbulence based upon a punched-plate grid for the Reynolds numbers varying between 10,000 and 20,000. In this instance the Reynolds

number was calculated for a characteristic length equal to the diameter of the hole in the grid. There was some indication that a small hole in the grid gave a slightly higher level of longitudinal turbulence than was obtained with a grid of larger scale and Corrsin (*52*) showed similar results. Such a behavior is to be expected since the smaller-diameter hole in the grid results in a larger change in static pressure across the grid in the equipment employed. The data submitted in Fig. VI-15 may be compared with the linear decrease in the square of the turbulence level predicted by a number of investigators (*23*, *53*, *54*) and expressed by

$$\frac{U^2}{\overline{u_{x,t}^2}} = \beta\left(\frac{X}{M} - \frac{X_0}{M}\right) = \beta\left(\frac{X}{M}\right) - \alpha_1 . \quad \text{(VI.40)}$$

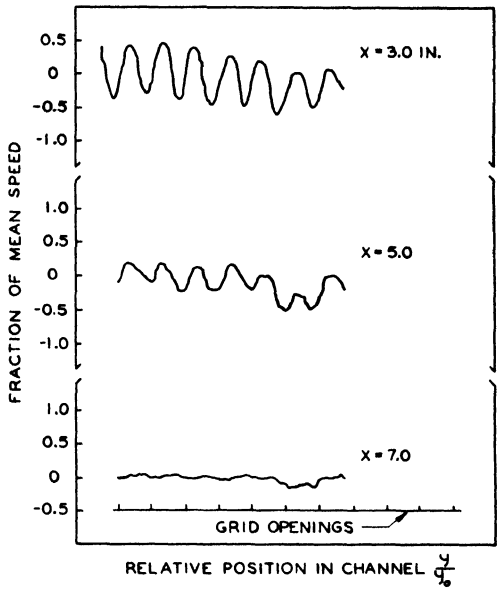

FIG. VI-14. Deviations from mean velocity distribution at three distances downstream from a grid in an air stream (*44*).

The use of the virtual origin (X_0/M) has been emphasized by the two constants β and α_1 in the form after the second equality. Figure VI-16 shows the variation in β of Eq. (VI.40) with downstream position as a function

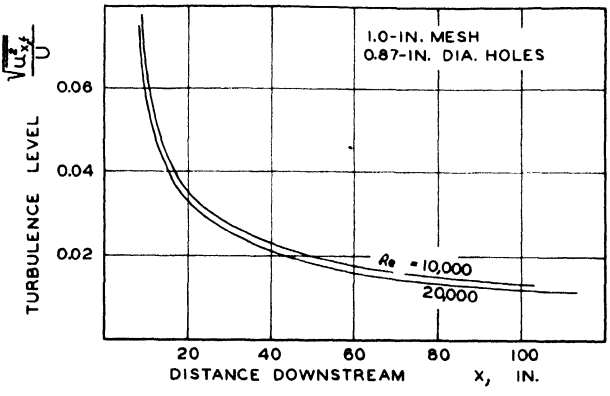

FIG. VI-15. Decay of longitudinal turbulence behind plate grid (*44*).

of the Reynolds number. In the evaluation of β, a value of (X_0/M) of 5 was employed. The agreement with the simple hypothesis of constant β expressed

in Eq. (VI.40) is not as good as might be desired. Kármán and Lin (*54*) and Frenkiel (*55*) suggested that in isotropic turbulence the energy associated with the random motion should decay proportionally to $\theta^{-10/7}$. Under these circumstances Eq. (VI.40) assumes the form

$$\left(\frac{U^2}{\overline{u_{x,f}^2}}\right)^{0.7} = \gamma\left(\frac{X}{M} - \frac{X_0}{M}\right) = \gamma\left(\frac{X}{M}\right) - \alpha_2 . \tag{VI.41}$$

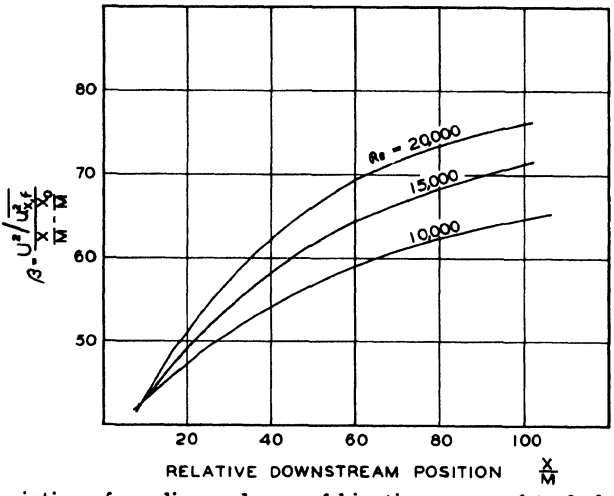

FIG. VI-16. Deviations from linear decay of kinetic energy of turbulence downstream of grid (*44*).

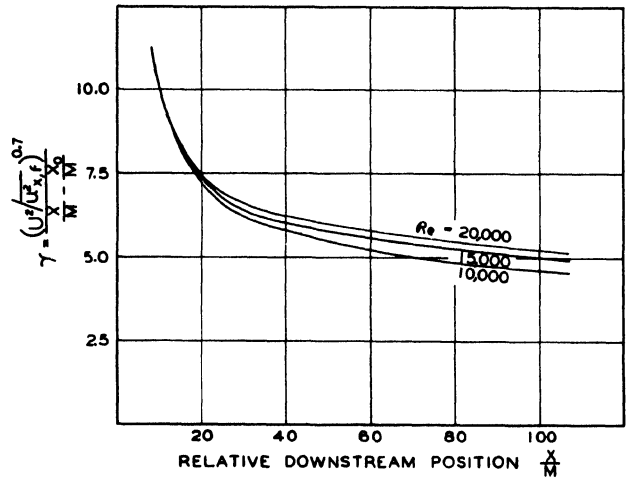

FIG. VI-17. Deviations from 0.7 power decay of kinetic energy of turbulence downstream of grid (*44*).

The variation in γ of Eq. (VI.40) with downstream distance and for different values of the Reynolds number is shown in Fig. VI-17. Equation (VI.41)

does not describe the behavior of the decay over as large a range of downstream distances as was found for Eq. (VI.40). Both Figs. VI-16 and VI-17 were based upon the data of Davis (*44*) for punched grids with 0.875-in. holes upon 1.0-in. centers.

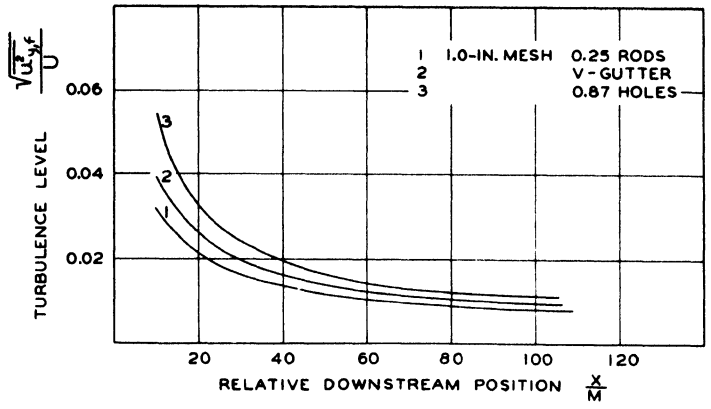

FIG. VI-18. Decay of transverse turbulence with downstream position at the Reynolds number of 20,000 (*44*).

The variations in the transverse random fluctuation at a Reynolds number of 20,000 are shown for three different grid spacings in Fig. VI-18. In this instance there is a rather rapid decrease in the transverse random

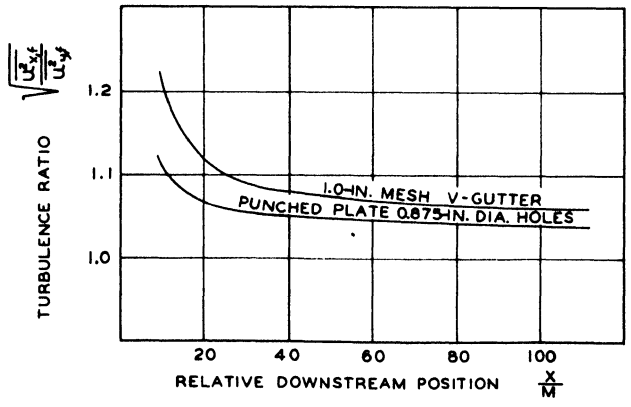

FIG. VI-19. Ratio of longitudinal and transverse turbulence at the Reynolds number of 20,000 (*44*).

velocity with downstream position and with the scale of the grid. Figure VI-19 presents the ratio of the average random fluctuation in the longitudinal and transverse directions. Throughout the decay period the turbulence is not isotropic. This type of behavior was found for other Reynolds numbers and

grid spacings. All the foregoing data were based upon the experimental work of Davis (*44*, *51*). As equilibrium is approached, marked deviations from linear decay of the turbulent kinetic energy with time are encountered. Experimental information was not available to the authors to present in detail the statistical approach to equilibrium, turbulent shear-flow. Equations (VI.40) and (VI.41), together with the data of Figs. VI-17 and VI-18, afford a reasonable means of empirically predicting the decay of turbulence under steady conditions of flow in one direction. There is no assurance that these data describe turbulent decay in two-dimensional flow. Information obtained, however, in connection with the temperature decay in a turbulent wake of a sphere (*56*) indicates that, even under three-dimensional conditions, the decay is not greatly different from that predicted by Eq. (VI.40).

VI-7. Temperature Fluctuations

In the discussion of turbulence, emphasis has been given to the fluctuations in velocity. The description of such behavior requires careful and extended treatment since velocity is a vector quantity and subject to the restrictions associated with vectors. There exist many other types of fluctuations in turbulent flow including temperature and composition. Since these quantities are scalar in nature their treatment can be somewhat simpler. Figure VI-20 shows the random fluctuations of temperature with time in a turbulent wake. These measurements were made at a gross velocity of 8 ft./sec. and at a point 0.125 in. above a heated wire. The measuring instrument was sufficiently coarse so as not to permit the detailed structure of the turbulence to be established.

Corrsin (*57*) applied dimensional considerations to the correlation equation and postulated several expressions for the isotropic, scalar temperature fluctuations for incompressible, homogeneous, isotropic turbulence. From such an approach the following expression was obtained to describe the three-dimensional, scalar temperature fluctuations:

$$\frac{\partial G}{\partial \theta} - 2k^2 K = -2\kappa k^2 G. \tag{VI.42}$$

The three-dimensional spectral-transfer function K may be defined by

$$K(k_1) = -2k_1 \frac{\partial K_1(k_1)}{\partial k_1}. \tag{VI.43}$$

From Eqs. (VI.42) and (VI.43) it follows that

$$\int_0^\infty k^2 K(k)\, dk = 0. \tag{VI.44}$$

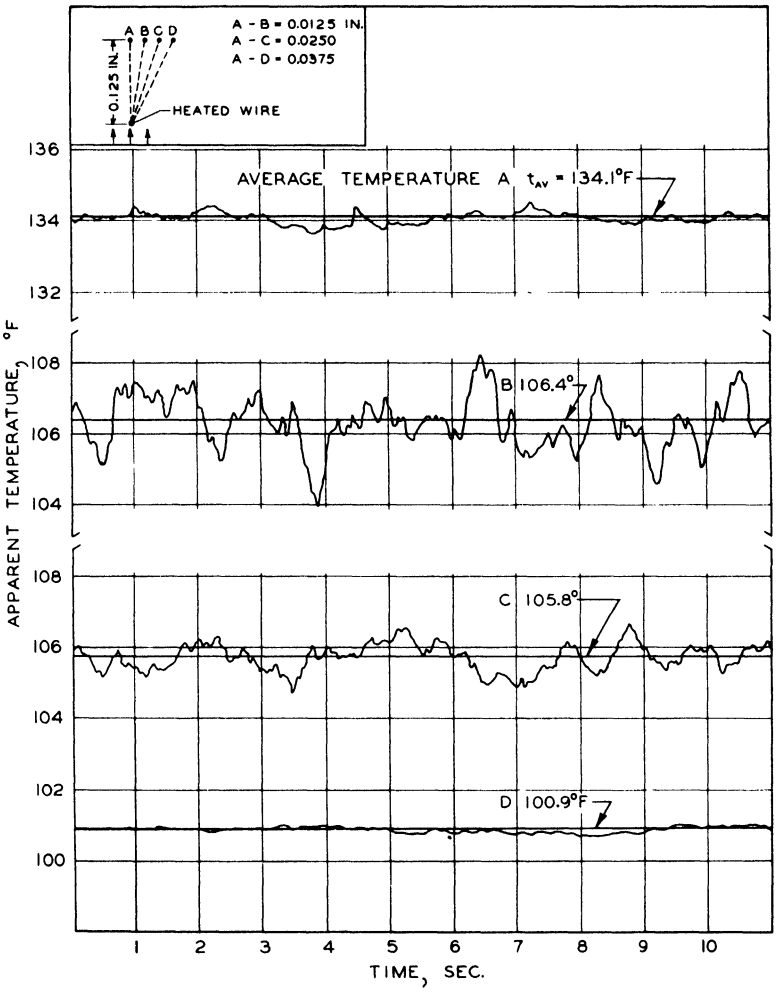

FIG. VI-20. Temperature fluctuations in wake of heated wire.

In Eq. (VI.43) it should be recognized that the subscript 1 applies to the measurable wave number in the one-dimensional spectrum. Equation (VI.42) is similar in many respects to the one which describes the velocity-spectral-transfer function [see Appendix II, Eq. (A II.322)].

At the present state of knowledge it is only possible to obtain a solution to this equation for small Peclet numbers. For many purposes the Peclet number may be defined as

$$\mathrm{Pe} = \mathrm{Re}\,\mathrm{Pr} = \frac{l_c U C_p \sigma}{k}. \tag{VI.45}$$

In this instance Kovasznay *et al.* (*58*) defined a local Peclet number in terms of the microscale of the temperature fluctuation:

$$\mathrm{Pe}_\lambda = \sqrt{\overline{u^2}_{x,t}}\,\lambda_t \frac{C_p \sigma}{k}. \tag{VI.46}$$

The microscale is defined in terms of the one-dimensional temperature spectrum by

$$\lambda_t = \sqrt{1 \Big/ \int_0^\infty k_1^2 G_1\, dk_1}. \tag{VI.47}$$

For small values of the Peclet number, the spectral-transfer term is negligible, and Eq. (VI.42) undergoes a marked simplification to

$$\frac{\partial G}{\partial \theta} = -2\frac{k}{C_p \sigma} k^2 G. \tag{VI.48}$$

This equation accounts only for the molecular conduction and describes the fashion in which an isotropic temperature-fluctuation distribution decays in a homogeneous field.

At extremely low wave numbers near $k_1 = 0$, it is possible to make a power series expansion for the one-dimensional energy

$$G_1(k_1) = G_1(0) + \frac{\partial^2 G_1(0)}{\partial k_1^2}\frac{k_1^2}{2!} + \frac{\partial^4 G_1(0)}{\partial k_1^4}\frac{k_1^4}{4!} + \cdots \tag{VI.49}$$

It should be noted that this form of the series expansion follows from the fact that the spectrum is an "even function." The combination of the analog of Eq. (VI.43) for $G(k)$ and Eq. (VI.49) shows that the following three-dimensional spectrum for low wave numbers is applicable:

$$G(k) = -\frac{\partial^2 G(0)}{\partial k^2}\frac{k^2}{2!} - \frac{\partial^4 G(0)}{\partial k^4}\frac{k^4}{4!} - \cdots \tag{VI.50}$$

It should be noted that the temperature spectrum in the vicinity of a wave number of zero is a parabolic distribution in contrast to the fourth-power

relation of the three-dimensional kinetic-energy spectrum (*33*, *34*) for isotropic velocity fluctuations.

In the high wave-number range, it is possible to establish expressions similar to those developed by Heisenberg (*41*, *51*) for the fluctuating velocity field. Under these circumstances, Corrsin (*57*) showed that for this portion of the temperature spectrum the functional relationship may be approximated by

$$G(k) \sim k^{-7}. \tag{VI.51}$$

This is similar to the seventh-power law for the velocity-fluctuation spectrum and only applies where molecular transport predominates. Further discussions of the significance of Eq. (VI.51) and its analog in the velocity fluctuation field were presented by Chandrasekhar (*60*, *61*).

In the intermediate wave-number range it is considered by analogy with the velocity-fluctuation field that the energy transport through this range of wave numbers is equal to the total rate of dissipation of temperature fluctuation. Under these circumstances, from dimensional reasoning, it follows that

$$G(k) = A\, k^{-5/3}\left[-2\frac{k}{C_p\sigma}\int_0^\infty k^2 G\, dk\right]\left[-2\nu\int_0^\infty k^2 \mathfrak{F}\, dk\right]^{-1/3}. \tag{VI.52}$$

Corrsin estimated that the constant A is of the order of unity (*57*).

The decay of temperature fluctuations was considered by Corrsin (*62*). He presented a rather elegant analysis of a complicated situation making use of an invariant analogous to that proposed by Loitsiansky (*63*) as to the product of the kinetic energy of turbulence and a moment of the velocity correlation. It was only possible to treat the cases of small and large Peclet numbers. In each case it was found that the decay of the temperature fluctuations proceeds more slowly than does the decay of the velocity fluctuations. In arriving at these conclusions Corrsin made use of the approach of Kármán and Howarth (*22*). The reader is referred to the discussion by Corrsin (*62*) for the detailed analysis of the decay of temperature fluctuations and to recent experimental work (*64*) by him and collaborators showing agreement with the theoretical analysis.

Corrsin (*47*) measured the temperature spectrum in a heated jet of air having an orifice diameter of 1 in. The results of these measurements are shown in Fig. VI-21. In this instance there is a noticeably higher value of the spectrum $G_1(k_1)$ on the axis of the jet than is found in the region of

maximum shear near the boundary of the stream. The data shown in Fig. VI-21 were obtained by Corrsin (*47*) at a distance 20 in. downstream from the end of the nozzle. These measurements were made under atmospheric pressure at a total head from between 3 and 5 in. of water. The correlation of the fluctuations in temperature at the same downstream distance is shown in Fig. VI-22. In this instance the correlation function is defined as

$$S_y = \frac{\overline{t_{f,1}\, t_{f,2}}}{\overline{t_f{}^2}}. \tag{VI.53}$$

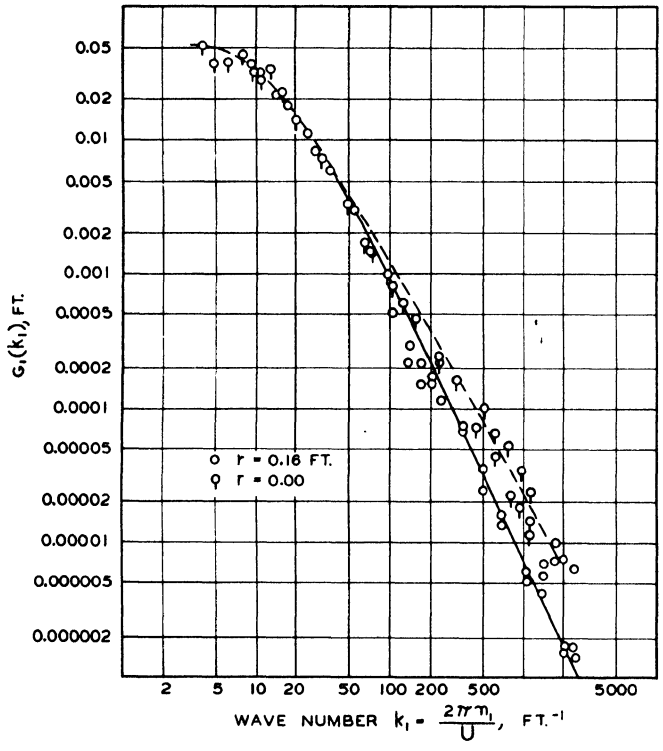

FIG. VI-21. One-dimensional spectrum of temperature fluctuations in a jet, 1 in. in diameter (*47*).

The subscripts 1 and 2 refer to symmetrical positions on opposite sides of the axis of the stream. In this instance there is a negative correlation for all distances greater than 1.3 in. It is of interest to note that the characteristic length Λ_y of the transverse temperature correlation was 0.303 in. which is somewhat larger than the corresponding characteristic correlation length L_y for the fluctuating velocity in the same jet. For the most part, the temperature spectrum yielded a somewhat larger value than was obtained for the

corresponding velocity spectrum. The longitudinal scale of the temperature spectrum may be defined by the following expression:

$$\Lambda_x = \frac{\pi}{2} G_1(0) = 0.86 \text{ in.} \tag{VI.54}$$

The temperature power-spectrum scale as defined by Eq. (VI.54) is somewhat smaller than the corresponding velocity power-spectrum scale.

Turbulence in Shear Flow

Throughout the following discussion attention will be focused upon the variation in the local characteristics of turbulence in shear flow as a function of position in the channel. The emphasis will be placed upon experimental measurements. The greater part of the experimental background utilized in this presentation will be based upon the work of Laufer (*65*) and experimental measurements made in the authors' laboratory which relate to the eddy properties of an air stream flowing between parallel plates (*66*). It is realized that such an approach does not cover the field exhaustively. Within the limited scope of this book it appears inadvisable to extend this discussion to include generalizations of fluid flow or the extensive background of information now available.

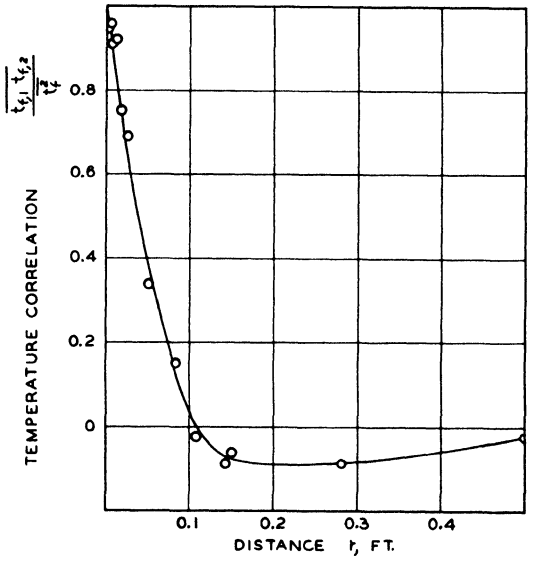

FIG. VI-22. Transverse temperature correlations in a heated jet, 1 in. in diameter (*47*).

VI-8. Eddy Viscosities

In considering the steady, uniform flow of a fluid under laminar conditions, the kinematic viscosity may be related to the velocity gradient by an expression of the following form which applies to the flow between parallel plates:

$$\nu = \frac{g_c}{\sigma} \frac{\tau_{yx}}{\left(\frac{du_x}{dy}\right)}. \tag{VI.55}$$

In a similar fashion, for flow in circular conduits, there is obtained

$$\nu = \frac{g_c}{\sigma} \frac{\tau_{rx}}{\left(\frac{du_x}{dr}\right)}. \tag{VI.56}$$

Analogous extensions of these relationships to include turbulent flow may be made. Boussinesq (*1*) first qualitatively suggested the idea, and others such as Kármán (*67*) and Taylor (*68*) expanded the concept. The so-called total viscosity for flow between parallel plates may then be defined as

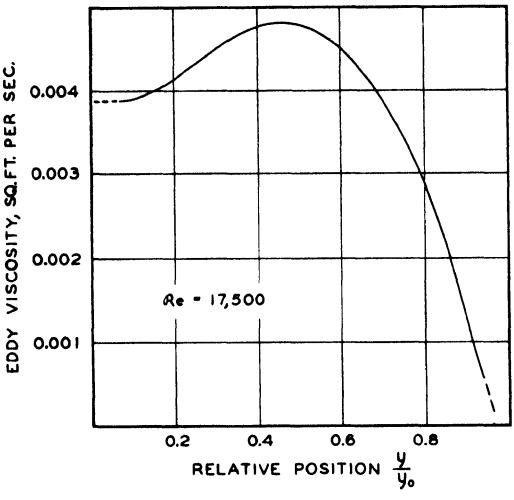

FIG. VI-23. Eddy viscosity as function of position in shear flow between parallel plates.

$$\epsilon_m = \frac{g_c}{\sigma} \frac{\tau_{yx}}{\left(\frac{du_x}{dy}\right)}. \tag{VI.57}$$

An expression analogous to Eq. (VI.57) exists for flow in a circular conduit. It is apparent that Eq. (VI.57) reduces to Eq. (VI.55) for laminar flow. For some purposes it is convenient to define the eddy viscosity as the difference between the total and kinematic viscosities as indicated in the following equation:

$$\varepsilon_m = \epsilon_m - \nu = \frac{g_c}{\sigma} \frac{\tau_{yx}}{\left(\frac{du_x}{dy}\right)} - \nu = \frac{g_c}{2\sigma y_0} \frac{(\tau_{yx})_0}{\left(\frac{du_x}{d(y^2)}\right)} - \nu. \tag{VI.58}$$

The variation in the eddy viscosity with position for the flow between parallel plates of air is shown in Fig. VI-23. This behavior is characteristic of all turbulent flows with incompressible fluid. The eddy viscosity is zero at the wall but increases rapidly to a maximum roughly midway between the wall and the center of the conduit.

Since both the shear and the velocity gradient vanish at the center of the channel, the ratio of these two quantities becomes indeterminate. If use is made of the fact that the shear varies linearly with position in the channel, this ratio and the eddy viscosity can be evaluated at the center of the channel by using the last terms in Eq. (VI.58).

Experimental work concerning the thermal transport across a turbulent stream (*69—71*) has indicated that the eddy conductivity is finite in the center of the stream. It may be shown (*69*) that the turbulent Prandtl number is related to the ratios of the total viscosity and total conductivity and molecular properties of the fluid stream as follows:

$$\mathrm{Pr}_e = \frac{\varepsilon_m}{\varepsilon_c} = \frac{\epsilon_m}{\epsilon_c}\left(1 + \frac{\kappa}{\varepsilon_c}\right) - \frac{\nu}{\varepsilon_c}. \tag{VI.59}$$

It appears most likely that the turbulent Prandtl number at the center of the stream will be similar to that at other points of the stream remote from the solid boundary.

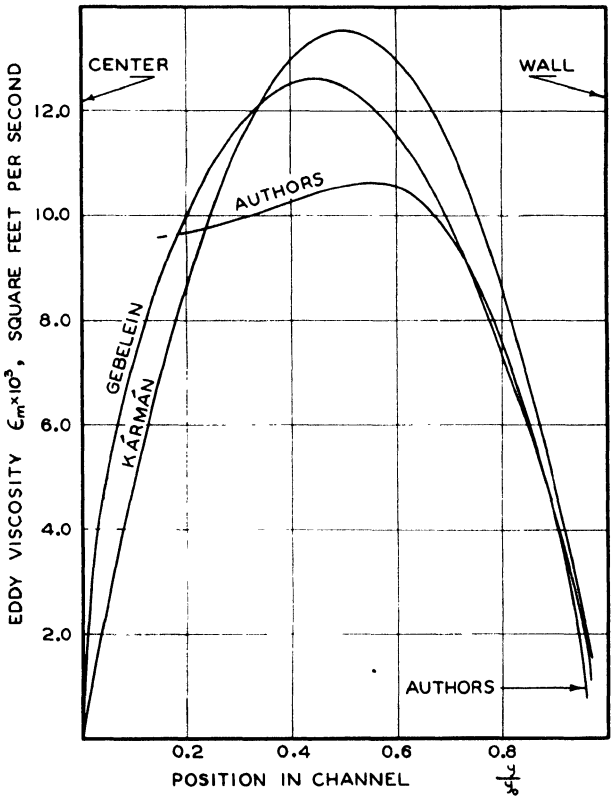

FIG. VI-24. Comparison of experimental and predicted eddy viscosity (*69*).

The behavior shown in Fig. VI-23 is in conflict with the prediction of Kármán (*67*) and of Prandtl (*72*) as is shown in Fig. VI-24. Both Kármán and Prandtl predicted zero values for the eddy viscosity at the center of the conduit which does not agree with the experimental information now available. In addition, Gebelein's (*73*) statistical predictions indicate a zero

value for the eddy viscosity at the center of the channel. It appears that this rather marked disagreement between theory and experiment in the case of eddy viscosity is one of the primary deficiencies in the earlier turbulence theory.

For many purposes it is convenient to consider a relative viscosity which is defined by

$$\epsilon_r = \frac{\epsilon_m}{\nu}. \tag{VI.60}$$

The relative viscosity is the ratio of the total viscosity to the kinematic viscosity and may be evaluated using equations that have been developed for correlation of velocities. Experimental data from Skinner (*74*), Deissler (*75*), and Nikuradse (*76*) have been generalized in terms of the velocity parameter u^+. The behavior in the laminar and transition boundary flow was described by

$$u^+ = \frac{1}{\sqrt{K_1}} \tanh\left(y_d^+ \sqrt{K_1}\right) = \frac{1}{0.0695} \tanh\left(0.0695\, y_d^+\right). \tag{VI.61}$$

This involved the proposal of Rannie, described by Dunn (*77*), concerning the relationship of u^+ and y_d^+ in the transition of boundary flow. In the fully developed turbulent stream the following expression was employed:

$$u^+ = K_3 + \frac{1}{K_2} \ln\left(y_d^+\right) = 5.5 + \frac{1}{0.4} \ln\left(y_d^+\right). \tag{VI.62}$$

The values of the coefficients shown in Eqs. (VI.61) and (VI.62) were based upon the experimental work described above. Equation (VI.61) is the same as Eq. (IV.07), and Eq. (VI.62) is the generalization of Eq. (IV.03). These relationships are not suitable for use with the Reynolds numbers below 20,000 (*78*), where it is necessary to take into account the influence of the Reynolds number upon the relationship of u^+ and y_d^+. At the higher Reynolds numbers, however, they yield the following expressions relating the relative viscosity to the gross velocity and the Fanning friction factor, which was described in Chapter III:

$$\begin{aligned} \frac{\epsilon_m}{\nu} = \frac{\epsilon_m + \nu}{\nu} &= \frac{y}{y_0} \cosh^2\left\{0.0695 \left(\frac{y_0 - y}{\nu}\right) \sqrt{(\tau_{yx})_0 \frac{g_c}{\sigma}}\right\} \\ &= \frac{y}{y_0} \cosh^2\left\{0.0695 \left(\frac{y_0 - y}{\nu}\right) U \sqrt{\frac{f}{2}}\right\}. \end{aligned} \tag{VI.63}$$

$$\frac{\epsilon_m}{\nu} = \frac{0.4}{\nu} \sqrt{(\tau_{yx})_0 \frac{g_c}{\sigma}} \left(\frac{y}{y_0}\right)(y_0 - y) = 0.4 \frac{U}{\nu} \sqrt{\frac{f}{2}} \left(\frac{y}{y_0}\right)(y_0 - y). \tag{VI.64}$$

Equation (VI.63) is applicable to the values of y_d^+ as large as 27 whereas Eq. (VI.61) may be employed from the edge of the boundary flow to approximately 2/3 of the way from the wall to the center of the conduit. Since Eq. (VI.64) is based on the logarithmic distribution shown in equation (VI.62), it yields a zero value for the relative viscosity at the center of the conduit. For this reason it is recommended that Eq. (VI.64) should not be used in the central third of the conduit and that it should be assumed constant throughout this region at a value corresponding to

$$\frac{y}{y_0} = 0.3 \tag{VI.65}$$

and

$$\frac{r}{r_0} = 0.3. \tag{VI.66}$$

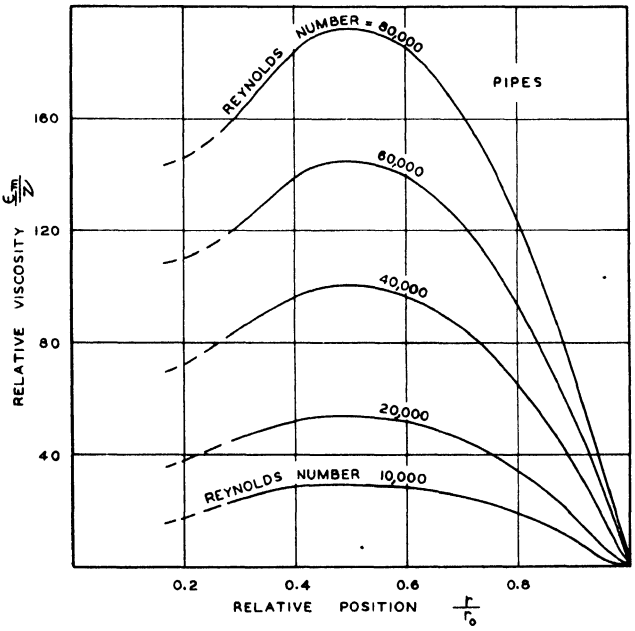

FIG. VI-25. Relative viscosity as a function of position in flow channel (*66*).

The behavior of Eqs. (VI.63) and (VI.64) for cylindrical conduits with y and y_0 replaced by r and r_0 is shown in Fig. VI-25. It is apparent that this behavior is very similar to that shown in Fig. VI-23 which was based upon experimental measurements. The dotted portion of the curve was based upon experimental indications (*66*).

Tables (VI-1) and (VI-2) record values of the relative viscosity for fluids in circular conduits and in flow between parallel plates. The Reynolds

number in circular conduits and parallel-plate conduits, respectively, is defined as

$$\mathrm{Re} = \frac{2\,U r_0}{\nu}, \tag{VI.67}$$

$$\mathrm{Re} = \frac{4\,U y_0}{\nu}. \tag{VI.68}$$

The information recorded in Tables (VI-1) and (VI-2) permits the relative viscosity to be determined from a knowledge of the Reynolds number and the position in the conduit. These values of relative viscosity may be employed to predict the macroscopic velocity distribution in a uniform, steady, turbulent stream from a knowledge of the shear. It should be emphasized that the definitions of the Reynolds number given in Eqs. (VI.67) and (VI.68) are based on the hydraulic radius and thus the relative viscosities differ by a factor of approximately 2 at the same value of the Reynolds number for flow in circular pipes and between parallel plates. The relative viscosities presented for the Reynolds numbers below 20,000 are not strictly applicable inasmuch as the empirical constants were evaluated primarily from information on air streams with the Reynolds numbers greater than this value.

VI-9. Structure of Turbulent Shear-Flow

In spite of the great industrial interest in turbulent shear-flow, only recently has the microscopic investigation of the behavior of turbulence in shear-flow been investigated in detail. Laufer (*65*) made one of the most complete investigations of the detailed characteristics of turbulence in steady, uniform flow of air in a circular conduit that has come to the authors' attention. The following discussion is based primarily on Laufer's measurements and the evaluation of supplemental references. The measurements to be discussed were made in a brass tube, having an outside diameter of 10 in. and a length of approximately 16 ft. The detailed characteristics of turbulence were studied with a platinum-rhodium wire

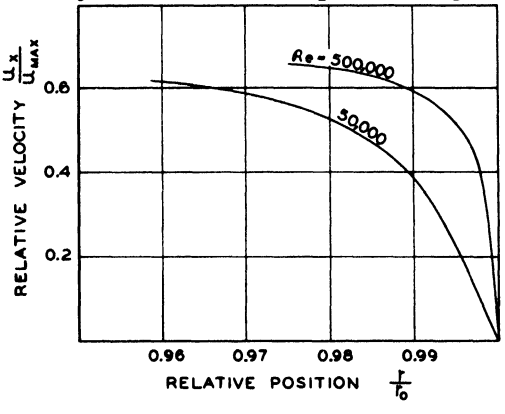

FIG. VI-26. Velocity distribution near wall in turbulent shear flow (*65*).

having a diameter of 0.0001 in. The details of the methods employed are available (*65*, *79*), and will not be given here. Near the wall appropriate corrections were made for the velocity fluctuations and their influence on the mean velocity and pressure measurements. In some instances these corrections amounted to as much as 10 per cent. The turbulence levels were determined by standard methods similar to those introduced by Dryden and Kuethe (*13*) and used by Corrsin and coworkers (*80*). The velocity distributions for a low and a high Reynolds number are shown for flow near the wall in Fig. VI-26. The marked decrease with the increasing Reynolds number of the region associated with boundary flow is clearly evident. The behavior shown in Fig. VI-26 is very similar to that found for other steady, uniform, turbulent flow.

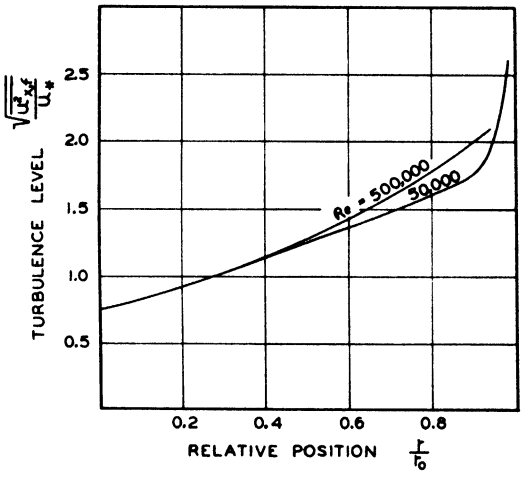

FIG. VI-27. Longitudinal velocity fluctuations in central portion of circular conduit (*65*).

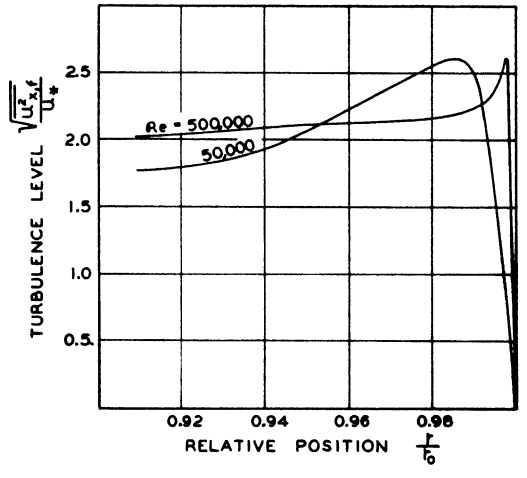

FIG. VI-28. Longitudinal velocity fluctuations near wall of circular conduit (*65*).

Following conventional methods, measurements were made (*65*) of the distribution of the fluctuating velocity and, in Fig. VI-27, it is expressed in terms of the friction velocity. (The friction velocity at Re = 500,000 was 3.5 ft./sec.) It is apparent from the information presented in Fig. VI-27 that the ratio of the fluctuating velocity to the friction velocity is defined by the following expression:

$$\frac{\sqrt{\overline{u^2_{x,f}}}}{u_*} = \sqrt{\frac{\sigma\,\overline{u^2_{x,f}}}{g_c(\tau_{yx})_0}} = \sqrt{\frac{2}{f}}\,\frac{\sqrt{\overline{u^2_{x,f}}}}{U}. \tag{VI.69}$$

The fluctuating velocity decreases as the center of the channel is approached. For all Reynolds numbers the fluctuating velocity shows a rather abrupt

TABLE (VI-1). Relative Viscosities[1] for Steady, Uniform Turbulent Flow in Pipes.

Position	Reynolds Number								
	5,000	7,500	10,000	12,500	15,000	17,500	20,000	25,000	30,000
0.3000	13.40	19.26	24.88	30.43	35.80	41.12	46.31	56.64	66.67
0.3500	14.54	20.92	27.02	33.04	38.87	44.64	50.28	61.50	72.38
0.4000	15.31	22.02	28.44	34.78	40.92	46.99	52.93	64.73	76.19
0.4500	15.82	22.75	29.39	35.94	42.28	48.56	54.69	66.89	78.73
0.5000	15.95	22.93	29.62	36.23	42.62	48.95	55.14	67.43	79.37
0.5500	15.82	22.75	29.39	35.94	42.28	48.56	54.69	66.89	78.73
0.6000	15.31	22.02	28.44	34.78	40.92	46.99	52.93	64.73	76.19
0.6500	14.54	20.92	27.02	33.04	38.87	44.64	50.28	61.50	72.38
0.7000	13.40	19.26	24.88	30.43	35.80	41.12	46.31	56.64	66.67
0.7500	11.99	17.25	22.28	27.24	32.05	36.81	41.46	50.71	59.69
0.8000	10.21	14.68	18.96	23.19	27.28	31.33	35.29	43.16	50.80
0.8400	7.71	12.29	15.88	19.42	22.85	26.24	29.55	36.14	42.54
0.8800	3.60	9.72	12.56	15.36	18.07	20.76	23.38	28.59	33.65
0.9200	1.85	3.42	6.67	10.72	12.62	14.49	16.32	19.96	23.49
0.9600	1.16	1.41	1.77	2.31	3.07	4.15	5.64	10.25	12.06
0.9800	1.03	1.08	1.16	1.25	1.37	1.51	1.68	2.12	2.74
0.9900	1.00	1.02	1.03	1.05	1.08	1.11	1.14	1.22	1.32
0.9920	1.00	1.01	1.02	1.03	1.05	1.07	1.09	1.14	1.20
0.9940	1.00	1.00	1.01	1.02	1.03	1.04	1.05	1.07	1.11
0.9960	1.00	1.00	1.00	1.01	1.01	1.01	1.02	1.03	1.05
0.9970	1.00	1.00	1.00	1.00	1.00	1.01	1.01	1.02	1.02
0.9980	1.00	1.00	1.00	1.00	1.00	1.00	1.00	1.01	1.01
0.9990	1.00	1.00	1.00	1.00	1.00	1.00	1.00	1.00	1.00
0.9995	1.00	1.00	1.00	1.00	1.00	1.00	1.00	1.00	1.00
1.0000	1.00	1.00	1.00	1.00	1.00	1.00	1.00	1.00	1.00

[1] Values are reported as the ratio of the total viscosity to the kinematic viscosity ϵ_m/ν.

TABLE (VI-1) Cont.

Position	Reynolds Number								
	35,000	40,000	45,000	50,000	60,000	70,000	80,000	90,000	100,000
0.3000	76.52	86.32	96.00	105.42	124.48	142.83	161.14	179.30	197.00
0.3500	83.08	93.72	104.23	114.46	135.14	155.07	174.95	194.67	213.89
0.4000	87.46	98.65	109.72	120.48	142.26	163.23	184.16	204.92	225.14
0.4500	90.73	101.94	113.37	124.50	147.00	168.67	190.30	211.75	232.65
0.5000	91.10	102.76	114.29	125.50	148.19	170.03	191.83	213.46	234.53
0.5500	90.37	101.94	113.37	124.50	147.00	168.67	190.30	211.75	232.65
0.6000	87.46	98.65	109.72	120.48	142.26	163.23	184.16	204.92	225.14
0.6500	83.08	93.72	104.23	114.46	135.14	155.07	174.95	194.67	213.89
0.7000	76.52	86.32	96.00	105.42	124.48	142.83	161.14	179.30	197.00
0.7500	68.51	77.28	85.95	94.38	111.44	127.86	144.26	160.52	176.36
0.8000	58.30	65.77	73.14	80.32	94.84	108.82	122.77	136.61	150.10
0.8400	48.83	55.08	61.26	67.27	79.43	91.14	102.82	114.41	125.71
0.8800	38.63	43.57	48.46	53.21	62.83	72.09	81.34	90.51	99.44
0.9200	26.97	30.42	33.83	37.15	43.86	50.33	56.78	63.18	69.42
0.9600	13.85	15.62	17.37	19.08	22.52	25.84	29.16	32.45	35.65
0.9800	3.59	4.77	6.38	8.51	11.85	13.60	15.35	17.08	18.76
0.9900	1.44	1.59	1.76	1.95	2.47	3.15	4.07	5.32	6.95
0.9920	1.27	1.35	1.45	1.56	1.83	2.18	2.62	3.18	3.88
0.9940	1.14	1.19	1.24	1.29	1.42	1.58	1.78	2.01	2.29
0.9960	1.06	1.08	1.10	1.12	1.17	1.24	1.31	1.39	1.48
0.9970	1.03	1.04	1.06	1.07	1.10	1.13	1.17	1.21	1.26
0.9980	1.01	1.02	1.02	1.03	1.04	1.05	1.07	1.09	1.11
0.9990	1.00	1.00	1.01	1.01	1.01	1.01	1.02	1.02	1.03
0.9995	1.00	1.00	1.00	1.00	1.00	1.00	1.00	1.01	1.01
1.0000	1.00	1.00	1.00	1.00	1.00	1.00	1.00	1.00	1.00

TABLE (VI-2). Relative Viscosities[1] for Steady, Uniform Turbulent Flow Between Parallel Plates.

Position	Reynolds Number								
	5,000	7,500	10,000	12,500	15,000	17,500	20,000	25,000	30,000
0.3000	6.70	9.63	12.44	15.22	17.90	18.84	20.94	28.32	33.33
0.3500	7.27	10.46	13.51	16.52	19.44	22.32	25.14	30.75	36.19
0.4000	7.65	11.01	14.22	17.39	20.46	21.52	23.91	32.37	38.10
0.4500	7.91	11.37	14.69	17.97	21.14	24.28	27.35	33.45	39.37
0.5000	7.97	11.47	14.81	18.11	21.31	22.42	24.91	33.72	39.68
0.5500	7.91	11.37	14.69	17.97	21.14	24.28	27.35	33.45	39.37
0.6000	7.65	11.01	14.22	17.39	20.46	21.52	23.91	32.37	38.10
0.6500	7.27	10.46	13.51	16.52	19.44	22.32	25.14	30.75	36.19
0.7000	6.70	9.63	12.44	15.22	17.90	18.84	20.94	28.32	33.33
0.7500	6.00	8.62	11.14	13.62	16.03	18.41	20.73	25.35	29.84
0.8000	2.26	5.26	9.48	11.59	13.64	14.37	15.98	21.58	25.40
0.8400	1.69	3.13	6.09	9.71	11.42	13.12	14.78	18.07	21.27
0.8800	1.33	1.96	3.06	4.97	8.14	9.56	10.62	14.30	16.83
0.9200	1.11	1.35	1.70	2.21	2.94	3.72	4.96	9.98	11.75
0.9600	1.01	1.06	1.13	1.23	1.34	1.44	1.58	2.08	2.69
0.9800	0.99	1.00	1.02	1.04	1.07	1.10	1.13	1.21	1.31
0.9900	0.99	1.00	1.00	1.01	1.01	1.02	1.03	1.05	1.07
0.9920	0.99	1.00	1.00	1.00	1.01	1.01	1.02	1.03	1.04
0.9940	1.00	1.00	1.00	1.00	1.00	1.00	1.01	1.01	1.02
0.9960	1.00	1.00	1.00	1.00	1.00	1.00	1.00	1.00	1.01
0.9970	1.00	1.00	1.00	1.00	1.00	1.00	1.00	1.00	1.00
0.9980	1.00	1.00	1.00	1.00	1.00	1.00	1.00	1.00	1.00
0.9990	1.00	1.00	1.00	1.00	1.00	1.00	1.00	1.00	1.00
0.9995	1.00	1.00	1.00	1.00	1.00	1.00	1.00	1.00	1.00
1.0000	1.00	1.00	1.00	1.00	1.00	1.00	1.00	1.00	1.00

[1] Values are reported as the ratio of the total viscosity to the kinematic viscosity ϵ_m/ν.

TABLE (VI-2) Cont.

Position	Reynolds Number								
	35,000	40,000	45,000	50,000	60,000	70,000	80,000	90,000	100,000
0.3000	32.98	43.16	48.00	42.78	62.24	71.41	80.57	89.65	98.50
0.3500	41.54	46.86	52.12	57.23	67.57	77.53	87.47	97.34	106.94
0.4000	37.68	49.32	54.86	48.83	71.13	81.61	92.08	102.46	112.57
0.4500	45.19	50.97	56.69	62.25	73.50	84.33	95.15	105.87	116.32
0.5000	39.24	51.38	57.14	50.85	74.09	85.02	95.92	106.73	117.26
0.5500	45.19	50.97	56.69	62.25	73.50	84.33	95.15	105.87	116.32
0.6000	37.68	49.32	54.86	48.83	71.13	81.61	92.08	102.46	112.57
0.6500	41.54	46.86	52.12	57.23	67.57	77.53	87.47	97.34	106.94
0.7000	32.98	43.16	48.00	42.78	62.24	71.41	80.57	89.65	98.50
0.7500	34.25	38.64	42.97	47.19	55.72	63.93	72.13	80.26	88.18
0.8000	25.16	32.88	36.57	32.61	47.42	54.41	61.39	68.31	75.05
0.8400	24.41	27.54	30.63	33.63	39.71	45.57	51.41	57.21	62.85
0.8800	16.72	21.79	24.23	21.68	31.42	36.05	40.67	45.25	49.72
0.9200	13.48	15.21	16.91	18.57	21.93	25.16	28.39	31.59	34.71
0.9600	3.16	4.67	6.25	6.92	11.26	12.92	14.58	16.22	17.82
0.9800	1.37	1.57	1.74	1.75	2.44	3.12	4.03	5.27	6.88
0.9900	1.09	1.12	1.15	1.19	1.28	1.38	1.50	1.64	1.81
0.9920	1.06	1.08	1.10	1.12	1.17	1.23	1.30	1.38	1.48
0.9940	1.03	1.04	1.05	1.06	1.09	1.12	1.16	1.20	1.25
0.9960	1.01	1.02	1.02	1.03	1.04	1.05	1.07	1.09	1.11
0.9970	1.01	1.01	1.01	1.01	1.02	1.03	1.04	1.05	1.06
0.9980	1.00	1.00	1.00	1.01	1.01	1.01	1.02	1.02	1.02
0.9990	1.00	1.00	1.00	1.00	1.00	1.00	1.00	1.00	1.01
0.9995	1.00	1.00	1.00	1.00	1.00	1.00	1.00	1.00	1.00
1.0000	1.00	1.00	1.00	1.00	1.00	1.00	1.00	1.00	1.00

increase near the wall. The details of the behavior near the wall of the ratio of the fluctuating velocity in the x-direction to the friction velocity are given in Fig. VI-28. As would be expected, there is a rapid decrease in the fluctuating velocity as the wall is approached still more closely. Similar

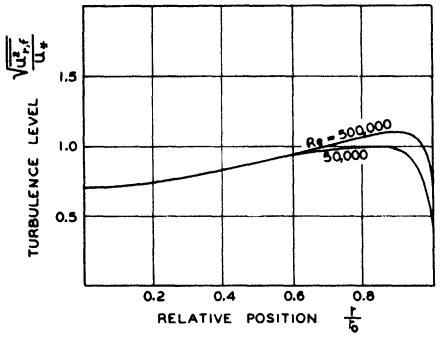

FIG. VI-29. Radial velocity fluctuations in circular conduits (*65*).

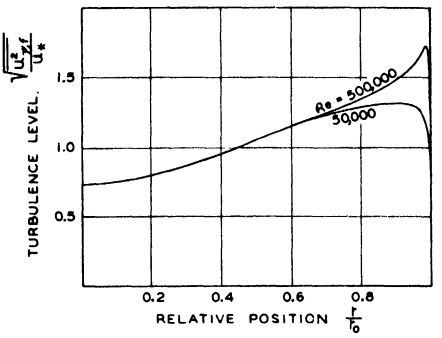

FIG. VI-30. Circumferential velocity fluctuations in circular conduits (*65*).

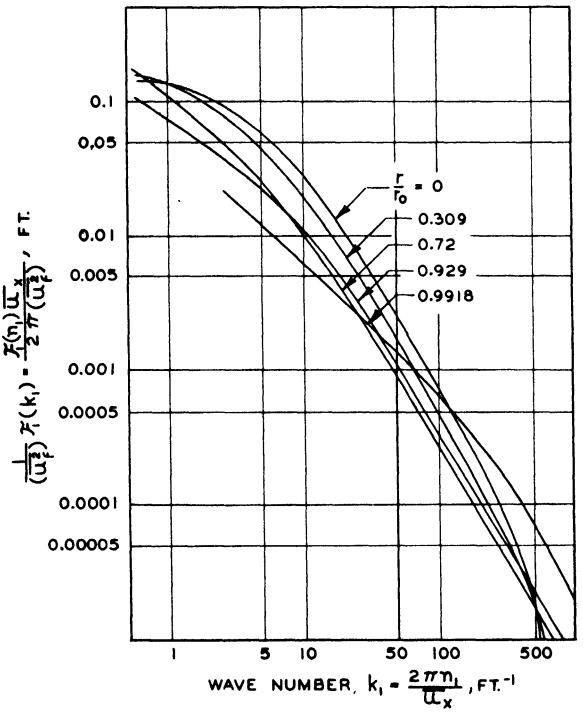

FIG. VI-31. Spectrum of longitudinal turbulence for several radial positions (*65*).

behavior in the boundary layer along a flat plate was observed by Klebanoff (*81*). This nearly linear decrease in the fluctuating velocity with position is apparently a characteristic of such boundary flow. The maximum

value of the ratio of the fluctuating velocity to the friction velocity is 2.6 which, apparently, is independent of the Reynolds number within the range covered by Laufer's investigation.

The corresponding distributions of the radial and circumferential fluctuating velocities are presented in Figs. VI-29 and VI-30, respectively. The fluctuating velocities in the radial and tangential directions are smaller than in the longitudinal direction. These measurements indicate the absence of any clear dividing line between turbulent and laminar flow in the boundary region.

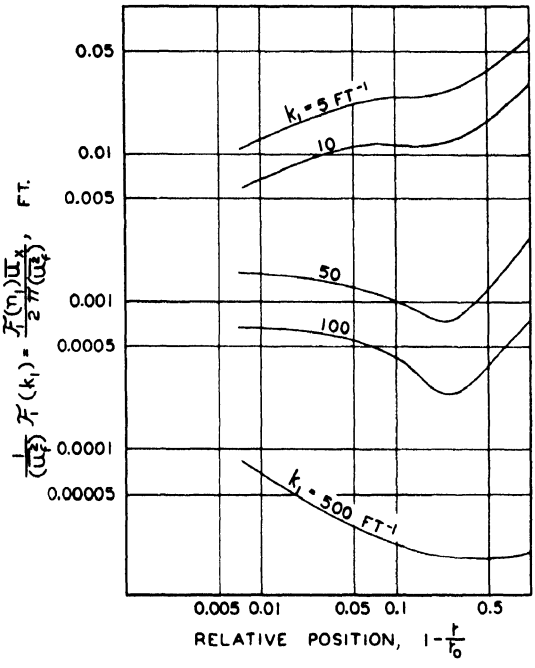

FIG. VI-32. Spectrum of kinetic energy of longitudinal turbulence as a function of position for several wave numbers (*65*).

The spectra of the longitudinal turbulence for several positions in the channel are shown in Fig. VI-31. These data were based upon the measurements of Laufer and do not indicate a marked change in the spectra from point to point in the stream although the change still is significant. The variation in the energy distribution for several wave numbers is presented in Fig. VI-32. There is not a marked influence of position in the channel on the energy at a particular wave number.

Nomenclature

A Constant, dimensionless

C Constant, ft.$^{8/3}$/lb.$^{2/3}$ sec.$^{4/3}$

C_P Isobaric heat capacity, B.t.u./lb.°F.

E Specific internal energy, B.t.u./lb.

E_v Internal energy density, B.t.u./cu.ft.

$\mathcal{E}_v$ Turbulent kinetic energy density, ft.lb./cu. ft.

$\dot{e}_v$ Dissipative function, ft.lb./cu.ft.sec.

f Fanning friction factor, dimensionless

$f(r)$ Longitudinal double velocity correlation scalar parameter, dimensionless

$f''(0)$ Second derivative of $f(r)$ evaluated at $r = 0$

$\mathfrak{F}(k)$ Kinetic energy spectrum, ft.^{3}/sec.^{2}

$\mathfrak{F}_0$ Empirical constant, ft.^{3}/sec.^{2}

$\mathfrak{F}_1(n_1)$ One-dimensional kinetic-energy spectrum, ft.^{2}/sec.

$\mathfrak{F}_1(k_1)$ One-dimensional kinetic-energy spectrum, ft.^{3}/sec.^{2}

$\mathfrak{F}_2(k_2)$ Transverse one-dimensional kinetic-energy spectrum, ft.^{3}/sec.^{2}

G Three-dimensional spectrum associated with the temperature fluctuations, ft.

$G_1(k_1)$ One-dimensional spectrum associated with the temperature fluctuations, ft.

$$G_1(k_1) = \frac{2}{\pi \overline{t_f^2}} \int_0^\infty \overline{t_f t_f'} \cos(k_1 r)\, dr$$

g Transverse double velocity correlation scalar parameter, dimensionless

g_c Acceleration due to gravity, ft./sec.^{2}

i $\sqrt{-1}$

K Three-dimensional spectral transfer function associated with temperature fluctuations, ft.^{3}/sec.

$K_0\{\ \}$ Modified Bessel function of second kind and of zero order

K_1 Empirical constant, dimensionless

$K_1(k_1)$ One-dimensional spectral transfer function associated with temperature fluctuations, ft.^{3}/sec.

$$K_1(k_1) = \frac{2}{\pi k_1 \overline{t_f^2}} \int_0^\infty \overline{t_f t_f' u_{r,f}} \sin(k_1 r)\, dr$$

K_2, K_3 Empirical constant, dimensionless

k Three-dimensional wave number, reciprocal ft.

k_0 Empirical constant, reciprocal ft.

k_1 One-dimensional wave number, reciprocal ft.

k Thermal conductivity, ft.lb./ft.sec.°F.

L_x Longitudinal scale of the fluctuating velocity, ft.

L_y Characteristic length associated with the transverse double velocity correlation, ft.

l_c Characteristic length, ft.

M Distance between centers of holes in grid, ft.

n Radial frequency of fluctuation, reciprocal sec.

n_1 One-dimensional frequency, reciprocal sec.

P Thermodynamic pressure, lb./ft.^{2}

Pe Peclet number, dimensionless

Pe_λ Local Peclet number, dimensionless

$\dot{Q}$ Heat flux, ft.lb./sq.ft.sec.

$\dot{Q}_L$ Heat flux, B.t.u./fl.sec.

R_{ij} ij component of the double velocity correlation tensor, dimensionless

R_y Correlation of axial velocity components between two points located symmetrically with respect to the axis of the jet, dimensionless

r Distance between the points $B(x_1, x_2, x_3)$ and $B'(x_1 + \xi_1, x_2 + \xi_2, x_3 + \xi_3)$, ft.

r Distance in the radial direction, ft.

Re Reynolds number, dimensionless

Re_c Characteristic Reynolds number, dimensionless

S_y Temperature correlation, dimensionless

T Absolute temperature, °R.; free stream temperature, °R.

T_{ijk} ijk component of the triple velocity correlation tensor, dimensionless

T_0 Temperature at the wall, °R.

t Temperature, °F.

t_{AV} Time-average point temperature, °F.

t_f Temperature fluctuation, °F.

U Gross velocity, ft./sec.

$\overline{u}$ Time-average velocity at a point, ft./sec.

u_c Characteristic velocity, ft./sec.

u_f Fluctuating velocity, ft./sec.

u_i Instantaneous velocity, ft./sec.

$u_{i,f}$ (x_1, x_2, x_3) Fluctuating velocity in the i-direction at the point $B(x_1, x_2, x_3)$, ft./sec.

$u'_{j,f}$ $(x_1 + \xi_1, x_2 + \xi_2, x_3 + \xi_3)$ Fluctuating component of velocity in the j-direction at the point $B'(x_1 + \xi_1, x_2 + \xi_2, x_3 + \xi_3)$, ft./sec.

$u_{\max}$ Maximum time-average velocity, ft./sec.

$\underline{u_x}$ Velocity in the x-direction, ft./sec.

$\overline{u_x}$ Time-average component of velocity in the x-direction, ft./sec.

$u_{x,f}$ Fluctuating component of velocity in the x-direction, ft./sec.

$u_{x,i}$ Instantaneous component of velocity in the x-direction, ft./sec.

$u_{y,f}$ Fluctuating component of velocity in the y-direction, ft./sec.

$u_{z,f}$ Fluctuating component of velocity in the z-direction, ft./sec.

$u_{\psi,f}$ Fluctuating velocity in the circumferential direction, ft./sec.

u^+ Velocity parameter, dimensionless

u_* Friction velocity, $\sqrt{(g_c/\sigma)(\tau_{yx})_0}$, ft./sec.

x Distance downstream from grid, ft.

x_a Distance downstream from axis of wire, ft.

x_0 Empirical constant, ft.

x_1, x_2, x_3 Coordinates of a point B in a turbulent stream, ft.

Y_c Characteristic width of temperature wake, ft.

y Distance from the plane of symmetry, ft.

y_a Distance from axis of temperature wake, ft.

y_d Distance from wall, ft.

y_d^+ Friction distance $y_d u_*/\nu$, dimensionless

$2y_0$ Separation of parallel plates, ft.

$y_{\Delta t_m/2}$ Distance from axis of temperature wake to point at which the temperature rise is half the maximum value, ft.

$\alpha_1, \alpha_2, \beta, \gamma$ Empirical constant, dimensionless

γ_1 Normalizing parameter, reciprocal ft.

Δt_m Maximum temperature rise, °F.

ϵ_c Eddy conductivity, ft.²/sec.

ϵ_m Eddy viscosity, ft.²/sec.

ϵ_m Total viscosity, ft.²/sec.

ϵ_r Relative viscosity, dimensionless

ζ Intensity of turbulence, dimensionless

η Absolute viscosity, lb.sec./ft.²

θ Time, sec.

κ Thermometric conductivity, ft.²/sec.

λ_t Microscale of the temperature fluctuation, ft.

Λ_x Characteristic length associated with temperature spectrum, ft.

Λ_y Characteristic length of the transverse temperature correlation, ft.

ν Kinematic viscosity, ft.²/sec.

ξ_1, ξ_2, ξ_3 Coordinates of a second point B' in a turbulent stream with respect to a reference point B in

	this stream, ft.
ρ	Density, lb.sec.^{2}/ft.^{4}
σ	Specific weight of fluid, lb./ft.^{3}
τ_{ij}	ij component of stress tensor, lb./ft.^{2}
τ_{rx}	Shear in the x-direction associated with a surface parallel with the wall, lb./ft.^{2}
τ_{yx}	Shear in the x-direction associated with a surface parallel to the walls, lb./ft.^{2}
$(\tau_{yx})_0$	Shear at the wall, lb./ft.^{2}
$\Phi()$	Function defined in Eq. (VI.25)
$\Phi_E()$	Function defined in Eq. (VI.27)
ψ	Angle defined in Eq. (VI.09), degree
ψ_m	Angle defined in Eq. (VI.08), degree
ψ_t	Angular width due to turbulence, degree
∇^2	Laplacian operator
$-$	Time average, used over a symbol

SUPERSCRIPTS

A	At upstream point
B	At downstream point
	Refers to the point B'

References

1. Boussinesq, J., "Essai sur la théorie des eaux courantes," memoires présentés par divers savants a l'Académie de l'Institut de France, **23** (1877).
2. Reynolds, O., *Phil. Trans. Roy. Soc.* **174**, 935 (1883).
3. von Kármán, T., *J. Aeronaut. Sci.* **4**, 131 (1937).
4. Taylor, G. I., *Proc. Roy. Soc.* **A 164**, 476 (1938).
5. Batchelor, G. K., "The Theory of Homogeneous Turbulence." Cambridge U. P., New York, 1953.
6. Liepmann, H., *J. Appl. Math. Phys.* **3**, 321 (1952).
7. von Kármán, T., Informal discussion, California Institute of Technology, Pasadena, 1954.
8. Wiener, N., "Extrapolation, Interpolation, and Smoothing of Stationary Time Series," Wiley, New York, 1950.
9. Rice, S. O., *Bell Tech. J.* **23**, 282 (1944); **24**, 46 (1945).
10. Goranson, R. W., "Thermodynamic Relations in Multi-Component Systems," Carnegie Institution, Washington, D. C., 1930.
11. Corrsin, S., *Am. J. Phys.* **18**, 467 (1950).
12. Kovasznay, L. S. G., "Techniques for the Optical Measurement of Turbulence in High Speed Flow," Heat Transfer and Fluid Mech. Inst. (ASME), Berkeley, California, 1949.
13. Dryden, H. L., and Kuethe, A. M., *Natl. Advisory Comm. Aeronaut. Tech. Rept.* **320** (1929).
14. King, L. V., *Phil. Trans. Roy. Soc.* **A 214**, 373 (1914).
15. Uberoi, M. S., and Kovasznay, L. S. G., Project Squid, Tech. Report 30. Johns Hopkins University, Baltimore, 1952.
16. Corrsin, S., *Natl. Advisory Comm. Aeronaut. Tech. Note* **1864** (1949).
17. Berry, V. J., Mason, D. M., and Sage, B. H., *Chem. Eng.Progr. Symposium Ser. No. 5*, **49**, 1 (1953).

18. Schubauer, G. B., *Natl. Advisory Comm. Aeronaut. Tech. Rept.* **524** (1935).
19. Drew, T. B., *Trans. Am. Inst. Chem. Engrs.* **26**, 26 (1931).
20. Townsend, A. A., *Proc. Roy. Soc.* **A 209**, 418 (1951).
21. Townsend, A. A., *Proc. Roy. Soc.* **A 224**, 487 (1954).
22. von Kármán, T., and Howarth, L., *Proc. Roy. Soc.* **A 164**, 192 (1938).
23. Michal, A. D., "Matrix and Tensor Analysis." Wiley, New York, 1947.
24. Taylor, G. I., *Proc. Roy. Soc.* **A 151**, 421 (1935).
25. von Kármán, T., *Mech. Eng.* **57**, 407 (1935).
26. Lamb, H., "Hydrodynamics," Section 329. Cambridge U. P., New York, 1932.
27. Uberoi, M. S., *Natl. Advisory Comm. Aeronaut. Tech. Note* **3116** (1954).
28. Batchelor, G. K., *Proc. Cambridge Phil. Soc.*, **47**, 359 (1951).
29. Millionshchikov, M., *Comp. rend. acad sci. U.R.S.S.* **32**, 615 (1941).
30. Dryden, H. L., *Quart. Appl. Math.* **1**, 7 (1943).
31. Corrsin, S., Thesis, California Institute of Technology, Pasadena, 1942.
32. Kovasznay, L. S. G., *J. Aeronaut. Sci.* **15**, 745 (1948).
33. Batchelor, G. K., and Townsend, A. A., *Proc. Roy. Soc.* **A 193**, 539 (1948).
34. Batchelor, G. K., and Townsend, A. A., *Proc. Roy. Soc.* **A 194**, 527 (1948).
35. Kolmogoroff, A. N., *Compt. rend. acad. sci. U.R.S.S.* **30**, 301 (1941).
36. Kolmogoroff, A. N., *Compt. rend. acad. sci. U.R.S.S.* **31**, 538 (1941).
37. Kolmogoroff, A. N., *Compt. rend. acad. sci. U.R.S.S.* **32**, 16 (1941).
38. Onsager, L., *Phys. Rev.* **37**, 405 (1931); **38**, 2265 (1931).
39. Onsager, L., *Phys. Rev.* **68**, 286 (1945).
40. Onsager, L., *Nuovo ciment.*, **6**, Suppl. **2**, 279 (1949).
41. Heisenberg, W., *Z. Physik* **124**, 628 (1948).
42. von Weizacker, C. F., *Z. Physik* **124**, 614 (1948).
43. Corrsin, S., *J. Aeronaut. Sci.* **20**, 853 (1953).
44. Davis, L., Jet Propulsion Laboratory Report No. 3—17, Pasadena, California (1952).
45. Stewart, R. W., and Townsend, A. A., *Phil. Trans. Roy. Soc.* **A 243**, 359 (1951).
46. Simmons, L. F. G., and Salter, C., *Proc. Roy. Soc.* **A 165**, 73 (1938).
47. Corrsin, S., and Uberoi, M. S., *Natl. Advisory Comm. Aeronaut. Tech. Note* **2124** (1950).
48. Ribner, H. S., and Tucker, M., *Natl. Advisory Comm. Aeronaut. Tech. Note* **2606** (1952).
49. Taylor, G. I., *Z. angew. Math. u. Mech.* **15**, 91 (1935 b).
50. Uberoi, M. S., Lecture at Institute of Aeronautical Sciences, January, 1954.
51. Davis, L., Jet Propulsion Laboratory Report No. 3—22, Pasadena, California (1950).
52. Corrsin, S., *Natl. Advisory Comm. Aeronaut. ACR No. 4H24 (WR W-90)* (1944).
53. Batchelor, G. K., *Quart. Appl. Math.* **6**, 97 (1948).
54. von Kármán, T., and Lin, C. C., *Advances in Appl. Mech.* **2**, 2 (1951).
55. Frenkiel, F. N., *J. Appl. Mech.* **5**, 311 (1948).
56. Baer, D. H., Schlinger, W. G., Berry, V. J., and Sage, B. H., *J. Appl. Mech.* **20**, 407 (1953).
57. Corrsin, S., *J. Appl. Phys.* **22**, 469 (1951).
58. Kovasznay, L. S. G., Uberoi, M. S., and Corrsin, S., *Phys. Rev.* **76**, 1263 (1949).
59. Heisenberg, W., *Proc. Roy. Soc.* **A 195**, 402 (1948).
60. Chandrasekhar, S., *Phys. Rev.* **75**, 896 (1949).
61. Chandrasekhar, S., *Proc. Roy. Soc.* **A 200**, 20 (1949).
62. Corrsin, S., *J. Aeronaut. Sci.* **18**, 417 (1951).

63. Loitsiansky, L. G., *Natl. Advisory Comm. Aeronaut. Tech. Mem.* **1079** (1945).
64. Kistler, A. L., O'Brien, V., and Corrsin, S., *Natl. Advisory Comm. Aeronaut. Research Mem.* **54D19** (1954).
65. Laufer, J., *Natl. Advisory Comm. Aeronaut. Tech. Note* **2954** (1953).
66. Schlinger, W. G., Berry, V. J., Mason, J. L., and Sage, B. H., *Ind. Eng. Chem.* **45**, 662 (1953).
67. von Kármán, T., *Trans. Am. Soc. Mech. Engrs.* **61**, 705 (1939).
68. Taylor, G. I., *Natl. Advisory Comm. Aeronaut. Tech. Rept.* **2** No. 272 (1916).
69. Page, F., Jr., Schlinger, W. G., Breaux, D. K., and Sage, B. H., *Ind. Eng. Chem.* **44**, 424 (1952).
70. Page, F., Jr., Corcoran, W. H., Schlinger, W. G., and Sage, B. H., *Ind. Eng. Chem.* **44**, 419 (1952).
71. Corcoran, W. H., Page, F., Jr., Schlinger, W. G., and Sage, B. H., *Ind. Eng. Chem.* **44**, 410 (1952).
72. Prandtl, L., *Physik. Z.* **29**, 487 (1928).
73. Gebelein, H., "Turbulenz." Springer, Berlin, 1935.
74. Skinner, G. T., Thesis, California Institute of Technology, Pasadena, 1950.
75. Deissler, R. G., *Natl. Advisory Comm. Aeronaut. Tech. Note* **2138** (1950).
76. Nikuradse, J., *Forsch. Gebiete Ingenieurw. Forschung.* **356** (1932).
77. Dunn, L. G., Powell, W. B., and Seifert, H. S., Heat transfer studies relating to rocket power-plant development. *Roy. Aeronaut. Soc. 3rd Anglo-American Aeronaut. Conf.*, 1951.
78. Schlinger, W. G., and Sage, B. H., *Ind. Eng. Chem.* **45**, 2636 (1953).
79. Kovasznay, L. S. G., *Natl. Advisory Comm. Aeronaut. Tech. Note* **2889** (1953).
80. Corrsin, S., and Uberoi, M. S., *Natl. Advisory Comm. Aeronaut. Tech. Rept.* **1040** (1951).
81. Klebanoff, P. S., *Natl. Advisory Comm. Aeronaut. Tech. Note* **3178** (1954).

Bibliography

Batchelor, G. K., Role of big eddies in homogeneous turbulence. *Proc. Roy. Soc.* **A 195**, 513 (1949).

Batchelor, G. K., Note on free turbulent flows, with special reference to the two-dimensional wake. *J. Aeronaut. Sci.* **17**, 441 (1950).

Klebanoff, P. S., and Diehl, Z. W., Some features of artificially thickened fully developed turbulent boundary layers with zero pressure gradients. *Natl. Advisory Comm. Aeronaut. Tech. Rept.* **1110** (1952).

Laufer, J., Investigation of turbulent flow in a two-dimensional channel. *Natl. Advisory Comm. Aeronaut. Rept.* **1053** (1951).

Rotta, J., Statistische Theorie nichthomogener Turbulenz. 1. Mitteilung. *Z. Physik* **129**, 547 (1951). 2. Mitteilung. *Z. Physik* **131**, 51 (1951).

Schubauer, G. B., and Klebanoff, P. S., Theory and application of hot-wire instruments in the investigation of turbulent boundary layers. *Natl. Advisory Comm. Aeronaut.* WR W-86 (1946).

Schubauer, G. B., and Klebanoff, P. S., Investigation of the separation of the turbulent boundary layer. *Natl. Advisory Comm. Aeronaut. Tech. Rept.* **1030** (1951).

Tchen, C. M., On the spectrum of energy in turbulent shear flow. RP **2388**, *J. Research Natl. Bur. Standards* **50**, 51 (1953).

Townsend, A. A., Measurements in the turbulent wake of a cylinder. *Proc. Roy. Soc.* **A 190**, 551 (1947).

Townsend, A. A., Local isotropy in the turbulent wake of a cylinder. *Australian J. Sci. Research* **A 1**, 161 (1948).

Townsend, A. A., Momentum and energy diffusion in the turbulent wake of a cylinder. *Proc. Roy. Soc.* **A 197**, 124 (1949).

Townsend, A. A., The fully developed turbulent wake of a circular cylinder. *Australian J. Sci. Research* **A 2**, 451 (1949).

Townsend, A. A., The eddy viscosity in turbulent shear flow. *Phil. Mag.* [7] **41**, 890 (1950).

Townsend, A. A., The structure of the turbulent boundary layer. *Proc. Cambridge Phil. Soc.* **47**, 375 (1951).

CHAPTER VII

BOUNDARY LAYER

One field of fluid mechanics that has received ever-increasing attention since the early days of Reynolds (*1*) is that relating to the turbulent and laminar flows in the vicinity of a solid boundary of a stream. Prandtl (*2*, *3*) was the first to consider these matters from an analytical standpoint, and his work together with the early studies of Kármán (*4*) and Pohlhausen (*5*) laid the basis for the quantitative interpretation of boundary flows. In reality, the term boundary layer means that there is a gradual change in the nature of the flow as the wall is approached rather than an abrupt transition. The term will be used here, however, because of its widespread acceptance in fluid mechanics.

It is the purpose of this chapter to describe some of the qualitative aspects of boundary flows for both compressible and incompressible fluids and to treat in some detail the laminar boundary layer for an incompressible fluid with constant physical properties. The latter situation is a useful approximation of many of the conditions encountered in the process industry but does not adequately describe the behavior of the flow around an immersed body at high velocity where the dissipation of kinetic energy results in a significant increase in the internal energy of the fluid. Under such circumstances it is necessary to take into account the variations in the physical properties of the fluid through that portion of the flow adjacent to the solid boundary of the stream. The mathematical treatment of boundary layers is somewhat more complicated than the consideration of steady, uniform flow, and for the most part the solution of the Navier-Stokes equations[1] yields nonlinear differential equations which have only particular solutions.

VII-1. Steady Uniform Flow

Figure VII-1 shows the velocity distribution near the wall for the steady, uniform flow of air between parallel plates. Three different gross velocities are shown. It was found experimentally (*6*, *7*) that the given velocity

[1] See Chapter V, Section V-9 for a discussion of the Navier-Stokes equations.

distributions in Fig. VII-1 were independent of the downstream position. The distributions at the entrance section of the channel were, however, nonuniform. Since there was shear in the flow as shown in Fig. VII-2,

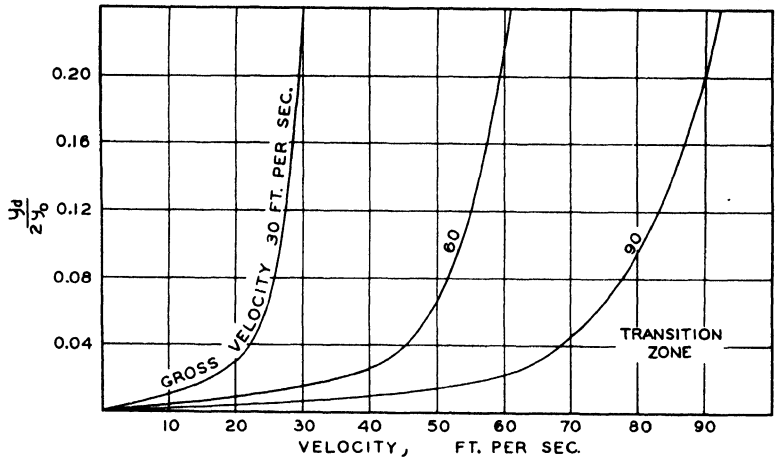

FIG. VII-1. Effect of position upon velocity in steady, uniform flow between parallel plates.

turbulence in the main body of the stream diffused into the laminar region near the wall. Uniform flow was then reached where the rate of dissipation of the turbulence as internal energy in the fluid adjacent to the wall just equaled its rate of migration into the boundary layer. There was then no change in the velocity distribution with downstream position.

As has been indicated earlier in this text,[2] the velocity distribution adjacent to the wall in steady, uniform turbulent flow may be generalized in terms of the velocity parameter u^+ and the distance parameter y_d^+. Sufficiently close to the wall, it may be readily shown that

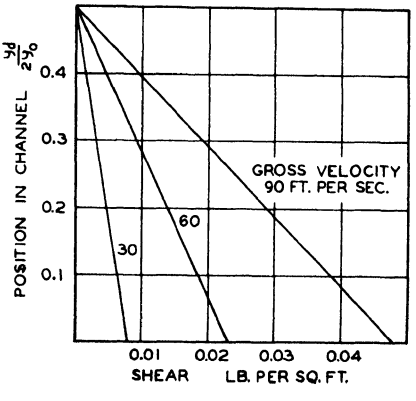

FIG. VII-2. Effect of position upon shear in steady, uniform flow.

$$u^+ = y_d^+. \qquad \text{(VII.01)}$$

Equation (VII.01) applies only in the laminar region and corresponds to the nearly straight line section of the velocity distribution near the origin

[2] See Chapter IV, Section IV-3 for a discussion of the velocity distribution in turbulent flow between parallel plates.

in Fig. VII-1 or VII-3. Throughout this region it follows from the definition of laminar flow that:

$$\tau_{yx} = \eta \frac{du_x}{dy_d} = (\tau_{yx})_0 + \frac{dP}{dx} y_d. \tag{VII.02}$$

In this discussion the symbol y_d will be employed to measure the normal distance from the boundary of interest to the point in the flow stream under consideration. If desired, Eq. (VII.02) may be rewritten as

$$\frac{du_x}{dy_d} = \frac{(\tau_{yx})_0 + \frac{dP}{dx} y_d}{\eta} = \frac{\left((\tau_{yx})_0 + \frac{dP}{dx} y_d\right) g_c}{(\nu + \varepsilon_m)\sigma} \tag{VII.03}$$

where the second equality has been included to show the form of the equation for turbulent flow. Integration of the second equality of Eq. (VII.02) yields the familiar parabolic velocity distribution of steady, uniform laminar flow. It is apparent from a consideration of Fig. VII-3 that the velocity deviates from the relationship described in Eq. (VII.01) at about $y_d^+ = 7$. The second equality of Eq. (VII.03) applies to the transition region indicated in Fig. VII-1 and beyond. Outside the laminar layer the total viscosity of the fluid is a function of position, and Eq. (VII.03) can only be integrated from a detailed knowledge of the variation of the eddy viscosity with position.

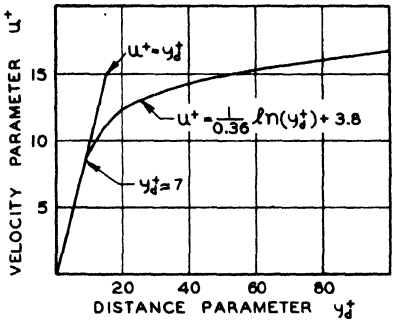

FIG. VII-3. Generalized velocity distribution for steady, uniform flow.

From the foregoing discussion it is apparent that there is a gradual transition from laminar flow adjacent to the wall to more fully developed turbulence in the center of the stream. In normal shear flow the presence of the wall controls the nature of the velocity distribution, and it is impossible to fix a definite sub-layer. It is usually conventional to consider the so-called laminar sub-layer as extending from a value of y_d^+ of zero to about 6.7 and the transition region from 6.7 to 23. The velocity distribution in these regions can be approximated by an empirical expression of the following form:[1]

[1] The details of the variation of the velocity distribution in turbulent flow have already been discussed in Chapter IV, Section 2. They have been repeated here in the interest of relating the behavior under steady, uniform flow to the behavior of a boundary layer in nonuniform flow.

$$u^+ = \frac{1}{\sqrt{K_1}} \tanh (y_d{}^+ \sqrt{K_1}) = \frac{1}{0.0695} \tanh (0.0695\, y_d{}^+). \quad \text{(VII.04)}$$

Equation (VII.04) is based upon a suggestion of Rannie as reported by Dunn (*8*). The coefficients were established from some recent experimental measurements upon the velocity distribution between parallel plates (*9*). It was found (*9*), however, that at Reynolds numbers below 20,000 there was a systematic variation with Reynolds number in the relationship of the velocity parameter u^+ to the distance parameter $y_d{}^+$. Therefore, it appears that even for steady, uniform flow the behavior near the boundary of a flowing turbulent stream is not understood in detail.

VII-2. Nonuniform Steady Boundary Flow

In many situations the behavior of a non-uniform boundary-flow is of practical interest. This is particularly true in connection with the aeroballistics of projectiles (*10*) and the behavior of aircraft in the atmosphere. In many industrial applications a knowledge of the flow around an immersed object is of interest, and the greater part of this chapter is concerned with this type of nonuniform boundary layer. The steady, uniform case which

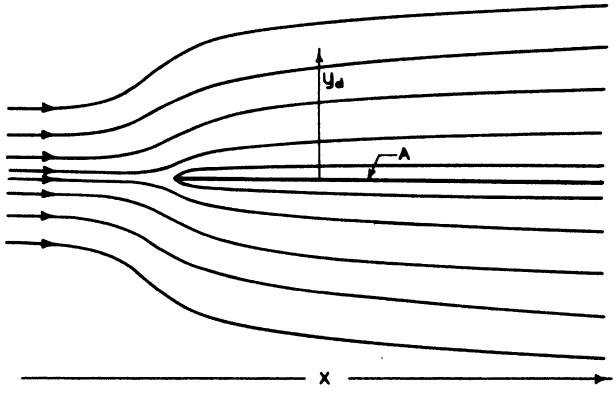

FIG. VII-4. Velocity distribution around a flat plate in potential flow.

has just been reviewed is an essential preliminary point of departure in the description of the over-all velocity distribution in such flows. In the nonuniform boundary flow the analysis of the behavior is more complicated and has been the subject of much research.

Figure VII-4 shows the velocity distribution around the plate A of indefinite length in the x-direction. The flow pattern is two-dimensional and was assumed to be potential in its approach to the plate and at a large normal distance from it. As indicated by the streamlines the stream is

displaced as a result of its flow around the plate. For relatively low velocities the fluid follows the laws of laminar motion in the vicinity of the plate, and it is possible to predict with reasonable accuracy the velocity distribution around such an object.

In many cases, particularly those involving projectiles and aircraft, it is convenient to neglect the changes in pressure in the direction of primary motion and to consider the entire process as isobaric. In the case of the flow in a conduit, however, there exists a pressure gradient as a result of the shear field, and it is not possible to analyze the flow around an object immersed in such a conduit on the basis of an isobaric system. For the purposes of most elementary analysis it is usually assumed that the pressure gradient in the x direction is determined by the conditions of flow in the main body of the fluid and is not influenced by the presence of the immersed body.

In the case where the approaching flow exhibits turbulent shear the situation is more complicated, and it is not possible to treat the behavior as laminar throughout the region where the flow is influenced by the immersed body. The analysis of such situations is much more complicated if it is desired to determine the time-average velocity as a function of position. The velocity distribution near the surface where the flow may be assumed to be laminar in character may, however, be empirically predicted by much the same methods as are used when the flow surrounding the object is potential. It is beyond the scope of the present discussion to consider the detailed analysis of a nonuniform boundary layer in turbulent flow where the transfer of momentum into the boundary flow as a result of turbulence is a significant part of the total momentum transport.

VII-3. Transition

At a distance from the leading edge of objects immersed in relatively high velocity streams, the initially laminar boundary layer becomes unstable to small disturbances and the boundary layer eventually becomes turbulent. The factors influencing the transition to turbulence are complicated and are not yet fully understood. Schlichting (*11*) presents some of the more important factors influencing separation. The pressure gradient is of particular importance. If it is positive along the boundary surface in the direction of flow, the laminar boundary layer becomes less stable and the onset of transition is to be expected.

The transition of the laminar boundary layer and the formation of a turbulent region behind is indicated in Fig. VII-5. The transition occurs at

point A, and it appears that the exact location of the point of transition from the leading edge of the plate B is sufficiently uncertain that it should properly be called a region of transition, and can be conveniently treated by statistical means (*12*). On this basis there is rapid alternation in the nature of the flow near the point A. The nature of the pressure distribution in the direction of flow exerts a pronounced influence upon the point at which this transition occurs. The velocity distribution in the turbulent region C

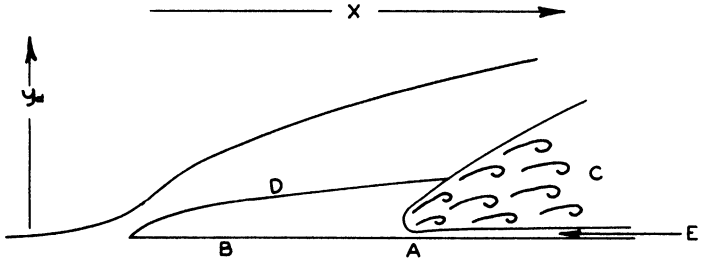

FIG. VII-5. Transition between laminar and turbulent boundary layer (*11, 15*).

is more nearly logarithmic as shown in Fig. VII-3 than is that in the laminar region at D. The turbulence in the boundary layer diffuses into other parts of the stream, as do all turbulent fluctuations. The laminar region or sublayer, as it is often called, may begin to grow after point A as indicated at E if the conditions are favorable for such types of flow. If the flow in the main body of the stream is turbulent, there usually is a blending of the turbulence diffusing inward in the main stream and that generated in the boundary layer after the initial point of transition at A in Fig. VII-5.

VII-4. Boundary Flows for Incompressible Fluids

Based upon the foregoing semi-quantitative discussion it is possible to consider the various types of flow that are encountered in the boundary regions. For convenience they may be divided into the two broad classes of incompressible and compressible flow, following the general precedent of writers on fluid mechanics. Incompressible fluids are limited to equations of state characterized by

$$V = K_2 \tag{VII.05}$$

for constant temperature. From the standpoint of the analysis of flow in the boundary layer it is possible to treat many gases as though they were incompressible. Situations arise, however, when the effect of deviations

from Eq. (VII.05) exerts a marked influence upon the behavior of a flowing system. For most of the conditions encountered in industrial practice velocities in the main stream are below the velocity of sound, and it is possible to treat the behavior of the flow in a boundary layer as involving an incompressible fluid. It is satisfactory to consider both laminar and turbulent boundary flow in such a manner. The influence of the laminar boundary region on the flow pattern of the stream can usually be estimated with sufficient accuracy under such an assumption. If high speed flow is encountered, the effects of dissipation of kinetic energy in the boundary layer as internal energy for both turbulent and laminar flow must be considered even though the fluid is treated as incompressible.

The transitions between laminar and turbulent boundary flow have been discussed. They are an important part of any general description of the behavior. As has been indicated, an analytical description of the factors influencing the transition of the boundary layer is difficult and has not been completely established. Throughout the greater part of the following discussion the behavior of boundary layers in incompressible flow will be considered.

Laminar Boundary Layers for Incompressible Fluids

Throughout this portion of the discussion attention will be focused upon the velocity distribution and the variations in pressure encountered in fluid adjacent to a boundary. Consideration will be given to such conditions of flow that the local accelerations of the fluid and the transfer of kinetic energy into internal energy as a result of mechanical dissipation do not influence the physical properties of the fluid significantly (*11*, *13*). Such situations are often encountered in industrial practice where the velocity of the stream is not large and there is neither thermal nor material transfer associated with the process. In the case of higher velocities the dissipation of kinetic energy results in marked changes in temperature in the boundary layer. These matters (*13*) will be considered briefly in another section, since much of the discussion which is presented here is applicable to the more general case of a compressible boundary layer. As a further simplification it will be assumed that the flow outside of the boundary region is potential in nature. Under actual conditions of flow in conduits such is not the case since shear exists and exerts a pronounced influence upon the gross velocity distribution and the existence of turbulent flow.

VII-5. Navier-Stokes Equations

The effects of the nature of the flow in the mainstream will be neglected in the present discussion and considered qualitatively after the analytical evaluation of the laminar boundary layer is presented. One of the simpler cases of laminar boundary layer is the flow over a flat plate with negligible pressure gradients. This case will be considered in some detail since it is upon this basic concept that most of the more complicated analysis of boundary flow is based. Before considering the detailed solution of the equations of motion for a particular boundary flow it is worth-while to describe the simplifications[1] that are permissible in the Navier-Stokes equations (*14*). In considering the simplifications it is convenient to use a relative velocity in the boundary layer by referring all velocities to the free stream velocity.

$$u_{x,b} = \frac{u_x}{u_\infty}; \qquad u_{y,b} = \frac{u_y}{u_\infty}. \tag{VII.06}$$

Correspondingly, the Reynolds number is given by

$$\mathrm{Re}_b = \frac{l \sigma u_\infty}{\eta g_c} \tag{VII.07}$$

in which l is a characteristic length of the solid boundary. When desirable, the pressure term may be considered dimensionless in the following way:

$$P_b = \frac{P g_c}{\sigma u_\infty^2}. \tag{VII.08}$$

Similarly, the time scale may be expressed in a dimensionless fashion as

$$\theta_b = \frac{\theta u_\infty}{l}. \tag{VII.09}$$

From dimensional reasoning it is possible to evaluate the relative magnitude of the principal terms in the Navier-Stokes equations (*15, 16*). The longitudinal velocity $u_{x,b}$ is of the order of unity as indicated in Eq. (VII.06). On the other hand, the boundary layer thickness δ is assumed to be much smaller than unity as indicated in Eq. (VII.10).

$$\frac{\delta}{l} \ll 1. \tag{VII.10}$$

---

[1] This discussion is based in part on the treatment of Schlichting (*11*) which is well suited to this consideration of boundary layer. No detailed references to this material are included as the subject is well known, and the presentation is rather conventional.

From the foregoing it may be shown that

$$\frac{\partial u_{x,b}}{\partial y_d} \cong \frac{1}{\delta}, \tag{VII.11}$$

$$\frac{\partial^2 u_{x,b}}{\partial y_d^2} \cong \frac{1}{\delta^2}. \tag{VII.12}$$

Since the boundary layer thickness is small, the gradient with respect to y_d of the longitudinal velocity $u_{x,b}$ and its first derivative are large. The derivatives of the longitudinal velocity with respect to x and the corresponding second derivatives are of the order of unity, as is the derivative of the normal velocity $u_{y,b}$ with respect to y_d. For these reasons the transverse velocity in the boundary layer $u_{y,b}$ may often be neglected in comparison to the longitudinal velocity $u_{x,b}$. Likewise it follows that:

$$\frac{\partial^2 u_{x,b}}{\partial x^2} \ll \frac{\partial^2 u_{x,b}}{\partial y_d^2}. \tag{VII.13}$$

From the foregoing reasoning it is apparent that all the terms in the Navier-Stokes equations describing the normal velocity $u_{y,b}$ are of the order of the boundary layer thickness and for this reason may be neglected as a first approximation. On the other hand, those relating to the longitudinal velocity are all, with but a single unimportant exception, of the order of unity. Under these circumstances the Navier-Stokes equations for an incompressible fluid in two-dimensional flow reduce to the following dimensional form:

$$\frac{\partial u_x}{\partial \theta} + u_x \frac{\partial u_x}{\partial x} + u_y \frac{\partial u_x}{\partial y_d} = -\frac{g_c}{\sigma}\frac{\partial P}{\partial x} + \frac{\eta g_c}{\sigma}\frac{\partial^2 u_x}{\partial y_d^2}. \tag{VII.14}$$

Equation (VII.14), together with the equation of continuity,

$$\frac{\partial u_x}{\partial x} + \frac{\partial u_x}{\partial y_d} = 0 \tag{VII.15}$$

is sufficient to define to a first degree of approximation the behavior of both steady and unsteady laminar boundary flows in an incompressible fluid. The boundary conditions for the foregoing expressions may be given as

at
$$y_d = 0, \tag{VII.16}$$

$$u_x = 0; \qquad u_y = 0, \tag{VII.17}$$

at
$$y_d = \infty, \tag{VII.18}$$

$$u_x = u_\infty. \tag{VII.19}$$

VII-6 Environmental Conditions

In determining the behavior of a laminar boundary layer it is necessary to establish the conditions of pressure and velocity which exist at a distance from the surface in question. In the case of steady potential flow at a distance from the boundary, it follows that:

$$-\frac{g_c}{\sigma}\frac{dP}{dx} = u_\infty \frac{du_\infty}{dx}. \tag{VII.20}$$

Equation (VII.20) applies only to steady flow. If it is desired to extend this to unsteady flow, there is obtained

$$-\frac{g_c}{\sigma}\frac{dP}{dx} = u_\infty \frac{du_\infty}{dx} + \frac{\partial u_\infty}{\partial \theta}. \tag{VII.21}$$

In the case of flows in which friction in other parts of the stream is important in establishing the pressure gradient it is necessary to extend Eq. (VII.20) for steady flow to include this dissipative quantity in the fashion that has been described in Chapter I. In most treatments of laminar boundary flows it is possible to neglect the effect of curvature at the boundary (*17*, *18*) except when the radius of the curvature becomes of the order of the thickness of the boundary layer. In addition, it is found expedient to neglect all pressure gradients normal to the boundary.

VII-7. Separation

In the case of boundary flows involving pressure gradients in the boundary or other variations in state there is a possibility of the separation of the fluids from the surface or a marked modification in the configuration of the flow pattern. For example, in the case of potential flow around a solid body immersed in the stream increasing pressures in the direction of flow are often encountered. These are a frequent cause of the phenomenon of separation of a laminar boundary layer. In Fig. VII-6 is shown a series of velocity distributions in such a boundary layer with a positive pressure gradient. In this instance the pressure gradient decelerated the flow near the wall and induced separation at the third section. The latter situation is characterized by

$$\left(\frac{\partial u_x}{\partial y_d}\right)_{y_d=0} = 0. \tag{VII.22}$$

At larger distances downstream there is a region adjacent to the wall where flow in the direction of decreasing pressure occurs. The designation of the behavior indicated at station 3 as "separation" involves only a modification of the flow pattern, not actual absence of fluid adjacent to the wall. In the case of flows with a positive pressure gradient the velocity distribution

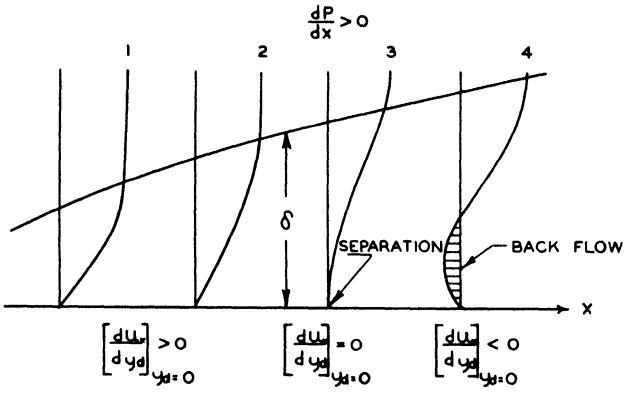

FIG. VII-6. Separation of boundary layer with a positive pressure gradient (*11*, *15*).

involves an inflection point where the second derivative of the velocity passes through zero. This inflection also characterizes the separation of the boundary layer. Such phenomena are not encountered in flows with negative pressure gradients.

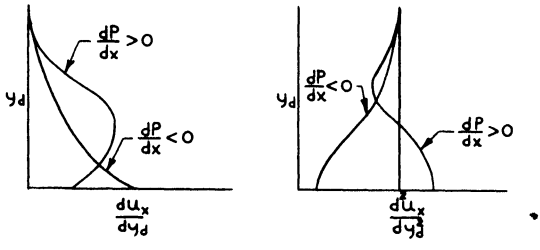

FIG. VII-7. Velocity gradients in boundary layer (*11*, *15*).

The first derivative of the velocity profile with positive and negative pressure gradients is shown in a part of Fig. VII-7 which also includes the second derivative of the velocity profile. It has been shown by Schlichting (*11*, *15*) that at the solid surface of all steady boundary layers the third derivative of the velocity with respect to the distance from the surface is zero as indicated in the following equation:

$$\left(\frac{\partial^3 u_x}{\partial y_d^3}\right)_{y_d = 0} = 0. \tag{VII.23}$$

Such behavior has been indicated qualitatively in Fig. VII-7 by the fashion in which the second derivative of the velocity with respect to normal distance approaches the wall.

VII-8. Drag on Immersed Bodies

In considering the frictional drag it is desirable to sum up the shear at all points on the surface of the body. This may be accomplished in the following way:

$$F_D = \oint (\tau_{yx})_0 \cos(\psi_*)\, ds. \tag{VII.24}$$

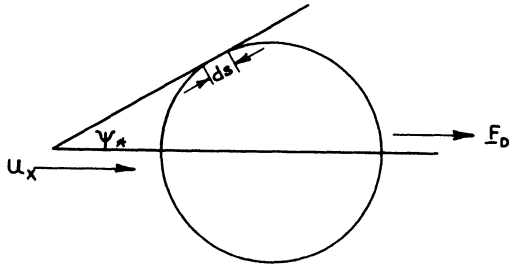

FIG. VII-8. Drag on immersed body of uniform cross section.

The significance of the symbols used in Eq. (VII.24) is indicated in Fig. VII-8. It should be realized that the quantity s represents the surface area of the cylinder of unit length whereas the angle ψ_* corresponds to the angle between a tangential plane and the direction of flow far from the body. Equation (VII.24) may be expanded to read

$$F_D = \oint \eta \left(\frac{\partial u_x}{\partial y_d}\right)_{y_d=0} \cos(\psi_*)\, ds = \eta \oint \left(\frac{\partial u_x}{\partial y_d}\right)_{y_d=0} \cos(\psi_*)\, ds. \tag{VII.25}$$

In Eq. (VII.25) y_d is taken as the direction normal to the surface at each point. If it is assumed that the viscosity is constant, the second equality of Eq. (VII.25) may be applied. It should be realized that Eq. (VII.25) gives only the friction drag, although the flow may be laminar or turbulent. For most immersed objects a separation occurs near the rear of the body and vortices with associated turbulence are encountered. For this reason it is not convenient to apply Eq. (VII.25) with the boundary layer theory to the prediction of the total drag of an object. However, if the velocity gradient and viscosity are known, Eq. (VII.25) becomes useful.

VII-9. Flow along a Flat Plate

Blasius (*14*) was the first to examine in detail the behavior of boundary flows along a flat plate. Since most of the theory of laminar boundary layer is based upon his analysis, it appears worth-while to examine it in some detail. No effort will be made to present the mathematical solutions of the differential equations which follow conventional series expansion methods (*19*). The results of the solutions of the nonlinear equations are presented in sufficient detail to permit specific solutions to be evaluated to at least the degree of accuracy that is usually desired. In addition, the approximate solutions to the boundary layer equation, which include an assumption as to velocity distribution, have been presented in a later section for more general application.

If it is assumed that the pressure is invariant and that steady-state conditions exist, Eq. (VII.14) assumes the following form:

$$u_x \frac{\partial u_x}{\partial x} + u_y \frac{\partial u_x}{\partial y_d} = \frac{\eta g_c}{\sigma} \frac{\partial^2 u_x}{\partial y_d^2}. \tag{VII.26}$$

The boundary conditions remain identical with those set forth in Eqs. (VII.16) through (VII.19). For unsteady conditions the Navier-Stokes equations yield the following expression if the flow is independent of the x coordinate:

$$\frac{\partial u_x}{\partial \theta} = \frac{\eta g_c}{\sigma} \frac{\partial^2 u_x}{\partial y_d^2} \tag{VII.27}$$

where $u_y = 0$ because of Eqs. (VII.15) and (VII.17) with $\partial u_x/\partial x = 0$. For a special case of a flat plate suddenly set into motion parallel to itself the boundary conditions for the solution[1] of this equation are

$$\theta \leqslant 0; \qquad 0 \leqslant y_d \leqslant \infty; \qquad u_x = 0, \tag{VII.28}$$

$$\theta > 0; \qquad y_d = 0; \qquad u_x = U_{x,P} = \text{constant}. \tag{VII.29}$$

In this instance it is convenient to consider the plate as moving relative to the stream. It may be shown (*20*) using the transformation

$$\zeta = \frac{y_d}{2\sqrt{\frac{\eta g_c \theta}{\sigma}}} \tag{VII.30}$$

[1] Equation (VII.27) is of the same form as the thermal conductivity expression for unsteady transport with constant thermal conductivity and neglect of thermal convection.

that a solution of Eq. (VII.27) is

$$u_x = \frac{2}{\sqrt{\pi}} U_{x,P} \int_{\zeta = \frac{y_d}{2\sqrt{\frac{\eta g_c \theta}{\sigma}}}}^{\infty} \exp\{-\zeta^2\}\, d\zeta = U_{x,P} \left\{1 - \operatorname{erf}\left(\frac{y_d}{2\sqrt{\frac{\eta g_c \theta}{\sigma}}}\right)\right\}. \quad \text{(VII.31)}$$

The integral is the complementary error function for which suitable tabulations are available (*20, 21*).

Example I

Development of Boundary Layer: It is desired to obtain values of u_x as a function of time and position for fluid in the vicinity of a flat plate suddenly set in motion with the velocity $U_{x,P}$ that is then maintained. The arrangement of the plate in the fluid is shown in Fig. VII-9. The viscosity of the fluid may be taken as 0.209×10^{-4} lb.sec./ft.^{2} which corresponds to that of water at room temperature. The specific volume of water is taken as 0.01613 cubic foot per pound for the temperature in question.

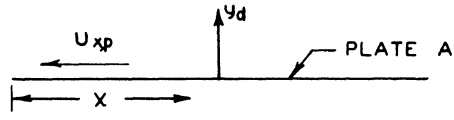

FIG. VII-9. Orientation of plate in fluid.

Equation (VII.31) may be written as

$$u_x = U_{x,P}\left[1 - \frac{2}{\sqrt{\pi}} \int_0^{\zeta_1} \exp\{-\zeta^2\}\, d\zeta\right] = U_{x,P}\left(1 - \operatorname{erf}(\zeta_1)\right). \quad \text{(1 E)}$$

Values of the probability integral or error function are readily available (*20, 21*) and may be used to obtain numerical values for the velocity as a function of the normal distance from the plate and time. The results of such calculations are set forth in Table VII-1 and in Fig. VII-10. In this instance the velocity has been presented as a ratio of that at the point in question to that of the plate.

Where there is flow past a flat plate that is infinitely long in the x-direction, the proportionality for the boundary layer thickness[1] may be written as

[1] Actually it is sometimes convenient to define the boundary layer thickness as that point where the local velocity has assumed some arbitrary fraction of that of the free stream.

$$\delta \sim \sqrt{\frac{\eta g_c \theta}{\sigma}} \sim \sqrt{\frac{\eta g_c}{\sigma} \frac{x}{u_\infty}}. \qquad \text{(VII.32)}$$

This relationship follows from Eq. (VII.30) rewritten for the steady or stationary plate. For much of the boundary layer discussion it is convenient to define a dimensionless thickness in the following way:

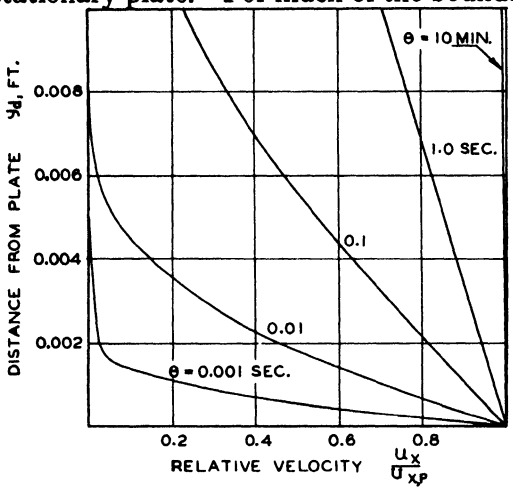

FIG. VII-10. Velocity distribution in vicinity of moving plate.

$$\frac{y_d}{\delta} \cong \psi. \qquad \text{(VII.33)}$$

A combination of Eqs. (VII.30), (VII.32), and (VII.33) with the replacement of $U_{x,P}$ by u_∞ yields

$$\psi = y_d \sqrt{\frac{\sigma}{\eta g} \frac{u_\infty}{x}}. \qquad \text{(VII.34)}$$

Equation (VII.34) yields an expression for the change in the relative position in the laminar

TABLE VII-1. $u_x/U_{x,P}$ as a Function of Time and Position near a Flat Plate.

θ, Time, Sec.

y_d, Distance From Plate, Ft.	0.001	0.01	0.1	1
0.00005	0.952	0.985	0.996	0.999
0.0001	0.904	0.970	0.990	0.997
0.0002	0.811	0.940	0.981	0.994
0.0005	0.549	0.850	0.952	0.985
0.001	0.231	0.704	0.904	0.970
0.002	0.016	0.448	0.811	0.940
0.005	0.000	0.058	0.549	0.850
0.01	0.0	0.0002	0.231	0.704
0.02	0.0	0.0	0.016	0.448
0.05	0.0	0.0	0.0000	0.058
0.1	0.0	0.0	0.0000	0.0002

boundary layer with distance from the leading edge. Differentiation of this expression with respect to x and y results in

$$\frac{\partial \psi}{\partial x} = -\frac{1}{2}\frac{\psi}{x}. \tag{VII.35}$$

$$\frac{\partial \psi}{\partial y_d} = \sqrt{\frac{\sigma}{\eta g_c}\frac{u_\infty}{x}}. \tag{VII.36}$$

As has been described in an earlier chapter, the equation of continuity may be integrated by the introduction of an appropriate stream function, χ, which is assumed here to be of the form,

$$\chi = \sqrt{\frac{\eta g_c}{\sigma} x u_\infty}\, \phi_2(\psi). \tag{VII.37}$$

By appropriate differentiation of Eq. (VII.37) there is obtained

$$u_x = \frac{\partial \chi}{\partial y_d} = \frac{\partial \chi}{\partial \psi}\frac{\partial \psi}{\partial y_d} = u_\infty \phi_2'(\psi). \tag{VII.38}$$

In Eq. (VII.38) the symbol $\phi_2'(\psi)$ signifies differentiation of $\phi_2(\psi)$ with respect to ψ. In a similar fashion it may be shown that

$$u_y = \frac{1}{2}\sqrt{\frac{\eta g_c}{\sigma}\frac{u_\infty}{x}}\,(\psi \phi_2'(\psi) - \phi_2(\psi)). \tag{VII.39}$$

Likewise, it is possible to establish the derivatives of the longitudinal velocity with respect to χ and y_d and the second derivative with respect to y_d. These are tabulated below.

$$\frac{\partial u_x}{\partial x} = \frac{1}{2}\frac{u_\infty}{x}\psi \phi_2''(\psi), \tag{VII.40}$$

$$\frac{\partial u_x}{\partial y_d} = u_\infty \sqrt{\frac{\sigma}{\eta g_c}\frac{u_\infty}{x}}\,\phi_2''(\psi), \tag{VII.41}$$

$$\frac{\partial^2 u_x}{\partial y_d^2} = \frac{\sigma}{\eta g_c}\frac{u_\infty^2}{x}\phi_2'''(\psi). \tag{VII.42}$$

A combination of the values of the longitudinal and transverse velocities together with their derivatives in Eq. (VII.26) results in

$$-\frac{u_\infty^2}{2x}\psi\phi_2'(\psi)\phi_2''(\psi) + \frac{u_\infty^2}{2x}(\psi\phi_2'(\psi) - \phi_2(\psi))\phi_2''(\psi) = \frac{\eta g_c}{\sigma}\frac{\sigma u_\infty^2}{\eta g_c x}\phi_2'''(\psi). \tag{VII.43}$$

Equation (VII.43) simplifies to

$$\phi_2(\psi)\phi_2''(\psi) + 2\phi_2'''(\psi) = 0. \tag{VII.44}$$

It should be realized that Eq. (VII.44) is an ordinary differential equation involving the stream function $\phi_2(\psi)$. It is known as the Blasius differential equation (*14*). From the boundary conditions and the defining relationships for the longitudinal and transverse velocities it follows that:

at
$$\psi = 0, \tag{VII.45}$$

$$\phi_2(0) = \phi_2'(0) = 0 \tag{VII.46}$$

at
$$\psi = \infty, \tag{VII.47}$$

$$\phi_2'(\infty) = 1. \tag{VII.48}$$

The foregoing transformation involving Eq. (VII.34) and the stream function χ has reduced a partial differential equation to an ordinary nonlinear differential equation of the third order. The three boundary conditions set forth by Eqs. (VII.44) and (VII.45) through (VII.48) permit a unique determination of the Blasius function $\phi_2(\psi)$. It may be shown from the theory of differential equations (*19*) that a particular solution to Eq. (VII.44) is of the form,

$$\phi_2(\psi) = \psi + k_3 \tag{VII.49}$$

where k_3 is independent of ψ. Equation (VII.49) corresponds to the behavior of Eq. (VII.44) in potential flow. It therefore satisfies the boundary conditions encountered at the edge of the boundary layer. Because of the nonlinear character of Eq. (VII.44) it is not possible to obtain a general solution in closed form, and it must be evaluated in particular cases by numerical methods (*22*) or by a series development. Blasius (*14*) obtained a reasonable solution in the vicinity of

$$\psi = 0 \tag{VII.50}$$

by use of a series expansion. By combining the appropriate series developments for the function $\phi_2(\psi)$ and its first and second derivatives it is possible to obtain the following solution to the Blasius equation:[1]

$$\phi_2(\psi) = \sum_{n=0}^{\infty} \left(-\frac{1}{2}\right)^n \frac{c_n \alpha^{n+1}}{(3n+2)!} \psi^{(3n+2)}. \tag{VII.51}$$

[1] A more detailed consideration of this development is available (*11*, *23*).

The coefficients α and C_n are determined by the boundary conditions. In a similar fashion an asymptotic solution (*14*) was obtained in the vicinity of

$$\psi = \infty, \tag{VII.52}$$

$$\phi_2(\psi) = \psi - \beta + \gamma \int_{\infty}^{\psi} d\psi \int_{\infty}^{\psi} \exp\left\{-\frac{1}{4}(\psi - \beta)^2\right\} d\psi. \tag{VII.53}$$

The integration constants are β and γ. Equations (VII.51) and (VII.53) may now be combined at some appropriate point where the value of ψ and the values of $\phi_2(\psi)$, $\phi_2'(\psi)$, and $\phi_2''(\psi)$ are equal for the series solution near the wall and the asymptotic solution at the outer edge of the laminar boundary layer. All of the higher derivatives will be satisfied by virtue of Eq. (VII.44). Howarth (*24*) and Blasius (*14*) obtained values for the three constants of Eqs. (VII.51) and (VII.53) and these are recorded in a part of Table VII-2. In addition, values of $\phi_2(\psi)$ and its first and second derivatives have been recorded from the calculations of Howarth and Blasius. A much more extended tabulation of the Blasius function and its derivative has been prepared by Emmons and Leigh (*25*). The data of Table VII-2 permit the direct solution of the velocity in the laminar boundary layer for the flow over a flat plate by use of Eqs. (VII.38) and (VII.39) for the longitudinal and transverse velocities. In the application of the data of Table VII-2 it should be realized that the quantities tabulated are functions of ψ which combines the relative position in the boundary layer with the flow conditions as noted in Eq. (VII.34). The second column gives the values of the function defined by Eq. (VII.37) whereas the third column gives the dimensionless velocity or Blasius function obtainable from Eq. (VII.38). The rate of change of velocity in the x-direction may be obtained from the second derivative of the Blasius function by application of Eq. (VII.40). The Blasius solution has been verified experimentally by Dhawan (*26*).

Example 2

Trajectory of a Particle in Boundary Layer: It is desired to determine the change in position of a particle near a flat plate as a result of the flow of a large body of fluid past the plate. In this instance it has been assumed that oil is approaching the plate at a bulk velocity of one foot per minute and is of a viscosity of 5 centipoises with a specific weight of 61 pounds per cubic foot. It is desired to determine the velocity-time relationships for particles located initially 0.02 and 0.003 inch from the plate. In addition, it is desired to determine the trajectories of these particles.

The velocity in the x and y_d directions may be obtained from the following expressions:

$$u_x = u_\infty \phi_2' \left(y_d \sqrt{\frac{u_\infty}{\nu x}} \right), \tag{1 E}$$

$$u_y = \frac{1}{2} \sqrt{\frac{\nu u_\infty}{x}} \left\{ y_d \sqrt{\frac{u_\infty}{\nu x}} \phi_2' \left(y_d \sqrt{\frac{u_\infty}{\nu x}} \right) - \phi_2 \left(y_d \sqrt{\frac{u_\infty}{\nu x}} \right) \right\}. \tag{2 E}$$

The values of the functions ϕ_2 and ϕ_2' are recorded in Table VII-2. The information stated in the problem permits values of u_x and u_y to be evaluated. The value of the position as a function of time at the two values of y_i indicated may be established from

$$x = \int_0^{\theta_1} u_x \, d\theta + x_i. \tag{3 E}$$

From a choice of θ_1 for Eq. (3 E) it is possible to solve Eqs. (1 E) and (2 E) iteratively and obtain the information as to the velocity in the x and y_d directions as functions of time for fixed values of y_d. Nothing is gained by combining Eqs. (1 E) and (2 E) separately with Eq. (3 E) since the variables are not separable. A choice of time intervals of approximately 0.1 second yields values of u_x and u_y with satisfactory accuracy.

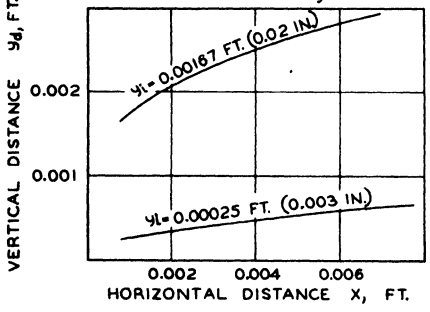

FIG. VII-11. Trajectories.

Since it is desired to determine the trajectory of a particle, Eqs. (1 E) and (2 E) must be solved simultaneously with Eqs. (3 E) and (4 E).

$$y_d = \int_0^{\theta_1} u_y \, d\theta + y_i. \tag{4 E}$$

The results of these calculations give simultaneous values of x and y_d along the trajectory. These trajectories are presented in Fig. VII-11. In the course of these calculations the corresponding values of u_x and u_y along the trajectories are obtained and have been shown in Figs. VII-12 and VII-13. Another approach to the whole problem is to note that the stream function χ in Eq. (VII.37) is constant on a trajectory.

The longitudinal velocity distribution in normalized coordinates is shown in Fig. VII-14 and the normalized transverse velocity in Fig. VII-15. It is

of interest to note that, at large distances from the plate, the data of Table VII-2 indicate that

$$u_y = u_{y\infty} = 0.865\, u_\infty \sqrt{\frac{\eta g_c}{\sigma}\frac{u_\infty}{x}}. \tag{VII.54}$$

Equation (VII.54) illustrates that even at an infinite distance from a flat plate the potential flow has been disturbed by the displacement resulting from the accumulation of additional material around the plate as a result

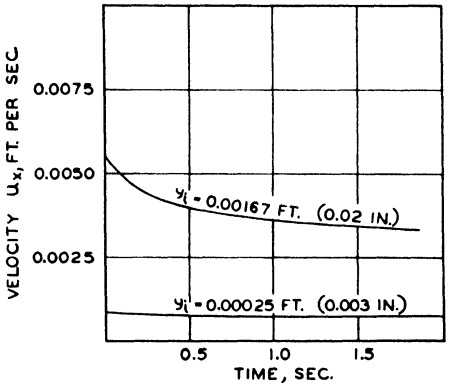

FIG. VII-12. X-Component velocity along trajectory.

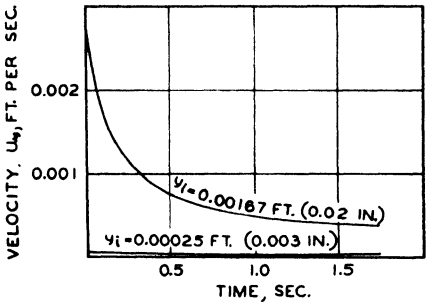

FIG. VII-13. Y-Component velocity along trajectory.

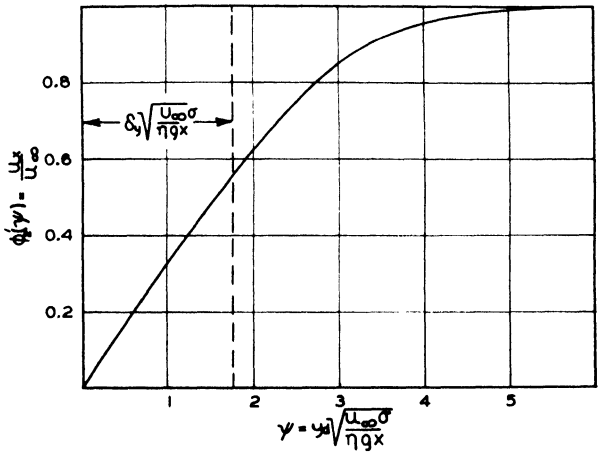

FIG. VII-14. Normalized longitudinal velocity distribution (*11*, *15*).

of the smaller longitudinal velocity. Although a consequence of Eq. (VII.15) this prediction constitutes a deficiency in the boundary layer theory as developed by Blasius (*14*) since it does not satisfy the condition that the transverse velocity approaches zero as y_d becomes large. It should be noted

that the data of Table VII-2 apply only to situations with a negligible pressure gradient. Kaplan (*16*) shows that this deficiency can be removed by solving the bundary-layer problem in a suitable coordinate system. The surface shear is unchanged.

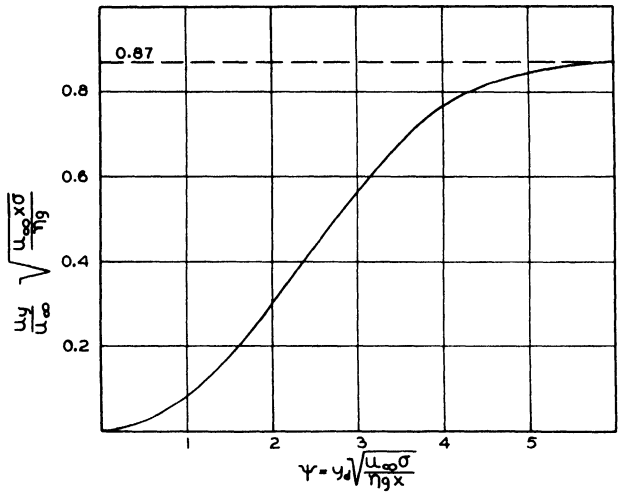

FIG. VII-15. Normalized transverse velocity distribution (*11*, *15*).

VII-10. Drag

It is often desirable to calculate the drag force or the shear at the boundary. Under these circumstances the longitudinal force acting on one side of a flat plate of width z may be established from Eq. (VII.24).

$$F_D = \oint (\tau_{yx})_0 \, ds = z \int_0^{x_1} (\tau_{yx})_0 \, dx. \tag{VII.55}$$

For a plate of constant width z it is possible to substitute the simple integral for the closed area integral of Eq. (VII.24) as has been done in the second equality of Eq. (VII.55). In this instance x represents the distance along the plate from the leading edge. The shear at the wall may be directly established from (*12*, *14*).

$$(\tau_{yx})_0 = \eta \left(\frac{\partial u_x}{\partial y_d} \right)_{y_d = 0}. \tag{VII.56}$$

A combination of Eqs. (VII.56) and (VII.41) results in

$$(\tau_{yx})_0 = \eta u_\infty \sqrt{\frac{\sigma}{\eta g_c} \frac{u_\infty}{x}} \, (\phi_2''(\psi))_{y_d = 0}. \tag{VII.57}$$

Equation (VII.57) may be rewritten in the following numerical form from the data of Table VII-2 for $(\phi_2''(\psi))_{y_d=0}$:

$$(\tau_{yx})_0 = 0.33206 \sqrt{\frac{\sigma \eta}{g_c} \frac{u_\infty^3}{x}}. \qquad \text{(VII.58)}$$

TABLE VII-2. Blasius Function $\phi_2(\psi)$ for Velocity Distribution Laminar, Incompressible Boundary Layer *11*

$\alpha = 0.332 \quad \beta = 1.73 \quad \gamma = 0.231$

ψ	$\phi_2(\psi)$	$\phi_2'(\psi)$	$\phi_2''(\psi)$	ψ	$\phi_2(\psi)$	$\phi_2'(\psi)$	$\phi_2''(\psi)$
0	0	0	0.33206	5.0	3.28329	0.99155	0.01591
0.2	0.00664	0.06641	0.33199	5.2	3.48189	0.99425	0.01134
0.4	0.02656	0.13277	0.33147	5.4	3.68094	0.99616	0.00793
0.6	0.05974	0.19894	0.33008	5.6	3.88031	0.99748	0.00543
0.8	0.10611	0.26471	0.32739	5.8	4.07990	0.99838	0.00365
1.0	0.16557	0.32979	0.32301	6.0	4.27964	0.99898	0.00240
1.2	0.23795	0.39378	0.31659	6.2	4.47948	0.99937	0.00155
1.4	0.32298	0.45627	0.30787	6.4	4.67938	0.99961	0.00098
1.6	0.42032	0.51676	0.29917	6.6	4.87931	0.99977	0.00061
1.8	0.52952	0.57477	0.28293	6.8	5.07928	0.99987	0.00037
2.0	0.65003	0.62977	0.26675	7.0	5.27926	0.99992	0.00022
2.2	0.78120	0.68132	0.24835	7.2	5.47925	0.99996	0.00013
2.4	0.92230	0.72899	0.22809	7.4	5.67924	0.99998	0.00007
2.6	1.07252	0.77246	0.20646	7.6	5.87924	0.99999	0.00004
2.8	1.23099	0.81152	0.18401	7.8	6.07923	1.00000	0.00002
3.0	1.39682	0.84605	0.16136	8.0	6.27923	1.00000	0.00001
3.2	1.56911	0.87609	0.13913	8.2	6.47923	1.00000	0.00001
3.4	1.74696	0.90177	0.11788	8.4	6.67923	1.00000	0.00000
3.6	1.92954	0.92333	0.09809	8.6	6.87923	1.00000	0.00000
3.8	2.11605	0.94112	0.08013	8.8	7.07923	1.00000	0.00000
4.0	2.30576	0.95552	0.06424				
4.2	2.49806	0.96696	0.05052				
4.4	2.69238	0.97587	0.03897				
4.6	2.88826	0.98269	0.02948				
4.8	3.08534	0.98779	0.02187				

From Eqs. (VII.55) and (VII.58) it may be seen that the force acting on one side of the plate may be established from integration of the following equation:

$$F_D = 0.33206\, z \sqrt{\frac{\sigma \eta}{g_c} u_\infty^3} \int_0^{x_1} \frac{dx}{\sqrt{x}}. \tag{VII.59}$$

If it is assumed that the physical properties remain unchanged throughout the boundary region, integration of Eq. (VII.59) results in

$$F_D = 0.66412\, z \sqrt{\frac{\sigma \eta}{g_c} u_\infty^3\, x}. \tag{VII.60}$$

It should be emphasized that Eq. (VII.60) yields only the drag force on one side of the plate. If it is desired to obtain the drag on both sides of the plate it assumes the form,

$$2F_D = 1.328\, z \sqrt{\frac{\sigma \eta}{g_c} u_\infty^3\, x}. \tag{VII.61}$$

For many purposes particularly in the field of aeronautics it is conventional to express the drag in terms of a dimensionless coefficient (*23*) which for these purposes may be defined as

$$C_D = \frac{2F_D g_c}{\sigma u_{x\infty}^2\, x\, z}. \tag{VII.62}$$

A combination of Eqs. (VII.61) and (VII.62) yields the following expression for the drag coefficient of the entire plate in terms of the conditions of flow:

$$C_D = 1.328 \sqrt{\frac{\eta g_c}{\sigma u_\infty x}} = \frac{1.328}{\sqrt{\mathrm{Re}}}. \tag{VII.63}$$

The total force on the plate may be directly obtained from rearrangement of Eq. (VII.62).

VII-11. Thickness of Boundary Layer

Steady laminar boundary layers actually are of infinite thickness but it is convenient to consider finite thicknesses of the boundary layer for purposes of practical calculations. For example, Fig. VII-16 shows the flow over a flat plate, and the boundary layer developing proportionally to the

square root of the distance from the leading edge at A. The potential flow is deflected outward away from the plate by some length quantity δ_y, which is called the displacement thickness. Following Schlichting (*11*) it is seen that if the limit of integration y_a is taken outside the effective boundary layer, the integration from the wall to y_a in the following expression illustrates the use of δ_y in describing the decrease of cross section of potential flow:

$$\int_0^{y_a} u_x \, dy_d = u_\infty (y_a - \delta_y). \quad \text{(VII.64)}$$

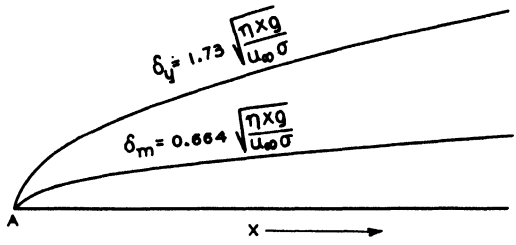

FIG. VII-16. Schematic arrangement of boundary layer on flat plate.

Equation (VII.64) is in reality the definition of the displacement thickness of the boundary layer when y_a becomes infinite and may be rewritten as

$$\delta_y = \int_0^\infty \left(1 - \frac{u_x}{u_\infty}\right) dy_d. \quad \text{(VII.65)}$$

A combination of Eqs. (VII.34), (VII.64), and (VII.38) results in

$$\delta_y = \sqrt{\frac{\eta g_c}{\sigma} \frac{x}{u_\infty}} \int_0^{\psi_1} [1 - \phi_2'(\psi)] \, d\psi = \sqrt{\frac{\eta g_c}{\sigma} \frac{x}{u_\infty}} [\psi_1 - \phi_2(\psi_1)]. \quad \text{(VII.66)}$$

If desired, it is possible to simplify Eq. (VII.66) still further by substitution of the following good approximation:

$$\phi_2(\psi_1) = \psi_1 - 1.73. \quad \text{(VII.67)}$$

Equation (VII.67) is the first term of the Blasius (*14*) asymptotic solution. A combination of Eqs. (VII.66) and (VII.67) results in

$$\delta_y = 1.73 \sqrt{\frac{\eta g_c}{\sigma} \frac{x}{u_\infty}} = \frac{1.73 \, x}{\sqrt{\mathrm{Re}}}. \quad \text{(VII.68)}$$

Equation (VII.68) yields the expression for the displacement thickness. It is apparent that δ_y increases directly with the square root of the downstream distance. This has been indicated in Fig. VII-16.

For some purposes it is convenient to define a momentum thickness of a boundary layer which is the thickness associated with the total loss in momentum of the flow as a result of the dissipation in the boundary layer. The momentum thickness is defined as

$$\delta_m = \int_0^\infty \frac{u_x}{u_\infty}\left(1 - \frac{u_x}{u_\infty}\right) dy_d. \tag{VII.69}$$

A combination of Eqs. (VII.34), (VII.69), and (VII.38) yields

$$\delta_m = \sqrt{\frac{\eta g_c}{\sigma}\frac{x}{u_\infty}} \int_0^\infty \phi_2'(\psi)\,(1 - \phi_2'(\psi))\, d\psi = 0.664 \sqrt{\frac{\eta g_c}{\sigma}\frac{x}{u_\infty}} = \frac{0.664\, x}{\sqrt{\mathrm{Re}}}. \tag{VII.70}$$

These expressions describe the variation in the characteristic dimension of the boundary layer with downstream position in terms of the properties of the flowing stream.

The momentum thickness is shown in Fig. VII-16. It does not appear worth-while to extend the discussion beyond the present point insofar as flat plates are concerned. The influence of curved boundary surfaces on such boundary layers has been investigated (*27*). It should be realized that there exists a definite limit of the Reynolds numbers beyond which a laminar boundary upon a flat plate does not persist in a stable form. It has been estimated (*12*), based upon the measurements of van der Hegge-Zijnen (*28*) and Hansen (*29*), that the probability of a laminar boundary layer existing continuously decreases rapidly at Reynolds numbers above 5×10^5 and none have been observed above 3×10^6 (*30*, *31*).

VII-12. Effect of Curvature

Some consideration has been given to the behavior of laminar boundary layers flowing along a surface whose radius of curvature lies in a direction normal to the flow. In such an instance the boundary layer is still two-dimensional and it has been found (*18*) that as long as the radius of curvature is large in comparison to the thickness of the boundary layer it is a reasonable approximation (*17*) to treat the boundary flow as though it were on a flat plate. It is desirable to differentiate clearly between the two-dimensional boundary layer flowing on a curved surface and a three-dimensional boundary layer such as is encountered in the flow over a sphere or some blunt object.

VII-13. Flow about Circular Cylinders

For many engineering purposes it is desired to predict the boundary flow around a cylinder. Hiemenz (*32*) was perhaps the first to consider this problem, and his attack was materially extended by Thom (*33*) and Howarth (*34*). In considering these problems the same primary differential equations as were employed for a flat plate were considered applicable. The pressure distribution around the cylinder may be estimated from the theory of potential flow or from experiment. By following much the same procedure as has been done in the case of flat plates Howarth (*34*) found a formulation which described the velocity distribution about a symmetrical cylinder.

In the case of a circular cylinder, Lamb (*35*) (see Appendix IV) has shown that the velocity distribution in potential flow around a cylinder may be described by

$$u_s = 2\,u_\infty \left[\frac{s}{r} - \frac{1}{3!}\left(\frac{s}{r}\right)^3 + \frac{1}{5!}\left(\frac{s}{r}\right)^5 - \frac{1}{7!}\left(\frac{s}{r}\right)^7 + \ldots\right]. \quad \text{(VII.71)}$$

In Eq. (VII.71) s is taken as the distance measured along the cylinder from the stagnation point. When the effects of viscosity are included, the velocity distribution in the boundary layer (*24*) is given by

$$\frac{1}{2}\frac{u_s}{u_\infty} = \frac{s}{r}\phi_1'(\psi_0) - \frac{4}{3!}\left(\frac{s}{r}\right)^3 \phi_3'(\psi_0) + \frac{1}{5!}\left(\frac{s}{r}\right)^5 (6\phi_5'(\psi_0) + 20\phi_1'(\psi_0)) + \ldots. \quad \text{(VII.72)}$$

The derivatives of the circular stream functions used in Eq. (VII.72) are given in Table VII-3 and permit the velocity at any point around the cylinder to be predicted. However, Eq. (VII.72) applies only to situations where no separation is involved. The circular stream function is defined by the following expression:

$$\psi_0 = \frac{y_d}{r}\sqrt{\frac{\sigma}{\eta g_c}\,2\,u_\infty\, r}. \quad \text{(VII.73)}$$

If desired, the point of separation, which is characterized by a zero velocity gradient at the surface, may be estimated. This point may be established by differentiation of the right side of Eq. (VII.72) and setting it equal to zero. Such action results in

$$\phi_1''(0)\frac{s_{sp}}{r} - \frac{4}{3!}\phi_3''(0)\left(\frac{s_{sp}}{r}\right)^3 + \ldots = 0. \quad \text{(VII.74)}$$

TABLE VII-3. Functions ϕ_1, ϕ_3, ϕ_5, ϕ_7 for Velocity Distribution. Laminar, Incompressible Boundary Layer for a Circular Cylinder (*11*)

ψ_0 [1]	$\phi_1(\psi_0)$	$\phi_1'(\psi_0)$	$\phi_1''(\psi_0)$	$\phi_3(\psi_0)$	$\phi_3'(\psi_0)$	$\phi_3''(\psi_0)$
0	0	0	1.23264	0	0	0.7244
0.1	0.0060	0.1183	1.1328	0.0035	0.0675	0.6249
0.2	0.0233	0.2266	1.0345	0.0132	0.1251	0.5286
0.3	0.0510	0.3252	0.9386	0.0282	0.1734	0.4375
0.4	0.0881	0.4144	0.8463	0.0476	0.2129	0.3539
0.5	0.1336	0.4946	0.7583	0.0705	0.2444	0.2780
0.6	0.1867	0.5662	0.6751	0.0962	0.2688	0.2112
0.7	0.2466	0.6298	0.5973	0.1240	0.2869	0.1530
0.8	0.3124	0.6859	0.5251	0.1534	0.2997	0.1037
0.9	0.3835	0.7350	0.4586	0.1838	0.3080	0.0626
1.0	0.4592	0.7778	0.3980	0.2149	0.3125	0.0292
1.1	0.5389	0.8149	0.3431	0.2462	0.3140	0.0028
1.2	0.6220	0.8467	0.2937	0.2776	0.3132	−0.0173
1.3	0.7081	0.8739	0.2498	0.3088	0.3107	−0.0320
1.4	0.7966	0.8968	0.2109	0.3397	0.3070	−0.0420
1.5	0.8873	0.9161	0.1769	0.3702	0.3025	−0.0482
1.6	0.9798	0.9324	0.1473	0.4002	0.2947	−0.0513
1.7	1.0738	0.9457	0.1218	0.4297	0.2923	−0.0518
1.8	1.1688	0.9569	0.0999	0.4587	0.2871	−0.0506
1.9	1.2650	0.9659	0.0814	0.4871	0.2822	−0.0480
2.0	1.3619	0.9732	0.0658	0.5151	0.2775	−0.0444
2.1	1.4596	0.9792	0.0528	0.5426	0.2733	−0.0402
2.2	1.5577	0.9841	0.0420	0.5698	0.2695	−0.0358
2.3	1.6563	0.9876	0.0332	0.5966	0.2662	−0.0314
2.4	1.7552	0.9905	0.0260	0.6230	0.2632	−0.0271
2.5	1.8543	0.9928	0.0202	0.6492	0.2607	−0.0230
2.6	1.9537	0.9946	0.0156	0.6752	0.2586	−0.0194
2.7	2.0533	0.9960	0.0119	0.7010	0.2568	−0.0160
2.8	2.1529	0.9971	0.0091	0.7266	0.2554	−0.0131
2.9	2.2528	0.9979	0.0068	0.7520	0.2542	−0.0106
3.0	2.3525	0.9985	0.0051	0.7774	0.2533	−0.0085
3.1	2.4523	0.9988	0.0036	0.8027	0.2525	−0.0067
3.2	2.5522	0.9992	0.0027	0.8279	0.2519	−0.0052
3.3	2.6521	0.9994	0.0023	0.8531	0.2515	−0.0041
3.4	2.7521	0.9996	0.0019	0.8782	0.2511	−0.0032
3.5	2.8520	0.9997	0.0014	0.9033	0.2508	−0.0024

[1] $\psi_0 = y_d \sqrt{a \frac{\sigma}{\eta g_c}}$; also the function ϕ_1 of the plane stagnation point.

TABLE VII-3. (Cont.)

ψ_0	$\phi_1(\psi_0)$	$\phi_1'(\psi_0)$	$\phi_1''(\psi_0)$	$\phi_3(\psi_0)$	$\phi_3'(\psi_0)$	$\phi_3''(\psi_0)$
3.6	2.9520	0.9998	0.0010	0.9284	0.2506	−0.0019
3.7	3.0519	0.9999	0.0008	0.9534	0.2504	−0.0014
3.8	3.1518	0.9999	0.0004	0.9785	0.2503	−0.0011
3.9	3.2518	0.9999	0.0003	1.0035	0.2502	−0.0008
4.0	3.3518	1.0000	0.0002	1.0285	0.2502	−0.0006
4.1	3.4518	1.0000	0.0001	1.0535	0.2501	−0.0004
4.2	3.5518	1.0000	0.0001	1.0785	0.2501	−0.0003
4.3	3.6518	1.0000	0.0000	1.1035	0.2500	−0.0002
4.4	—	—	—	1.1285	0.2500	−0.0001

ψ_0	$\phi_5(\psi_0)$	$\phi_5'(\psi_0)$	$\phi_5''(\psi_0)$	$\phi_7(\psi_0)$	$\phi_7'(\psi_0)$	$\phi_7''(\psi_0)$
0	0	0	0.6348	0	0	0.1192
0.2	0.0114	0.1072	0.4402	0.0017	0.0141	0.0249
0.4	0.0405	0.1778	0.2717	0.0045	0.0117	−0.0436
0.6	0.0806	0.2184	0.1408	0.0057	−0.0010	−0.0783
0.8	0.1264	0.2367	0.0483	0.0039	−0.0176	−0.0833
1.0	0.1742	0.2399	−0.0106	−0.0012	−0.0330	−0.0680
1.2	0.2218	0.2342	−0.0431	−0.0090	−0.0441	−0.0423
1.4	0.2676	0.2239	−0.0567	−0.0185	−0.0498	−0.0149
1.6	0.3112	0.2123	−0.0580	−0.0286	−0.0503	0.0088
1.8	0.3526	0.2012	−0.0522	−0.0384	−0.0468	0.0256
2.0	0.3918	0.1916	−0.0432	−0.0472	−0.0406	0.0351
2.2	0.4293	0.1839	−0.0335	−0.0546	−0.0331	0.0380
2.4	0.4655	0.1781	−0.0245	−0.0604	−0.0257	0.0361
2.6	0.5007	0.1740	−0.0171	−0.0649	−0.0189	0.0312
2.8	0.5352	0.1712	−0.0114	−0.0681	−0.0133	0.0249
3.0	0.5692	0.1694	−0.0072	−0.0703	−0.0089	0.0187
3.2	0.6030	0.1682	−0.0043	−0.0717	−0.0058	0.0132
3.4	0.6365	0.1676	−0.0026	−0.0726	−0.0036	0.0089
3.6	0.6700	0.1672	−0.0015	−0.0732	−0.0021	0.0057
3.8	0.7034	0.1669	−0.0010	−0.0735	−0.0012	0.0036
4.0	0.7368	0.1668	−0.0004	−0.0737	−0.0006	0.0022
4.2	0.7701	0.1667	−0.0001	−0.0738	−0.0003	0.0012
4.4	0.8035	0.1667	−0.0001	−0.0738	−0.0001	0.0007

In Eq. (VII.74) the position of separation has been identified by the subscript sp. The values of the functions, $\phi_1, \phi_1', \phi_1''$; $\phi_3, \phi_3', \phi_3''$; $\phi_5, \phi_5', \phi_5''$; and $\phi_7, \phi_7', \phi_7''$, of ψ_0 are recorded in Table VII-3. The solution of Eq. (VII.74) from the tabulated functions of Table VII-3 yields a value s_{sp}/r of 1.60 which corresponds to an angular displacement of 92° from the point of stagnation. Such a theoretical value differs significantly from that found by experiment *32*). This divergence has been attributed by Schlichting (*11*) to the disagreement between the pressure distribution predicted by the potential theory and that obtained in an actual flow for a rather blunt body of revolution such as a circular cylinder.

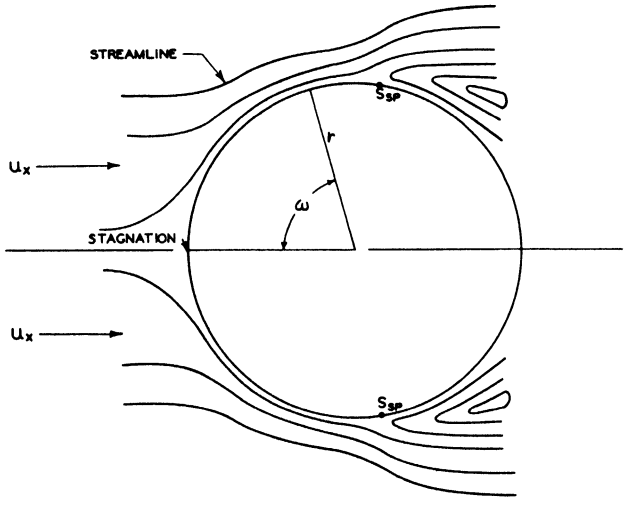

FIG. VII-17. Flow around a circular cylinder (*11*, *15*).

The significance of the symbols in Eqs. (VII.71), (VII.72), (VII.73), and (VII.74) is shown in Fig. VII-17 which illustrates qualitatively the point of separation of the flow at s_{sp}. It should be emphasized that the nature of the flow approaching the cylinder as well as the relative dimensions of the channel and the cylinder influence this behavior.

Fig. VII-18 shows the air speed field (*36*) in the wake of a steel cylinder 0.190 in. in diameter which was located between parallel plates with a separation of 0.75 in. It should be emphasized that the data of Fig. VII-18 are air speed and no indication of the direction of motion is included. These data are an illustration of the complexity of the flow fields existing in the wake of cylinders when separation occurs. If fully developed laminar flow existed throughout the flow field and no separation occurred, the pressure

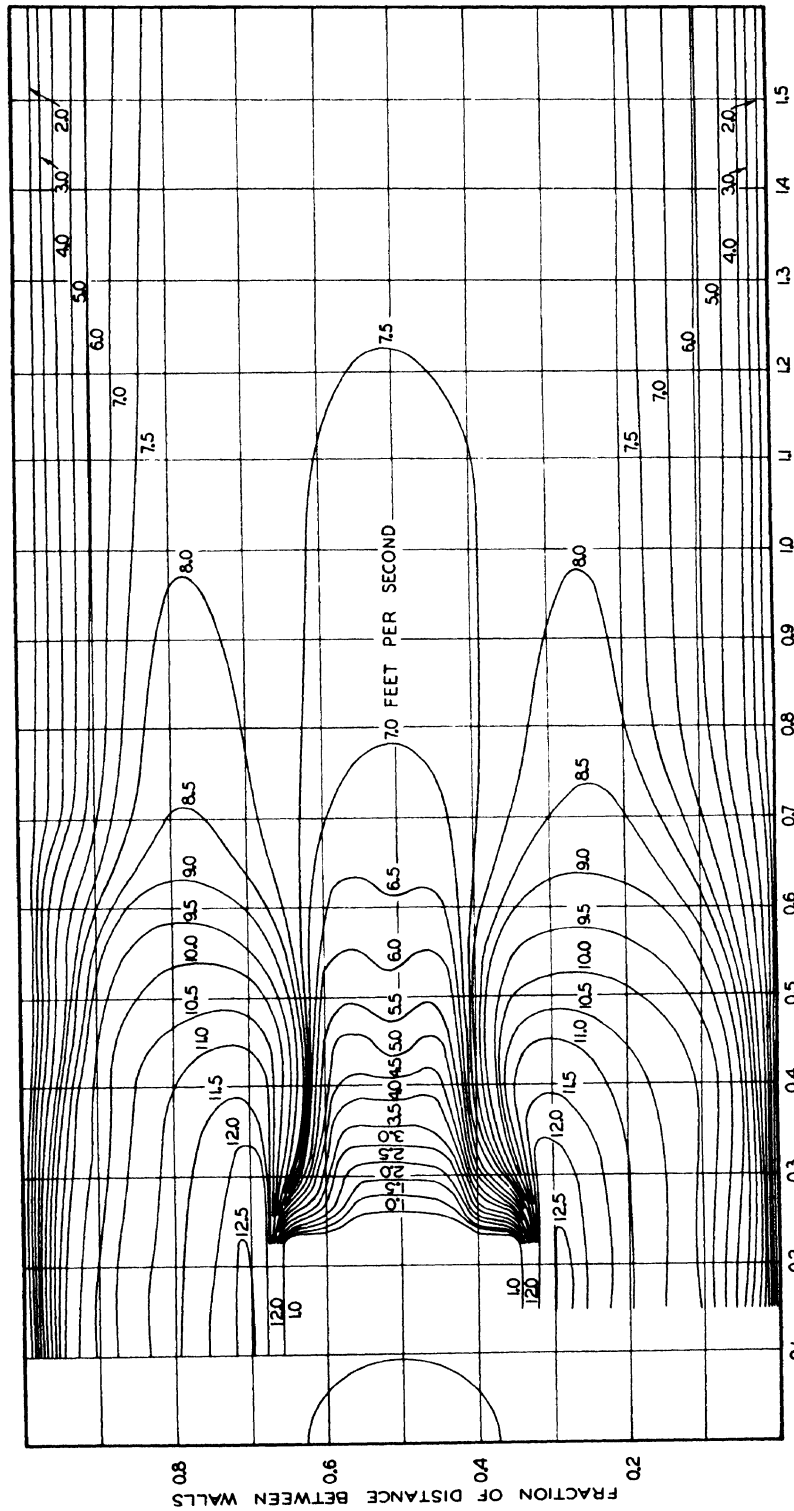

FIG. VII-18. Air speed field in wake of heated steel cylinder at bulk air velocity of 6.99 ft./sec. (*36*).

distribution predicted for potential flow would apply over the entire surface of the cylinder.[1]

It is possible to extend the solution of the laminar boundary layer to a number of other cases including symmetrical and unsymmetrical air foils (*34*). Furthermore, the same line of reasoning may be used to predict approximately the dissipation and velocity distribution in a free jet. These applications are typified by the work of Schlichting (*15*), Bickley (*38*), Pai (*39*), and Donoughe (*40*). It is beyond the scope of this discussion to consider such special applications in detail.

Example 3

Boundary Layer Around a Cylinder: A circular cylinder two inches in diameter with its axis normal to a stream of oil flowing at a velocity of 10 feet per second develops boundary flow. If it is assumed that the flow in the main body of the stream of oil may be treated as potential and if the oil has an absolute viscosity of 15 centipoises and a specific gravity relative to water at its maximum specific weight of 0.86, determine the following:

1. Pressure distribution at outer edge of boundary layer in accordance with potential theory
2. Local velocity distribution in boundary flow
3. Momentum and displacement thickness of boundary flow.

The pressure distribution in potential flow may be shown (*15*) to be the following function of the angular position around the cylinder where s/r is expressed in radians:

$$P = \frac{\sigma u_\infty^2}{2 g_c}\left\{1 - 4\left(\frac{s}{r}\right)^2 + \frac{4}{3}\left(\frac{s}{r}\right)^4 - \frac{24}{270}\left(\frac{s}{r}\right)^6 + \cdots\right\} = \frac{\sigma u_\infty^2}{2 g_c}\left[1 - 4\sin^2\left(\frac{s}{r}\right)\right]. \tag{1 E}$$

In this instance the point of reference is taken coincident with the stagnation point. It should be emphasized that Eq. (1 E) takes no account of separation

[1] It has been found (*37*) that such behavior may be experienced in practice by removing a small amount of the fluid from the boundary layer by use of a permeable surface.

of the boundary flow, and since this was found to be in the neighborhood of 90°, the calculations based on Eq. (1 E) are not significant beyond this value. Figure VII-19 shows the pressure expressed in pounds per square foot above and below the ambient pressure of the stream as a function of angular position. It assumes a value of zero at 30° since Eq. (1 E) under these circumstances may be rewritten as

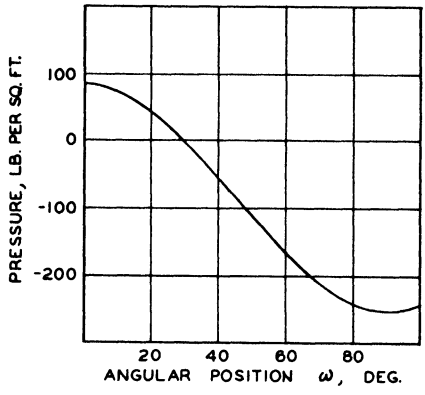

FIG. VII-19. Pressure distribution around cylinder.

$$P = \frac{\sigma u_\infty^2}{2 g_c}\left[1 - 4\left(\frac{1}{2}\right)^2\right] = 0. \quad (2\,E)$$

The minimum pressure occurs at an angular position of 90°. Following the methods that have been described in the present chapter the velocity tangent to the surface may be established from Eq. (VII.72) which in the present instance may be written as

$$u_s = 2 u_\infty \left[\{\phi_1'(\psi_0)\}\left(\frac{s}{r}\right) - \frac{4}{3!}\{\phi_3'(\psi_0)\}\left(\frac{s}{r}\right)^3 + \frac{6}{5!}\left\{\phi_5'(\psi_0) + \frac{10}{3}\phi_7'(\psi_0)\right\}\left(\frac{s}{r}\right)^5 + \ldots\right]. \quad (3\,E)$$

The solution of Eq. (3 E) for several different angular displacements is shown in Fig. VII-20. It is apparent that the boundary layer increases in thickness with the angular displacement. In this instance the calculations were extended to 105° which is beyond the predicted point of separation. It was shown in Eq. (VII.22) that separation would occur under such conditions that

$$\left(\frac{\partial u_s}{\partial y_d}\right)_{y_d = 0} = 0. \quad (4\,E)$$

A combination of Eqs. (4 E) and (3 E) indicates a point of separation of 92°. The details of the solution of Eqs. (3 E) and (4 E) are set forth in Table VII-4.

From the definition of displacement and momentum thicknesses given by Eqs. (VII.65) and (VII.69) respectively it follows that the displacement and momentum thicknesses may be described by:

$$\delta_y = \int_0^\infty \left(1 - \frac{u_s}{u_\infty}\right) dy_d, \tag{5 E}$$

$$\delta_m = \int_0^\infty \frac{u_s}{u_\infty}\left(1 - \frac{u_s}{u_\infty}\right) dy_d. \tag{6 E}$$

The evaluation of Eqs. (5 E) and (6 E) may be accomplished numerically utilizing the information given in Table VII-4. The results of these calculations are summarized in Fig. VII-21. In this instance it should be realized that the thickness shown at stagnation has no real significance. These calculations based upon a pressure distribution ascribed to potential flow are subject to some uncertainty. The method could be extended to a pressure distribution determined experimentally.

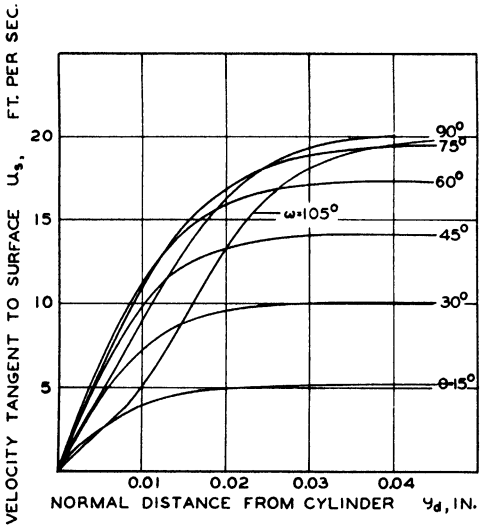

FIG. VII-20. Velocity distribution around cylinder.

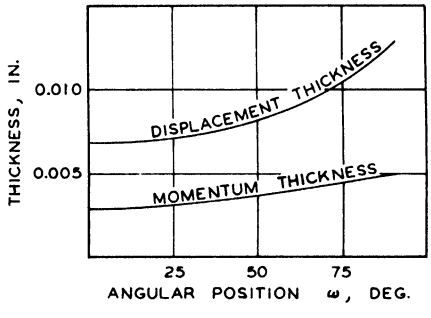

FIG. VII-21. Displacement and momentum thicknesses of boundary layer.

Approximate Solution to the Boundary Layer

In the foregoing sections nearly exact solutions to the laminar incompressible boundary flows were obtained for situations in which the physical properties of the fluid are considered invariant. It was indicated that mathematical difficulties are encountered in attempting to obtain general solutions to the Navier-Stokes equations, even as simplified for application to the conditions near the boundary. For many engineering applications, particularly those involving thermal and material transport, it is desirable to be able to predict the characteristics of boundary layers with and without pressure gradients for a variety of conditions of flow and configurations of

TABLE VII-4. Velocity Distribution in Boundary Flow around a Cylinder

y_d Inch	s Inch	$57.3\frac{s}{r}=\omega$ Degree	$u_s(s, y_d)$ Ft/Sec	y_d Inch	s Inch	$57.3\frac{s}{r}=\omega$ Degree	$u_s(s, y_d)$ Ft/Sec
0.002123	0	0	0	0.02548	0	0	0
($\psi_0 = 0.2$)	0.262	15	1.16	($\psi_0 = 2.4$)	0.262	15	5.127
	0.524	30	2.141		0.524	30	9.879
	0.785	45	2.799		0.785	45	13.882
	1.047	60	3.029		1.047	60	16.830
	1.309	75	2.785		1.309	75	18.380
	1.571	90	2.150		1.571	90	18.420
	1.833	105	1.600		1.833	105	16.600
0.006369	0	0	0	0.03609	0	0	0
($\psi_0 = 0.6$)	0.262	15	2.906	($\psi_0 = 3.4$)	0.262	15	5.18
	0.524	30	5.414		0.524	30	10.01
	0.785	45	7.232		0.785	45	14.13
	1.047	60	8.011		1.047	60	17.28
	1.309	75	7.587		1.309	75	19.25
	1.571	90	5.970		1.571	90	19.93
	1.833	105	3.130		1.833	105	19.20
0.01061	0	0	0	∞	0	0	0
($\psi_0 = 1.0$)	0.262	15	4.0	($\psi_0 = \infty$)	0.262	15	5.18
	0.524	30	7.555		0.524	30	10.01
	0.785	45	10.234		0.785	45	14.14
	1.047	60	11.673		1.047	60	17.32
	1.309	75	11.500		1.309	75	19.44
	1.571	90	9.572		1.571	90	20.00
	1.833	105	5.530				
0.01698	0	0	0				
($\psi_0 = 1.6$)	0.262	15	4.809				
	0.524	30	9.197				
	0.785	45	12.733				
	1.047	60	15.056				
	1.309	75	15.750				
	1.571	90	14.485				
	1.833	105	10.900				

the boundary. In such instances approximations must be made in order to solve the appropriate equations of motion. A most far-reaching assumption involving the form of the velocity profiles in the boundary layer is usually made (*5*).

Various approximations for this velocity profile can be used with varying degrees of success (*11*). The following discussion follows closely the methods developed by Kármán (*4*) and Pohlhausen (*5*) and reviewed by Schlichting (*11*). It should be emphasized that these methods represent only an approximation which has proved to be useful in predicting the characteristics of laminar boundary layers under a variety of conditions of restraint.

VII-14. The Momentum Theorem

The Navier-Stokes equations may be reduced (*11*) to the following form for a steady laminar-boundary-layer:

$$u_x \frac{\partial u_x}{\partial x} + u_y \frac{\partial u_x}{\partial y_d} = -\frac{g_c}{\sigma}\frac{\partial P}{\partial x} + \frac{\eta g_c}{\sigma}\frac{\partial^2 u_x}{\partial y_d^2}. \tag{VII.75}$$

The equation of continuity for an incompressible fluid assumes the familiar form,

$$\frac{\partial u_x}{\partial x} + \frac{\partial u_y}{\partial y_d} = 0. \tag{VII.76}$$

Equation (VII.75) may be integrated from the wall in a direction normal to the interface to some point in the stream outside the boundary region. The order of integration of the first term may be inverted since the limit y_a is assumed not to be a function of x. Under these circumstances and assuming an incompressible fluid Eq. (VII.75) assumes the form,

$$\frac{1}{2}\frac{d}{dx}\int_0^{y_a} u_x^2\, dy_d + \int_0^{y_a} u_y \frac{\partial u_x}{\partial y_d}\, dy_d = -y_a \frac{g_c}{\sigma}\frac{dP}{dx} + \frac{\eta g_c}{\sigma}\left[\frac{\partial u_x}{\partial y_d}\right]_{y_d=0}^{y_d=y_a}. \tag{VII.77}$$

The second term of Eq. (VII.77) may be integrated by parts to yield

$$\int_0^{y_a} u_y \frac{\partial u_x}{\partial y_d}\, dy_d = u_\infty (u_y)_{y_d=y_a} - \int_0^{y_a} u_x \frac{\partial u_y}{\partial y_d}\, dy_a. \tag{VII.78}$$

From the equation of continuity as expressed in Eq. (VII.76) it follows that:

$$(u_y)_{y_d=y_a} = -\int_0^{y_a} \frac{\partial u_x}{\partial x}\, dy_d. \tag{VII.79}$$

Equation (VII.79) assumes that the velocity at the boundary of the stream is zero and therefore all types of slip flow (*15*) cannot be treated in this fashion. A combination of Eqs. (VII.78) and (VII.79) results in

$$\int_0^{y_a} u_y \frac{\partial u_x}{\partial y_d} dy_d = - u_\infty \int_0^{y_a} \frac{\partial u_x}{\partial x} dy_d + \int_0^{y_a} u_x \frac{\partial u_x}{\partial x} dy_d. \tag{VII.80}$$

If the shear is assumed to be zero at $y_d \geqslant y_a$ as is often done in calculations in the boundary region, then

$$\eta \left[\frac{\partial u_x}{\partial y_d} \right]_{y_d = 0}^{y_d = y_a} = - (\tau_{yx})_0. \tag{VII.81}$$

A combination of Eqs. (VII.80) and (VII.81) with Eq. (VII.77) results in the following integral equation:

$$\frac{d}{dx} \int_0^{y_a} u_x^2 dy_d - u_\infty \int_0^{y_a} \frac{\partial u_x}{\partial x} dy_d = - \frac{y_a g_c}{\sigma} \frac{dP}{dx} - \frac{g_c}{\sigma} (\tau_{yx})_0. \tag{VII.82}$$

Equation (VII.82) represents the integral condition first proposed by Kármán (*4*) which is applicable to both potential and turbulent flow in the stream and boundary region.

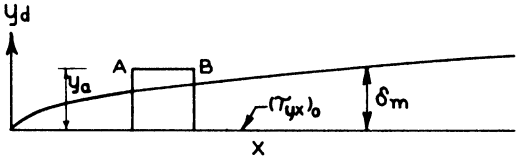

FIG. VII-22. Physical significance of momentum conditions at boundary.

It is of interest to consider the over-all implications of Eq. (VII.82) which may be rewritten in the following form:

$$\frac{d}{dx} \int_0^{y_a} \frac{\dot{m}_x}{g_c} u_x dy_d + \frac{\dot{m}_\infty}{g} \int_0^{y_a} \frac{\partial u_x}{\partial y_d} dy_d = \frac{1}{z} \frac{dF}{dx}. \tag{VII.83}$$

The first term represents the rate of change per unit length in the direction of flow of the flux of momentum entering and leaving the control volume shown in Fig. VII-22 for the case of two-dimensional flow. The second term represents the momentum transport across the surface AB as the result of the difference in velocity between the fluid in the boundary layer and in the

main body of the stream. The third term represents the net force acting upon the section as a result of the shear at the wall $(\tau_{yx})_0$ and the pressure gradient dP/dx acting on the projected area y_a. It is perhaps easier to visualize the behavior of the momentum fluxes by reference to Eq. (VII.77). If desired, the equivalent of Eq. (VII.82) may be written immediately from the phenomenological consideration of the situation described in Fig. VII-22.

It is convenient to rewrite the definition of the displacement and momentum thicknesses of the boundary layer in the following slightly modified form:

$$u_\infty \delta_y = \int_0^\infty (u_\infty - u_x)\, dy_d, \tag{VII.84}$$

$$u_\infty{}^2 \delta_m = \int_0^\infty u_x(u_\infty - u_x)\, dy_d. \tag{VII.85}$$

If it is assumed that local potential flow exists exterior to the boundary layer, it follows directly from Bernoulli's equation[1] or from Eq. (VII.75) with $\partial u_x/\partial y_d = 0$ and $\eta = 0$ which give the boundary layer approximation that

$$\frac{g_c}{\sigma}\frac{dP}{dx} = -u_\infty \frac{du_\infty}{dx} = -\frac{du_\infty{}^2}{dx} + u_\infty \frac{du_\infty}{dx}. \tag{VII.86}$$

The integration of Eq. (VII.86) from the wall to some point outside the boundary region yields the following:

$$\frac{y_a g_c}{\sigma}\frac{dP}{dx} = -\frac{d}{dx}\int_0^{y_a} u_\infty{}^2\, dy_d + u_\infty \frac{d}{dx}\int_0^{y_a} u_\infty\, dy_d. \tag{VII.87}$$

Equation (VII.87) may now be substituted in Eq. (VII.82), and after some rearrangement there is obtained

$$\frac{g_c}{\sigma}(\tau_{yx})_0 = \frac{d}{dx}\int_0^{y_a} (u_\infty{}^2 - u_x{}^2)\, dy_d - u_\infty \frac{d}{dx}\int_0^{y_a} (u_\infty - u_x)\, dy_d. \tag{VII.88}$$

---

[1] Bernoulli's equation is discussed in Appendix I.

Equation (VII.88) may be expressed in still another form by application of integration by parts.

$$\frac{g_c}{\sigma}(\tau_{yx})_0 = \frac{d}{dx}\int_0^{y_a}(u_\infty - u_x)\,u_x\,dy_a + \left(\int_0^{y_a}(u_\infty - u_x)\,dy_a\right)\frac{du_\infty}{dx}. \quad \text{(VII.89)}$$

A combination of Eq. (VII.89) with Eqs. (VII.84) and (VII.85) results in the following expressions involving the displacement and momentum thicknesses of the incompressible boundary layer:

$$\frac{g_c}{\sigma}(\tau_{yx})_0 = \frac{d}{dx}(u_\infty{}^2\,\delta_m) + u_\infty\,\delta_y\frac{du_\infty}{dx}, \quad \text{(VII.90)}$$

$$\frac{g_c}{\sigma}(\tau_{yx})_0 = u_\infty{}^2\frac{d\delta_m}{dx} + (2\,\delta_m + \delta_y)\,u_\infty\frac{du_\infty}{dx}. \quad \text{(VII.91)}$$

Equation (VII.91) is a convenient expression relating the change in momentum thickness of the boundary layer with distance along the surface and applies equally well to laminar and to turbulent flows. In the case of zero pressure gradient, where du_∞/dx becomes zero, Eq. (VII.91) assumes the following form if potential flow exists outside of the boundary region:

$$\frac{g_c}{\sigma}(\tau_{yx})_0 = u_\infty{}^2\frac{d\delta_m}{dx}. \quad \text{(VII.92)}$$

Equation (VII.92) expresses in a simple manner the variation in the momentum thickness with distance as long as the shear at the wall is known. This shear is directly related to the viscosity and to the velocity gradient which is to be assumed. Before considering some of the simplifications that result from the assumption of simple velocity distributions, it is desirable to consider a rather general approach to the problem that has found widespread acceptance.

VII-15. A Polynomial Velocity Distribution

Pohlhausen (*5*) considered these matters in some detail and in order to satisfy the necessary boundary conditions of a laminar boundary layer such as are given in Eqs. (VII.16) through (VII.22) he proposed a velocity distribution of the following general form:

$$\frac{u_x}{u_\infty} = a\psi_P + b\psi_P{}^2 + c\psi_P{}^3 + e\psi_P{}^4. \quad \text{(VII.93)}$$

In Eq. (VII.93) the quantity ψ_P was defined by Pohlhausen (*5*) as

$$\psi_P = \frac{y_d}{\delta_P} \tag{VII.94}$$

where δ_P is the thickness of the boundary layer in Pohlhausen's model. It is desirable to introduce a form function which describes the nature of the velocity distribution. For present purposes this function λ may be defined

$$\lambda = \frac{\delta_P{}^2 \sigma}{\eta g_c} \frac{du_\infty}{dx}. \tag{VII.95}$$

From a consideration of the appropriate boundary conditions that apply to any laminar boundary layer it has been shown by Pohlhausen (*5*) that the four coefficients of Eq. (VII.93) are mutually related by four independent equations. The solution of these equations reduces Eq. (VII.93) to

$$\frac{u_x}{u_\infty} = (2\psi_P - 2\psi_P^3 + \psi_P^4) + \frac{\lambda}{6}(\psi_P - 3\psi_P^2 + 3\psi_P^3 - \psi_P^4). \tag{VII.96}$$

Equation (VII.96) may be rewritten (*5*) in terms of two functions of the relative position in the boundary layer ψ_P and the form factor λ.

$$\frac{u_x}{u_\infty} = \phi_8(\psi_P) + \lambda\phi_9(\psi_P), \tag{VII.97}$$

when

$$\lambda = 0; \quad \frac{dP}{dx} = 0, \tag{VII.98}$$

when

$$\lambda = -12; \quad \left(\frac{\partial u_x}{\partial y_d}\right)_{y_d = 0} = 0. \tag{VII.99}$$

The values of the two functions designated as $\phi_8(\psi_P)$ and $\phi_9(\psi_P)$ are shown in Table VII-5. These values are based upon the calculations of Pohlhausen (*5*) and Howarth (*34*). In applying the data of Table VII-5 it should be realized that the form parameter λ is limited to values between -12 and $+12$. From the original definition of λ it follows that when it assumes a value of zero, there is no pressure gradient, and when it assumes the value of -12, the normal velocity gradient at the wall is zero. For values of λ greater than 12, fictitious values of the velocity which are greater than in the free stream value are obtained.[1]

---

[1] Li and Nagamatsu (*41*) report solutions of the laminar boundary layer for a compressible fluid which yield higher velocities than that in the free stream in the case of a heated solid surface.

The ratio of the displacement thickness of the boundary layer to the empirical Pohlhausen thickness of the boundary layer δ_P may be obtained by a combination of Eqs. (VII.84), (VII.94), and (VII.97).

$$\frac{\delta_y}{\delta_P} = \int_0^1 [1 - \phi_8(\psi_P) - \lambda\phi_9(\psi_P)]\, d\psi_P = \frac{3}{10} - \frac{\lambda}{120}. \quad \text{(VII.100)}$$

In a similar fashion the combination of Eqs. (VII.85), (VII.94), and (VII.97) results in the ratio of the momentum thickness of the boundary layer and the Pohlhausen thickness.

$$\frac{\delta_m}{\delta_P} = \int_0^1 [\phi_8(\psi_P) + \lambda\phi_9(\psi_P)]\,[1 - \phi_8(\psi_P) - \lambda\phi_9(\psi_P)]\, d\psi_P$$

$$= \frac{37}{315} - \frac{\lambda}{945} - \frac{\lambda^2}{9072}. \quad \text{(VII.101)}$$

It should be noted that both Eqs. (VII.100) and (VII.101) yield explicit values for the definite integrals in terms of the form factor λ.

In a similar fashion the shear at the boundary may be established by a combination of Eqs. (VII.56), (VII.94), and (VII.96).

$$(\tau_{yx})_0 = \left(\frac{12 + \lambda}{6}\right)\frac{\eta}{\delta_P} u_\infty. \quad \text{(VII.102)}$$

It is apparent that the shear at the boundary is a function of the form factor λ, the viscosity, the Pohlhausen thickness, and the free stream velocity.

TABLE VII-5. Functions for the Pohlhausen Velocity Distribution (*11*)

$\psi_P = \frac{y_d}{\delta_P}$	$\phi_8(\psi_P)$	$\phi_9(\psi_P)$
0	0	0
0.1	0.1981	0.01215
0.2	0.3856	0.01725
0.3	0.5541	0.01715
0.4	0.6976	0.0144
0.5	0.8125	0.0104
0.6	0.8976	0.0064
0.7	0.9541	0.00315
0.8	0.9856	0.00105
0.9	0.9981	0.00015
1.0	1.0000	0.00000

TABLE VII-5 (Cont.)

λ	$\frac{\sigma \delta_m^2}{\eta g_c} \frac{du_\infty}{dx}$	$\phi_{10}(\lambda)$	$\phi_{11}(\lambda)$	$\phi_{12}(\lambda)$
15	0.0885	−0.0657	2.279	0.345
14	0.0920	−0.0814	2.262	0.351
13	0.0941	−0.0913	2.253	0.354
12	0.0948	−0.0946	2.250	0.356
11	0.0941	−0.0911	2.253	0.354
10	0.0920	−0.0806	2.260	0.351
9	0.0882	−0.0608	2.273	0.346
8	0.0831	−0.0332	2.289	0.340
7.8	0.0820	−0.0271	2.293	0.338
7.6	0.0807	−0.0203	2.297	0.337
7.4	0.0794	−0.0132	2.301	0.335
7.2	0.0780	−0.0051	2.305	0.333
7.052	0.0770	0	2.308	0.332
7	0.0767	0.0021	2.309	0.331
6.9	0.0760	0.0061	2.312	0.330
6.8	0.0752	0.0102	2.314	0.330
6.7	0.0744	0.0144	2.316	0.329
6.6	0.0737	0.0186	2.318	0.328
6.5	0.0729	0.0230	2.321	0.327
6.4	0.0721	0.0274	0.323	0.326
6.3	0.0713	0.0319	2.326	0.325
6.2	0.0706	0.0365	2.328	0.324
6.1	0.0697	0.0412	2.331	0.322
6	0.0689	0.0459	2.333	0.321
5	0.0599	0.0978	2.361	0.310
4	0.0497	0.1579	2.392	0.297
3	0.0385	0.2255	2.427	0.283
2	0.0264	0.3000	2.466	0.268
1	0.0135	0.3820	2.508	0.252
0	0	0.4698	2.554	0.235
−1	−0.0140	0.5633	2.604	0.217
−2	−0.0284	0.6616	2.658	0.199
−3	−0.0429	0.7640	2.716	0.179
−4	−0.0575	0.8698	2.779	0.160
−5	−0.0720	0.9780	2.847	0.140
−6	−0.0862	1.0853	2.921	0.119
−7	−0.0999	1.1981	2.999	0.100
−8	−0.1130	1.3078	3.084	0.079
−9	−0.1255	1.4173	3.177	0.059
−10	−0.1369	1.5231	3.276	0.039
−11	−0.1474	1.6251	3.383	0.019
−12	−0.1567	1.7237	3.500	0
−13	−0.1648	1.8159	3.627	−0.019
−14	−0.1715	1.9020	3.765	−0.037
−15	−0.1767	1.9821	3.920	−0.054

It is convenient to rewrite Eq. (VII.91) in somewhat different form for further extension of the empirical approach to the analysis of boundary flows. This may be accomplished by rearrangement of Eq. (VII.91).

$$\frac{\delta_m}{\eta u_\infty}(\tau_{yx})_0 = \frac{\sigma}{\eta g_c} u_\infty \delta_m \frac{d\delta_m}{dx} + \left(2 + \frac{\delta_v}{\delta_m}\right)\frac{\sigma}{\eta g_c}\delta_m{}^2 \frac{du_\infty}{dx}. \quad \text{(VII.103)}$$

It is of interest to note that Eq. (VII.103) does not contain the Pohlhausen boundary layer thickness and is in reality a statement of the relationship between the displacement and momentum boundary layer thicknesses. This fact suggests that the momentum thickness δ_m is a more fundamental quantity than δ_p.

It has been shown (*11*, *15*) that the derivative of the change in the square of momentum thickness with distance may be evaluated from an expression of the following form:

$$\frac{d(\delta_m{}^2)}{dx} = \frac{\phi_{10}(\lambda)}{u_\infty}\frac{\eta g_c}{\sigma} \quad \text{(VII.104)}$$

where $\eta g_c/\sigma$ is constant. In Eq. (VII.104) the quantity $\phi_{10}(\lambda)$ is given by the following expression:

$$\phi_{10}(\lambda) = 2\left(\frac{37}{315} - \frac{\lambda}{945} - \frac{\lambda^2}{9072}\right)\left[2 - \frac{116}{315}\lambda + \left(\frac{2}{945} + \frac{1}{120}\right)\lambda^2 + \frac{2}{9072}\lambda^3\right]. \quad \text{(VII.105)}$$

Equations (VII.100) and (VII.101) may be combined to yield

$$\frac{\delta_v}{\delta_m} = \frac{\left(\frac{3}{10} - \frac{\lambda}{120}\right)}{\left(\frac{37}{315} - \frac{\lambda}{945} - \frac{\lambda^2}{9072}\right)} = \phi_{11}(\lambda). \quad \text{(VII.106)}$$

From Eqs. (VII.102) and (VII.101) it follows that:

$$\frac{\delta_m}{\eta u_\infty}(\tau_{yx})_0 = \left(\frac{12+\lambda}{6}\right)\left(\frac{37}{315} - \frac{\lambda}{945} - \frac{\lambda^2}{9072}\right) = \phi_{12}(\lambda). \quad \text{(VII.107)}$$

It thus becomes possible to integrate the boundary flow from stagnation to any point where the laminar behavior is stable by use of Eqs. (VII.104), (VII.105), (VII.106), and (VII.107). These relations apply to the boundary

flows with and without pressure gradient. The appropriate values of ϕ_{10}, ϕ_{11}, and ϕ_{12} are recorded in a part of Table VII-5 as a function of λ.

Equation (VII.104) is a nonlinear differential equation of the first order. It has been found convenient to initiate its solution at the stagnation point which is often the origin of the coordinate system as well. At the stagnation point

$$x = 0 \tag{VII.108}$$

and

$$u_x = 0, \tag{VII.109}$$

$$\phi_{10}(\lambda_{st}) = 0. \tag{VII.110}$$

It follows from Eq. (VII.105) that if $\phi_{10}(\lambda)$ is zero at the stagnation point then:

$$\lambda_{st} = 7.052. \tag{VII.111}$$

Where λ_{st} is 7.052, the following is obtained at the stagnation point:

$$\delta_m = \frac{0.0770}{\left(\frac{du_\infty}{dx}\right)_{st}} \frac{\eta g_c}{\sigma}, \tag{VII.112}$$

$$\frac{d(\delta_m{}^2)}{dx} = -0.0652 \frac{\eta g_c}{\sigma} \frac{\left(\frac{d^2u_\infty}{dx^2}\right)_{st}}{\left(\frac{du_\infty}{dx}\right)_{st}}. \tag{VII.113}$$

After these initial values are utilized, it is a relatively simple matter to carry out the integration of Eq. (VII.104). The solution of this equation permits a direct evaluation of the change in thickness of the momentum boundary layer as a function of downstream distance. It is worth while to emphasize that the values of λ must be predicted from the behavior of the free stream for each of the particular conditions of flow encountered in the treatment of the laminar boundary layer. The values of λ for specified conditions of flow are set forth in Table VII-6 and are also useful in evaluating the behavior at stagnation and separation. The values of the form function λ may be obtained from the relationship

$$\frac{\sigma}{\eta g_c} \delta_m{}^2 \frac{du_\infty}{dx} = \left(\frac{37}{315} - \frac{\lambda}{945} - \frac{\lambda^2}{9072}\right)^2 \lambda. \tag{VII.114}$$

An example illustrating the application of the Pohlhausen method for flow over a flat plate with no pressure gradient is given below.

TABLE VII-6. Form Factor for Characteristic Conditions of Boundary Layer[1]

Case	λ	$\frac{\sigma \delta_m^2}{\eta g_c} \frac{du_\infty}{dx}$	$\phi_{10}(\lambda)$
Stagnation point	7.052	0.0770	0
Velocity maximum	0.000	0.0000	0.4698
Separation point	−12.000	−0.1567	—
Separation	−10.000	−0.1369	1.523

[1] See ref. *11*.

Example 4

Evaluation of Velocity Distribution Along a Flat Plate: In order to apply the Pohlhausen method to the flow about a flat plate it is necessary to establish the conditions associated with the primary flow. In the present instance it will be assumed that the primary flow about the plate is potential and uniform. As a result there is no pressure gradient in the direction of flow. From Eq. (VII.95) it follows immediately that the form factor λ is zero throughout the flow. This also results directly from Eq. (VII.114).

Substituting the appropriate values of the functions from Table VII-5 in Eq. (VII.104) there is obtained

$$\frac{d(\delta_m^2)}{dx} = \frac{\eta g_c}{\sigma} \frac{\phi_{10}(0)}{u_\infty} = \frac{0.4698}{u_\infty} \frac{\eta g_c}{\sigma}. \tag{1 E}$$

If the value of the momentum thickness is zero at the leading edge of the plate and if Eq. (1 E) is integrated, there results

$$\delta_m^2 = \frac{0.4698}{u_\infty} \frac{\eta g_c}{\sigma} x \tag{2 E}$$

or

$$\delta_m = 0.685 \sqrt{\frac{\eta g_c}{\sigma} \frac{x}{u_\infty}}. \tag{3 E}$$

Equation (3 E) may be compared with Eq. (VII.70), and it is seen that the agreement is fairly satisfactory. In a similar fashion it is possible to evaluate the displacement thickness from Eq. (VII.106) in the following way:

$$\delta_y = \frac{\delta_y}{\delta_m} \delta_m = 0.685 \sqrt{\frac{\eta g_c}{\sigma} \frac{x}{u_\infty}} \phi_{11}(0). \tag{4 E}$$

The combination of Eqs. (VII.106) and (4 E) yields the second equality indicated. Substitution of the appropriate value of $\phi_{11}(0)$ in Eq. (4 E) yields

$$\delta_y = (2.554)\ (0.685)\sqrt{\frac{\eta g_c}{\sigma}\frac{x}{u_\infty}} = 1.75\sqrt{\frac{\eta g_c}{\sigma}\frac{x}{u_\infty}}. \qquad (5\text{ E})$$

Equation (5 E) may be compared with Eq. (VII.68), and it is again seen that the Pohlhausen approximation is a reasonably satisfactory description of the behavior of an incompressible laminar boundary layer insofar as the evaluation of the displacement thickness is concerned. However, it does not give the detailed velocity distribution available with the Blasius solution (*14*) of this special case.

In a similar fashion the shear at the wall may be established from

$$(\tau_{yx})_0 = \frac{\eta u_\infty}{\delta_m}\phi_{12}(\lambda) = \frac{0.235\,\eta u_\infty}{0.685\sqrt{\frac{\eta g_c}{\sigma}\frac{x}{u_\infty}}} = 0.343\sqrt{\frac{\eta\sigma}{g_c}\frac{u_\infty^3}{x}}. \qquad (6\text{ E})$$

This may be compared with the more exact value obtained for the Blasius boundary layer that is presented in Eq. (VII.58).

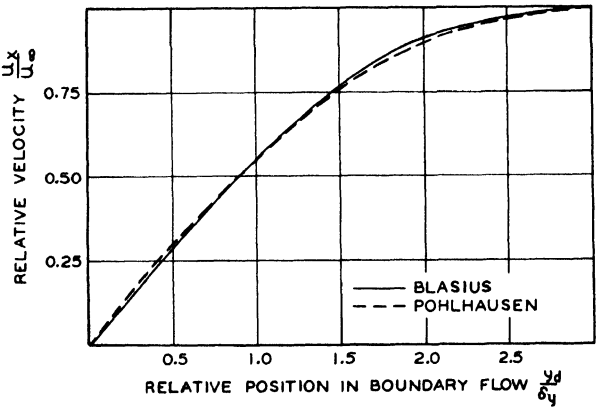

FIG. VII-23. Velocity distribution in boundary layer.

Further calculation of the velocity distribution in terms of the displacement thickness can be made. The results of these calculations following the methods which have been described are recorded in Table VII-7 For comparison the Pohlhausen approximation and the Blasius solution have been included in this table and are depicted in Fig. VII-23.

TABLE VII-7. Comparison of Blasius and Pohlhausen Solutions of Boundary Layer Equations

$\frac{y_d}{\delta_y}$	$y_d\sqrt{\frac{u_\infty}{\nu_x}}$	Blasius	Pohlhausen	
		$\frac{u_x}{u_\infty}$	$\frac{u_x}{u_\infty}$	Error Per cent
—	0	0	0	—
0.2286	0.4	0.13277	0.13650	2.81
0.4571	0.8	0.26471	0.26944	1.79
0.6857	1.2	0.39378	0.39575	0.50
0.9143	1.6	0.51676	0.51289	-0.75
1.1429	2.0	0.62977	0.61885	-1.73
1.7143	3.0	0.84605	0.82643	-2.32
2.2857	4.0	0.95552	0.94770	-0.82
2.8571	5.0	0.99155	0.99475	0.32
3.4286	6.0	0.99898	1.00039	0.14
4.5714	8.0	1.00000	1.12223	12.22

VII-16. Estimation of Separation

The Pohlhausen method of laminar boundary calculation may be used to estimate the point of separation. In this instance the original concept of Prandtl (*2*) concerning the existence of back flow, which was described earlier in this chapter, will be employed as the criterion of the onset of separation. In order that separation may be possible it is necessary that the form function λ be negative. As a second approximation the suggestions of Schlichting (*11*) will be followed and it will be assumed that the form function λ does not change after the onset of separation. From experience (*11*) it appears that a value of λ of -10 will be the limiting negative form function for stable laminar flow in a practical situation when perturbations are encountered in the flow. The corresponding values of the associated functions are recorded in a part of Table VII-6 for a value of λ of -10.

From values of the function corresponding to the practical limits of laminar flow without separation it follows that:

$$\frac{\sigma}{\eta g_c}\delta_m^2 = -\frac{0.1369}{\left(\frac{\partial u_\infty}{\partial x}\right)}. \qquad \text{(VII.115)}$$

The change in momentum thickness with downstream distance may be established as

$$\frac{\partial(\delta_m^2)}{\partial x} = 0.1369 \frac{\eta g_c}{\sigma} \frac{\left(\frac{\partial^2 u_\infty}{\partial x^2}\right)}{\left(\frac{\partial u_\infty}{\partial x}\right)^2}. \tag{VII.116}$$

It has already been established from Eq. (VII.104) that in the normal growth of the boundary layer after separation

$$\frac{\partial(\delta_m^2)}{\partial x} = \frac{\phi_{10}(\lambda)}{u_\infty} \frac{\eta g_c}{\sigma} = \frac{1.523}{u_\infty} \frac{\eta g_c}{\sigma}. \tag{VII.117}$$

If the form parameter is not to increase negatively in a particular flow, it is necessary that the following conditions exist:

$$\frac{\left(\frac{\partial^2 u_\infty}{\partial x^2}\right)}{\left(\frac{\partial u_\infty}{\partial x}\right)^2} \geqslant \frac{1.523}{0.1369\, u_\infty} > \frac{11}{u_\infty}. \tag{VII.118}$$

Equation (VII.118) constitutes an approximation of the limiting change in velocity in the main part of the stream which may be permitted without separation. The limiting case where

$$\frac{\partial^2 u_\infty}{\partial x^2} = 0 \qquad \text{and} \qquad \frac{\partial u_\infty}{\partial x} < 0 \tag{VII.119}$$

always leads to separation if the flow is continued. It appears (*11*) that Eq. (VII.118) may be used to advantage as a first approximation to establish the limiting conditions of stable flow on any type of surface involving an incompressible laminar boundary layer as long as the situation conforms to the basic assumption made in simplifying the Navier-Stokes equation.

Further calculations of this nature indicate that in order to satisfy the conditions set forth by Eq. (VII.118) only very small decreases in the free stream velocity with position are permissible without separation. For example, it can be shown (*11*) that the boundary layer is continually on the verge of separation if the velocity at a distance from the boundary satisfies the following expression:

$$u_\infty \geqslant u_\infty{}^0\, x^{-0.091}. \tag{VII.120}$$

Equation (VII.120) indicates the extremely small rate of retardation permissible along a surface to maintain an attached boundary layer with no removal of fluid from the boundary flow. Pohlhausen (*5*) has shown that separation is associated with any divergent flow and predicts it to take place at a specified distance from the virtual origin of the flow. The point of separation in divergent flow is indicated in the following expression:

$$\frac{x}{x_2} = 1.213 \tag{VII.121}$$

where x_2 is the distance from the virtual origin to the beginning of the divergent section. The schematic arrangement of a diverging channel corresponding to the situation typified by Eqs. (VII.120) and (VII.121) is

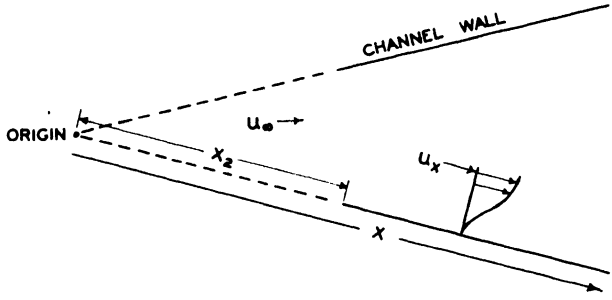

FIG. VII-24. Boundary flow in a divergent channel.

presented in Fig. VII-24. It is possible to extend the treatment of separation somewhat further but it is evident that laminar boundary layers do not remain stable in practical, positive pressure gradients. Therefore, it is to be expected that the flow in diffusers will not form stable boundary layers and that the flow around immersed bodies will introduce separation in regions where there exists a significant positive pressure gradient for a reasonable portion of the time. This is one reason why it is difficult to design diffusers with small frictional losses.

Boundary Layers with Material Transport across the Surface

As has been described, one method of increasing the stability of a boundary layer is to remove that portion of it which is unstable and in which back flow is incipient. It has been found that marked improvement in the stability of laminar boundary layers can be made by withdrawing a small amount of material from the layer through a porous surface of the plate. This phenomenon is shown in Fig. VII-25. In the upper part of the figure a

boundary layer is shown in which fluid is withdrawn continuously along the surface. The dotted curve corresponds to the behavior with an impervious boundary, whereas the full curve shows the variation in the displacement thickness with position from the leading edge with the removal of material from the boundary. It is seen that with the removal of fluid the boundary layer becomes thinner, as would be expected.

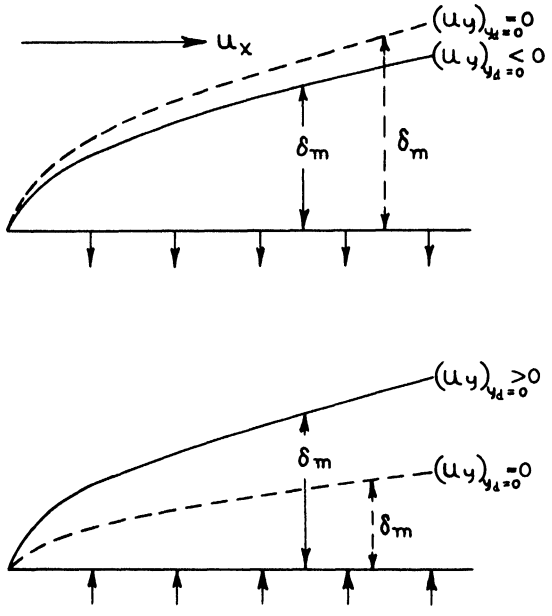

FIG. VII-25. Momentum thickness for flows with material transport at the interface.

In the lower part of the figure is shown the behavior of a boundary layer into which fluid is introduced. In this instance the displacement thickness of the so-called "blowing boundary layer" is greater than that of the boundary layer on an impermeable surface. For large values of downstream distance the boundary layer increases in nearly a linear fashion for situations in which the effect of the added material at the interface is large compared to the normal growth of the boundary layer.

VII-17. Analysis

In situations where there is a net transport of material across the interface, Eq. (VII.79) may be written as

$$(u_y)_{y_d=y_a} = (u_y)_{y_d=0} - \int_0^{y_a} \frac{\partial u_x}{\partial x}\, dy_d. \tag{VII.122}$$

In a similar fashion it may be shown that Eq. (VII.91) assumes the form,

$$\frac{g_c}{\sigma}(\tau_{yx})_0 = u_\infty{}^2 \frac{d\delta_m}{dx} + (2\,\delta_m + \delta_y)\,u_\infty \frac{du_\infty}{dx} - u_\infty (u_y)_{y_d=0}. \qquad \text{(VII.123)}$$

In the case of a flat plate with zero pressure gradient and with potential flow at an infinite distance from it there is obtained

$$\frac{du_\infty}{dx} = 0. \qquad \text{(VII.124)}$$

Furthermore it will be assumed for the present analysis that the flow into or from the boundary layer is invariant with distance along the plate, which may be indicated by

$$\left(\frac{\partial u_y}{\partial x}\right)_{y_d=0} = 0. \qquad \text{(VII.125)}$$

Following the same procedures as were employed in the earlier section, Eq. (VII.123) may be reduced to

$$\frac{g_c}{\sigma}(\tau_{yx})_0 = u_\infty{}^2 \frac{d\delta_m}{dx} - u_\infty (u_y)_{y_d=0} = \frac{\eta\, g_c}{\sigma}\left(\frac{\partial u_x}{\partial y_d}\right)_{y_d=0} \qquad \text{(VII.126)}$$

If a dimensionless form parameter D is employed and it is assumed that the parameter is not a function of x, i.e.,

$$\frac{\partial D}{\partial x} = 0, \qquad \text{(VII.127)}$$

it is possible to write the velocity gradient at the boundary in the following form:

$$\left(\frac{\partial u_x}{\partial y_d}\right)_{y_d=0} = D\,\frac{u_\infty}{\delta_m}. \qquad \text{(VII.128)}$$

In a way, Eq. (VII.128) is a definition of the form function D. A combination of Eqs. (VII.126) and (VII.128), when the significance of Eq. (VII.127) is taken into account, results in

$$\frac{1}{2}\frac{d\delta_m{}^2}{dx} = \frac{\eta\, g_c}{\sigma}\frac{D}{u_\infty} + \frac{\delta_m}{u_\infty}(u_y)_{y_d=0}. \qquad \text{(VII.129)}$$

The following boundary conditions exist for a flat plate:

$$\delta_m = 0 \tag{VII.130}$$

at

$$x = 0. \tag{VII.131}$$

If it is desired to determine the conditions yielding a constant momentum thickness of the boundary layer with downstream distance, the following boundary condition is applied:

$$\frac{d\delta_m}{dx} = 0. \tag{VII.132}$$

Under these circumstances Eq. (VII.129) reduces to

$$(\delta_m)_{x=\infty} = -D\frac{\eta g}{\sigma}\frac{1}{(u_y)_{y_d=0}}. \tag{VII.133}$$

Likewise, an asymptotic solution for a blowing boundary layer may be obtained

$$(\delta_m)_{x=\infty} = \frac{x}{u_\infty}(u_y)_{y_d=0}. \tag{VII.134}$$

It is seen that Eq. (VII.133) establishes the extent of the removal of the boundary layer necessary to maintain a uniform thickness whereas Eq. (VII.134) establishes the rate of growth of a blowing boundary layer at a large distance from the leading edge. The foregoing solutions represent a relatively simple approach to the analysis of boundary layer with material transport. They do not permit an evaluation of the velocity distribution throughout the boundary region as may be obtained with the Blasius solution of the equations of motion for an impervious wall.

Emmons and Leigh (*25*) applied the laminar jet mixing solutions of the simplified Navier-Stokes equations obtained by Lock (*42*) to the behavior of boundary flows with material transport. They recorded an extensive set of tabulations of these solutions to the Blasius equation for a number of different values of the mass flow coefficient, defined as the value of the Blasius function $\phi_2(\psi)$ at the solid boundary which may be obtained as the solution of the following equation:

$$\frac{\dot{m}_y}{\sigma u_\infty} = \frac{1}{2}\{\psi\phi_2'(\psi) - \phi_2(\psi)\}\sqrt{\frac{\eta g_c}{\sigma}\frac{u_\infty}{x}}. \tag{VII.135}$$

In Eq. (VII.135) the symbol $\dot{m}_y$ represents the weight rate at which the fluid is introduced per unit area of interface. These data were in good agreement with the earlier calculations of Schlichting and Bussmann (*43*) for the same situation. The mass flow coefficients investigated (*25*) covered values from -1.23849, corresponding to the minimum coefficient at which a boundary layer remains in blowing normal to the boundary, to 10, which is in the region for suction. It is beyond the scope of the present work to consider in detail the solution of laminar incompressible boundary layers involving material transport at the interface (*44*). It is of interest to note the marked effect found by Pankhurst and Thwaites (*37*) of the removal of gas from the boundary layer on the separation of the flow around a cylinder. The pressure distribution around a cylinder is shown in Fig. VII-26. The full curve represents potential flow and follows the pressure distribution predicted by Lamb (*35*), whereas the dotted curve represents the pressure distribution as measured by Pankhurst and Thwaites (*37*) with normal separation and no boundary fluid removal. The dashed curve corresponds to their measurements with boundary fluid removal. In this instance the agreement between the pressure distribution for potential flow as predicted from Lamb's analysis and the measured pressure distribution with boundary fluid removal is satisfactory. It appears that the removal of a portion of the boundary layer exerts a marked influence on the separation phenomena.

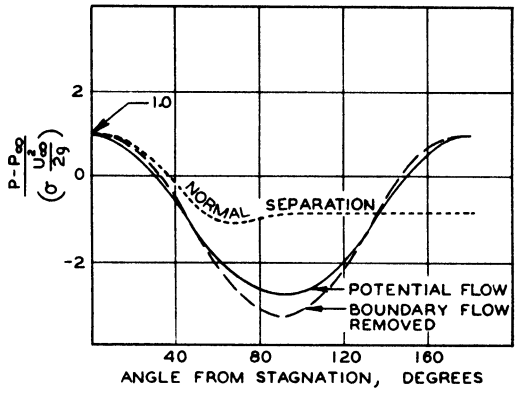

FIG. VII-26. Pressure distribution around a circular cylinder in an air stream with low level of turbulence (*37*).

VII-18. Turbulent Boundary Layers

It is possible to introduce a turbulent boundary layer in an otherwise laminar region by various types of protuberances on the surface of the immersed body or on the wall of the flow channel. In experimental work it is often convenient to initiate artificially a turbulent boundary layer by the use of small wires fastened to the solid boundary perpendicular to the direction of flow. The difference in the velocity distribution encountered in a laminar boundary layer and a turbulent boundary layer is shown in

Fig. VII-27. These experimental measurements were taken from the work of Chapman and Kester (*45*), and Dhawan's data (*26*) could be used for a similar comparison. It is apparent that on this cylinder the turbulent boundary layer diffuses out into the free stream much more rapidly than does the laminar boundary layer as indicated by the approach to the free stream velocity at a much larger distance from the solid boundary. In the case of the turbulent boundary layer a distance of about 0.04 in. was required

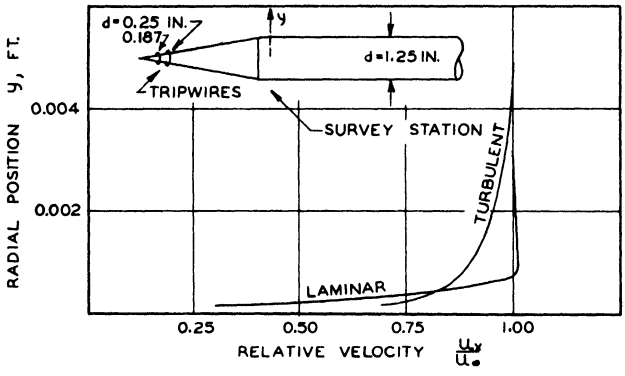

FIG. VII-27. Comparison of velocity distribution in turbulent and laminar boundary layer (*45*).

in order to reach the free stream velocity whereas a radial distance of about only 0.01 in. was required to reach the free stream velocity under laminar conditions. The measurements shown in Fig. VII-27 were obtained with supersonic flow in the main stream but serve to illustrate a marked difference in the nature of laminar and turbulent boundary layers. In the case of the data of Fig. VII-27 the boundary layer was tripped into the turbulent region by the location of two wires 0.05 in. in diameter at points on the approach cone corresponding to diameters of 0.187 and 0.25 in. The free stream velocity corresponded to twice the velocity of sound and for a one-inch length of cylinder the Reynolds number was 0.64×10^6. In dealing with bodies immersed in a flowing stream it is convenient to measure the Reynolds number in terms of a characteristic dimension of the body. In boundary layer problems the distance from the leading edge is often employed. Thus the Reynolds number increases directly with the downstream distance along the body when all the other characteristics of flow are uniform.

It is possible to solve for some of the characteristics of the turbulent boundary flows around a flat plate by the momentum equation of Kármán (*4*) and Pohlhausen (*5*). In this instance it is desirable to make use of the Reynolds concept of average values of the fluctuating components of velocity.

Schlichting (*46*) and Rotta (*47*) presented satisfactory derivations of the differential equations describing turbulent boundary flows based upon the Navier-Stokes equations. Except for the inclusion of the Reynolds stresses these expressions are similar to the steady-state form of the Navier-Stokes equations when applied to incompressible laminar boundary flows in the absence of potential fields and may be written as

$$\overline{u_x}\frac{\partial \overline{u_x}}{\partial x} + \overline{u_y}\frac{\partial \overline{u_x}}{\partial y_d} = -\frac{g_c}{\sigma}\frac{\partial P}{\partial x} + \frac{\partial}{\partial x}\left(\nu\frac{\partial \overline{u_x}}{\partial x} - \overline{u^2_{x,f}}\right) + \frac{\partial}{\partial y_d}\left(\nu\frac{\partial \overline{u_x}}{\partial y_d} - \overline{u_{x,f}\,u_{y,f}}\right), \tag{VII.136}$$

$$\overline{u_x}\frac{\partial \overline{u_y}}{\partial x} + \overline{u_y}\frac{\partial \overline{u_y}}{\partial y_d} = -\frac{g_c}{\sigma}\frac{\partial P}{\partial y_d} + \frac{\partial}{\partial x}\left(\nu\frac{\partial \overline{u_y}}{\partial x} - \overline{u_{x,f}\,u_{y,f}}\right) + \frac{\partial}{\partial y_d}\left(\nu\frac{\partial \overline{u_y}}{\partial y_d} - \overline{u^2_{y,f}}\right), \tag{VII.137}$$

$$\frac{\partial}{\partial x}\left(\overline{u_{x,f}\,u_{z,f}}\right) = -\frac{\partial}{\partial y_d}\left(\overline{u_{y,f}\,u_{z,f}}\right). \tag{VII.138}$$

These relations assume that the mean flow, although not the turbulence, is two-dimensional. When the above expressions are supplemented by the equation of continuity in two dimensions,

$$\frac{\partial \overline{u_x}}{\partial x} + \frac{\partial \overline{u_y}}{\partial y_d} = 0; \qquad \frac{\partial u_{x,f}}{\partial x} + \frac{\partial u_{y,f}}{\partial y_d} + \frac{\partial u_{z,f}}{\partial z} = 0, \tag{VII.139}$$

there are sufficient relations to permit the integration of the Kármán momentum equation for boundary flow. Goldschmied (*48*) integrated Eqs. (VII.136) through (VII.139) following Kármán's procedure and obtained rather lengthy equations describing the balance of momentum in the boundary flow. In connection with such integrations it is convenient to follow the conventional representation of the Reynolds stresses.

$$-\frac{\sigma}{g_c}\overline{u^2_{x,f}} = \tau_{xx} - 2\eta\frac{\partial \overline{u_x}}{\partial x}, \tag{VII.140}$$

$$-\frac{\sigma}{g_c}\overline{u_{y,f}\,u_{x,f}} = \tau_{yx} - \eta\left(\frac{\partial \overline{u_x}}{\partial y_d} + \frac{\partial \overline{u_y}}{\partial x}\right), \tag{VII.141}$$

$$\frac{\sigma}{g_c}\overline{u_{x,f}\,u_{y,f}} = \tau_{xy} - \eta\left(\frac{\partial \overline{u_y}}{\partial x} + \frac{\partial \overline{u_x}}{\partial y_d}\right), \tag{VII.142}$$

$$\frac{\sigma}{g_c}\overline{u^2_{y,f}} = \tau_{yy} - 2\eta\frac{\partial \overline{u_y}}{\partial y_d}. \tag{VII.143}$$

If the definitions of the Reynolds stresses are used, Eq. (VII.137) may be transformed and differentiated (*48*) with respect to x yielding, when the order of differentiation is interchanged, the expression

$$\frac{\partial}{\partial y}\left(\frac{\partial P}{\partial x}\right) = \frac{\partial^2 \tau_{xy}}{\partial x^2} + \frac{\partial}{\partial y}\left(\frac{\partial \tau_{yy}}{\partial x}\right) - \frac{\sigma}{g_c}\frac{\partial}{\partial x}\left(\overline{u_x}\frac{\partial \overline{u_y}}{\partial x} - \overline{u_y}\frac{\partial \overline{u_x}}{\partial x}\right). \quad \text{(VII.144)}$$

Equation (VII.144) may be integrated with respect to y in the conventional fashion across the boundary layer using as limit of integration the streamline at the value of y where the pressure gradient is known. Under these circumstances Eq. (VII.144) assumes the form,

$$\left\{\left(\frac{\partial P}{\partial x}\right)_{y_d} - \left(\frac{\partial P}{\partial x}\right)_{y_0}\right\} = \int_{y_0}^{y_d} \frac{\partial^2 \tau_{xy}}{\partial x^2}\, dy_d \quad \text{(VII.145)}$$

$$- \frac{\sigma}{g_c}\int_{y_0}^{y_d} \frac{\partial}{\partial x}\left(\overline{u_x}\frac{\partial \overline{u_y}}{\partial x} - \overline{u_y}\frac{\partial \overline{u_x}}{\partial x}\right) dy_d + \left\{\left(\frac{\partial \tau_{yy}}{\partial x}\right)_{y_d} - \left(\frac{\partial \tau_{yy}}{\partial x}\right)_{y_0}\right\}.$$

Goldschmied (*48*) related the pressure gradient to the position in the stream by means of Bernoulli's equation for potential flow.

$$\frac{dP_\infty}{dx} = -\frac{\sigma}{g_c} u_\infty \frac{du_\infty}{dx}. \quad \text{(VII.146)}$$

For many purposes it is convenient to determine the behavior on the basis of the pressure gradient along the wall rather than in the free stream. The two pressure gradients are related by Eq. (VII.145) using the wall and the edge of the boundary layer as the limits of integration. Under these circumstances Eq. (VII.145) simplifies to

$$\frac{dP_\infty}{dx} = -\frac{\sigma}{g_c} u_\infty \frac{du_\infty}{dx} = \frac{dP_0}{dx} + \int_0^\delta \frac{\partial^2 \tau_{xy}}{\partial x^2}\, dy_d \quad \text{(VII.147)}$$

$$- \frac{\sigma}{g_c}\int_0^\delta \frac{\partial}{\partial x}\left(\overline{u_x}\frac{\partial \overline{u_y}}{\partial x} - \overline{u_y}\frac{\partial \overline{u_x}}{\partial x}\right) dy_d + \left(\frac{\partial \tau_{yy}}{\partial x}\right)_{y_d=\delta} - \left(\frac{\partial \tau_{yy}}{\partial x}\right)_{y_d=0}.$$

Following these procedures Ross (*49*) obtained the following expression for the change in momentum thickness with downstream distance:

$$\frac{d\delta_m}{dx} = \frac{g_c}{\sigma u_\infty^2}(\tau_{yx})_0 + \frac{(2\delta_m + \delta_y) g_c}{\sigma u_\infty^2}\frac{dP_0}{dx} + \frac{g_c}{\sigma u_\infty^2}\int_0^\delta \frac{\partial(\tau_{yy} - \tau_{xx})}{\partial x}\, dy_d$$

$$+ 2(\delta_m + \delta_y)\frac{g_c}{\sigma u_\infty^2}\int_0^\delta \frac{\partial^2 \tau_{xy}}{\partial x^2}\, dy_d - \frac{g_c}{\sigma u_\infty^2}\int_0^\delta\int_y^\delta \frac{\partial^2 \tau_{xy}}{\partial x^2}\, dy_1\, dy_d$$

$$- (\delta - 2\delta_m - \delta_y)\frac{g_c}{\sigma u_\infty^2}\left(\frac{\partial \tau_{yy}}{\partial x}\right)_{y_d = \infty} \qquad \text{(VII.148)}$$

$$- \frac{(2\delta_m + \delta_y)}{u_\infty^2}\int_0^\delta \left(\overline{u}_x \frac{\partial^2 \overline{u}_y}{\partial x^2} - \overline{u}_y \frac{\partial^2 \overline{u}_x}{\partial x^2}\right) dy_d$$

$$+ \frac{1}{u_\infty^2}\int_0^\delta\int_{y_d}^\delta \left(\overline{u}_x \frac{\partial^2 \overline{u}_y}{\partial x^2} - \overline{u}_y \frac{\partial^2 \overline{u}_x}{\partial x^2}\right) dy_1\, dy_d.$$

Equation (VII.148) is sufficiently complicated to be inconvenient for numerical calculations. It is similar to the relationships found by Goldschmied (*48*) except that it involves the conventional definition of the momentum thickness given in Eq. (VII.69). Likewise the displacement thickness of the boundary layer follows the conventional definition of Eq. (VII.64).

Combination of Eqs. (VII.141) through (VII.143) with (VII.148) may be written as

$$\frac{d\delta_m}{dx} = \frac{g_c}{\sigma u_\infty^2}(\tau_{yx})_0 + (2\delta_m + \delta_y)\frac{g_c}{\sigma u_\infty^2}\frac{dP_0}{dx} + A_1 + A_2 + A_3 + A_4. \qquad \text{(VII.149)}$$

Consideration of the above equation indicates that it has the same form as the Kármán momentum equation used for laminar boundary flows (*4*) except for the correction terms identified as A_1 to A_4 inclusive. It was suggested by Ross (*49*) that only A_1, which depends upon the anisotropy of the turbulence, is important at the present state of knowledge of such flows.

VII-19. Effect of Anisotropic Turbulence

In the rearrangement of Eq. (VII.148) to give Eq. (VII.149) the term A_1 has been defined as

$$A_1 = \frac{1}{u_\infty{}^2} \int_0^\delta \frac{\partial(\overline{u^2_{x,f}} - \overline{u^2_{y,f}})}{\partial x} dy_d. \tag{VII.150}$$

Recent experimental work by Dryden (*50*) and Schubauer (*51*) indicates that it is possible to evaluate this correction term, which is associated with the anisotropy of the normal Reynolds stresses. Such evaluation may be conveniently accomplished in the following way:

$$\overline{u^2_{x,f}} - \overline{u^2_{y,f}} = -\frac{2\,\overline{u_{x,f}\,u_{y,f}}}{\tan(2\phi_\tau)}. \tag{VII.151}$$

In this equation the anisotropy of the turbulence was related to the turbulent shear stress by means of the direction of the principal axis of the fluctuating stress tensor (*49*). Assuming from Dryden's observation that $\tan(2\phi_\tau)$ has a constant value of approximately 0.75, it is possible to write Eq. (VII.150) in the following rather simple form:

$$A_1 \cong -2.7 \frac{g_c}{\sigma u_\infty} \frac{d}{dx} \int_0^\delta \left(\frac{\sigma}{g_c} \overline{u_{x,f}\,u_{y,f}}\right) dy_d \cong 0.016 \frac{d\delta_y}{dx} - 0.016 \frac{2\,\delta_y\,g_c}{\sigma\,u_\infty{}^2} \frac{dP}{dx}. \tag{VII.152}$$

The numerical coefficients shown in Eq. (VII.152) were based upon Granville's integration (*52*) of the shear stress across the turbulent boundary flow.

$$\frac{g_c}{\sigma\,u_\infty{}^2} \int_0^{\delta_y} \left(\frac{\sigma}{g_c} \overline{u_{x,f}\,u_{y,f}}\right) dy_d \cong -0.006. \tag{VII.153}$$

Here the shear in the boundary layer was evaluated from the fluctuating velocities and the effect of the kinematic viscosity was neglected. In some instances this correction for anisotropy of the normal stresses in a turbulent boundary layer may amount to as much as 10% of the total rate of change of momentum thickness with downstream position. The work of Newman (*53*) and Bidwell (*54*) confirmed that the inclusion of the correction term A_1 brings the predicted wall shear stress in fair agreement with that determined experimentally.

VII-20. Minor Correction Terms

The remainder of the correction terms are usually of minor importance and may be defined in the following way:

$$A_2 = \frac{1}{u_\infty{}^2}\int_0^\delta\int_{y_d}^\delta \frac{\partial^2(\overline{u_{x,f}\,u_{y,f}})}{\partial x^2}\,dy_1\,dy_d - \frac{(2\,\delta_m + \delta_y)}{u_\infty{}^2}\int_0^\delta \frac{\partial^2(\overline{u_{x,f}\,u_{y,f}})}{\partial x^2}\,dy_d, \tag{VII.154}$$

$$A_3 = \frac{1}{u_\infty{}^2}\int_0^\delta\int_{y_d}^\delta \left(\overline{u_x}\,\frac{\partial^2\overline{u_y}}{\partial x^2} - \overline{u_y}\,\frac{\partial^2\overline{u_x}}{\partial x^2}\right)dy_1\,dy_d \tag{VII.155}$$

$$- \frac{(2\,\delta_m + \delta_y)}{u_\infty{}^2}\int_0^\delta \left(\overline{u_x}\,\frac{\partial^2 u_y}{\partial x^2} - \overline{u_y}\,\frac{\partial^2 u_x}{\partial x^2}\right)dy_d,$$

$$A_4 = 2\,\frac{\nu}{u_\infty{}^2}\left(\frac{\partial\overline{u_y}}{\partial x}\right)_{y_d=0} + \frac{\nu}{u_\infty{}^2}(\delta - 2\,\delta_m - \delta_y)\left(\frac{\partial^2\overline{u_x}}{\partial x^2}\right)_{y_d=\infty} \tag{VII.156}$$

The correction A_2 is associated with the rate of change of the shear gradient in the direction of primary flow and is negligible except when the boundary flow approaches separation (*55*). The corrections identified as A_3 and A_4 are associated with the neglect of velocities normal to the boundary and should be included in both laminar and turbulent flows. They appear to be less important for turbulent than for laminar flows. Ross (*49*) estimated that the flow corrections under isobaric conditions are approximately 2% of the total and with an adverse pressure gradient may amount to as much as 10%. It should be realized that Eq. (VII.149) does not account for all the discrepancy that is found between the normal Kármán integral equation for boundary flows and experiment. The deviations are particularly significant in connection with the experimental work of Rubert and Persh (*56*). Clauser (*57*) suggests that such discrepancies arise from the flow really being three-dimensional.

Clauser (*57*) considered the velocity distribution in turbulent boundary layers with adverse pressure gradients and suggested a universal diagram for the velocity distribution for a variety of gradients. These matters were not sufficiently far advanced to justify detailed consideration here. However, the use of a modified friction velocity defined as

$$\frac{u_x - u_\infty}{u_*} = u^+ - \frac{u_\infty}{u_*} \tag{VII.157}$$

appears to be a satisfactory means of correlating the velocity distribution for a variety of turbulent boundary flows under a particular pressure gradient. Such behavior is not unexpected since the normal velocity parameter u^+ is nearly a single-valued function of the distance parameter y_d^+ in steady, uniform boundary-shear-flows such as were considered by Laufer (*58*).

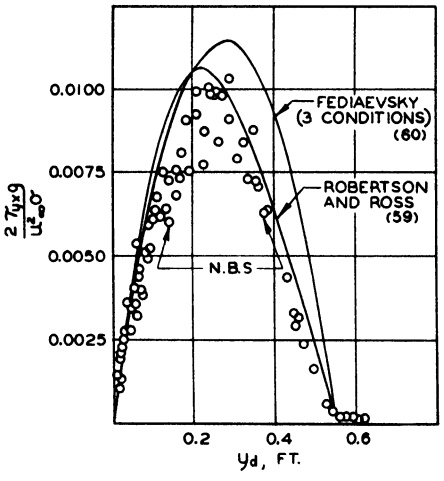

FIG. VII-28. Distribution of shear in turbulent boundary layer (*59*).

Ross and Robertson (*59*) extended Fediaevsky's (*60*) analysis of the shear-stress distribution in a turbulent boundary layer for a variety of pressure gradients. Progress is being made in the explanation of the distribution of shear stress in a turbulent boundary layer under pressure gradients for which back flow is approached. It should be realized that in the case of an adverse pressure gradient the shear is no longer a linear function of position and may in fact change sign. Figure VII-28 compares the Fediaevsky and Ross theories with the experimental data obtained by Dryden (*50*). As a matter of interest the shear distribution predicted by Ross and Robertson (*59*) may be evaluated from

$$\tau_{yx} = \tau_w \frac{\delta}{\partial_0}\left(1 - \frac{y_d}{\delta}\right) - \left(\delta \frac{dP}{dx} + \tau_{w0}\frac{\delta}{\delta_0}\right)\left(1 - \frac{y_d}{\delta}\right)^q + \left(\delta \frac{dP}{dx} + \tau_w\right)\left(1 - \frac{y_d}{\delta}\right)^{q+1}. \tag{VII.158}$$

The value of the exponent q may be obtained from

$$q = \frac{2\,\delta \dfrac{dP}{dx} + \tau_{w0}\dfrac{\delta}{\delta_0} + \tau_w}{\tau_{w0}\dfrac{\delta}{\delta_0} - \tau_{w0}}. \tag{VII.159}$$

It should be noted that at the beginning of a region of adverse pressure gradients the exponent $(q + 1)$ is large and Eq. (VII.158) yields a nearly linear distribution of shear as would be expected in steady, uniform flow. As the boundary flow increases in thickness the linear term is important only near the outer edge of the flow. Equations (VII.158) and (VII.159) require

a knowledge of the thickness of the boundary flow for their solution. Recent experimental work has contributed materially to an understanding of the behavior and stability of turbulent boundary layers under adverse pressure gradients (*48*, *56*, *57*, *61*).

Locke (*62*) recently reviewed the drag coefficients with turbulent boundary layers and recommends the following implicit expression for the drag coefficient:

$$0.242 = \sqrt{C_D} \log (\mathrm{Re}\, C_D). \qquad \text{(VII.160)}$$

This relationship is the same as that proposed earlier by Schoenherr (*63*) and appears to be much more representative of experiment than the power functions and polynomials often employed. The above expression is recommended for use at Reynolds numbers as high as 10^{10}. Its application for lower Reynolds number is limited inasmuch as few data are available for Reynolds numbers as low as 5×10^4, and in the region of low Reynolds numbers there is a difficulty in precisely defining a Reynolds number for the turbulent boundary layer (*64*).

Laminar Boundary Flows in Three Dimensions

For some purposes it is desirable to consider the behavior of fluid flow in three dimensions. Such considerations are of particular importance in understanding the behavior of rotating machinery involving fluids when operating under relatively high pressure gradients. Experience indicates that most turbo-machines usually operate satisfactorily only at pressure gradients markedly below those predicted from cascade and single-stage measurements. The deficiency in existing simple theories describing the performance of such equipment lies in a large measure in the lack of a proper evaluation of the behavior of boundary flows in three dimensions such as are encountered on turbine and compressor blades. In the case of three-dimensional boundary flows the secondary motion adjacent to solid boundaries and the effects of viscosity are of importance.

The mathematical treatment of such problems is difficult and usually leads to a consideration of perturbation theory as applied to the conditions in the boundary flow. Howarth (*65*), Hayes (*66*), and Moore (*67*) considered the nature of boundary flows without attempting the detailed solution of the equations of motion applying to this situation. Such results have been of importance in understanding the behavior of rotating machinery and have permitted a marked improvement in the design of some equipment. If a velocity distribution is assumed, as was done by Pohlhausen (*5*), the

momentum integral method may be applied to the evaluation of three-dimensional boundary layers. Timman (*68*) considered the laminar boundary layer with conventional assumptions as to the velocity distribution and Mager (*69*) treated the turbulent boundary layer for the three-dimensional case in a satisfactory method for practical application. There are a number of additional investigations involving special cases in which the change in the properties of the stream with respect to the coordinate system is negligible and where the effect of one of the velocity characterization parameters may be neglected.

More recently Mager (*70*) reviewed three-dimensional boundary behavior limited to rather small crossflows. He applied the perturbation theory to the normal boundary layer equations and developed examples illustrating the solution of his analysis. These expressions were unable to predict the point of separation although it was indicated that variations in crossflow exerted an important effect upon point of separation. These effects were found in oblique cylinders and flow in ducts of more complex curvature. Sharply varying, lateral, concave curvatures contribute markedly to the separation of the basic flow. In addition Mager proposed the solution of equations describing three-dimensional boundary layers by assuming that the outer part of the boundary flow is nonviscous. It is beyond the scope of the present discussion to consider the solution of the perturbation equations although such solutions can be accomplished in a manner similar to that employed for the basic flow.

The equations describing three-dimensional boundary flows differ from the two-dimensional theory by the presence of additional terms involving changes in the z-direction and by the change in the order of the pressure gradient normal to the primary flow and parallel to the surface. This gradient can no longer be neglected because of its need to balance the centripetal and Coriolis forces, and it is the critical factor in three-dimensional flows responsible for change in flow direction in the boundary layer. Likewise the change in pressure through the boundary layer normal to the wall is one order larger than in the two-dimensional case but can still be neglected in a first-order approximation.

VII-21. Effects of Dissipation and Thermal Transfer

Throughout most of the foregoing discussion no regard was taken of the variation in temperature or other properties in the boundary flow. Because of the change in temperature with density in compressible fluids and the dissipation of kinetic energy in the boundary layer as a result of either viscous

or turbulent shear, there exists a marked increase in the temperature in the boundary layer in high-speed adiabatic flow. There also is a difference between the temperature distribution in the boundary layer for turbulent and laminar flows, although the surface temperature of an immersed body under adiabatic conditions is always higher than that of the free stream. It is convenient to consider the surface temperature in relation to the gross velocity in the following way. The stagnation temperature may be established from the definition

$$T_{st} = T + \frac{u_\infty{}^2}{2\, g_c\, C_P{}^*}. \tag{VII.161}$$

It is of interest to note that the stagnation temperature, T_{st}, is not a function of the thermodynamic path followed between the free stream and the boundary. In Eq. (VII.161) the heat capacity is the average value applying to the fluid in the boundary flow and may be defined as

$$C_P{}^* = \frac{H_{st} - H}{T_{st} - T}. \tag{VII.162}$$

The temperature at an adiabatic interface is not equal to the stagnation temperature because of the thermal transport through the gas phase and because of the dissipation of kinetic energy in the flowing stream near the surface.

VII-22. Temperature Recovery Factors

In order to take these effects into account in an empirical way it is convenient to define a temperature recovery factor (*67*) in the following way:

$$r' = \frac{T_0 - T}{T_{st} - T}. \tag{VII.163}$$

The effect of the type of boundary flow upon the recovery factor is shown in Fig. VII-29, for nearly adiabatic conditions. It is apparent that there exists a transition in the temperature distribution in the boundary region as a result of the change from laminar to turbulent flow. The data shown in Fig. VII-29 were based upon measurements of Evvard, Tucker, and Burgess (*12*) for the flow of air along a 10° cone, with primary flow parallel to the axis of the cone. These measurements were made at free stream velocities above that of sound but there did not appear to be any significant local shock waves to complicate the flow pattern. The recovery factors

were determined from measurements of the surface temperature of the cone under nearly adiabatic conditions.

The marked variation in temperature in the boundary layer in high speed flow is an indication of the need of considering the effect of compressibility and kinetic-energy dissipation upon the behavior of the boundary layer. As an indication of the practical aspects of this matter, reference is made to the recent work of Low (*71*)[1] who established the extent of the thermal transport at the boundary necessary to stabilize a laminar boundary layer. Such calculations were based upon the earlier work of Lees (*72, 73*).

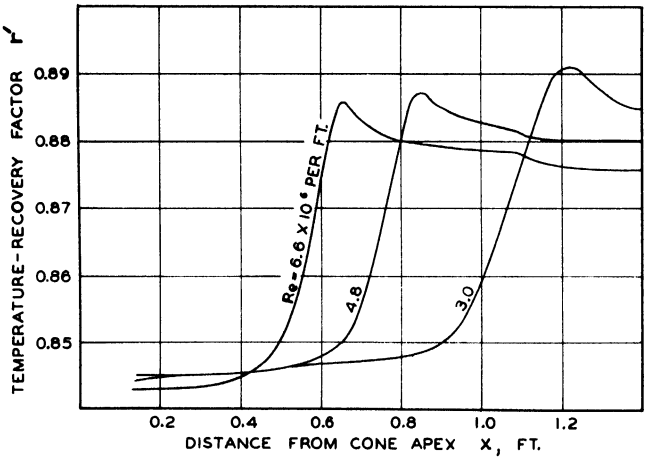

FIG. VII-29. Temperature recovery factor.

Boundary Flows for Compressible Fluids

Throughout the foregoing discussions of boundary flows, no regard was taken of the effect of changes in specific volume of the fluid with change in position in the boundary layer nor was any consideration given to the changes in temperature resulting from the changes in pressure under adiabatic, and in some cases nearly isentropic, conditions. The changes in temperature result in changes in both the specific volume and viscosity of the fluid, thus changing the velocity distribution in the boundary layer. Furthermore the earlier discussions of laminar and turbulent boundary flows did not take into account the effect of thermal transfer on the behavior of the boundary layer. These matters, except as they influence the velocity, shear, and momentum distribution in the boundary layer will not be considered beyond the brief

[1] See also van Driest (*73 a, 73 b*) for a discussion of recovery factor and heat-transfer coefficient for laminar and turbulent boundary layers.

discussion of the foregoing section relating to the influence of dissipative effects on the behavior of fluids. The present section will relate to a description of the behavior of boundary flows under conditions in which the changes in specific volume and temperature cannot be neglected.

VII-23. Laminar Flow

In dealing with a compressible fluid it is usually assumed that the phase is a perfect gas, and an equation of state of the following form is employed:

$$P V = b T. \tag{VII.164}$$

It does not increase the complexity of the basic analysis to any great extent to consider more complex equations of state such as those of van der Waals (*74*) and of Beattie and Bridgeman (*75*). Until more is learned concerning the mechanics of boundary flows it usually suffices to employ Eq. (VII.164) to describe the volumetric behavior of gases. In situations involving fluids at high pressures it may be desirable, however, to take into account any deviations from the behavior of perfect gases. The primary difference in the analysis of the behavior of compressible and incompressible fluids in boundary flows rests in the large effect of pressure upon the adiabatic change in temperature of a gas in comparison to that found for liquids. Under such circumstances it is desirable to consider directly the interrelation of velocity and internal energy. Thus the energy balance (*76*) may be written as

$$\sigma u_x \frac{\partial}{\partial x}\left(H + \frac{u_x^2}{2g}\right) + \sigma u_y \frac{\partial}{\partial y_d}\left(H + \frac{u_x^2}{2g}\right) = \frac{\partial}{\partial y_d}\left\{\frac{k}{C_P}\frac{\partial}{\partial y_d}\left(H + \Pr\frac{u_x^2}{2g}\right)\right\}. \tag{VII.165}$$

Equation (VII.165) applies only to laminar flows since no regard was taken of the energy transport as a result of turbulence. In evaluating the thermal transport normal to the direction of flow it is desirable to employ the stagnation temperature rather than the thermodynamic temperature of the free stream as a measure of the potential of transport. In the derivation of Eq. (VII.165) thermal conduction in the direction of flow was neglected, as were changes in the y_d or z components of velocity with position. These assumptions are compatible with those normally employed in laminar-boundary-flow theory.

The corresponding expression for the conservation of momentum may be written according to Eq. (VII.75) as

$$\frac{\sigma u_x}{g_c}\frac{\partial u_x}{\partial x} + \frac{\sigma u_y}{g_c}\frac{\partial u_x}{\partial y_d} = \frac{\partial}{\partial y_d}\left(\eta \frac{\partial u_x}{\partial y_d}\right), \tag{VII.166}$$

for steady, uniform flow with no change in pressure. If Eqs. (VII.165) and (VII.166) are combined with the equation of continuity for a compressible fluid they form a set of equations which permits the solution of the boundary flow of a compressible fluid. In this instance it is convenient to write the equation of continuity in the following form:

$$\frac{\partial \sigma u_x}{\partial x} + \frac{\partial \sigma u_y}{\partial y_d} = 0. \tag{VII.167}$$

Most of the analytical effort associated with compressible boundary flows was concerned with the solutions of these three equations which are nonlinear in character.

Crocco (*77*) gave the classic treatment of laminar boundary flows for compressible fluids. He carried out the solution of the above equations by numerical methods and gave a large number of graphical representations and tabular records of the behavior of laminar compressible boundary flows. Kuerti (*78*) gave a very excellent discussion of the laminar boundary layer in compressible flow. Monaghan (*76*) obtained approximate solutions for Eqs. (VII.165), (VII.166), and (VII.167) on the assumption that the enthalpy and velocity of the fluid are dependent only upon local conditions. The analytical results obtained appear to be in satisfactory agreement with Crocco's more accurate numerical computation. Johnson (*79*) considered the behavior of a laminar boundary flow of a compressible fluid on a curved adiabatic surface. He followed some of the methods of Pohlhausen (*80*) and extended them to apply to curved surfaces. The influence of upstream disturbances on compressible boundary flows was reviewed by Lighthill (*81*). Much of this work is based on the early considerations of Crocco (*77*) and Howarth (*82*). Young (*83*) presented an excellent nonmathematical review of compressible boundary flows and included a useful bibliography. The effect of shock waves upon the separation or near separation of compressible boundary flows was described by Young, who indicated that for most situations the shock waves do not induce complete separation, as is accomplished by means of a step in the solid boundary. The effect of shock waves on the separation of boundary flows was recently reviewed by Lange (*84*). The effects of arbitrary surface temperature and pressure gradients upon the behavior of laminar boundary flows have been considered by Morris and Smith (*85*) whereas the influence of varying properties of the fluid including chemical dissociation was considered by Moore (*86*). Young and Janssen (*87*) considered broadly the nature of boundary flows for a compressible fluid from a nonmathematical standpoint.

A number of specific solutions to Eqs. (VII.165), (VII.166), and (VII.167) have been obtained. Among these the work of Hantzsche and Wendt (*88*, *89*) is of particular interest in situations involving thermal transport. Emmons and Brainerd (*90*, *91*) also contributed to the study of the influence of temperature gradients upon laminar flows for a compressible fluid. The large background of experimental and theoretical work that has recently accumulated makes it possible to review only the more important contributions. The calculations of Kármán and Tsien (*92*) have proved to be of unusual utility and are in reasonable agreement with much more recent predictions.

In predicting the behavior in a laminar compressible boundary flow it is important to evaluate the properties of primary interest as a function of position near the boundary of a stream. For present purposes the equation of state to be employed will be that of a perfect gas. The effect of temperature upon the viscosity is of direct importance. As a first approximation it was assumed for the present analysis that the viscosity was directly proportional to the absolute temperature (*93*) as indicated in the following equation:

$$\frac{\eta}{\eta_\infty} = B\frac{T}{T_\infty}. \tag{VII.168}$$

Such an assumption is satisfactory for many gases where no changes in chemical composition occur near the boundary and where the differences in temperatures are not great.

Following the methods of Monaghan (*76*) the following summary of algebraic expressions is submitted for the approximate solution of a boundary flow for a compressible fluid under isobaric conditions. These expressions apply only to a perfect gas with values of the Prandtl number varying from 0.5 to 3. The Prandtl number as used here is defined as

$$\mathrm{Pr} = \frac{C_P \eta g_c}{k}. \tag{VII.169}$$

In order to simplify the tabulation of the results, a number of symbolic functions will be defined

$$B_1 = \frac{T_0}{T_\infty}, \tag{VII.170}$$

$$B_2 = \mathrm{Pr}^{1/3}\left[\frac{T_0}{T_\infty} - 1 - \mathrm{Pr}^{1/2}\left(\frac{C_P}{2C_v} - \frac{1}{2}\right)M_\infty^2\right], \tag{VII.171}$$

$$B_3 = \mathrm{Pr}\left[\frac{C_P}{2C_v} - \frac{1}{2}\right]M_\infty^2, \tag{VII.172}$$

$$F = C_\tau \sqrt{\mathrm{Re}}, \tag{VII.173}$$

$$F_0 = C_D \sqrt{\mathrm{Re}} = 0.664 \sqrt{B} \tag{VII.174}$$

where

$$C_D = \frac{2 g_c}{\sigma u_\infty^2} (\tau_{yx})_0. \tag{VII.175}$$

In these functions it will be assumed that the average value of the Prandtl number and of the ratio of the isobaric to isochoric heat capacities will be employed. The Mach number is that of the free stream and involves its conventional meaning of the ratio of the stream velocity to the velocity of sound in the fluid at that point. Finally,

$$C_\tau = \frac{2 g_c}{\sigma u_\infty^2} \tau_{yx}. \tag{VII.176}$$

The velocity distribution in the laminar boundary layer was presented (*76*) in the following expression, which must be solved implicitly:

$$\frac{y_d}{2x} \sqrt{\mathrm{Re}} = \frac{B}{F_0} \left[\left(B_1 - \frac{B_3}{2} \right) \sin^{-1} \left(\frac{u_x}{u_\infty} \right) + \left(\frac{B_3 u_x}{2 u_\infty} + B_2 \right) \left(1 - \frac{u_x^2}{u_\infty^2} \right)^{1/2} - B_2 \right]. \tag{VII.177}$$

The distribution of shear is given by

$$\frac{\tau_{yx}}{(\tau_{yx})_0} = \sqrt{1 - \frac{u_x^2}{u_\infty^2}} = \frac{F}{F_0}, \tag{VII.178}$$

whereas the temperature distribution may be obtained from

$$\frac{T}{T_\infty} = B_1 - B_2 \frac{u_x}{u_\infty} - B_3 \frac{u_x^2}{u_\infty^2}. \tag{VII.179}$$

In these equations u_x is the point velocity parallel to the free stream velocity. The quantity B of Eq. (VII.168) may be established from

$$B = \left(\frac{T_b}{T_\infty} \right)^{1/2} \frac{1 + \dfrac{T_c}{T_\infty}}{\dfrac{T_b}{T_\infty} + \dfrac{T_c}{T_\infty}}. \tag{VII.180}$$

The ratio T_b/T_∞ appearing in Eq. (VII.180) is obtained by evaluating

$$\frac{T_b}{T_\infty} = B_1 - 0.468 B_2 - 0.273 B_3. \tag{VII.181}$$

The quantity T_c is a characteristic temperature for the gas and is 208.8° R. for air. The foregoing semi-empirical expressions based directly on the work of Monaghan (*76*) permit the temperature, velocity, and shear to be determined as a function of position in the boundary layer.

As an illustration, the variation in shear as a function of position is shown in Fig. VII-30. In this instance the normal position for the surface has been shown as a fraction of the downstream distance corresponding to a particular Reynolds number. The behavior of an incompressible boundary layer with constant physical properties of the fluid has been included for comparison. The latter information was based upon the calculations of Blasius (*14*). As a second illustration the temperature distribution in the compressible boundary layer is shown as a function of the same variable in Fig. VII-31. Similar shear and temperature distributions are shown in Figs. VII-32 and VII-33 for a situation in which the absolute temperature

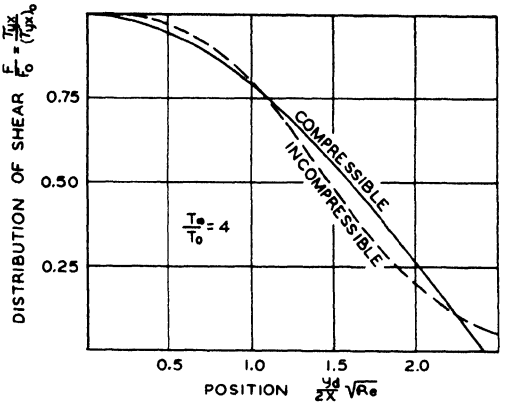

FIG. VII-30. Distribution of shear in compressible boundary with adiabatic wall (*12*).

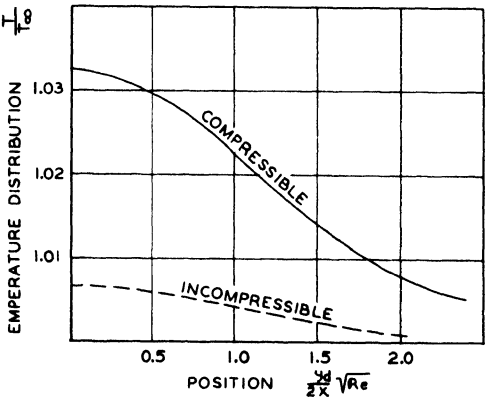

FIG. VII-31. Temperature distribution in compressible laminar boundary with adiabatic wall.

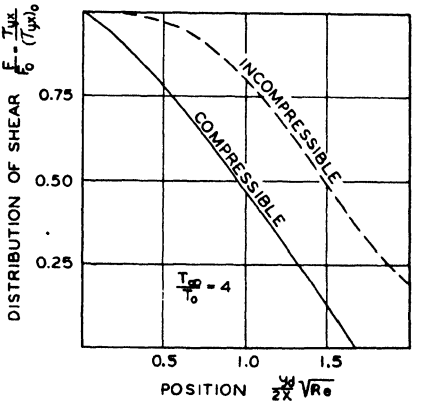

FIG. VII-32. Distribution of shear in compressible laminar boundary with thermal transfer.

of the boundary was only one fourth that of the free stream. There is little difference in the shear distributions in the two cases. Because of a rapid thermal transport to the wall, however, a markedly different temperature

distribution in the boundary flow results. A similar comparison is made in Figs. VII-34 and VII-35 for the velocity distribution in the adiabatic and thermal transport cases. The information presented in Figs. VII-30 through VII-35 was based on Eqs. (VII.170) through (VII.181). Sufficient identifying information was included on each diagram to define the conditions for which the boundary flow applied. The data of all these figures were associated with the properties of air at a free stream temperature of 70° F.

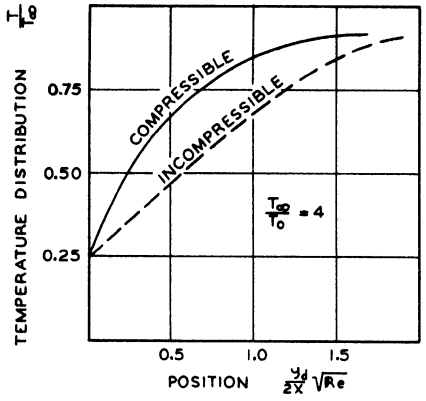

FIG. VII-33. Temperature distribution in compressible laminar boundary with thermal transfer.

It is apparent from the foregoing figures that changes in surface temperature exert a pronounced effect upon the behavior of a laminar compressible boundary flow. It is beyond the scope of the present work to consider the many methods of analysis which have been applied with varying success to the prediction of the properties of such boundary flows. The effect of the compressibility of the fluid on the behavior of the flow is usually small at free stream velocities less than half

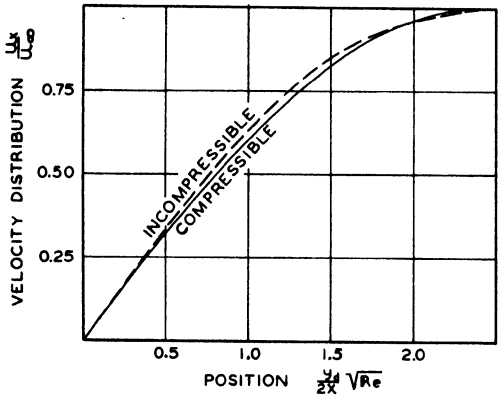

FIG. VII-34. Velocity distribution in compressible laminar boundary with adiabatic wall.

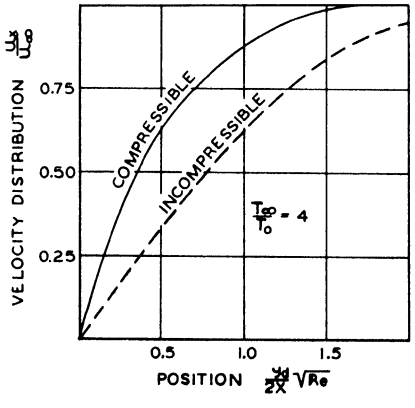

FIG. VII-35. Velocity distribution in compressible laminar boundary with thermal transfer.

that of the velocity of sound. The reader is referred to the excellent treatment by Howarth (*94*) for a more detailed consideration of high-speed flow in which the effect of compressibility is of particular importance. In many

such circumstances shock phenomena become controlling, and in some instances the rate of change of state is great enough to introduce significant deviations from the local or microscopic equilibrium behavior of the fluid (*95*).

VII-24. Slip Flow

As the pressure is decreased, the nature of the flow may undergo change as the dimensions of the boundary layer approach the same order as that of the mean free path of the molecule. Mirels (*96*) reviewed the effect of slip flow on compressible laminar boundary layers and defined a number of regimes of flow. Whenever the ratio of the Reynolds number to the one-half power to the Mach number of the free stream is less than 0.1, there is free molecular flow. Under these conditions the motion of each individual molecule is not restricted. When this ratio is between unity and 100, slip flow exists in which it is difficult to assign a specific velocity of boundary flow relative to the interface. For values of the ratio greater than 100 the effect of the statistical nature of the gas can be neglected and the normal methods of continuum mechanics may be applied. Maslen (*97*) considered further approximations in evaluating the behavior of laminar compressible boundary behavior under conditions in which slip flow is important. The background of the statistical treatment of gases was well laid by Chapman and Cowling (*98*).

VII-25. Turbulent Flow

As has been described, laminar boundary layers in high-speed flow often undergo a transition into turbulent boundary layers (*71*). The introduction of "spoilers" in a laminar boundary flow will rèsult in an early transition to a turbulent flow. The analysis of compressible turbulent boundary flows has not advanced to the extent that has been realized in the analysis of laminar boundary flows of compressible fluids. Donaldson (*99*) discussed some of the characteristics of turbulent boundary layers and Cope (*100*) presented some of the basic relationships and their approximate solution. Primary emphasis has been directed to the evaluation of the drag coefficients experienced with turbulent boundary layers. The development of turbulent flows has been considered in compressible flow by Tucker (*101*) and Wilson (*102*). Chapman and Kester (*103*) and Coles (*104*) have considered turbulent boundary flows in sufficient detail to be of value in the prediction of their behavior. In addition, Schlichting (*46*) reviewed turbulent boundary flows for incom-

pressible fluids, and the behavior of such fluids affords a satisfactory limit to the characteristics of compressible turbulent boundary layers.

As was described in connection with the introduction to incompressible fluids it is usually necessary where a general solution to the equations of motion cannot be obtained to rely on an over-all evaluation of the behavior of the boundary flows. In the case of a turbulent compressible boundary flow there exist fluctuations in specific weight, temperature, pressure, viscosity, thermal conductivity, and velocity with time throughout the flow.

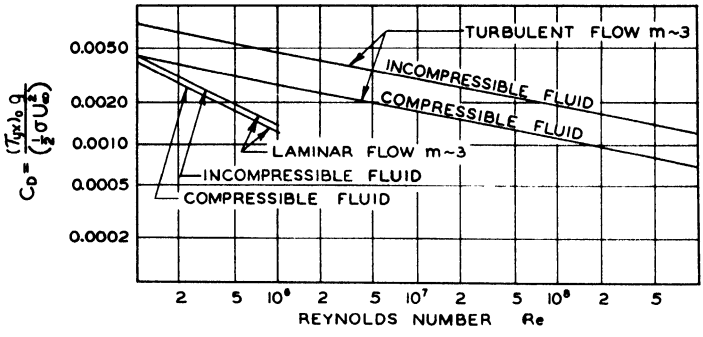

FIG. VII-36. Drag coefficients (*100*).

In the case of incompressible flow only the latter fluctuation is encountered. The greater part of the exchange of momentum and energy is a result of these fluctuations and is not associated with molecular transport as is the case with laminar flow. In the case of a turbulent boundary flow there exists a marked change in the character of the motion along the wall from that encountered for incompressible flow. This is emphasized when consideration is given to the marked difference in the velocity distribution encountered. Donaldson (*99*) and also Cope (*100*) assumed that the macroscopic velocity in the turbulent boundary may be described by an expression of the form

$$\frac{u_x}{u_\infty} = \left(\frac{y_d}{\delta}\right)^{\frac{1}{m}}. \tag{VII.182}$$

In Eq. (VII.182) the exponent m controls the form of the velocity distribution. On the basis of Eq. (VII.182) it is a relatively straightforward matter to determine an approximate value of the drag coefficient on a flat plate as a function of Reynolds number. The results of such an analysis of the drag coefficient are set forth in Fig. VII-36. It is noted that in incompressible flow a somewhat larger drag coefficient is obtained.

At present the treatment of turbulent boundary layers follows the methods developed by Kármán (*4*) and Pohlhausen (*5*). These momentum

considerations may be written in the form previously shown in Eq. (VII.82). It is necessary to ascertain the velocity profile in order to evaluate the integrals shown in Eq. (VII.82). As has been described the velocity distribution is a function of the local Reynolds number. However, it has been found possible to estimate the velocity distribution in terms of a single parameter as shown in Eq. (VII.182). Furthermore, it has been found that

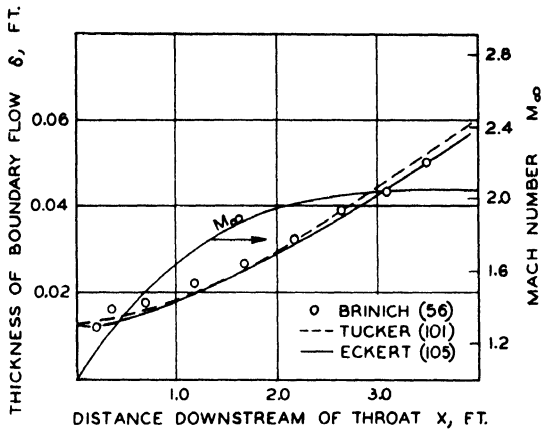

FIG. VII-37. Thickness of turbulent boundary layer in a de Laval nozzle (*105*).

under adverse pressure gradients where compressible turbulent boundary layers become unstable, Eq. (VII.82) is not particularly useful (*105*). The choice of the power law distribution presented in Eq. (VII.182) is based primarily on the ease of analytical treatment and allows the use of tabulated functions of Tucker (*101*), although the agreement with experiment in the case of pressure gradients does not appear to be as satisfactory as had originally been expected (*97*). As an indication of the agreement of theory and experiment, the variation in the effective turbulent boundary layer thickness in a two-dimensional Laval nozzle is shown in Fig. VII-37. In this diagram the experimental thickness of the boundary layer based upon Brinich's measurements (*55*) and the predictions of Tucker (*101*) and Eckert (*105*) were included. In addition, the Mach number of the average free flow is presented as a matter of interest. The reader is referred to the work of Tucker (*101*), Donaldson (*99*) and Eckert (*105*) together with the more general treatment of Howarth (*94*) for a more complete consideration of turbulent boundary flows of compressible fluids.

Nomenclature

A_1, A_2, A_3, A_4 Correction terms for the Kármán momentum equation
a Constant
B Constant
B_1, B_2, B_3, F, F_0 Parameters in Monaghan's formulation of the compressible boundary layer problem, dimensionless
b Specific gas constant, ft./°R.
C_D Drag coefficient, dimensionless
C_n A coefficient in the Blasius function
C_P Isobaric heat capacity, ft./°R.
C_P^* Average isobaric heat capacity, ft./°R.
C_τ Analog of drag coefficient in the boundary layer, dimensionless
D Dimensionless form parameter
d Diameter
$\boldsymbol{F}$ Force, lb.
$\boldsymbol{F}_D$ Drag force, lb.
g_c Acceleration due to gravity, ft./sec.^{2}
H Enthalpy, ft.
H_{st} Enthalpy at T_{st}, ft.
K_1 An empirical constant, dimensionless
K_2 Constant
K_3 Constant
K_4 Constant
k Thermal conductivity, lb./sec.°R.
l Characteristic length of the solid boundary, ft.
M_∞ Free stream Mach number, dimensionless
m Empirical constant
$\dot{m}_x$ Material flux in the x-direction, lb./ft.^{2}sec.
$\dot{m}_y$ Material flux in the y-direction, lb./ft.^{2}sec.
$\dot{m}_\infty$ Free stream material flux, lb./ft.^{2}sec.
P Thermodynamic pressure, lb./ft.^{2}
P_b Dimensionless pressure
P_0 Pressure at the solid boundary, lb./ft.^{2}
P_∞ Free stream thermodynamic pressure, lb./ft.^{2}
Pr Prandtl number, dimensionless
q A parameter of Ross' equation
r Radius of cylinder, ft.
r' Temperature-recovery factor, dimensionless
Re Reynolds number for boundary layer, $x\, u_\infty\, (\sigma/\eta\, g_c)$
Re_b Boundary layer Reynolds number, dimensionless
s Distance from the stagnation point along the surface of a cylinder, ft.
T Thermodynamic temperature, °R.
T_b Parameter in Monaghan's formulation of the compressible boundary layer problem, °R.
T_0 Temperature at the solid boundary, °R.
T_{st} Stagnation temperature, °R.
T_∞ Thermodynamic temperature of the free stream, °R.
$U_{x,P}$ Velocity of plate, ft./sec.
u^+ Velocity to friction velocity ratio for x-direction, dimensionless
u_s Velocity tangential to the surface of a cylinder, ft./sec.
u_x x-component of velocity, ft./sec.
$u_{x,b}$ Dimensionless velocity in x-direction
u_y y-component of velocity, ft./sec.
$u_{y,b}$ Dimensionless velocity in y-direction
$u_{y\infty}$ Velocity in y-direction in region remote from boundary, ft./sec.
u_∞ Free stream velocity, ft./sec.
$u^0{}_\infty$ Constant
u_* Friction velocity, $\sqrt{g_c/\sigma(\tau_{yx})_0}$, ft./sec.
V Specific volume, cu.ft./lb.
x Distance along the direction of flow, ft.
x_2 Distance from virtual origin of flow, ft.
y Distance in direction perpendicular to the direction of flow, ft.
y_a An arbitrary value of $y_d \gg \delta$
y_d Distance from wall, ft.
$y_d{}^+$ Friction distance parameter, dimensionless

$2\,y_0$ Separation of parallel plates, ft.
z Width of solid boundary, ft.
α A coefficient in the Blasius function
β A coefficient in the Blasius function
γ A coefficient in the Blasius function
δ Boundary layer thickness, ft.
δ_m Momentum thickness, ft.
δ_0 Boundary layer thickness at the start of the positive pressure gradient, ft.
δ_p Pohlhausen boundary layer thickness, ft.
δ_y Displacement thickness, ft.
ε_m Eddy viscosity, ft.^{2}/sec.
ζ The dimensionless variable $y_d/2\sqrt{\sigma/(\eta\, g_c\, \theta)}$
η Absolute viscosity, lb.sec./ft.^{2}
η_0 Absolute viscosity evaluated at the wall, lb.sec./ft.^{2}
θ Time, sec.
θ_b Dimensionless time scale
λ Pohlhausen's form function, dimensionless
λ_{st} Value of λ at the stagnation point
ν Kinematic viscosity, ft.^{2}/sec.
σ Specific weight, lb./ft.^{3}
σ_0 Specific weight evaluated at the wall, lb./ft.^{3}
τ_{xx} Component of stress in the x-direction exerted on a plane perpendicular to the direction of flow, lb./ft.^{2}
τ_{xy} Component of stress in the y-direction exerted on a plane perpendicular to the direction of flow, lb./ft.^{2}
τ_{yx} Component of stress in the x-direction lying in a plane parallel to the wall, lb./ft.^{2}
τ_{yy} Component of stress in the y-direction exerted on a plane parallel to the wall, lb./ft.^{2}
$(\tau_{yx})_0$ Component of shear in the x-direction exerted by the fluid on the wall, lb./ft.^{2}
τ_w Variable shear at the wall, lb./ft.^{2}
τ_{w0} Value of τ_w at the start of the positive pressure gradient, lb./ft.^{2}
$\phi_1(\psi_0)$, $\phi_3(\psi_0)$, $\phi_5(\psi_0)$, $\phi_7(\psi_0)$ Functions of the boundary layer on a cylinder, dimensionless
$\phi_2(\psi)$ Blasius function, dimensionless
$\phi_8(\psi_P)$, $\phi_9(\psi_P)$, $\phi_{10}(\lambda)$, $\phi_{11}(\lambda)$, $\phi_{12}(\lambda)$ Pohlhausen boundary layer functions, dimensionless
ϕ_τ A parameter
χ Stream function, dimensionless
ψ Dimensionless boundary layer thickness
ψ_0 Dimensionless parameter for describing boundary layer on a cylinder
ψ_* Angle of tangential plane to the direction of flow
ψ_P Pohlhausen parameter, dimensionless
Ω Modified Reynolds number, dimensionless

Superscripts and Subscripts

Derivative with respect to indicated variable
$-$ Time average quantity
f Fluctuating component
i Initial
o Evaluated at solid boundary
sp Evaluated at separation point
st Evaluated at stagnation point
$x = \infty$ Quantity applies only for large X
$y_d = 0$ Evaluated at $y_d = 0$
$y_d = y_a$ Evaluated at $y_d = y_a$
1 = To distinguish limit of integration from variable of integration

References

1. Reynolds, O. S., *Proc. Manchester Lit. and Phil. Soc.* **14**, 7 (1874); "Papers on Mechanical and Physical Subjects," Vol. 1, p. 81. Cambridge U. P., New York, 1890.
2. Prandtl, L., Div. *G in "Aerodynamic Theory"* (W. F. Durand, ed. 1943), Vol. 3. Springer, Berlin, 1934.
3. Prandtl, L., *Verhandl. Dritten Intern. Math. Kongr. Heidelberg*, p. 484 (1904).
4. von Kármán, T., *Z. angew. Math. u. Mech.* **1**, 233 (1921).
5. Pohlhausen, K., *Z. angew. Math. u. Mech.* **1**, 252 (1921).
6. Page, F., Jr., Corcoran, W. H., Schlinger, W. G., and Sage, B. H., *Ind. Eng. Chem.* **44**, 419 (1952).
7. Page, F., Jr., Schlinger, W. C., Breaux, D. K., and Sage, B. H., *Ind. Eng. Chem.* **44**, 424 (1952).
8. Dunn, L. G., Powell, W. B., and Seifert, H. S., Heat transfer studies relating to power plant development. *Roy. Aeronaut. Soc. Brighton, England, 3rd Anglo-American Aeronaut. Conf.* (1951).
9. Schlinger, W. G., and Sage, B. H., *Ind. Eng. Chem.* **45**, 2636 (1953).
10. McShane, E. J., Kelley, J. L., and Reno, F. V., "Exterior Ballistics." Univ. of Denver Press, Denver, 1953.
11. Schlichting, H., *Natl. Advisory Comm. Aeronaut. Tech. Mem.* **1217** (1949).
12. Evvard, J. C., Tucker, M., and Burgess, W. C., Jr., *Natl. Advisory Comm. Aeronaut. Tech. Note* **3100** (1954).
13. Levy, S., and Seban, R., *J. Appl. Mech.* **20**, 415 (1953).
14. Blasius, H., *Z. Math. u. Phys.* **56**, 1 (1908).
15. Schlichting, H., "Grenzschicht-Theorie." Braun, Karlsruhe, 1951.
16. Kaplun, S., *Z. angew. Math. u. Phys.* **5**, 111 (1954).
17. Murphy, J. S., *J. Aeronaut. Sci.* **20**, 338 (1953).
18. Millikan, C. B., A critical discussion of turbulent flows in channels and circular tubes. *Proc. 5th Intern. Congr. Appl. Mech. Cambridge* (1938).
19. Kamke, E., "Differentialgleichungen, Lösungsmethoden und Lösungen," Vol. 1. Chelsea, New York, 1948.
20. Carslaw, H. S., and Jaeger, J. C., "Conduction of Heat in Solids." Oxford U. P., New York, 1947.
21. Jahnke, E., and Emde, F., "Tables of Functions with Formulae and Curves." Dover, New York, 1945.
22. Hartree, D. R., *Proc. Cambridge Phil. Soc.* Part II, **33**, 223 (1937).
23. Goldstein, S., "Modern Developments in Fluid Dynamics," Vol. 1. Oxford U. P., New York, 1938.
24. Howarth, L., *Proc. Roy. Soc.* **A 164**, 547 (1938).
25. Emmons, H. W., and Leigh, D. C., *Current Paper 157. Aeronaut. Research Council London* (1954).
26. Dhawan, S., *Natl. Advisory Comm. Aeronaut. Tech. Note* **2567** (1952).
27. Mager, A., and Hansen, A. C., *Natl. Advisory Comm. Aeronaut. Tech. Note* **2658** (1952).
28. van der Hegge-Zijnen, B. G., Measurements of the Velocity Distribution in the Boundary Layer Along a Plane Surface, Thesis, Delft, Holland, 1924.
29. Hansen, W., *Z. angew. Math. u. Mech.* **8**, 185 (1928).

30. Schubauer, G. B., and Skramstead, H. K., *Natl. Advisory Comm. Aeronaut. Tech. Rept.* **909** (1948).
31. Hall, A. A., and Hislop, G. S., *Reports and Memoranda* **No. 1848**, *Aeronaut. Research Council London* (1938).
32. Hiemenz, K., *Dinglers Polytech. J.* **326**, 321 (1911).
33. Thom, A., *Proc. Roy. Soc.* **A 141**, 651 (1933).
34. Howarth, L., *Aeronaut. Research Council Rept.* **1632** (1935).
35. Lamb, H., "Hydrodynamics." Cambridge U. P., New York, 1932.
36. Billman, G. W., Mason, D. M., and Sage, B. H., *Chem. Eng. Progr.* **46**, 625 (1950).
37. Pankhurst, R. C., and Thwaites, B., *Reports and Memoranda* **No. 2787**, *Roy. Aeronaut. Council London* (1952).
38. Bickley, W., *Phil. Mag.* [7] **23**, 727 (1937).
39. Pai, S. I., 2nd Midwest Conf. on Fluid Mechanics, Ohio State Univ. (March, 1952).
40. Donoughe, P. L., and Prasse, E. I., *Natl. Advisory Comm. Aeronaut. Tech. Note* **2942** (1953).
41. Li, T. Y., and Nagamatsu, H. T., Similar Solutions of Compressible Boundary Layer Equations, CALCIT Report, Preprint, Heat Transfer and Fluid Mechanics Institute, Berkeley, 1954.
42. Lock, R. C., *Quart. J. Mech. and Appl. Math.* **4**, Part 1, 42 (1951).
43. Schlichting, H., and Bussman, K., *Schriften deut. Akad. Luftfahrtforsch.* **7 b**, Heft 2 (1943).
44. Libby, P. A., Kaufman, L., and Harrington, R. P., *J. Aeronaut. Sci.* **19**, 127 (1952).
45. Chapman, D. R., and Kester, R. H., *Natl. Advisory Comm. Aeronaut. Tech. Note* **3097** (1954).
46. Schlichting, H., *Natl. Advisory Comm. Aeronaut. Tech. Mem.* **1218** (1949).
47. Rotta, J., *Natl. Advisory Comm. Aeronaut. Tech. Mem.* **8411** (1953).
48. Goldschmied, F. B., *Natl. Advisory Comm. Aeronaut. Tech. Note* **2431** (1951).
49. Ross, D., Integration of the Reynolds Equations for Incompressible Turbulent Boundary Layers, Ordnance Research Lab., Pennsylvania State College, May 29, 1953.
50. Dryden, H. L., *Natl. Advisory Comm. Aeronaut. Tech. Note* **1168** (1947).
51. Schubauer, G. B., and Klebanoff, P. S., *Natl. Advisory Comm. Aeronaut. Tech. Note* **2133** (1950).
52. Granville, P. S., *David Taylor Model Basin Report* **752** (1951).
53. Newman, B. G., *Report A 64 of the Aeronaut. Research Labs. Australia* (1949).
54. Bidwell, J. M., *Natl. Advisory Comm. Aeronaut. Tech. Note* **2571** (1951).
55. Brinich, P. F., *Natl. Advisory Comm. Aeronaut. Tech. Note* **2203** (1950).
56. Rubert, K. F., and Persh, J., *Natl. Advisory Comm. Aeronaut. Tech. Note* **2478** (1951).
57. Clauser, F. H., *J. Aeronaut. Sci.* **21**, 91 (1954).
58. Laufer, J., *Natl. Advisory Comm. Aeronaut. Tech. Note* **2954** (1953).
59. Ross, D., and Robertson, J. M., Ordnance Research Lab., Pennsylvania State College Lab., Pennsylvania State College, May 29, 1953.
60. Fediaevsky, K., *Natl. Advisory Comm. Aeronaut. Tech. Mem.* **822** (1937); *J. Aeronaut. Sci.* **4**, 491 (1937).
61. Sandborn, V. A., *Natl. Advisory Comm. Aeronaut. Tech. Note* **3031** (1953).
62. Locke, F. W. S., Jr., *NAVAER DR Rept.* **No. 1415**, Navy Dept. Bureau Aeronaut. (1952).

63. Schoenherr, K. E., *Trans. Soc. Naval Architects and Marine Engrs.* **40**, 279 (1932).
64. Coles, D., *Z. angew. Math. u. Phys.* **5**, 181 (1954).
65. Howarth, L., *Phil. Mag.* [7] **42**, 239 (1951).
66. Hayes, W. D., *NAVORD Rept.* **1813**, NOTS 38, U. S. Naval Ordnance Training Station (1951).
67. Moore, F. K., *Natl. Advisory Comm. Aeronaut. Tech. Note* **2279** (1951).
68. Timman, R., *Natl. Luchtvaartlab., Amsterdam, Rept. F* **66** (1951).
69. Mager, A., *Natl. Advisory Comm. Aeronaut. Tech. Rept.* **1067** (1952).
70. Mager, A., Doctoral Thesis, California Institute of Technology, Pasadena, 1953.
71. Low, G. M., *Natl. Advisory Comm. Aeronaut. Tech. Note* **3103** (1954).
72. Lees, L., and Lin, C. C., *Natl. Advisory Comm. Aeronaut. Tech. Note* **1115** (1946).
73. Lees, L., *Natl. Advisory Comm. Aeronaut. Tech. Rept.* **876** (1947).
73a. van Driest, E. R., Report No. AL-1866, Missile and Control Equipment Dept., North American Aviation (1954).
73b. van Driest, E. R., Report No. AL-1914, Missile and Control Equipment Dept., North American Aviation (1954).
74. van der Waals, J. D., *Z. physik. Chem.* **38**, 257 (1901).
75. Beattie, J. A., and Bridgeman, O. C., *Proc. Am. Acad. Arts. Sci.* **63**, 229 (1928).
76. Monaghan, R. J., *Reports and Memoranda* **No. 2760**, *Aeronaut. Research Council London* (1953).
77. Crocco, L., Associazone Culturale Aeronautica Monografie Scientifiche di Aeronautica, No. 3, Rome, December, 1946. Royal Aircraft Establishment Library Translation No. 218, December, 1947, Aeronaut. Research Council 11, 453; Translation Aerophysics Laboratory Report CF 1038, North American Aviation, July 15, 1948.
78. Kuerti, G., *Advances in Appl. Mech.* **2**, 21—92 (1951).
79. Johnson, A. F., *Tech. Rept.* **No. HS-5**, Department of Mechanical Engineering, Stanford University (1953).
80. Pohlhausen, E., *Z. angew. Math. u. Mech.* **1**, 115 (1921).
81. Lighthill, M. J., *Fluid Motion. 1805, Aeronaut. Research Council London* (1952).
82. Howarth, L., *Proc. Roy. Soc.* **A 194**, 16 (1948).
83. Young, A. D., *J. Roy. Aeronaut. Soc.* **55**, 285 (1951).
84. Lange, R. H., *Natl. Advisory Comm. Aeronaut. Tech. Note* **3065** (1954).
85. Morris, D. N., and Smith, J. W., *J. Aeronaut. Sci.* **20**, 805 (1953).
86. Moore, L. L., *J. Aeronaut. Sci.* **19**, 505 (1952).
87. Young, G. B. W., and Janssen, E., *J. Aeronaut. Sci.* **19**, 229 (1952).
88. Hantzsche, W., and Wendt, H., *Jahrb. deut. Luftfahrtsforsch.* **1**, 517 (1940).
89. Hantzsche, W., and Wendt, H., *Jahrb. deut. Luftfahrtsforsch.* **1**, 40 (1941).
90. Emmons, H. W., and Brainerd, J. G., *J. Appl. Mech.* **63**, A 105 (1941).
91. Emmons, H. W., and Brainerd, J. G., *J. Appl. Mech.* **64**, A 1 (1942).
92. von Kármán, T., and Tsien, H. S., *J. Aeronaut. Sci.* **5**, 227 (1938).
93. Chapman, D. R., *Natl. Advisory Comm. Aeronaut. Tech. Rept.* **958** (1950).
94. Howarth, L., "Modern Developments in Fluid Dynamics, High Speed Flow," Vols. 1 and 2. Oxford U. P., New York, 1953.
95. Kirkwood, J. G., and Crawford, B., Jr., *J. Phys. Chem.* **56**, 1048 (1952).
96. Mirels, H., *Natl. Advisory Comm. Aeronaut. Tech. Note* **2609** (1952).
97. Maslen, S. H., *Natl. Advisory Comm. Aeronaut. Tech. Note* **2818** (1952).
98. Chapman, S., and Cowling, T. G., "The Mathematical Theory of Non-Uniform Gases," Cambridge U. P., New York, 1939.

99. Donaldson, C. du P., *Natl. Advisory Comm. Aeronaut. Tech. Note* **2692** (1952).
100. Cope, W. F., *Reports and Memoranda* **No. 2840**, *Aeronaut. Research Council London* (1950).
101. Tucker, M., *Natl. Advisory Comm. Aeronaut. Tech. Note* **2337** (1951).
102. Wilson, R. E., *J. Aeronaut. Sci.* **17**, 585 (1950).
103. Chapman, D. R., and Kester, R. H., *J. Aeronaut. Sci.* **20**, 441 (1953).
104. Coles, D., *J. Aeronaut. Sci.* **21**, 433 (1954).
105. Eckert, H. U., *Tech. Note* **WCRR 53-3**, Wright Air Development Center (1953).

APPENDIX I

A Derivation of Bernoulli's Equation

Bernoulli's equation is often derived from the concept of "conservation of mechanical energy." A precise definition of mechanical energy is difficult to establish and, as a result, the above-mentioned approach leaves much to be desired in the way of precision. Bernoulli's equation is usually written in the following differential form:

$$dh + \frac{u\,du}{g} + V\,dP + w' + j' = 0. \tag{A I.01}$$

This equation offers a useful means of evaluating friction or work from a knowledge of the path of a flow process.

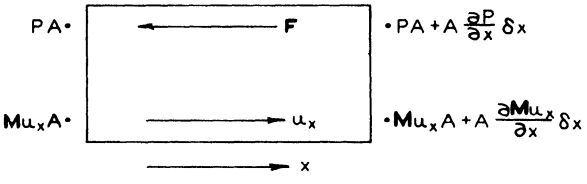

Fig. AI-1. Element of conduit showing orientation of fluxes and forces.

Consider a section of a conduit whose axis lies in the direction x and through which a compressible fluid is flowing at steady state. The directions of the several forces and fluxes of interest are indicated in Fig. A I-1.

No accelerations are present in this system at steady state. This situation is described precisely in the following restricted statement of the principle of the "conservation of momentum":

$$A\,\frac{\partial M u_x}{\partial x}\,\delta x + F + A\,\frac{\partial P}{\partial x}\,\delta x = 0. \tag{A I.02}$$

This equation assumes that the flow is potential and that there exist no components of velocity perpendicular to the x-direction. If these assumptions are not made, the form of Eq. (A I.02) becomes considerably more complicated since the momentum transport in the directions orthogonal to x must also be considered. These assumptions imply that the conduit is of uniform cross section over the length δx. For the present purposes, this

restriction is of no concern because the length δx will be considered to be infinitesimal, in which case the contributions of momentum fluxes perpendicular to x will be negligible.

If the terms of Eq. (A I.02) are divided by δx, then

$$A\frac{\partial M u_x}{\partial x} + \frac{F}{\delta x} + A\frac{\partial P}{\partial x} = 0. \tag{A I.03}$$

Consequently,

$$\frac{\partial M u_x}{\partial x} + \frac{F}{A\,\delta x} + \frac{\partial P}{\partial x} = 0. \tag{A I.04}$$

But

$$\frac{\sigma u_x}{g} = M = \frac{\dot{m}}{g} \tag{A I.05}$$

and

$$\delta V = A\,\delta x. \tag{A I.06}$$

Therefore,

$$\frac{1}{g}\frac{\partial \sigma u_x^2}{\partial x} + \frac{F}{\delta V} + \frac{\partial P}{\partial x} = 0. \tag{A I.07}$$

Under the steady state assumption, the equation of continuity which expresses the principle of "conservation of mass" states

$$u_x\frac{\partial \sigma}{\partial x} = -\sigma\frac{\partial u_x}{\partial x}. \tag{A I.08}$$

So

$$\frac{\partial \sigma u_x^2}{\partial x} = u_x u_x\frac{\partial \sigma}{\partial x} + 2\sigma u_x\frac{\partial u_x}{\partial x} = \sigma u_x\frac{\partial u_x}{\partial x}. \tag{A I.09}$$

Thus

$$\frac{u_x}{g}\frac{\partial u_x}{\partial x} + \frac{F}{\delta m} + V\frac{\partial P}{\partial x} = 0. \tag{A I.10}$$

For a closed system consisting of a weight δm of material under a force F being moved a distance dx in the direction of that force, the work done per 1 lb. of system may be expressed as follows:

$$w' = \frac{F}{\delta m}dx - j'. \tag{A I.11}$$

If the properties of the fluid are uniform in the directions orthogonal to x, then

$$\frac{u_x}{g} du_x + V\,dP + w' + j' = 0, \tag{A I.12}$$

which is a statement of Bernoulli's equation for fluids flowing without change in elevation. If the flow is in the vertical direction, the analog of Eq. (A I.04) would be

$$\frac{\partial M u_y}{\partial y} + \frac{F}{A\,\delta m} + \frac{\partial P}{\partial y} + \sigma \frac{\partial h}{\partial y} = 0. \tag{A I.13}$$

By an argument similar to that used to obtain Eq. (A I.12), Eq. (A I.13) reduces to

$$\frac{u_y}{g} du_y + V\,dP + w' + j' + dh = 0. \tag{A I.14}$$

Both Eqs. (A I.12) and (A I.14) are total differential expressions the terms of which are independent of the direction of flow and may, therefore, be combined to give Eq. (A I.01). The fact that the terms of Eq. (A I.01) have the dimensions of energy is coincidental rather than a consequence of Eq. (A I.01) expressing an energy conservation principle. This fact is at the same time the essence of what makes Eq. (A I.01) of great utility. The integration of Eq. (A I.01) may be performed along a conduit of any shape of cross section since it is a total differential expression and j' depends upon the condition of flow. The quantity j' is a measure of the dissipation of kinetic energy as the fluid passes through the conduit and, so, this dependence upon configuration is not unexpected.

Nomenclature

A	ft.^{2}
F	Shear force at the wall = $[(\tau_{yx})_0\,\delta x]$ times perimeter, lb.
g	Gravitational constant, ft./sec.^{2}
h	Elevation, ft.
j'	Friction, ft.lb./lb. = ft.
M	Momentum per unit volume, lb.sec./ft.^{3}
$\dot{m}$	Weight rate of flow, lb./ft.^{2}sec.
m	Total weight, lb.
δm	$\sigma\,\delta V$
u_x	x-component of velocity, ft./sec.
u_y	y-component of velocity, ft./sec.
V	Specific volume, ft.^{3}/lb.
V	Total volume, ft.^{3}
w'	Work, ft.lb./lb. = ft.
x	Distance in the x-direction, ft.
y	Distance in the y-direction, ft.
σ	Specific weight, lb./ft.^{3}
$(\tau_{yx})_0$	Shear stress at wall, lb./ft.^{2}

All dimensions are expressed in the force-length-time system.

APPENDIX II

An Introduction to Tensors and the Statistical Theory of Turbulence

AII-1. An Introduction to Tensors

Tensor analysis has been developed to a large extent for the purpose of expressing physical "laws" in forms which do not imply a particular coordinate system. A law which expresses a particular relationship among tensors is invariant under a transformation of coordinates. A temperature field is an example of a tensor field of rank zero. Scalar fields are tensor fields of rank zero. A temperature gradient field forms a tensor field of rank one. Vector fields form tensor fields of rank one. A velocity gradient field is a tensor field of rank two. In any of these examples, of course, the physical distribution of the property is independent of the coordinate system used to define the field.

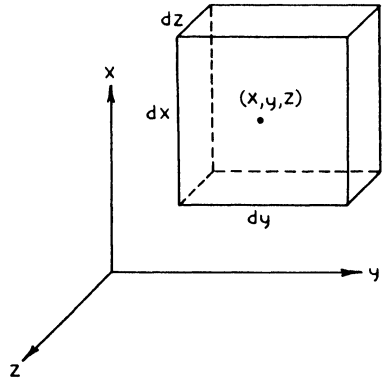

FIG. A II-1. Rectangular Cartesian coordinates.

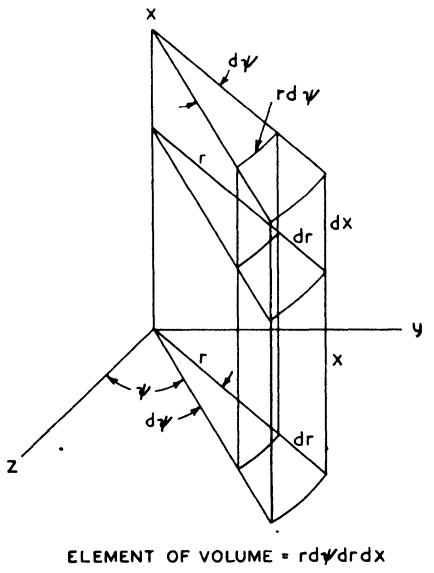

FIG. A II-2. Polar cylindrical coordinates.

Similarly the square of the arc length of a space curve is invariant under a change of coordinates. Let ds be an element of arc length; then

$$(ds)^2 = (dx)^2 + (dy)^2 + (dz)^2. \qquad \text{(A II.01)}$$

By the definition of the partial derivative,

$$\begin{aligned} dx &= \frac{\partial x}{\partial r}\,dr + \frac{\partial x}{\partial \psi}\,d\psi + \frac{\partial x}{\partial x}\,dx, \\ dy &= \frac{\partial y}{\partial r}\,dr + \frac{\partial y}{\partial \psi}\,d\psi + \frac{\partial y}{\partial x}\,dx, \\ dz &= \frac{\partial z}{\partial r}\,dr + \frac{\partial z}{\partial \psi}\,d\psi + \frac{\partial z}{\partial x}\,dx. \end{aligned} \tag{A II.02}$$

Substitution of Eqs. (A II.02) into (A II.01) will give an expression for $(ds)^2$ in polar cylindrical coordinates.

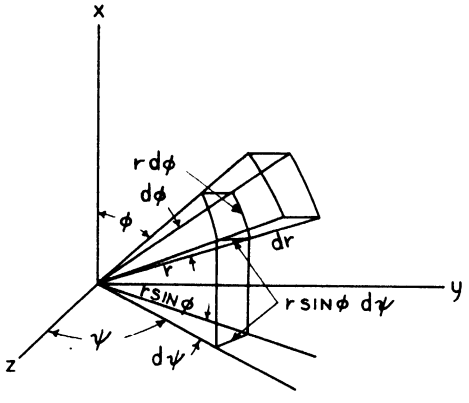

ELEMENT OF VOLUME = $r^2 \sin\phi\ dr\ d\psi\ d\phi$

FIG. A II-3. Polar spherical coordinates.

Obviously

$$\begin{aligned} (dx)^2 = {} & \frac{\partial x}{\partial r}\frac{\partial x}{\partial r}\,dr\,dr + \frac{\partial x}{\partial r}\frac{\partial x}{\partial \psi}\,dr\,d\psi + \frac{\partial x}{\partial r}\frac{\partial x}{\partial x}\,dr\,dx \\ & + \frac{\partial x}{\partial \psi}\frac{\partial x}{\partial r}\,d\psi\,dr + \frac{\partial x}{\partial \psi}\frac{\partial x}{\partial \psi}\,d\psi\,d\psi + \frac{\partial x}{\partial \psi}\frac{\partial x}{\partial x}\,d\psi\,dx \\ & + \frac{\partial x}{\partial x}\frac{\partial x}{\partial r}\,dx\,dr + \frac{\partial x}{\partial x}\frac{\partial x}{\partial \psi}\,dx\,d\psi + \frac{\partial x}{\partial x}\frac{\partial x}{\partial x}\,dx\,dx. \end{aligned} \tag{A II.03}$$

$$\begin{aligned} (dy)^2 = {} & \frac{\partial y}{\partial r}\frac{\partial y}{\partial r}\,dr\,dr + \frac{\partial y}{\partial r}\frac{\partial y}{\partial \psi}\,dr\,d\psi + \frac{\partial y}{\partial r}\frac{\partial y}{\partial x}\,dr\,dx \\ & + \frac{\partial y}{\partial \psi}\frac{\partial y}{\partial r}\,d\psi\,dr + \frac{\partial y}{\partial \psi}\frac{\partial y}{\partial \psi}\,d\psi\,d\psi + \frac{\partial y}{\partial \psi}\frac{\partial y}{\partial x}\,d\psi\,dx \\ & + \frac{\partial y}{\partial x}\frac{\partial y}{\partial r}\,dx\,dr + \frac{\partial y}{\partial x}\frac{\partial y}{\partial \psi}\,dx\,d\psi + \frac{\partial y}{\partial x}\frac{\partial y}{\partial x}\,dx\,dx. \end{aligned} \tag{A II.04}$$

$$(dz)^2 = \frac{\partial z}{\partial r}\frac{\partial z}{\partial r}dr\,dr + \frac{\partial z}{\partial r}\frac{\partial z}{\partial \psi}dr\,d\psi + \frac{\partial z}{\partial r}\frac{\partial z}{\partial x}dr\,dx$$
$$+ \frac{\partial z}{\partial \psi}\frac{\partial z}{\partial r}d\psi\,dr + \frac{\partial z}{\partial \psi}\frac{\partial z}{\partial \psi}d\psi\,d\psi + \frac{\partial z}{\partial \psi}\frac{\partial z}{\partial x}d\psi\,dx \qquad \text{(A II.05)}$$
$$+ \frac{\partial z}{\partial x}\frac{\partial z}{\partial r}dx\,dr + \frac{\partial z}{\partial x}\frac{\partial z}{\partial \psi}dx\,d\psi + \frac{\partial z}{\partial x}\frac{\partial z}{\partial x}dx\,dx.$$

After collection of terms,

$$(ds)^2 = \left(\frac{\partial x}{\partial r}\frac{\partial x}{\partial r} + \frac{\partial y}{\partial r}\frac{\partial y}{\partial r} + \frac{\partial z}{\partial r}\frac{\partial z}{\partial r}\right)dr\,dr$$
$$+ \left(\frac{\partial x}{\partial r}\frac{\partial x}{\partial \psi} + \frac{\partial y}{\partial r}\frac{\partial y}{\partial \psi} + \frac{\partial z}{\partial r}\frac{\partial z}{\partial \psi}\right)dr\,d\psi$$
$$+ \left(\frac{\partial x}{\partial r}\frac{\partial x}{\partial x} + \frac{\partial y}{\partial r}\frac{\partial y}{\partial x} + \frac{\partial z}{\partial r}\frac{\partial z}{\partial x}\right)dr\,dx \qquad \text{(A II.06)}$$
$$+ \left(\frac{\partial x}{\partial \psi}\frac{\partial x}{\partial r} + \frac{\partial y}{\partial \psi}\frac{\partial y}{\partial r} + \frac{\partial z}{\partial \psi}\frac{\partial z}{\partial r}\right)d\psi\,dr$$
$$+ \quad . \quad . \quad . \quad + \quad . \quad . \quad .$$
$$+ \left(\frac{\partial x}{\partial x}\frac{\partial x}{\partial x} + \frac{\partial y}{\partial x}\frac{\partial y}{\partial x} + \frac{\partial z}{\partial x}\frac{\partial z}{\partial x}\right)dx\,dx.$$

Now let[1]

$$\begin{aligned} y^1 &= z, & x^1 &= r, \\ y^2 &= y, & x^2 &= \psi, \\ y^3 &= x, & x^3 &= x \end{aligned} \qquad \text{(A II.07)}$$

and define

$$g_{ij} = \left(\frac{\partial y^1}{\partial x^i}\frac{\partial y^1}{\partial x^j} + \frac{\partial y^2}{\partial x^i}\frac{\partial y^2}{\partial x^j} + \frac{\partial y^3}{\partial x^i}\frac{\partial y^3}{\partial x^j}\right) = g_{ji}. \qquad \text{(A II.08)}$$

Then, in general

$$(ds)^2 = \sum_{i=1}^{3}\sum_{j=1}^{3} g_{ij}\,dx^i\,dx^j. \qquad \text{(A II.09)}$$

---

[1] Superscripts are distinguishing indices. Exponents are $(\,)^n$.

In the case of polar cylindrical coordinates:

$$\begin{aligned} z &= r\cos\psi, & y^1 &= x^1\cos x^2, \\ y &= r\sin\psi, & y^2 &= x^1\sin x^2, \\ x &= x, & y^3 &= x^3, \\ r &= \sqrt{(z)^2+(y)^2}, & x^1 &= \sqrt{(y^1)^2+(y^2)^2}, \\ \psi &= \arcsin\left(y/\sqrt{(z)^2+(y)^2}\right), & x^2 &= \arcsin\left(y^2/\sqrt{(y^1)^2+(y^2)^2}\right), \\ x &= x, & x^3 &= y^3. \end{aligned} \tag{A II.10}$$

From Eqs. (A II.07) and transformations (A II.10), it can be shown that

$$\begin{aligned} g_{11} &= 1, \\ g_{22} &= (x^1)^2 = (r)^2, \\ g_{33} &= 1, \\ \text{all other} \quad g_{ij} &= 0. \end{aligned} \tag{A II.11}$$

Thus, for polar cylindrical coordinates

$$(ds)^2 = (dr)^2 + (r)^2\,(d\psi)^2 + (dx)^2. \tag{A II.12}$$

Notice that the $(r)^2$ in Eq. (A II.12) arose in a very natural way to maintain the dimensional homogeneity of the expression for $(ds)^2$ under a transformation from a dimensionally homogeneous coordinate system to one lacking dimensional homogeneity. The quantities g_{ij} are called the components of the Euclidean metric tensor. As Eq. (A II.08) shows, this tensor is symmetric in its indices, i.e. $g_{ij} = g_{ji}$. The components of the Euclidean metric tensor as defined by Eq. (A II.08) can be evaluated in any coordinate system (this coordinate system and the rectangular Cartesian coordinate system must transform into one another uniquely) provided that $y^k\,(k = 1, 2, 3)$ is interpreted as the rectangular Cartesian coordinate. If, for example,

$$\begin{aligned} x^1 &= z = y^1, \\ x^2 &= y = y^2, \\ x^3 &= x = y^3 \end{aligned} \tag{A II.13}$$

then

$$\begin{aligned} g_{11} &= g_{22} = g_{33} = 1 \\ \text{all other } g_{ij} &= 0. \end{aligned} \tag{A II.14}$$

Or, if

$$\begin{aligned} x^1 &= r, & y^1 &= r\sin\phi\cos\psi, \\ x^2 &= \phi, & y^2 &= r\sin\phi\sin\psi, \\ x^3 &= \psi, & y^3 &= r\cos\phi \end{aligned} \tag{A II.15}$$

then

$$\begin{aligned} g_{11} &= 1, \\ g_{22} &= (r)^2, \\ g_{33} &= (r)^2\sin^2\phi \\ \text{all other } g_{ij} &= 0 \end{aligned} \tag{A II.16}$$

and

$$(ds)^2 = (dr)^2 + (r)^2\,(d\phi)^2 + (r)^2\sin^2\phi\,(d\psi)^2. \tag{A II.17}$$

Notice that the components of the Euclidean metric tensor supply even more than dimensional homogeneity in the case of polar spherical coordinates.

While relations among tensors are invariant under transformations of coordinates, the components of the tensors do change and change in a characteristic way:

rectangular Cartesian	polar cylindrical	polar spherical
transformation		
$z = z,$	$z = r\cos\psi,$	$z = r\sin\phi\cos\psi,$
$y = y,$	$y = r\sin\psi,$	$y = r\sin\phi\sin\psi,$
$x = x,$	$x = x,$	$x = r\cos\phi$
inverse transformation		
$z = z,$	$r = \sqrt{(z)^2 + (y)^2},$	$r = \sqrt{(z)^2 + (y)^2 + (x)^2},$
$y = y,$	$\psi = \arcsin\left(y/\sqrt{(z)^2 + (y)^2}\right),$	$\psi = \arctan(y/z),$
$x = x,$	$x = x,$	$\phi = \arccos\left(x/\sqrt{(x)^2 + (y)^2 + (z)^2}\right)$

(A II.18) (A II.19)

components of Euclidean metric tensor

$$
\begin{array}{lll}
g_{11}=1, & g_{11}=1, & g_{11}=1, \\
g_{22}=1, & g_{22}=(r)^2, & g_{22}=(r)^2, \\
g_{33}=1, & g_{33}=1, & g_{33}=(r)^2\sin^2\phi, \\
\text{all other} & \text{all other} & \text{all other} \\
g_{ij}=0, & g_{ij}=0, & g_{ij}=0.
\end{array}
\qquad \text{(A II.20)}
$$

Now assume that an expression, e.g. Eq. (A II.12), is known for the square of the element of arc length in polar cylindrical coordinates but the expression in polar spherical coordinates is desired. Let $\overline{g_{ij}}$ represent the components of the Euclidean metric tensor in polar spherical coordinates while $g_{\alpha\beta}$ represents the components of this tensor in polar cylindrical coordinates. Then

$$
(ds)^2=\sum_{i=1}^{3}\sum_{j=1}^{3}\overline{g_{ij}}\,d\overline{x}^i\,d\overline{x}^j=\sum_{\alpha=1}^{3}\sum_{\beta=1}^{3}g_{\alpha\beta}\,dx^\alpha\,dx^\beta. \qquad \text{(A II.21)}
$$

To determine the relationship between $\overline{g_{ij}}$ and $g_{\alpha\beta}$, relations between $d\overline{x}^i$ and dx^α must be applied:

$$
\begin{aligned}
dx^\alpha &= \frac{\partial x^\alpha}{\partial \overline{x}^1}d\overline{x}^1+\frac{\partial x^\alpha}{\partial \overline{x}^2}d\overline{x}^2+\frac{\partial x^\alpha}{\partial \overline{x}^3}d\overline{x}^3, \\
dx^\beta &= \frac{\partial x^\beta}{\partial \overline{x}^1}d\overline{x}^1+\frac{\partial x^\beta}{\partial \overline{x}^2}d\overline{x}^2+\frac{\partial x^\beta}{\partial \overline{x}^3}d\overline{x}^3.
\end{aligned}
\qquad \text{(A II.22)}
$$

Substitution of Eqs. (A II.22) into (A II.21) gives

$$
\begin{aligned}
\sum_{i=1}^{3}\sum_{j=1}^{3}\overline{g_{ij}}\,d\overline{x}^i\,d\overline{x}^j &= \overline{g}_{11}\,d\overline{x}^1\,d\overline{x}^1+\overline{g}_{22}\,d\overline{x}^2\,d\overline{x}^2+\overline{g}_{33}\,d\overline{x}^3\,d\overline{x}^3 \\
&\quad +2\,\overline{g}_{12}\,d\overline{x}^1\,d\overline{x}^2+2\,\overline{g}_{13}\,d\overline{x}^1\,d\overline{x}^3+2\,\overline{g}_{23}\,d\overline{x}^2\,d\overline{x}^3 \\
&= \sum_{\alpha=1}^{3}\sum_{\beta=1}^{3}g_{\alpha\beta}\left(\frac{\partial x^\alpha}{\partial \overline{x}^1}\frac{\partial x^\beta}{\partial \overline{x}^1}d\overline{x}^1\,d\overline{x}^1+\frac{\partial x^\alpha}{\partial \overline{x}^1}\frac{\partial x^\beta}{\partial \overline{x}^2}d\overline{x}^1\,d\overline{x}^2\right. \\
&\quad \left.+\frac{\partial x^\alpha}{\partial \overline{x}^1}\frac{\partial x^\beta}{\partial \overline{x}^3}d\overline{x}^1\,d\overline{x}^3+\frac{\partial x^\alpha}{\partial \overline{x}^2}\frac{\partial x^\beta}{\partial \overline{x}^1}d\overline{x}^2\,d\overline{x}^1\right.
\end{aligned}
$$

$$+\frac{\partial x^\alpha}{\partial \bar{x}^2}\frac{\partial x^\beta}{\partial \bar{x}^2}d\bar{x}^2\,d\bar{x}^2+\frac{\partial x^\alpha}{\partial \bar{x}^2}\frac{\partial x^\beta}{\partial \bar{x}^3}d\bar{x}^2\,d\bar{x}^3$$
$$+\frac{\partial x^\alpha}{\partial \bar{x}^3}\frac{\partial x^\beta}{\partial \bar{x}^1}d\bar{x}^3\,d\bar{x}^1+\frac{\partial x^\alpha}{\partial \bar{x}^3}\frac{\partial x^\beta}{\partial \bar{x}^2}d\bar{x}^3\,d\bar{x}^2$$
$$+\frac{\partial x^\alpha}{\partial \bar{x}^3}\frac{\partial x^\beta}{\partial \bar{x}^3}d\bar{x}^3\,d\bar{x}^3\Bigg) \qquad \text{(A II.23)}$$
$$=\sum_{i=1}^{3}\sum_{j=1}^{3}\left(\sum_{\alpha=1}^{3}\sum_{\beta=1}^{3}g_{\alpha\beta}\frac{\partial x^\alpha}{\partial \bar{x}^i}\frac{\partial x^\beta}{\partial \bar{x}^j}\right)d\bar{x}^i\,d\bar{x}^j.$$

Consequently

$$\bar{g}_{ij}=\sum_{\alpha=1}^{3}\sum_{\beta=1}^{3}g_{\alpha\beta}\frac{\partial x^\alpha}{\partial \bar{x}^i}\frac{\partial x^\beta}{\partial \bar{x}^j} \qquad \text{(A II.24)}$$

which illustrates the fundamental distinguishing property of tensors, *viz.*, the transformation law. It shows how the components of the Euclidean metric tensor $\bar{g}_{ij}$ in the coordinates $\bar{x}^1, \bar{x}^2, \bar{x}^3$ are related to the Euclidean metric tensor evaluated in the coordinates x^1, x^2, x^3. The tensor g_{ij} is invariant under a transformation of coordinates but its components form a different set of quantities in each coordinate system just as a point in space does not change position under a transformation of coordinates though the components of position do change, e.g., the point is at (x, y, z) in rectangular Cartesian coordinates but at (r, ψ, ϕ) in polar spherical coordinates.

A quantity is called a scalar field if in each coordinate system there exists a function, called a component, such that the relationship between the component evaluated in coordinates $\bar{x}^1, \bar{x}^2, \bar{x}^3$ and evaluated in x^1, x^2, x^3 is

$$\bar{s}(\bar{x}^1, \bar{x}^2, \bar{x}^3)=s(x^1, x^2, x^3). \qquad \text{(A II.25)}$$

This states that a scalar field is invariant under a transformation of coordinates. Temperature is a familiar example of a scalar field. A scalar field is a tensor field of rank zero.

A quantity is called a covariant vector field if in each coordinate system there exists a set of three functions, called components, such that the relationship between the components in any two coordinate systems is given by

$$\bar{v}_i(\bar{x}^1, \bar{x}^2, \bar{x}^3)=\sum_{\alpha=1}^{3}v_\alpha(x^1, x^2, x^3)\frac{\partial x^\alpha}{\partial \bar{x}^i}. \qquad \text{(A II.26)}$$

With every covariant vector field there is associated a contravariant vector field such that

$$v_i = \sum_{j=1}^{3} g_{ij} v^j. \tag{A II.27}$$

A velocity field is an example of a contravariant vector field. A contravariant vector field transforms as follows:

$$\overline{v}^i(\overline{x}^1, \overline{x}^2, \overline{x}^3) = \sum_{\alpha=1}^{3} v^\alpha(x^1, x^2, x^3) \frac{\partial \overline{x}^i}{\partial x^\alpha}. \tag{A II.28}$$

The convention will be followed that contravariant vector fields (tensor fields of rank one) will bear upper indices and covariant vector fields will bear lower ones.

The transformation law for covariant tensor fields is given by Eq. (A II.24). With the Euclidean metric tensor is associated a contravariant tensor of rank two and a determinant g. This determinant has the elements g_{ij}.

$$g = |g_{ij}| \tag{A II.29}$$

in *rectangular Cartesian coordinates,*

$$g = \begin{vmatrix} 1 & 0 & 0 \\ 0 & 1 & 0 \\ 0 & 0 & 1 \end{vmatrix} = 1 \tag{A II.30}$$

in polar cylindrical coordinates,

$$g = \begin{vmatrix} 1 & 0 & 0 \\ 0 & (r)^2 & 0 \\ 0 & 0 & 1 \end{vmatrix} = (r)^2 \tag{A II.31}$$

and in *polar spherical coordinates,*

$$g = \begin{vmatrix} 1 & 0 & 0 \\ 0 & (r)^2 & 0 \\ 0 & 0 & (r)^2 \sin^2\phi \end{vmatrix} = (r)^4 \sin^2\phi. \tag{A II.32}$$

The cofactor of an element g_{ij} in a determinant[1] is the determinant obtained by striking out row i and column j and multiplying the $(-1)^{i+j}$. Define the contravariant tensor of rank two g^{ij} as

[1] Note: A determinant always has *a* numerical value, a tensor of rank one or greater, *never*. A tensor consists of a set of functions called components which may or may not vary from point to point in space. Of course, the determinant may also be dependent upon position.

$$g^{ij} = \frac{\text{cofactor of } g_{ji} \text{ in } g}{g}. \tag{A II.33}$$

By the familiar theorem for evaluating a determinant by expansion in terms of cofactors, it can be shown (*1*) that

$$\sum_{i=1}^{3}\sum_{j=1}^{3} g^{ij} g_{jk} = \delta^i_k = \begin{cases} 0, & i \neq k \\ 1, & i = k \end{cases}. \tag{A II.34}$$

The term δ^i_k is called the Kronecker delta. Using this contravariant tensor on Eq. (A II.27) gives

$$\begin{aligned} \sum_{i=1}^{3} g^{ki} v_i &= \sum_{i=1}^{3} g^{ki} \sum_{j=1}^{3} g_{ij} v^j \\ &= \sum_{i=1}^{3}\sum_{j=1}^{3} g^{ki} g_{ij} v^j = \sum_{i=1}^{3}\sum_{j=1}^{3} \delta^k_j v^j = v^k \end{aligned} \tag{A II.35}$$

which represents the inverse of Eq. (A II.27).

If in Eq. (A II.35) the convention is adopted that, if a term in an equation contains an index which appears twice, once in the contravariant position and once in the covariant position ("contravariant" indices in the denominator of partial derivatives are considered to be covariant indices), this index is to be summed over its range of values, e.g.,

$$g^{ij} v_i = \sum_{i=1}^{3} g^{ij} v_i = g^{1j} v_1 + g^{2j} v_2 + g^{3j} v_3. \tag{A II.36}$$

In the remainder of this section the *summation convention* just described will be used wherever applicable. This convention is one of the most elegant features of the tensor notation. Most treatises (*1*) start the discussion of tensor analysis with the introduction of this convention, and some discussions (*2*) of fluid mechanics presume it without specific statement. Using the summation (sometimes called Einstein) convention, Eq. (A II.21) becomes

$$(ds)^2 = \bar{g}_{ij}\, d\bar{x}^i\, d\bar{x}^j = g_{\alpha\beta}\, dx^\alpha\, dx^\beta, \tag{A II.37}$$

Eq. (A II.24),

$$\bar{g}_{ij} = g_{\alpha\beta} \frac{\partial x^\alpha}{\partial \bar{x}^i} \frac{\partial x^\beta}{\partial \bar{x}^j}, \tag{A II.38}$$

Eq. (A II.26),

$$\overline{v}_i = v_\alpha \frac{\partial x^\alpha}{\partial \overline{x}^i}, \tag{A II.39}$$

Eq. (A II.27),

$$v_i = g_{ij} v^j, \tag{A II.40}$$

Eq. (A II.28),

$$\overline{v}^i = v^\alpha \frac{\partial \overline{x}^i}{\partial x^\alpha}, \tag{A II.41}$$

and Eq. (A II.35),

$$g^{ki} v_i = g^{ki} g_{ij} v^j = \delta^k_j v^j = v^k. \tag{A II.42}$$

The partial derivative of a tensor field of rank one or greater is not a tensor since it does not transform under a change of coordinates in the manner illustrated by Eqs. (A II.38), (A II.39), and (A II.41). Thus a relationship between partial derivatives (with respect to the coordinates) which is true in one coordinate system is not necessarily true in all coordinate systems.

This situation implies that partial derivatives alone are insufficient to describe the physical facts associated with the potential theory. If ξ^i is a contravariant tensor field of rank one (a velocity field for example), then it can be shown that

$$\xi^i_{,\alpha} = \frac{\partial \xi^i (x^1, x^2, x^3)}{\partial x^\alpha} + \Gamma^i_{\sigma\alpha} (x^1, x^2, x^3)\, \xi^\sigma (x^1, x^2, x^3) \tag{A II.43}$$

is a mixed tensor, i.e. a covariant and contravariant tensor of rank two. The quantity $\xi^i_{,\alpha}$ is called the covariant derivative of the tensor field ξ^i. The quantities $\Gamma^i_{\sigma\alpha}$ (sometimes written $\left\{ {i \atop \sigma\alpha} \right\}$) are the Euclidean-Christoffel symbols. These quantities, like the partial derivatives, are *not* tensors. They are defined

$$\Gamma^i_{\sigma\alpha} = \Gamma^i_{\alpha\sigma} = \frac{1}{2} g^{i\beta} \left(\frac{\partial g_{\beta\alpha}}{\partial x^\sigma} + \frac{\partial g_{\sigma\beta}}{\partial x^\alpha} - \frac{\partial g_{\sigma\alpha}}{\partial x^\beta} \right) \tag{A II.44}$$

in *rectangular Cartesian coordinates*:

$$\begin{aligned} &x^1 = z, && g_{11} = g_{22} = g_{33} = 1, \\ &x^2 = y, && g^{11} = g^{22} = g^{33} = 1, \qquad \text{all } \Gamma^i_{jk} \equiv 0. \\ &x^3 = x, && \text{all other } g_{ij} \text{ and } g^{ij} = 0, \end{aligned} \tag{A II.45}$$

The Euclidean-Christoffel symbols are identically zero in all Cartesian coordinates whether rectangular or oblique (Cartesian coordinates are number sets used to locate points relative to intersecting straight lines). Consequently the partial derivative, with respect to the coordinates, of a tensor field is the covariant derivative when evaluated in Cartesian coordinates.

In *polar cylindrical coordinates*:

$$\begin{array}{llll} x^1 = r, \text{ radius}, & g_{11} = 1, & g^{11} = 1, & \Gamma^1_{22} = -r, \\ x^2 = \psi, \text{ azimuth}, & g_{22} = (r)^2, & g^{22} = (r)^{-2}, & \Gamma^2_{12} = \Gamma^2_{21} = (r)^{-1}, \\ x^3 = x, \text{ altitude}, & g_{33} = 1, & g^{33} = 1, & \text{all other } \Gamma^i_{jk} \equiv 0, \end{array}$$

$$\text{all other } g_{ij} \text{ and } g^{ij} = 0. \qquad \text{(A II.46)}$$

In certain cases the partial and covariant derivatives differ in polar coordinates. It is the covariant derivative which is used in the potential theory.

In *polar spherical coordinates*:

$$\begin{array}{llll} & & & \Gamma^1_{22} = -r, \\ & & & \Gamma^2_{12} = \Gamma^2_{21} = (r)^{-1}, \\ x^1 = r, \text{ radius}, & g_{11} = 1, & g^{11} = 1, & \Gamma^1_{33} = -r\sin^2\phi, \\ x^2 = \phi, \text{ colatitude}, & g_{22} = (r)^2, & g^{22} = (r)^{-2}, & \Gamma^2_{33} = -\sin\phi\cos\phi, \\ x^3 = \psi, \text{ azimuth}, & g_{33} = (r)^2\sin^2\phi, & g^{33} = (r)^{-2}\sin^{-2}\phi, & \Gamma^3_{13} = \Gamma^3_{31} = (r)^{-1}, \\ & \text{all other } g_{ij}, g^{ij} = 0, & & \Gamma^3_{23} = \Gamma^3_{32} = \cot\phi, \\ & & & \text{all other } \Gamma^i_{jk} \equiv 0. \end{array} \qquad \text{(A II.47)}$$

The second covariant derivative is defined as the covariant derivative of $\xi^i_{,\alpha}$ and is written $\xi^i_{,\alpha,\beta}$ for a contravariant vector field or $\xi_{i,\alpha,\beta}$ for a covariant vector field, where

$$\xi_{i,\alpha} = \frac{\partial \xi_i}{\partial x^\alpha} - \Gamma^\sigma_{i\alpha}\xi_\sigma. \qquad \text{(A II.48)}$$

In Euclidean (or flat) space, the second covariant derivative is symmetric in its differentiation indices, i.e.,

$$\xi^i_{,\alpha,\beta} = \xi^i_{,\beta,\alpha}, \qquad \text{(A II.49)}$$

$$\xi_{i,\alpha,\beta} = \xi_{i,\beta,\alpha}. \qquad \text{(A II.50)}$$

This symmetry is a distinguishing property of Euclidean space. For a contravariant vector field such as the velocity field:

grad u	has components	$u^i_{,\alpha}$,
div u	is a scalar field	$u^\alpha_{,\alpha} = \delta^\alpha_i u^i_{,\alpha} = g^{\alpha k} g_{ki} u^i_{,\alpha}$,
curl u	has components	$\frac{1}{\sqrt{g}}(u^k g_{ik})_{,j} - (u^l g_{jl})_{,i} = 2\omega_{ij}$
		$= \frac{1}{\sqrt{g}}\left\{\frac{\partial(g_{ik}u^k)}{\partial x^j} - \frac{\partial(g_{jl}u^l)}{\partial x^i}\right\}$.

Laplacian $\Phi = \operatorname{div}\operatorname{grad}\Phi = g^{ij}\Phi_{,i,j}$ = scalar field (Φ is scalar).
Laplacian $\xi^i = g^{\alpha\beta}\xi^i_{,\alpha,\beta}$.

Expansion of $g^{\alpha\beta}\xi^i_{,\alpha,\beta}$ will show that Laplacian ξ^1 contains terms in ξ^2 and ξ^3. Similarly Laplacian ξ^2 contains terms in ξ^1 and ξ^3, and so on, when evaluated in coordinate systems which are not Cartesian. Equation of continuity,

$$\frac{\partial\rho}{\partial\theta} + (\rho u^i)_{,i} = 0, \tag{A II.51}$$

equation of motion,

$$\tau^{ij}_{,j} = \rho(a^i - \Phi^i). \tag{A II.52}$$

Newtonian stress tensor,

$$\tau^i_j = -\left(P + \frac{2}{3}\eta u^\beta_{,\beta}\right)\delta^i_j + \eta g^{ki}(u_{k,j} + u_{j,k}). \tag{A II.53}$$

Navier-Stokes equation,

$$a^i = \Phi^i - \frac{1}{\rho}g^{i\alpha}\frac{\partial P}{\partial x^\alpha} + \frac{\nu}{3}g^{i\alpha}\frac{\partial}{\partial x^\alpha}(u^\beta_{,\beta}) + \nu g^{\alpha\beta}u^i_{,\alpha,\beta}. \tag{A II.54}$$

AII-2. Newtonian Stress Tensor

The stresses on an element of fluid form a mixed tensor field of rank two. If the fluid is homogeneous and isotropic (*3*), the number of independent viscosity coefficients reduces to two. If the Stokes (*4*) hypothesis is assumed (the mean pressure in a flowing viscous fluid is the same function of stress field as it is in a fluid at rest) for a homogeneous and isotropic fluid, the stress tensor has the components

$$\tau_j^i = -\left(P - \lambda u^{\beta}_{,\beta}\right)\delta_j^i + \eta\, g^{ki}\,(u_{k,j} + u_{j,k}). \qquad \text{(A II.55)}$$

The two viscosity coefficients are λ and η. Under the Stokes hypothesis

$$P = -\frac{1}{3} g_{ij} g^{kj} \tau_k^i = -\frac{1}{3}\delta_i^k \tau_k^i = -\frac{1}{3}(\tau_1^1 + \tau_2^2 + \tau_3^3). \qquad \text{(A II.56)}$$

Thus

$$\begin{aligned} \delta_i^j \tau_j^i + 3P &= 0, \\ &= 3\lambda u^{\beta}_{,\beta} + \eta\, \delta_i^j g^{ki}\,(u_{k,j} + u_{j,k}) \\ &= 3\lambda u^{\beta}_{,\beta} + \eta\,(\delta_i^j u^i_{,j} + g^{ki} u_{i,k}) \\ &= 3\lambda u^{\beta}_{,\beta} + \eta\,(u^j_{,j} + u^k_{,k}) \\ &= (3\lambda + 2\eta)\, u^{\beta}_{,\beta} \end{aligned} \qquad \text{(A II.57)}$$

and therefore

$$\lambda = -\frac{2}{3}\eta.$$

Application of the Stokes hypothesis to Eq. (A II.55) gives the Newtonian stress tensor components,

$$\tau_j^i = -\left(P + \frac{2}{3}\eta\, u^{\beta}_{,\beta}\right)\delta_j^i + \eta\, g^{ki}\,(u_{k,j} + u_{j,k}) \qquad \text{(A II.58)}$$

in *rectangular Cartesian coordinates*:

$$\begin{aligned} &u^1 = u_z, \quad x^1 = z, \quad g_{11} = g_{22} = g_{33} = 1, \\ &u^2 = u_y, \quad x^2 = y, \quad g^{11} = g^{22} = g^{33} = 1, \quad \text{all } \Gamma^i_{jk} \equiv 0. \\ &u^3 = u_x, \quad x^3 = x, \quad \text{all other } g_{ij}, g^{ij} = 0, \end{aligned} \qquad \text{(A II.59)}$$

Thus

$$\begin{aligned} \tau_1^1 &= -P - \frac{2}{3}\eta\left(\frac{\partial u_z}{\partial z} + \frac{\partial u_y}{\partial y} + \frac{\partial u_x}{\partial x}\right) + 2\eta\frac{\partial u_z}{\partial z} = \tau^{11}, \\ \tau_2^1 = \tau_1^2 &= \eta\left(\frac{\partial u_y}{\partial z} + \frac{\partial u_z}{\partial y}\right) = \tau^{12} = \tau^{21}, \\ \tau_3^1 = \tau_1^3 &= \eta\left(\frac{\partial u_x}{\partial z} + \frac{\partial u_z}{\partial x}\right) = \tau^{13} = \tau^{31}, \end{aligned} \qquad \text{(A II.60)}$$

$$\tau_2^2 = -P - \frac{2}{3}\eta\left(\frac{\partial u_z}{\partial z} + \frac{\partial u_y}{\partial y} + \frac{\partial u_x}{\partial x}\right) + 2\eta\frac{\partial u_y}{\partial y} = \tau^{22},$$

$$\tau_3^2 = \tau_2^3 = \eta\left(\frac{\partial u_z}{\partial y} + \frac{\partial u_y}{\partial x}\right) = \tau^{23} = \tau^{32},$$

$$\tau_3^3 = -P - \frac{2}{3}\eta\left(\frac{\partial u_z}{\partial z} + \frac{\partial u_y}{\partial y} + \frac{\partial u_x}{\partial x}\right) + 2\eta\frac{\partial u_x}{\partial x} = \tau^{33},$$

in *polar cylindrical coordinates*:

$$u^1 = u_r, \quad x^1 = r, \quad g_{11} = g_{33} = g^{11} = g^{33} = 1, \quad \Gamma_{22}^1 = -r,$$
$$u^2 = (r)^{-1}u_\psi, \quad x^2 = \psi, \quad g_{22} = (r)^2 \quad g^{22} = (r)^{-2}, \quad \Gamma_{12}^2 = \Gamma_{21}^2 = (r)^{-1},$$
$$u^3 = u_x, \quad x^3 = x, \quad \text{all other } g_{ij}, g^{ij} = 0, \quad \text{all other } \Gamma_{jk}^i \equiv 0. \tag{A II.61}$$

$$u^\beta_{,\beta} = \frac{\partial u^\beta}{\partial x^\beta} + \Gamma^\beta_{\sigma\beta}u^\sigma = \frac{\partial u_r}{\partial r} + \frac{u_r}{r} + \frac{1}{r}\frac{\partial u_\psi}{\partial \psi} + \frac{\partial u_x}{\partial x} \tag{A II.62}$$
$$= \frac{1}{r}\frac{\partial u_r r}{\partial r} + \frac{1}{r}\frac{\partial u_\psi}{\partial \psi} + \frac{\partial u_x}{\partial x},$$

$$\begin{aligned} u_1 &= g_{1i}u^i = g_{11}u^1 = u^1 = u_r, \\ u_2 &= g_{2i}u^i = g_{22}u^2 = u^2(r)^2 = r\,u_\psi, \\ u_3 &= g_{3i}u^i = g_{33}u^3 = u^3 = u_x. \end{aligned} \tag{A II.63}$$

$$u_{i,k} = \frac{\partial u_i}{\partial x^k} - \Gamma^\sigma_{ik}u_\sigma. \tag{A II.64}$$

$$\begin{aligned} u_{1,1} &= \frac{\partial u_1}{\partial x^1} = \frac{\partial u_r}{\partial r}, \\ u_{1,2} &= \frac{\partial u_1}{\partial x^2} - \Gamma_{12}^2 u_2 = \frac{\partial u_r}{\partial \psi} - u_\psi, \\ u_{1,3} &= \frac{\partial u_1}{\partial x^3} = \frac{\partial u_r}{\partial x}, \\ u_{2,1} &= \frac{\partial u_2}{\partial x^1} - \Gamma_{12}^2 u_2 = \frac{\partial u_\psi r}{\partial r} - u_\psi, \\ u_{2,2} &= \frac{\partial u_2}{\partial x^2} - \Gamma_{22}^1 u_1 = \frac{\partial u_\psi r}{\partial \psi} + r\,u_r, \\ u_{2,3} &= \frac{\partial u_2}{\partial x^3} = \frac{\partial u_\psi r}{\partial x}, \end{aligned} \tag{A II.65}$$

$$u_{3,1} = \frac{\partial u_3}{\partial x^1} = \frac{\partial u_x}{\partial r},$$

$$u_{3,2} = \frac{\partial u_3}{\partial x^2} = \frac{\partial u_x}{\partial \psi},$$

$$u_{3,3} = \frac{\partial u_3}{\partial x^3} = \frac{\partial u_x}{\partial x}.$$

$$g^{ki}(u_{k,j} + u_{j,k}) = g^{1i}(u_{1,j} + u_{j,1}) + g^{2i}(u_{2,j} + u_{j,2}) + g^{3i}(u_{3,j} + u_{j,3}). \quad \text{(A II.66)}$$

$$g^{11}(u_{1,1} + u_{1,1}) = 2\frac{\partial u_r}{\partial r}$$

$$g^{11}(u_{1,2} + u_{2,1}) = \frac{\partial u_r}{\partial \psi} - 2u_\psi + \frac{\partial u_\psi r}{\partial r} = r\left[r\frac{\partial}{\partial r}\left(\frac{u_\psi}{r}\right) + \frac{1}{r}\frac{\partial u_r}{\partial \psi}\right],$$

$$g^{11}(u_{1,3} + u_{3,1}) = \frac{\partial u_r}{\partial x} + \frac{\partial u_x}{\partial r},$$

$$g^{22}(u_{2,1} + u_{1,2}) = \frac{1}{r}\left[r\frac{\partial}{\partial r}\left(\frac{u_\psi}{r}\right) + \frac{1}{r}\frac{\partial u_r}{\partial \psi}\right],$$

$$g^{22}(u_{2,2} + u_{2,2}) = \frac{2}{(r)^2}\left(\frac{\partial u_\psi r}{\partial \psi} + r\,u_r\right) = 2\left(\frac{1}{r}\frac{\partial u_\psi}{\partial \psi} + \frac{u_r}{r}\right), \quad \text{(A II.67)}$$

$$g^{22}(u_{2,3} + u_{3,2}) = \frac{1}{(r)^2}\left(\frac{\partial u_\psi r}{\partial x} + \frac{\partial u_x}{\partial \psi}\right) = \frac{1}{r}\left(\frac{1}{r}\frac{\partial u_x}{\partial \psi} + \frac{\partial u_\psi}{\partial x}\right),$$

$$g^{33}(u_{3,1} + u_{1,3}) = \frac{\partial u_r}{\partial x} + \frac{\partial u_x}{\partial r},$$

$$g^{33}(u_{3,2} + u_{2,3}) = r\left(\frac{1}{r}\frac{\partial u_x}{\partial \psi} + \frac{\partial u_\psi}{\partial x}\right),$$

$$g^{33}(u_{3,3} + u_{3,3}) = 2\frac{\partial u_x}{\partial x}.$$

$$\tau_1^1 = -P - \frac{2}{3}\eta\left(\frac{1}{r}\frac{\partial u_r r}{\partial r} + \frac{1}{r}\frac{\partial u_\psi}{\partial \psi} + \frac{\partial u_x}{\partial x}\right) + 2\eta\frac{\partial u_r}{\partial r}$$

$$\tau_2^1 = \eta r\left[r\frac{\partial}{\partial r}\left(\frac{u_\psi}{r}\right) + \frac{1}{r}\frac{\partial u_r}{\partial \psi}\right],$$

$$\tau_3^1 = \eta\left(\frac{\partial u_r}{\partial x} + \frac{\partial u_x}{\partial r}\right),$$

$$\tau_1^2 = \eta\frac{1}{r}\left[r\frac{\partial}{\partial r}\left(\frac{u_\psi}{r}\right) + \frac{1}{r}\frac{\partial u_r}{\partial \psi}\right],$$

$$\tau_2^2 = -P - \frac{2}{3}\eta\left(\frac{1}{r}\frac{\partial u_r r}{\partial r} + \frac{1}{r}\frac{\partial u_\psi}{\partial \psi} + \frac{\partial u_x}{\partial x}\right) + 2\eta\left(\frac{1}{r}\frac{\partial u_\psi}{\partial \psi} + \frac{u_r}{r}\right) \qquad \text{(A II.68)}$$

$$\tau_3^2 = \eta\frac{1}{r}\left(\frac{1}{r}\frac{\partial u_x}{\partial \psi} + \frac{\partial u_\psi}{\partial x}\right),$$

$$\tau_1^3 = \eta\left(\frac{\partial u_r}{\partial x} + \frac{\partial u_x}{\partial r}\right),$$

$$\tau_2^3 = \eta\, r\left(\frac{1}{r}\frac{\partial u_x}{\partial \psi} + \frac{\partial u_\psi}{\partial x}\right),$$

$$\tau_3^3 = -P - \frac{2}{3}\eta\left(\frac{1}{r}\frac{\partial u_r r}{\partial r} + \frac{1}{r}\frac{\partial u_\psi}{\partial \psi} + \frac{\partial u_x}{\partial x}\right) + 2\eta\frac{\partial u_x}{\partial x}.$$

Note that the mixed tensor, the components of which are τ_j^i, is neither symmetric nor dimensionally homogeneous when its components are evaluated in polar cylindrical coordinates. However, the contravariant tensor with components τ^{ij} is symmetric in these coordinates:

$$\tau^{11} = g^{11}\tau_1^1 = -P - \frac{2}{3}\eta\, u^\beta_{,\beta} + 2\eta\frac{\partial u_r}{\partial r} = -P - \frac{2}{3}\eta\, u^\beta_{,\beta} + \eta\, e_{rr},$$

$$\tau^{12} = g^{22}\tau_2^1 = \frac{\eta}{r}\left[r\frac{\partial}{\partial r}\left(\frac{u_\psi}{r}\right) + \frac{1}{r}\frac{\partial u_r}{\partial \psi}\right] = \frac{\eta}{r}\, e_{r\psi},$$

$$\tau^{13} = g^{33}\tau_3^1 = \eta\left(\frac{\partial u_r}{\partial x} + \frac{\partial u_x}{\partial r}\right) = \eta\, e_{rx},$$

$$\tau^{21} = g^{11}\tau_1^2 = \frac{\eta}{r}\left[r\frac{\partial}{\partial r}\left(\frac{u_\psi}{r}\right) + \frac{1}{r}\frac{\partial u_r}{\partial \psi}\right) = \frac{\eta}{r}\, e_{r\psi},$$

$$\tau^{22} = g^{22}\tau_2^2 = -\frac{P}{(r)^2} - \frac{2}{3}\frac{\eta}{(r)^2}\, u^\beta_{,\beta} + 2\frac{\eta}{(r)^2}\left(\frac{1}{r}\frac{\partial u_\psi}{\partial \psi} + \frac{u_r}{r}\right) \qquad \text{(A II.69)}$$

$$= \frac{1}{(r)^2}\left\{-P - \frac{2}{3}\eta\, u^\beta_{,\beta} + \eta\, e_{\psi\psi}\right\},$$

$$\tau^{23} = g^{33}\tau_3^2 = \frac{\eta}{r}\left(\frac{1}{r}\frac{\partial u_x}{\partial \psi} + \frac{\partial u_\psi}{\partial x}\right) = \frac{\eta}{r}\, e_{\psi x},$$

$$\tau^{31} = g^{11}\tau_1^3 = \eta\left(\frac{\partial u_r}{\partial x} + \frac{\partial u_x}{\partial r}\right) = \eta\, e_{rx},$$

$$\tau^{32} = g^{22}\tau_2^3 = \frac{\eta}{r}\left(\frac{1}{r}\frac{\partial u_x}{\partial \psi} + \frac{\partial u_\psi}{\partial x}\right) = \frac{\eta}{r}\, e_{\psi x},$$

$$\tau^{33} = g^{33}\tau_3^3 = -P - \frac{2}{3}\eta\, u^\beta_{,\beta} + 2\eta\frac{\partial u_x}{\partial x} = -P - \frac{2}{3}\eta\, u^\beta_{,\beta} + \eta\, e_{xx}.$$

The contravariant tensor of rank two denoted by e_{ij} is dimensionally homogeneous. It is unfortunate that the subscripts are used on this contravariant tensor, but superscripts would be even more confusing. The notation conforms with that of Goldstein (*5*) (p. 104).

The following covariant derivatives will be required later:

$$\tau^{1j}_{,j} = \frac{\partial \tau^{11}}{\partial x^1} + \frac{\partial \tau^{12}}{\partial x^2} + \Gamma^1_{22}\tau^{22} + \Gamma^2_{12}\tau^{11} + \frac{\partial \tau^{13}}{\partial x^3},$$

$$\tau^{1j}_{,j} = -\frac{\partial P}{\partial r} - \frac{2}{3}\eta\frac{\partial}{\partial r}u^{\beta}_{,\beta} + \eta\frac{\partial e_{rr}}{\partial r} + \frac{\eta}{r}\frac{\partial e_{r\psi}}{\partial \psi} - \frac{\eta}{r}e_{\psi\psi} + \frac{\eta}{r}e_{rr} + \eta\frac{\partial e_{rx}}{\partial x},$$

$$\tau^{1j}_{,j} = -\frac{\partial P}{\partial r} - \frac{2}{3}\eta\frac{\partial}{\partial r}u^{\beta}_{,\beta} + \frac{\eta}{r}\frac{\partial r\, e_{rr}}{\partial r} + \frac{\eta}{r}\frac{\partial e_{r\psi}}{\partial \psi} + \frac{\eta}{r}\frac{\partial r\, e_{rx}}{\partial x} - \frac{\eta}{r}e_{\psi\psi},$$

$$\tau^{2j}_{,j} = \frac{\partial \tau^{21}}{\partial x^1} + \Gamma^2_{21}\tau^{21} + \frac{\partial \tau^{22}}{\partial x^2} + 2\Gamma^2_{12}\tau^{12} + \frac{\partial \tau^{23}}{\partial x^3},$$

$$\tau^{2j}_{,j} = \eta\frac{\partial}{\partial r}\left(\frac{e_{r\psi}}{r}\right) + \eta\frac{e_{r\psi}}{(r)^2} + \frac{1}{(r)^2}\frac{\partial e_{\psi\psi}}{\partial \psi} - \frac{1}{(r)^2}\frac{\partial P}{\partial \psi} \qquad \text{(A II.70)}$$

$$- \frac{2}{3}\frac{\eta}{(r)^2}\frac{\partial}{\partial \psi}u^{\beta}_{,\beta} + \frac{2}{(r)^2}e_{r\psi} + \frac{\eta}{r}\frac{\partial e_{\psi x}}{\partial x},$$

$$\tau^{2j}_{,j} = \frac{1}{r}\left\{-\frac{1}{r}\frac{\partial P}{\partial \psi} - \frac{2}{3}\frac{\eta}{r}\frac{\partial}{\partial \psi}u^{\beta}_{,\beta} + \frac{\eta}{r}\frac{\partial r\, e_{r\psi}}{\partial r} + \frac{\eta}{r}\frac{\partial e_{\psi\psi}}{\partial \psi} + \frac{\eta}{r}\frac{\partial r\, e_{\psi x}}{\partial x} + \frac{\eta}{r}e_{r\psi}\right\},$$

$$\tau^{3j}_{,j} = \frac{\partial \tau^{31}}{\partial x^1} + \frac{\partial \tau^{32}}{\partial x^2} + \Gamma^2_{12}\tau^{13} + \frac{\partial \tau^{33}}{\partial x^3},$$

$$\tau^{3j}_{,j} = \eta\frac{\partial e_{rx}}{\partial r} + \frac{\eta}{r}\frac{\partial}{\partial \psi}e_{\psi x} + \frac{\eta}{r}e_{rx} + \eta\frac{\partial}{\partial x}e_{xx} - \frac{\partial P}{\partial x} - \frac{2}{3}\eta\frac{\partial}{\partial x}u^{\beta}_{,\beta},$$

$$\tau^{3j}_{,j} = -\frac{\partial P}{\partial x} - \frac{2}{3}\eta\frac{\partial}{\partial x}u^{\beta}_{,\beta} + \frac{\eta}{r}\frac{\partial r\, e_{rx}}{\partial r} + \frac{\eta}{r}\frac{\partial e_{\psi x}}{\partial \psi} + \frac{\eta}{r}\frac{\partial r\, e_{xx}}{\partial x}.$$

Therefore:

$$\tau^{1j}_{,j} = -\frac{\partial P}{\partial r} - \frac{2}{3}\eta\frac{\partial}{\partial r}u^{\beta}_{,\beta} + \frac{\eta}{r}\left\{\frac{\partial r\, e_{rr}}{\partial r} + \frac{\partial e_{r\psi}}{\partial \psi} + \frac{\partial r\, e_{rx}}{\partial x} - e_{\psi\psi}\right\},$$

$$r\,\tau^{2j}_{,j} = -\frac{1}{r}\frac{\partial P}{\partial \psi} - \frac{2}{3}\frac{\eta}{r}\frac{\partial}{\partial \psi}u^{\beta}_{,\beta} + \frac{\eta}{r}\left\{\frac{\partial r\, e_{r\psi}}{\partial r} + \frac{\partial e_{\psi\psi}}{\partial \psi} + \frac{\partial r\, e_{\psi x}}{\partial x} + e_{r\psi}\right\},$$

$$\tau^{3j}_{,j} = -\frac{\partial P}{\partial x} - \frac{2}{3}\eta\frac{\partial}{\partial x}u^{\beta}_{,\beta} + \frac{\eta}{r}\left\{\frac{\partial r\, e_{rx}}{\partial r} + \frac{\partial e_{\psi x}}{\partial \psi} + \frac{\partial r\, e_{xx}}{\partial x}\right\}. \qquad \text{(A II.71)}$$

So:

$$\tau^{1j}_{,j} = -\frac{\partial P}{\partial r} - \frac{2}{3}\eta\frac{\partial}{\partial r}u^{\beta}_{,\beta} + \frac{\eta}{r}\left\{2\frac{\partial}{\partial r}\left(r\frac{\partial u_r}{\partial r}\right) + \frac{\partial}{\partial \psi}\left[r\frac{\partial}{\partial r}\left(\frac{u_\psi}{r}\right) + \frac{1}{r}\frac{\partial u_r}{\partial \psi}\right] + r\frac{\partial}{\partial x}\left(\frac{\partial u_r}{\partial x} + \frac{\partial u_x}{\partial r}\right) - \frac{2}{r}\frac{\partial u_\psi}{\partial \psi} - 2\frac{u_r}{r}\right\}$$

$$= -\frac{\partial P}{\partial r} - \frac{2}{3}\eta\frac{\partial}{\partial r}u^{\beta}_{,\beta} + \frac{\eta}{r}\left\{2r\frac{\partial^2 u_r}{\partial r^2} + 2\frac{\partial u_r}{\partial r} + r\frac{\partial}{\partial r}\left(\frac{1}{r}\frac{\partial u_\psi}{\partial \psi}\right) + \frac{1}{r}\frac{\partial^2 u_r}{\partial \psi^2} + r\frac{\partial^2 u_r}{\partial x^2} + r\frac{\partial}{\partial r}\frac{\partial u_x}{\partial x} - \frac{2}{r}\frac{\partial u_\psi}{\partial \psi} - 2\frac{u_r}{r}\right\} \quad \text{(A II.72)}$$

$$= -\frac{\partial P}{\partial r} + \frac{\eta}{3}\frac{\partial u^{\beta}_{,\beta}}{\partial r} + \eta\left\{\frac{\partial^2 u_r}{\partial r^2} + \frac{1}{r}\frac{\partial u_r}{\partial r} + \frac{1}{(r)^2}\frac{\partial^2 u_r}{\partial \psi^2} + \frac{\partial^2 u_r}{\partial x^2} - \frac{u_r}{(r)^2} - \frac{2}{(r)^2}\frac{\partial u_\psi}{\partial \psi}\right\}.$$

$$r\tau^{2j}_{,j} = -\frac{1}{r}\frac{\partial P}{\partial \psi} - \frac{2}{3}\frac{\eta}{r}\frac{\partial}{\partial \psi}u^{\beta}_{,\beta} + \frac{\eta}{r}\left\{\frac{\partial}{\partial r}\left[(r)^2\frac{\partial}{\partial r}\left(\frac{u_\psi}{r}\right) + \frac{\partial u_r}{\partial \psi}\right] + 2\frac{\partial}{\partial \psi}\left(\frac{1}{r}\frac{\partial u_\psi}{\partial \psi} + \frac{u_r}{r}\right) + \frac{\partial}{\partial x}\left(\frac{\partial u_x}{\partial \psi} + r\frac{\partial u_\psi}{\partial x}\right) + r\frac{\partial}{\partial r}\left(\frac{u_\psi}{r}\right) + \frac{1}{r}\frac{\partial u_r}{\partial \psi}\right\}$$

$$= -\frac{1}{r}\frac{\partial P}{\partial \psi} + \frac{\eta}{3}\frac{1}{r}\frac{\partial u^{\beta}_{,\beta}}{\partial \psi} + \eta\left\{\frac{\partial^2 u_\psi}{\partial r^2} + \frac{1}{r}\frac{\partial u_\psi}{\partial r} + \frac{1}{(r)^2}\frac{\partial^2 u_\psi}{\partial \psi^2} + \frac{\partial^2 u_\psi}{\partial x^2} - \frac{u_\psi}{(r)^2} + \frac{2}{(r)^2}\frac{\partial u_r}{\partial \psi}\right\}. \quad \text{(A II.73)}$$

$$\tau^{3j}_{,j} = \eta\left\{\frac{\partial^2 u_r}{\partial r\,\partial x} + \frac{\partial^2 u_x}{\partial r^2} + \frac{1}{r}\frac{\partial u_r}{\partial x} + \frac{1}{r}\frac{\partial u_x}{\partial r} + \frac{1}{(r)^2}\frac{\partial^2 u_x}{\partial \psi^2} + \frac{1}{r}\frac{\partial u_\psi}{\partial \psi\,\partial x} + 2\frac{\partial^2 u_x}{\partial x^2}\right\} - \frac{\partial P}{\partial x} - \frac{2}{3}\eta\frac{\partial}{\partial x}u^{\beta}_{,\beta}$$

$$= -\frac{\partial P}{\partial x} + \frac{\eta}{3}\frac{\partial u^{\beta}_{,\beta}}{\partial x} + \eta\left\{\frac{\partial^2 u_x}{\partial r^2} + \frac{1}{r}\frac{\partial u_x}{\partial r} + \frac{1}{(r)^2}\frac{\partial^2 u_x}{\partial \psi^2} + \frac{\partial^2 u_x}{\partial x^2}\right\}. \quad \text{(A II.74)}$$

In *polar spherical coordinates:*

$$u^1 = u_r, \quad x^1 = r, \quad g_{11} = 1, \quad g^{11} = 1,$$
$$u^2 = u_\phi(r)^{-1}, \quad x^2 = \phi, \quad g_{22} = (r)^2, \quad g^{22} = (r)^{-2},$$
$$u^3 = u_\psi/r\sin\phi, \quad x^3 = \psi, \quad g_{33} = (r)^2\sin^2\phi, \quad g^{33} = (r)^{-2}\sin^{-2}\phi$$
$$\text{all other } g_{ij}, g^{ij} = 0. \quad \text{(A II.75)}$$

$$\Gamma^1_{22} = -r, \qquad \Gamma^1_{33} = -r\sin^2\phi,$$

$$\Gamma^2_{12} = \Gamma^2_{21} = (r)^{-1}, \qquad \Gamma^3_{13} = \Gamma^3_{31} = (r)^{-1}, \qquad \text{all other } \Gamma^i_{jk} \equiv 0.$$

$$\Gamma^2_{33} = -\sin\phi\cos\phi, \qquad \Gamma^3_{23} = \Gamma^3_{32} = \cot\phi.$$

$$u^\beta_{,\beta} = \frac{\partial u^\beta}{\partial x^\beta} + \Gamma^\beta_{\sigma\beta} u^\sigma = \frac{\partial u_r}{\partial r} + \frac{u_r}{r} + \frac{1}{r}\frac{\partial u_\phi}{\partial \phi} + \frac{1}{r\sin\phi}\frac{\partial u_\psi}{\partial \psi} + \frac{u_r}{r} + \frac{u_\phi}{r}\cot\phi$$

$$= \frac{1}{(r)^2}\frac{\partial}{\partial r}\left((r)^2 u_r\right) + \frac{1}{r\sin\phi}\frac{\partial}{\partial \phi}(u_\phi \sin\phi) + \frac{1}{r\sin\phi}\frac{\partial u_\psi}{\partial \psi}. \tag{A II.76}$$

$$\begin{aligned} u_1 &= g_{1i} u^i = g_{11} u^1 = u^1 &&= u_r, \\ u_2 &= g_{2i} u^i = g_{22} u^2 = (r)^2 u^2 &&= r u_\phi, \\ u_3 &= g_{3i} u^i = g_{33} u^3 = (r)^2 \sin^2\phi\, u_3 &&= r u_\psi \sin\phi. \end{aligned} \tag{A II.77}$$

$$u_{i,k} = \frac{\partial u_i}{\partial x^k} - \Gamma^\sigma_{ik} u_\sigma. \tag{A II.78}$$

$$\begin{aligned} u_{1,1} &= \frac{\partial u_1}{\partial x^1} &&= \frac{\partial u_r}{\partial r}, \\ u_{1,2} &= \frac{\partial u_1}{\partial x^2} - \Gamma^2_{12} u_2 &&= \frac{\partial u_r}{\partial \phi} - u_\phi, \\ u_{1,3} &= \frac{\partial u_1}{\partial x^3} - \Gamma^3_{13} u_3 &&= \frac{\partial u_r}{\partial \psi} - u_\psi \sin\phi, \\ u_{2,1} &= \frac{\partial u_2}{\partial x^1} - \Gamma^2_{21} u_2 &&= \frac{\partial r u_\phi}{\partial r} - u_\phi, \\ u_{2,2} &= \frac{\partial u_2}{\partial x^2} - \Gamma^1_{22} u_1 &&= \frac{\partial r u_\phi}{\partial \phi} + r u_r, \\ u_{2,3} &= \frac{\partial u_2}{\partial x^3} - \Gamma^3_{23} u_3 &&= \frac{\partial r u_\phi}{\partial \phi} - r u_\psi \cos\phi, \\ u_{3,1} &= \frac{\partial u_3}{\partial x^1} - \Gamma^3_{31} u_3 &&= \frac{\partial r u_\psi \sin\phi}{\partial r} - u_\psi \sin\phi, \\ u_{3,2} &= \frac{\partial u_3}{\partial x^2} - \Gamma^3_{23} u_3 &&= \frac{\partial r u_\psi \sin\phi}{\partial \phi} - r u_\psi \cos\phi, \\ u_{3,3} &= \frac{\partial u_3}{\partial x^3} - \Gamma^1_{33} u_1 - \Gamma^2_{33} u_2 &&= \frac{\partial r u_\psi \sin\phi}{\partial \psi} + r\sin\phi(u_r \sin\phi + u_\phi \cos\phi). \end{aligned} \tag{A II.79}$$

$$g^{11}(u_{1,1}+u_{1,1}) = 2\frac{\partial u_r}{\partial r},$$

$$g^{11}(u_{1,2}+u_{2,1}) = \frac{\partial u_r}{\partial \phi} - 2u_\phi + \frac{\partial r\, u_\phi}{\partial r} = r\left[\frac{1}{r}\frac{\partial u_r}{\partial \phi} + r\frac{\partial}{\partial r}\left(\frac{u_\phi}{r}\right)\right],$$

$$g^{11}(u_{1,3}+u_{3,1}) = \frac{\partial u_r}{\partial \psi} - 2u_\psi \sin\phi + \frac{\partial r\, u_\psi}{\partial r}\sin\phi$$
$$= r\sin\phi\left[\frac{1}{r\sin\phi}\frac{\partial u_r}{\partial \psi} + r\frac{\partial}{\partial r}\left(\frac{u_\psi}{r}\right)\right],$$

$$g^{22}(u_{2,1}+u_{1,2}) = \frac{1}{(r)^2}\left(\frac{\partial r\, u_\phi}{\partial r} - 2u_\phi + \frac{\partial u_r}{\partial \phi}\right) = \frac{1}{r}\left[\frac{1}{r}\frac{\partial u_r}{\partial \phi} + r\frac{\partial}{\partial r}\left(\frac{u_\phi}{r}\right)\right],$$

$$g^{22}(u_{2,2}+u_{2,2}) = \frac{2}{(r)^2}\left(\frac{\partial r\, u_\phi}{\partial \phi} + r\,u_r\right) = \frac{2}{r}\left(\frac{\partial u_\phi}{\partial \phi} + u_r\right),$$

$$g^{22}(u_{2,3}+u_{3,2}) = \frac{1}{(r)^2}\left(\frac{\partial r\, u_\phi}{\partial \psi} - 2r\,u_\psi\cos\phi + \frac{\partial r\, u_\psi \sin\phi}{\partial \phi}\right) \qquad \text{(A II.80)}$$
$$= \frac{\sin\phi}{r}\left[\frac{1}{\sin\phi}\frac{\partial u_\phi}{\partial \psi} + \sin\phi\,\frac{\partial}{\partial \phi}\left(\frac{u_\psi}{\sin\phi}\right)\right]$$

$$g^{33}(u_{3,1}+u_{1,3}) = \frac{1}{(r)^2\sin^2\phi}\left(\frac{\partial u_r}{\partial \psi} - 2u_\psi\sin\phi + \frac{\partial r\, u_\psi \sin\phi}{\partial r}\right)$$
$$= \frac{1}{r\sin\phi}\left[\frac{1}{r\sin\phi}\frac{\partial u_r}{\partial \psi} + r\frac{\partial}{\partial r}\left(\frac{u_\psi}{r}\right)\right],$$

$$g^{33}(u_{3,2}+u_{2,3}) = \frac{1}{(r)^2\sin^2\phi}\left(\frac{\partial r\, u_\psi \sin\phi}{\partial \psi} - 2r\,u_\psi\cos\phi + \frac{\partial r\, u_\phi}{\partial \psi}\right)$$
$$= \frac{1}{r\sin\phi}\left[\frac{1}{\sin\phi}\frac{\partial u_\phi}{\partial \psi} + \sin\phi\,\frac{\partial}{\partial \phi}\left(\frac{u_\psi}{\sin\phi}\right)\right],$$

$$g^{33}(u_{3,3}+u_{3,3}) = \frac{2}{(r)^2\sin^2\phi}\left(\frac{\partial r\, u_\psi \sin\phi}{\partial \psi} + r\sin\phi(u_r\sin\phi + u_\phi\cos\phi)\right)$$
$$= 2\left(\frac{1}{r\sin\phi}\frac{\partial u_\psi}{\partial \psi} + \frac{u_r}{r} + \frac{u_\psi}{r}\cot\phi\right).$$

$$\tau_1^1 = -P - \frac{2}{3}\eta\, u^{\beta}_{,\beta} + 2\eta\frac{\partial u_r}{\partial r},$$

$$\tau_2^1 = \eta r\left[\frac{1}{r}\frac{\partial u_r}{\partial \phi} + r\frac{\partial}{\partial r}\left(\frac{u_\phi}{r}\right)\right],$$

$$\tau_3^1 = \eta r\sin\phi\left[\frac{1}{r\sin\phi}\frac{\partial u_r}{\partial \psi} + r\frac{\partial}{\partial r}\left(\frac{u_\psi}{r}\right)\right],$$

$$\tau_1^2 = \frac{\eta}{r}\left[\frac{1}{r}\frac{\partial u_r}{\partial \phi} + r\frac{\partial}{\partial r}\left(\frac{u_\phi}{r}\right)\right],$$

$$\tau_2^2 = -P - \frac{2}{3}\eta\, u^{\beta}_{,\beta} + 2\frac{\eta}{r}\left(\frac{\partial u_\phi}{\partial \phi} + u_r\right), \qquad \text{(A II.81)}$$

$$\tau_3^2 = \eta\frac{\sin\phi}{r}\left[\frac{1}{\sin\phi}\frac{\partial u_\phi}{\partial \psi} + \sin\phi\frac{\partial}{\partial \phi}\left(\frac{u_\psi}{\sin\phi}\right)\right],$$

$$\tau_1^3 = \frac{\eta}{r\sin\phi}\left[\frac{1}{r\sin\phi}\frac{\partial u_r}{\partial \psi} + r\frac{\partial}{\partial r}\left(\frac{u_\psi}{r}\right)\right],$$

$$\tau_2^3 = \frac{\eta}{\sin\phi}\left[\frac{1}{r\sin\phi}\frac{\partial u_\phi}{\partial \psi} + \frac{\sin\phi}{r}\frac{\partial}{\partial \phi}\left(\frac{u_\psi}{\sin\phi}\right)\right],$$

$$\tau_3^3 = -P - \frac{2}{3}\eta\, u^{\beta}_{,\beta} + 2\eta\left(\frac{1}{r\sin\phi}\frac{\partial u_\psi}{\partial \psi} + \frac{u_r}{r} + \frac{u_\phi}{r}\cot\phi\right).$$

$$\tau^{11} = g^{11}\tau_1^1 = -P - \frac{2}{3}\eta\, u^{\beta}_{,\beta} + 2\eta\frac{\partial u_r}{\partial r} = -P - \frac{2}{3}\eta\, u^{\beta}_{,\beta} + \eta\, e_{rr},$$

$$\tau^{12} = g^{22}\tau_2^1 = \frac{\eta}{r}\left[\frac{1}{r}\frac{\partial u_r}{\partial \phi} + r\frac{\partial}{\partial r}\left(\frac{u_\phi}{r}\right)\right] = \frac{\eta}{r}\, e_{r\phi},$$

$$\tau^{13} = g^{33}\tau_3^1 = \frac{\eta}{r\sin\phi}\left[\frac{1}{r\sin\phi}\frac{\partial u_r}{\partial \psi} + r\frac{\partial}{\partial r}\left(\frac{u_\psi}{r}\right)\right] = \frac{\eta}{r\sin\phi}\, e_{r\psi}, \qquad \text{(A II.82)}$$

$$\tau^{21} = g^{11}\tau_1^2 = \frac{\eta}{r}\left[\frac{1}{r}\frac{\partial u_r}{\partial \phi} + r\frac{\partial}{\partial r}\left(\frac{u_\phi}{r}\right)\right] = \frac{\eta}{r}\, e_{r\phi},$$

$$\tau^{22} = g^{22}\tau_2^2 = -\frac{P}{(r)^2} - \frac{2}{3}\frac{\eta}{(r)^2}\, u^{\beta}_{,\beta} + 2\frac{\eta}{(r)^2}\left(\frac{1}{r}\frac{\partial u_\phi}{\partial \phi} + \frac{u_r}{r}\right)$$

$$= -\frac{P}{(r)^2} - \frac{\frac{2}{3}\eta\, u^{\beta}_{,\beta}}{(r)^2} + \frac{\eta}{(r)^2}\, e_{\phi\phi},$$

$$\tau^{23} = g^{33}\tau_3^2 = \frac{\eta}{(r)^2\sin\phi}\left[\frac{1}{r\sin\phi}\frac{\partial u_\phi}{\partial \psi} + \frac{\sin\phi}{r}\frac{\partial}{\partial \phi}\left(\frac{u_\psi}{\sin\phi}\right)\right] = \frac{\eta}{(r)^2\sin\phi}\, e_{\phi\psi},$$

$$\tau^{31} = g^{11}\tau_1^3 = \frac{\eta}{r\sin\phi}\left[\frac{1}{r\sin\phi}\frac{\partial u_r}{\partial \psi} + r\frac{\partial}{\partial r}\left(\frac{u_\psi}{r}\right)\right] = \frac{\eta}{r\sin\phi}\, e_{r\psi},$$

$$\tau^{32} = g^{22}\tau_2^3 = \frac{\eta}{(r)^2\sin\phi}\left[\frac{1}{r\sin\phi}\frac{\partial u_\phi}{\partial \psi} + \frac{\sin\phi}{r}\frac{\partial}{\partial \phi}\left(\frac{u_\psi}{\sin\phi}\right)\right] = \frac{\eta}{(r)^2\sin\phi}\, e_{\phi\psi}.$$

$$\tau^{33} = g^{33}\tau^3_3 = -\frac{P}{(r)^2\sin^2\phi} - \frac{\frac{2}{3}\eta u^{\beta}_{,\beta}}{(r)^2\sin^2\phi} + \frac{2\eta}{(r)^2\sin^2\phi}\left(\frac{1}{r\sin\phi}\frac{\partial u_\psi}{\partial\psi} + \frac{u_r}{r} + \frac{u_\phi}{r}\cot\phi\right)$$

$$= -\frac{P}{(r)^2\sin^2\phi} - \frac{\frac{2}{3}\eta u^{\beta}_{,\beta}}{(r)^2\sin^2\phi} + \frac{\eta e_{\psi\psi}}{(r)^2\sin^2\phi}.$$

Note that ηe_{ij} has the dimensions of pressure while τ^{ij} has heterogeneous dimensions. The "divergence" of τ^{ij} is

$$\tau^{1j}_{,j} = \frac{\partial\tau^{11}}{\partial x^1} + \frac{\partial\tau^{12}}{\partial x^2} + \Gamma^1_{22}\tau^{22} + \Gamma^2_{12}\tau^{11} + \frac{\partial\tau^{13}}{\partial x^3} + \Gamma^1_{33}\tau^{33} + \Gamma^3_{13}\tau^{11} + \Gamma^3_{23}\tau^{12}$$

$$= -\frac{\partial P}{\partial r} - \frac{2}{3}\eta\frac{\partial}{\partial r}u^{\beta}_{,\beta} + \eta\frac{\partial e_{rr}}{\partial r} + \frac{\eta}{r}\frac{\partial e_{r\phi}}{\partial\phi} + \frac{P}{r} + \frac{2}{3}\frac{\eta}{r}u^{\beta}_{,\beta}$$

$$- \frac{\eta}{r}e_{\phi\phi} - \frac{P}{r} - \frac{2}{3}\frac{\eta}{r}u^{\beta}_{,\beta} + \frac{\eta}{r}e_{rr} + \frac{\eta}{r\sin\phi}\frac{\partial e_{r\psi}}{\partial\psi}$$

$$+ \frac{P}{r} + \frac{2}{3}\frac{\eta}{r}u^{\beta}_{,\beta} - \frac{\eta}{r}e_{\psi\psi} - \frac{P}{r} - \frac{2}{3}\frac{\eta}{r}u^{\beta}_{,\beta} + \frac{\eta}{r}e_{rr} + \frac{\eta}{r}e_{r\phi}\cot\phi$$

$$= -\frac{\partial P}{\partial r} - \frac{2}{3}\eta\frac{\partial}{\partial r}u^{\beta}_{,\beta} + \frac{\eta}{r}\frac{\partial r\, e_{rr}}{\partial r} + \frac{\eta}{r}e_{rr} + \frac{\eta}{r\sin\phi}\frac{\partial}{\partial\phi}(e_{r\phi}\sin\phi) \qquad \text{(A II.83)}$$

$$+ \frac{\eta}{r\sin\phi}\frac{\partial e_{r\psi}}{\partial\phi} - \frac{\eta}{r}(e_{\phi\phi} + e_{\psi\psi})$$

$$= -\frac{\partial P}{\partial r} - \frac{2}{3}\eta\frac{\partial}{\partial r}u^{\beta}_{,\beta} + \eta\left\{\frac{1}{(r)^2}\frac{\partial(r)^2 e_{rr}}{\partial r} + \frac{1}{r\sin\phi}\frac{\partial}{\partial\phi}(e_{r\phi}\sin\phi)\right.$$

$$\left. + \frac{1}{r\sin\phi}\frac{\partial e_{r\psi}}{\partial\psi} - \frac{e_{\phi\phi} + e_{\psi\psi}}{r}\right\}$$

$$= -\frac{\partial P}{\partial r} + \frac{1}{3}\eta\frac{\partial}{\partial r}\left\{\frac{1}{(r)^2}\frac{\partial(r)^2 u_r}{\partial r} + \frac{1}{r\sin\phi}\frac{\partial}{\partial\phi}(u_\phi\sin\phi) + \frac{1}{r\sin\phi}\frac{\partial u_\psi}{\partial_\psi}\right\}$$

$$+ \eta\left\{\frac{1}{(r)^2}\frac{\partial}{\partial r}\left((r)^2\frac{\partial u_r}{\partial r}\right) + \frac{1}{(r)^2\sin\phi}\frac{\partial}{\partial\phi}\left(\sin\phi\frac{\partial u_r}{\partial\phi}\right) + \frac{1}{(r)^2\sin^2\phi}\frac{\partial^2 u_r}{\partial\psi^2}\right\}$$

$$- \frac{2\eta}{(r)^2}\left\{u_r + \frac{\partial u_\phi}{\partial\phi} + u_\phi\cot\phi + \frac{1}{\sin\phi}\frac{\partial u_\psi}{\partial\psi}\right\},$$

$$\tau^{2j}_{,j} = \frac{\partial \tau^{21}}{\partial x^1} + \Gamma^2_{21}\tau^{21} + \frac{\partial \tau^{22}}{\partial x^2} + 2\,\Gamma^2_{12}\tau^{12} + \frac{\partial \tau^{23}}{\partial x^3} + \Gamma^2_{33}\tau^{33} + \Gamma^3_{13}\tau^{21} + \Gamma^3_{23}\tau^{22}$$

$$= \frac{\eta}{r}\frac{\partial e_{r\phi}}{\partial r} - \frac{\eta}{(r)^2}e_{r\phi} + \frac{\eta}{(r)^2}e_{r\phi} - \frac{1}{(r)^2}\frac{\partial P}{\partial \phi} - \frac{2}{3}\frac{\eta}{(r)^2}\frac{\partial}{\partial \phi}u^{\beta}_{,\beta} + \frac{\eta}{(r)^2}\frac{\partial e_{\phi\phi}}{\partial \phi}$$

$$+ \frac{2\eta}{(r)^2}e_{r\phi} + \frac{\eta}{(r)^2\sin\phi}\frac{\partial e_{\phi\psi}}{\partial \psi} - \eta\frac{\cot\phi}{(r)^2}e_{\psi\psi} + \frac{\eta}{(r)^2}e_{r\phi} + \eta\frac{\cot\phi}{(r)^2}e_{\phi\phi}$$

$$= \frac{\eta}{r}\frac{\partial e_{r\phi}}{\partial r} + \frac{3}{(r)^2}e_{r\phi} + \frac{\eta}{(r)^2}\frac{\partial e_{\phi\phi}}{\partial \phi} + \frac{\eta}{(r)^2\sin\phi}\frac{\partial e_{\phi\psi}}{\partial \psi} - \frac{\cot\phi}{(r)^2}e_{\psi\psi} + \frac{\cot\phi}{(r)^2}e_{\phi\phi}$$

$$- \frac{1}{(r)^2}\frac{\partial P}{\partial \phi} - \frac{2}{3}\frac{\eta}{(r)^2}\frac{\partial}{\partial \phi}u^{\beta}_{,\beta}$$

$$= -\frac{1}{(r)^2}\frac{\partial P}{\partial \phi} - \frac{2}{3}\frac{\eta}{(r)^2}\frac{\partial}{\partial \phi}u^{\beta}_{,\beta} + \eta\left\{\frac{1}{(r)^4}\frac{\partial (r)^3 e_{r\phi}}{\partial r} + \frac{1}{(r)^2\sin\phi}\frac{\partial}{\partial \phi}(e_{\phi\phi}\sin\phi)\right.$$

$$\left. + \frac{1}{(r)^2\sin\phi}\frac{\partial e_{\phi\psi}}{\partial \psi} - \frac{e_{\psi\psi}}{(r)^2}\cot\phi\right\}$$

$$= -\frac{1}{(r)^2}\frac{\partial P}{\partial \phi} - \frac{2}{3}\frac{\eta}{(r)^2}\frac{\partial}{\partial \phi}u^{\beta}_{,\beta} + \eta\left\{\frac{1}{(r)^2}\frac{\partial}{\partial \phi}\left(\frac{1}{(r)^2}\frac{\partial r^2 u_r}{\partial r}\right) + \frac{1}{(r)^3}\frac{\partial}{\partial r}\left((r)^2\frac{\partial u_\phi}{\partial r}\right)\right.$$

$$- \frac{2u_\phi}{(r)^3} + \frac{1}{(r)^3\sin\phi}\frac{\partial}{\partial \phi}\left(\sin\phi\frac{\partial u_\phi}{\partial \phi}\right) + \frac{1}{(r)^2}\frac{\partial}{\partial \phi}\left[\frac{1}{r\sin\phi}\frac{\partial}{\partial \phi}(u_\phi\sin\phi)\right]$$

$$+ \frac{u_\phi}{(r)^3\sin^2\phi} + \frac{2}{(r)^3}\frac{\partial u_r}{\partial \phi} + \frac{2u_r}{(r)^3}\cot\phi + \frac{1}{(r)^3\sin^2\phi}\frac{\partial^2 u_\phi}{\partial \psi^2}$$

$$\left. + \frac{1}{(r)^2}\frac{\partial}{\partial \phi}\left(\frac{1}{r\sin\phi}\frac{\partial u_\psi}{\partial \psi}\right) - \frac{2\cos\phi}{(r)^3\sin^2\phi}\frac{\partial u_\psi}{\partial \psi} - \frac{2u_r}{(r)^3}\cot\phi - \frac{2u_\phi}{(r)^3}\cot^2\phi\right\},$$

$$r\,\tau^{2j}_{,j} = -\frac{1}{r}\frac{\partial P}{\partial \phi} + \frac{1}{3}\frac{\eta}{r}\frac{\partial}{\partial \phi}u^{\beta}_{,\beta} + \eta\left\{\frac{1}{(r)^2}\frac{\partial}{\partial r}\left((r)^2\frac{\partial u_\phi}{\partial r}\right) + \frac{1}{(r)^2\sin\phi}\frac{\partial}{\partial \phi}\left(\sin\phi\frac{\partial u_\phi}{\partial \phi}\right)\right.$$

$$\left. + \frac{1}{(r)^2\sin^2\phi}\frac{\partial^2 u_\phi}{\partial \psi^2}\right\} + \frac{2\eta}{(r)^2}\left\{\frac{\partial u_r}{\partial \phi} - \frac{u_\phi}{2\sin^2\phi} - \frac{\cos\phi}{\sin^2\phi}\frac{\partial u_\psi}{\partial \psi}\right\}$$

$$\tau^{3j}_{,j} = \frac{\partial \tau^{31}}{\partial x^1} + \Gamma^3_{31}\tau^{31} + \frac{\partial \tau^{32}}{\partial x^2} + \Gamma^2_{12}\tau^{31} + \Gamma^3_{32}\tau^{32} + \frac{\partial \tau^{33}}{\partial x^3} + 2\,\Gamma^3_{13}\tau^{13} + 2\,\Gamma^3_{23}\tau^{23}$$

$$= \frac{\partial \tau^{31}}{\partial x^1} + 4\frac{\tau^{31}}{x^1} + \frac{\partial \tau^{32}}{\partial x^2} + 3\cot\phi\,\tau^{32} + \frac{\partial \tau^{33}}{\partial x^3}$$

$$= \frac{1}{(r)^4}\frac{\partial (r)^4\tau^{31}}{\partial r} + \frac{1}{\sin^3\phi}\frac{\partial \sin^3\phi\,\tau^{32}}{\partial \phi} + \frac{\partial \tau^{33}}{\partial x^3}$$

$$= \frac{\eta}{(r)^4}\frac{\partial}{\partial r}\left(\frac{(r)^2}{\sin\phi}e_{r\psi} + \frac{\eta}{(r)^2\sin^3\phi}\frac{\partial}{\partial\phi}(\sin^2\phi\, e_{\phi\psi}) + \frac{\eta}{(r)^2\sin^2\phi}\frac{\partial e_{\psi\psi}}{\partial\psi}\right.$$

$$\left. - \frac{1}{(r)^2\sin^2\phi}\frac{\partial P}{\partial\psi} - \frac{\frac{2}{3}\eta}{(r)^2\sin^2\phi}\frac{\partial}{\partial\psi}u_{,\beta}^{\beta}\right)$$

$$r\sin\phi\,\tau_{,i}^{3i} = \frac{\eta}{(r)^3}\frac{\partial}{\partial r}((r)^3 e_{r\psi}) + \frac{\eta}{r\sin^2\phi}\frac{\partial}{\partial\phi}(\sin^2\phi\, e_{\phi\psi}) + \frac{\eta}{r\sin\phi}\frac{\partial e_{\psi\psi}}{\partial\psi}$$

$$- \frac{1}{r\sin\phi}\frac{\partial P}{\partial\psi} - \frac{\frac{2}{3}\eta}{r\sin\phi}\frac{\partial}{\partial\psi}u_{,\beta}^{\beta}$$

$$= -\frac{1}{r\sin\phi}\frac{\partial P}{\partial\psi} - \frac{\frac{2}{3}\eta}{r\sin\phi}\frac{\partial}{\partial\psi}u_{,\beta}^{\beta} + \eta\left\{\frac{1}{(r)^3}\frac{\partial}{\partial r}((r)^3 e_{r\psi})\right.$$

$$\left. + \frac{1}{r\sin^2\phi}\frac{\partial}{\partial\phi}(\sin^2\phi\, e_{\phi\psi}) + \frac{1}{r\sin\phi}\frac{\partial e_{\psi\psi}}{\partial\psi}\right\}$$

$$= -\frac{1}{r\sin\phi}\frac{\partial P}{\partial\psi} - \frac{\frac{2}{3}\eta}{r\sin\phi}\frac{\partial}{\partial\psi}u_{,\beta}^{\beta} + \eta\left\{\frac{1}{r\sin\phi}\frac{\partial}{\partial\psi}\left(\frac{1}{(r)^2}\frac{\partial}{\partial r}((r)^2 u_r)\right.\right.$$

$$+ \frac{1}{(r)^2}\frac{\partial}{\partial r}\left((r)^2\frac{\partial u_\psi}{\partial r}\right) - \frac{2u_\psi}{(r)^2} + \frac{1}{r\sin\phi}\frac{\partial}{\partial\psi}\left(\frac{1}{r\sin\phi}\frac{\partial}{\partial\phi}(\sin\phi\, u_\psi)\right)$$

$$+ \frac{1}{(r)^2\sin\phi}\frac{\partial}{\partial\phi}\left(\sin\phi\frac{\partial u_\psi}{\partial\phi}\right) - \cot^2\phi\frac{u_\psi}{(r)^2} + \frac{u_\psi}{(r)^2}$$

$$\left.\left. + \frac{2}{(r)^2\sin^2\phi}\frac{\partial^2 u_\psi}{\partial\psi^2} + \frac{2}{(r)^2\sin\phi}\frac{\partial u_r}{\partial\psi} + \frac{2\cos\phi}{(r)^2\sin^2\phi}\frac{\partial u_\phi}{\partial\psi}\right\}\right.$$

$$= -\frac{1}{r\sin\phi}\frac{\partial P}{\partial\psi} + \frac{\eta}{3}\frac{1}{r\sin\phi}\frac{\partial}{\partial\psi}u_{,\beta}^{\beta} + \eta\left\{\frac{1}{(r)^2}\frac{\partial}{\partial r}\left((r)^2\frac{\partial u_\psi}{\partial r}\right)\right.$$

$$+ \frac{1}{(r)^2\sin\phi}\frac{\partial}{\partial\phi}\left(\sin\phi\frac{\partial u_\psi}{\partial\phi}\right) + \frac{1}{(r)^2\sin^2\phi}\frac{\partial^2 u_\psi}{\partial\psi^2} - \frac{u_\psi}{(r)^2\sin^2\phi}$$

$$\left. + \frac{2}{(r)^2\sin\phi}\frac{\partial u_r}{\partial\psi} + \frac{2\cos\phi}{(r)^2\sin^2\phi}\frac{\partial u_\phi}{\partial\psi}\right\}.$$

Summary of Stress Tensor Formulas

Rectangular Cartesian Coordinates

$$u^{\beta}_{,\beta} = \frac{\partial u_x}{\partial x} + \frac{\partial u_y}{\partial y} + \frac{\partial u_z}{\partial z}. \tag{A II.84}$$

$$\begin{aligned}
\tau^{11} &= -P - \frac{2}{3}\eta\, u^{\beta}_{,\beta} + 2\eta \frac{\partial u_z}{\partial z}, \\
\tau^{21} = \tau^{12} &= \eta\left(\frac{\partial u_y}{\partial z} + \frac{\partial u_z}{\partial y}\right), \\
\tau^{31} = \tau^{13} &= \eta\left(\frac{\partial u_z}{\partial x} + \frac{\partial u_x}{\partial z}\right), \\
\tau^{22} &= -P - \frac{2}{3}\eta\, u^{\beta}_{,\beta} + 2\eta \frac{\partial u_y}{\partial y}, \\
\tau^{23} = \tau^{32} &= \eta\left(\frac{\partial u_x}{\partial y} + \frac{\partial u_y}{\partial x}\right), \\
\tau^{33} &= -P - \frac{2}{3}\eta\, u^{\beta}_{,\beta} + 2\eta \frac{\partial u_x}{\partial x}.
\end{aligned} \tag{A II.85}$$

$$\begin{aligned}
\tau^{1j}_{,j} &= -\frac{\partial P}{\partial z} + \frac{1}{3}\eta \frac{\partial}{\partial z} u^{\beta}_{,\beta} + \eta\left(\frac{\partial^2 u_z}{\partial z^2} + \frac{\partial^2 u_z}{\partial y^2} + \frac{\partial^2 u_z}{\partial x^2}\right), \\
\tau^{2j}_{,j} &= -\frac{\partial P}{\partial y} + \frac{1}{3}\eta \frac{\partial}{\partial y} u^{\beta}_{,\beta} + \eta\left(\frac{\partial^2 u_y}{\partial z^2} + \frac{\partial^2 u_y}{\partial y^2} + \frac{\partial^2 u_y}{\partial x^2}\right), \\
\tau^{3j}_{,j} &= -\frac{\partial P}{\partial x} + \frac{1}{3}\eta \frac{\partial}{\partial x} u^{\beta}_{,\beta} + \eta\left(\frac{\partial^2 u_x}{\partial z^2} + \frac{\partial^2 u_x}{\partial y^2} + \frac{\partial^2 u_x}{\partial x^2}\right).
\end{aligned} \tag{A II.86}$$

Polar Cylindrical Coordinates

$$u^{\beta}_{,\beta} = \frac{1}{r}\frac{\partial}{\partial r}(r\, u_r) + \frac{1}{r}\frac{\partial u_\psi}{\partial \psi} + \frac{\partial u_x}{\partial x}. \tag{A II.87}$$

$$\begin{aligned}
\tau^{11} &= -P - \frac{2}{3}\eta\, u^{\beta}_{,\beta} + 2\eta \frac{\partial u_r}{\partial r} && = -P - \frac{2}{3}\eta\, u^{\beta}_{,\beta} + \eta\, e_{rr}, \\
r\,\tau^{12} = r\,\tau^{21} &= \eta\left[r \frac{\partial}{\partial r}\left(\frac{u_\psi}{r}\right) + \frac{1}{r}\frac{\partial u_r}{\partial \psi}\right] && = \eta\, e_{r\psi} = \eta\, e_{\psi r}, \\
\tau^{13} = \tau^{31} &= \eta\left(\frac{\partial u_r}{\partial x} + \frac{\partial u_x}{\partial r}\right) && = \eta\, e_{rx} = \eta\, e_{xr}, \\
(r)^2\tau^{22} &= -P - \frac{2}{3}\eta\, u^{\beta}_{,\beta} + 2\eta\left(\frac{1}{r}\frac{\partial u_\psi}{\partial \psi} + \frac{u_r}{r}\right) = -P - \frac{2}{3}\eta\, u^{\beta}_{,\beta} + \eta\, e_{\psi\psi},
\end{aligned} \tag{A II.88}$$

$$r\tau^{23} = r\tau^{32} = \eta\left(\frac{1}{r}\frac{\partial u_x}{\partial \psi} + \frac{\partial u_\psi}{\partial x}\right) \qquad = \eta\, e_{\psi x} = \eta\, e_{x\psi},$$

$$\tau^{33} = -P - \frac{2}{3}\eta\, u^{\beta}_{,\beta} + 2\eta\frac{\partial u_x}{\partial x} \qquad = -P - \frac{2}{3}\eta\, u^{\beta}_{,\beta} + \eta\, e_{xx}.$$

$$\tau^{1j}_{,j} = -\frac{\partial P}{\partial r} - \frac{2}{3}\eta\frac{\partial}{\partial r}u^{\beta}_{,\beta} + \frac{\eta}{r}\left\{\frac{\partial r\, e_{rr}}{\partial r} + \frac{\partial e_{r\psi}}{\partial \psi} + \frac{\partial r\, e_{rx}}{\partial x} - e_{\psi\psi}\right\},$$

$$r\,\tau^{2j}_{,j} = -\frac{1}{r}\frac{\partial P}{\partial \psi} - \frac{2}{3}\frac{\eta}{r}\frac{\partial}{\partial \psi}u^{\beta}_{,\beta} + \frac{\eta}{r}\left\{\frac{\partial r\, e_{r\psi}}{\partial r} + \frac{\partial e_{\psi\psi}}{\partial \psi} + \frac{\partial r\, e_{\psi x}}{\partial x} + e_{r\psi}\right\},$$

$$\tau^{3j}_{,j} = -\frac{\partial P}{\partial x} - \frac{2}{3}\eta\frac{\partial}{\partial x}u^{\beta}_{,\beta} + \frac{\eta}{r}\left\{\frac{\partial r\, e_{rx}}{\partial r} + \frac{\partial e_{\psi x}}{\partial \psi} + \frac{\partial r\, e_{xx}}{\partial x}\right\},$$

$$\tau^{1j}_{\ j} = -\frac{\partial P}{\partial r} + \frac{\eta}{3}\frac{\partial}{\partial r}u^{\beta}_{,\beta} \qquad \text{(A II.89)}$$

$$+ \eta\left\{\frac{\partial^2 u_r}{\partial r^2} + \frac{1}{r}\frac{\partial u_r}{\partial r} + \frac{1}{(r)^2}\frac{\partial^2 u_r}{\partial \psi^2} + \frac{\partial^2 u_r}{\partial x^2} - \frac{u_r}{(r)^2} - \frac{2}{(r)^2}\frac{\partial u_\psi}{\partial \psi}\right\},$$

$$r\,\tau^{2j}_{,j} = -\frac{1}{r}\frac{\partial P}{\partial \psi} + \frac{\eta}{3r}\frac{\partial}{\partial \psi}u^{\beta}_{,\beta}$$

$$+ \eta\left\{\frac{\partial^2 u_\psi}{\partial r^2} + \frac{1}{r}\frac{\partial u_\psi}{\partial r} + \frac{1}{(r)^2}\frac{\partial^2 u_\psi}{\partial \psi^2} + \frac{\partial^2 u_\psi}{\partial x^2} - \frac{u_\psi}{(r)^2} + \frac{2}{(r)^2}\frac{\partial u_r}{\partial \psi}\right\},$$

$$\tau^{3j}_{,j} = -\frac{\partial P}{\partial x} + \frac{\eta}{3}\frac{\partial}{\partial x}u^{\beta}_{,\beta} + \eta\left\{\frac{\partial^2 u_x}{\partial r^2} + \frac{1}{r}\frac{\partial u_x}{\partial r} + \frac{1}{(r)^2}\frac{\partial^2 u_x}{\partial \psi^2} + \frac{\partial^2 u_x}{\partial x^2}\right\}.$$

Polar Spherical Coordinates

$$u^{\beta}_{,\beta} = \frac{1}{(r)^2}\frac{\partial}{\partial r}\left((r)^2 u_r\right) + \frac{1}{r\sin\phi}\frac{\partial}{\partial \phi}\left(u_\phi \sin\phi\right) + \frac{1}{r\sin\phi}\frac{\partial u_\psi}{\partial \psi}. \qquad \text{(A II.90)}$$

$$\tau^{11} = -P - \frac{2}{3}\eta\, u^{\beta}_{,\beta} + 2\eta\frac{\partial u_r}{\partial r} \qquad = -P - \frac{2}{3}\eta\, u^{\beta}_{,\beta} + \eta\, e_{rr},$$

$$r\,\tau^{12} = r\,\tau^{21} = \eta\left[\frac{1}{r}\frac{\partial u_r}{\partial \phi} + r\frac{\partial}{\partial r}\left(\frac{u_\phi}{r}\right)\right] \qquad = \eta\, e_{r\phi} = \eta\, e_{\phi r},$$

$$r\sin\phi\,\tau^{13} = r\sin\phi\,\tau^{31} = \eta\left[\frac{1}{r\sin\phi}\frac{\partial u_r}{\partial \psi} + r\frac{\partial}{\partial r}\left(\frac{u_\psi}{r}\right)\right]$$

$$= \eta\, e_{r\psi} = \eta\, e_{\psi r},$$

$$(r)^2\tau^{22} = -P - \frac{2}{3}\eta\, u^{\beta}_{,\beta} + 2\eta\left(\frac{1}{r}\frac{\partial u_\phi}{\partial \phi} + \frac{u_r}{r}\right) \qquad \text{(A II.91)}$$

$$= -P - \frac{2}{3}\eta\, u^{\beta}_{,\beta} + \eta\, e_{\phi\phi},$$

$$(r)^2 \sin\phi\, \tau^{23} = (r)^2 \sin\phi\, \tau^{32} = \eta\left[\frac{1}{r\sin\phi}\frac{\partial u_\phi}{\partial \psi} + \frac{\sin\phi}{r}\frac{\partial}{\partial\phi}\left(\frac{u_\psi}{\sin\phi}\right)\right]$$
$$= \eta\, e_{\phi\psi} = \eta e_{\psi\phi},$$

$$(r)^2 \sin^2\phi\, \tau^{33} = -P - \frac{2}{3}\eta\, u^{\beta}_{,\beta} + 2\eta\left(\frac{1}{r\sin\phi}\frac{\partial u_\psi}{\partial\psi} + \frac{u_r}{r} + \frac{u_\phi}{r}\cot\phi\right)$$
$$= -P - \frac{2}{3}\eta\, u^{\beta}_{,\beta} + \eta\, e_{\psi\psi}.$$

$$\tau^{1j}_{,j} = -\frac{\partial P}{\partial r} - \frac{2}{3}\eta\frac{\partial}{\partial r}u^{\beta}_{,\beta} + \eta\left\{\frac{1}{(r)^2}\frac{\partial (r)^2 e_{rr}}{\partial r} + \frac{1}{r\sin\phi}\frac{\partial}{\partial\phi}(e_{r\phi}\sin\phi)\right.$$
$$\left. + \frac{1}{r\sin\phi}\frac{\partial e_{r\psi}}{\partial\psi} - \frac{e_{\phi\phi}+e_{\psi\psi}}{r}\right\},$$

$$r\,\tau^{2j}_{,j} = -\frac{1}{r}\frac{\partial P}{\partial\phi} - \frac{2}{3}\frac{\eta}{r}\frac{\partial}{\partial\phi}u^{\beta}_{,\beta} + \eta\left\{\frac{1}{(r)^3}\frac{\partial (r)^3 e_{r\phi}}{\partial r} + \frac{1}{r\sin\phi}\frac{\partial}{\partial\phi}(e_{\phi\phi}\sin\phi)\right.$$
$$\left. + \frac{1}{r\sin\phi}\frac{\partial e_{\phi\psi}}{\partial\psi} - \frac{e_{\psi\psi}}{r}\cot\phi\right\},$$

$$r\sin\phi\,\tau^{3j}_{,j} = -\frac{1}{r\sin\phi}\frac{\partial P}{\partial\psi} - \frac{2}{3}\frac{\eta}{r\sin\phi}\frac{\partial}{\partial\psi}u^{\beta}_{,\beta} + \eta\left\{\frac{1}{(r)^3}\frac{\partial (r)^3 e_{r\psi}}{\partial r}\right. \qquad \text{(A II.92)}$$
$$\left. + \frac{1}{r\sin^2\phi}\frac{\partial}{\partial\phi}(e_{\phi\psi}\sin^2\phi) + \frac{1}{r\sin\phi}\frac{\partial e_{\psi\psi}}{\partial\psi}\right\},$$

$$\tau^{1j}_{,j} = -\frac{\partial P}{\partial r} + \frac{\eta}{3}\frac{\partial}{\partial r}u^{\beta}_{,\beta} + \eta\left\{\frac{1}{(r)^2}\frac{\partial}{\partial r}\left((r)^2\frac{\partial u_r}{\partial r}\right) + \frac{1}{(r)^2\sin\phi}\frac{\partial}{\partial\phi}\left(\sin\phi\frac{\partial u_r}{\partial\phi}\right)\right.$$
$$\left. + \frac{1}{(r)^2\sin^2\phi}\frac{\partial^2 u_r}{\partial\psi^2} - \frac{2\,u_r}{(r)^2} - \frac{2}{(r)^2}\frac{\partial u_\phi}{\partial\phi} - \frac{2\,u_\phi}{(r)^2}\cot\phi - \frac{2}{(r)^2\sin\phi}\frac{\partial u_\psi}{\partial\psi}\right\},$$

$$r\,\tau^{2j}_{,j} = -\frac{1}{r}\frac{\partial P}{\partial r} + \frac{\eta}{3\,r}\frac{\partial}{\partial\phi}u^{\beta}_{,\beta} + \eta\left\{\frac{1}{(r)^2}\frac{\partial}{\partial r}\left((r)^2\frac{\partial u_\phi}{\partial r}\right) + \frac{1}{(r)^2\sin\phi}\frac{\partial}{\partial\phi}\left(\sin\phi\frac{\partial u_\phi}{\partial\phi}\right)\right.$$
$$\left. + \frac{1}{(r)^2\sin^2\phi}\frac{\partial^2 u_\phi}{\partial\psi^2} + \frac{2}{(r)^2}\frac{\partial u_r}{\partial\phi} - \frac{u_\phi}{(r)^2\sin^2\phi} - \frac{2\cos\phi}{(r)^2\sin^2\phi}\frac{\partial u_\psi}{\partial\psi}\right\},$$

$$r\sin\phi\,\tau^{3j}_{,j} = -\frac{1}{r\sin\phi}\frac{\partial P}{\partial\psi} + \frac{\eta}{3\,r\sin\phi}\frac{\partial}{\partial\psi}u^{\beta}_{,\beta} + \eta\left\{\frac{1}{(r)^2}\frac{\partial}{\partial r}\left((r)^2\frac{\partial u_\psi}{\partial r}\right)\right.$$
$$+ \frac{1}{(r)^2\sin\phi}\frac{\partial}{\partial\phi}\left(\sin\phi\frac{\partial u_\psi}{\partial\phi}\right) + \frac{1}{(r)^2\sin^2\phi}\frac{\partial^2 u_\psi}{\partial\psi^2} - \frac{u_\psi}{(r)^2\sin^2\phi}$$
$$\left. + \frac{2}{(r)^2\sin\phi}\frac{\partial u_r}{\partial\psi} + \frac{2\cos\phi}{(r)^2\sin^2\phi}\frac{\partial u_\phi}{\partial\psi}\right\}.$$

AII-3. Acceleration in Generalized Coordinates

The contravariant acceleration field is the intrinsic derivative of the contravariant velocity field with respect to time:

$$\begin{aligned} a^i = \frac{\delta u^i}{\delta\theta} &= \frac{du^i}{d\theta} + \Gamma^i_{jk} u^j \frac{dx^k}{d\theta} \\ &= \frac{\partial u^i}{\partial\theta} + u^k \frac{\partial u^i}{\partial x^k} + \Gamma^i_{jk} u^j u^k \\ &= \frac{\partial u^i}{\partial\theta} + u^k \left(\frac{\partial u^i}{\partial x^k} + \Gamma^i_{jk} u^j \right) \\ &= \frac{\partial u^i}{\partial\theta} + u^k u^i_{,k} . \end{aligned} \tag{A II.93}$$

In *rectangular Cartesian coordinates,* the acceleration is the substantial derivative of the velocity:

$$\begin{aligned} a^i = \frac{du^i}{d\theta} = \frac{\partial u^i}{\partial\theta} + u^k u^i_{,k} &= \frac{\partial u^i}{\partial\theta} + u_x u^i_{,x} + u_y u^i_{,y} + u_z u^i_{,z} \\ &= \frac{\partial u^i}{\partial\theta} + u_x \frac{\partial u^i}{\partial x} + u_y \frac{\partial u^i}{\partial y} + u_z \frac{\partial u^i}{\partial z} . \end{aligned} \tag{A II.94}$$

In *polar cylindrical coordinates:*

$$\begin{aligned} a^1 = a_r &= \frac{\partial u^1}{\partial\theta} + u^1 u^1_{,1} + u^2 u^1_{,2} + u^3 u^1_{,3} \\ &= \frac{\partial u_r}{\partial\theta} + u_r \frac{\partial u_r}{\partial r} + \frac{u_\psi}{r} \left(\frac{\partial u_r}{\partial\psi} + \Gamma^1_{22} \frac{u_\psi}{r} \right) + u_x \frac{\partial u_r}{\partial x} \\ &= \frac{\partial u_r}{\partial\theta} + u_r \frac{\partial u_r}{\partial r} + \frac{u_\psi}{r} \frac{\partial u_r}{\partial\psi} + u_x \frac{\partial u_r}{\partial x} - \frac{u^2_\psi}{r} . \end{aligned}$$

$$\begin{aligned} a^2 = \frac{a_\psi}{r} = \frac{\partial u^2}{\partial\theta} &+ u^1 u^2_{,1} + u^2 u^2_{,2} + u^3 u^2_{,3} \\ &= \frac{\partial u^2}{\partial\theta} + u^1 \left(\frac{\partial u^2}{\partial x^1} + \Gamma^2_{21} u^2 \right) + u^2 \left(\frac{\partial u^2}{\partial x^2} + \Gamma^2_{21} u^1 \right) + u^3 \frac{\partial u^2}{\partial x^3} \\ &= \frac{1}{r} \frac{\partial u_\psi}{\partial\theta} + u_r \left[\frac{\partial}{\partial r} \left(\frac{u_\psi}{r} \right) + \frac{u_\psi}{(r)^2} \right] + \frac{u_\psi}{r} \left(\frac{1}{r} \frac{\partial u_\psi}{\partial\psi} + \frac{u_r}{r} \right) + \frac{u_x}{r} \frac{\partial u_x}{\partial x} , \end{aligned} \tag{A II.95}$$

$$a_\psi = \frac{\partial u_\psi}{\partial\theta} + u_r \frac{\partial u_\psi}{\partial r} + \frac{u_\psi}{r} \frac{\partial u_\psi}{\partial\psi} + u_x \frac{\partial u_\psi}{\partial x} + \frac{u_r u_\psi}{r} ,$$

$$a^3 = a_x = \frac{\partial u^3}{\partial \theta} + u^1 u^3_{,1} + u^2 u^3_{,2} + u^3 u^3_{,3}$$

$$= \frac{\partial u_x}{\partial \theta} + u_r \frac{\partial u_x}{\partial r} + \frac{u_\psi}{r} \frac{\partial u_x}{\partial \psi} + u_x \frac{\partial u_x}{\partial x}.$$

In *polar spherical coordinates:*

$$a^1 = a_r = \frac{\partial u^1}{\partial \theta} + u^1 u^1_{,1} + u^2 u^1_{,2} + u^3 u^1_{,3}$$

$$= \frac{\partial u_r}{\partial \theta} + u_r \frac{\partial u_r}{\partial r} + \frac{u_\phi}{r}\left(\frac{\partial u_r}{\partial \phi} - u_\phi\right) + \frac{u_\psi}{r \sin\phi}\left(\frac{\partial u_r}{\partial \psi} - \frac{r \sin^2\phi}{r \sin\phi} u_\psi\right)$$

$$= \frac{\partial u_r}{\partial \theta} + u_r \frac{\partial u_r}{\partial r} + \frac{u_\phi}{r} \frac{\partial u_r}{\partial \phi} + \frac{u_\psi}{r \sin\phi} \frac{\partial u_r}{\partial \psi} - \frac{u_\phi^2 + u_\psi^2}{r},$$

$$a^2 = \frac{a_\phi}{r} = \frac{\partial u^2}{\partial \theta} + u^1 u^2_{,1} + u^2 u^2_{,2} + u^3 u^2_{,3}$$

$$= \frac{1}{r} \frac{\partial u_\phi}{\partial \theta} + u_r\left[\frac{\partial}{\partial r}\left(\frac{u_\phi}{r}\right) + \Gamma^2_{21} \frac{u_\phi}{r}\right] + \frac{u_\phi}{r}\left[\frac{\partial}{\partial \phi}\left(\frac{u_\phi}{r}\right) + \Gamma^2_{12} u_r\right]$$

$$+ \frac{u_\psi}{r \sin\phi}\left[\frac{\partial}{\partial \psi}\left(\frac{u_\phi}{r}\right) + \Gamma^2_{33} u^3\right]$$

$$= \frac{1}{r} \frac{\partial u_\phi}{\partial \theta} + \frac{u_r}{r} \frac{\partial u_\phi}{\partial r} - \frac{u_r u_\phi}{(r)^2} + \frac{u_r u_\phi}{(r)^2} + \frac{u_\phi}{(r)^2} \frac{\partial u_\phi}{\partial \phi}$$

$$+ \frac{u_\phi u_r}{(r)^2} + \frac{u_\psi}{(r)^2 \sin\phi} \frac{\partial u_\phi}{\partial \psi} - \frac{u_\psi^2 \cos\phi}{(r)^2 \sin\phi},$$

$$a_\phi = \frac{\partial u_\phi}{\partial \theta} + u_r \frac{\partial u_\phi}{\partial r} + \frac{u_\phi}{r} \frac{\partial u_\phi}{\partial \phi} + \frac{u_\psi}{r \sin\phi} \frac{\partial u_\phi}{\partial \psi} + \frac{u_r u_\phi}{r} - \frac{u_\psi^2 \cot\phi}{r}. \quad \text{(A II.96)}$$

$$a^3 = \frac{a_\psi}{r \sin\phi} = \frac{\partial u^3}{\partial \theta} + u^1 u^3_{,1} + u^2 u^3_{,2} + u^3 u^3_{,3}$$

$$= \frac{1}{r \sin\phi} \frac{\partial u_\psi}{\partial \theta} + u_r\left[\frac{\partial}{\partial r}\left(\frac{u_\psi}{r \sin\phi}\right) + \Gamma^3_{31} u^3\right]$$

$$+ \frac{u_\phi}{r}\left[\frac{\partial}{\partial \phi}\left(\frac{u_\psi}{r \sin\phi}\right) + \Gamma^3_{32} u^3\right] + \frac{u_\psi}{r \sin\phi}\left[\frac{\partial}{\partial \psi}\left(\frac{u_\psi}{r \sin\phi}\right)\right.$$

$$\left. + \Gamma^3_{13} u^1 + \Gamma^3_{23} u^2\right]$$

$$= \frac{1}{r\sin\phi}\frac{\partial u_\psi}{\partial\theta} + \frac{u_r}{r\sin\phi}\frac{\partial u_\psi}{\partial r} - \frac{u_r u_\psi}{(r)^2\sin\phi} + \frac{u_r u_\psi}{(r)^2\sin\phi}$$

$$+ \frac{u_\phi}{(r)^2\sin\phi}\frac{\partial u_\psi}{\partial\phi} - \frac{u_\phi u_\psi\cos\phi}{(r)^2\sin^2\phi} + \frac{u_\phi u_\psi\cot\phi}{(r)^2\sin\phi}$$

$$+ \frac{u_\psi}{(r)^2\sin^2\phi}\frac{\partial u_\psi}{\partial\psi} + \frac{u_r u_\psi}{(r)^2\sin\phi} + \frac{u_\phi u_\psi\cot\phi}{(r)^2\sin\phi},$$

$$a_\psi = \frac{\partial u_\psi}{\partial\theta} + u_r\frac{\partial u_\psi}{\partial r} + \frac{u_\phi}{r}\frac{\partial u_\psi}{\partial\phi} + \frac{u_\psi}{r\sin\phi}\frac{\partial u_\psi}{\partial\psi}$$

$$+ \frac{u_r u_\psi}{r} + \frac{u_\psi u_\phi}{r}\cot\phi\,.$$

AII-4. Components of Vorticity

The angular velocity of rotation at any point in a velocity field is equal to one-half the curl of the velocity field at that point. The curl of a velocity field is a covariant tensor of rank two [Margenau and Murphy (*6*), p. 192]. In Cartesian rectangular coordinates for three-dimensional space, the curl of a vector field has the algebraic properties associated with a vector field (tensor field of rank one) and is considered to be a vector in the Gibbs-Wilson notation. In "absolute differential calculus," the curl is defined to be a skew-symmetric tensor of rank two, whose components are

$$(\text{curl}\,u)_{ij} = 2\,\omega_{ij} = \frac{1}{\sqrt{g}}\left(\frac{\partial u_i}{\partial x^j} - \frac{\partial u_j}{\partial x^i}\right). \qquad \text{(A II.97)}$$

But

$$u_i = g_{ik}\,u^k \qquad \text{and} \qquad u_j = g_{ik}\,u^k \qquad \text{(A II.98)}$$

so

$$2\,\omega_{ij} = \frac{g_{ij}}{\sqrt{g}}\frac{\partial u^k}{\partial x^j} - \frac{g_{il}}{\sqrt{g}}\frac{\partial u^l}{\partial x^i} + \left(\frac{u^k}{\sqrt{g}}\frac{\partial g_{ik}}{\partial x^j} - \frac{u^l}{\sqrt{g}}\frac{\partial g_{jl}}{\partial x^i}\right), \qquad \text{(A II.99)}$$

In *rectangular Cartesian coordinates:*

$$\begin{aligned} u^1 &= u_z, & x^1 &= z, & \sqrt{g} &= 1, \\ u^2 &= u_y, & x^2 &= y, & g_{11} = g_{22} &= g_{33} = 1, \\ u^3 &= u_x, & x^3 &= x, & \text{all other } g_{ij} &= 0. \end{aligned} \qquad \text{(A II.100)}$$

Thus

$$
\begin{aligned}
2\,\omega_{11} &= 2\,\omega_{22} = 2\,\omega_{33} = 0,\\
2\,\omega_{12} &= -\,2\,\omega_{21} = \frac{\partial u^1}{\partial x^2} - \frac{\partial u^2}{\partial x^1} = \frac{\partial u_x}{\partial y} - \frac{\partial u_y}{\partial z},\\
2\,\omega_{23} &= -\,2\,\omega_{32} = \frac{\partial u^2}{\partial x^3} - \frac{\partial u^3}{\partial x^2} = \frac{\partial u_y}{\partial x} - \frac{\partial u_x}{\partial y},\\
2\,\omega_{31} &= 2\,\omega_{13} = \frac{\partial u^3}{\partial x^1} - \frac{\partial u^1}{\partial x^3} = \frac{\partial u_z}{\partial z} - \frac{\partial u_z}{\partial x}.
\end{aligned}
\tag{A II.101}
$$

In the Gibbs-Wilson notation:

$$
\begin{aligned}
\omega^1 = \omega_{32} &= \frac{1}{2}\left(\frac{\partial u_x}{\partial y} - \frac{\partial u_y}{\partial x}\right) = -\,\omega_z,\\
\omega^2 = \omega_{13} &= \frac{1}{2}\left(\frac{\partial u_z}{\partial x} - \frac{\partial u_x}{\partial z}\right) = -\,\omega_y,\\
\omega^3 = \omega_{21} &= \frac{1}{2}\left(\frac{\partial u_y}{\partial z} - \frac{\partial u_z}{\partial y}\right) = -\,\omega_x,
\end{aligned}
\tag{A II.102}
$$

In *polar cylindrical coordinates:*

$$
\begin{aligned}
&u^1 = u_r, && x^1 = r, && g_{11} = g_{33} = 1,\\
&u^2 = u_\psi (r)^{-1}, && x^2 = \psi, && g_{22} = (r)^2, \qquad \sqrt{g} = r,\\
&u^3 = u_z, && x^3 = x, && \text{all other } g_{ij} = 0,
\end{aligned}
\tag{A II.103}
$$

Thus

$$
\begin{aligned}
2\,\omega_{11} &= 2\,\omega_{22} = 2\,\omega_{33} = 0,\\
2\,\omega_{12} &= -\,2\,\omega_{21} = \frac{g_{11}}{r}\frac{\partial u^1}{\partial x^2} - \frac{g_{22}}{r}\frac{\partial u^2}{\partial x^1} + \left(\frac{u^1}{r}\frac{\partial g_{11}}{\partial x^2} - \frac{u^2}{r}\frac{\partial g_{22}}{\partial x^1}\right)\\
&= \frac{1}{r}\frac{\partial u_r}{\partial \psi} - r\,\frac{\partial}{\partial r}\left(\frac{u_\psi}{r}\right) - 2\,\frac{u_\psi}{r}\\
&= \frac{1}{r}\frac{\partial u_r}{\partial \psi} - \frac{\partial u_\psi}{\partial r} - \frac{u_\psi}{r} = \frac{1}{r}\frac{\partial u_r}{\partial \psi} - \frac{1}{r}\frac{\partial r\,u_\psi}{\partial r},
\end{aligned}
\tag{A II.104}
$$

$$
\begin{aligned}
2\,\omega_{23} &= -\,2\,\omega_{32} = \frac{g_{22}}{r}\frac{\partial u^2}{\partial x^3} - \frac{g_{33}}{r}\frac{\partial u^3}{\partial x^2} + \left(\frac{u^2}{r}\frac{\partial g_{22}}{\partial x^3} - \frac{u^3}{r}\frac{\partial g_{33}}{\partial x^2}\right)\\
&= r\,\frac{\partial}{\partial x}\left(\frac{u_\psi}{r}\right) - \frac{1}{r}\frac{\partial u_z}{\partial \psi} = \frac{\partial u_\psi}{\partial x} - \frac{1}{r}\frac{\partial u_z}{\partial \psi},
\end{aligned}
$$

$$
2\,\omega_{31} = -\,2\,\omega_{13} = \frac{g_{33}}{r}\frac{\partial u^3}{\partial x^1} - \frac{g_{11}}{r}\frac{\partial u^1}{\partial x^3} = \frac{1}{r}\frac{\partial u_z}{\partial r} - \frac{1}{r}\frac{\partial u_r}{\partial x}
$$

or

$$\omega^1 = \omega_{32} = \frac{1}{2}\left(\frac{1}{r}\frac{\partial u_x}{\partial \psi} - \frac{\partial u_\psi}{\partial x}\right) = \omega_r,$$

$$\omega^2 = r\,\omega_{13} = \frac{1}{2}\left(\frac{\partial u_r}{\partial x} - \frac{\partial u_x}{\partial r}\right) = \omega_\psi, \qquad \text{(A II.105)}$$

$$\omega^3 = \omega_{21} = \frac{1}{2}\left(\frac{1}{r}\frac{\partial r\,u_\psi}{\partial r} - \frac{1}{r}\frac{\partial u_r}{\partial \psi}\right) = \omega_x,$$

in *polar spherical coordinates:*

$$u^1 = u_r, \qquad x^1 = r, \qquad g_{11} = 1,$$

$$u^2 = u_\phi/r, \qquad x^2 = \phi, \qquad g_{22} = (r)^2, \qquad \sqrt{g} = (r)^2 \sin\phi.$$

$$u^3 = u_\psi/r\sin\phi, \qquad x^3 = \psi, \qquad g_{33} = (r)^2\sin^2\phi, \qquad \text{(A II.106)}$$

Thus:

$$2\,\omega_{11} = 2\,\omega_{22} = 2\,\omega_{33} = 0,$$

$$2\,\omega_{12} = -\,2\,\omega_{21} = \frac{g_{11}}{(r)^2\sin\phi}\frac{\partial u^1}{\partial x^2} - \frac{g_{22}}{(r)^2\sin\phi}\frac{\partial u^2}{\partial x^1} + \left(\frac{u^1}{(r)^2\sin\phi}\frac{\partial g_{11}}{\partial x^2} - \frac{u^2}{(r)^2\sin\phi}\frac{\partial g_{22}}{\partial x^1}\right)$$

$$= \frac{1}{(r)^2\sin\phi}\frac{\partial u_r}{\partial\phi} - \frac{1}{\sin\phi}\frac{\partial}{\partial r}\left(\frac{u_\phi}{r}\right) - \frac{2\,u_\phi}{(r)^2\sin\phi}$$

$$= \frac{1}{r\sin\phi}\left(\frac{1}{r}\frac{\partial u_r}{\partial\phi} - \frac{1}{r}\frac{\partial r\,u_\phi}{\partial r}\right),$$

$$2\,\omega_{23} = -\,2\,\omega_{32} = \frac{g_{22}}{(r)^2\sin\phi}\frac{\partial u^2}{\partial x^3} - \frac{g_{33}}{(r)^2\sin\phi}\frac{\partial u^3}{\partial x^2} + \left(\frac{u^2}{(r)^2\sin\phi}\frac{\partial g_{22}}{\partial x^3} - \frac{u^3}{(r)^2\sin\phi}\frac{\partial g_{33}}{\partial x^2}\right)$$

$$= \frac{1}{\sin\phi}\frac{\partial}{\partial\psi}\left(\frac{u_\phi}{r}\right) - \sin\phi\frac{\partial}{\partial\phi}\left(\frac{u_\psi}{r\sin\phi}\right) - \frac{2\,u_\psi\,(r)^2}{(r)^3\sin^2\phi}\sin\phi\cos\phi$$

$$= \frac{1}{r\sin\phi}\frac{\partial u_\phi}{\partial\psi} - \frac{\sin\phi}{r}\frac{\partial}{\partial\phi}\left(\frac{u_\psi}{\sin\phi}\right) - \frac{2\,u_\psi}{r\sin\phi}\cot\phi \qquad \text{(A II.107)}$$

$$= \frac{1}{r\sin\phi}\left\{\frac{\partial u_\phi}{\partial\psi} - \left[\sin\phi\frac{\partial}{\partial\phi}\left(\frac{u_\psi}{\sin\phi}\right) + 2\,u_\psi\cot\phi\right]\right\}$$

$$= \frac{1}{r\sin\phi}\left\{\frac{\partial u_\phi}{\partial\psi} - \frac{\partial u_\psi\sin\phi}{\partial\phi}\right\},$$

$$2\,\omega_{31} = -\,2\,\omega_{13} = \frac{g_{33}}{(r)^2 \sin\phi}\frac{\partial u^3}{\partial x^1} - \frac{g_{11}}{(r)^2 \sin\phi}\frac{\partial u^1}{\partial x^3}$$

$$+\left(\frac{u^3}{(r)^2 \sin\phi}\frac{\partial g_{33}}{\partial x^1} - \frac{u^1}{(r)^2 \sin\phi}\frac{\partial g_{11}}{\partial x^3}\right)$$

$$= \sin\phi\,\frac{\partial}{\partial r}\left(\frac{u_\psi}{r\sin\phi}\right) - \frac{1}{(r)^2 \sin\phi}\frac{\partial r}{\partial \psi} + \frac{2\,u_\psi}{(r)^3 \sin^2\phi}\,r\sin^2\phi$$

$$= \frac{1}{r\sin\phi}\left\{r\sin^2\phi\,\frac{\partial}{\partial r}\left(\frac{u_\psi}{r\sin\phi}\right) - \frac{1}{r}\frac{\partial u_r}{\partial \psi} + \frac{2\,u_\psi}{r}\sin\phi\right\}$$

$$= \frac{1}{(r)^2 \sin\phi}\left\{\sin\phi\,\frac{\partial r\,u_\psi}{\partial r} - \frac{\partial u_r}{\partial \psi}\right\},$$

or

$$\omega^1 = \omega_{32} = \frac{1}{2\,r\sin\phi}\left(\frac{\partial u_\psi \sin\phi}{\partial \phi} - \frac{\partial u_\phi}{\partial \psi}\right) = \omega_r,$$

$$\omega^2 = r\,\omega_{13} = \frac{1}{2\,r\sin\phi}\left(\frac{\partial u_r}{\partial \psi} - \frac{\partial r\,u_\psi \sin\phi}{\partial r}\right) = \omega_\phi, \qquad \text{(A II.108)}$$

$$\omega^3 = (r\sin\phi)\,\omega_{21} = \frac{1}{2\,r}\left(\frac{\partial r\,u_\phi}{\partial r} - \frac{\partial u_r}{\partial \phi}\right) = \omega_\psi.$$

AII-5. Navier-Stokes Equation

If $\rho\,\Phi^i\,\delta V$ are the components of body force on the matter contained in a volume element of infinitesimal size, then at any time θ D'Alembert's (*4*) principle may be applied to give

$$\rho\,a^i = \rho\,\Phi^i + \tau^{ij}_{,j}. \qquad \text{(A II.109)}$$

This is a very general statement of the principle of conservation of momentum. It states that the product of mass and acceleration for a specific quantity of matter is equal to the sum of the surface and body forces acting upon this matter. For a Newtonian fluid D'Alembert's principle becomes the Navier-Stokes equation. Thus

$$a^i = \Phi^i + \frac{1}{\rho}\tau^{ij}_{,j}, \qquad \text{(A II.110)}$$

in *rectangular Cartesian coordinates:*

$$a_z = \Phi_z - \frac{1}{\rho}\frac{\partial P}{\partial z} + \frac{\nu}{3}\frac{\partial}{\partial z}u^{\beta}_{,\beta} + \nu\left(\frac{\partial^2 u_z}{\partial z^2} + \frac{\partial^2 u_z}{\partial y^2} + \frac{\partial^2 u_z}{\partial x^2}\right),$$

$$a_y = \Phi_y - \frac{1}{\rho}\frac{\partial P}{\partial y} + \frac{\nu}{3}\frac{\partial}{\partial y}u^{\beta}_{,\beta} + \nu\left(\frac{\partial^2 u_y}{\partial z^2} + \frac{\partial^2 u_y}{\partial y^2} + \frac{\partial^2 u_y}{\partial x^2}\right), \quad \text{(A II.111)}$$

$$a_x = \Phi_x - \frac{1}{\rho}\frac{\partial P}{\partial z} + \frac{\nu}{3}\frac{\partial}{\partial x}u^{\beta}_{,\beta} + \nu\left(\frac{\partial^2 u_x}{\partial z^2} + \frac{\partial^2 u_x}{\partial y^2} + \frac{\partial^2 u_x}{\partial x^2}\right).$$

$$u^{\beta}_{,\beta} = \frac{\partial u_z}{\partial z} + \frac{\partial u_y}{\partial y} + \frac{\partial u_x}{\partial x}. \quad \text{(A II.112)}$$

$$a_z = \frac{\partial u_z}{\partial \theta} + u_z\frac{\partial u_z}{\partial z} + u_y\frac{\partial u_z}{\partial y} + u_x\frac{\partial u_z}{\partial x},$$

$$a_y = \frac{\partial u_y}{\partial \theta} + u_z\frac{\partial u_y}{\partial z} + u_y\frac{\partial u_y}{\partial y} + u_x\frac{\partial u_y}{\partial x}, \quad \text{(A II.113)}$$

$$a_x = \frac{\partial u_x}{\partial \theta} + u_z\frac{\partial u_x}{\partial z} + u_x\frac{\partial u_x}{\partial y} + u_x\frac{\partial u_x}{\partial x},$$

in *polar cylindrical coordinates:*

$$a_r = \Phi_r - \frac{1}{\rho}\frac{\partial P}{\partial r} + \frac{\nu}{3}\frac{\partial}{\partial r}u^{\beta}_{,\beta} + \nu\left\{\frac{\partial^2 u_r}{\partial r^2} + \frac{1}{r}\frac{\partial u_r}{\partial r} + \frac{1}{(r)^2}\frac{\partial^2 u_r}{\partial \psi^2} + \frac{\partial^2 u_r}{\partial x^2} - \frac{u_r}{(r)^2} - \frac{2}{(r)^2}\frac{\partial u_\psi}{\partial \psi}\right\},$$

$$a_\psi = \Phi_\psi - \frac{1}{\rho r}\frac{\partial P}{\partial \psi} + \frac{\nu}{3r}\frac{\partial}{\partial \psi}u^{\beta}_{,\beta} + \nu\left\{\frac{\partial^2 u_\psi}{\partial r^2} + \frac{1}{r}\frac{\partial u_\psi}{\partial r} + \frac{1}{(r)^2}\frac{\partial^2 u_\psi}{\partial \psi^2} + \frac{\partial^2 u_\psi}{\partial x^2} - \frac{u_\psi}{(r)^2} + \frac{2}{(r)^2}\frac{\partial u_r}{\partial \psi}\right\}, \quad \text{(A II.114)}$$

$$a_x = \Phi_x - \frac{1}{\rho}\frac{\partial P}{\partial x} + \frac{\nu}{3}\frac{\partial}{\partial x}u^{\beta}_{,\beta} + \nu\left\{\frac{\partial^2 u_x}{\partial r^2} + \frac{1}{r}\frac{\partial u_x}{\partial r} + \frac{1}{(r)^2}\frac{\partial^2 u_x}{\partial \psi^2} + \frac{\partial^2 u_x}{\partial x^2}\right\},$$

$$u^{\beta}_{,\beta} = \frac{1}{r}\frac{\partial}{\partial r}(r\,u_r) + \frac{1}{r}\frac{\partial u_\psi}{\partial \psi} + \frac{\partial u_x}{\partial x}, \quad \text{(A II.115)}$$

$$a_r = \frac{\partial u_r}{\partial \theta} + u_r\frac{\partial u_r}{\partial r} + \frac{u_\psi}{r}\frac{\partial u_r}{\partial \psi} + u_x\frac{\partial u_r}{\partial x} - \frac{{u_\psi}^2}{r},$$

$$a_\psi = \frac{\partial u_\psi}{\partial \theta} + u_r\frac{\partial u_\psi}{\partial r} + \frac{u_\psi}{r}\frac{\partial u_\psi}{\partial \psi} + u_x\frac{\partial u_\psi}{\partial x} + \frac{u_r u_\psi}{r}, \quad \text{(A II.116)}$$

$$a_x = \frac{\partial u_x}{\partial \theta} + u_r\frac{\partial u_x}{\partial r} + \frac{u_\psi}{r}\frac{\partial u_x}{\partial \psi} + u_x\frac{\partial u_x}{\partial x},$$

in *polar spherical coordinates:*

$$a_r = \Phi_r - \frac{1}{\rho}\frac{\partial P}{\partial r} + \frac{\nu}{3}\frac{\partial}{\partial r}u^{\beta}_{,\beta} + \nu\left\{\frac{1}{(r)^2}\frac{\partial}{\partial r}\left((r)^2\frac{\partial u_r}{\partial r}\right) + \frac{1}{(r)^2\sin\phi}\frac{\partial}{\partial\phi}\left(\sin\phi\frac{\partial u_r}{\partial\phi}\right)\right.$$
$$\left. + \frac{1}{(r)^2\sin^2\phi}\frac{\partial^2 u_r}{\partial\phi^2} - \frac{2u_r}{(r)^2} - \frac{2}{(r)^2}\frac{\partial u_\phi}{\partial\phi} - \frac{2u_\phi\cot\phi}{(r)^2} - \frac{2}{(r)^2\sin\phi}\frac{\partial u_\psi}{\partial\psi}\right\},$$

$$a_\phi = \Phi_\phi - \frac{1}{\rho r}\frac{\partial P}{\partial\phi} + \frac{\nu}{3r}\frac{\partial}{\partial\phi}u^{\beta}_{,\beta} + \nu\left\{\frac{1}{(r)^2}\frac{\partial}{\partial r}\left((r)^2\frac{\partial u_\phi}{\partial r}\right)\right.$$
$$+ \frac{1}{(r)^2\sin\phi}\frac{\partial}{\partial\phi}\left(\sin\phi\frac{\partial u_\phi}{\partial\phi}\right) + \frac{1}{(r)^2\sin^2\phi}\frac{\partial^2 u_\phi}{\partial\psi^2} \qquad \text{(A II.117)}$$
$$\left. + \frac{2}{(r)^2}\frac{\partial u_r}{\partial\phi} - \frac{u_\phi}{(r)^2\sin^2\phi} - \frac{2\cos\phi}{(r)^2\sin^2\phi}\frac{\partial u_\psi}{\partial\psi}\right\},$$

$$a_\psi = \Phi_\psi - \frac{1}{\rho r\sin\phi}\frac{\partial P}{\partial\psi} + \frac{\nu}{3r\sin\phi}\frac{\partial}{\partial\psi}u^{\beta}_{,\beta} + \nu\left\{\frac{1}{(r)^2}\frac{\partial}{\partial r}\left((r)^2\frac{\partial u_\psi}{\partial r}\right)\right.$$
$$+ \frac{1}{(r)^2\sin\phi}\frac{\partial}{\partial\phi}\left(\sin\phi\frac{\partial u_\psi}{\partial\phi}\right) + \frac{1}{(r)^2\sin^2\phi}\frac{\partial^2 u_\psi}{\partial\psi^2} - \frac{u_\psi}{(r)^2\sin^2\phi}$$
$$\left. + \frac{2}{(r)^2\sin\phi}\frac{\partial u_r}{\partial\psi} + \frac{2\cos\phi}{(r)^2\sin^2\phi}\frac{\partial u_\phi}{\partial\psi}\right\},$$

$$u^{\beta}_{,\beta} = \frac{1}{(r)^2}\frac{\partial}{\partial r}\left((r)^2 u_r\right) + \frac{1}{r\sin\phi}\frac{\partial}{\partial\phi}\left(u_\phi\sin\phi\right) + \frac{1}{r\sin\phi}\frac{\partial u_\psi}{\partial\psi}, \qquad \text{(A II.118)}$$

$$a_r = \frac{\partial u_r}{\partial\theta} + u_r\frac{\partial u_r}{\partial r} + \frac{u_\phi}{r}\frac{\partial u_r}{\partial\phi} + \frac{u_\psi}{r\sin\phi}\frac{\partial u_r}{\partial\psi} - \frac{u_\phi{}^2 + u_\psi{}^2}{r},$$

$$a_\phi = \frac{\partial u_\phi}{\partial\theta} + u_r\frac{\partial u_\phi}{\partial r} + \frac{u_\phi}{r}\frac{\partial u_\phi}{\partial\phi} + \frac{u_\psi}{r\sin\phi}\frac{\partial u_\phi}{\partial\psi} + \frac{u_r u_\phi}{r} - \frac{u_\psi{}^2\cot\phi}{r}, \qquad \text{(A II.119)}$$

$$a_\psi = \frac{\partial u_\psi}{\partial\theta} + u_r\frac{\partial u_\psi}{\partial r} + \frac{u_\phi}{r}\frac{\partial u_\psi}{\partial\phi} + \frac{u_\psi}{r\sin\phi}\frac{\partial u_\psi}{\partial\psi} + \frac{u_r u_\psi}{r} - \frac{u_\phi u_\psi\cot\phi}{r}.$$

A II-6. Reynolds Stresses

In a stream

$$\frac{\partial\sigma u^i}{\partial\theta} + (\sigma u^i u^j)_{,j} = g_c\tau^{ij}_{,j} + \sigma\Phi^i \qquad \text{(A II.120)}$$

expresses the principle of conservation of momentum (7). This may be rewritten as

$$\frac{\partial\sigma u^i}{\partial\theta} = (g_c\tau^{ij} - \sigma u^i u^j)_{,j} + \sigma\Phi^i. \qquad \text{(A II.121)}$$

In the Reynolds transformation the following substitution is made:

$$\sigma = \overline{\sigma} + \sigma_f, \tag{A II.122}$$

$$u^i = \overline{u}^i + u_f \tag{A II.123}$$

to give

$$\frac{\partial}{\partial\theta}(\overline{\sigma}\,\overline{u}^i + \overline{\sigma}\,\overline{u_f^i} + \sigma_f\,\overline{u}^i + \sigma_f u_f) = \overline{\sigma}\,\Phi^i + \sigma_f \Phi^i + (g_c\,\tau^{ij} - \overline{\sigma}\,\overline{u}^i\,\overline{u}^j \tag{A II.124}$$
$$- \overline{\sigma}\,\overline{u}^i\,u_f^j - \overline{\sigma}\,u_f^i\,\overline{u}^j - \overline{\sigma}\,\overline{u_f^i\,u_f^j} - \sigma_f\,\overline{u}^i\,\overline{u}^j - \sigma_f\,\overline{u}^i\,u_f^j - \sigma_f u_f\,\overline{u}^j - \sigma_f\,\overline{u_f^i\,u_f^j})_{,j}.$$

Now

$$\overline{u}^i = \frac{1}{\theta}\int_{\theta_0-\frac{1}{2}\theta}^{\theta_0+\frac{1}{2}\theta} u^i\,d\vartheta \qquad \text{and} \qquad \overline{\sigma} = \frac{1}{\theta}\int_{\theta_0-\frac{1}{2}\theta}^{\theta_0+\frac{1}{2}\theta} \sigma\,d\vartheta\,. \tag{A II.125}$$

Consequently, if A and B are dependent variables being averaged and s is one of the independent variables,

$$\begin{aligned} \overline{\frac{\partial A}{\partial s}} &= \frac{\partial \overline{A}}{\partial s}, \\ \overline{A_{,j}} &= \overline{A}_{,j}, \\ \overline{\overline{A}\,B} &= \overline{A}\,\overline{B}, \\ \overline{A_f} &= 0. \end{aligned} \tag{A II.126}$$

thus

$$\frac{\partial}{\partial\theta}(\overline{\sigma}\,\overline{u}^i + \overline{\sigma_f\,u_f^i}) = \sigma\,\Phi^i + (g_c\,\overline{\tau}^{ij} - \overline{\sigma}\,\overline{u}^i\,\overline{u}^j - \overline{\sigma}\,\overline{u_f^i\,u_f^j} - \overline{u}^i\,\overline{\sigma_f\,u_f^j} \tag{A II.127}$$
$$- u^j\,\overline{\sigma_f\,u_f^i} - \overline{\sigma_f\,u_f^i\,u_f^j})_{,j}$$

If the fluid is "incompressible with respect to the turbulent fluctuations", then $\sigma_f \equiv 0$ and

$$\frac{\partial(\overline{\sigma}\,\overline{u}^i)}{\partial\theta} = \sigma\,\Phi^i + (g_c\,\overline{\tau}^{ij} - \overline{\sigma}\,\overline{u}^i\,\overline{u}^j - \overline{\sigma}\,\overline{u_f^i u_f^j})_{,j} \tag{A II.128}$$

the quantities $-\overline{\sigma}\,\overline{u_f^i\,u_f^j}/g_c$ are called the "Reynolds stresses." Let $\overline{\rho} = \overline{\sigma}/g_c$ If τ^{ij} is the Newtonian stress tensor, then

$$\tau^{ij} = g^{kj}\,\tau_k^i = -\left(P + \frac{2}{3}u^{\beta}_{,\beta}\right)\delta_k^i\,g^{kj} + \eta\,g^{kj}\,g^{il}\,(u_{l,k} + u_{k,l}) \tag{A II.129}$$

and

$$\bar{\tau}^{ij} = -\left(P + \frac{2}{3}\bar{u}^{\beta}_{,\beta}\right)\delta^i_k g^{kj} + \eta\, g^{kj}\, g^{il}\,(\bar{u}_{l,k} + \bar{u}_{k,l}). \qquad \text{(A II.130)}$$

The quantity $(\bar{\tau}^{ij} - \bar{\sigma}\,\overline{u'^i_f u'^j_f})/g_c)$ is the turbulent stress tensor. The expression

$$\frac{\partial(\bar{\sigma}\,\bar{u}^i)}{\partial\theta} + (\bar{\sigma}\,\bar{u}^i\,\bar{u}^j)_{,j} = \bar{\sigma}\,\frac{\partial\bar{u}^i}{\partial\theta} + \bar{u}^i\,(\bar{\sigma}\,\bar{u}^j)_{,j} + \bar{u}^j\,\bar{\sigma}\,\bar{u}^i_{,j} + \bar{u}^i\,\frac{\partial\bar{\sigma}}{\partial\theta} \qquad \text{(A II.131)}$$

reduces to

$$\frac{\partial(\bar{\sigma}\,\bar{u}^i)}{\partial\theta} + (\bar{\sigma}\,\bar{u}^i\,\bar{w}^j)_{,j} = \bar{\sigma}\,\bar{a}^i. \qquad \text{(A II.132)}$$

since

$$u^i\left(\frac{\partial\bar{\sigma}}{\partial\theta} + (\bar{\sigma}\,\bar{u}^j)_{,j}\right) = 0 \qquad \text{(A II.133)}$$

by the equation of continuity. If external force fields are neglected

$$\bar{\rho}\,\bar{a}^i = \left(\bar{\tau}^{ij} - \bar{\rho}\,\overline{(u'^i_f u'^j_f)}\right)_{,j}. \qquad \text{(A II.134)}$$

For idealized flow $\bar{a}^i = 0$ and $\bar{\rho}$ = constant,

$$\rho\,\overline{(u'^i_f u'^j_f)}_{,j} = \tau^{ij}_{,j}, \qquad \text{(A II.135)}$$

$$(u'^i_f u'^j_f)_{,j} = \frac{\partial}{\partial x^j}\overline{(u'^i_f u'^j_f)} + \Gamma^i_{kj}\,\overline{(u'^k_f u'^j_f)} + \Gamma^j_{kj}\,\overline{(u'^i_f u'^k_f)}. \qquad \text{(A II.136)}$$

Idealized Flow Between Infinite Parallel Plates

Idealized flow between infinite parallel plates may be defined by the following relationship:

$$\begin{gathered}\bar{u}_y = 0,\\ \bar{u}_z = 0,\\ \Gamma^i_{kj} \equiv 0,\\ \frac{\partial}{\partial x^1}\overline{(u'^i_f u'^1_f)} = 0,\\ \frac{\partial}{\partial x^3}\overline{(u'^i_f u'^3_f)} = 0,\\ \frac{\partial P}{\partial y} = \frac{\partial P}{\partial z} = 0\end{gathered} \qquad \text{(A II.137)}$$

because the coordinates are rectangular Cartesian, i.e.,

$$\begin{aligned} x^1 &= z, \\ x^2 &= y, \\ x^3 &= x \end{aligned} \tag{A II.138}$$

and because the average quantities are uniform in the x- and z-directions. The flow is in the x-direction and the plate separation is $2\,y_0$. Thus

$$\begin{aligned} \rho\,\overline{(u_f^1 u_f^j)}_{,j} &= \rho\,\frac{\partial}{\partial x^2}\,\overline{(u_f^1 u_f^2)} = \overline{\tau^{1j}_{,j}} = \frac{\partial \tau^{11}}{\partial x^1} + \frac{\partial \tau^{12}}{\partial x^2} + \frac{\partial \tau^{13}}{\partial x^3} = 0, \\ \rho\,\overline{(u_f^2 u_f^j)}_{,j} &= \rho\,\frac{\partial}{\partial x^2}\,\overline{(u_f^2 u_f^2)} = \overline{\tau^{2j}_{,j}} = \frac{\partial \tau^{21}}{\partial x^1} + \frac{\partial \tau^{22}}{\partial x^2} + \frac{\partial \tau^{23}}{\partial x^3} = 0, \\ \rho\,\overline{(u_f^3 u_f^j)}_{,j} &= \rho\,\frac{\partial}{\partial x^2}\,\overline{(u_f^3 u_f^2)} = \overline{\tau^{3j}_{,j}} = \frac{\partial \tau^{31}}{\partial x^1} + \frac{\partial \tau^{32}}{\partial x^2} + \frac{\partial \tau^{33}}{\partial x^3} = -\frac{\partial P}{\partial x} + \frac{\partial}{\partial y}\left(\eta\,\frac{\partial \overline{u_x}}{\partial y}\right). \end{aligned} \tag{A II.139}$$

Since $\partial P/\partial x$ is independent of y, these equations may be integrated to give

$$\begin{aligned} \rho\,\overline{u_f^1 u_f^2} &= A(x), \\ \rho\,\overline{u_f^2 u_f^2} &= B(x), \\ \rho\,\overline{u_f^3 u_f^2} &= \eta\,\frac{\partial \overline{u_x}}{\partial y} - y\,\frac{\partial P}{\partial x} + C(x). \end{aligned} \tag{A II.140}$$

When $y = 0$, $u_f^1 u_f^2$ and $u_f^3 u_f^2$ are just as likely to be negative as positive because of the symmetry of flow. Hence $\overline{u_f^1 u_f^2}$ and $\overline{u_f^3 u_f^2}$ are zero at $y = 0$; consequently $A(x)$ and $C(x) = 0$. Since time averages are independent of x, $B(x) =$ constant > 0. Thus

$$\begin{aligned} \rho\,\overline{(u_{xf}\,u_{yf})} &= 0, \\ \rho\,\overline{(u_{yf}\,u_{yf})} &= B > 0, \\ \rho\,\overline{(u_{yf}\,u_{xf})} &= \eta\,\frac{\partial \overline{u_x}}{\partial y} - y\,\frac{\partial P}{\partial x}. \end{aligned} \tag{A II.141}$$

Let

$$\overline{u_{yf}\,u_{yf}} = (U_y)^2 \qquad \text{and} \qquad \overline{u_{xf}\,u_{xf}} = (U_x)^2. \tag{A II.142}$$

The coefficient of correlation is R_{xy}, where

$$R_{xy} = \frac{\overline{u_{yf}\,u_{xf}}}{U_y\,U_x}. \tag{A II.143}$$

Since U_y is nearly equal to U_x, $R_{xy} \approx \overline{u_{yf} u_{xf}}/U_x^2$ or

$$R_{xy} \approx R'_{xy} = \frac{\eta}{U_x^2}\frac{\partial \overline{u_x}}{\partial y} - \frac{y}{U_x^2}\frac{\partial P}{\partial x}. \qquad \text{(A II.144)}$$

Goldstein (*5*) (p. 194) presents the information in Fig. A II-4 where curves (a) and (b) represent the results of two different investigators.

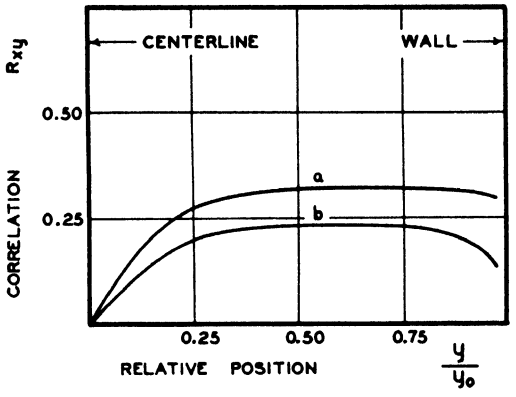

FIG. A II-4. Correlation in turbulent flow.

Idealized Flow in a Circular Conduit

Idealized flow in a circular conduit may be defined by the following relationship:

$$\begin{aligned} u^1 &= u_r, & x^1 &= r, & \Gamma^1_{22} &= -r, \\ u^2 &= u_\psi (r)^{-1}, & x^2 &= \psi, & \Gamma^2_{21} &= \Gamma^2_{12} = 1/r, \\ u^3 &= u_x, & x^3 &= x, & \text{all other } \Gamma^i_{jk} &\equiv 0, \end{aligned} \qquad \text{(A II.145)}$$

$$\begin{aligned} \overline{u_r} &= 0, & \frac{\partial}{\partial x^2}\overline{(u^i_f u^2_f)} &= 0, & \frac{\partial P}{\partial x^2} &= 0, \\ \overline{u_\psi} &= 0, & \frac{\partial}{\partial x^3}\overline{(u^i_f u^3_f)} &= 0, & \frac{\partial P}{\partial x^1} &= 0 \end{aligned} \qquad \text{(A II.146)}$$

because time average quantities are uniform in the ψ- and x-directions. Thus:

$$\rho\,\overline{(u^i_f u^j_f)}_{,j} = \overline{\tau}^{ij}_{,j} \qquad \text{(A II.147)}$$

$$\overline{\rho(u_f^1 u_f^j)_{,j}} = \rho \frac{\partial}{\partial x^1} \overline{(u_f^1 u_f^1)} + \rho \Gamma_{22}^1 \overline{(u_f^2 u_f^2)} + \rho \Gamma_{12}^2 \overline{(u_f^1 u_f^1)}$$

$$= \rho \frac{\partial}{\partial r} \overline{(u_f^1 u_f^1)} - \rho r \overline{(u_f^2 u_f^2)} + \frac{\rho}{r} \overline{(u_f^1 u_f^1)} = -\frac{\partial P}{\partial r} = 0,$$

$$\overline{\rho(u_f^2 u_f^j)_{,j}} = \rho \frac{\partial}{\partial x^1} \overline{(u_f^2 u_f^1)} + 3\rho \Gamma_{12}^2 \overline{(u_f^1 u_f^2)} = \rho \frac{\partial}{\partial r} \overline{(u_f^2 u_f^1)} + \frac{3\rho}{r} \overline{(u_f^1 u_f^2)} = 0,$$

$$\overline{\rho(u_f^3 u_f^j)_{,j}} = \rho \frac{\partial}{\partial x^1} \overline{(u_f^3 u_f^1)} + \rho \Gamma_{12}^2 \overline{(u_f^3 u_f^1)} \tag{A II.148}$$

$$= \rho \frac{\partial}{\partial r} \overline{(u_f^3 u_f^1)} + \frac{\rho}{r} \overline{(u_f^3 u_f^1)} = \frac{\rho}{r} \frac{\partial}{\partial r} \overline{(r u_f^3 u_f^1)}$$

$$= -\frac{\partial P}{\partial x} + \frac{\partial}{\partial r}\left(\eta \frac{\partial \overline{u_x}}{\partial r}\right) + \frac{\eta}{r} \frac{\partial \overline{u_x}}{\partial r} = -\frac{\partial P}{\partial x} + \frac{1}{r} \frac{\partial}{\partial r}\left(\eta r \frac{\partial \overline{u_x}}{\partial r}\right).$$

These equations may be rewritten as follows:

$$\frac{\partial}{\partial r} \overline{(r u_f^1 u_f^1)} = (r)^2 \overline{(u_f^2 u_f^2)}$$

$$\frac{\partial}{\partial r} \overline{(u_f^2 u_f^1)} = -\frac{3}{r} \overline{(u_f^2 u_f^1)} \tag{A II.149}$$

$$\rho \frac{\partial}{\partial r} \overline{(r u_f^3 u_f^1)} = \frac{\partial}{\partial r}\left(\eta r \frac{\partial \overline{u_x}}{\partial r}\right) - r \frac{\partial P}{\partial x}.$$

The third equation may be integrated to give

$$\rho r \overline{(u_{xf} u_{rf})} = \eta r \frac{\partial \overline{u_x}}{\partial r} - \frac{r^2}{2} \frac{\partial P}{\partial x} + C(x), \tag{A II.150}$$

because time averages are uniform in the ψ- and x-directions. The quantity $C(x)$ is a constant; because of symmetry $C(x) \equiv 0$. Hence

$$\rho \overline{u_{xf} u_{rf}} = \eta \frac{\partial \overline{u_x}}{\partial r} - \frac{r}{2} \frac{\partial P}{\partial x}. \tag{A II.151}$$

AII-7. Bernoulli's Equation

The equations of motion for an invariant unit mass of material embedded in a continuous medium may be expressed (*4*)

$$\Phi^i + \frac{\tau^{ij}_{,j}}{\rho} = a^i \tag{A II.152}$$

where a^i is the ith-component of acceleration of this unit mass of material. Newton's second law of motion requires that a^i also be the ith-component of the total force impressed upon this unit mass to produce the acceleration. $\rho \Phi^i$ is the ith-component of the force which acts directly upon the mass of this closed system due to its position in a force field, and $(\tau^{ij}_{,j}/\rho)$ represents ith-component of the resultant surface force acting at the boundary of this closed system of unit mass with its surroundings.

The element of work w_v done by a force F^i in producing a displacement δx^j is defined

$$w_v = g_{ij} F^i \delta x^j. \tag{A II.153}$$

Here w_v is a scalar quantity and represents energy which has been transferred by the action of a force through a distance. The rate at which work is performed upon the unit mass system is

$$\lim_{\delta\theta \to 0} \frac{w_v}{\delta\theta} = \lim_{\delta\theta \to 0} \rho a^i \frac{\delta x^j}{\delta\theta} g_{ij} = \rho g_{ij} a^i w^j. \tag{A II.154}$$

Thus

$$g_{ij} a^i w^j = g_{ij} \Phi^i w^j + \frac{\tau^{ik}_{,k}}{\rho} g_{ij} w^j \tag{A II.155}$$

or

$$a^i u_i = \Phi^i u_i + \frac{\tau^{ik}_{,k}}{\rho} u_i = \Phi^i u_i + \frac{\tau^{ij}_{,j}}{\rho} u_i. \tag{A II.156}$$

The acceleration is the intrinsic derivative of the velocity. That is,

$$a^i = \frac{du^i}{d\theta} + \Gamma^i_{jk} w^j \frac{dx^k}{d\theta} = \frac{du^i}{d\theta} + \Gamma^i_{jk} w^j u^k. \tag{A II.157}$$

Therefore

$$u_i du^i + \Gamma^i_{jk} w^j u^k u_i d\theta = \Phi^i u_i d\theta + \frac{\tau^{ij}_{,j}}{\rho} u_i d\theta \tag{A II.158}$$

or

$$u_i du^i + g_{il} \Gamma^i_{jk} w^j u^k dx^l = g_{il} \Phi^i dx^l + \frac{\tau^{ij}_{,j}}{\rho} g_{il} dx^l. \tag{A II.159}$$

If the force field is assumed to be conservative and of uniform and invariant direction, then

$$g_{il}\Phi^i dx^l = \Phi_l dx^l = -g_c dh \tag{A II.160}$$

where h is the distance into the field in the direction of increasing potential energy. If this field is gravity, the g_c is the gravitational constant; further

$$u_i du^i = \frac{du_i u^i}{2} = \frac{d(u)^2}{2}. \tag{A II.161}$$

For a stream of fluid with uniform velocity profile,

$$\begin{gathered} w^j = u^k = 0, \\ g_{il}\Gamma^i_{jk} w^j u^k dx^l = 0. \end{gathered} \tag{A II.162}$$

Consequently

$$g_c dh + \frac{d(u)^2}{2} = d\left(g_c h + \frac{(u)^2}{2}\right) = \frac{\tau^{ij}_{,j}}{\rho} g_{il} dx^l = \frac{\tau^{ij}_{,j}}{\rho} u_i d\theta. \tag{A II.163}$$

Thus

$$\left\{g_c h + \frac{(u)^2}{2} - \int \frac{\tau^{ij}_{,j}}{\rho} g_{il} dx^l\right\}$$

is an invariant of the motion. If the substitution

$$(\tau^{ij} u_i)_{,j} = \tau^{ij}_{,j} u_i + \tau^{ij} u_{i,j} \tag{A II.164}$$

is made, then

$$d\left(g_c h + \frac{(u)^2}{2}\right) = \frac{(\tau^{ij} u_i)_{,j}}{\rho} d\theta - \frac{\tau^{ij} u_{i,j}}{\rho} d\theta. \tag{A II.165}$$

For a Newtonian fluid,

$$\begin{aligned} \tau^{ij} &= -\left(P + \frac{2}{3}\eta u^\beta_{,\beta}\right)\delta^i_l g^{lj} + \eta g^{lj} g^{ki}(u_{k,l} + u_{l,k}), \\ (\tau^{ij} u_{i,j}) &= -\left(P + \frac{2}{3}\eta u^\beta_{,\beta}\right) u_{i,j}\, \delta^i_l g^{lj} + \eta u_{i,j} g^{lj} g^{ki}(u_{k,l} + u_{l,k}) \\ &= -P g^{ij} u_{i,j} - \frac{2}{3}\eta u^\beta_{,\beta} u^j_{,j} + \eta u^k_{,j} g^{lj}(u_{k,l} + u_{l,k}), \end{aligned} \tag{A II.166}$$

$$(\tau^{ij} u_i)_{,j} = -(P u_i)_{,j}\, \delta^i_l g^{lj} - \frac{2}{3}\eta (u^\beta_{,\beta} u_i)_{,j}\, \delta^i_l g^{lj} + \eta g^{lj} g^{ki}(u_{k,l} u_i + u_{l,k} u_i)_{,j}, \tag{A II.167}$$

$$(\tau^{ij}u_i)_{,j} - (\tau^{ij}u_{i,j}) = -u_i P_{,j} g^{ij} - \frac{2}{3}\eta(u^{\beta}_{,\beta} u_i)_{,j} g^{ij} + \eta g^{lj} g^{ki}(u_{k,l} u_i + u_{l,k} u_i)_{,j}$$

$$+ \frac{2}{3}\eta(u^{\beta}_{,\beta})^2 - \eta g^{lj} u^{k}_{,j}(u_{k,l} + u_{l,k}). \qquad \text{(A II.168)}$$

But

$$u_i P_{,j} g^{ij} d\theta = g^{ij}\frac{\partial P}{\partial x^j} g_{il} dx^l = \frac{\partial P}{\partial x^j}\delta^j_l dx^l = \frac{\partial P}{\partial x^j} dx^j. \qquad \text{(A II.169)}$$

Thus

$$\frac{d}{d\theta}\left(h + \frac{(u)^2}{2g_c}\right) + V\frac{\partial P}{\partial x^j}\frac{dx^j}{d\theta} = -\frac{2}{3}\frac{\eta}{\sigma}(u_i u^{\beta}_{,\beta})_{,j} g^{ij} + \frac{\eta}{\sigma} g^{lj} g^{ki}(u_{k,l} u_i + u_{l,k} u_i)_{,j} - \mathring{j} \qquad \text{(A II.170)}$$

where

$$\mathring{j} = -\frac{2}{3}\frac{\eta}{\sigma}(u^{\beta}_{,\beta})^2 + \frac{\eta}{\sigma} g^{lj} u^{k}_{,j}(u_{k,l} + u_{l,k}) \qquad \text{(A II.171)}$$

which equals the Reynolds dissipation function (8). Writing j' for $\mathring{j}\, d\theta$

$$dh + \frac{d(u)^2}{2g_c} + V\frac{\partial P}{\partial x^j} dx^j + j' = -\zeta \qquad \text{(A II.172)}$$

where

$$\zeta = \left(\frac{2}{3}\frac{\eta}{\sigma}(u_i u^{\beta}_{,\beta})_{,j} g^{ij} - \frac{\eta}{\sigma} g^{lj} g^{ki}(u_i u_{k,l} + u_i u_{l,k})_{,j}\right) d\theta. \qquad \text{(A II.173)}$$

Clearly

$$\zeta = -(u_i \tau^{ij} + u_i P \delta^i_l g^{lj})_{,j}\, d\theta \qquad \text{(A II.174)}$$

by Gauss' theorem (divergence theorem)

$$\int_V (\tau^{ij} u_i + u_i P \delta^i_j g^{lj})_{,j}\, dV = \int_\Sigma u_i(\tau^{ij} + P\delta^i_l g^{lj}) n_j\, d\Sigma = \int_\Sigma u_i(\tau^i_l + P\delta^i_l)\, n^l\, d\Sigma \qquad \text{(A II.175)}$$

where n^l is the unit normal to the boundary surface Σ. But $-u_i(\tau^i_l + P\delta^i_l)\, n^l$ is the rate at which the unit mass system does work on its surroundings as the consequence of velocity gradients existing at the boundary. Thus

$$dh + \frac{d(u)^2}{2\,g_c} + V\frac{\partial P}{\partial x^j}dx^j + j' + \zeta' = 0 \qquad \text{(A II.176)}$$

for a closed system which flows along with the fluid stream provided that the velocity profile is uniform in the direction of flow. In the integration of this equation, h and $(u)^2/2\,g_c$ depend only upon the initial and final states of the system, i.e., dh and $d(u)^2/2\,g_c$ are exact differentials. The integrals of the other three terms depend upon the trajectory.

In practical applications, the unit mass of fluid is assumed to have properties which correspond to the bulk average properties of the stream. The boundary of the stream is so chosen that the net work due to velocity gradients is zero; however, when work is done on the stream at some point between the entrance and exit sections, account must be taken of it as though it arose through the action of the viscosity and velocity gradients simply because work is not changed in character by changes in its origin.

In such cases j' must be interpreted as including all irreversible effects associated with such work in addition to the Reynolds dissipation function. If x^j is the direction of flow for such a system, then, replacing ζ by w',

$$dh + \frac{d(u)^2}{2\,g_c} + V\,dP + j' + w' = 0 \qquad \text{(A II.177)}$$

which is the familiar Bernoulli equation.

AII-8. Definition of Isotropic Turbulence

Assume that the velocity components in an infinite incompressible fluid may be measured and assume that the mean values of the velocity components are zero. This assumption implies that the coordinate system moves with the hydrodynamic velocity of the system and that the velocity profile of the system is a straight line. Homogeneous, isotropic turbulence may be defined (*9*) in mathematical terms by the assumptions (1) that the mean values of the squares and products of the velocity components and their derivatives are independent of the position of the point of observation and (*2*) that these mean values are also invariant with respect to rotation and reflection of the coordinate axes. While the mean values are, in general, functions of time, it may be assumed that the fluctuations are so rapid that the mean values can be determined over time intervals during which the variation of mean values is negligible.

In the following discussion of isotropic turbulence all tensors will be evaluated in rectangular Cartesian coordinates. The need for distinguishing between covariant and contravariant tensors is thereby circumvented.

Accordingly, the tensor indices have been moved to the covariant position to make the notation similar to that now in general use in discussions of isotropic turbulence. To avoid possible misinterpretation the summation convention has not been used subsequently. Since only fluctuating quantities are considered, the subscript f will be omitted.

AII-9. Derivation (10) of the Correlation Tensor for Isotropic Turbulence

Figure A II-5 shows the magnitudes and directions of the fluctuating components of velocity at the points B and B' referred to the rectangular Cartesian coordinates x_1, x_2, x_3. The distance from B to B' is r. If the turbulence is isotropic, then the probability of a fluctuation of size u is independent of direction and hence $\overline{u^2}$ is uniform in direction and may be

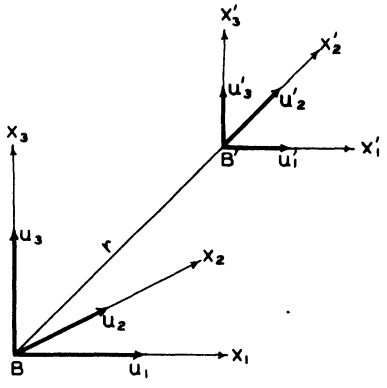

FIG. A II-5. General rectangular Cartesian coordinates.

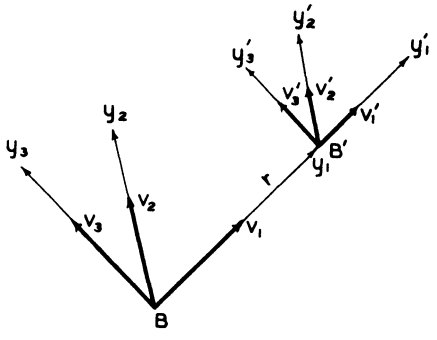

FIG. A II-6. Special rectangular Cartesian coordinates.

considered constant from B to B'. Figure A II-6 shows a particular rectangular Cartesian coordinate system so chosen that B' lies on one of the axes. If the components of the fluctuating velocity referred to a coordinate system obtained from that of Fig. A II-6 by rotation about the line BB' through π radians are designated V_1, V_2, V_3 and the coordinates Y_1, Y_2, Y_3, then

$$\begin{aligned} Y_1 &= y_1, & V_1 &= v_1, \\ Y_2 &= -y_2, & V_2 &= -v_2, \\ Y_3 &= -y_3, & V_3 &= -v_3 \end{aligned} \qquad \text{(A II.178)}$$

and hence

$$\begin{aligned} \overline{v_1 v_2'} &= -\overline{V_1 V_2'}, \\ \overline{v_1 v_3'} &= -\overline{V_1 V_3'}. \end{aligned} \qquad \text{(A II.179)}$$

Since the turbulence has been assumed to be isotropic, the change in sign obtained in this rotation of coordinates implies that

$$\overline{v_1 v_2'} \equiv \overline{v_1 v_3'} \equiv 0. \tag{A II.180}$$

Similarly, if the y_2-axis is reflected through the plane of y_1 and y_3, then

$$V_2 = -v_2 \qquad \text{and} \qquad \overline{V_3 V_2'} = -\overline{v_3 v_2'} \tag{A II.181}$$

which implies that

$$\overline{V_3 V_2'} = -\overline{v_3 v_2'} \equiv 0 \tag{A II.182}$$

by the assumption of isotropic turbulence. Clearly the identities expressed in Eqs. (A II.180) and (A II.182) presume that the coordinate system is chosen so that one of the axes lies along BB' and that the turbulence is isotropic. Only in such a coordinate system can the rotations and reflections which are required in the definition of isotropic turbulence be performed and yet leave the coordinates of B with respect to B' invariant.

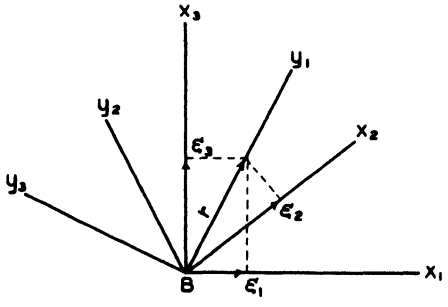

FIG. A II-7. General rectangular Cartesian coordinates.

Generally, the hydrodynamic problem is more interesting when expressed in the more general coordinates x_1, x_2, x_3. Figure A II-7 illustrates the transformation from the coordinates x_1, x_2, x_3 to the coordinates y_1, y_2, y_3 and the inverse transformation. The equations of transformation are

$$\begin{aligned} y_1 &= x_1 \cos\alpha_1 + x_2 \cos\beta_1 + x_3 \cos\gamma_1, \\ y_2 &= x_1 \cos\alpha_2 + x_2 \cos\beta_2 + x_3 \cos\gamma_2, \\ y_3 &= x_1 \cos\alpha_3 + x_2 \cos\beta_3 + x_3 \cos\gamma_3 \end{aligned} \tag{A II.183}$$

and

$$\begin{aligned} x_1 &= y_1 \cos\alpha_1 + y_2 \cos\alpha_2 + y_3 \cos\alpha_3 \\ x_2 &= y_1 \cos\beta_1 + y_2 \cos\beta_2 + y_3 \cos\beta_3, \\ x_3 &= y_1 \cos\gamma_1 + y_2 \cos\gamma_2 + y_3 \cos\gamma_3. \end{aligned} \tag{A II.184}$$

The equations may be written more conveniently in the form

$$\begin{bmatrix} y_1 \\ y_2 \\ y_3 \end{bmatrix} = \begin{bmatrix} \cos\alpha_1 & \cos\beta_1 & \cos\gamma_1 \\ \cos\alpha_2 & \cos\beta_2 & \cos\gamma_2 \\ \cos\alpha_3 & \cos\beta_3 & \cos\gamma_3 \end{bmatrix} \begin{bmatrix} x_1 \\ x_2 \\ x_3 \end{bmatrix} = \begin{bmatrix} l_1 & l_2 & l_3 \\ m_1 & m_2 & m_3 \\ n_1 & n_2 & n_3 \end{bmatrix} \begin{bmatrix} x_1 \\ x_2 \\ x_3 \end{bmatrix} \tag{A II.183'}$$

$$\begin{bmatrix} x_1 \\ x_2 \\ x_3 \end{bmatrix} = \begin{bmatrix} l_1 & m_1 & n_1 \\ l_2 & m_2 & n_2 \\ l_3 & m_3 & n_3 \end{bmatrix} \begin{bmatrix} y_1 \\ y_2 \\ y_3 \end{bmatrix}. \tag{A II.184'}$$

Substitution of (A II.184') into (A II.183') leads to

$$\begin{bmatrix} y_1 \\ y_2 \\ y_3 \end{bmatrix} = \begin{bmatrix} l_1 & l_2 & l_3 \\ m_1 & m_2 & m_3 \\ n_1 & n_2 & n_3 \end{bmatrix} \begin{bmatrix} l_1 & m_1 & n_1 \\ l_2 & m_2 & n_2 \\ l_3 & m_3 & n_3 \end{bmatrix} \begin{bmatrix} y_1 \\ y_2 \\ y_3 \end{bmatrix} = \begin{bmatrix} 1 & 0 & 0 \\ 0 & 1 & 0 \\ 0 & 0 & 1 \end{bmatrix} \begin{bmatrix} y_1 \\ y_2 \\ y_3 \end{bmatrix}. \tag{A II.185}$$

Carrying through the indicated matrix multiplication gives

$$\begin{aligned} l_1^2 + l_2^2 + l_3^2 &= 1, \\ m_1^2 + m_2^2 + m_3^2 &= 1, \\ n_1^2 + n_2^2 + n_3^2 &= 1, \\ l_1 m_1 + l_2 m_2 + l_3 m_3 &= 0, \\ l_1 n_1 + l_2 n_2 + l_3 n_3 &= 0, \\ m_1 n_1 + m_2 n_2 + m_3 n_3 &= 0. \end{aligned} \tag{A II.186}$$

Substitution of (A II.183') into (A II.184') leads to the following relations among the direction cosines:

$$\begin{aligned} l_1^2 + m_1^2 + n_1^2 &= 1, \\ l_2^2 + m_2^2 + n_2^2 &= 1, \\ l_3^2 + m_3^2 + n_3^2 &= 1, \\ l_1 l_2 + m_1 m_2 + n_1 n_2 &= 0, \\ l_1 l_3 + m_1 m_3 + n_1 n_3 &= 0, \\ l_2 l_3 + m_2 m_3 + n_2 n_3 &= 0. \end{aligned} \tag{A II.187}$$

Thus only three of the nine direction cosines are independent. Let these three be l_1, l_2, l_3. From Fig. A II-7,

$$\begin{aligned} l_1 &= \cos\alpha_1 = \xi_1/r, \\ l_2 &= \cos\beta_1 = \xi_2/r, \\ l_3 &= \cos\gamma_1 = \xi_3/r. \end{aligned} \tag{A II.188}$$

Differentiation of Eqs. (A II.183′) and (A II.184′) with respect to time gives the relationships among the components of velocity in the two coordinate systems:

$$\begin{bmatrix} v_1 \\ v_2 \\ v_3 \end{bmatrix} = \begin{bmatrix} l_1 & l_2 & l_3 \\ m_1 & m_2 & m_3 \\ n_1 & n_2 & n_3 \end{bmatrix} \begin{bmatrix} u_1 \\ u_2 \\ u_3 \end{bmatrix}, \tag{A II.189}$$

$$\begin{bmatrix} u_1 \\ u_2 \\ u_3 \end{bmatrix} = \begin{bmatrix} l_1 m_1 n_1 \\ l_2 m_2 n_2 \\ l_3 m_3 n_3 \end{bmatrix} \begin{bmatrix} v_1 \\ v_2 \\ v_3 \end{bmatrix}. \tag{A II.190}$$

The dyadic of the fluctuating velocity at B with that at B' is

$$\begin{bmatrix} u_1 \\ u_2 \\ u_3 \end{bmatrix} [u_1' \; u_2' \; u_3'] = \begin{bmatrix} u_1 u_1' & u_1 u_2' & u_1 u_3' \\ u_2 u_1' & u_2 u_2' & u_2 u_3' \\ u_3 u_1' & u_3 u_2' & u_3 u_3' \end{bmatrix}, \tag{A II.191}$$

$$\begin{bmatrix} u_1 \\ u_2 \\ u_3 \end{bmatrix} [u_1' \; u_2' \; u_3'] = \begin{bmatrix} l_1 m_1 n_1 \\ l_2 m_2 n_2 \\ l_3 m_3 n_3 \end{bmatrix} \begin{bmatrix} v_1 v_1' & v_1 v_2' & v_1 v_3' \\ v_2 v_1' & v_2 v_2' & v_2 v_3' \\ v_3 v_1' & v_3 v_2' & v_3 v_3' \end{bmatrix} \begin{bmatrix} l_1 & l_2 & l_3 \\ m_1 & m_2 & m_3 \\ n_1 & n_2 & n_3 \end{bmatrix}. \tag{A II.192}$$

The time average is defined

$$\overline{v_i v_j'} = \frac{1}{\theta} \int_{\theta_0 - \theta/2}^{\theta_0 + \theta/2} v_i v_j' \, d\theta. \tag{A II.193}$$

Since the direction cosines are independent of time,

$$\begin{bmatrix} \overline{u_1u_1'} & \overline{u_1u_2'} & \overline{u_1u_3'} \\ \overline{u_2u_1'} & \overline{u_2u_2'} & \overline{u_2u_3'} \\ \overline{u_3u_1'} & \overline{u_3u_2'} & \overline{u_3u_3'} \end{bmatrix} = \begin{bmatrix} l_1m_1n_1 \\ l_2m_2n_2 \\ l_3m_3n_3 \end{bmatrix} \begin{bmatrix} \overline{v_1v_1'} & 0 & 0 \\ 0 & \overline{v_2v_2'} & 0 \\ 0 & 0 & \overline{v_3v_3'} \end{bmatrix} \begin{bmatrix} l_1 & l_2 & l_3 \\ m_1 & m_2 & m_3 \\ n_1 & n_2 & n_3 \end{bmatrix} \tag{A II.194}$$

Use has been made of Eqs. (A II.182) and (A II.183) in writing Eq. (A II.194). From the symmetry shown in Fig. A II-6, it is apparent that

$$\overline{v_2v_2'} = \overline{v_3v_3'}. \tag{A II.195}$$

Thus

$$\begin{bmatrix} \overline{u_1u_1'} & \overline{u_1u_2'} & \overline{u_1u_3'} \\ \overline{u_2u_1'} & \overline{u_2u_2'} & \overline{u_2u_3'} \\ \overline{u_3u_1'} & \overline{u_3u_2'} & \overline{u_3u_3'} \end{bmatrix} = \begin{bmatrix} l_1\overline{v_1v_1'} & m_1\overline{v_2v_2'} & n_1\overline{v_2v_2'} \\ l_2\overline{v_1v_1'} & m_2\overline{v_2v_2'} & n_2\overline{v_2v_2'} \\ l_3\overline{v_1v_1'} & m_3\overline{v_2v_2'} & n_3\overline{v_2v_2'} \end{bmatrix} \begin{bmatrix} l_1 & l_2 & l_3 \\ m_1 & m_2 & m_3 \\ n_1 & n_2 & n_3 \end{bmatrix}$$

$$= \begin{bmatrix} l_1^2\,\overline{v_1v_1'} + m_1^2\,\overline{v_2v_2'} + n_1^2\,\overline{v_2v_2'} & l_1l_2\overline{v_1v_1'} + m_1m_2\overline{v_2v_2'} + n_1n_2\overline{v_2v_2'} \\ l_2l_1\overline{v_1v_1'} + m_2m_1\overline{v_2v_2'} + n_2n_1\overline{v_2v_2'} & l_2^2\,\overline{v_1v_1'} + m_2^2\,\overline{v_2v_2'} + n_2^2\,\overline{v_2v_2'} \\ l_3l_1\overline{v_1v_1'} + m_3m_1\overline{v_2v_2'} + n_3n_1\overline{v_2v_2'} & l_3l_2\overline{v_1v_1'} + m_3m_2\overline{v_2v_2'} + n_3n_2\overline{v_2v_2'} \end{bmatrix}$$

$$\begin{bmatrix} l_1l_3\,\overline{v_1v_1'} + m_1m_3\overline{v_2v_2'} + n_1n_3\overline{v_2v_2'} \\ l_2l_3\,\overline{v_1v_1'} + m_2m_3\overline{v_2v_2'} + n_2n_3\overline{v_2v_2'} \\ l_3^2\,\overline{v_1v_1'} + m_3^2\,\overline{v_2v_2'} + n_3^2\,\overline{v_2v_2'} \end{bmatrix} \tag{A II.196}$$

Substitution of Eqs. (A II.187) into Eq. (A II.196) gives

$$\begin{bmatrix} \overline{u_1u_1'} & \overline{u_1u_2'} & \overline{u_1u_3'} \\ \overline{u_2u_1'} & \overline{u_2u_2'} & \overline{u_2u_3'} \\ \overline{u_3u_1'} & \overline{u_3u_2'} & \overline{u_3u_3'} \end{bmatrix}$$

$$\begin{bmatrix} l_1^2\,(\overline{v_1v_1'} - \overline{v_2v_2'}) + \overline{v_2v_2'}, & l_1l_2\,(\overline{v_1v_1'} - \overline{v_2v_2'}) & l_1l_3\,(\overline{v_1v_1'} - \overline{v_2v_2'}), \\ l_2l_1\,(\overline{v_1v_1'} - \overline{v_2v_2'}), & l_2^2\,(\overline{v_1v_1'} - \overline{v_2v_2'}) + \overline{v_2v_2'}, & l_2l_3\,(\overline{v_1v_1'} - \overline{v_2v_2'}) \\ l_3l_1\,(\overline{v_1v_1'} - \overline{v_2v_2'}), & l_3^2\,(\overline{v_1v_1'} - \overline{v_2v_2'}), & l_3^2\,(\overline{v_1v_1'} - \overline{v_2v_2'}) + \overline{v_2v_2'} \end{bmatrix} \tag{A II.197}$$

$$= (\overline{v_1 v_1'} - \overline{v_2 v_2'}) \begin{bmatrix} l_1^2 & l_1 l_2 & l_1 l_3 \\ l_2 l_1 & l_2^2 & l_2 l_3 \\ l_3 l_1 & l_3 l_2 & l_3^2 \end{bmatrix} + \overline{v_2 v_2'} \begin{bmatrix} 1 & 0 & 0 \\ 0 & 1 & 0 \\ 0 & 0 & 1 \end{bmatrix} \quad \text{(A II.198)}$$

Substitution of Eqs. (A II.188) into Eq. (A II.198) gives

$$\begin{bmatrix} \overline{u_1 u_1'} & \overline{u_1 u_2'} & \overline{u_1 u_3'} \\ \overline{u_2 u_1'} & \overline{u_2 u_2'} & \overline{u_2 u_3'} \\ \overline{u_3 u_1'} & \overline{u_3 u_2'} & \overline{u_3 u_3'} \end{bmatrix} = \frac{(\overline{v_1 v_1'} - \overline{v_2 v_2'})}{(r)^2} \begin{bmatrix} (\xi_1)^2 & \xi_1 \xi_2 & \xi_1 \xi_3 \\ \xi_2 \xi_1 & (\xi_2)^2 & \xi_2 \xi_3 \\ \xi_3 \xi_1 & \xi_3 \xi_2 & (\xi_3)^2 \end{bmatrix} + \overline{v_2 v_2'} \begin{bmatrix} 1 & 0 & 0 \\ 0 & 1 & 0 \\ 0 & 0 & 1 \end{bmatrix} \quad \text{(A II.199)}$$

The two-point correlation tensor (*1*) for isotropic turbulence is defined to be R_{ij}, where

$$R_{ij} = \frac{1}{\overline{u^2}} \begin{bmatrix} \overline{u_1 u_1'} & \overline{u_1 u_2'} & \overline{u_1 u_3'} \\ \overline{u_2 u_1'} & \overline{u_2 u_2'} & \overline{u_2 u_3'} \\ \overline{u_3 u_1'} & \overline{u_3 u_2'} & \overline{u_3 u_3'} \end{bmatrix} = \frac{(f-g)}{(r)^2} \begin{bmatrix} (\xi_1)^2 & \xi_1 \xi_2 & \xi_1 \xi_3 \\ \xi_2 \xi_1 & (\xi_2)^2 & \xi_2 \xi_3 \\ \xi_3 \xi_1 & \xi_3 \xi_2 & (\xi_3)^2 \end{bmatrix} + g \begin{bmatrix} 1 & 0 & 0 \\ 0 & 1 & 0 \\ 0 & 0 & 1 \end{bmatrix} \quad \text{(A II.200)}$$

Equation (A II.200) shows that the correlation tensor may be expressed in terms of two scalar quantities f and g. (The symbols f and g are most frequently used in the literature on the correlation tensor but some authors (*11*) have preferred to use R_1 and R_2, respectively, for these quantities.)

Figures A II-5 and A II-7 show that the coordinates of B' in the (x_1, x_2, x_3)-system are ξ_1, ξ_2, ξ_3. For an *incompressible* fluid,

$$\frac{\partial u_1'}{\partial \xi_1} + \frac{\partial u_2'}{\partial \xi_2} + \frac{\partial u_3'}{\partial \xi_3} = 0. \quad \text{(A II.201)}$$

This equation is true irrespective of the location of the origin of the (x_1, x_2, x_3)-system and consequently also of the direction and magnitude of r or the location of the point B. Thus

$$u_j \frac{\partial u_1'}{\partial \xi_1} + u_j \frac{\partial u_2'}{\partial \xi_2} + u_j \frac{\partial u_3'}{\partial \xi_3} = 0. \quad \text{(A II.202)}$$

Since the velocities at B are independent of the location of the point B', it follows that

$$\frac{\partial}{\partial \xi_1}(\overline{u_j u_1'}) + \frac{\partial}{\partial \xi_2}(\overline{u_j u_2'}) + \frac{\partial}{\partial \xi_3}(\overline{u_j u_3'}) = 0. \quad \text{(A II.203)}$$

From Eq. (A II.193) the averaging operation is permissible since the length of time over which the average is taken is independent of the coordinates. The quantity $\overline{u^2}$ has been assumed to be uniform by the assumption of isotropic turbulence. Thus

$$\frac{\partial}{\partial \xi_1}\left(\frac{\overline{u_j u_1'}}{\overline{u^2}}\right) + \frac{\partial}{\partial \xi_2}\left(\frac{\overline{u_j u_2'}}{\overline{u^2}}\right) + \frac{\partial}{\partial \xi_3}\left(\frac{\overline{u_j u_3'}}{\overline{u^2}}\right) = \frac{\partial R_{j1}}{\partial \xi_1} + \frac{\partial R_{j2}}{\partial \xi_2} + \frac{\partial R_{j3}}{\partial \xi_3} = 0. \tag{A II.204}$$

The equation of continuity expressed in (A II.204) may now be applied to Eq. (A II.200):

$$\frac{\partial R_{11}}{\partial \xi_1} = 2\frac{(f-g)}{(r)^2}\xi_1 + \frac{(\xi_1)^2}{(r)^2}\left(\frac{\partial f}{\partial \xi_1} - \frac{\partial g}{\partial \xi_1}\right) + \frac{\partial g}{\partial \xi_1} - 2\frac{(f-g)}{(r)^4}(\xi_1)^3, \tag{A II.205}$$

$$\frac{\partial R_{12}}{\partial \xi_2} = \frac{(f-g)}{(r)^2}\xi_1 + \frac{\xi_1 \xi_2}{(r)^2}\left(\frac{\partial f}{\partial \xi_2} - \frac{\partial g}{\partial \xi_2}\right) - 2\frac{(f-g)}{(r)^4}\xi_1(\xi_2)^2, \tag{A II.206}$$

$$\frac{\partial R_{13}}{\partial \xi_3} = \frac{(f-g)}{(r)^2}\xi_1 + \frac{\xi_1 \xi_3}{(r)^2}\left(\frac{\partial f}{\partial \xi_3} - \frac{\partial g}{\partial \xi_3}\right) - 2\frac{(f-g)}{(r)^4}\xi_1(\xi_3)^2. \tag{A II.207}$$

Since Eq. (A II.204) is true in all orientations of the coordinate system, it will be true in the one shown in Fig. A II-6 in this particular coordinate system.

$$\begin{aligned} \xi_1 &= r, \\ \xi_2 &= 0, \\ \xi_3 &= 0 \end{aligned} \tag{A II.208}$$

$$\frac{\partial R_{11}}{\partial \xi_1} = \frac{2(f-g)}{r} + \frac{\partial f}{\partial r} - \frac{2(f-g)}{r}, \tag{A II.209}$$

$$\frac{\partial R_{12}}{\partial \xi_2} = \frac{f-g}{r}, \tag{A II.210}$$

$$\frac{\partial R_{13}}{\partial \xi_3} = \frac{f-g}{r}, \tag{A II.211}$$

$$\frac{\partial R_{ij}}{\partial \xi_j} = 0, \quad \text{if} \quad i \neq 1. \tag{A II.212}$$

Thus

$$r\frac{\partial f}{\partial r} + 2(f-g) = 0. \tag{A II.213}$$

This equation relates f and g. Therefore the correlation tensor is determined by one scalar function of r and r itself. As $B' \to B$ or as $r \to 0$, $v_1' \to v_1$ and $v_2' \to v_2$ or $f \to 1$ and $g \to 1$. Thus, near the origin ($r = 0$) f and g are even functions of r:

$$f = 1 + f''_{r=0} \frac{(r)^2}{2!} + f''''_{r=0} \frac{(r)^4}{4!} + \dots, \tag{A II.214}$$

$$g = 1 + g''_{r=0} \frac{(r)^2}{2!} + g''''_{r=0} \frac{(r)^4}{4!} + \dots. \tag{A II.215}$$

Substitution of (A II.214) and (A II.215) into (A II.213) gives

$$-f''_{r=0} \frac{2(r)^2}{2!} - f''''_{r=0} \frac{4(r)^4}{4!} = 2(f''_{r=0} - g''_{r=0}) \frac{(r)^2}{2!} + 2(f''''_{r=0} - g''''_{r=0}) \frac{(r)^4}{4!} + \dots \tag{A II.216}$$

or

$$4(f''_{r=0} - 2g''_{r=0}) \frac{(r)^2}{2!} + (6f''''_{r=0} - 2g''''_{r=0}) \frac{(r)^4}{4!} + \dots = 0. \tag{A II.217}$$

Thus

$$2f''_{r=0} = g''_{r=0}, \tag{A II.218}$$

$$3f''''_{r=0} = g''''_{r=0}. \tag{A II.219}$$

Substitution of (A II.218) into (A II.215) and (A II.214) and (A II.215) into (A II.200) gives, *for small values of r*,

$$R_{ij} = -\frac{f''_{r=0}}{2} \begin{bmatrix} (\xi_1)^2 & \xi_1\xi_2 & \xi_1\xi_3 \\ \xi_2\xi_1 & (\xi_2)^2 & \xi_2\xi_3 \\ \xi_3\xi_1 & \xi_3\xi_2 & (\xi_3)^2 \end{bmatrix} + (1 + f''_{r=0}(r)^2) \begin{bmatrix} 1 & 0 & 0 \\ 0 & 1 & 0 \\ 0 & 0 & 1 \end{bmatrix}. \tag{A II.220}$$

From Eq. (A II.220) the following results may be obtained:

$$\left(\frac{\partial^2 R_{ij}}{\partial\xi_k\,\partial\xi_l}\right)\Big|_{\xi_1=0,\xi_2=0,\xi_3=0} = f''_{r=0} \quad \text{if} \quad i=j=k=l, \tag{A II.221}$$

$$\left(\frac{\partial^2 R_{ij}}{\partial\xi_k\,\partial\xi_l}\right)\Big|_{\xi_1=0,\xi_2=0,\xi_3=0} = 2f''_{r=0} \quad \text{if} \quad i=j\neq k=l, \tag{A II.222}$$

$$\left(\frac{\partial^2 R_{ij}}{\partial\xi_k\,\partial\xi_l}\right)\Big|_{\xi_1=0,\xi_2=0,\xi_3=0} = -\frac{1}{2} f''_{r=0} \quad \text{if} \quad k=i\neq l=j \text{ or } k=j\neq l=i. \tag{A II.223}$$

Otherwise

$$\left(\frac{\partial^2 R_{ij}}{\partial \xi_k \partial \xi_l}\right)\Bigg|_{\xi_1=0,\,\xi_2=0,\,\xi_3=0} = 0. \tag{A II.224}$$

AII-10. Correlation Coefficients Between the Derivatives of the Velocities

If we differentiate the components of the correlation tensor with respect to the coordinates of B,

$$\frac{\partial}{\partial x_i}\overline{(u_k\, u_l')} = \overline{u^2}\frac{\partial R_{kl}}{\partial x_i} = -\overline{u^2}\frac{\partial R_{kl}}{\partial \xi_i}. \tag{A II.225}$$

The velocity fluctuations at B' are independent of the coordinates of B, and, since space differentiation and average over a uniform time interval are commutative,

$$-\overline{u^2}\frac{\partial R_{kl}}{\partial \xi_i} = \overline{\frac{\partial u_k}{\partial x_i}\, u_l'} \tag{A II.226}$$

which may now be differentiated with respect to the coordinates of B',

$$-\overline{u^2}\frac{\partial^2 R_{kl}}{\partial \xi_i\, \partial \xi_j} = \overline{\frac{\partial u_k}{\partial x_i}\frac{\partial u_l'}{\partial \xi_j}} \tag{A II.227}$$

as B and B' move into coincidence.

$$-\overline{u^2}\left(\frac{\partial^2 R_{kl}}{\partial \xi_i\, \partial \xi_j}\right)\Bigg|_{\xi_1=\xi_2=\xi_3=0} = \overline{\frac{\partial u_k}{\partial x_i}\frac{\partial u_l}{\partial x_j}}. \tag{A II.228}$$

From Eqs. (A II.228), (A II.221), (A II.222), and (A II.223) the following useful results are obtained:

$$\overline{\left(\frac{\partial u_1}{\partial x_1}\right)^2} = -\overline{u^2} f''_{r=0}, \tag{A II.229}$$

$$\overline{\left(\frac{\partial u_1}{\partial x_2}\right)^2} = -2\overline{u^2} f''_{r=0}, \tag{A II.230}$$

$$\overline{\frac{\partial u_1}{\partial x_1}\frac{\partial u_2}{\partial x_2}} = \overline{\frac{\partial u_1}{\partial u_2}\frac{\partial x_2}{\partial x_1}} = \frac{1}{2}\overline{u^2} f''_{r=0} = -\frac{1}{2}\overline{\left(\frac{\partial u_1}{\partial x_1}\right)^2} = -\frac{1}{4}\overline{\left(\frac{\partial u_1}{\partial x_2}\right)^2}. \tag{A II.231}$$

Similar analysis leads to the following results (*10*):

$$\overline{\left(\frac{\partial^2 u_1}{\partial x_1^2}\right)^2} = \overline{u^2} f''''_{r=0}, \tag{A II.232}$$

$$\overline{\left(\frac{\partial^2 u_1}{\partial x_2^2}\right)^2} = 3\,\overline{u^2} f''''_{r=0}, \tag{A II.233}$$

$$\overline{\frac{\partial^2 u_1}{\partial x_1^2}\frac{\partial^2 u_1}{\partial x_2^2}} = \overline{\left(\frac{\partial^2 u_1}{\partial x_1\,\partial x_2}\right)^2} = \frac{2}{9}\overline{\left(\frac{\partial^2 u_1}{\partial x_2^2}\right)^2} = \frac{2}{3}\overline{\left(\frac{\partial^2 u_1}{\partial x_1^2}\right)^2}. \tag{A II.234}$$

AII-11. Expression of Mean Values by Integrals

The velocity field in a fluid can be separated into two parts. One part has no divergence and one part no curl. Let, for the moment, X be the part with no divergence and Y the part with no curl. The velocity field is then the sum of the two vector fields $X + Y$ and

$$\begin{aligned} \nabla \times X &= 0, \\ \nabla \times Y &= 0. \end{aligned} \tag{A II.235}$$

Consider a scalar function φ and a vector function Ξ, related to X and Y as follows:

$$\begin{aligned} X &= \nabla \times \Xi, \\ Y &= -\nabla\varphi. \end{aligned} \tag{A II.236}$$

Then the velocity field is $(\nabla \times \Xi - \nabla\varphi)$. From vector analysis

$$\nabla \cdot \nabla \times \Xi = 0, \tag{A II.237}$$

$$\nabla \times \nabla\varphi = 0. \tag{A II.238}$$

Thus the divergence of the velocity field is $-\nabla^2\varphi$. For an incompressible fluid $\nabla^2\varphi = 0$. If the velocity field is without sources or sinks and of infinite extension, then $\varphi = 0$. The curl of the velocity field is $\nabla(\nabla \cdot \Xi) - \nabla^2 \Xi$ which is also a vector field. Since Ξ is as yet undetermined, it may be assumed to be divergenceless. The components of the curl of the velocity field are equal to twice the components of the vorticity, ω_1, ω_2, ω_3, so that

$$2\omega = -\nabla^2 \Xi. \tag{A II.239}$$

This is Poisson's equation and if the fluid is of infinite extension then the solution may be written

$$\Xi = \frac{2}{4\pi}\int\int\int \frac{\omega}{r}\, dx_1\, dx_2\, dx_3 \tag{A II.240}$$

where the integration extends throughout the fluid.
If the components of Ξ are F, G, H, then

$$F = \frac{2}{4\pi}\int\int\int \frac{\omega_1'}{r}\, dx_1'\, dx_2'\, dx_3', \tag{A II.241}$$

$$G = \frac{2}{4\pi}\int\int\int \frac{\omega_2'}{r}\, dx_1'\, dx_2'\, dx_3', \tag{A II.242}$$

$$H = \frac{2}{4\pi}\int\int\int \frac{\omega_3'}{r}\, dx_1'\, dx_2'\, dx_3', \tag{A II.243}$$

$$r = (x_1 - x_1')^2 + (x_2 - x_2')^2 + (x_3 - x_3')^2. \tag{A II.244}$$

The primes are used to distinguish the variables of integration from the coordinates of the point at which F, G, H are being evaluated. So

$$\nabla \cdot \Xi = \frac{\partial F}{\partial x_1} + \frac{\partial G}{\partial x_2} + \frac{\partial H}{\partial x_3} = \frac{2}{4\pi}\int\int\int \nabla \cdot \left(\frac{\omega'}{r}\right) dx_1'\, dx_2'\, dx_3', \tag{A II.245}$$

$$\nabla \cdot \Xi = \frac{2}{4\pi}\int\int \omega' \cdot \frac{dS}{r} = 0 \tag{A II.246}$$

where the surface with element dS is any bounding surface lying entirely within the fluid at a uniform distance from (x, y, z). For a fluid of infinite extension, r may be taken infinitely large. Since ω is a solenoidal vector, exactly as many vortex filaments enter the surface as leave it, thus confirming the assumption that Ξ is divergenceless, i.e., solenoidal.

Since the velocity field is $(\nabla \times \Xi - \nabla\varphi)$ and φ is 0 for an infinite, incompressible fluid without sources or sinks

$$u_1 = \frac{\partial H}{\partial x_2} - \frac{\partial G}{\partial x_3} \tag{A II.247}$$

$$u_2 = \frac{\partial F}{\partial x_3} - \frac{\partial H}{\partial x_1} \tag{A II.248}$$

$$u_3 = \frac{\partial G}{\partial x_1} - \frac{\partial F}{\partial x_2} \tag{A II.249}$$

hence

$$\frac{\partial u_3}{\partial x_2} = \frac{\partial^2 G}{\partial x_1 \partial x_2} - \frac{\partial^2 F}{\partial x_2^2} \tag{A II.250}$$

$$\frac{\partial u_3}{\partial x_2} = \frac{1}{2\pi}\left\{\frac{\partial^2}{\partial x_1 \partial x_2}\int\int\int \frac{\omega_2'}{r}\,dx_1'\,dx_2'\,dx_3' - \frac{\partial^2}{\partial x_2^2}\int\int\int \frac{\omega_1'}{r}\,dx_1'\,dx_2'\,dx_3'\right\}, \tag{A II.251}$$

$$\frac{\partial u_3}{\partial x_2} = \frac{1}{2\pi}\int\int\int\left[\frac{3\,(x_1' - x_1)\,(x_2' - x_2)}{(r)^5}\,\omega_2' - \left\{\frac{3\,(x_2' - x_2)^2}{(r)^5} - \frac{1}{(r)^3}\right\}\omega_1'\right] dx_1'\,dx_2'\,dx_3'. \tag{A II.252}$$

Thus

$$\overline{\omega_1 \frac{\partial u_3}{\partial x_2}} = \frac{1}{2\pi}\int\int\int\left[\frac{3\,(x_1' - x)\,(x_2' - x_2)}{(r)^5}\,\overline{\omega_1\,\omega_2'} - \left\{\frac{3\,(x_2' - x_2)^2}{(r)^5} - \frac{1}{(r)^3}\right\}\overline{\omega_1\,\omega_1'}\right] dx_1'\,dx_2'\,dx_3'. \tag{A II.253}$$

A correlation tensor for the vorticity components may be defined in a manner analogous to that for the velocity components. Thus

$$\overline{\omega_1 \frac{\partial u_3}{\partial x_2}} = \frac{2\,\omega_x^2}{4\pi}\int\int\int\left[\frac{3\,(x_1' - x)\,(x_2' - x)}{(r)^5}\,V_{12} - \left\{\frac{3\,(x_2' - x_2)}{(r)^5} - \frac{1}{(r)^3}\right\}V_{11}\right] dx_1'\,dx_2'\,dx_3'. \tag{A II.254}$$

The analysis leading to Eqs. (A II.200) and (A II.213) may be applied directly to vorticity fluctuations so that the following substitutions may be made in Eqs. (A II.200) and (A II.213):

$$R_{ij} = V_{ij},$$

$$f \to f_\omega,$$

$$g \to g_\omega.$$

When the turbulence is isotropic, the result expressed in (A II.254) may be obtained more easily from Eq. (A II.231),

$$\overline{\omega_1 \frac{\partial u_3}{\partial x_2}} = \overline{\frac{\partial u_3}{\partial x_2}\frac{\partial u_3}{\partial x_2}} - \overline{\frac{\partial u_2}{\partial x_3}\frac{\partial u_3}{\partial x_2}} = \overline{\frac{\partial u_3}{\partial x_2}\frac{\partial u_3}{\partial x_2}} - \overline{\frac{\partial u_2}{\partial x_3}\frac{\partial u_3}{\partial x_2}}. \tag{A II.255}$$

AII-12. Correlation Between Pressure and Velocity

Let P be the pressure at the point $B(x, y, z)$ (Fig. A II-6). Since the turbulence is assumed to be isotropic, the correlations $\overline{P v_3'}$ and $\overline{P v_2'}$ vanish as they would change sign when the coordinate system is reflected through any plane containing r. Let

$$\overline{P v_1'} = \{\overline{P^2}\}^{1/2} \{\overline{u^2}\}^{1/2} s(r). \tag{A II.256}$$

From Eq. (A II.189)

$$\begin{aligned} u_1' &= l_1 v_1' + m_1 v_2' + n_1 v_3', \\ u_2' &= l_2 v_1' + m_2 v_2' + n_2 v_3', \\ u_3' &= l_3 v_1' + m_3 v_2' + n_3 v_3'. \end{aligned} \tag{A II.257}$$

Therefore

$$\begin{aligned} \overline{P u_1'} &= \{\overline{P^2}\}^{1/2} \{\overline{u^2}\}^{1/2} l_1 s(r), \\ \overline{P u_2'} &= \{\overline{P^2}\}^{1/2} \{\overline{u^2}\}^{1/2} l_2 s(r), \\ \overline{P u_3'} &= \{\overline{P^2}\}^{1/2} \{\overline{u^2}\}^{1/2} l_3 s(r). \end{aligned} \tag{A II.258}$$

By the equation of continuity (A II.201),

$$\overline{\frac{P}{\{\overline{P^2}\}^{1/2} \{\overline{u^2}\}^{1/2}} \sum_{i=1}^{3} \frac{\partial u_i'}{\partial \xi_i}} = \sum_{i=1}^{3} \frac{\partial}{\partial \xi_i} \left(\frac{\overline{P u_i'}}{\{\overline{P^2}\}^{1/2} \{\overline{u^2}\}^{1/2}} \right) = \sum_{i=1}^{3} \frac{\partial}{\partial \xi_i} (l_i s(r)) = 0. \tag{A II.259}$$

Thus

$$\sum_{i=1}^{3} \left(s(r) \frac{\partial l_i}{\partial \xi_i} + l_i \frac{\partial s(r)}{\partial \xi_i} \right) = \sum_{i=1}^{3} \left(\frac{s(r)}{r} \{1 - l_i^2\} + l_i^2 \frac{\partial s(r)}{\partial r} \right) = 0. \tag{A II.260}$$

Since $\partial r / \partial \xi_i = l_i$ by Eq. (A II.188), hence

$$\frac{\partial s(r)}{\partial r} + 2 \frac{s(r)}{r} = 0. \tag{A II.261}$$

Since $s(r)$ is finite the appropriate solution is

$$s(r) = 0. \tag{A II.262}$$

Therefore

$$\overline{P u_j'} = 0; \qquad (j = 1, 2, 3). \tag{A II.263}$$

Since pressure is a scalar quantity, it might appear that reflection of the coordinate y_1 in the plane of y_2 and y_3 would change the sign of the correlation $\overline{P v_1'}$ and thereby show $\overline{P v_1'} = 0$ for isotropic turbulence. Such is not the case, however, because the coordinates of the point B would also change sign under such a reflection. The situation in the resulting coordinate system would be equivalent to shifting the origin of the original coordinate system to B and considering the correlation $\overline{P' v_1}$. Because of the symmetry of the points B and B' in the definition of the correlation

$$\overline{P v_1'} = \overline{P' v_1}. \tag{A II.264}$$

Since Eq. (A II.259) is true in all orientations of the coordinates ξ_1, ξ_2, ξ_3, it will be true when evaluated in the coordinate system shown in Fig. A II-6. Thus

$$\frac{1}{\{\overline{P^2}\}^{1/2}\{\overline{u^2}\}^{1/2}} \frac{\partial \overline{P v_1'}}{\partial r} = \frac{\partial s(r)}{\partial r} = 0. \tag{A II.265}$$

The solution of this equation is a constant. Since $\overline{P v_1'}$ must approach zero as r becomes large without limit, this constant must be zero, thus confirming Eq. (A II.263).

AII-13. Triple Correlations

We define a tensor of rank 3, T_{ijk}, as follows:

$$\overline{v_i v_j v_k'} = \{\overline{u^2}\}^{3/2} T_{ijk}. \tag{A II.266}$$

Consider again the coordinate system of Fig. A II-6. All of the quantities $\overline{v_i v_j v_k'}$ belong to one of the following six groups:

$$\overline{v_1^2 v_k'}, \qquad \overline{v_1^2 v_1'},$$

$$\overline{v_i v_j v_k'}, \qquad \overline{v_i v_j v_1'},$$

$$\overline{v_1 v_j v_1'}, \qquad \overline{v_1 v_j v_k'}$$

where i, j, k may be either 2 or 3. By reflection of either y_2 or y_3, $\overline{v_1^2 v_k'}$, $\overline{v_i v_j v_k'}$, $\overline{v_1 v_j v_1'}$ change sign and hence must be zero for isotropic turbulence.

Unless $j = k$ or $i = j$, $\overline{v_1 v_j v_k'}$ and $\overline{v_i v_j v_1'}$ vanish for the same reason. Because of isotropy

$$\begin{aligned} \overline{v_1 v_2 v_2'} &= \overline{v_1 v_3 v_3'}, \\ \overline{(v_2)^2 v_1'} &= \overline{(v_3)^2 v_1'}. \end{aligned} \tag{A II.267}$$

Reflection of the y_1-axis does not change the sign of the remaining correlations because of the situation discussed above under the subject of pressure-velocity correlations. Thus only three independent components of the triple correlation tensor remain different from zero.
Define

$$\begin{aligned} k(r) &= \overline{(v_1)^2 v_1'}/\{\overline{u^2}\}^{3/2}, \\ q(r) &= \overline{v_1 v_2 v_2'}/\{\overline{u^2}\}^{3/2}, \\ h(r) &= \overline{(v_2)^2 v_1'}/\{\overline{u^2}\}^{3/2}. \end{aligned} \tag{A II.268}$$

If, for small r, v_1' is expanded in Taylor's series about the point B in the reference frame of Fig. A II-6,

$$\overline{(v_1)^2 v_1'} = \overline{(v_1)^3} + \overline{(v_1)^2 \frac{\partial v_1}{\partial r}} r + \frac{1}{2} \overline{(v_1)^2 \frac{\partial^2 v'}{\partial r^2}} r^2 + \ldots . \tag{A II.269}$$

Reflection of the y_1-axis changes the signs of the coefficients of all even-numbered terms and consequently they must be zero for isotropic turbulence. For homogeneous turbulence,

$$\overline{(v_1)^2 \frac{\partial v_1}{\partial r}} = \frac{1}{3} \frac{\partial \overline{(v_1)^3}}{\partial r} = 0. \tag{A II.270}$$

Thus the expansion of $\overline{(v_1)^2 v_1'}$ starts with $\frac{1}{6} (v_1)^2 \frac{\partial^3 v_1}{\partial r^3} (r)^3$

and

$$k(r) = k'''_{r=0} \frac{(r)^3}{3!} + k^{\mathrm{v}}_{r=0} \frac{(r)^5}{5!} + \ldots . \tag{A II.271}$$

Using Eq. (A II.190)

$$\begin{aligned} \overline{(u_1)^2 u_1'} = l_1^3 \overline{(v_1)^2 v_1'} + l_1 m_1^2 \overline{(v_2)^2 v_1'} + l_1 n_1^2 \overline{v_3^2 v_1'} \\ + 2 l_1 m_1^2 \overline{v_1 v_2 v_2'} + 2 l_1 n_1^2 \overline{v_1 v_3 v_3'}, \end{aligned} \tag{A II.272}$$

$$\overline{(u_1)^2 u_1'} = \{\overline{u^2}\}^{3/2} [l_1^3 k + l_1 (m_1^2 + n_1^2) h + 2 l_1 (m_1^2 + n_1^2) q], \quad \text{(A II.273)}$$

$$\overline{(u_1)^2 u_1'} = \{\overline{u^2}\}^{3/2} [l_1^3 k + (l_1 - l_1^3) h + 2 (l_1 - l_1^3) q], \quad \text{(A II.274)}$$

$$\overline{(u_1)^2 u_1'} = \{\overline{u^2}\}^{3/2} [l_1^3 (k - h - 2q) + l_1 h + 2 l_1 q], \quad \text{(A II.275)}$$

$$\overline{(u_1)^2 u_1'} = \{\overline{u^2}\}^{3/2} \left[\xi_1^3 \frac{(k - h - 2q)}{(r)^3} + \frac{\xi_1 h}{r} + 2 \xi_1 \frac{q}{r}\right]. \quad \text{(A II.276)}$$

Similar analysis leads to the general result

$$\overline{u_i u_j u_k'} = \{\overline{u^2}\}^{3/2} T_{ijk} = \{\overline{u^2}\}^{3/2} \left[\xi_i \xi_j \xi_k \frac{(k - h - 2q)}{(r)^3} + \delta_{ij} \xi_k \frac{h}{r} + \delta_{ik} \xi_j \frac{q}{r} + \delta_{jk} \xi_i \frac{q}{r}\right] \quad \text{(A II.277)}$$

where $\delta_{ij} = 1$ when $i = j$ and $\delta_{ij} = 0$ when $i \neq j$. Equation (A II.277) shows that shifting the origin of the coordinate system to B' without changing the orientation of the axes changes the coordinates of B to $(-\xi_1, -\xi_2, -\xi_3)$. Consequently

$$\overline{u_i u_j' u_k'} = -\{\overline{u^2}\}^{3/2} T_{ijk} = -\overline{u_i' u_j u_k}. \quad \text{(A II.278)}$$

Since the velocity fluctuations at B are independent of the coordinates of B', the equation of continuity may be written

$$\sum_{k=1}^{3} \frac{\partial}{\partial \xi_k} \overline{(u_i u_j u_k')} = 0. \quad \text{(A II.279)}$$

Hence also

$$\sum_{k=1}^{3} \frac{\partial}{\partial \xi_k} T_{ijk} = 0. \quad \text{(A II.280)}$$

From Eq. (A II.277)

$$T_{111} = (\xi_1)^3 \frac{(k - h - 2q)}{(r)^3} + \xi_1 \frac{h}{r} + 2 \xi_1 \frac{q}{r}$$

$$T_{112} = (\xi_1)^2 \xi_2 \frac{(k - h - 2q)}{(r)^3} + \xi_2 \frac{h}{r}, \quad \text{(A II.281)}$$

$$T_{113} = (\xi_1)^2 \xi_3 \frac{(k - h - 2q)}{(r)^3} + \xi_3 \frac{h}{r},$$

$$\frac{\partial T_{111}}{\partial \xi_1} = 3(\xi_1)^2 \frac{(k-h-2q)}{(r)^3} - 3(\xi_1)^4 \frac{(k-h-2q)}{(r)^5} + \frac{(\xi_1)^4}{(r)^4}(k'-h'-2q') + \frac{h}{r} + 2\frac{q}{r} + \frac{(\xi_1)^2}{(r)^2}(h'+2q') - \frac{(\xi_1)^2}{(r)^3}(h+2q),$$

$$\frac{\partial T_{112}}{\partial \xi_2} = (\xi_1)^2 \frac{(k-h-2q)}{(r)^3} + \frac{h}{r} + \frac{(\xi_1)^2(\xi_2)^2}{(r)^4}(k'-h'-2q') + \frac{(\xi_2)^2}{(r)^2}h' - \frac{3(\xi_1)^2(\xi_2)^2}{(r)^5}(k-h-2q) - \frac{(\xi_2)^2}{(r)^3}h,$$

$$\frac{\partial T_{113}}{\partial \xi_3} = (\xi_1)^2 \frac{(k-h-2q)}{(r)^3} + \frac{h}{r} + \frac{\xi_1(\xi_3)^2}{(r)^4}(k'-h'-2q') + \frac{(\xi_2)^2}{(r)^2}h' - \frac{3(\xi_1)^2(\xi_3)^2}{(r)^5}(k-h-2q) - \frac{(\xi_3)^2}{(r)^3}h. \tag{A II.282}$$

These derivatives may be evaluated in the coordinates of Fig. A II-6 and then substituted into Eq. (A II.280) resulting in

$$\sum_{k=1}^{3} \frac{\partial T_{11k}}{\partial \xi_k} = k'-h'-2q' + \frac{2k-2h-4q}{r} + h' + 2q' + 2\frac{h}{r} \tag{A II.283}$$

$$= \left\{k'-h'+\frac{2k-2h-6q}{r}\right\} + \left\{h'+2\frac{h}{r}+2\frac{q}{r}\right\} = 0.$$

Again from Eq. (A II.277)

$$T_{221} = \xi_1(\xi_2)^2 \frac{(k-h-2q)}{(r)^3} + \xi_1 \frac{h}{r},$$

$$T_{222} = (\xi_2)^3 \frac{(k-h-2q)}{(r)^3} + \xi_2 \frac{h}{r} + 2\xi_2 \frac{q}{r}, \tag{A II.284}$$

$$T_{223} = (\xi_2)^2 \xi_3 \frac{(k-h-2q)}{(r)^3} + \xi_3 \frac{h}{r}.$$

The following expressions are obtained by differentiation and evaluation in the coordinate system shown in Fig. A II-6:

$$\frac{\partial T_{221}}{\partial \xi_1} = h',$$

$$\frac{\partial T_{222}}{\partial \xi_2} = \frac{h}{r} + 2\frac{q}{r}, \tag{A II.285}$$

$$\frac{\partial T_{223}}{\partial \xi_3} = \frac{h}{r}.$$

Substitution into Eq. (A II.280) gives

$$h' + 2\frac{h}{r} + 2\frac{q}{r} = 0 \qquad \text{(A II.286)}$$

and from (A II.283) and (A II.286)

$$k' - h' + \frac{2k - 2h - 6q}{r} = 0. \qquad \text{(A II.287)}$$

Therefore

$$q = -h - \frac{r}{2}\frac{dh}{dr}, \qquad k = -2h. \qquad \text{(A II.288)}$$

It can be shown that the other seven equations obtainable from (A II.280) and (A II.277) reduce to the trivial result that zero equals zero or Eq. (A II.286). The equation of continuity shows that the triple correlation tensor may be expressed in terms of a single scalar $h(r)$.

AII-14. Propagation of the Correlation

At the point $B(x_1, x_2, x_3)$ the principle of conservation of momentum in an incompressible Newtonian fluid of uniform, molecular, kinematic viscosity may be expressed in the form of the Navier-Stokes equations of motion:

$$\frac{\partial u_i}{\partial \theta} + \sum_{j=1}^{3} \frac{\partial u_i}{\partial x_j} = -\frac{1}{\rho}\frac{\partial P}{\partial x_i} + \nu \nabla^2 u_i\,; \qquad (i = 1, 2, 3). \qquad \text{(A II.289)}$$

This equation may be multiplied by the k-component of the fluctuating velocity at the point B' and averaged:

$$\overline{u_k'\frac{\partial u_i}{\partial \theta}} + \sum_{j=1}^{3} \overline{u_k' u_j \frac{\partial u_i}{\partial x_j}} = -\overline{\frac{u_k'}{\rho}\frac{\partial P}{\partial x_i}} + \overline{\nu u_k' \nabla^2 u_i} \qquad \text{(A II.290)}$$

which may be reduced to

$$\overline{u_k'\frac{\partial u_i}{\partial \theta}} + \sum_{j=1}^{3} \overline{u_k' u_j \frac{\partial u_i}{\partial x_j}} = \nu \nabla^2 \overline{(u_k' u_i)} \qquad \text{(A II.291)}$$

since the pressure-velocity correlations are all zero. Now

$$\sum_{j=1}^{3} \frac{\partial}{\partial x_j} (u_i u_j u_k') = u_k' \left\{ \sum_{j=1}^{3} u_i \frac{\partial u_j}{\partial x_j} + \sum_{j=1}^{3} u_j \frac{\partial u_i}{\partial x_j} \right\} = \sum_{j=1}^{3} u_k u_j \frac{\partial u_i}{\partial x_j} \tag{A II.292}$$

by the equation of continuity. The quantity $\overline{u_i u_j u_k'}$ is a function of ξ_1, ξ_2, ξ_3, the coordinates of B referred to the system of Fig. A II-5 translated to the point B'. Thus

$$\frac{\partial}{\partial x_j} \overline{(u_i u_j u_k')} = - \frac{\partial}{\partial \xi_j} \overline{(u_i u_j u_k')}. \tag{A II.293}$$

Thus

$$\overline{u_k' \frac{\partial u_i}{\partial \theta}} - \sum_{j=1}^{3} \overline{(u_i u_j u_k')} = \nu \nabla^2 \overline{(u_i u_k')}. \tag{A II.294}$$

Since the definition of the correlation of fluctuating velocities is symmetrical

$$\overline{u_i \frac{\partial u_k'}{\partial \theta}} + \sum_{j=1}^{3} \frac{\partial}{\partial \xi_j} \overline{(u_i u_j' u_k')} = \nu \nabla^2 \overline{(u_i u_k')}. \tag{A II.295}$$

By Eq. (A II.278)

$$\overline{u_i \frac{\partial u_k'}{\partial \theta}} - \sum_{j=1}^{3} \frac{\partial}{\partial \xi_j} \overline{(u_j u_k u_i')} = \nu \nabla^2 \overline{(u_i u_k')}. \tag{A II.296}$$

Adding Eq. (A II.294) to (A II.296) yields

$$\frac{\partial \overline{(u_i u_k')}}{\partial \theta} - \sum_{j=1}^{3} \frac{\partial}{\partial \xi_j} \overline{(u_i u_j u_k' + u_j u_k u_i')} = 2 \nu \nabla^2 \overline{(u_i u_k')}. \tag{A II.297}$$

Equations (A II.200) and (A II.286) may be substituted into (A II.297) to give

$$\frac{\partial (\overline{u^2} R_{ik})}{\partial \theta} - \{\overline{u^2}\}^{3/2} \sum_{j=1}^{3} \frac{\partial}{\partial \xi_j} (T_{ijk} + T_{kji}) = 2 \nu \overline{u^2} \nabla^2 R_{ik} \tag{A II.298}$$

Equation (A II.298) may be expressed in terms of f and h in the following manner. Let $i = k$, then

$$R_{11} = f + \frac{r}{2}\frac{\partial f}{\partial r}\left\{1 - \frac{(\xi_1)^2}{(r)^2}\right\}. \tag{A II.299}$$

When evaluated in the coordinate system of Fig. A II-6,

$$\nabla^2 R_{11} = \frac{\partial^2 f}{\partial r^2} + \frac{4}{r}\frac{\partial f}{\partial r}, \tag{A II.300}$$

$$\frac{\partial(\overline{u^2} R_{11})}{\partial \theta} = \frac{\partial(\overline{u^2} f)}{\partial \theta}. \tag{A II.301}$$

Also

$$T_{111} = (\xi_1)^3 \frac{k - h - 2q}{(r)^3} + \frac{\xi_1}{r}(h + 2q) = -\left\{\frac{(\xi_1)^3}{(r)^3}(h - r h') + \frac{\xi_1}{r}(h + r h')\right\}, \tag{A II.302}$$

$$T_{121} = \xi_2\left\{(\xi_1)^2 \frac{k - h - 2q}{(r)^3} + \frac{q}{r}\right\}, \tag{A II.303}$$

$$T_{131} = \xi_3\left\{(\xi_1)^2 \frac{k - h - 2q}{(r)^3} + \frac{q}{r}\right\}. \tag{A II.304}$$

When evaluated in the coordinate system of Fig. A II-6,

$$\sum_{j=1}^{3} \frac{\partial}{\partial \xi_1}(T_{ijk} + T_{kji}) = -2\left\{\frac{\partial h}{\partial r} + \frac{4}{r}h\right\}. \tag{A II.305}$$

Thus Eq. (A II.298) may be written

$$\frac{\partial(\overline{u^2} f)}{\partial \theta} + 2\{\overline{u^2}\}^{3/2}\left(\frac{\partial h}{\partial r} + \frac{4}{r}h\right) = 2\nu\overline{u^2}\left(\frac{\partial^2 f}{\partial r^2} + \frac{4}{r}\frac{\partial f}{\partial r}\right). \tag{A II.306}$$

Equation (A II.298) implies eight other equations of the form of (A II.306) by choosing $(i, j = 1, 2, 3)$. These equations all reduce to (A II.306) identically or to the trivial result zero equals zero when evaluated in the coordinate system of Fig. A II-6.

AII-15. Relation Between Correlation and Spectral Theories (12)

The spectral tensor $\mathcal{F}_{ik}(k_1, k_2, k_3)$ may be defined as the Fourier transform of the correlation tensor $R_{ik}(\xi_1, \xi_2, \xi_3)$:

$$\mathcal{F}_{ik}(k_1, k_2, k_3) = \frac{1}{(2\pi)^3} \int_{-\infty}^{\infty} \int_{-\infty}^{\infty} \int_{-\infty}^{\infty} \overline{u^2}\, R_{ik}(\xi_1, \xi_2, \xi_3)\, e^{i(\xi_1 k_1 + \xi_2 k_2 + \xi_3 k_3)}\, d\xi_1\, d\xi_2\, d\xi_3. \tag{A II.307}$$

From the theory of the Fourier transformation,

$$\overline{u^2}\, R_{ik}(\xi_1, \xi_2, \xi_3) = \int_{-\infty}^{\infty} \int_{-\infty}^{\infty} \int_{-\infty}^{\infty} \mathcal{F}_{ik}(k_1, k_2, k_3)\, e^{-i(\xi_1 k_1 + \xi_2 k_2 + \xi_3 k_3)}\, dk_1\, dk_2\, dk_3. \tag{A II.308}$$

The quantities k_1, k_2, k_3 are the components of the wave number in units of reciprocal length. Let $i = j$; then

$$\sum_{j=1}^{3} \overline{u^2}\, R_{ii}(\xi_1, \xi_2, \xi_3) = \overline{u^2} \left\{ \frac{f - g}{(r)^2} \sum_{i=1}^{3} (\xi_i)^2 + 3g \right\}, \tag{A II.309}$$

$$= \overline{u^2} \left\{ f + 2g \right\}. \tag{A II.310}$$

As $r \to 0$; $f \to g \to 1$ so that

$$\overline{u^2} = \frac{1}{3} \int_{-\infty}^{\infty} \int_{-\infty}^{\infty} \int_{-\infty}^{\infty} \sum_{i=1}^{3} \mathcal{F}_{ii}(k_1, k_2, k_3)\, dk_1\, dk_2\, dk_3. \tag{A II.311}$$

The quantity

$$\frac{1}{2} \sum_{i=1}^{3} \mathcal{F}_{ii}(k_1, k_2, k_3)$$

is thus the density of turbulent kinetic energy in wave-number space. Define

$$\mathcal{W}_{ijk}(k_1, k_2, k_3) = \tag{A II.312}$$

$$\frac{1}{(2\pi)^3} \int_{-\infty}^{\infty} \int_{-\infty}^{\infty} \int_{-\infty}^{\infty} \{\overline{u^2}\}^{3/2}\, T_{ijk}(\xi_1, \xi_2, \xi_3)\, e^{i(\xi_1 k_1 + \xi_2 k_2 + \xi_3 k_3)}\, d\xi_1\, d\xi_2\, d\xi_3.$$

so that

$$\{\overline{u^2}\}^{3/2} T_{ijk} = \int_{-\infty}^{\infty}\int_{-\infty}^{\infty}\int_{-\infty}^{\infty} \mathcal{W}_{ijk}(k_1, k_2, k_3)\, e^{-i(\xi_1 k_1 + \xi_2 k_2 + \xi_3 k_3)}\, dk_1\, dk_2\, dk_3. \tag{A II.313}$$

The Fourier transform of Eq. (A II.298) becomes

$$\frac{\partial \mathcal{F}_{ik}}{\partial \theta} + \mathcal{W}_{ik} = -2\nu k^2 \mathcal{F}_{ik} \tag{A II.314}$$

where

$$\mathcal{W}_{ik} = i k_j \sum_{j=1}^{3} (\mathcal{W}_{ijk} + \mathcal{W}_{kji}) \tag{A II.315}$$

and where

$$k^2 = (k_1)^2 + (k_2)^2 + (k_3)^2 \qquad \text{or} \qquad k = ((k_1)^2 + (k_2)^2 + (k_3)^2)^{1/2}. \tag{A II.316}$$

Define

$$\mathcal{F} = \frac{4\pi k^2}{3} \sum_{i=1}^{3} \mathcal{F}_{ii}. \tag{A II.317}$$

Equation (A II.311) may be rewritten using spherical polar coordinates

$$\overline{u^2} = \int_0^{\infty}\int_0^{\pi}\int_0^{2\pi} \left\{\sum_{i=1}^{3} \frac{1}{3} \mathcal{F}_{ii}\right\} k^2 \sin\phi\, dk\, d\phi\, d\psi \tag{A II.318}$$

$$\overline{u^2} = \int_0^{\infty}\int_0^{\pi} \left\{\frac{2}{3}\pi \sum_{i=1}^{3} \mathcal{F}_{ii}\right\} k^2 \sin\phi\, d\phi\, dk = \int_0^{\infty} \left\{\frac{4}{3}\pi \sum_{i=1}^{3} \mathcal{F}_{ii}\right\} k^2\, dk \tag{A II.319}$$

$$\overline{u^2} = \int_0^{\infty} \mathcal{F}(k)\, dk. \tag{A II.320}$$

Define

$$\mathcal{W} = \frac{4}{3}\pi (k)^2 \sum_{i=1}^{3} \mathcal{W}_{ii}. \tag{A II.321}$$

Equation (A II.314) reduces to

$$\frac{\partial \mathcal{J}}{\partial \theta} + \mathcal{W} = -2\,\nu(k)^2\,\mathcal{J}\,. \tag{A II.322}$$

Since k has dimension of reciprocal length, $\mathcal{J}(k)$ must have dimensions of length cubed divided by time squared. From Eq. (A II.317)

$$\sum_{i=1}^{3} \mathcal{J}_{ii} = \frac{3\,\mathcal{J}}{4\pi(k)^2} \tag{A II.323}$$

and from Eq. (A II.307)

$$\frac{8\pi^3}{\overline{u^2}}\,\frac{3\,\mathcal{J}}{4\pi(k)^2} = \frac{6\pi^2}{(k)^2}\,\frac{\mathcal{J}}{\overline{u^2}} = \int_{-\infty}^{\infty}\int_{-\infty}^{\infty}\int_{-\infty}^{\infty} \sum_{i=1}^{3} R_{ii}(r)\, e^{i(\xi_1 k_1 + \xi_2 k_2 + \xi_3 k_3)}\, d\xi_1\, d\xi_2\, d\xi_3 \tag{A II.324}$$

$$= \int_0^{\infty}\int_0^{\pi}\int_0^{2\pi} \sum_{i=1}^{3} R_{ii}(r)\, e^{ikr\cos\phi}\,(r)^2 \sin\phi\, d\psi\, d\phi\, dr \tag{A II.325}$$

$$= 2\pi \int_0^{\infty} \left\{(r)^2 \sum_{i=1}^{3} R_{ii}(r)\right\} \frac{2\sin k\,r}{k\,r}\, dr. \tag{A II.326}$$

Therefore

$$\frac{3}{2}\,\frac{\pi}{\overline{u^2}}\,\frac{\mathcal{J}}{(k)^2} = \frac{1}{(k)^2}\int_0^{\infty} \sum_{i=1}^{\infty} R_{ii}(r)\, k\, r \sin k\, r\, dr \tag{A II.327}$$

or

$$\mathcal{J} = \frac{2}{3\pi}\int_0^{\infty} \overline{u^2} \sum_{i=1}^{\infty} R_{ii}(r)\, k\, r \sin k\, r\, dr. \tag{A II.328}$$

The sine transform is

$$\overline{u^2} \sum_{i=1}^{3} R_{ii}(r) = 3\int_0^{\infty} \mathcal{J}\,\frac{\sin k\,r}{k\,r}\, dk. \tag{A II.329}$$

Now

$$\sum_{i=1}^{3} R_{ii}(r) = 3f + r\,\frac{df}{dr}. \tag{A II.330}$$

by combining Eqs. (A II.200) and (A II.213). Combination of Eqs. (A II.328) and (A II.330) gives

$$\mathfrak{F} = \frac{2}{3\pi}\int_0^\infty \overline{u^2}\,(3f)\,k r \sin k r\, dr + \frac{2}{3\pi}\int_0^\infty \overline{u^2}\,k(r)^2 \sin k r\, df. \tag{A II.331}$$

Since f is finite at $r = 0$ and approaches zero as r becomes large,

$$\int_{r=0}^{r=\infty} \overline{u^2}\, d(k(r)^2 f \sin k r) = 0. \tag{A II.332}$$

Thus

$$\mathfrak{F} = \frac{2}{3\pi}\overline{u^2}\int_0^\infty \{3 f k r \sin k r - 2 f k r \sin k r - f(k r)^2 \cos k r\}\, dr. \tag{A II.333}$$

Or

$$\mathfrak{F} = \frac{2}{3\pi}\overline{u^2}\int_0^\infty f(k r)^2 \left(\frac{\sin k r}{k r} - \cos k r\right) dr. \tag{A II.334}$$

By similar reasoning Eq. (A II.329) may be rewritten

$$\overline{u^2} f = 3\int_0^\infty \mathfrak{F}(k r)^{-2} \left(\frac{\sin k r}{k r} - \cos k r\right) dk. \tag{A II.335}$$

The longitudinal one-dimensional spectrum which is measured in the experiments on turbulence is

$$\mathfrak{F}_1(k_1) = \int_{-\infty}^\infty \int_{-\infty}^\infty \mathfrak{F}_{11}\, dk_2\, dk_3, \tag{A II.336}$$

$$\mathfrak{F}_1(k_1) = \frac{1}{\pi}\int_{-\infty}^\infty \overline{u^2}\, R_{11}(\xi_1, 0, 0)\, e^{i k_1 \xi_1}\, d\xi_1 = \frac{\overline{u^2}}{\pi}\int_{-\infty}^\infty f \cos k_1 \xi_1\, d\xi_1 \tag{A II.337}$$

or

$$\mathfrak{F}_1(k_1) = \frac{\overline{u^2}}{\pi}\int_{-\infty}^\infty f \cos k_1 r\, dr = 2\frac{\overline{u^2}}{\pi}\int_0^\infty f \cos k_1 r\, dr. \tag{A II.338}$$

The cosine transform of Eq. (A II.338) is

$$\overline{u^2} f = \int_0^\infty \mathcal{F}_1(k_1) \cos k_1 r \, dk_1. \tag{A II.339}$$

Differentiation of Eq. (A II.338) leads to the results

$$(k)^3 \frac{d}{dk}\left[\frac{1}{k}\frac{d\mathcal{F}_1(k)}{dk}\right] = 2\frac{\overline{u^2}}{\pi}\int_0^\infty f(kr)^2\left(\frac{\sin kr}{kr} - \cos kr\right)dr, \tag{A II.340}$$

$$(k)^3 \frac{d}{dk}\left[\frac{1}{k}\frac{d\mathcal{F}_1(k)}{dk}\right] = 3\mathcal{F} = (k)^2\frac{d^2\mathcal{F}_1(k)}{dk^2} - k\frac{d\mathcal{F}_1(k)}{dk}. \tag{A II.341}$$

Integration of Eq. (A II.341) leads to

$$\mathcal{F}_1(k_1) = 3\int_{k_1}^\infty \left[1 - \left(\frac{k_1}{k}\right)^2\right]\frac{\mathcal{F}(k)}{k}\,dk. \tag{A II.342}$$

The lateral spectrum function is

$$\mathcal{F}_2(k_1) = 2\frac{\overline{u^2}}{\pi}\int_0^\infty g \cos k_1 r \, dr, \tag{A II.343}$$

$$\mathcal{F}_2(k_1) = \frac{1}{2}\left\{\mathcal{F}_1(k_1) - k_1\frac{d_1\mathcal{F}_1(k_1)}{dk_1}\right\}. \tag{A II.344}$$

Nomenclature

A, B, C Parameters

a^i ith component of acceleration in generalized coordinates

a_x x-component of acceleration, ft./sec.^{2}

a_y y-component of acceleration, ft./sec.^{2}

a_z z-component of acceleration, ft./sec.^{2}

a_r r-component of acceleration, ft./sec.^{2}

a_ϕ ϕ-component of acceleration, ft./sec.^{2}

a_ψ ψ-component of acceleration, ft./sec.^{2}

e_{ij} ijth-component of deformation, sec.$^{-1}$

F x_1-component of Ξ

F^i ith-component of force, lb.

$\mathcal{F}$ Spectral function defined by Eq. (A II.317), ft.^{3}/sec.^{2}

$\mathcal{F}_{ik}(k_1, k_2, k_3)$ ikth-component of the spectral tensor, ft.^{5}/sec.^{2}

$\mathcal{F}_1(k_1)$ Longitudinal one-dimensional spectrum, ft.^{3}/sec.^{2}

$\mathcal{F}_2(k_1)$ Lateral one-dimensional spectrum, ft.^{3}/sec.^{2}

f Longitudinal velocity correlation scalar parameter

$f''_{r=0}$ Second derivative of f evaluated at $r = 0$

$f''''_{r=0}$ Fourth derivative of f evaluated at $r = 0$

G x_2-component of Ξ defined by Eq. (A II.242)

g Lateral velocity correlation scalar parameter

g_c Acceleration due to gravity, ft./sec.^{2}

$g''_{r=0}$ Second derivative of g evaluated at $r = 0$

$g''''_{r=0}$ Fourth derivative of g evaluated at $r = 0$

$|g_{ij}|$ Determinant whose elements are g_{ij}

g Determinant associated with Euclidean metric tensor

g_{ij} ijth-component of the Euclidean metric tensor

g^{ij} ijth-component of contravariant tensor associated with the Euclidean metric tensor

g_ω Lateral vorticity correlation scalar parameter

H x_3-component of Ξ

$h(r)$ Triple velocity correlation scalar parameter, dimensionless

h' Derivative of h with respect to r

h Distance in a conservative force field in the direction of increasing potential energy, ft.

$\mathring{j}$ The Reynolds dissipation function

j' Friction resulting from irreversible processes in a turbulent stream, ft. lb./lb.

k' Derivative of k with respect to r

k^2 The square of the absolute magnitude of the wave number, ft.$^{-2}$

k_1, k_2, k_3 Rectangular Cartesian coordinates in wave-number space, ft.$^{-1}$

$k(r)$ Triple velocity correlation scalar parameter, dimensionless

$k'''_{r=0}$ Third derivative of $k(r)$ evaluated at $r = 0$

$k^{v}_{r=0}$ Fifth derivative of $k(r)$ evaluated at $r = 0$

l, m, n Direction cosines used in defining relative orientation of two coordinate systems

n^j jth-component of unit normal vector to boundary surface

P Thermodynamic pressure, lb./ft.^{2}

$q(r)$ Triple velocity correlation scalar parameter, dimensionless

q' Derivative of q with respect to r

R_{ij} ijth-component of the correlation tensor, dimensionless

R_{xy} Coefficient of correlation between velocity fluctuation in x- and y-directions

R_1 f

R_2 g

r Position vector of point B' with respect to the point B; Radius, ft.

S Area of a bounding surface

s Distance along space curve, ft.

$s(r)$ A function of r defined in Eq. (A II.256)

$s(x^1, x^2, x^3)$ Scalar function of x^1, x^2, x^3

T_{ijk} ijkth-component of the triple velocity correlation tensor, dimensionless

U_x Root-mean-square velocity fluctuation in the x-direction

U_y Root-mean-square velocity fluctuation in the y-direction

u Velocity fluctuation, ft./sec.

u^i ith-component of the contravariant velocity field, ft./sec.

u_1, u_2, u_3 Velocity components, ft./sec.

$\overline{u^2}$ Mean square velocity fluctuation, ft.^{2}/sec.^{2}

V Specific volume, ft.^{3}/lb.

V Total volume, ft.^{3}

$\overline{V}_{ij}$ ijth-component of the vorticity correlation tensor

V_1, V_2, V_3 Velocity components, ft./sec.

v_1, v_2, v_3 Velocity components, ft./sec.

v_i ith-component of a covariant vector field

$\mathcal{W}_{ijk}$ ijkth-component of the Fourier transform of the triple correlation tensor, ft.^{6}/sec.^{3}

$\mathcal{W}$ Function defined in Eq. (A II.321), ft.^{4}/sec.^{3}

$\mathcal{W}_{ik}$ Function defined in Eq. (A II.315), ft.^{6}/sec.^{3}

w_v Infinitesimal element of work, ft. lb./ft.^{3}

w' Infinitesimal quantity of work in a flow system, ft. lb./lb.

X Divergenceless part of the velocity field

x Rectangular Cartesian coordinate, ft. Altitude in polar cylindrical coordinates, ft.

x_1, x_2, x_3 Rectangular Cartesian coordinates, ft.

x^i ith generalized curvilinear coordinate

Y Nonrotational part of the velocity field

y Rectangular Cartesian coordinate, ft.

y^i ith rectangular Cartesian coordinate, ft.

y_1, y_2, y_3 Rectangular Cartesian coordinate, ft.

z Rectangualr Cartesian coordinate, ft.

α, β, γ Angles used in defining relative orientation of two coordinate systems

Γ^i_{jk} ijkth Euclidean-Christoffel symbol

ζ An energy transfer function, ft. lb./lb.

η Absolute viscosity, lb. sec./ft.^{2}

θ Time, seconds

θ_0 Reference time, seconds

ϑ Time variable of integration, sec.

λ A viscosity coefficient

ν Kinematic viscosity, ft.^{2}/sec.

Ξ Defined in Eq. (A II.236)

ξ^i ith-component of a general contravariant vector field

ξ_1, ξ_2, ξ_3 Rectangular Cartesian components of the vector r

ρ Density, lb. sec.^{2}/ft.^{4}

Ξ Surface area

σ Specific weight, lb./ft.^{3}

τ^i_j ijth-component of the Newtonian stress tensor

Φ A scalar field

Φ^i ith-component of acceleration due to a conservative external field of force, ft./sec.^{2}

φ Defined in Eq. (A II.236)

ϕ Colatitude of polar spherical coordinates, radians

ψ Azimuth in polar cylindrical and polar spherical coordinate systems, radians

ω Vorticity vector with components $\omega_1, \omega_2, \omega_3$

ω_{ij} ijth-component of vorticity, sec.$^{-1}$

∇ Operator del of vector analysis. In rectangular Cartesian coordinates, this operator has the components $\partial/\partial x, \partial/\partial y, \partial/\partial z$

δ^i_k Kronecker delta

δ Variation operator

Intrinsic derivative operator

$| |$ Indicates that the number array constitutes a determinant

$[\ ]$ Indicates that the number array constitutes a matrix

$-$ Distinguishes two sets of coordinates

Indicates time-average value. Placed over symbols

SUPERSCRIPTS

i, j, α, β Contravariant tensor indices

SUBSCRIPTS

f Indicates fluctuating quantity

r, x, y, z, ϕ, ψ Components

i, j, α, β Covariant tensor indices

Symbol indicating covariant differentiation of tensor with respect to the coordinate whose index follows this symbol

References

1. Michal, A. D., "Matrix and Tensor Analysis." Wiley, New York, 1947.
2. Corrsin, S., *J. Aeronaut. Sci.* **20**, 853 (1953).
3. Jeffreys, H., "Cartesian Tensors." Cambridge U. P., New York, 1931.
4. Sokolnikoff, I. S., "Tensor Analysis." Wiley, New York, 1951.
5. Goldstein, S., "Modern Developments in Fluid Mechanics," Vol. 1. Oxford U. P., 1938.
6. Margenau, H., and Murphy, G. M., "The Mathematics of Physics and Chemistry." Van Nostrand, New York, 1943.
7. Kirkwood, J. G., and Crawford, B., Jr., *J. Phys. Chem.* **56**, 1048 (1952).
8. Lamb, H., "Hydrodynamics." Cambridge U. P., New York, 1932.
9. von Kármán, T., *J. Aeronaut. Sci.* **4**, 131 (1937).
10. von Kármán, T., and Howarth, L., *Proc. Roy. Soc.* **A 164**, 192 (1938).
11. Kovasznay, L. S. G., *J. Aeronaut. Sci.* **15**, 745 (1948).
12. Batchelor, G. K., "The Theory of Homogeneous Turbulence." Cambridge U. P., New York, 1953.

APPENDIX III

Constants and Conversion Factors

Dimensions

The quantitative description of nature requires a systematic set of dimensions and a consistent set of units. The basis for the present tabulation is the force-length-time system of dimensions with the addition of the undefined concept, temperature (*1*). On this basis the quantity of material is measured in terms of its weight in a standard gravitational field. In accordance with Newton's second law applied to a constant-mass system, mass is the quotient of this weight and the standard acceleration due to gravity is 32.1740 ft./sec.^{2}. As a matter of definition, the unit of mass in the mass-length-time system of dimensions exerts, in a standard gravitational field, a unit of force in the force-length-time system. This choice of reference standard results primarily from the reproducibility and precision with which the acceleration of gravity upon a fixed quantity of material may be determined experimentally.

The set of fundamental physical constants given in Table A III—1 has been taken from available tabulations and is not necessarily restricted to the force-length-time system of dimensions. However, all units associated with the mass-length-time system have been indicated by asterisks. In Tables A III—2 to A 3—V 8, which are concerned with conversion factors, the force-length-time system has been retained. Both the constants and conversion factors were based on values recommended by the National Bureau of Standards (*2*, *3*) and the Subcommittee on Physical Constants of the National Research Council (*4*). They compare favorably with data presented by Du Mond and Cohen (*5*).

TABLE A III-1. Physical Constants (*6*).

Force	
1 pound (lb.) avoirdupois	= 453.5924277 grams (g.)
Length	
1 U.S. inch (in.)	= 1/0.3937 centimeters
	= 2.54000508 centimeters (cm.)
	= 1/12 U.S. foot (ft.)
Time	
1 mean solar second (sec.)	= 1.00273791 sidereal second
	= 1/86,400 mean solar day
Volume	
1 liter (l.)	= 1000.028 ± 0.004 cm.^{3}
1 U.S. gallon (gal.)	= 231 in.^{3}
Energy	
1 dyne cm.	= 1 g. cm.^{2}/sec.^{2}
1 erg	= 1 dyne cm.
1 absolute (abs.) joule	= 10^7 erg
1 abs. joule	= 0.999835 ± 0.000052 int. joule (N.B.S.)
1 abs. electron volt	= $(1.60200 \pm 0.00060) \times 10^{12}$ erg
1 thermochemical calorie (cal.)	= 4.1840 abs. joule
	= 41.2929 cm.^{3} atm.
1 I.T. (International Steam Tables) cal.	= 1.000654 cal., thermochemical (N.B.S.)
	= $1/860 \pm 0.00116279$ int. watt-hour
1 I.T. British Thermal Unit (B.t.u.)	= 252.161 cal., thermochemical (N.B.S.)
Power	
1 abs. joule/sec.	= 1 abs. watt
1 abs. watt	= 0.999835 ± 0.000052 int. watt (N.B.S.)
1 horsepower (hp.)	= 550 ft. lb./sec.
	= 745.701 abs. watt
Acceleration Due to Gravity — Standard	
g_c	= 980.665 cm./sec.^{2}
	= 32.1740 ft./sec.^{2}
Pressure	
1 standard atmosphere (atm.)	= 1.013250×10^6 dyne/cm.^{2}
1 standard millimeter (mm.) mercury (at 32° F. and standard gravity)	= 1/760 = 0.0013157895 atm.

Temperature

1 degree centigrade (°C.)	= 1.8° Fahrenheit (°F.)
$T_{0°C}$	= 273.160 ± 0.010° Kelvin (°K.)
$T_{0°F}$	= 459.688 ± 0.018° Rankine (°R.)
$T_{32°F}$	= 491.688 ± 0.018° Rankine (°R.)

Universal Gas Constant

$$R = 8.31439 \pm 0.00034 \frac{\text{abs. joules}}{(°\text{K.})\ (\text{g. mole})}$$

TABLE A III-2. Length (*6*).

Units	cm.	m.	in.	ft.
1 cm.	1	0.01	0.3937	0.032808333
1 m.	100	1	39.37	3.2808333
1 in.	2.5400051	0.025400051	1	0.083333333
1 ft.	30.480061	0.30480061	12	1

1 micron (μ) = 10^{-4} cm.; 1 angstrom unit (Å.) = 10^{-8} cm.

TABLE A III-3. Area (*6*).

Units	$cm.^2$	$m.^2$	$in.^2$	$ft.^2$
1 $cm.^2$	1	10^{-4}	0.15499969	1.0763867×10^{-3}
1 $m.^2$	10^4	1	1549.9969	10.763867
1 $in.^2$	6.4516258	6.4516258×10^{-4}	1	6.9444444×10^{-3}
1 $ft.^2$	929.03412	0.092903412	144	1

TABLE A III-4. Volume (*6*).

Units	$cm.^3$	$in.^3$	$ft.^3$	liter	gal.
1 $cm.^3$	1	0.061023378	3.5314455×10^{-5}	0.9999720×10^{-3}	2.6417047×10^{-4}
1 $in.^3$	16.387162	1	5.7870370×10^{-4}	1.638670×10^{-2}	4.3290043×10^{-3}
1 $ft.^3$	28317.016	1728	1	28.31622	7.4805195
1 liter	1000.028	61.02509	0.03531544	1	0.2641779
1 gal.	3785.4345	231	0.13368056	3.785329	1

TABLE III-5. Weight (*6*).

Unit	g.	lb.	ton
1 g.	1	2.2046223×10^{-3}	1.1023112×10^{-6}
1 lb.	453.59243	1	0.0005
1 ton	907184.86	2000	1

TABLE A III-6. Specific Weight (*6*).

Units	$g./cm.^3$	g./ml	$lb./in.^3$	$lb./ft.^3$	lb./gal.
1 $g./cm.^3$	1	1.000028	0.036127504	62.428327	8.3454534
1 g./ml.	0.9999720	1	0.03612649	62.42658	8.345220
1 $lb./in.^3$	27.679742	27.68052	1	1728	231
1 $lb./ft.^3$	0.016018369	0.01601882	5.7870370×10^{-4}	1	0.13368056
1 lb./gal.	0.11982572	0.1198291	4.3290043×10^{-3}	7.4805195	1

TABLE A III-7. Pressure (*6*).

Units	dyne/cm.^{2}	atm.	kg./cm.^{2}	mm. Hg	in. Hg	lb./in.^{2}
1 dyne/cm.^{2}	1	0.9869233×10^{-6}	1.0197162×10^{-6}	7.500617×10^{-4}	2.952993×10^{-5}	1.4503830×10^{-5}
1 atm.	1013250.0	1	1.0332275	760.0	29.92120	14.696006
1 kg./cm.^{2}	980665.0	0.9678411	1	735.5592	28.95897	14.223398
1 mm. Hg	1333.2237	1.3157895×10^{-3}	1.3595098×10^{-3}	1	0.03937	0.019336850
1 in. Hg	33863.95	0.03342112	0.03453162	25.400051	1	0.4911570
1 lb./in.^{2}	68947.31	0.06804570	0.07030669	51.71473	2.036009	1

1 bar = 10^6 dyne/cm.^{2}.

TABLE A III-8. Energy (*2*).

	B.t.u.	therms	ft. lb.	hp. hr.	kw. hr.
1 British thermal unit (B.t.u.)	1	1×10^{-5}	778.173	3.93017×10^{-4}	2.93074×10^{-4}
1 therm	1×10^{5}	1	7.78173×10^{7}	39.3017	29.3074
1 foot pound (ft .lb.)	1.28506×10^{-3}	1.28506×10^{-8}	1	5.050505×10^{-7}	3.76618×10^{-7}
1 horsepower hour (hp. hr.)	2.54442×10^{3}	2.54442×10^{-2}	1.98000×10^{6}	1	0.745703
1 absolute kilowatthour (kw. hr.)	3412.11	3.41211×10^{-2}	2.65521×10^{6}	1.34102	1
1 metric horsepower hour (cv. hr.)	2509.57	2.50957×10^{-2}	1.95288×10^{6}	0.98630	0.735490
1 kilogram meter (kg. m.)	9.2947×10^{-3}	9.2947×10^{-8}	7.23288	3.65298×10^{-6}	2.72403×10^{-6}
1 calorie (cal.) (thermochemical)	3.96562×10^{-3}	3.96562×10^{-8}	3.08594	1.55855×10^{-6}	1.16222×10^{-6}
1 International Steam Table calorie (I.T.cal.)	3.96832×10^{-3}	3.96832×10^{-8}	3.08804	1.55962×10^{-6}	1.16301×10^{-6}
1 absolute joule (j.)	9.4780×10^{-4}	9.4780×10^{-9}	0.737552	3.72502×10^{-7}	2.77778×10^{-7}

	cv. hr.	kg. m.	cal.	I.T.cal.	j.
1 British thermal unit (B.t.u.)	3.98474×10^{-4}	107.588	252.167	251.996	1055.07
1 therm	39.8474	1.07588×10^{7}	2.52167×10^{7}	2.51996×10^{7}	1.05507×10^{8}
1 foot pound (ft. lb.)	5.12063×10^{-7}	0.138257	0.324050	3.323830	1.35583
1 horsepower hour (hp. hr.)	1.01388	2.73749×10^{5}	6.41619×10^{5}	6.41184×10^{5}	2.68454×10^{6}
1 absolute kilowatthour (kw. hr.)	1.35964	3.67102×10^{5}	8.60421×10^{5}	8.5984×10^{5}	3.60000×10^{6}
1 metric horsepower hour (cv. hr.)	1	2.70000×10^{5}	6.32831×10^{5}	6.32402×10^{5}	2.64777×10^{6}
1 kilogram meter (kg. m.)	3.70370×10^{-6}	1	2.34382	2.34223	9.80665
1 calorie (cal.) (thermochemical)	1.58020×10^{-6}	0.426653	1	0.99932	4.18400
1 International Steam Table calorie (I.T.cal.)	1.58127×10^{-6}	0.426944	1.00068	1	4.18684
1 absolute joule (j.)	3.77674×10^{-7}	0.1019716	0.2390057	0.238842	1

TABLE A III-9. Miscellaneous Derived Equivalents (*6*).

P.V. Product for Ideal Gas

$(P.V.)^{p\ 0}_{T_{0°C.}\ \text{or}\ T_{32°F.}}$	= 2271.16 abs. joule/g. mole
	= 22,414.6 (cm.^{3}) (atm.)/g. mole
	= 22.4140 (liter) (atm.)/g. mole
	= 3.69300 (ft. lb.)/(lb. mole)
	= 4.74584×10^{-3} B.t.u./(lb. mole)
	= 2.56458×10^{-2} (ft.^{3}) (psi.)/(lb. mole)

Gas Constant

$R\dfrac{(P.V.)^{p\ 0}_{T_{0°C.}\ \text{or}\ T_{32°F.}}}{T_{0°C.}\ \text{or}\ T_{32°F.}}$	= 8.31439[1] abs. joule/(°K.) (g. mole)
	= 1.98719 cal./(°K.) (g. mole)
	= 82.0567 (cm.^{3}) (atm.)/(°K.) (g. mole)
	= 0.0820544 (liter) (atm.)/(°K.) (g. mole)
	= 1545.33 (ft. lb.)/(lb. mole) (°R.)
	= 1.98589 B.t.u./(lb. mole) (°R.)
	= 10.73147 (ft.^{3}) (psi.)/(lb. mole) (°R.)

Standard Atmosphere of Pressure

P	= 14.69601 lb./in.^{2}

Horsepower

1 hp.	= 745.701 watts
	= 550 (ft. lb.)/sec.
	= 0.706799 B.t.u./sec.

---

[1] Du Mond and Cohen (*5*) give 8.31667 joules/(°K.) (g. mole). This corresponds to 10.73441 [(lb./in.^{2}) (ft.^{3})]/[(°R.) (lb. mole)].

TABLE A III-10. Numerical Constants and Mathematical Relationships.

Numerical Constants (7).

Constant	Value	Constant	Value
π	3.14159 26536	e	2.71828 18285
π^{-1}	0.3183 0989	e^{-1}	0.3678 7944
π^2	9.8696 0440	e^2	7.3890 5610
π^{-2}	0.1013 2118	e^{-2}	0.1353 3528
$\pi^{1/2}$	1.7724 5385	$e^{1/2}$	1.6487 2127
$\pi^{-1/2}$	0.5641 8958	$e^{-1/2}$	0.6065 3066
π^3	31.0062 767		
π^{-3}	0.0322 5153	1 radian	57° 17′ 44.80625″
$\pi^{1/3}$	1.4645 9189		57.29577 95131°
$\pi^{-1/3}$	0.6827 8406	1 degree	0.01745 32925 199 radian

Logarithmic Constants

$$\log_{10} e = 0.43429\ 44819$$

$$\log_e 10 = 2.30258\ 50930$$

$$\log_a x = \log_b x / \log_b a$$

$$\log_{10} x = \log_e x / \log_e 10 = 0.4342944819 \log_e x$$

$$\log_e x = \log_{10} x / \log_{10} e = 2.3025850930 \log_{10} x$$

TABLE A III-11. International Atomic Weights.

[Chemical Scale 1953 Revision (*8*)].

Element	Symbol	Atomic Number	Atomic Weight[1]	Element	Symbol	Atomic Number	Atomic Weight[1]
Actinium	Ac	89	227	Curium	Cm	96	[245]
Aluminum	Al	13	26.98	Dysprosium	Dy	66	162.46
Americium	Am	95	[243]	Erbium	Er	68	167.2
Antimony	Sb	51	121.76	Europium	Eu	63	152.0
Argon	A	18	39.944	Fluorine	F	9	19.00
Arsenic	As	33	74.91	Francium	Fr	87	[223]
Astatine	At	85	[210]	Gadolinium	Gd	64	156.9
Barium	Ba	56	137.36	Gallium	Ga	31	69.72
Berkelium	Bk	97	[245]	Germanium	Ge	32	72.60
Beryllium	Be	4	9.013	Gold	Au	79	197.0
Bismuth	Bi	83	209.00	Hafnium	Hf	72	178.6
Boron	B	5	10.82	Helium	He	2	4.003
Bromine	Br	35	79.916	Holmium	Ho	67	164.94
Cadmium	Cd	48	112.41	Hydrogen	H	1	1.0080
Calcium	Ca	20	40.08	Indium	In	49	114.76
Californium	Cf	98	[248]	Iodine	I	53	126.91
Carbon	C	6	12.011	Iridium	Ir	77	192.2
Cerium	Ce	58	140.13	Iron	Fe	26	55.85
Cesium	Cs	55	132.91	Krypton	Kr	36	83.80
Chlorine	Cl	17	35.457	Lanthanum	La	57	138.92
Chromium	Cr	24	52.01	Lead	Pb	82	207.21
Cobalt	Co	27	58.94	Lithium	Li	3	6.940
Columbium				Lutetium	Lu	71	174.99
(See Niobium)				Magnesium	Mg	12	24.32
Copper	Cu	29	63.54	Manganese	Mn	25	54.94

Element	Symbol	Atomic Number	Atomic Weight[1]	Element	Symbol	Atomic Number	Atomic Weight[1]
Mercury	Hg	80	200.61	Samarium	Sm	62	150.43
Molybdenum	Mo	42	95.95	Scandium	Sc	21	44.96
Neodymium	Nd	60	144.27	Selenium	Se	34	78.96
Neptunium	Np	93	[237]	Silicon	Si	14	28.09
Neon	Ne	10	20.183	Silver	Ag	47	107.880
Nickel	Ni	28	58.69	Sodium	Na	11	22.991
Niobium (Columbium)	Nb	41	92.91	Strontium	Sr	38	87.63
Nitrogen	N	7	14.008	Sulfur	S	16	32.066[2]
Osmium	Os	76	190.2	Tantalum	Ta	73	180.95
Oxygen	O	8	16	Technetium	Tc	43	99
Palladium	Pd	46	106.7	Tellurium	Te	52	127.61
Phosphorus	P	15	30.975	Terbium	Tb	65	158.93
Platinum	Pt	78	195.23	Thallium	Tl	81	204.39
Plutonium	Pu	94	[242]	Thorium	Th	90	232.05
Polonium	Po	84	210	Thulium	Tm	69	168.94
Potassium	K	19	39.100	Tin	Sn	50	118.70
Praseodymium	Pr	59	140.92	Titanium	Ti	22	47.90
Promethium	Pm	61	[145]	Tungsten	W	74	183.92
Protactinium	Pa	91	231	Uranium	U	92	238.07
Radium	Ra	88	226.05	Vanadium	V	23	50.95
Radon	Rn	86	222	Xenon	Xe	54	131.3
Rhenium	Re	75	186.31	Ytterbium	Yb	70	173.04
Rhodium	Rh	45	102.91	Yttrium	Y	39	88.92
Rubidium	Rb	37	85.48	Zinc	Zn	30	65.38
Ruthenium	Ru	44	101.1	Zirconium	Zr	40	91.22

[1] A value given in brackets denotes the mass number of the isotope of longest known half-life.

[2] Because of natural variations in the relative abundance of the isotopes of sulfur, the atomic weight of this element has a range of $\pm$ 0.003.

TABLE A III-12. Atomic Weight Multiples.

Carbon		Hydrogen	
C 1	12.010	H 1	1.0080
2	24.020	2	2.0160
3	36.030	3	3.0240
4	48.040	4	4.0320
5	60.050	5	5.0400
6	72.060	6	6.0480
7	84.070	7	7.0560
8	96.080	8	8.0640
9	108.09	9	9.0720
C 10	120.10	H 10	10.080
11	132.11	11	11.088
12	144.12	12	12.096
13	156.13	13	13.104
14	168.14	14	14.112
15	180.15	15	15.120
16	192.16	16	16.128
17	204.17	17	17.136
18	216.18	18	18.144
19	228.19	19	19.152
C 20	240.20	H 20	20.160
Nitrogen		**Oxygen**	
N 1	14.008	O 1	16.0000
2	28.016	2	32.0000
3	42.024	3	48.0000
4	56.032	4	64.0000
5	70.040	5	80.0000

Nomenclature

$F(z) = F(w)$ Complex velocity potential
$F'(z)$ Derivative of $F(z)$ with respect to the variable z
r Radius in polar coordinates, ft.
u_x Component of velocity in the x-direction, ft./sec.
u_y Component of velocity in the y-direction, ft./sec.
u_∞ Free stream velocity, ft./sec.
w A second position variable in the complex plane
x Rectangular Cartesian coordinate, ft.
y Rectangular Cartesian coordinate, ft.
θ Azimuth in polar coordinates, radius
ϕ Velocity potential, ft.^{2}/sec.
ψ Stream function, ft.^{2}/sec.
$| \, |$ Absolute value
$\bar{\ }$ Complex conjugate. Placed over symbols

References

1. Bridgman, P. W., "The Logic of Modern Physics." Macmillan, New York, 1938.
2. Private communication from D. D. Wagman, Chemistry, Division of Natl. Bur. Standards, Sept. 10, 1954.
3. "Announcement of Changes in Electrical and Photometric Units," *Natl. Bur. Standards Circ.* C 459 (1948).
4. Rossini, F. D., Gucker, F. T., Jr., Johnston, H. L., Pauling, L., and Vinal, G. W., *J. Am. Chem. Soc.* 74, 2699 (1952).
5. Du Mond, J. W. M., and Cohen, E. R., *Am. Scientist* 40, 447 (1952).
6. Rossini, F. D., "Selected Values of Properties of Hydrocarbons," *Natl. Bur. Standards Circ.* C 461 [1947].
7. Hodgman, C., D. [ed.], "Handbook of Chemistry and Physics." Chemical Rubber Publishing, Cleveland, 1948.
8. Report of the committee on atomic weights of the American Chemical Society, *J. Am. Chem. Soc.* 76, 2033 [1954].

APPENDIX IV

Analysis of Potential Flow Across a Cylinder

The assumption of potential flow in two dimensions involves the assumption that there exists a potential function ϕ, called the velocity potential such that

$$u_x = \frac{\partial \phi}{\partial x}, \tag{A IV.01}$$

$$u_y = \frac{\partial \phi}{\partial y}. \tag{A IV.02}$$

By the equation of continuity for an incompressible fluid

$$\frac{\partial u_x}{\partial x} + \frac{\partial u_y}{\partial y} = \frac{\partial^2 \phi}{\partial x^2} + \frac{\partial^2 \phi}{\partial y^2} = 0. \tag{A IV.03}$$

Consequently the velocity potential is a solution of Laplace's equation in two dimensions. From the theory of functions of a complex variable (*1*), there exists a function $\psi(x, y)$ such that

$$u_x = \frac{\partial \phi}{\partial x} = \frac{\partial \psi}{\partial y} \tag{A IV.04}$$

and

$$u_y = \frac{\partial \phi}{\partial y} = -\frac{\partial \psi}{\partial x}. \tag{A IV.05}$$

Let

$$F(z) = F(x + i\,y) = \phi + i\,\psi. \tag{A IV.06}$$

Then

$$F'(z) = \frac{\partial \phi}{\partial x} + i\frac{\partial \psi}{\partial y} = \frac{\partial \phi}{\partial x} - i\frac{\partial \phi}{\partial y} = u_x - i\,u_y \tag{A IV.07}$$

and the velocity is the complex conjugate of $F'(z)$,

$$u_x + i\,u_y = \overline{F'(z)}. \tag{A IV.08}$$

When the flow is uniform in the direction of positive x,

$$u_x = \frac{\partial \phi}{\partial x} = u_\infty = \frac{\partial \psi}{\partial y} \tag{A IV.09}$$

or

$$\phi = u_\infty\, x \tag{A IV.10}$$

and

$$\psi = u_\infty\, y. \tag{A IV.11}$$

If a solid wall exists at $(y = 0)$, then slippage occurs at the wall in order to satisfy Eq. (A IV.09).

The lines of constant ϕ (equipotentials) are always perpendicular to the lines of constant ψ (streamlines) because of Eqs. (A IV.04) and (A IV.05) (*1*). Thus, if the boundary conditions at $(y = 0)$ are transformed to the same boundary conditions at $(x^2 + y^2 = 1)$, the equipotentials will still be perpendicular to the streamlines and potential flow will still obtain. Under such a transformation one streamline lies along the circle $(x^2 + y^2 = 1)$. The transformation which achieves this result is:

$$z = w + \frac{1}{w} = x + i\,y. \tag{A IV.12}$$

From Eq. (A IV.12) it follows that

$$F(z) = u_\infty\, x + i\,u_\infty\, y = u_\infty\left(w + \frac{1}{w}\right) = F(w), \tag{A IV.13}$$

$$\frac{dF(w)}{dw} = F'(w) = u_\infty\left(1 - \frac{1}{w^2}\right) \tag{A IV.14}$$

and

$$\begin{aligned}\overline{F'(w)} &= \overline{u_\infty\left(1 - \frac{1}{w^2}\right)} = u_\infty\left(1 - \frac{1}{\bar{w}^2}\right) = u_\infty\left(1 - \frac{1}{r^2 e^{-2i\theta}}\right) \\ &= u_\infty\left(1 - \frac{e^{2i\theta}}{r^2}\right) = u_\infty\left(1 - \frac{\cos 2\theta}{r^2} - i\,\frac{\sin 2\theta}{r^2}\right).\end{aligned} \tag{A IV.15}$$

The speed along the path ($x^2 + y^2 = r^2 = 1$) is

$$|F'(w)| = u_\infty \sqrt{(1 - \cos 2\theta)^2 + \sin^2 2\theta}, \tag{A IV.16}$$

$$= u_\infty \sqrt{1 - 2\cos 2\theta + \cos^2 2\theta + \sin^2 2\theta} \tag{A IV.17}$$

$$= u_\infty \sqrt{2(1 - \cos 2\theta)} = u_\infty \sqrt{4 \sin^2 \theta} \tag{A IV.18}$$

$$= 2 u_\infty |\sin \theta|. \tag{A IV.19}$$

Equation (A IV.19) shows that in potential flow perpendicular to a cylinder, the speed along the streamline adjacent to the cylinder reaches a maximum of twice the free stream value.

References

1. Churchill, R. V., "Introduction to Complex Variables and Applications," McGraw-Hill, New York, 1948.

Subject Index